



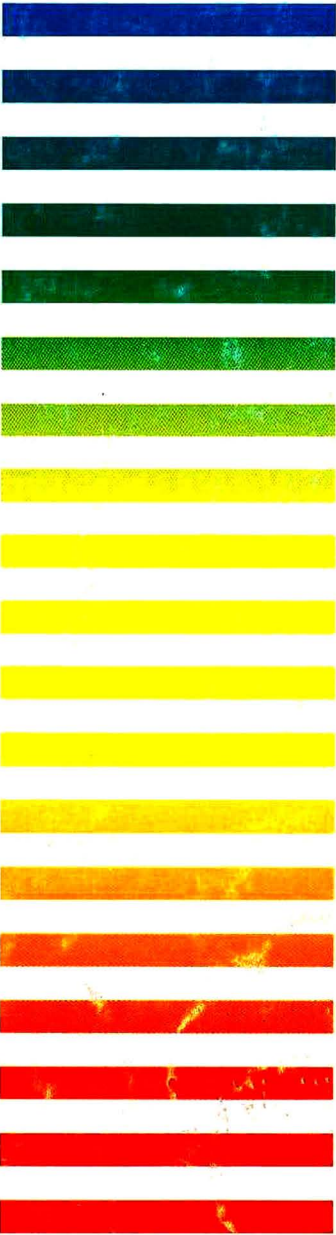
VOL. **603** NOS. **1 + 2** JUNE 19, 1992

COMPLETE IN ONE ISSUE

JOURNAL OF

# CHROMATOGRAPHY

INCLUDING ELECTROPHORESIS AND OTHER SEPARATION METHODS



## EDITORS

U. A. Th. Brinkman (Amsterdam)  
R. W. Giese (Boston, MA)  
J. K. Haken (Kensington, N.S.W.)  
K. Macek (Prague)  
L. R. Snyder (Orinda, CA)

EDITORS, SYMPOSIUM VOLUMES,  
E. Heftmann (Orinda, CA), Z. Deyl (Prague)

## EDITORIAL BOARD

D. W. Armstrong (Rolla, MO)  
W. A. Aue (Halifax)  
P. Boček (Brno)  
A. A. Boulton (Saskatoon)  
P. W. Carr (Minneapolis, MN)  
N. H. C. Cooke (San Ramon, CA)  
V. A. Davankov (Moscow)  
Z. Deyl (Prague)  
S. Dilli (Kensington, N.S.W.)  
F. Erni (Basle)  
M. B. Evans (Hatfield)  
J. L. Glajch (N. Billerica, MA)  
G. A. Guiochon (Knoxville, TN)  
P. R. Haddad (Kensington, N.S.W.)  
I. M. Hais (Hradec Králové)  
W. S. Hancock (San Francisco, CA)  
S. Hjertén (Uppsala)  
Cs. Horváth (New Haven, CT)  
J. F. K. Huber (Vienna)  
K.-P. Hupe (Waldbronn)  
T. W. Hutchens (Houston, TX)  
J. Janák (Brno)  
P. Jandera (Pardubice)  
B. L. Karger (Boston, MA)  
J. J. Kirkland (Wilmington, DE)  
E. sz. Kováts (Lausanne)  
A. J. P. Martin (Cambridge)  
L. W. McLaughlin (Chestnut Hill, MA)  
E. D. Morgan (Keele)  
J. D. Pearson (Kalamazoo, MI)  
H. Poppe (Amsterdam)  
F. E. Regnier (West Lafayette, IN)  
P. G. Righetti (Milan)  
P. Schoenmakers (Eindhoven)  
R. Schwarzenbach (Dübendorf)  
R. E. Shoup (West Lafayette, IN)  
A. M. Siouffi (Marseille)  
D. J. Strydom (Boston, MA)  
N. Tanaka (Kyoto)  
S. Terabe (Hyogo)  
K. K. Unger (Mainz)  
R. Verpoorte (Leiden)  
Gy. Vigh (College Station, TX)  
J. T. Watson (East Lansing, MI)  
B. D. Westerlund (Uppsala)

## EDITORS, BIBLIOGRAPHY SECTION

Z. Deyl (Prague), J. Janák (Brno), V. Schwarz (Prague)

ELSEVIER

# JOURNAL OF CHROMATOGRAPHY

INCLUDING ELECTROPHORESIS AND OTHER SEPARATION METHODS

**Scope.** The *Journal of Chromatography* publishes papers on all aspects of chromatography, electrophoresis and related methods. Contributions consist mainly of research papers dealing with chromatographic theory, instrumental development and their applications. The section *Biomedical Applications*, which is under separate editorship, deals with the following aspects: developments in and applications of chromatographic and electrophoretic techniques related to clinical diagnosis or alterations during medical treatment; screening and profiling of body fluids or tissues with special reference to metabolic disorders; results from basic medical research with direct consequences in clinical practice; drug level monitoring and pharmacokinetic studies; clinical toxicology; analytical studies in occupational medicine.

**Submission of Papers.** Manuscripts (in English; four copies are required) should be submitted to: Editorial Office of *Journal of Chromatography*, P.O. Box 681, 1000 AR Amsterdam, Netherlands, Telefax (+31-20) 5862 304, or to: The Editor of *Journal of Chromatography, Biomedical Applications*, P.O. Box 681, 1000 AR Amsterdam, Netherlands. Review articles are invited or proposed by letter to the Editors. An outline of the proposed review should first be forwarded to the Editors for preliminary discussion prior to preparation. Submission of an article is understood to imply that the article is original and unpublished and is not being considered for publication elsewhere. For copyright regulations, see below.

**Publication.** The *Journal of Chromatography* (incl. *Biomedical Applications*) has 39 volumes in 1992. The subscription prices for 1992 are:

*J. Chromatogr.* (incl. *Cum. Indexes, Vols. 551-600*) + *Biomed. Appl.* (Vols. 573-611):

Dfl. 7722.00 plus Dfl. 1209.00 (p.p.h.) (total ca. US\$ 4880.25)

*J. Chromatogr.* (incl. *Cum. Indexes, Vols. 551-600*) only (Vols. 585-611):

Dfl. 6210.00 plus Dfl. 837.00 (p.p.h.) (total ca. US\$ 3850.75)

*Biomed. Appl.* only (Vols. 573-584):

Dfl. 2760.00 plus Dfl. 372.00 (p.p.h.) (total ca. US\$ 1711.50).

**Subscription Orders.** The Dutch guilder price is definitive. The US\$ price is subject to exchange-rate fluctuations and is given as a guide. Subscriptions are accepted on a prepaid basis only, unless different terms have been previously agreed upon. Subscriptions orders can be entered only by calendar year (Jan.-Dec.) and should be sent to Elsevier Science Publishers, Journal Department, P.O. Box 211, 1000 AE Amsterdam, Netherlands. Tel. (+31-20) 5803 642, Telefax (+31-20) 5803 598, or to your usual subscription agent. Postage and handling charges include surface delivery except to the following countries where air delivery via SAL (Surface Air Lift) mail is ensured: Argentina, Australia, Brazil, Canada, China, Hong Kong, India, Israel, Japan\*, Malaysia, Mexico, New Zealand, Pakistan, Singapore, South Africa, South Korea, Taiwan, Thailand, USA. \*For Japan air delivery (SAL) requires 25% additional charge of the normal postage and handling charge. For all other countries airmail rates are available upon request. Claims for missing issues must be made within three months of our publication (mailing) date, otherwise such claims cannot be honoured free of charge. Back volumes of the *Journal of Chromatography* (Vols. 1-572) are available at Dfl. 217.00 (plus postage). Customers in the USA and Canada wishing information on this and other Elsevier journals, please contact Journal Information Center, Elsevier Science Publishing Co. Inc., 655 Avenue of the Americas, New York, NY 10010, USA, Tel. (+1-212) 633 3750, Telefax (+1-212) 633 3990.

**Abstracts/Contents Lists** published in Analytical Abstracts, Biochemical Abstracts, Biological Abstracts, Chemical Abstracts, Chemical Titles, Chromatography Abstracts, Clinical Chemistry Lookout, Current Awareness in Biological Sciences (CABS), Current Contents/Life Sciences, Current Contents/Physical, Chemical & Earth Sciences, Deep-Sea Research/Part B: Oceanographic Literature Review, Excerpta Medica, Index Medicus, Mass Spectrometry Bulletin, PASCAL-CNRS, Pharmaceutical Abstracts, Referativnyi Zhurnal, Research Alert, Science Citation Index and Trends in Biotechnology.

**US Mailing Notice.** *Journal of Chromatography* (main section ISSN 0021-9673, *Biomedical Applications* section ISSN 0378-4347) is published (78 issues/year) by Elsevier Science Publishers (Sara Burgerhartstraat 25, P.O. Box 211, 1000 AE Amsterdam, Netherlands). Annual subscription price in the USA US\$ 4880.25 (subject to change), including air speed delivery. Application to mail at second class postage rate is pending at Jamaica, NY 11431. **USA POSTMASTERS:** Send address changes to *Journal of Chromatography*, Publications Expediting, Inc., 200 Meacham Avenue, Elmont, NY 11003. Airfreight and mailing in the USA by Publication Expediting.

See inside back cover for Publication Schedule, Information for Authors and information on Advertisements.

© 1992 ELSEVIER SCIENCE PUBLISHERS B.V. All rights reserved.

0021-9673/92/\$05.00

No part of this publication may be reproduced, stored in a retrieval system or transmitted in any form or by any means, electronic, mechanical, photocopying, recording or otherwise, without the prior written permission of the publisher, Elsevier Science Publishers B.V., Copyright and Permissions Department, P.O. Box 521, 1000 AM Amsterdam, Netherlands.

Upon acceptance of an article by the journal, the author(s) will be asked to transfer copyright of the article to the publisher. The transfer will ensure the widest possible dissemination of information.

Submission of an article for publication entails the authors' irrevocable and exclusive authorization of the publisher to collect any sums or considerations for copying or reproduction payable by third parties (as mentioned in article 17 paragraph 2 of the Dutch Copyright Act of 1912 and the Royal Decree of June 20, 1974 (S. 351) pursuant to article 16 b of the Dutch Copyright Act of 1912) and/or to act in or out of Court in connection therewith.

**Special regulations for readers in the USA.** This journal has been registered with the Copyright Clearance Center, Inc. Consent is given for copying of articles for personal or internal use, or for the personal use of specific clients. This consent is given on the condition that the copier pays through the Center the per-copy fee stated in the code on the first page of each article for copying beyond that permitted by Sections 107 or 108 of the US Copyright Law. The appropriate fee should be forwarded with a copy of the first page of the article to the Copyright Clearance Center, Inc., 27 Congress Street, Salem, MA 01970, USA. If no code appears in an article, the author has not given broad consent to copy and permission to copy must be obtained directly from the author. All articles published prior to 1980 may be copied for a per-copy fee of US\$ 2.25, also payable through the Center. This consent does not extend to other kinds of copying, such as for general distribution, resale, advertising and promotion purposes, or for creating new collective works. Special written permission must be obtained from the publisher for such copying.

No responsibility is assumed by the Publisher for any injury and/or damage to persons or property as a matter of products liability, negligence or otherwise, or from any use or operation of any methods, products, instructions or ideas contained in the materials herein. Because of rapid advances in the medical sciences, the Publisher recommends that independent verification of diagnoses and drug dosages should be made.

Although all advertising material is expected to conform to ethical (medical) standards, inclusion in this publication does not constitute a guarantee or endorsement of the quality or value of such product or of the claims made of it by its manufacturer.

This issue is printed on acid-free paper.

Printed in the Netherlands

## CONTENTS

(Abstracts/Contents Lists published in Analytical Abstracts, Biochemical Abstracts, Biological Abstracts, Chemical Abstracts, Chemical Titles, Chromatography Abstracts, Current Contents/Life Sciences, Current Contents/Physical, Chemical & Earth Sciences, Deep-Sea Research/Part B: Oceanographic Literature Review, Excerpta Medica, Index Medicus, Mass Spectrometry Bulletin, PASCAL-CRNS, Referativnyi Zhurnal, Research Alert and Science Citation Index)

## REGULAR PAPERS

*Column Liquid Chromatography*

- Comparison of the various kinetic models of non-linear chromatography  
by S. Golshan-Shirazi and G. Guiochon (Knoxville and Oak Ridge, TN, USA) (Received February 12th, 1992) . . . . . 1
- Comparison between the hodograph transform method and frontal chromatography for the measurement of binary competitive adsorption isotherms  
by Z. Ma and G. Guiochon (Knoxville and Oak Ridge, TN, USA) (Received February 5th, 1992) . . . . . 13
- Batch dynamic adsorption of dipeptides onto reversed-phase silica gel  
by T. S. Nguyen, S.-G. Hu and D. D. Do (Brisbane, Australia) (Received March 10th, 1992) . . . . . 27
- The *S* index in the retention equation in reversed-phase high-performance liquid chromatography  
by N. Chen, Y. Zhang and P. Lu (Dalian, China) (Received February 11th, 1992) . . . . . 35
- Dispersion in stacked-membrane chromatography  
by D. D. Frey, R. Van de Water and B. Zhang (New Haven, CT, USA) (Received February 25th, 1992) . . . . . 43
- Reduction in large-scale adsorption chromatography unit costs by use of 30-Å Sorbsil C30 silica  
by I. Chappell and P. Baines (Warrington, UK) and P. K. Carpenter (Bracknell, UK) (Received January 31st, 1992) . . . . . 49
- Solvent-stationary phase interactions in normal bonded phase high-performance liquid chromatographic columns. I. Investigation of system peaks in amino bonded phase columns  
by C. W. Hsu and W. T. Cooper (Tallahassee, FL, USA) (Received February 25th, 1992) . . . . . 63
- Support for liquid-liquid partition chromatography in aqueous two-phase systems: a comparison of Superdex and LiParGel  
by C. Wingren, U.-B. Hansson and K. Andersson (Lund, Sweden) (Received February 17th, 1992) . . . . . 73
- Systematic study on the resolution of derivatized amino acids enantiomers on different cyclodextrin-bonded stationary phases  
by S. H. Lee, A. Berthod and D. W. Armstrong (Rolla, MO, USA) (Received February 21st, 1992) . . . . . 83
- Protein purification using combined streptavidin (or avidin)-Sepharose and thiopropyl-Sepharose affinity chromatography  
by F. Desarnaud, J. Marie, R. Larguier, C. Lombard, S. Jard and J.-C. Bonnafous (Montpellier, France) (Received February 7th, 1992) . . . . . 95
- Conalbumin-conjugated silica gel, a new chiral stationary phase for high-performance liquid chromatography  
by N. Mano and Y. Oda (Ibaraki, Japan), T. Miwa (Gifu, Japan) and N. Asakawa, Y. Yoshida and T. Sato (Ibaraki, Japan) (Received February 12th, 1992) . . . . . 105
- High-performance affinity chromatography of oligonucleotides on nucleic acid analogue immobilized silica gel columns  
by E. Yashima, T. Shiiba, T. Sawa, N. Miyauchi and M. Akashi (Kagoshima, Japan) (Received February 5th, 1992) . . . . . 111
- Practical approach to the miniaturization of chiral separations in liquid chromatography using packed fused-silica capillary columns  
by H. Wännman, A. Walhagen and P. Erlandsson (Lund, Sweden) (Received March 16th, 1992) . . . . . 121
- Enantiomeric separation of racemic isoflavanones and related compounds on (+)-poly(triphenylmethyl methacrylate)-coated silica gel  
by S. Antus (Budapest, Hungary), R. Bauer (Munich, Germany), Á. Gottsegen (Budapest, Hungary) and H. Lotter, O. Seligmann and H. Wagner (Munich, Germany) (Received February 18th, 1992) . . . . . 133
- Separation of oligogalacturonic acids by high-performance gel filtration chromatography on silica gel with diol radical  
by J. Naohara (Okayama, Japan) and M. Manabe (Kagawa, Japan) (Received February 6th, 1992) . . . . . 139
- Determination of hydroxylamine in aqueous solutions of pyridinium aldoximes by high-performance liquid chromatography with UV and fluorometric detection  
by W. D. Korte (Aberdeen Proving Ground, MD, USA) (Received March 3rd, 1992) . . . . . 145

(Continued overleaf)

Contents (continued)

Separation of benz[ <i>f</i> ]isoindole derivatives of amino acid and amino acid amide enantiomers on a $\beta$ -cyclodextrin-bonded phase by A. L. L. Duchateau, G. M. P. Heemels, L. W. Maesen and N. K. de Vries (Geleen, Netherlands) (Received February 11th, 1992)	151
High-performance liquid chromatography–thermospray mass spectrometry of gibberellins by E. B. Hansen, Jr., J. Abian and T. A. Getek (Jefferson, AR, USA), J. S. Choinski, Jr. (Conway, AR, USA) and W. A. Korfmacher (Jefferson, AR, USA) (Received February 7th, 1992)	157
High-performance liquid chromatographic investigations of stillingia oil by K. Aitzetmüller, Y. Xin, G. Werner and M. Grönheim (Münster, Germany) (Received February 10th, 1992)	165
<i>Gas Chromatography</i>	
Comparison of gas chromatographic–mass spectrometric methods for screening of chlorotriazine pesticides in soil by G. Durand (Barcelona, Spain), P. Gille and D. Fraisse (Vernaison, France) and D. Barceló (Barcelona, Spain) (Received January 3rd, 1992)	175
Solventless determination of caffeine in beverages using solid-phase microextraction with fused-silica fibers by S. B. Hawthorne and D. J. Miller (Grand Forks, ND, USA) and J. Pawliszyn and C. L. Arthur (Waterloo, Canada) (Received February 11th, 1992)	185
<i>Supercritical Fluid Chromatography</i>	
Characterization of a supercritical fluid chromatographic retention process with a large pressure drop by the temporal average density by X. Zhang and D. E. Martire (Washington, DC, USA) and R. G. Christensen (Gaithersburg, MD, USA) (Received February 27th, 1992)	193
Retention characteristics of high-molecular-weight compounds in capillary supercritical fluid chromatography by L. D. Giddings, S. V. Olesik and L. A. Pekay (Columbus, OH, USA) and E. Marti (Dublin, OH, USA) (Received March 3rd, 1992)	205
<i>Planar Chromatography</i>	
Reversed-phase thin-layer chromatography of diacylglycerols in the presence of silver ions by V. P. Pchelkin and A. G. Vereshchagin (Moscow, Russia) (Received December 19th, 1991)	213
Fluorescence reactions of inorganic cations heated on a porous glass sheet for thin-layer chromatography by M. Yoshioka and H. Araki (Osaka, Japan) and M. Seki, T. Miyazaki, T. Utsuki, T. Yaginuma and M. Nakano (Tokyo, Japan) (Received February 21st, 1992)	223
Formation of zinc complexes during chromatography of porphyrins on fluorescent thin-layer plates by K. Saitoh, C. Kiyohara and N. Suzuki (Miyagi, Japan) (Received March 5th, 1992)	231
<i>Electrophoresis</i>	
Theoretical aspects of chiral separation in capillary electrophoresis. I. Initial evaluation of a model by S. A. C. Wren and R. C. Rowe (Macclesfield, UK) (Received February 12th, 1992)	235
Chromogenic substrate for <i>endo</i> -polygalacturonase detection in gels by O. Markovič, D. Mislovičová, P. Biely and K. Heinrichová (Bratislava, Czechoslovakia) (Received February 26th, 1992)	243
High-performance capillary electrophoretic analysis of chloramphenicol acetyl transferase activity by J. P. Landers, M. D. Schuchard, M. Subramaniam, T. P. Sismelich and T. C. Spelsberg (Rochester, MN, USA) (Received February 12th, 1992)	247
Separation of sulphonamides and determination of the active ingredients in tablets by micellar electrokinetic capillary chromatography by Q.-X. Dang (Xian, China) and Z.-P. Sun and D.-K. Ling (Beijing, China) (Received February 6th, 1992)	259
Qualitative analysis of environmental samples for aromatic sulfonic acids by high-performance capillary electrophoresis by W. C. Brumley (Las Vegas, NV, USA) (Received March 12th, 1992)	267

## SHORT COMMUNICATIONS

### *Column Liquid Chromatography*

- Multiple ligand applications in high-performance immunoaffinity chromatography  
by J. B. Wheatley (Berkeley, CA, USA) (Received April 3rd, 1992) . . . . . 273
- Novel polymeric reagent for synthesizing 9-fluorenylmethoxycarbonyl L-prolinyl derivatives for chiral high-performance liquid chromatography of amino acids  
by Z. Zhang, G. Malikin and S. Lam (Bronx, NY, USA) (Received March 30th, 1992) . . . . . 279
- Automated liquid chromatographic determination of ochratoxin A in cereals and animal products using immunoaffinity column clean-up  
by M. Sharman, S. MacDonald and J. Gilbert (Norwich, UK) (Received April 3rd, 1992) . . . . . 285

### *Gas Chromatography*

- Automation of a clean-up procedure for determination of trichothecenes in cereals using a charcoal-alumina column  
by W. Langseth and P.-E. Clasen (Oslo, Norway) (Received February 24th, 1992) . . . . . 290
- Gas chromatographic-mass spectrometric detection of trace amounts of organic compounds in the intravenous solution Infusio Darrowi  
by J. Lesko, T. Jakubik and A. Michalkova (Bratislava, Czechoslovakia) (Received March 3rd, 1992) . . . . . 294

### *Electrophoresis*

- Quantitation of *l*-epinephrine and determination of the *d*-/*l*-epinephrine enantiomer ratio in a pharmaceutical formulation by capillary electrophoresis  
by T. E. Peterson and D. Trowbridge (Fort Worth, TX, USA) (Received April 1st, 1992) . . . . . 298

*Author Index* . . . . . 302

*Errata* . . . . . 304



JOURNAL OF CHROMATOGRAPHY

VOL. 603 (1992)



# JOURNAL of CHROMATOGRAPHY

INCLUDING ELECTROPHORESIS AND OTHER SEPARATION METHODS

## EDITORS

U. A. Th. BRINKMAN (Amsterdam), R. W. GIESE (Boston, MA), J. K. HAKEN (Kensington, N.S.W.), K. MACEK (Prague),  
L. R. SNYDER (Orinda, CA)

## EDITORS, SYMPOSIUM VOLUMES

E. HEFTMANN (Orinda, CA), Z. DEYL (Prague)

## EDITORIAL BOARD

D. W. Armstrong (Rolla, MO), W. A. Aue (Halifax), P. Boček (Brno), A. A. Boulton (Saskatoon), P. W. Carr (Minneapolis, MN),  
N. H. C. Cooke (San Ramon, CA), V. A. Davankov (Moscow), Z. Deyl (Prague), S. Dilli (Kensington, N.S.W.), F. Erni (Basle), M.  
B. Evans (Hatfield), J. L. Glajch (N. Billerica, MA), G. A. Guiochon (Knoxville, TN), P. R. Haddad (Kensington, N.S.W.), I. M.  
Hais (Hradec Králové), W. S. Hancock (San Francisco, CA), S. Hjertén (Uppsala), Cs. Horváth (New Haven, CT), J. F. K. Huber  
(Vienna), K.-P. Hupe (Waldbronn), T. W. Hutchens (Houston, TX), J. Janák (Brno), P. Jandera (Pardubice), B. L. Karger  
(Boston, MA), J. J. Kirkland (Wilmington, DE), E. sz. Kováts (Lausanne), A. J. P. Martin (Cambridge), L. W. McLaughlin  
(Chestnut Hill, MA), E. D. Morgan (Keele), J. D. Pearson (Kalamazoo, MI), H. Poppe (Amsterdam), F. E. Regnier (West  
Lafayette, IN), P. G. Righetti (Milan), P. Schoenmakers (Eindhoven), R. Schwarzenbach (Dübendorf), R. E. Shoup (West  
Lafayette, IN), A. M. Siouffi (Marseille), D. J. Strydom (Boston, MA), N. Tanaka (Kyoto), S. Terabe (Hyogo), K. K. Unger  
(Mainz), R. Verpoorte (Leiden), Gy. Vigh (College Station, TX), J. T. Watson (East Lansing, MI), B. D. Westerlund (Uppsala)

## EDITORS, BIBLIOGRAPHY SECTION

Z. Deyl (Prague), J. Janák (Brno), V. Schwarz (Prague)



ELSEVIER

AMSTERDAM — LONDON — NEW YORK — TOKYO

*J. Chromatogr.*, Vol. 603 (1992)

ห้องสมุดกรมวิทยาศาสตร์บริการ

© 1992 ELSEVIER SCIENCE PUBLISHERS B.V. All rights reserved.

0021-9673/92/\$05.00

No part of this publication may be reproduced, stored in a retrieval system or transmitted in any form or by any means, electronic, mechanical, photocopying, recording or otherwise, without the prior written permission of the publisher, Elsevier Science Publishers B.V., Copyright and Permissions Department, P.O. Box 521, 1000 AM Amsterdam, Netherlands.

Upon acceptance of an article by the journal, the author(s) will be asked to transfer copyright of the article to the publisher. The transfer will ensure the widest possible dissemination of information.

Submission of an article for publication entails the authors' irrevocable and exclusive authorization of the publisher to collect any sums or considerations for copying or reproduction payable by third parties (as mentioned in article 17 paragraph 2 of the Dutch Copyright Act of 1912 and the Royal Decree of June 20, 1974 (S. 351) pursuant to article 16 b of the Dutch Copyright Act of 1912) and/or to act in or out of Court in connection therewith.

**Special regulations for readers in the USA.** This journal has been registered with the Copyright Clearance Center, Inc. Consent is given for copying of articles for personal or internal use, or for the personal use of specific clients. This consent is given on the condition that the copier pays through the Center the per-copy fee stated in the code on the first page of each article for copying beyond that permitted by Sections 107 or 108 of the US Copyright Law. The appropriate fee should be forwarded with a copy of the first page of the article to the Copyright Clearance Center, Inc., 27 Congress Street, Salem, MA 01970, USA. If no code appears in an article, the author has not given broad consent to copy and permission to copy must be obtained directly from the author. All articles published prior to 1980 may be copied for a per-copy fee of US\$ 2.25, also payable through the Center. This consent does not extend to other kinds of copying, such as for general distribution, resale, advertising and promotion purposes, or for creating new collective works. Special written permission must be obtained from the publisher for such copying.

No responsibility is assumed by the Publisher for any injury and/or damage to persons or property as a matter of products liability, negligence or otherwise, or from any use or operation of any methods, products, instructions or ideas contained in the materials herein. Because of rapid advances in the medical sciences, the Publisher recommends that independent verification of diagnoses and drug dosages should be made.

Although all advertising material is expected to conform to ethical (medical) standards, inclusion in this publication does not constitute a guarantee or endorsement of the quality or value of such product or of the claims made of it by its manufacturer.

This issue is printed on acid-free paper.

Printed in the Netherlands

# Comparison of the various kinetic models of non-linear chromatography

Sadroddin Golshan-Shirazi and Georges Guiochon

*Department of Chemistry, University of Tennessee, Knoxville, TN 37996-1501, and Division of Analytical Chemistry, Oak Ridge National Laboratory, Oak Ridge, TN 37831 (USA)*

(First received November 5th, 1991; revised manuscript received February 12th, 1992)

---

## ABSTRACT

It is not possible to separate simply the influences of a slow mass transfer kinetics and of a slow kinetics of adsorption–desorption on the elution profile of a component. Four kinetic models of chromatography are studied: (i) the Thomas or reaction model, which assumes Langmuir kinetics of adsorption–desorption and no axial dispersion; (ii) the reaction-dispersive model, which uses the same Langmuir kinetics as the Thomas model but assumes a finite axial dispersion; (iii) a transport model, which uses the linear solid film driving force model to account for a slow kinetics of mass transfer and assumes no axial dispersion; and (iv) a transport-dispersive model, using the same mass transfer kinetics as the transport model and assumes finite axial dispersion. The analytical solution of the Thomas model can be fitted, with an accuracy which exceeds the precision of experimental measurements, on bands calculated using either one of the other three kinetic models of chromatography. Thus, the Thomas model, which assumes a slow adsorption–desorption kinetics and infinitely fast mass transfer kinetics, accounts very well for profiles calculated with a model making the reverse assumption. However, the values of the lumped kinetic coefficient obtained by curve fitting depend on the sample amount. Thus, the examination of an elution profile and its fitting to a model do not permit an easy solution of the inverse problem of chromatography.

---

## INTRODUCTION

A number of different kinetic models have been introduced in linear chromatography [1–4]. Closed-form solutions for these models or their solutions in the Laplace domain have been derived, the general equations of chromatography being greatly simplified by the assumption of a linear isotherm. It has been shown that, provided the number of transfer units is not very small, the results of all these models are equivalent and that their solution is well approximated by a Gaussian profile [4–7]. Further, this common result is equivalent to the results of the equilibrium-dispersive model [1,8,9] and of the plate theory [5,10], provided that the proper apparent number of transfer units be used.

The elution profile of a component is the distribution of the residence times of its molecules. As for all distributions, a variance can be defined for the elution profile. Glueckauf [7] showed that a contribution to this variance can be calculated for each independent source of band broadening and that these contributions are simply additive. Van Deemter *et al.* [5] also established this rule of additivity. They simplified the analytical solution of Lapidus and Amundson [1] in the case of a non-equilibrium model of linear chromatography and showed that, if the rate-controlling step of the mass transfer kinetics in the chromatographic column is not very slow, this solution can be reduced to a Gaussian profile. By comparing their simplified solution with that of the plate theory [10], they derived a landmark relationship between the height equivalent to a theoretical plate of the plate model, the axial dispersion coefficient and the lumped mass transfer coefficient of their linear driving force model.

---

*Correspondence to:* Professor G. Guiochon, Department of Chemistry, University of Tennessee, Knoxville, TN 37996-1501, USA.

Using a completely different approach, the moment analysis, Kucera [2] and Kubin [3] demonstrated also the additivity of the different contributions to band broadening. This demonstration is based on the solution of the general rate model of linear chromatography in the Laplace domain. The solution cannot be inverted into the time domain, but the moments of the distribution in the time domain can be calculated. Giddings [6], using the rate theory, derived the same additivity rule. The most general analysis of the dependence of the height equivalent to a theoretical plate in linear chromatography on the experimental conditions is due to Horvath and Lin [11]. Contributions for all the known contributions to the mass transfer resistance have been discussed.

In the course of these investigations, several general kinetic models have been used. These models can be extended to non-linear chromatography, where the isotherm is no longer linear. The purpose of this work is a comparison between the results given by these different models in non-linear chromatography and the search for whether, and under which conditions, they could be equivalent, as they are in linear chromatography.

## THEORY

Chromatography is a complex combination of phenomena, involving the dynamic transfer, under conditions which are often close to equilibrium but never achieve it, of a pulse of a mixture of components along a column. In this study, however, we consider only the simplest possible case, the migration of a pulse of a pure compound. The column is packed with porous particles between which flows a mobile phase in which the component is soluble. The component has free access to the inside of the porous particles. During its migration, the component experiences transfer between the mobile phase and the surface of an adsorbent. The band profile depends on the equilibrium isotherm and on the different phenomena which act to broaden the band, axial dispersion, diffusion across the mobile phase stream, resistance to mass transfer across the external film around the particles, intraparticle diffusion and kinetics of adsorption-desorption.

Different chromatographic models attempt to model the band migration in different ways. They

can be grouped in two classes of models. The general rate models consider a more or less complex array of kinetic equations and make a detailed analysis of the various steps involved in the chromatographic process. The lumped rate models consider only one kinetic process, regarded as the rate-controlling step, or at most a few such processes, and they lump in the rate constant the contributions of the kinetics of the other processes.

### General rate model

A general rate model of chromatography uses two mass balance equations, one in the mobile phase outside the particle and the other in the stagnant mobile phase inside a particle, and two kinetic equations, one relating the two mobile phase concentrations (mass transfer kinetics) and the other relating the stagnant mobile phase and the stationary phase concentrations (kinetics of adsorption-desorption).

*External mass balance equation.* The differential mass balance equation of the solute in the stream of mobile phase around the particles can be written as

$$u \cdot \frac{\partial C}{\partial z} + \frac{\partial C}{\partial t} + F \cdot \frac{\partial \bar{C}_s}{\partial t} = D_L \cdot \frac{\partial^2 C}{\partial z^2} \quad (1)$$

where  $u$  is the mobile phase linear velocity,  $F = (1 - \varepsilon_e)/\varepsilon_e$  is the phase ratio,  $\varepsilon_e$  is the external porosity of the column,  $D_L$  is the axial dispersion coefficient,  $C$  is the mobile phase concentration in the interparticle stream,  $\bar{C}_s$  is the stationary phase concentration averaged over the entire particles and  $\partial \bar{C}_s / \partial t$  is the rate of adsorption averaged over an entire particle. For a spherical particle,

$$\bar{C}_s = \frac{3}{R_p^3} \int_0^{R_p} r^2 C_s dr \quad (2)$$

where  $R_p$  is the particle radius. For a spherical particle, we have

$$\frac{\partial \bar{C}_s}{\partial t} = \frac{3}{R_p} \cdot N_0 \quad (3)$$

where  $N_0$  is the mass flux of solute from the bulk solution through the external surface of the particle. The boundary condition at the external particle surface is given by

$$N_0 = D_p \cdot \frac{\partial C_p}{\partial r} \Big|_{r=R_p} = k_f(C - C_p \Big|_{r=R_p}) \quad (4a)$$

where  $k_f$  is the external mass transfer coefficient.

The Danckwerts-type initial and boundary conditions in the mobile phase are given by

$$C(z, 0) = 0 \quad (4b)$$

$$\frac{\partial C}{\partial z} \Big|_{z=L} = 0 \quad (4c)$$

$$uC(0, t) = uC_0(t) + D_L \cdot \frac{\partial C}{\partial z} \Big|_{z=0} \quad (4d)$$

*Intraparticle mass balance equation.* The differential mass balance equation of the solute in the particle yields

$$\varepsilon_p \cdot \frac{\partial C_p}{\partial t} + (1 - \varepsilon_p) \frac{\partial C_s}{\partial t} = D_p \left( \frac{\partial^2 C_p}{\partial r^2} + \frac{2}{r} \cdot \frac{\partial C_p}{\partial r} \right) \quad (5)$$

where  $\varepsilon_p$  is the internal porosity of the packed bed,  $D_p$  is the diffusion coefficient of the solute inside the pores of the particles and  $C_p$  and  $C_s$  are the solute concentrations in the solution inside the pores and in the stationary phase, respectively. The boundary conditions for the particle is the symmetrical condition

$$\frac{\partial C_p}{\partial r} \Big|_{r=0} = 0 \quad (6a)$$

The initial condition is

$$C_p = C_p(r, 0) \text{ at } t = 0 \quad (6b)$$

For a pulse injection, we have

$$C(0, t) = C_0 \text{ for } 0 \leq t \leq t_p \quad (7a)$$

$$C(0, t) = 0 \text{ for } t_p \leq t \quad (7b)$$

*Kinetic equation.* If we may assume that the kinetics of adsorption-desorption are infinitely fast, the concentrations of the solute in the mobile phase contained in the pores and in the stationary phase are related through the equilibrium isotherm,  $C_s = f(C_p)$ . If these kinetics are slow, they are related through the kinetic equation. For example, for a linear isotherm and slow kinetics of adsorption-desorption with a first-order rate, we have

$$\frac{\partial C_s}{\partial t} = k_{ads}(C_p - C_p^*) = k_{ads}(C_p - C_s/K_a) \quad (8)$$

where  $k_{ads}$  and  $K_a$  are the adsorption rate constant and the adsorption equilibrium constant (Henry constant), respectively, and  $C_p^*$  is the liquid concentration in equilibrium with the stationary phase concentration,  $C_p^* = C_s/K_a$ .

*Solution of the general rate model.* Kubin [3] and Kucera [2] derived in the Laplace domain the analytical solution of the system of eqns. 1-8 of the general rate model of linear chromatography just presented. This solution cannot be inverted in the time domain, but they could derive from it the moments of the retention time distribution which constitute the elution band profile. More recently, Lenhoff [4] calculated the elution band profile in the time domain by numerical evaluation of the inverse Laplace transform.

General rate models coupled to a non-linear isotherm have been studied in detail by Wang and co-workers [12-14], using the method of orthogonal collocation for the numerical calculation of solutions. The general rate model considering an infinite rate of adsorption-desorption and a non-linear isotherm was solved numerically by Yu and Wang [12] and by Lee *et al.* [13]. Later, this model was extended to the case of slow adsorption-desorption, possibly involving also reactions in the mobile or stationary phases, with a slow reaction rate [14]. Lin and Ma [15] solved numerically, by orthogonal collocation, a simpler pore diffusion model, considering only intraparticle diffusion and axial dispersion, ignoring the diffusion through the external film around the particles, but including the influence of non-uniform particle size by taking the particle size distribution into account.

#### *Lumped model of chromatography*

The general rate model of chromatography just discussed is a complete and correct model of the chromatographic process. It accounts for all the known contributions, whether of thermodynamic or kinetic origins, to the elution band profile. Unfortunately, the prediction of the band profiles in any real case requires the prior knowledge, determination or evaluation of a number of parameters (*e.g.*, isotherm coefficients, rate constants, mass transfer coefficients). Accordingly, the optimization of the experimental conditions for maximum production rate (let alone for minimum production cost!) becomes extremely complex when using this

model. To simplify the solution of the problem of non-linear chromatography, several simpler kinetic models have been introduced. These models are extensions of models which were successfully used in linear chromatography.

**Thomas model.** The simplest lumped model is due to Thomas [16]. Like the ideal model, the Thomas model ignores the axial dispersion (*i.e.*,  $D_L = 0$  in eqn. 1) and the mass transfer kinetics. It could be called a reaction model. It assumes, however, that the rates of adsorption and desorption are finite and given by the second-order Langmuir kinetics:

$$\frac{\partial C_s}{\partial t} = k_a(q_s - C_s)C - k_d C_s \quad (9)$$

where  $k_a$  and  $k_d$  are the rate constants of adsorption and desorption, respectively, and  $q_s$  is the specific saturation capacity of the adsorbent, or amount needed to form a saturated monolayer. Because of the difference between the kinetic models used, there is no reason for  $k_{ads}$  (eqn. 8) to be equivalent to  $k_a$  (eqn. 9). As we assume that the mass transfer kinetics are very fast,  $C$  (eqn. 1) and  $C_p$  (eqn. 5) are equivalent. Thomas derived a closed-form solution for his model in the case of a step function input, *i.e.*, for the frontal analysis problem [16]. Later, Goldstein [17] derived an analytical solution of the Thomas model in the case of a pulse injection of any width, finite or not. More recently, Wade *et al.* [18] studied the solution of the Dirac problem, in which case the input function is an impulse or rectangular pulse of infinitely narrow width. They found that this problem has a solution simpler than Goldstein's, and compared it with experimental results obtained in affinity chromatography, a mode of separation in which the effects of a slow adsorption-desorption kinetics may often offset the effects of both axial dispersion and the resistances to mass transfer.

In the case of an impulse input, the solution given by Wade *et al.* [18] can be written as [19]

$$\frac{C}{C_0} = \frac{1 - e^{-N_{rea}L_f}}{k'_0 N_{rea} L_f} \cdot \frac{N_{rea} \sqrt{\frac{1}{\tau}} I_1(2N_{rea} \sqrt{\tau}) e^{-N_{rea}(\tau+1)}}{1 - T(N_{rea}, N_{rea}\tau)(1 - e^{-N_{rea}L_f})} \quad (10a)$$

or

$$\frac{C}{C_{di,0}} = \frac{1 - e^{-N_{rea}L_f}}{N_{rea} L_f} \cdot \frac{N_{rea} \sqrt{\frac{1}{\tau}} I_1(2N_{rea} \sqrt{\tau}) e^{-N_{rea}(\tau+1)}}{1 - T(N_{rea}, N_{rea}\tau)(1 - e^{-N_{rea}L_f})} \quad (10b)$$

where  $\tau = (t - t_0)/(t_{R,0} - t_0)$  is a dimensionless time,  $C_0 = A_p/t_0 = n/\varepsilon SL$  and  $C_{di,0}$  is a reference, dimensionless concentration obtained by dividing the amount injected by the product of the column hold-up volume and the retention factor of the component studied at infinite dilution, also equal to the ratio of the area of the input profile to the net retention time at infinite dilution [ $C_{di,0} = n/\varepsilon SLk'_0 = A_p/k'_0 t_0 = C_p t_p/(t_{R,0} - t_0) = C_p \tau_0$ ].  $n$  (mol) is the amount of solute injected,  $S$  and  $L$  are the column cross-section area and length, respectively,  $A_p = C_p t_p$  is the area (conservative) of the rectangular pulse of solute injected,  $C_p$  being the solute concentration, and  $t_p$  the time width. In eqns. 10,  $I_1(x)$  is the first-order modified Bessel function of the first kind, and  $T(u,v)$  is a Bessel function integral [17-19]. Eqn. 10b is convenient as it gives a normalized profile depending only on two parameters, and we see that the dimensionless elution profile (*i.e.*, the plot of  $C/C_{di,0}$  versus  $\tau$ ) depends only on two parameters, the loading factor,  $L_f$  [19], and the reaction (or adsorption-desorption) number of transfer units,  $N_{rea} = k'_0 k_d L/u$ . If the pulse width is finite, the solution derived by Goldstein [17] applies, and it depends on one additional parameter, the reduced injection pulse width,  $\tau_0 = t_p/(t_{R,0} - t_0)$ .

**Reaction-dispersive model.** More recently, an extension of the Thomas model, the reaction-dispersive model of chromatography, has been suggested [19]. In this model, we use a single mass balance equation and a kinetic equation. The mass balance equation is written as

$$u \cdot \frac{\partial C}{\partial z} + \frac{\partial C}{\partial t} + F \cdot \frac{\partial C_s}{\partial t} = D_a \cdot \frac{\partial^2 C}{\partial z^2} \quad (11)$$

where  $C$  and  $C_s$  are the concentrations of the component in the mobile and stationary phases, respectively, and  $D_a$  is the apparent dispersion coefficient, related to the axial dispersion coefficient,  $D$ , and to the lumped mass transfer coefficient,  $k_f$ . Any proper kinetic equation can be used in this model. For the sake of comparison with the Thomas model, we may assume the Langmuir kinetic equation, eqn. 9. The model has no analytical solution. A numerical solution can be obtained easily, using the finite difference method [19,20]. The solutions of the reaction-dispersive model for a narrow injection pulse depend on three parameters, the loading factor,  $L_f$ , and two kinetic parameters, the reaction

number of transfer units,  $N_{rea} = k'_0 k_d L / u$ , and the dispersion number of transfer units,  $N_{Disp} = Lu / 2D_a$ . When  $D_a = 0$ , the reaction-dispersive model reduces to the Thomas model and the solution is obtained using either the Goldstein (finite pulse width) or the Wade *et al.* (impulse) solution.

*Transport and transport-dispersive models.* Instead of assuming slow kinetics of adsorption-desorption and very fast kinetics of mass transfer, we may as well assume very fast kinetics of adsorption-desorption and slow kinetics of mass transfer. An attractive kinetic model of chromatography combines a mass balance equation (eqn. 11) and the kinetic equation of the solid film linear driving force model [21,22]. Now, we have the following system:

$$u \cdot \frac{\partial C}{\partial z} + \frac{\partial C}{\partial t} + F \cdot \frac{\partial C_s}{\partial t} = D_L \cdot \frac{\partial^2 C}{\partial z^2} \quad (12a)$$

$$\frac{\partial C_s}{\partial t} = k_f (q^* - C_s) \quad (12b)$$

where  $k_f$  is the lumped mass transfer coefficient and  $q^*$  is the stationary phase concentration in equilibrium with the local mobile phase concentration, as given by the isotherm equation. The analytical solution of this model in the case of a linear isotherm has been derived [1,5]. In the case of a non-linear isotherm, numerical solutions have been obtained using a finite difference procedure [20,23,24]. In this case, the band profile depends on  $L_f$ ,  $N_{Disp}$  and another kinetic parameter, the number of transfer units,  $N_m = k'_0 St$ , where  $St$  is the Stanton number,  $St = k_f L / u_0$ . If we assume  $D_L = 0$  in eqn. 12a, we have a transport model, and the band profile depends only on  $L_f$  and  $N_m$ . If  $D_L$  is different from 0, we have a transport-dispersive model.

Thus, we have a series of similar models, which differ essentially by the nature of the step in the global mass transfer which is considered as the slowest and may control the entire kinetics of the chromatographic process and depending on whether the axial dispersion is neglected or not. We now compare the solutions of these models for a non-linear isotherm.

## RESULTS AND DISCUSSION

In all the cases discussed here, we have assumed in the calculations a narrow injection plug width, 20  $\mu$ l,

so we can compare directly the profiles obtained by numerical integration and by the Wade *et al.* [18] equation. For wider injection plugs, the Goldstein equation [17] could also be used, but it requires the evaluation of four Bessel function integrals instead of one, rendering the numerical calculation as complex and possibly slower than straightforward numerical integration of the system of partial differential equations.

### Comparison between the Thomas model and the reaction-dispersive model

In Fig. 1, we compare two band profiles corresponding to the same experimental conditions with a loading factor  $L_f = 1\%$  and obtained as analytical solution of the Thomas model (dotted line) and numerical solution of the reaction-dispersive model

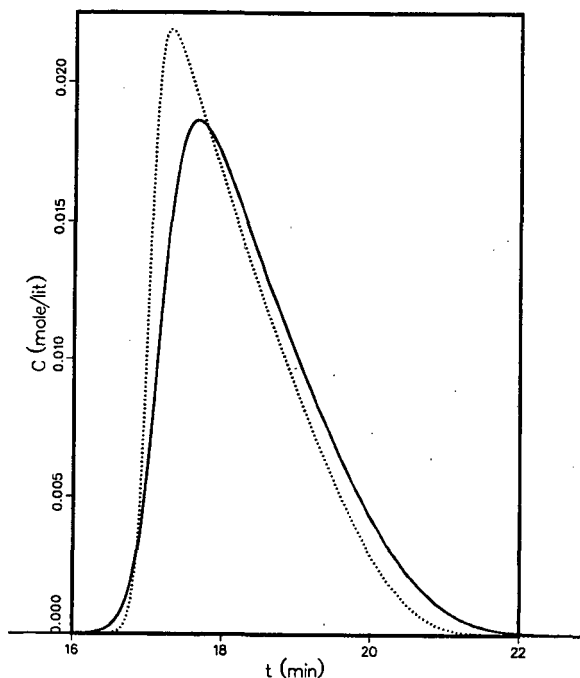


Fig. 1. Comparison between the numerical solution of the reaction-dispersive model of chromatography (solid line) and the analytical solution of the Thomas model (dotted line). Values of parameters; loading factor,  $L_f = 1\%$ ; retention factor,  $k'_0 = 5$ ; Thomas number,  $N_{rea} = k'_0 k_d L / u = 2000$ ; corrected efficiency, for the reaction-dispersive model:

$$2N_{Disp} \left( \frac{k'_0}{1+k'_0} \right)^2 = P_{e,z} \left( \frac{k'_0}{1+k'_0} \right)^2 = \frac{Lu}{D_a} \left( \frac{k'_0}{1+k'_0} \right)^2 = 2000,$$

for the Thomas model,  $N_{Disp} = \infty$ .

(solid line). The dimensionless number characterizing the kinetics of adsorption-desorption or number of reaction units,  $N_{\text{rea}}$ , is equal to 2000. The dimensionless number characterizing the axial dispersion in the reaction-dispersive model is

$$2N_{\text{Disp}} \left( \frac{k'_0}{1+k'_0} \right)^2 = Pe \left( \frac{k'_0}{1+k'_0} \right)^2 = 2000 \quad (13)$$

with  $Pe = uL/D_a$ . As expected, the two band profiles are different, as the reaction-dispersive model takes into account the axial dispersion (axial diffusion and mass transfer kinetics) whose effects have been neglected in the Thomas model.

It is interesting to examine now whether it would be possible to lump together the two main contributions to band broadening, the adsorption-desorption kinetics and the axial dispersion. If this is possible, we could fit a solution of the Thomas model on the solid line in Fig. 1. Of course, the values of the kinetic parameters leading to the best fit would be different from those corresponding to the strict Thomas model. We call  $N_{\text{rea}}^{\text{app}}$  this apparent value of the number of reaction units which corresponds to an apparent rate parameter and includes the effects of both slow adsorption-desorption and finite axial dispersion.

The calculations were carried out using a three-dimensional simplex algorithm with  $k'_0$ ,  $L_f$  and  $N_{\text{rea}}^{\text{app}}$  as the parameters, and fitting the Wade *et al.* [18] equation for the Thomas model (eqn. 10a) to the profile calculated by numerical integration of the reaction-dispersive model. In the modified simplex approach used [25-27], a method of successive estimation of the three parameters ( $k'_0$ ,  $L_f$  and  $N_{\text{rea}}$ ) was designed. The band profile computed with the Thomas model from a set of values of the three parameters is compared with the profile generated by the other model by calculating a score measuring the degree of similarity between the two profiles. Then, an algorithm generates a new set of parameters leading to a new profile. The simplex algorithm assures convergence of the similarity between the profiles and selects the best set.

The result of this exercise is shown in Fig. 2, for various values of the loading factor,  $L_f = 1, 5, 10$  and 20%. There is excellent agreement between the two curves. In all instances an excellent fit was achieved. The best values of the three parameters are

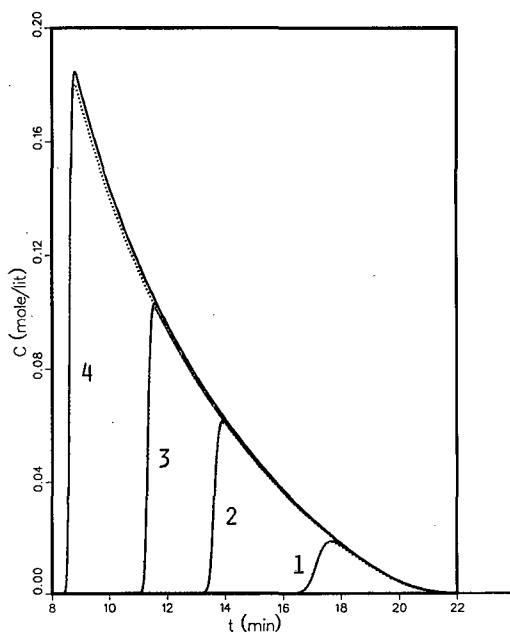


Fig. 2. Same as Fig. 1, except that the parameters of the Thomas model were obtained by a best fit of eqn. 10a to the numerical solution of the reaction-dispersive model (see Table I). Value of the loading factor,  $L_f$ : (1) 1%; (2) 5%; (3) 10%; (4) 20%.

given in Table I. There is excellent agreement between the "true" values of the retention and the loading factors used for the numerical calculation of the solutions of the reaction-dispersive model and the "best-fit" values derived from the fitting of the

TABLE I

BEST PARAMETERS OBTAINED BY FITTING BAND PROFILES CALCULATED WITH THE REACTION-DISPERSIVE MODEL<sup>a</sup> TO THE THOMAS MODEL<sup>b</sup>

$k'_0$	$L_f$ (%)	$k'_0$ <sup>c</sup>	$L_f$ <sup>c</sup>	$N_{\text{rea}}^{\text{app}}$ <sup>c</sup>
5	1	4.994	0.98	954
5	5	4.992	4.91	865
1	5	0.993	4.93	865
20	5	19.98	4.92	865
5	10	4.986	9.81	798
5	20	4.968	19.54	690

<sup>a</sup> Parameters of the generated profiles:  $2[k'_0/(1+k'_0)]^2 N_{\text{Disp}} = 2000$ ,  $N_{\text{rea}} = k'_0 k_d L/u = 2000$ . Hence,  $N_{\text{rea}}^{\text{app}} = 1000$ .

<sup>b</sup> Parameter of the Thomas model:  $N_{\text{Disp}} = \infty$ .

<sup>c</sup> Best values of the parameters obtained by curve fitting.

Thomas model to these profiles. The relative differences between the true and the calculated values of the loading factor and the retention factors are constant and close to 2 and 0.5%, respectively. As they are constant, they are probably due to the fitting process itself. This agreement is better than what can be expected when actual experimental data are fitted to a correct model. In a case like that, no model error can be detected. On the other hand, as expected, the value of  $N_{\text{rea}}^{\text{app}}$  is smaller than  $N_{\text{rea}}$ . This theoretical result is supported by data published by Lucy *et al.* [28]. They recorded experimental band profiles at increasing sample sizes for a series of compounds and fitted them to the Thomas model. They found that the best values obtained for the retention factor,  $k'_0$ , and the column saturation capacity are nearly independent of the sample size while the kinetic parameter is concentration dependent, which is in agreement with our results.

The variances of the various contributions to band broadening in linear chromatography are additive. Thus, in linear chromatography we may write

$$H = H_{\text{Disp}} + H_{\text{m,t}} + H_{\text{reac.}}$$

or

$$\frac{1}{N_{\text{rea}}^{\text{app}}} = \frac{1}{2} \left( \frac{1 + k'_0}{k'_0} \right)^2 \frac{1}{N_{\text{Disp}}} + \frac{1}{N_{\text{m}}} + \frac{1}{N_{\text{rea}}} \quad (14)$$

where  $N_{\text{rea}}^{\text{app}}$  is the apparent number of reaction transfer units and  $H$ ,  $H_{\text{Disp}}$ ,  $H_{\text{m,t}}$  and  $H_{\text{reac}}$  are the total height equivalent to a theoretical plate of the column and the contributions of the axial dispersion, the mass transfer kinetics and the adsorption-desorption kinetics, respectively. According to eqn. 14, the apparent number of transfer units in linear chromatography as derived from the reaction-dispersive model (eqns. 1-7) would be  $N_{\text{rea}}^{\text{app}} = 1000$ . The data in Table I suggest that  $N_{\text{rea}}^{\text{app}}$  is not constant in non-linear chromatography, but decrease with increasing value of the loading factor.

Attempts were also made to fit the Thomas model to solutions of the reaction-dispersive model corresponding to lower values of the loading factor, *e.g.*, 0.2% or less. The agreement between the two profiles (not shown) becomes increasingly less satisfactory with decreasing values of the loading factor. Also, the value of the loading factor obtained by curve fitting was increasingly more different from

the value used in the numerical calculation. The same problem was already observed by Lucy *et al.* [28] when attempting to fit experimental band profiles on the Thomas model at low values of the loading factor. Obviously, at high loading factors, the influence of the thermodynamics on the band profiles is major and the kinetic influence moderate, unless the rates are very slow. When the loading factor is small, chromatography is becoming linear and the band broadening contributions of kinetic origin are dominant. The fitting procedure then fails to determine the correct value of the loading factor. We conclude that, if isotherm parameters are to be determined by fitting an experimental profile to a model, the best results will be obtained when using a large sample size and strong column overload.

Similarly, if we change the retention factor, from 5 to 20 or 1 (results not shown), while keeping the

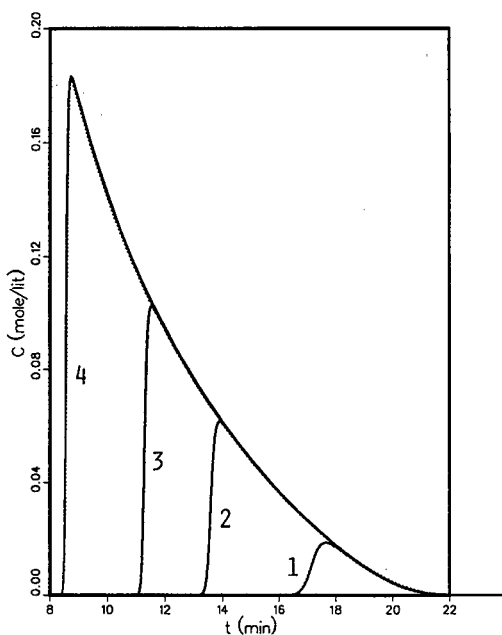


Fig. 3. Comparison between a profile obtained as numerical solution of the transport model of chromatography (solid line) and a profile given by the analytical solution of the Thomas model (dotted line). Experimental conditions for the linear driving force model: loading factor,  $L_r = 1\%$ ; limit retention factor,  $k'_0 = 5$ ; number of mass transfer stages,  $N_m = k'_0 k_r L/u = 1000$ ; coefficient of axial dispersion,  $D_L = 0$ ,  $N_{\text{Disp}} = \infty$ . The parameters of the Thomas model were obtained by fitting eqn. 10a to the profile obtained by numerical integration of the linear driving force model (see coefficients in Table II). Values of the loading factor,  $L_r$ : (1) 1%; (2) 5%; (3) 10%; (4) 20%.

other parameters constant, we can also achieve an excellent fit. The values of the parameters obtained by this curve fitting are also reported in Table I. The change in  $k'_0$  does not have any effect on the best values of either  $L_t$  or  $N_{\text{rea}}^{\text{app}}$ . This was expected as the retention factor has no influence on the dimensionless profile of the band [19].

#### Comparison between the Thomas model and the transport model

In Fig. 3 we compare two series of band profiles. The first (solid lines) are calculated using the solid film linear driving force model kinetic equation (eqn. 12b) and the mass balance of the ideal model (eqn. 12a with  $D_L = 0$ , transport model). These calculations were performed assuming a number of transfer units,  $N_m = k'_0 k_f L/u$ , equal to 1000. The second series of profiles (dotted lines) were calculated using the equation derived by Wade *et al.* [18] as solution of the Thomas model (eqn. 10a). The three coefficients of these Thomas profiles are selected so as to minimize the difference between the two profiles, using a simplex program. The corresponding parameters of the Thomas model are compared in Table II with the parameters used in the calculation of the profiles with the linear driving force model. A similar comparison is shown in Fig. 4. In this case, however, the calculated profile was obtained with the transport-dispersive model (eqns. 12a and 12b), with a number of transfer units,  $N_m$ ,

TABLE II  
BEST PARAMETERS OBTAINED BY FITTING THE BAND PROFILES CALCULATED WITH THE TRANSPORT<sup>a</sup> AND TRANSPORT-DISPERSIVE MODELS<sup>b</sup> TO THE THOMAS MODEL<sup>c</sup>

$k'_0$	$L_t$ (%)	$k'_0$ <sup>d</sup>	$L_t$ <sup>d</sup>	$N_{\text{rea}}^{\text{app}}$ <sup>d</sup>
5	1	5.0	0.991	954 <sup>a</sup>
5	5	4.996	4.952	886 <sup>a</sup>
5	5	4.998	4.87	823 <sup>b</sup>
5	10	4.993	9.91	828 <sup>a</sup>
5	20	4.995	19.82	727 <sup>a</sup>

<sup>a</sup> Parameters of the generated profiles:  $N_{\text{Disp}} = \infty$  and  $N_m = k'_0 k_f L/u = 1000$ . Hence  $N_{\text{rea}}^{\text{app}} = 1000$ .

<sup>b</sup> Parameters of the generated profiles:  $2[k'_0/(1 + k'_0)]^2 N_{\text{Disp}} = 2000$  and  $N_m = k'_0 k_f L/u = 2000$ . Hence  $N_{\text{rea}}^{\text{app}} = 1000$ .

<sup>c</sup> Parameter of the Thomas model:  $N_{\text{Disp}} = \infty$ .

<sup>d</sup> Best values of the parameters obtained by curve fitting.

equal to 2000, and a finite coefficient of axial dispersion, such that

$$\frac{uL}{D_L} \left( \frac{k'_0}{1 + k'_0} \right)^2 = 2N_{\text{Disp}} \left( \frac{k'_0}{1 + k'_0} \right)^2 = 2000$$

Thus, in linear chromatography the column efficiency and the band profiles would be the same as for the conditions selected for Fig. 3 (see eqn. 14, which gives  $N_{\text{rea}}^{\text{app}} = 1000$ ).

Figs. 3 and 4 show that the band profiles obtained with the transport and the transport-dispersive models can be fitted accurately enough to the Thomas model. The data in Table II show a very small error, of the order of 0.1%, for the retention factor,  $k'_0$ . For the loading factor, the error is *ca.* 1%. Both errors are independent of the loading factor. On the other hand, the value obtained for  $N_{\text{rea}}^{\text{app}}$  is not constant. It is significantly lower than 1000 and it decreases with increasing loading factor, whereas in

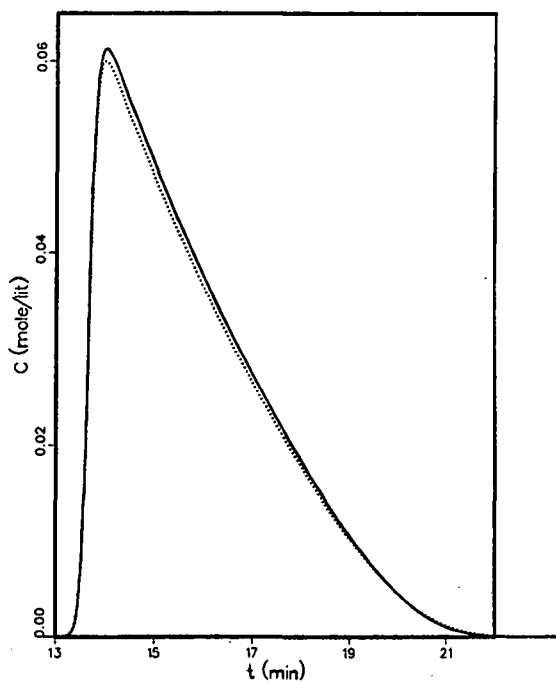


Fig. 4. Comparison between a profile obtained as numerical solution of the transport-dispersive model of chromatography (solid line) and a profile given by the analytical solution of the Thomas model (dotted line). Same conditions as in Fig. 3 for  $L_t = 5\%$ , except  $N_m = k'_0 k_f L/u = 2000$ , and  $2N_{\text{Disp}}[k'_0/(1 + k'_0)]^2 = 2000$ . In linear chromatography, the overall band broadening would be the same in Figs. 3 and 4.

linear chromatography, and from eqn. 14, this value would be 1000 for Figs. 3 and 4.

We conclude from this comparison that it is possible to fit experimental data to any of the simple kinetic models. Different models will give approximately the same values for the limit retention factor at infinite dilution,  $k'_0$ , and for the loading factor,  $L_f$ . However, the lumped kinetic parameters derived in the process will not remain constant. These parameters appear to be concentration dependent and to decrease with increasing concentration or sample size. In the following, we discuss the fundamental reason why the rate constant determined by fitting an experimental profile to a lumped kinetic model is concentration dependent.

#### *Dependence of the lumped kinetic coefficients on the sample size*

The dependence of the apparent kinetic parameter on the concentration was discussed by Rhee and Amundson [29] in an analysis of the properties of the shock layer in frontal analysis. We know that the ideal model predicts a concentration shock whenever the equilibrium isotherm is not linear [30]. The shock takes place on the band front in the case of a convex upward isotherm, the most frequent in liquid chromatography. This is due to the fact that, in the ideal model, each concentration propagates at its own velocity, related to the slope of the isotherm for the concentration considered. This velocity increases with increasing concentration for a convex upward isotherm. The faster high concentrations cannot pass the slower low concentrations and a concentration discontinuity or shock appears instead [30,31]. For an actual column, however, a concentration shock is impossible. This corresponds to an infinitely steep concentration gradient, generating an infinite mass flux by diffusion. A very steep front appears instead, the shock layer.

If we assume [29] the existence of a shock layer (region of very rapid variation of the concentration with the position in the column), write the mass balance equation and assume a linear driving force model for the kinetic equation of chromatography (eqns. 12a and 12b), it is possible to derive, by combination of the mass balance and the kinetic equation, the following relationship:

$$-\frac{\lambda}{PeSt} \frac{\partial^2 C}{\partial \eta^2} + \left[ \frac{1}{Pe} + \frac{\lambda(1-\lambda)}{St} \right] \frac{\partial C}{\partial \eta} = F\lambda f(C; C^f, C^i) \quad (15)$$

where  $\lambda$  is the migration velocity of the shock layer:

$$\lambda = \frac{1}{1 + F\Delta q/\Delta C} \quad (16)$$

$F$  is the phase ratio,  $\Delta q$  and  $\Delta C$  are the amplitude of the concentration change (*i.e.*, shock) in the stationary and mobile phases, respectively, and  $\eta$  is a new variable:

$$\eta = x - \lambda t_d \quad (17)$$

with  $x = z/L$  and  $t_d = ut/L$ , dimensionless variables, and the function  $f$  is given by

$$f(C; C^f, C^i) = \frac{\Delta q}{\Delta C} (C - C^f) - q(C^i) + q(C^f) \quad (18)$$

where  $C^i$  and  $C^f$  are the initial and final concentrations of the breakthrough curve and  $\Delta C = C^f - C^i$ .

Rhee and Amundson [29] showed that the velocity of the shock layer is the same as the velocity predicted for the shock in the ideal model. It is independent of the values of the axial dispersion coefficient and the kinetic coefficients. Thus, the elution of the mid-point of the breakthrough curve is independent of all kinetic influence and depends only on the thermodynamics. As can be seen, the axial dispersion term,  $Pe$ , and the mass transfer resistance term,  $St$ , have equivalent roles in eqn. 15. Their individual contributions add in the first-order differential term. In addition, however, there is a coupled, second-order differential term. In the practice of chromatography, both the Peclet and Stanton numbers are large. Hence the first term in the left-hand side of eqn. 15 is very small and can be neglected. The effects of the axial dispersion and the kinetics of mass transfer resistances are additive. The band profiles calculated by the equilibrium-dispersive model (infinitely fast mass transfer kinetics but finite axial dispersion) and the solid film driving force model are the same, provided the axial Peclet number of the kinetic model is replaced in the equilibrium-dispersive model with an apparent Peclet number related to the Peclet and Stanton numbers of the linear driving force model by

$$\frac{1}{Pe_{app}} = \frac{1}{Pe} + \frac{\lambda(1-\lambda)}{St} \quad (19a)$$

or

$$H = \frac{2D_L}{u} + 2 \left( \frac{K}{1+K} \right)^2 \frac{u}{Kk_f} \quad (19b)$$

where  $K = F(\Delta q/\Delta C)$  is the slope of the chord, which is concentration dependent.

This important result demonstrates that, in non-linear as in linear chromatography, the effects of axial dispersion and mass transfer resistances are additive. Since  $\lambda$  and  $K$  are concentration dependent, however, the apparent axial dispersion term also depends on the concentration. This makes the situation much more complex in non-linear than in linear chromatography.

We have shown above that the additivity of the contributions of the axial dispersion and the mass transfer resistances valid in linear chromatography also holds in non-linear chromatography, but the retention factor,  $k'_0$  should be replaced with the slope of the chord,  $F(\Delta q/\Delta C)$ . In linear chromatography, this slope is equal to  $k'_0$  and eqn. 19 becomes

$$\frac{1}{Pe_{app}} = \frac{1}{Pe} + \frac{k'_0}{(1 + k'_0)^2 St} \quad (20a)$$

or

$$H = \frac{2D_L}{u} + \frac{2k'_0 u}{(1 + k'_0)^2 k_f} \quad (20b)$$

Eqn. 20, which is valid only for linear chromatography, is exactly the result obtained by Van Deemter *et al.* [5].

The previous analysis applies to the combination of a finite axial dispersion and slow mass transfer kinetics, which can be accounted for using the solid film linear driving force model. When the mass transfer kinetics are fast but the kinetics of adsorption-desorption are slow and can be accounted for by the Langmuir model (eqn. 9), we can let  $b = k_a/k_d$  and rewrite the second-order Langmuir kinetics as

$$\begin{aligned} \frac{\partial C_s}{\partial t} &= k_d [bCq_s - C_s(1 + bC)] = k_d(1 + bC) \\ &\quad \left[ \frac{bCq_s}{1 + bC} - C_s \right] \\ &= k_d(1 + bC)(q^* - C_s) \end{aligned} \quad (21)$$

where  $q^*$  is the stationary phase concentration in equilibrium with the mobile phase concentration  $C$ . For a linear isotherm (*i.e.*,  $bC \rightarrow 0$ ), eqn. 21 is exactly the solid film linear driving force model (eqn.

8), with  $k_f = k_d$ . These two models are identical in linear chromatography. Eqn. 21 shows that, with a non-linear isotherm, the Langmuir kinetic model can still be written under the general form of the solid film linear driving force model, but with a kinetic coefficient

$$k_f = k_d(1 + bC) \quad (22a)$$

or, conversely, a linear driving force model can be written under the general form of the Langmuir kinetic model, but with a rate constant

$$k_d = \frac{k_f}{1 + bC} \quad (22b)$$

In both instances, however, the new rate constant is concentration dependent. This is why when a band profile is simulated using the transport model (*i.e.*,  $D = 0$  and solid film linear driving force kinetics), the profile can be fitted to the Thomas model ( $D = 0$  and Langmuir kinetics). However, the parameters supplied by the regression,  $k_d$  and  $N_{rea}^{app}$ , are concentration dependent and decrease with increasing concentration.

The equivalence between the kinetic equations of the Langmuir model (eqn. 9) and the linear driving force model (eqn. 12) has been shown previously by Hiester and Vermeulen [32] in the case of the breakthrough curve (Riemann problem). They also showed that the equivalent rate parameter is concentration dependent. Arnold and Blanch [33] suggested that, when slow mass transfer kinetics and slow adsorption-desorption kinetics coexist, the solution of the Thomas model can still be applied. In this instance, however, the apparent number of reaction units used should be related to the numbers of reaction units and mass transfer units by

$$\frac{1}{N_{rea}^{app}} = \frac{1}{N_{rea}} + \frac{1}{N_m} \quad (23)$$

As in non-linear chromatography  $N_m$  depends on the concentration, the apparent number of transfer units also depends on the concentration. The concentration dependence of the kinetic parameter is more consequential in frontal analysis and in displacement chromatography where the variation of concentration is much more important. The maximum concentration of a band in elution chromatography is smaller than the step height in the other two

methods. Hence the profile of an elution band calculated without accounting for the concentration dependence of the kinetic parameter is close to the actual band profile, especially when the column efficiency is significant [34].

All these results explain why we can fit band profiles calculated with a model to the formalism of another model and determine satisfactory values for the parameters of this other model. It explains also why, in this instance, the kinetic parameter of the other model depends on the concentration range of the band, *i.e.*, on the sample size.

#### CONCLUSIONS

Experimental band profiles acquired in non-linear chromatography can be fitted to many different models. The values supplied by the curve-fitting procedure for the thermodynamic parameters, the limit retention factor,  $k'_0$ , and the loading factor,  $L_f$ , are accurate with all models. The differences between the values derived from different models are probably not significant, but less than the experimental error. On the other hand, the lumped kinetic coefficient is concentration dependent. The values obtained differ, depending on the model used and on the loading factor corresponding to the experiment.

In a further paper we shall consider the dependence of the kinetic parameters on the concentration range studied and on the column efficiency [34], and investigate the differences between the various models at very low column efficiency.

#### ACKNOWLEDGEMENTS

We gratefully acknowledge fruitful discussions with Eric Dose (UTK) regarding the procedures for implementation of the simplex algorithm to our particular problem. This work was supported in part by grant CHE-8901382 from the National Science Foundation and by the cooperative agreement between the University of Tennessee and the Oak Ridge National Laboratory. We acknowledge support of our computational effort by the University of Tennessee Computing Center.

#### REFERENCES

- 1 L. Lapidus and N. R. Amundson, *J. Phys. Chem.*, 56 (1952) 984.
- 2 E. Kucera, *J. Chromatogr.*, 19 (1965) 237.
- 3 M. Kubin, *Collect. Czech. Chem. Commun.*, 30 (1965) 2900.
- 4 A. M. Lenhoff, *J. Chromatogr.*, 384 (1987) 285.
- 5 J. J. Van Deemter, F. J. Zuiderweg and A. Klinkenberg, *Chem. Eng. Sci.*, 5 (1956) 271.
- 6 J. C. Giddings, *Dynamics of Chromatography*, Marcel Dekker, New York, 1965.
- 7 E. Glueckauf, *Ion Exchange and its Applications*, Metcalfe and Cooper, London, 1955.
- 8 J. J. Carberry and R. H. Bretton, *AIChE J.*, 4 (1958) 367.
- 9 C. N. Reilly, G. P. Hildebrand and J. W. Ashley, *Anal. Chem.*, 34 (1962) 1198.
- 10 A. J. P. Martin and R. L. M. Synge, *Biochem. J.*, 35 (1941) 1358.
- 11 Cs. Horváth and H. J. Lin, *J. Chromatogr.*, 149 (1978) 43.
- 12 Q. Yu and N.-H. L. Wang, *Comput. Chem. Eng.*, 13 (1989) 915.
- 13 C. K. Lee, Q. Yu, S. U. Kim and N.-H. L. Wang, *J. Chromatogr.*, 484 (1989) 29.
- 14 R. D. Whitley, K. E. Van Cott, J. A. Berninger and N.-H. L. Wang, *AIChE J.*, 37 (1991) 555.
- 15 Y. S. Lin and Y. H. Ma, *AIChE J.*, 36 (1990) 1569.
- 16 H. C. Thomas, *J. Am. Chem. Soc.*, 66 (1944) 1664.
- 17 S. Goldstein, *Proc. R. Soc. London, Ser. A*, 219 (1953) 151.
- 18 J. L. Wade, A. F. Bergold and P. W. Carr, *Anal. Chem.*, 59 (1987) 1286.
- 19 S. Golshan-Shirazi and G. Guiochon, *J. Phys. Chem.*, 95 (1991) 6390.
- 20 B. C. Lin, S. Golshan-Shirazi and G. Guiochon, *J. Phys. Chem.*, 93 (1989) 3363.
- 21 E. Glueckauf and J. I. Coates, *J. Chem. Soc.*, 1315 (1947).
- 22 A. S. Michaels, *Ind. Eng. Chem.*, 44 (1952) 1922.
- 23 S. Golshan-Shirazi, B. C. Lin and G. Guiochon, *Anal. Chem.*, 61 (1989) 1960.
- 24 M. W. Phillips, G. Subramanian and S. M. Cramer, *J. Chromatogr.*, 454 (1988) 1.
- 25 J. A. Nelder and R. Mead, *Comput. J.*, 7 (1965) 308.
- 26 E. R. Aberg and G. T. Gustavsson, *Anal. Chim. Acta*, 144 (1982) 39.
- 27 E. Dose, *Anal. Chem.*, 59 (1987) 2420.
- 28 C. A. Lucy, J. L. Wade and P. W. Carr, *J. Chromatogr.*, 484 (1989) 61.
- 29 H.-K. Rhee and N. R. Amundson, *Chem. Eng. Sci.*, 27 (1972) 199.
- 30 R. Aris and N. R. Amundson, *Mathematics in Chemical Engineering*, Prentice-Hall, Englewood Cliffs, NJ, 1973.
- 31 B. C. Lin, S. Golshan-Shirazi, Z. Ma and G. Guiochon, *Anal. Chem.*, 60 (1988) 2647.
- 32 N. K. Hiester and T. Vermeulen, *Chem. Eng. Prog.*, 48 (1952) 505.
- 33 F. H. Arnold and H. W. Blanch, *J. Chromatogr.*, 355 (1986) 13.
- 34 S. Golshan-Shirazi and G. Guiochon, in preparation.



# Comparison between the hodograph transform method and frontal chromatography for the measurement of binary competitive adsorption isotherms

Zidu Ma and Georges Guiochon

Department of Chemistry, University of Tennessee, Knoxville, TN 37996-1501 and Division of Analytical Chemistry, Oak Ridge National Laboratory, Oak Ridge, TN 37831-6120 (USA)

(First received October 7th, 1991; revised manuscript received February 5th, 1992)

---

## ABSTRACT

Frontal analysis is an accurate method of isotherm determination. However, for the study of binary competitive isotherms, it requires a large number of measurements, it is time consuming and it needs excessive amounts of pure chemicals. The hodograph transform method is of considerable interest because it uses much smaller amounts of chemicals. It requires validation. In this work, the potential precision and accuracy of the two methods were compared and the optimum experimental conditions for each were determined on the basis of simulation study.

---

## INTRODUCTION

The determination of multi-component adsorption isotherms and the investigation of their properties are important in several different areas. In physical chemistry, these isotherms offer another angle for the study of adsorbate–adsorbate and adsorbate–surface interactions. In chemical engineering, a knowledge of competitive adsorption isotherms is essential for process design. With the development of high-performance liquid chromatography (HPLC) and of its preparative applications, the study of competitive isotherms is gaining increasing attention as liquid–solid adsorption is one of the most important retention mechanisms. The competitive adsorption isotherms permit a better understanding of the phenomena responsible for retention and separation. Further, a method for the rapid, precise and accurate determination of com-

petitive adsorption isotherms would permit the rapid optimization of the design and operating conditions of a preparative chromatograph for performing a given purification. This is currently a crucial need in the pharmaceutical and biotechnical industries.

There are currently three types of methods for the determination of competitive isotherms, frontal analysis [1], pulse methods [2–4] and the application of the non-linear wave theory known as the hodograph plot [5–7]. Frontal analysis uses to advantage the formation and propagation of self-sharpening fronts in a chromatographic column as a response to the injection of a concentration step. If the isotherm is convex upward, these sharp fronts are observed for positive steps whereas they are recorded with negative steps with concave upward isotherms. For a binary mixture, Jacobson *et al.* [1] have shown how the measurement of the retention volumes of these self-sharpening fronts permits the determination of the amount of each component adsorbed at equilibrium with a solution of given composition, using an integral mass balance equation. This method is

---

Correspondence to: Professor G. Guiochon, Department of Chemistry, University of Tennessee, Knoxville, TN 37996-1501, USA.

accurate but tedious and requires large amount of materials. It remains the most frequently used.

Helfferich and Peterson [2] have shown that the equilibrium isotherm can be related to the retention times of pulses of the mixture components injected on a concentration plateau. Two types of procedures have been developed, depending whether the pulses can be identified by using isotopically labeled components or not. In the former procedure, the elution pulse is identified using a radioactivity detector (radiolabeled components), an LC–mass spectrometric or LC–NMR instrument (stable isotopes) and the retention time of the pulse of the material actually injected in the column is measured. It gives directly, in a single experiment, the stationary-to-mobile phase partition coefficients of all tagged solutes at the mobile phase composition of the experiment, hence  $q_i(C_1, C_2)$ , the isotherm. Because of current safety regulations, however, the use of radioactive isotopes has become extremely cumbersome; the use of stable isotopes requires complex and expensive equipment which is difficult to tune and rarely available. Finally, in all instances, the synthesis of the appropriately labeled compounds needed is required. All these requirements combined make the tracer pulse method too expensive to be practical in an academic laboratory.

In the latter procedure, the injection of a small amount of one component on a concentration plateau of both components generates a series of peaks as the response of the column, the system peaks [8]. There are as many system peaks as there are degrees of freedom in the composition of the system. This number is equal to the total number of components of the eluent minus one, as we inject one of the mobile phase components. The retention time of the system peak gives the slope of the tangent to the corresponding isotherm,  $\partial q_i / \partial C_i$ . Thus, the method does not provide enough information to calculate the competitive isotherms as the four derivatives,  $\partial q_i / \partial C_j$ , are required.

Recently, a new method for the determination of the competitive equilibrium isotherms of binary mixtures has been introduced [5–7]. This method employs the non-linear wave effect which takes place when the column is overloaded both in concentration and in volume, to the degree that a concentration plateau at the feed composition is eluted between the band front and its rear. Under such

conditions, we have a non-linear wave solution of the system of partial differential equations made of the mass balances of the sample components [5,9–11]. It can be shown that, under such conditions, the hodograph transform of the band profiles, *i.e.*, a plot of the concentration of the first component *versus* the concentration of the second at the same time (see below), is made of two lines (one for the band front and the other for its rear) which intersect at the point corresponding to the feed composition (constant state). This plot is called the hodograph plot or hodogram [5–7,11–13]. The theory of partial differential equations shows that the hodogram contains all the information regarding the interaction of the mixture components, but no information on the extent of adsorption [11].

When the competitive isotherms of the components of a binary mixture follow the competitive Langmuir model, the hodogram consists of two straight lines. The slopes and intercepts of these two lines are simply related to the four parameters of the competitive Langmuir isotherms [5]. As a conventional chromatographic system with an automatic fraction collector and an autoinjector system [6] permits a rapid determination of the individual elution profiles, this provides a convenient method for the determination of these coefficients [5,7]. When the competitive Langmuir isotherm model fails, however, the lines are no longer straight and more experimental data are required in order to determine the isotherms. Repeating the experiment while varying the composition of the wide pulse can provide these data.

Among the obvious advantages of the new method compared with frontal analysis are the much smaller amount of material needed and the lesser dependence of the accuracy on some important experimental conditions, such as the column efficiency and the column dead volume. Conversely, a serious disadvantage is the need for an isotherm equation to which the data have to be fitted. The derivation of a direct isotherm plot from the hodogram is not possible. We present here a theoretical comparison between data obtained by frontal analysis and by the hodograph method.

## THEORY

The mass balance equation of the two compo-

nents of a binary mixture in a chromatographic system is

$$\frac{\partial C_i}{\partial t} + F \cdot \frac{\partial q_i}{\partial t} + u_0 \cdot \frac{\partial C_i}{\partial x} = D_a \cdot \frac{\partial^2 C_i}{\partial x^2} \quad (1)$$

As usual in the non-ideal or equilibrium-dispersive model of chromatography, the stationary phase concentration,  $q_i$ , and the mobile phase concentration,  $C_i$ , are related by the equilibrium isotherm;  $F$  is the phase ratio and  $u_0$  the mobile phase velocity. The apparent dispersion coefficient,  $D_a$ , accounts for axial diffusion and for the mass transfer kinetics [14]. This assumption is valid as long as the column efficiency exceeds a few hundred theoretical plates [11,14]. The initial and boundary conditions of the problem are

$$C_i(t, x = 0) = \phi_i(t) \quad (2a)$$

$$C_i(t = 0, x) = 0 \quad (2b)$$

with  $i = 1, 2$ . In practice, we assume a rectangular injection of a mixture of constant composition,  $C_{1,0}$ ,  $C_{2,0}$ , during a time  $t_p$ .

In the case of a competitive Langmuir isotherm:

$$q_i = \frac{a_i C_i}{1 + \sum_{j=1}^2 b_j C_j} \quad (3a)$$

When  $C_i$  becomes large,  $q_i$  tends towards a limit, the column saturation capacity,  $q_{si} = a_i/b_i$ . We can simplify the equations in the following derivation by letting  $\bar{Q}_i = q_i/q_{si}$ ,  $\bar{C}_i = b_i C_i$ . Eqn. 3a becomes

$$\bar{Q}_i = \frac{\bar{C}_i}{1 + \sum_{j=1}^2 \bar{C}_j} \quad (3b)$$

*Frontal chromatography method*

In this method, a solution of the two components is pumped into a column previously equilibrated with the pure mobile phase. A front of the first component is eluted, followed by a front of the second component. When the eluent composition is constant and equal to the feed composition, the experience is repeated, the feed solution being replaced with a more concentrated solution of the two components, usually keeping constant the ratio of these two components. Because of the competi-

tion between the two components, an intermediate plateau appears after the elution of the front of the first component. During the elution of this intermediate plateau, the eluent concentration of the first component is higher than its concentration in the new feed while the eluent concentration of the second component is intermediate between its concentrations in the old and the new feed (see Fig. 1).

In the assumption of ideal chromatography (*i.e.*, if  $D_a = 0$ ), the integral mass balance equations of

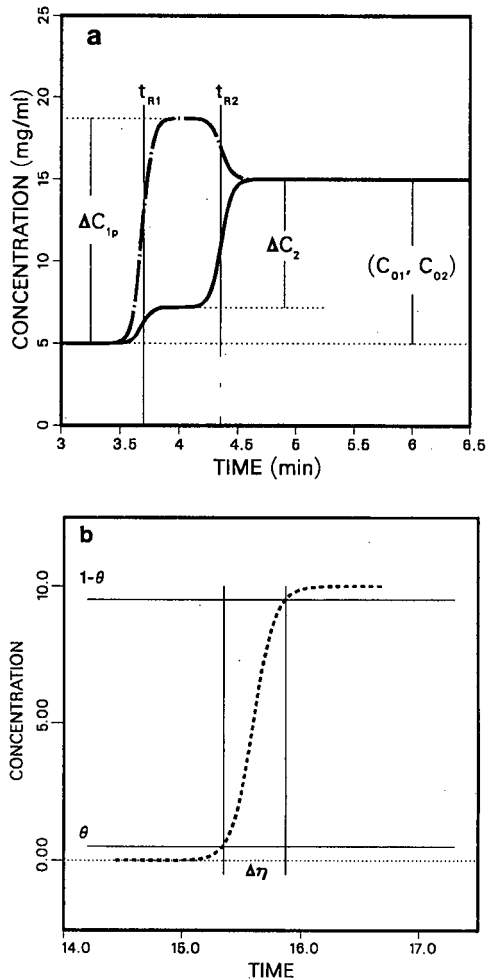


Fig. 1. Breakthrough profiles of the two components in frontal analysis and definition of symbols. (a) Schematic diagram of the individual breakthrough profiles in binary frontal analysis (assuming  $C_{01} = C_{02}$ ), and definitions. (b) Schematic diagram of a shock layer and definition of its thickness. All figures: concentration is in mg/ml; time is in min.

the two components are written (see Symbols and Fig. 1a)

$$\frac{t_{R1} - t_0}{Ft_0} = \frac{\Delta q_1}{\Delta C_{1p}} \quad (4a)$$

$$\frac{t_{R2} - t_0}{Ft_0} = \frac{\Delta q_2}{\Delta C_2} \quad (4b)$$

where  $\Delta q_i$  and  $\Delta C_i$  are the amplitudes of the concentration shock in the stationary and the mobile phases, respectively. The relationship which was derived by Jacobson *et al.* [1] as an integral mass balance equation can also be derived from the above equations which relate the retention times of the two breakthrough curves, the mobile phase concentration jumps of each solute corresponding to the injection step and the corresponding changes of each solute concentration in the stationary phase. However, when accounting for experimental data, different results are obtained when fitting these data to eqns. 4 or to the equations reported in ref. 1. The differences can be significant if the data are not very precise.

In practice,  $D_a$  is different from zero. The axial dispersion and the finite rate of mass transfer combine to erode the concentration discontinuities predicted by the ideal model. As these shocks are caused by non-linear thermodynamic effects which are constantly at work, the fronts remain very steep. Shock layers appear, which propagate at the same velocity as the shocks of the ideal model but have a finite width [9,11,15]. As a result, the formation of the intermediate concentration plateau is not instantaneous and this plateau is narrower than predicted by the ideal model [13], as allowance must be made for the thickness of the two shock layers.

The thickness of the shock layer was calculated by Rhee and Amundson [16]. They showed that a steep but steady concentration change, the shock layer, propagates along a real column (*i.e.*, a column where  $D_a$  is different from zero), that it propagates at the same velocity as the concentration shock would propagate along an ideal column with the same isotherms and they calculated the thickness of this shock layer. The velocity of a shock depends only on its height and is given by the equation

$$U_s = \frac{u_0}{1 + Fa_i \cdot \frac{\Delta \bar{Q}_i}{\Delta \bar{C}_i}} \quad (5)$$

From the study performed by Rhee and Amundson, we can derive the width,  $\Delta \eta$ , of the shock layer on the front of the first component band in frontal analysis and the time,  $\Delta t$ , needed for the formation of the intermediate plateau [13]. The width of the shock layer depends on the fractional height,  $\theta$ , at which it is measured. It is given by

$$\Delta \eta(\theta) = D_a \cdot \frac{(1+K)^2}{K} \cdot \frac{2 + \bar{C}_0}{\bar{C}_0} \cdot \ln\left(\frac{1-\theta}{\theta}\right) \approx \frac{H(1+K)^2}{2u_0K} \cdot \frac{2 + C_0}{C_0} |\ln \theta| \quad (6)$$

with

$$K = k'_0/(1 + \bar{C}_0) \quad (7a)$$

$$\theta = \frac{C_1^* - C_1}{C_1^* - C_r^*} = \frac{C_r - C_r^*}{C_1^* - C_r^*} \quad (7b)$$

$k'_{1,0} = a_1 F$  is the retention factor of the first component at infinite dilution;  $C_1^*$  and  $C_r^*$  are the concentrations at the left and right of the shock which are used to define  $\theta$  and indicate at which fractional height of the shock layer we measure its width (see Fig. 1b). In eqn. 7b, either the true concentrations or the dimensionless concentrations (eqn. 3b) can be used. As the front of the first component elutes pure, we calculate the thickness of the first shock by combining eqns. 6 and 7a with

$$\begin{aligned} \bar{C}_0 &= \bar{C}_{1,0} \\ k'_0 &= Fa_1 \\ D_a &= H/2u_0 \end{aligned} \quad (8a)$$

where  $H$  is the column height equivalent to a theoretical plate. It would probably be more exact to use  $D_a = H/2u_0 + U_s(u_0 - U_s)/k_f$ , where  $k_f$  is the lumped mass transfer coefficient [17].

This question deserves a more thorough investigation, currently undergone in connection with an experimental study. For the thickness of the second component, we use

$$\bar{C}_0 = \bar{C}_{2,0}$$

$$k'_0 = \frac{Fa_2}{1 + b_1 \cdot \frac{1 - \alpha}{\alpha b_1 + b_2/\xi}} \quad (8b)$$

where  $\xi$  is the solution of the second degree algebraic eqn. 12a in ref. 13. This equation is also eqn. 10 in the next section of this paper.

From the combination of eqns. 6 and 8a, it results that the shock layer thickness increases in proportion to the column HETP [11,13]. This conclusion is supported by experimental results [13].

The time required before stabilization of the elution front of the first component and formation of the enriched plateau is

$$\Delta t = \frac{1}{2} \cdot \frac{\Delta C_{1p}(\Delta\eta_1 + \Delta\eta_2)}{C_{1,0}U_{s1} - C_{2,0}U_{s2}} \quad (9)$$

where  $\Delta C_{1p}$  is the concentration height of the enriched plateau of the first component,  $\Delta\eta_{s,1}$  and  $\Delta\eta_{s,2}$  are the width of the shock layers before and after the enriched plateau and  $U_{s,1}$  and  $U_{s,2}$  are the shock velocities of the two injection concentrations,  $C_{1,0}$  and  $C_{2,0}$ , respectively.

From eqn. 9, we can derive the conditions required for an accurate determination of the amounts of the two components adsorbed at equilibrium with the concentrations  $C_{1,0}$  and  $C_{2,0}$  in the mobile phase. The column length and efficiency must be such that the elution of the band front takes a time longer than  $\Delta t$  under all the experimental conditions investigated, so the intermediate plateau is always formed and its composition can be measured.

#### Hodograph method

As demonstrated previously [9,11,18–20], the following relationship can be derived between the derivatives and differentials of the concentrations, when the apparent diffusion coefficient is zero:

$$\xi^2 f_{21} + \xi(f_{22} - f_{11}) - f_{12} = 0 \quad (10)$$

where

$$\xi = dC_1/dC_2 \quad (11a)$$

and

$$f_{i,j} = \partial q_i / \partial C_j \quad i, j = 1, 2 \quad (11b)$$

$\xi$  is the derivative associated with the characteristic direction in the  $C_1, C_2$  space [9,18,19]; it defines the

slope of the lines in the hodograph plot. Eqn. 10 is a Clairaut differential equation with respect to  $dC_1/dC_2$ . Its solutions are well known [9]: they consist of two families of straight lines whose slopes and ordinates are related to the partial differentials of the isotherm, which are the characteristics in the concentration domain. Each of the two roots defines a family of characteristic lines in each point of the  $(C_1, C_2)$  plane having the slopes  $\xi_+$ ,  $\xi_-$ , where  $\xi_+$  and  $\xi_-$  are the positive and negative roots of eqn. 10, respectively. In the case of the competitive Langmuir isotherm, combining eqns. 3 and 10 gives

$$C_1 = \xi_+ C_2 + \frac{a_1 - a_2}{a_2 b_1 + a_1 b_2 / \xi_+} \quad (12a)$$

$$C_1 = \xi_- C_2 - \frac{a_1 - a_2}{a_2 b_1 + a_1 b_2 / \xi_-} \quad (12b)$$

The hodogram, *i.e.*, the plot of  $C_1$  versus  $C_2$  during the elution of the band, is made of two straight lines intersecting at the point of coordinates  $C_{1,0}$ ,  $C_{2,0}$ , corresponding to the feed composition [5,11–16]. These lines are the characteristics of the point  $C_{1,0}$ ,  $C_{2,0}$ . As a consequence, the product of their slopes is

$$\xi_- \xi_+ = -\frac{a_1 b_2}{a_2 b_1} \cdot \frac{C_{1,0}}{C_{2,0}} = \frac{1}{R_{q_s} R_{C_0}} \quad (13)$$

where  $R_{q_s}$  and  $R_{C_0}$  are the ratios  $q_{s,2}/q_{s,1}$  and  $C_{2,0}/C_{1,0}$ , respectively [21]. This equation is derived directly from eqn. 10. Thus, if experiments are made with the same two components ( $R_{q_s}$  constant) and the same composition ( $R_{C_0}$  constant), the product of the two slopes should remain constant if the competitive isotherm is accounted for by the Langmuir isotherm.

An interesting question on which calculations may shed useful light is whether or not the accurate determination of isotherm data by the hodograph method requires experimental conditions under which the intermediate plateau of the first component is formed, which is an absolute requirement with the frontal analysis procedure. We have calculated the elution profile of a wide rectangular band at the end of columns of increasing lengths (Fig. 2a) and otherwise identical (*e.g.*, same height equivalent to a theoretical plate). For the sake of clarity, only the front part of these bands is shown. We see that the intermediate plateau is formed progressively, the height of the first component front increasing until it

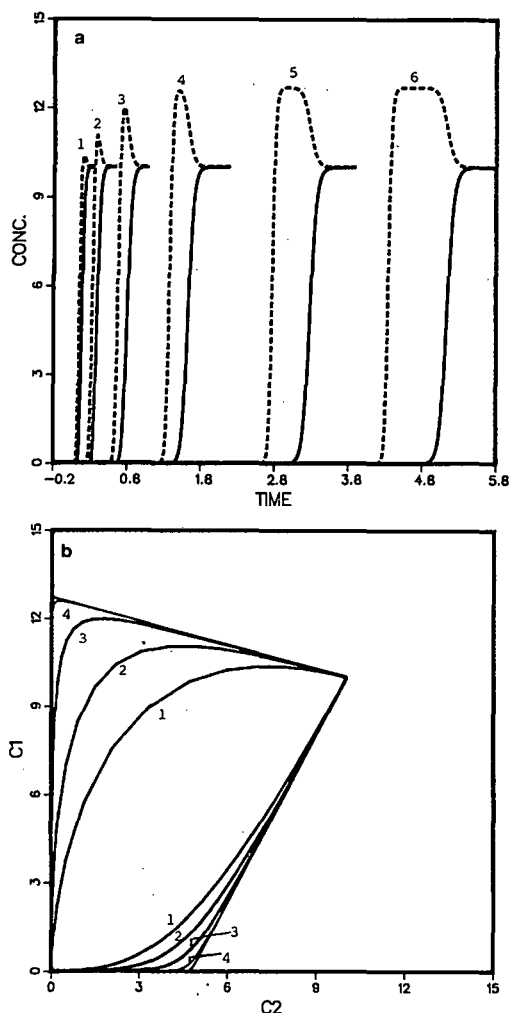


Fig. 2. Influence of the width of the intermediate plateau on the accuracy of the hodograph plot method. (a) Band profiles for a wide rectangular injection of a binary mixture at the exit of columns of increasing lengths. Column length: (1) 1 cm; (2) 2 cm; (3) 4 cm; (4) 8 cm; (5) 16 cm; (6) 25 cm. The rear boundaries of the elution profiles are not shown. (b) Hodograph plots corresponding to the elution profiles shown in (a). The plots corresponding to the elution profiles detected at 16 and 25 cm are superimposed on each other and cannot be distinguished.

reaches the plateau concentration, which it does for the fourth profile. The minimum column length required in frontal analysis is that corresponding to the fourth profile. In practice, a longer column would be needed as the plateau has to be wide enough to permit grabbing an eluent sample for its analysis. In Fig. 2b, the hodograph transform of

these bands is shown. The plot corresponding to the fourth profile permits essentially the same accuracy as any further experiment for which the intermediate plateau is fully developed. Satisfactory results could be obtained from the hodogram corresponding to the third profile, provided that about a third of the experimental data points, near the two concentration axes, be eliminated when the data processing is done to estimate the isotherm parameters.

#### Comparison between the frontal analysis and the hodogram methods for isotherm determination

Both methods are based on the solution of the mass balance eqns. 1 in the assumption of the ideal model. The errors made will derive from the consequences of having to use real, non-ideal columns and they will strike differently.

In frontal analysis, we assume that the two shock layers, at the front of the first component band and between the bands of the first and second components, have had time to form before the breakthrough of the concentration step. The formation of two stable shock layers and of a plateau wide enough to be recorded and collected is necessary to permit the determination of the concentrations of the two components on this intermediate plateau. This measure, in turn, is necessary for the calculation of the integral mass balance of the two components of the binary mixture. Under non-ideal conditions, this phenomenon takes a finite time, as mass transfers are no longer infinitely fast. This is especially true with a mixture, as the concentration of the first component at the breakthrough time is higher than in the injected feed [1]. The time,  $\Delta t$  (eqn. 9), required for the formation of this plateau depends on the column efficiency, on the relative retention of the components and on the injection profile. As a consequence, the minimum time required for the determination of a series of competitive isotherms at different relative concentrations  $R_{C_0}$  depends strongly on the efficiency of the column used and on the relative retention of the components studied.

The accuracy of the mass balances measured by frontal analysis relies on the assumption that the shock layers are symmetrical, so the retention time of the inflection point of the breakthrough profile is also the retention time of the mass center of the front. If the kinetics of mass transfer or of the retention mechanism are slow, this assumption may

lead to a significant error. This kind of error seems insignificant in most determinations carried out with most HPLC systems, where the kinetics are fast. It might be significant in affinity chromatography or in other applications involving biopolymers.

These limitations similarly affect the hodograph method. This method is valid only if the intermediate plateau at the front of the first component band has fully developed. Otherwise, there would not be any meaning to the slope and intercept of the first straight line of the hodogram. Although the method is fairly immune to slow mass transfer or reaction kinetics, if one of these types of kinetics is slow enough to generate a strongly unsymmetrical shock layer, it will render meaningless the parts of the plot close to the concentration axis and make it nearly impossible to select the experimental points which must be kept in the calculation of the slopes and intercepts of the two straight lines.

If we consider eqns. 4 and 12, we observe that frontal analysis requires the determination of the retention times of the two fronts, the phase ratio and the concentrations of the intermediate plateau. Both methods require the determination of the dead time (the hodograph method, in order to derive the value of the  $a_i$  coefficients). The hodograph method requires the collection of a large number of fractions and the accurate determination of their composition. Further, frontal analysis gives a single point of the isotherm for each breakthrough curve, while the hodogram samples the isotherm over an entire arc, *i.e.*, over a wide composition range, using a much smaller amount of sample and mobile phase in the process.

Experimentally, the hodograph method requires the acquisition of a large number of fractions and their analysis. A number of experimental problems have to be solved. A fast fraction collector is needed to collect enough fractions during the elution of the second shock layer (the elution of the first one does not give useful hodograph data). The collected fractions must be analyzed rapidly and accurately. Practical solutions have been discussed previously [6,7]. The errors made on the fraction concentrations result in a significant scatter of the data points [5–7,22], which limits the accuracy of the coefficients obtained by fitting the hodogram to an isotherm model that is more sophisticated than the competitive Langmuir equation. This is probably the most important drawback of the method.

Finally, the experimental data acquired in frontal analysis are transformed directly into isotherm points. The experimental data supplied by the hodogram cannot be transformed directly into isotherm points. They may be fitted to the equation of an isotherm model and used to calculate the best estimates of the parameters of this model. A model is necessary; the fitting of the isotherm data points to a spline is impossible as there are no isotherm data points.

In summary, the two methods have similar requirements regarding the column characteristics. The equipment needed for the hodograph method is standard whereas two chromatographs must be used in binary frontal analysis, the second for the analysis of a sample of the intermediate plateau. The hodograph transform is more precise, faster and uses much smaller amounts of chemicals but the data it collects are more difficult to process and require an isotherm model. Binary frontal analysis is very accurate but requires tight control of experimental conditions. A comparison between the accuracies of the two methods is difficult. The hodograph method does not require the determination of  $t_0$ , whereas frontal analysis does. Flow-rate fluctuations during the experiment affect the frontal analysis measurement if made after the recording of detector signal *versus* time. They will not affect the hodogram, which merely uses the two concentrations.

The two methods appear to have complementary natures. An attractive synthesis would be to conduct a series of experiments designed for the hodograph method, injecting different concentration steps, with different concentration ratios. The retention times of the fronts of the breakthrough curves can be used to calculate the concentrations of each solute in the stationary phase, using eqns. 4, while the concentration profiles of the whole bands can be used with the hodograph method. This would provide some check on consistency and accuracy.

#### *Simulation experiments*

Using the computer programs previously developed for the calculation of solutions of the equilibrium-dispersive model [21–24], we have calculated the elution profiles for a series of four wide band injections of a binary mixture (concentration  $C_1^0 = 15.0, 10.0, 5.0$  and  $2.5$  mM, respectively, with

$C_1^0/C_2^0 = 1$ ) and the breakthrough profiles for various steps of the same mixture [5]. A fraction of the points (one every 80) is kept as a data point. To each of these data points, a number taken from a simulated noise sequence is added. The uniform distribution random number generator DRNUN of

the IMSL library gives random numbers between 0 and 1. A random number series of appropriate length is scaled to a mean of 0 and a standard deviation of 5% of the height of the rectangular pulse or of the concentration step injected.

The elution profiles of the four wide rectangular pulses considered are shown in Figs. 3a-6a. In these figures, the points are the "experimental" results of the simulated experimental data obtained as just

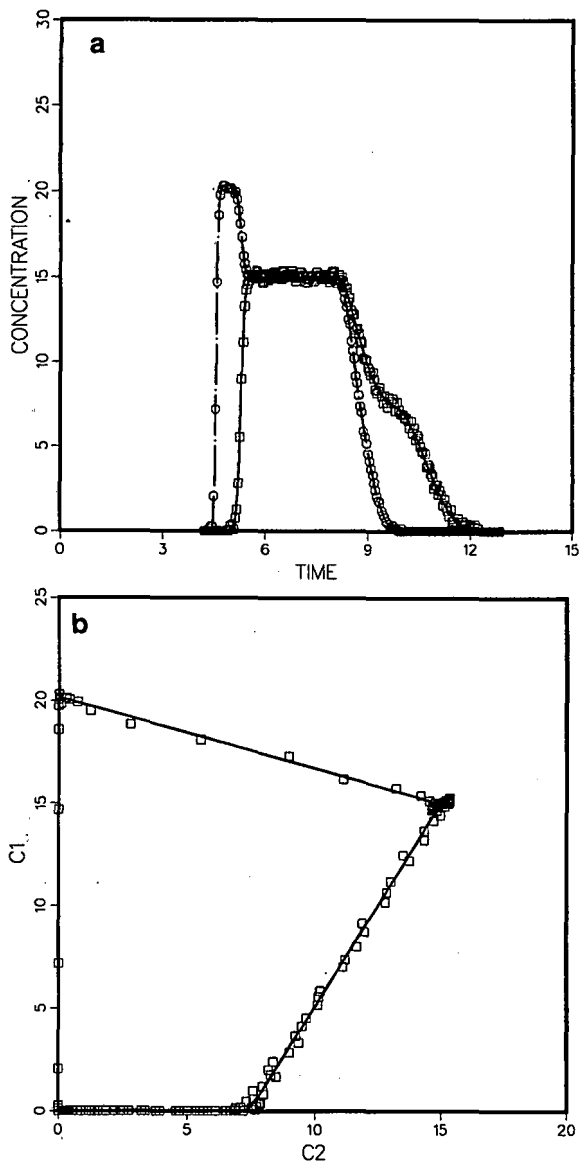


Fig. 3. Elution profiles and hodograph plot of experiment No. 1 shown in Table I. (a) Elution profiles. The points are simulated experiment points and the lines are the theoretical lines. (b) Hodograph plot corresponding to the elution profiles shown in (a).

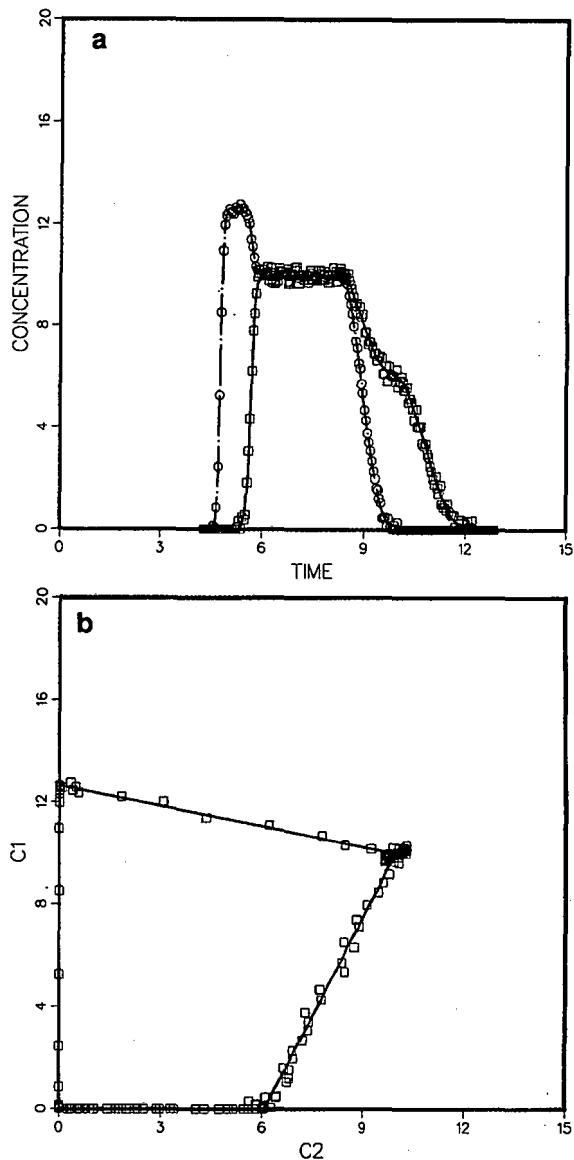


Fig. 4. As Fig. 3 for experiment No. 2 shown in Table I.

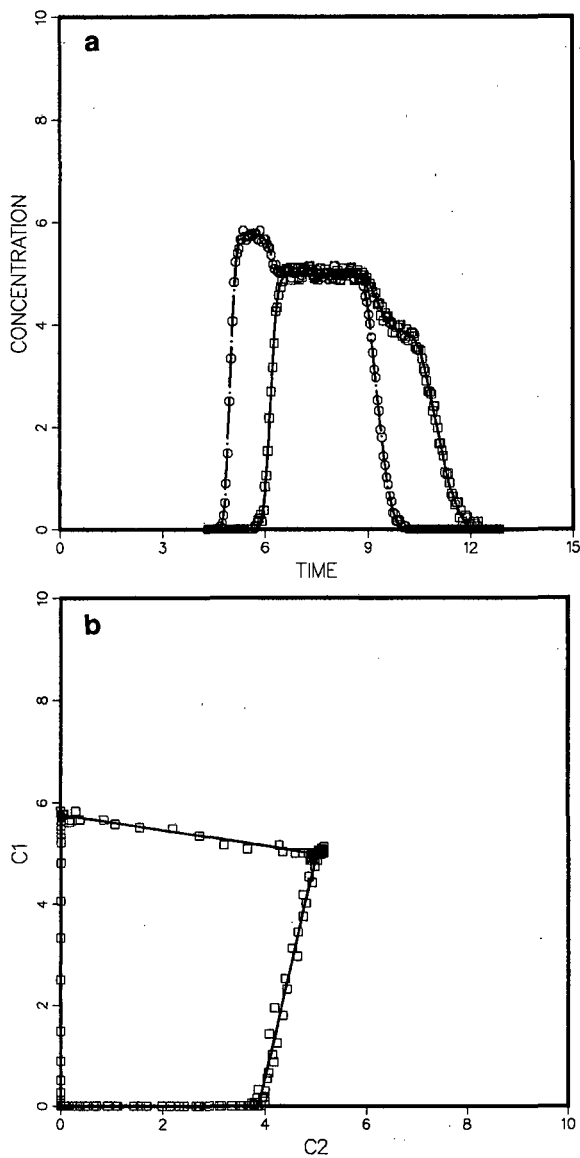


Fig. 5. As Fig. 3 for experiment No. 3 shown in Table I.

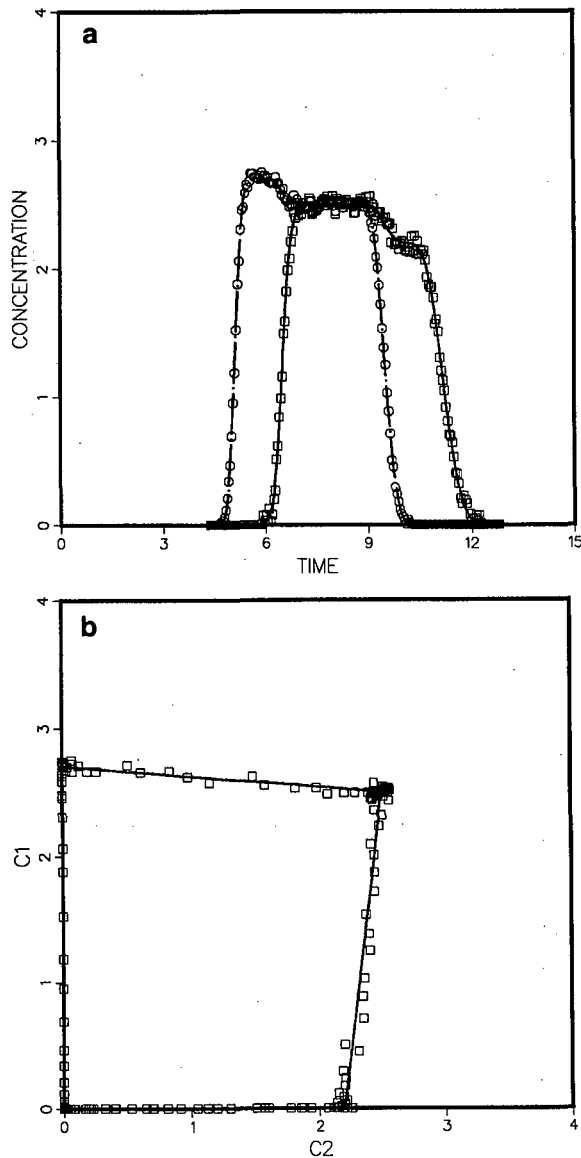


Fig. 6. As Fig. 3 for experiment No. 4 shown in Table I.

described. The data points obtained for the elution of a wide rectangular pulse are sorted into two groups. The former includes the points for which the second component concentration is positive and the first component concentration is larger than the injection concentration augmented with the largest noise number. This set of data is used to calculate the negative slope,  $\xi_-$ , and the corresponding intercept

(Table I) by fitting the points to a straight line. The latter data group includes the points for which the first component concentration is positive and the second component concentration is lower than the injection concentration less the smallest random number. This second set of data is used to calculate the positive slope,  $\xi_+$ , and the corresponding intercept (Table I). The hodograph plots and the best

TABLE I  
SLOPES AND INTERCEPTS

Concentrations of the rectangular injection plug,  $C_1^0 = C_2^0$ : (1) 15 mM; (2) 10.0 mM; (3) 5.0 mM; (4) 2.5 mM.  $A_+$  and  $A_-$  are the intercept of the straight lines shown in Fig. 3a, corresponding to the positive and the negative slope, respectively. Column length,  $L = 25$  cm; flow-rate, 1 ml/min; hold-up time, 3.00 min; phase ratio,  $F = 0.35$ ; column efficiency, 2500 theoretical plates. True values:  $a_1 = 2.1556$ ,  $a_2 = 3.7566$ ,  $b_1 = 0.0216$ ,  $b_2 = 0.0256$ .

No.	$\xi_-$	$\xi_+$	$A_+$	$A_-$	$b_1$	$b_2$
1	0.3381	1.9594	14.3714	20.0927	0.02217	0.02556
2	0.2585	2.4854	14.9240	12.6399	0.02268	0.02541
3	0.1461	4.2905	16.4198	5.7550	0.02266	0.02463
4	0.07730	7.3592	15.9042	2.6922	0.02487	0.02468

straight lines obtained for the four simulated experiments are shown in Figs. 3b–6b.

The data points from the breakthrough curve are used to calculate the retention times of the two fronts and the intermediate concentration (Table II). Then, the equations in ref. 1 were used to calculate the corresponding stationary phase concentrations for the two components. To fit the frontal analysis data to the equations of the model, we used the SYSNLIN procedure from the SAS package. This program permits the fitting of a set of experimental data to more than one equation.

## RESULTS AND DISCUSSION

As indicated in the previous section, a comparison

of the accuracies of the two methods based on the use of experimental data is difficult, as the exact isotherm can never be known. A comparison based on the use of simulated data is useful to search for possible bias or errors. Experimental data comparing the precisions of the two methods will be reported later [25].

The parameters of the Langmuir isotherms are derived from the slopes and intercepts of the two straight lines of the hodograph plots (Table I) [5]. The deviations between the values of the parameters obtained with the hodograph method and the theoretical values increase from 2.6% to 15% for  $b_1$  and from 0.2 to 3.6% for  $b_2$  when the pulse concentration decreases from 15 to 2.5 mM. The results derived from the three highest concentration injec-

TABLE II  
FRONTAL ANALYSIS RESULTS

Nos. 1–10 are the ten steps of a frontal analysis experiment. The concentrations  $C_{int}$  are the intermediate mobile phase concentrations of the first component corresponding to its mobile phase concentration on the intermediate plateau. From eqn. 4a,  $Q_1$  and  $Q_2$  are the stationary phase concentrations of the first and the second component corresponding to the mobile phase concentration of the injected step. All concentrations are in mM and all times in min. A hold-up time of 2.97 min was used to calculate the stationary concentrations.

No.	$t_{R1}$	$t_{R2}$	$C_{int}$	$Q_1$	$Q_2$
1	4.581	5.192	19.920	20.552	32.385
2	4.757	5.706	12.832	14.751	26.588
3	4.915	6.063	5.849	8.503	15.028
4	5.042	6.625	2.762	4.631	8.879
5	4.635	5.632	16.184	23.120	12.933
6	5.026	6.316	7.948	14.420	8.128
7	5.180	6.589	3.959	7.766	4.396
8	4.991	5.693	8.014	7.761	39.691
9	5.103	6.274	3.266	4.310	24.076
10	5.315	6.358	1.446	2.699	12.346

TABLE III  
PARAMETERS OBTAINED BY FITTING THE EXPERIMENTAL RESULTS TO VARIOUS ISOTHERMS

Isotherm	Parameters					
	$a_1$	$a_2$	$b_1$	$b_2$	$R^2$	
(a) Competitive Langmuir isotherm equation, using eqn. 4						
					$Q_1$	$Q_2$
	2.3568	3.9007	0.0269	0.0234	0.9976	0.9978
(b) Langmuir isotherm equation, using eqn. 4			$b_1$	$b_2$	$R^2$	
					$Q_1$	$Q_2$
			0.0198	0.02236	0.9967	0.9951
(c) Competitive Langmuir isotherm equation	$a_1$	$a_2$	$b_1$	$b_2$	$R^2$	
					$Q_1$	$Q_2$
	2.3389	3.9075	0.0233	0.0276	0.9944	0.9979
(d) Langmuir isotherm equation			$b_1$	$b_2$	$R^2$	
					$Q_1$	$Q_2$
			0.0221	0.0214	0.9925	0.9961

tions are all within 5% of the true value. Thus, when the adsorption behavior of the binary mixture is well described by the Langmuir model, the determination of the model parameters is reasonably accurate.

Table II gives the results of a frontal analysis experiment involving the simulation of ten consecutive steps. For each step, the values of the intermediate concentration of the first component and of the retention times of the two fronts contain a random error resulting from the noise added to the detector signal, as explained in the previous section. The largest error made on the intermediate concentration is 2.2% and that made on the retention time of the two fronts is 2.3%. We have used two methods to fit these results to a Langmuir model. The data in Table III(a) and (c) were obtained using eqn. 4. First, the data for the first component are fitted to the single-component Langmuir equation, using  $C_{int}$  as the concentration in the mobile phase, and calculating the stationary phase concentration from eqn. 4a. The data for the second component are then

fitted to the competitive Langmuir equation, using the injection concentrations as mobile phase concentrations and deriving the stationary phase concentrations from eqn. 4b. The data in Table III(b) and (d) were obtained by determining the coefficients  $a_1$  and  $a_2$  from the infinite retention times and deriving the coefficients  $b_1$  and  $b_2$  by fitting the data in Table II using the equations derived by Jacobson *et al.* [1].

The largest deviation is about 24% [Table III(a)]. The best results are in Table III(c) (ca. 8% error for  $a_1$ ,  $b_1$  and  $b_2$  and 4% for  $a_2$ ). We conclude that in the case of a true Langmuir isotherm, the frontal analysis data are slightly less accurate than the hodograph data. From this numerical comparison, we may conclude that the two methods give comparable performances. Both require fast mass transfer in the column for an accurate determination of the isotherm data. From a theoretical viewpoint, frontal analysis has the advantage of supplying as an intermediate result the absolute concentrations of the two solutes in the stationary phase at equilib-

rium. The hodograph method cannot give this result. With this second method, an isotherm model is always required, so the experimental data can be fitted to this equation. On the other hand, the hodograph method does not need the prior determination of the dead time whereas frontal analysis does. However, this advantage is due to the fact that the hodograph method supplies only the ratio  $\alpha = a_2/a_1$ , not the value of each of these two coefficients, so the measurement of  $t_0$  is eventually necessary. Finally, only random errors on the composition of the collected fractions affect the results of the hodograph method. Random errors on the flow-rate and the influence of the signal noise on the error made in the determination of the retention time of the breakthrough curve affect the results of frontal analysis. This could sometimes be an advantage.

From a practical point of view, the hodograph method has several important advantages over the frontal analysis method. (1) The experimental procedure is simpler than that described in ref. 1 and it is much easier to automate. The equipment required includes an ordinary liquid chromatograph, an automatic fraction collector and an automated analyzer. (2) The requirements for the control of the experimental conditions are less demanding than for frontal analysis. For example, flow-rate fluctuations do not affect the results of the hodograph method whereas they directly affect the results of frontal analysis. (3) Finally, but most important, the amount of sample needed for the determination of an isotherm is much less than in frontal analysis, often several orders of magnitude less. (4) On the other hand, the data processing required for the application of the hodograph method is much more complicated than the simple fit of the stationary phase concentrations to an adsorption equation needed in frontal analysis. This is especially true in the case of non-Langmuir isotherms. If the isotherm function has one or several inflection points, however, unexpected difficulties arise in the use of the frontal analysis method, *i.e.*, in the identification of the self-sharpening boundary and in the measurement of the correct retention time [26]. The hodograph method is easier to apply if the isotherms of the two components are similar.

## SYMBOLS

$a_i$	first coefficient of the Langmuir isotherm (eqn. 3)
$b_i$	second coefficient of the Langmuir isotherm (eqn. 3)
$C_{i,0}$	concentration of the component $i$ in a rectangular injection pulse (eqn. 2)
$C_i$	mobile phase concentration of the component $i$ ( $i = 1$ or $2$ ) (eqn. 1)
$\bar{C}_i$	normalized mobile phase concentration of the component $i$ (eqn. 3)
$C_1^*$	concentration of the plateau before the shock layer (eqn. 7b)
$C_2^*$	concentration of the plateau after the shock layer (eqn. 7b)
$D_a$	coefficient of axial dispersion (eqn. 1)
$F$	phase ratio [ $F = (1 - \varepsilon)/\varepsilon$ ] (eqn. 1)
$H$	column HETP (eqn. 6)
$K$	retention parameter, eqn. 7a
$i$	rank of the component (here, $i = 1$ or $2$ ) (eqn. 1)
$\bar{Q}_i$	normalized stationary phase concentration of the component $i$ (eqn. 3)
$q_i$	stationary phase concentration of the component $i$ ( $i = 1$ or $2$ ) (eqn. 1)
$q_{si}$	column saturation capacity for the component $i$ (eqn. 3)
$t$	time (eqn. 1)
$t_0$	hold-up time (eqn. 4)
$t_p$	width of a rectangular injection profile (eqn. 2)
$t_{Ri}$	retention time of the component $i$ (elution time of the center of the breakthrough curve)
$U_s$	velocity of a shock (eqn. 5)
$u_0$	mobile phase velocity (eqn. 1)
$x$	distance along the column (eqn. 1)

## Greek symbols

$\alpha$	relative retention of the two components, $\alpha = a_2/a_1$ (eqn. 8b)
$\varepsilon$	total column porosity
$\Delta C_i$	amplitude of the concentration shock or step in the mobile phase (eqn. 4)
$\Delta C_{1p}$	concentration height of the intermediate plateau (eqn. 9)
$\Delta q_i$	amplitude of the concentration shock or step in the stationary phase (eqn. 4)
$\Delta t$	time necessary to form the intermediate pla-

- teau in the case of frontal analysis of a binary mixture (eqn. 9)
- $\Delta\eta$  shock layer thickness (eqn. 6)
- $\phi_i(t)$  injection profile (eqn. 2)
- $\theta$  reduced concentration during the passage of the shock layer (eqn. 7b)
- $\xi$  solution of eqn. 10. There are two roots,  $\xi_+$  and  $\xi_-$

## ACKNOWLEDGEMENTS

This work was supported in part by Grant CHE-8901382 of the National Science Foundation and by the cooperative agreement between the University of Tennessee and the Oak Ridge National Laboratory. We acknowledge support of our computational effort by the University of Tennessee Computing Center.

## REFERENCES

- 1 J. M. Jacobson, J. H. Frenz and Cs. Horváth, *Ind. Eng. Chem. Res.*, 26 (1987) 43.
- 2 F. Helfferich and D. L. Peterson, *Science (Washington, D.C.)*, 142 (1963) 661.
- 3 F. I. Stalkup and F. Kobayashi, *AIChE J.*, 9 (1963) 121.
- 4 S. H. Hyun and R. P. Denner, *AIChE J.*, 31 (1985) 1077.
- 5 Z. Ma, B. C. Lin, A. M. Katti and G. Guiochon, *J. Phys. Chem.*, 94 (1990) 6911.
- 6 A. M. Katti and G. Guiochon, *Am. Lab. (Fairfield, Conn.)*, 21(10) (1989) 17.
- 7 A. M. Katti, Z. Ma and G. Guiochon, *AIChE J.*, 36 (1990) 1722.
- 8 S. Golshan-Shirazi and G. Guiochon, *Anal. Chem.*, 62 (1990) 923.
- 9 R. Aris and N. R. Amundson, *Mathematical Methods in Chemical Engineering*, Prentice-Hall, Englewood Cliffs, NJ, 1973.
- 10 J. H. Seinfeld and L. Lapidus, *Mathematical Methods in Chemical Engineering*, Vol. 3, Prentice-Hall, Englewood Cliffs, NJ, 1974.
- 11 B. C. Lin, Z. Ma, S. Golshan-Shirazi and G. Guiochon, *J. Chromatogr.*, 500 (1990) 185.
- 12 Z. Ma and G. Guiochon, *Anal. Chem.*, 62 (1990) 2330.
- 13 Z. Ma and G. Guiochon, submitted for publication in *J. Chromatogr.*
- 14 S. Golshan-Shirazi and G. Guiochon, *J. Chromatogr.*, 506 (1990) 495.
- 15 B. C. Lin, S. Golshan-Shirazi, Z. Ma and G. Guiochon, *Anal. Chem.*, 60 (1988) 2647.
- 16 H.-K. Rhee and N. R. Amundson, *Chem. Eng. Sci.*, 29 (1974) 2049.
- 17 S. Golshan-Shirazi and G. Guiochon, *J. Chromatogr.*, 603 (1992) 1.
- 18 G. B. Whitham, *Linear and Nonlinear Waves*, Wiley, New York, 1974.
- 19 A. Jeffrey, *Quasilinear Hyperbolic Systems and Waves*, Pitman, London, 1976.
- 20 S. Golshan-Shirazi and G. Guiochon, *J. Phys. Chem.*, 93 (1990) 4143.
- 21 M. Z. El Fallah, S. Golshan-Shirazi and G. Guiochon, *J. Chromatogr.*, 511 (1990) 1.
- 22 Z. Ma and G. Guiochon, *Comput. Chem. Eng.*, 15 (1990) 415.
- 23 G. Guiochon, S. Golshan-Shirazi and A. Jaulmes, *Anal. Chem.*, 60 (1988) 1856.
- 24 M. Czok and G. Guiochon, *Anal. Chem.*, 62 (1990) 189.
- 25 Z. Ma and G. Guiochon, in preparation.
- 26 M. Diack and G. Guiochon, *Anal. Chem.*, 63 (1991) 2608.



# Batch dynamic adsorption of dipeptides onto reversed-phase silica gel

T. S. Nguyen, S.-G. Hu and D. D. Do

*Department of Chemical Engineering, University of Queensland, Brisbane, Qld. 4072 (Australia)*

(First received November 26th, 1991; revised manuscript received March 10th, 1992)

---

## ABSTRACT

Batch adsorption kinetics of two dipeptides, N-carbobenzoxy-L-leucyl-glycine and N-carbobenzoxy-glycyl-L-phenylalanine, onto the reversed-phase C<sub>18</sub> silica gel has been experimentally and theoretically studied in this paper. This dynamic adsorption process was described with a rate-equation model, in which the surface interaction rates is considered to be finite and follows an intrinsic kinetics of Langmuir type. The model is validated with the experimental batch kinetics data. The model parameters, rate constants and pore diffusivity, were estimated by matching the experimental data with the theoretical predictions obtained from numerical solution of the model equations. The dependence of these parameters on various factors including initial solute concentration, ratio of solution volume to adsorbent mass, pH and methanol content were examined.

---

## INTRODUCTION

Reversed-phase liquid chromatography is a powerful technique for the purification of peptides and proteins from natural and synthetic sources. Mathematical modelling to predict the process performance of a full scale column is essential for the design and optimisation of such chromatographic processes. The application of such approach requires model parameters, which characterise the thermodynamics and kinetics of the process. Since the intraparticle mass transfer and surface interaction are independent of operation mode, the parameters such as pore diffusivity and rate constants for surface interaction can be estimated using the batch experimental data [1,2]. Compared with column operation mode, the batch mode taking place in a finite bath has the main advantages of less expensive and less computational effort involved in the parameter estimation.

Most of previous works has been concerned with the retention factor in reversed-phase liquid chromatography [3–5]. However, the use of retention coefficients only addresses the thermodynamics of the process and it is not possible to assess the bandspreading in the column process. Furthermore, slow binding kinetics was observed in reverse phase chromatographic system and the activation energies for binding and dissociation were clearly commensurate with those involved in the rupture of weak chemical bonds [6]. In a column dynamic study, we also found that the bandspreading in a reversed-phase column can be well interpreted with the intrinsic kinetics mechanism [7].

In this work, batch dynamic adsorption of two dipeptides onto reversed-phase C<sub>18</sub> silica gel was experimentally studied. A rate-equation model, incorporated with the intrinsic adsorption kinetics, was proposed to describe the adsorption process. The experimental data were used to validate the proposed model and to extract the relevant model parameters. The dependence of model parameters, rate constants and pore diffusivity, on various factors has been examined. These factors include the

---

*Correspondence to:* Dr. D. D. Do, Department of Chemical Engineering, University of Queensland, Brisbane, Qld. 4072, Australia.

initial solute concentration, the ratio of solution volume to sorbent mass, pH and the methanol content in the mixed solvent.

## THEORETICAL

### Model equation

Under consideration is the batch uptake process taking place in a finite bath, in which porous adsorbent particles with uniform spherical shape and size are suspended in the bath liquid by mechanical means, and the solution is stirred such as the bulk concentration is uniform through the bath. A rate-equation model is developed to describe this batch dynamic adsorption process. This model takes into account external diffusion in the stagnant film around the adsorbent particle, pore diffusion through the void in the particle and the interaction between adsorbates and pore surface.

In formulating this model, we have assumed isothermal behaviour and constant liquid volume in the bath. The film mass transfer coefficient is taken to be constant. The pore diffusivity is also assumed to be independent of solute concentration.

Having made the above assumptions, we can write the mass balance equation for the solute  $k$  in the particle phase as follows

$$\varepsilon_m \cdot \frac{\partial C(k)}{\partial t} + (1 - \varepsilon_m) \cdot \frac{\partial C_\mu(k)}{\partial t} = \varepsilon_m D_p(k) \frac{1}{r^2} \cdot \frac{\partial}{\partial r} \cdot \left( r^2 \cdot \frac{\partial C_\mu(k)}{\partial r} \right) \quad (1)$$

where  $\partial C_\mu / \partial t$  is governed by the following Langmuir kinetic equation:

$$\frac{\partial C_\mu(k)}{\partial t} = k_a(k) C(k) \left[ 1 - \sum_{j=1}^{NC} \frac{C_\mu(j)}{C_{\mu s}(j)} \right] - k_d(k) \left[ \frac{C_\mu(k)}{C_{\mu s}(k)} \right] \quad (2)$$

where  $k_a$  is the adsorption rate constant (1/s);  $k_d$  is the desorption rate constant (mmol/ml · s), and  $C_{\mu s}$  is the sorbent capacity.

Eqns. 1 and 2 are subject to following initial and boundary conditions:

$$\begin{aligned} t = 0; C(k) = 0; C_\mu(k) = 0 \\ t = 0; \frac{\partial C(k)}{\partial r} = 0 \end{aligned} \quad (3)$$

$$r = R_0; \varepsilon_m D_p(k) \cdot \frac{\partial C(k)}{\partial r} = k_m(k) [C_b(k) - C(k)]$$

The mass balance equation for the finite bath is written as

$$V \cdot \frac{dC_b(k)}{dt} = - \left( \frac{m}{\rho_p} \right) \left( \frac{3}{R_0} \right) \left( \varepsilon_m D_p(k) \cdot \frac{\partial C(k)}{\partial r} \Big|_{R_0} \right) \quad (4)$$

The initial condition for eqn. 4 is given by

$$t = 0, C_b(k) = C_b^0(k) \quad (5)$$

At equilibrium, the following Langmuir isotherm is obtained by setting the right-hand side of eqn. 2 to zero:

$$C_\mu(k) = \frac{C_{\mu s}(k) b(k) C(k)}{1 + \sum_{j=1}^{NC} b(j) C(j)} \quad (6)$$

where  $b$  is the Langmuir constant, which is the ratio of adsorption to the desorption rate constants. The isotherm parameters  $b$  and  $C_{\mu s}$  were determined by independent batch experiments and details of which can be found in ref. 8.

### Solution method

The partial differential equation for particle phase (eqn. 1) was reduced to ordinary differential equations using the orthogonal collocation technique [9]. The resulting equations are in the form of coupled differential and algebraic equations and they were then solved with DASSL, a Differential/Algebraic System Solver [10]. The values of the kinetic parameters and diffusivities were estimated by matching the theoretical predictions of this model with the experimental concentration decay versus time curves. The optimisation method of Powell's conjugated direction method (see ref. 11) and the subroutine PCD [12] were used in this matching procedure.

## EXPERIMENTAL

### Materials

Two dipeptides, N-Cbz-L-leucyl-glycine (Cbz = carbobenzoxy) (pI 5.97) and N-Cbz-glycyl-L-phenylalanine (pI 5.72) (Sigma, St. Louis, MO, USA), were used as adsorbates in batch uptake experiments. The choice of the dipeptides is mainly based

on the consideration that these two dipeptides have relatively similar adsorption behavior under the selected conditions. The adsorbent is 5- $\mu\text{m}$  Adsorbphere C<sub>18</sub> silica gel with 80 Å pore size, 12% carbon loaded, 200 m<sup>2</sup>/g surface area, which was completely end capped (Alltech, IL, USA). The Na<sub>2</sub>HPO<sub>4</sub>, NaH<sub>2</sub>PO<sub>4</sub>·2H<sub>2</sub>O, H<sub>3</sub>PO<sub>4</sub> and HPLC-grade methanol were purchased from BDH (Victoria, Australia). All these chemicals were used as received.

#### Analytical apparatus

Analytical Beckman System Gold (San Ramon, CA, USA) was employed. It consists of a dual-pump programmable solvent module 126, a rapid scanning dual-wavelength monitoring detector module 167, a Model 210A sample injection valve and an analog module 406. The Beckman Serial Interface card is used to provide the communication between the computer and the high-performance liquid chromatography (HPLC) modules. A 250 × 4.6 mm I.D. stainless-steel column packed with 5- $\mu\text{m}$  reverse phase silica gel C<sub>18</sub> was employed.

#### Mobile phase

Both batch dynamic experiments and analysis were carried out using solutions containing 45% to 55% (v/v) HPLC-grade methanol in 75 mM phosphate buffer. The buffer solution was prepared with analytical UNIVAR reagent-grade sodium dihydrogenorthophosphate, disodium hydrogenorthophosphate and Millipore deionised water. The pH of the solutions were adjusted to about 2.98, 3.18, 3.42 and 4.18 with H<sub>3</sub>PO<sub>4</sub> in presence of pure methanol. The mobile phase used in chromatographic analysis procedure was filtered by 0.45- $\mu\text{m}$  cellulose acetate filters (Sartorius, Göttingen, Germany) and degassed under vacuum.

#### Experimental description

The transient uptake experiments were carried out for both single components and binary mixtures for various pH and methanol contents using 1.5-ml micro test tubes (Eppendorf, Hamburg, Germany). A quantities of pre-weighed silica gel was added to a series of dipeptide solutions of predetermined initial concentrations. The ratio of sorbent mass to solution volume was kept about 42 mg per ml. At the moment of sorbate-sorbent contact, mixing is start-

ed and the tube was gently rotated for a given period of time. At a certain time a small sample was withdrawn and the two dipeptides concentrations were measured by analytical HPLC Beckman System Gold at 238 nm and 254 nm.

In this work, a series of runs were carried out to investigate the effect of initial dipeptide concentrations, the amount of sorbents, pH and methanol concentration in solution. The ratio of initial concentration for the two dipeptides in finite batch is 1:1 and have limited diluted value about 30 mM. The range of methanol concentrations from 45% to 55% and pH ranged from 2.98 to 4.20 were chosen. The small range of methanol concentration is because when the methanol concentration is greater than 55% the two dipeptides have very close affinity, hence separation is not possible. On the other hand, if the methanol concentration is less than 45%, the affinities of the two dipeptides are widely different but too high. As a result, the two peaks are eluted so far apart with problems of wasting carrier fluid and longer cycle time. The similar effects of pH with those of methanol composition on retention time are also observed.

#### RESULTS AND DISCUSSION

Transient uptake experiments were carried out for a binary mixture of dipeptides except the cases in Fig. 1 where single component systems are studied. The initial adsorbate concentration in finite bath for both dipeptides is about 18 mM. The film mass

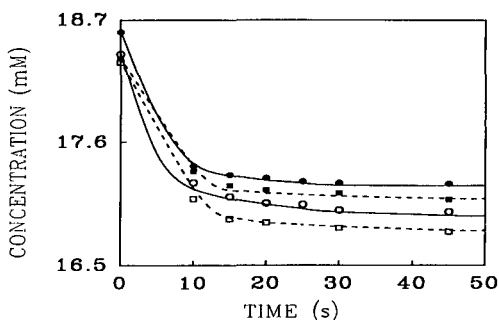


Fig. 1. Comparison between experimental data (symbols) and the finite rate model (dashed lines) to single and binary component batch adsorption systems. Symbols: filled symbols, Cbz-Leu-Gly; open symbols, Cbz-Gly-Phe; ■, □: single component; ●, ○: binary component.

TABLE I  
EXPERIMENTAL CONDITIONS

$V$ (ml)	1.2
pH	3.42
$m$ (mg)	42
Methanol content (%)	55

transfer coefficient was evaluated from correlation [13]. Other conditions used in the experiments are given in Table I unless otherwise indicated in figures or figure captions.

In Fig. 1 the proposed model (*i.e.* intrinsic kinetics model) for the description of the batch dynamic adsorption of dipeptides onto reversed-phase silica gel is fitted to the experimental uptake data. The parameter values for the pore diffusivity and the rate constants, as given in Table II, were obtained from the fitting between the model prediction and experimental data. As shown in this figure, the intrinsic kinetics model yields a reasonable fit. The pore diffusivity and sorption rate constants extracted from these batch experiments have been used to successfully predict the column elution profile [7]. It was also found that the intrinsic kinetics could contribute significantly to the bandspreading. An exact explanation for the slow surface interaction is currently not available. However, this could be due to the high activation energy for interaction between the hydrophobic groups of dipeptides and the immobilised hydrocarbonaceous groups.

The data in Table II suggest that the rate constants and pore diffusivity for the single component

systems are quite close to those for the corresponding binary component system. This seems to indicate that the sorption rate constants and pore diffusivity for a given species is basically not influenced by other species. This feature would facilitate the parameter evaluation. That is to say that batch experiment for single component can be used to obtain the kinetic parameters and pore diffusivity for multicomponent system. However, for the system having an adsorption kinetics other than Langmuir type, the kinetic parameters for single component systems may be different from those for binary mixtures because of the possible existence of lateral interaction between adsorbed solutes. The adsorption behavior of the system in this work is well described by the kinetics and isotherm of Langmuir type, and therefore the interaction between adsorbed solutes is not significant.

Fig. 2 shows the effect of initial solute concentration on the transient uptake of the binary mixture of dipeptide. The experimental data and predicted curves from the intrinsic kinetics model are displayed in this figure. The best fit values of the parameters for various initial solute concentrations are given in Table III. It is seen from this table that the initial solute concentration appears to have no effects on the parameter values. Small difference may be attributed to the experimental error. Therefore, the assumption that the pore diffusivity is independent of solute concentration is justified. Due to the solubility of the dipeptides, experiments with higher initial concentration are not possible.

The transient uptake under different ratio of bath solution volume to sorbent amount ( $V/m$ ) is shown

TABLE II  
PARAMETERS FOR CASES IN FIG. 1

		Intrinsic kinetics			Local equilibrium	Isotherm	
		$D_p \times 10^7$ (cm/s)	$k_a$ (l/s)	$k_d \times 10^2$ (mmol/ml · s)	$D_p \times 10^7$ (cm/s)	$C_{\mu s}$	$b$ (ml/mmol)
Single solute	Leu-Gly	1.18	0.689	3.042	1.020	0.183	22.96
	Gly-Phe	1.69	1.043	2.893	1.351	0.254	36.08
Binary mixture	Leu-Gly	0.995	0.634	2.871	0.992	0.166	22.08
	Gly-Phe	1.48	0.991	2.713	1.415	0.235	36.58

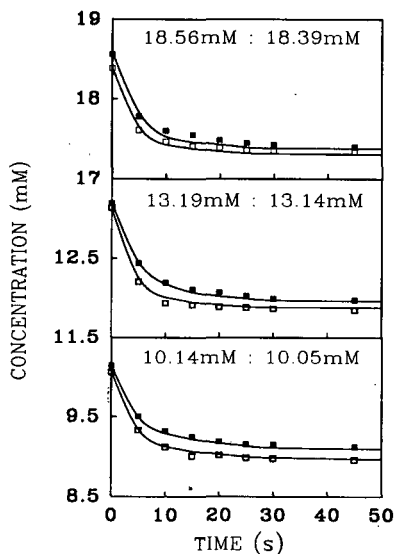


Fig. 2. Effect of initial solute concentrations with fixed concentration ratio Cbz-Leu-Gly/Cbz-Gly-Phe = 1:1. Symbols: ■ = Cbz-Leu-Gly; □ = Cbz-Gly-Phe.

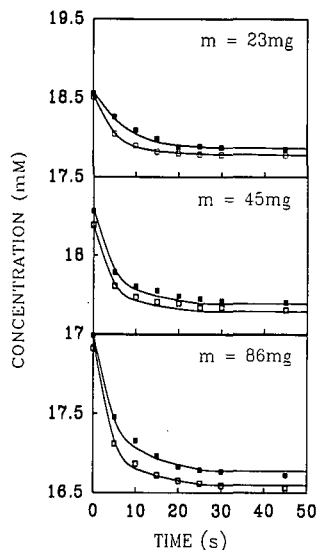


Fig. 3. Effect of ratio  $V/m$  on transient uptake. Symbols as in Fig. 2.

in Fig. 3. The parameter values extracted from these experimental data are given in Table IV. The data in Table IV indicate that the effect of  $V/m$  is negligible.

In order to elucidate the dependence of binding kinetics on the pH and organic modifier content, transient uptake experiments were carried out for a range of pH values and methanol contents. Representative uptake curves are shown in Figs. 4 and 5. For given pH value and methanol content, the adsorption isotherm of the binary mixture was measured experimentally and equilibrium parameters were extracted for the Langmuir isotherm

equation [8]. The batch dynamic data were then fitted using the intrinsic kinetics model proposed in this paper to obtain the parameter estimates for rate constants  $k_a$ ,  $k_d$  and pore diffusivity  $D_p$ .

Generally, the variation of the kinetic parameters due to the change of pH and organic modifier content in solution is not clearly known. Some reasons for this trend could be explained by: (1) the change of physico-chemical properties of solute molecules (*e.g.* net charge, reformation, aggregation change,  $pI$  and polar state), and (2) surface diffusion may be involved in the overall process.

TABLE III  
EFFECT OF INITIAL CONCENTRATION ( $C_b^0$ ) ON PARAMETERS

	Leu-Gly			Gly-Phe		
	$C_b^0$ (mM)			$C_b^0$ (mM)		
	18.56	13.19	10.14	18.39	13.14	10.05
$D_p \times 10^7$ (cm/s)	1.94	1.85	1.75	2.74	2.69	2.65
$k_a$ (1/s)	0.671	0.679	0.681	0.532	0.541	0.543
$k_d \times 10^2$ (mmol/ml · s)	3.86	3.83	3.82	3.22	3.12	3.10

TABLE IV  
EFFECT OF  $V/m$  ON PARAMETERS

	Leu-Gly			Gly-Phe		
	$V/m$ (ml/mg)			$V/m$ (ml/mg)		
	0.052	0.027	0.014	0.052	0.027	0.014
$D_p \times 10^7$ (cm/s)	1.89	1.94	1.98	2.69	2.74	2.81
$k_a$ (l/s)	0.675	0.671	0.671	0.534	0.532	0.531
$k_d \times 10^2$ (mmol/ml·s)	3.89	3.85	3.85	3.20	3.22	3.21

In Figs. 6 and 7, the adsorption rate constant,  $k_a$  and desorption rate constant,  $k_d$  are plotted as a function of pH for the different methanol content. It is noted that  $k_a$  decreases linearly with increasing pH. The predominant effect of increasing pH is to increase the degree of ionisation of dipeptide molecules, and thus the dipeptide molecules carry more associated ions. In such instance, the frequency for the efficient collision between solute molecules and immobilised hydrocarbonaceous groups is reduced. The adsorption rate constant is, therefore, decreased with increasing pH. At a given pH value,  $k_a$  is also decreased with an increase in the methanol content.

This is because the dipeptide molecules are less excluded from the solute at a higher organic solvent content.

The effect of pH and methanol content on the desorption rate constant ( $k_d$ ) is shown in Fig. 7. It can be seen from this figure that  $k_d$  is decreased with increasing pH except the case for Cbz-Gly-Phe at the methanol content of 45%. It is believed that ionised solutes may bind to the hydrocarbonaceous group bound surface with the charges oriented away from the surface. The net charge at low pH value may favour the desorption. As a consequence, the  $k_d$  is higher at lower pH. However, raising the methanol

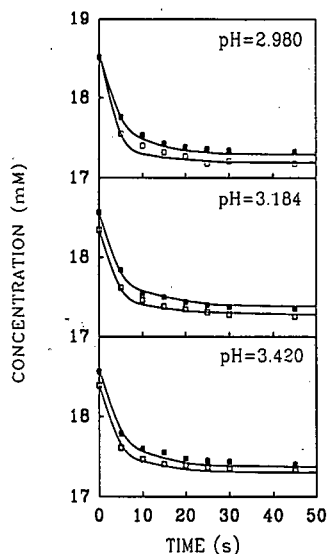


Fig. 4. Effect of pH values on transient uptake. Symbols as in Fig. 2.

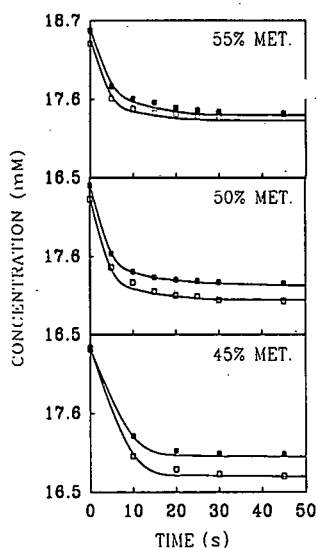


Fig. 5. Effect of methanol (MET.) contents on transient uptake. Symbols as in Fig. 2.

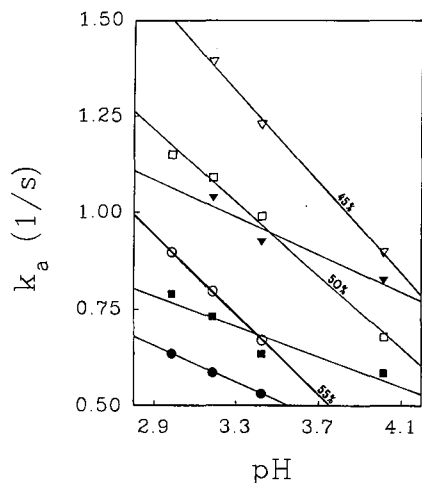


Fig. 6. Adsorption constant *versus* solution pH for various methanol contents (55, 50 and 45%). Symbols:  $\nabla$ ,  $\square$ ,  $\circ$  = Cbz-Gly-Phe;  $\blacktriangledown$ ,  $\blacksquare$ ,  $\bullet$  = Cbz-Leu-Gly.

content enhances the hydrophobicity of the mixed solvent. This effect reduces the energy needed for a solute to desorb from the surface. Therefore, the desorption rate constant is increased with increasing methanol content.

The pore diffusivity ( $D_p$ ) determined from the batch uptake measurement for various pH values and methanol contents are shown in Fig. 8. It is seen that the  $D_p$  linearly decreases with an increase in pH.

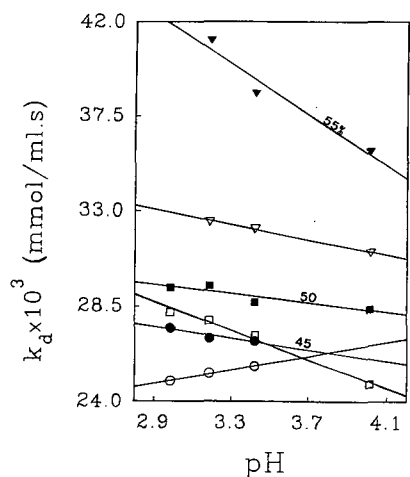


Fig. 7. Desorption rate constant *versus* solution pH for various methanol contents (55, 50 and 45%). Symbols as in Fig. 6.

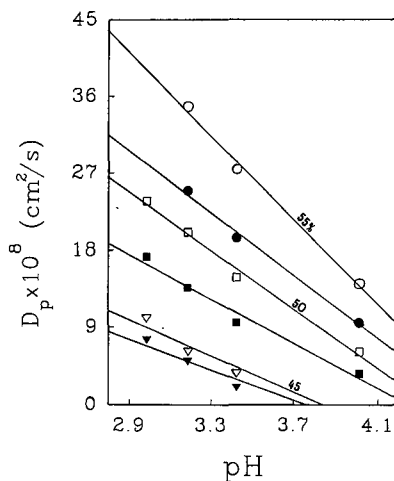


Fig. 8. Diffusivity value *versus* pH for various methanol contents (55, 50 and 45%). Symbols as in Fig. 6.

This observation could be explained again by the ionisation of dipeptide molecule. With the pH increased from 3 to 4, the degree of ionisation of the solutes is enhanced. Thus, more counter-ions are associated with the dipeptide molecules, and this results in a larger resistance for the solute molecules to diffuse in the pore liquid phase. The methanol content also has profound effect on the pore diffusivity. As shown in this figure,  $D_p$  is increased with increasing methanol content. Such variation of  $D_p$  is unlikely resulted from the reduction of the viscosity, since the viscosity only slightly changes in the methanol content range of 45–55% [14]. One of the possible explanations is that the higher methanol content reduces the electrostatic interaction between the solutes and solvent, and consequently the dipeptide molecules have a higher mobility. As already shown, the pore diffusivity is sensitivity to the variation of both pH and methanol content. The implication of this is that when modelling the reversed-phase liquid chromatographic process under any gradient elution mode, the dependence of  $D_p$  on pH and organic modifier content must be taken into account.

## CONCLUSIONS

The batch dynamic adsorption of a binary mix-

ture of dipeptides has been experimentally studied. The results obtained from these experiments were fitted well by the proposed model which is incorporated with an intrinsic adsorption kinetics of Langmuir type. For the system under consideration, the pore diffusivity is independent of solute concentration. It is also found that rate constants ( $k_a$ ,  $k_d$ ) and pore diffusivity ( $D_p$ ) for a multicomponent system can be approximated by those from the corresponding single component systems. These extracted parameters,  $k_a$ ,  $k_d$  and  $D_p$  exhibit a linear dependence on the pH value of the solution and methanol content in the mixed solvent.

#### SYMBOLS

$b$	Langmuir affinity constant
$C$	concentration in pore fluid phase
$C_b$	concentration in bulk fluid of finite bath
$C_b^0$	initial concentration in bulk fluid of finite bath
$C_\mu$	concentration in adsorbed phase
$C_{\mu s}$	sorbent capacity
$D_p$	pore diffusivity
$j$	solute $j$
$k$	solute $k$
$k_a$	adsorption rate constant
$k_d$	desorption rate constant
$k_m$	film mass transfer coefficient
$m$	sorbent mass in finite bath
$NC$	number of solute
$r$	radial coordinate
$R_0$	particle radius
$t$	time
$V$	solution volume in finite bath

#### Greek symbols

$\epsilon_m$	particle porosity
$\rho_p$	particle density

#### ACKNOWLEDGEMENT

Support from Research Excellence Grant Scheme of University of Queensland is gratefully acknowledged.

#### REFERENCES

- 1 B. H. Arve and A. I. Liapis, *AIChE J.*, 33 (1987) 179–193.
- 2 M. A. McCoy and A. I. Liapis, *J. Chromatogr.*, 548 (1991) 25–60.
- 3 W. R. Melander and Cs. Horváth, in Cs. Horváth (Editor), *High-Performance Liquid Chromatography — Advances and Perspectives*, Vol. 2, Academic Press, New York, 1980, p. 113.
- 4 M. T. W. Hearn and M. I. Aguilar, in A. Neuberger and L. L. M. van Deenan (Editors), *Modern Physical Methods in Biochemistry*, Part B, Elsevier, Amsterdam, 1988, p. 107.
- 5 Á. Bartha, J. Ståhlberg and F. Szokoli, *J. Chromatogr.*, 552 (1991) 13–22.
- 6 Cs. Horváth and H.-J. Lin, *J. Chromatogr.*, 149 (1978) 43–70.
- 7 T. S. Nguyen, S.-G. Hu and D. D. Do, *Biochem. J.*, in press.
- 8 T. S. Nguyen, Q. Yu and D. D. Do, *J. Chromatogr.*, submitted for publication.
- 9 J. Villadsen and M. I. Michelsen, *Solution of Differential Equation Models by Polynomial Approximation*, Prentice-Hall, Englewood Cliffs, NJ, 1978.
- 10 L. R. Petzold, *A Description of DASSL: a Differential/Algebraic System Solver*, Sandia Technical Report Sand 81-8637, CA, 1982.
- 11 G. V. Reklaitis, A. Ravindran and K. M. Ragsdell, *Engineering Optimization: Method and Application*, Wiley, New York, 1982.
- 12 G. A. Gabriele and K. M. Ragsdell, *OPLIB: an Optimization Program Library*, Purdue University, West Lafayette, IN, 1979.
- 13 C. J. Geankoplis, *Transport Process and Unit Operations*, Allyn & Bacon, Boston, MA, 1983.
- 14 H. Colin, J. C. Diez-Masa, G. Guiochon, T. Czajkowska and I. Miedziak, *J. Chromatogr.*, 167 (1978) 41–65.

# The $S$ index in the retention equation in reversed-phase high-performance liquid chromatography

Nong Chen, Yukui Zhang and Peichang Lu

National Chromatographic R. & A. Centre, Dalian Institute of Chemical Physics, Chinese Academy of Sciences, 116011 Dalian (China)

(First received July 1st, 1991; revised manuscript received February 11th, 1992)

## ABSTRACT

The empirical retention equation  $\log k' = \log k'_w - S\phi$  in reversed-phase high-performance liquid chromatography (RP-HPLC) was investigated to evaluate the properties of the parameter  $S$ . The  $S$  index, which is defined as the slope of  $\log k'$  versus volume fraction of the organic modifier ( $\phi$ ) was systematically examined as a function of bonded phase density, column type and temperature in RP-HPLC. The  $S$  index for a particular solute was observed to be nearly constant even when column systems with different  $C_{18}$  packing materials are used. The dependence of  $\log k'$  on eluent composition was found to be represented by parallel lines for a given solute for a variety of different stationary phases. The  $S$  index remains constant for a given solute despite the prolonged use of  $C_{18}$  column. The results showed that the  $S$  index is determined mainly by the interaction between the solute and the mobile phase. It was observed to decrease with the increasing column temperature for non-ionic solutes. Other factors influencing the measurement of the  $S$  index are discussed.

## INTRODUCTION

The mechanism governing solute retention in reversed-phase high-performance liquid chromatography (RP-HPLC) is of considerable research interest [1–16]. Most of the proposed models have constructed a retention scheme and the corresponding equilibrium constants. By combining these constants with empirical relationships, equations are obtained for the capacity factors as a function of different variables, of which eluent composition is one of the most important factors in RP-HPLC. At present, the best and most rigorous description of RP-HPLC retention is the solvophobic model developed by Horváth and co-workers [1,2], which has explained many fundamental retention behaviours observed in RP-HPLC.

The stoichiometric displacement model (SDM), which was developed by Geng and Regnier [3,4], is

also important in the development of reversed-phase retention theory. They developed a double logarithmic plot to represent the dependence of retention on solvent composition and this has been widely applied in both RP-HPLC and hydrophobic interaction chromatography (HIC). According to the solubility parameter concept [5,6], a quadratic dependence of the retention on mobile phase composition has been derived and been predicted theoretically [14]. This general equation was found to describe precisely the retention over a wide range of concentrations of the mobile phase.

As the rigorous theoretical study of retention mechanisms is very complicated [12–16], it is more practical to approximate the retention behaviour of a solute by using empirical relationships. In RP-HPLC, the linear approximation of the relationship between the logarithm of capacity factors and the eluent composition has commonly been used and has been found to be fairly reliable in practical RP-HPLC applications [10] (see eqn. 2). However, it must be pointed that deviations from linearity have been observed and not all solvent systems are

Correspondence to: Dr. N. Chen, National Chromatographic R. & A. Centre, Dalian Institute of Chemical Physics, Chinese Academy of Sciences, 116011 Dalian, China.

equally suitable [5,6]. This empirical retention equation has been shown to be strictly valid for methanol–water mobile phase.

The parameter  $S$  in the empirical retention equation plays an important role in computer simulations in RP-HPLC [11]. It has been suggested that  $S$  is a characteristic constant of an organic solvent depending only on the strength of the organic modifier used. It has been found that  $S$  is not invariant with solutes. In several studies,  $S$  tended to increase with increasing solute retention and to be a function of the functional groups in the solute [11].

This paper systematically describes the  $S$  index as a function of bonded phase density, column type and temperature based on the empirical retention equation  $\log k' = \log k'_w - S\varphi$  in RP-HPLC.

#### RETENTION EQUATION TO DESCRIBE THE EFFECT OF ORGANIC MODIFIER CONCENTRATION ON CAPACITY FACTORS IN RP-HPLC

A linear approximation of the retention equation to describe the effect of organic modifier concentration on the logarithm of the capacity factor ( $k'$ ) in RP-HPLC has been widely accepted in practical RP-HPLC and no significant errors in retention prediction have been found. It is expressed as

$$\log k' = \log k'_w - S\varphi \quad (1)$$

where  $\log k'_w$  and  $S$  are constants for a given column system. The  $S$  index is defined as the slope of  $\log k'$  versus volume fraction of organic modifier ( $\varphi$ ). A thermodynamic explanation of  $S$  can be attempted if the free-energy of the interaction between the solute and solvent molecules is taken as a linear function of eluent composition [1,2]. We have used a thermodynamic method in combination with an empirical relationship to derive the retention equation  $\log k' = \log k'_w - S\varphi$ ; the parameters  $\log k'_w$  and  $S$  can be expressed as

$$\log k'_w = \log \beta + (\Delta G_{A,C}^0 - \Delta G_{A,L}^0)/RT \quad (2)$$

$$S = (\Delta G_{A,C}^0 - \Delta G_{A,B}^0)/RT \quad (3)$$

where  $R$  is the gas constant,  $T$  is the absolute temperature,  $\beta$  is phase ratio, the subscripts A, B, C and L refer to solute, strong solvent, weak solvent and hydrocarbonaceous ligands, respectively,  $\Delta G_{A,B}^0$  and  $\Delta G_{A,C}^0$  are the non-electrostatic free-energy

changes for solute–strong solvent and solute–weak solvent, respectively, and  $\Delta G_{A,L}^0$  is the non-electrostatic free-energy change for solute–hydrocarbonaceous ligands. As can be seen,  $S$  is determined mainly by the interactions in the mobile phase. The  $S$  index characterizes the properties of the mobile phase and approaches a constant for a certain solute with different  $C_{18}$  packing materials.

The statistical mechanics theory described by Dill [14] and Lu and Lu [15] also showed that  $S$  was mainly determined by the interaction between the solute and the mobile phase.

#### EXPERIMENTAL

The liquid chromatograph was constructed in our laboratory and consisted of a YSB-2 pump (Shanghai Instrumental Plant, Shanghai, China), a Model 7010 injector (Rheodyne, Cotati, CA, USA), and a Uvidec-100-III UV detector (Jasco, Tokyo, Japan) operating at 254 nm. Reversed-phase packing materials YWG- $C_{18}$  (Tianjin Chemical Reagent Factory, Tianjin, China), ES- $C_{18}$  (ES Industries, Marlton, NJ, USA), Nucleosil- $C_{18}$ , LiChrosorb RP- $C_{18}$ , B4- $C_{18}$  and B8- $C_{18}$  with 5- $\mu$ m particle diameter were employed. B4- $C_{18}$  and B8- $C_{18}$  are laboratory-made silica-based  $C_{18}$  packing materials, prepared from monochlorodimethyloctadecylsilane. Dry silica was suspended with toluene and pyridine and within 1 h the silane agent was added, then the mixture was refluxed for 12 h. The product was washed with acetone, chloroform, acetone and methanol. Energetically homogeneously distributed  $C_{18}$  bonded phases were obtained.

We used six ODS columns (250  $\times$  4.6 mm I.D.) which were packed in our laboratory. A column (200  $\times$  4.0 mm I.D.) containing Polygosil- $C_{18}$  reversed-phase packing material with 5- $\mu$ m particle diameter was also used.

The factors influencing the reproducibility of  $k'$  on a given  $C_{18}$  column were systematically investigated.

Mobile phase mixtures were prepared from individually measured volumes of methanol and deionized water in the range 50–90%. All solutes were of analytical-reagent grade.

The column dead time,  $t_0$ , was determined using sodium nitrite as a non-retained compound. All HPLC measurements were performed at room temperature.

Other experimental results utilized in this work were taken from papers by Petrovic and Lomic [17,18], Smith and Burr [19], Braumann *et al.* [20,21], Engelhardt and co-workers [22,23], Jinno and Kuwajima [24] and Hafkenscheid and Tomlinson [25], which give exact descriptions of the analytical conditions employed.

## RESULTS AND DISCUSSION

As is well known, the variation of  $k'$  for a specific solute over a prolonged period on the  $C_{18}$  column is considerable even under closely controlled chromatographic conditions [19]. Tables I and II compare

TABLE I  
COMPARISON OF LONG-TERM REPRODUCIBILITIES OF  $k'$  AND  $S$  INDEX OVER A 2-YEAR PERIOD WITH METHANOL–WATER AS MOBILE PHASE

Column, Spherisorb  $C_{18}$ ; eluent, methanol–buffer. Data were recalculated from ref. 19.

Com- pound	Methanol concentration (%, v/v)	$k'$			
		Mean	Max.	Min.	S.D. <sup>a</sup>
Phenol	40	2.24	2.80	2.02	0.21
	50	1.26	1.29	1.14	0.10
	60	0.71	0.83	0.75	0.02
	70	0.56	0.57	0.50	0.02
	80	0.34	0.39	0.33	0.02
$S$		2.01	2.07	1.93	0.07
Benzene	40	12.27	13.22	11.38	0.60
	50	6.56	6.99	5.91	0.50
	60	3.55	3.86	3.22	0.15
	70	1.97	2.09	1.75	0.07
	80	1.11	1.21	1.06	0.04
$S$		2.61	2.60	2.59	0.01
Toluene	40	29.83	31.80	27.25	1.07
	50	13.92	16.07	13.32	0.90
	60	7.13	7.81	5.54	0.84
	70	3.24	3.46	2.40	0.28
	80	1.66	1.89	1.56	0.07
$S$		3.14	3.16	3.23	0.05

<sup>a</sup> The standard deviations of the mean of the capacity factors were determined by 20–30 individual measurements at each eluent composition over the 2-year period; the standard deviations of the  $S$  index were determined by only three measurements.

of the reproducibilities of  $k'$  and  $S$  over a 2-year period of extensive use of a  $C_{18}$  column with methanol–water and acetonitrile–water mobile phases. The results illustrate that the prolonged use of the columns does not affect the  $S$  values for a specific solute despite a considerable variation in the retention values for each of the compounds. The reproducibility of the  $S$  index for a given solute within the same laboratory on a certain  $C_{18}$  column is generally of the order of 0.05.

It is generally observed that the retention values differ significantly when column systems with the same mobile phase concentration but with  $C_{18}$  packing materials from different sources or even

TABLE II  
COMPARISON OF LONG-TERM REPRODUCIBILITIES OF  $k'$  AND  $S$  INDEX OVER A 2-YEAR PERIOD WITH ACETONITRILE–WATER AS MOBILE PHASE

Column, Spherisorb  $C_{18}$ ; eluent, acetonitrile–buffer. Data were recalculated from ref. 19.

Com- pound	Acetonitrile concentration (%, v/v)	$k'$			
		Mean	Max.	Min.	S.D. <sup>a</sup>
Phenol	30	2.46	2.48	1.84	0.21
	40	1.51	1.64	1.38	0.07
	50	0.96	1.09	0.84	0.18
	60	0.65	0.68	0.63	0.02
	70	0.44	0.47	0.42	0.01
80	0.31	0.39	0.24	0.05	
$S$		1.79	1.76	1.74	0.03
Benzene	30	13.76	15.38	11.99	1.02
	40	6.90	7.79	6.14	0.57
	50	3.70	4.27	2.98	0.37
	60	2.14	2.28	2.03	0.10
	70	1.31	1.40	1.29	0.05
80	0.84	0.95	0.74	0.06	
$S$		2.42	2.44	2.36	0.04
Toluene	30	29.75	31.98	25.27	2.19
	40	12.78	14.37	11.31	1.20
	50	6.12	7.01	4.94	0.59
	60	3.18	3.41	3.01	0.15
	70	1.87	1.98	1.73	0.08
80	1.17	1.26	1.09	0.09	
$S$		2.83	2.83	2.71	0.07

<sup>a</sup> See Table I.

TABLE III  
S VALUES OF EIGHTEEN COMPOUNDS AS A FUNCTION OF THE SURFACE COVERAGE WITH METHANOL-WATER AS MOBILE PHASE

Column, LiChrosorb C<sub>18</sub>; eluent, methanol-water (methanol from 10 to 100%, v/v). Data were recalculated from refs. 17 and 18.

Compound	Coverage (mmol/g)				Mean ± S.D.
	0.255	0.335	0.499	0.690	
Pentane	3.70	3.79	3.67	3.74	3.73 ± 0.05
Hexane	4.30	4.35	4.28	4.26	4.30 ± 0.04
Heptane	4.90	4.92	4.82	4.82	4.87 ± 0.05
Octane	5.47	5.49	5.41	5.43	5.45 ± 0.04
Nonane	6.05	6.08	6.01	6.06	6.05 ± 0.03
Decane	6.66	6.74	6.62	6.62	6.66 ± 0.06
Benzene	2.67	2.64	2.72	2.74	2.69 ± 0.05
Toluene	3.23	3.25	3.23	3.28	3.25 ± 0.03
Ethylbenzene	3.91	3.90	3.92	3.86	3.90 ± 0.03
<i>n</i> -Propylbenzene	4.52	4.54	4.54	4.41	4.50 ± 0.06
<i>n</i> -Butylbenzene	5.07	5.08	5.03	4.87	5.01 ± 0.10
<i>n</i> -Pentylbenzene	5.62	5.69	5.55	5.37	5.56 ± 0.14
<i>n</i> -Hexylbenzene	6.21	6.26	6.14	6.06	6.17 ± 0.09
1-Butanol	1.84	1.94	1.93	1.89	1.90 ± 0.05
1-Pentanol	2.34	2.47	2.47	2.41	2.42 ± 0.06
1-Hexanol	2.92	2.95	2.96	2.93	2.94 ± 0.02
1-Heptanol	3.40	3.50	3.49	3.45	3.46 ± 0.05
1-Octanol	3.93	4.00	4.01	3.98	3.98 ± 0.04
Acetophenone	2.63	2.66	2.77	2.73	2.70 ± 0.06
<i>o</i> -Cresol	2.68	2.78	2.81	2.72	2.75 ± 0.06
Benzyl alcohol	2.27	2.36	2.31	2.33	2.32 ± 0.04
Phenol	2.29	2.31	2.25	2.30	2.29 ± 0.03
Aniline	2.10	2.14	2.11	2.18	2.13 ± 0.04

from the same source but different batches are used. This causes difficulties in using retention data from the literature. It has been observed that the *S* index can eliminate the difference between C<sub>18</sub> packing materials and can act as an important parameter for the standardization of different C<sub>18</sub> packing materials.

Table III gives the *S* values of some compounds on different C<sub>18</sub> packing materials with surface coverages ranging from 0.255 to 0.690 mmol/g with methanol-water as mobile phase. Although a considerable variation in *k'* on the different C<sub>18</sub> bonded phases was observed, the *S* index remains a characteristic constant for a given compound. *S* is independent of the bonded phase density for the solutes

tested. The standard deviations of the *S* index for a specific solute are about 0.05.

The *S* index for a particular solute can make the standardization of different C<sub>18</sub> packing materials possible. The difference between different C<sub>18</sub> bonded phases can be compensated for by using the *S* index, and therefore the retention data with different compositions of the mobile phase on different C<sub>18</sub> packings can be standardized. As *S* value that characterizes the interactions in the mobile phase for a certain solute is independent of different C<sub>18</sub> packing materials with the same mobile phase, which makes it possible to transfer *k'* values from one packing material to another with different compositions of the mobile phase with only one isocratic experiment from which the difference in log *k'*<sub>w</sub> for two kinds of C<sub>18</sub> packing materials can be determined [26]. Therefore, this will allow us to transfer separation results from one C<sub>18</sub> column to another. Details will be given elsewhere.

Tables IV and V give other examples of the *S* index as a function of different column systems with different reversed-phase packing materials.

It can be seen that although *k'* measured with a certain mobile phase composition on different C<sub>18</sub> packing materials varies considerably, the *S* value for a given solute is not affected by the packing material used and reflects the properties of the solute. It is nearly constant even when column systems with different C<sub>18</sub> packing materials are used, which means that the dependence of log *k'* on eluent composition results in parallel lines for a given solute on different reversed-phase packing materials. This parallel behaviour has been observed in many other studies.

Czok and Engelhardt [22] used four constants, *A*, *B*, *C* and *D*, to describe the retention of homologous series in RP-HPLC:

$$\ln k' = A + Bn + CX + DnX \quad (4)$$

where *X* is the concentration of methanol in the mobile phase and *n* is the chain length of a homologous series. Our interest is in the values of *C* and *D*, where *C* shows the change in log *k'* with increasing water content for the basis of the homologous series with *n* = 0. They found that for all reversed-phase packings *C* has about the same values with an average of 5.5 with a relative standard deviation of 6%. Parameter *D* shows the variation of methylene

TABLE IV

EFFECT OF DIFFERENT C<sub>18</sub> PACKING MATERIALS ON S INDEX WITH METHANOL-WATER AS MOBILE PHASE

For experimental conditions, see text. Eluent, methanol-water (methanol from 60 to 90%, v/v).

Compound	C <sub>18</sub> packing <sup>a</sup>						Mean ± S.D. <sup>1</sup>
	1	2	3	4	5	6	
Benzene	2.74	2.68	2.74	2.84	2.81	2.73	2.76 ± 0.06
Toluene	—	—	—	—	3.32	3.24	3.28 ± 0.06
Naphthalene	3.60	3.57	3.70	3.70	3.83	3.69	3.73 ± 0.09
Biphenyl	4.24	4.20	4.36	4.35	4.49	4.30	4.32 ± 0.10
Phenanthrene	4.44	4.43	4.40	4.46	4.69	4.55	4.50 ± 0.11
Anthracene	4.54	4.61	4.49	—	—	—	4.55 ± 0.06
Chrysene	5.24	5.20	5.28	—	—	—	5.24 ± 0.04
p-Terphenyl	5.73	5.68	5.71	—	—	—	5.71 ± 0.03
Anisole	2.74	2.69	2.79	2.85	2.88	2.72	2.78 ± 0.08
Benzyl alcohol	2.11	2.01	2.08	2.18	—	—	2.10 ± 0.07
Benzophenone	2.39	2.29	2.38	—	—	—	2.35 ± 0.06
p-Nitrotoluene	3.05	3.03	3.10	—	—	—	3.06 ± 0.04
n-Butyl benzoate	4.16	4.11	4.20	—	—	—	4.16 ± 0.05

<sup>a</sup> 1 = YWG-C<sub>18</sub>; 2 = ES-C<sub>18</sub>; 3 = Nucleosil-C<sub>18</sub>; 4 = LiChrosorb RP-C<sub>18</sub>; 5 = B4-C<sub>18</sub>; 6 = B8-C<sub>18</sub>.

selectivity with solvent composition, and they found that *D* is also largely constant for all of the packing materials investigated, its average values being 0.88 with a relative standard deviation of 9%.

As *C* and *D* determine the values of *S*, *S* therefore remains constant for all the packings for a specific

solute, and all the stationary phases exhibit parallel behaviour.

In ref. 23, Fig. 6 illustrated the variation of the retention of ethylbenzene with the concentration of water on different alkyl-bonded phases with chain lengths ranging from methyl to octadecyl, and

TABLE V

EFFECT OF DIFFERENT REVERSED-PHASE PACKING MATERIALS ON S INDEX WITH METHANOL-WATER AS MOBILE PHASE

Data are from ref. 20. Eluent, methanol-water (methanol from 00 to 00%, v/v).

corrected to 35

(methanol from 61 to 83% v/v)

Compound	C <sub>18</sub> packing <sup>a</sup>						Mean ± S.D. <sup>1</sup>
	1	2	3	4	5	6	
Toluene	3.41	3.36	3.72	3.49	3.38	3.34	2.45 ± 0.14 → 3.45 ± 0.14
Chlorobenzene	3.52	3.48	3.82	3.62	3.52	3.44	3.57 ± 0.14
Fluorobenzene	3.21	3.20	3.37	3.19	3.19	3.16	3.22 ± 0.08
Benzene	2.97	2.97	3.12	3.07	2.97	2.92	3.00 ± 0.08
Nitrobenzene	2.88	2.85	4.04	2.88	2.99	2.80	2.91 ± 0.09
Benzyl alcohol	2.53	2.57	2.52	3.04	2.53	2.48	2.53 ± 0.03
Phenol	2.55	2.54	2.66	2.55	2.55	2.50	2.56 ± 0.05

<sup>a</sup> 1 = LiChrosorb RP-C<sub>18</sub>; 2 = LiChrosorb RP-C<sub>18</sub>; 3 = LiChrosorb RP-Select B-5; 4 = Kieselgel 60 C<sub>18</sub>; 5 = Biosil-55 RP-18; 6 = Polygosil 60 RP-18.

showed an identical dependence of  $\log k'$  on the eluent concentration [23]. The almost exactly parallel lines on the plot of  $\ln k'$  vs.  $\phi$  demonstrated that the  $S$  index for a specific compound is nearly constant. As an example, for toluene in Fig. 6 in ref. 23  $S = 6.4$  for RP-8 and  $S = 6.6$  for RP-18 and for ethylbenzene  $S = 7.3$  and  $7.5$ , respectively. Braumann [24] also observed this parallel retention behaviour for benzene on six alkyl-bonded packing materials, which demonstrates that  $S$  reflects the property of a given solute for a certain binary mobile phase.

All the results showed that the  $S$  index was determined mainly by the interaction between the solute and the mobile phase. The  $S$  index for a specific solute obtained with the same LC system shows little deviation, but it may diverge slightly from laboratory to laboratory. We compared the  $S$  values given in numerous publications for a similar concentration range of methanol in water for a specific compound. The average standard deviation of the mean  $S$  values is about 0.15.

Factors influencing the  $S$  values may mainly include the homogeneity of the bonded stationary phases, the linearity of the relationship between  $\log k'$  and  $\phi$ , the column temperature and solute structure parameters. The solute structure parameters are one of the most important variables in determining  $S$  values, which will be discussed elsewhere.

The homogeneity of the bonded phases affects the linearity of the  $\log k'$  versus  $\phi$  relationship, which therefore leads to a change in  $S$  values [16,27]. If solute retention is governed by a hydrophobic mechanism, the reproducibility of  $S$  values for a particular solute can be achieved in a given eluent system by using energetically homogeneously distributed bonded phases. The reproducibility of the  $S$  index for a particular solute can serve as a useful parameter for comparison of the energetic homogeneity between different  $C_{18}$  bonded phases. When a compound is extreme polar or ionizable in an aqueous mobile phase, a parabolic shape of the  $\log k'$  versus  $\phi$  plot has been observed [27] and demonstrated different retention mechanisms over the whole concentration range of the mobile phase. This implies an inhomogeneous character of the stationary phase (silanophilic interaction) and of the molecular solute itself (ionic interaction), which means that  $S$  values are difficult to ascertain for these

TABLE VI

EFFECT OF BUFFER ON  $S$  VALUES FOR SOME AROMATIC COMPOUNDS

Column, Hypersil-ODS; eluent, methanol–water. Data are from ref. 25.

Compound	$S^a$	$S^b$
Benzene	2.79	2.77
Chlorobenzene	3.46	3.46
Phenol	2.66	2.59
Benzoic acid	—	3.27
4-Chlorobenzoic acid	—	3.86
4-Chlorotoluene	3.98	3.99
1,4-Dinitrobenzene	2.87	2.80
2-Hydroxypropane	1.37	1.35
2-Nitropropane	1.98	1.94
2-Chloropropane	2.70	2.78

<sup>a</sup> Methanol–water.<sup>b</sup> Methanol–phosphate buffer (pH 2.15).

compounds. Therefore, during the practical separation of ionizable compounds, suppression agents or buffers should be added to the mobile phase to suppress the ionization of these compounds in order to enhance solute–hydrocarbonaceous ligand hydrophobic interactions, and therefore the pH should be strictly controlled when determining  $S$  values for these compounds. The presence of buffer in the mobile phase does not affect the  $S$  values for non-electrolytes, as shown in Table VI.

Temperature plays an important role in RP-HPLC separations. The column temperature should be carefully controlled when determining  $S$  values [24,28,29]. A detailed study of the  $S$  index as a function of column temperature for some non-ionic compounds is summarized in Tables VII and VIII. In the temperature range investigated the  $S$  values were observed to decrease with increasing column temperature, which can be clearly explained by eqn. 3. As the difference in the solute–weak solvent and solute–strong solvent free energy change characterizes the solute interactions in the mobile phase and approaches a constant value for a particular solute with different column temperatures, the value of  $ST$  approaches a constant value for non-ionic compounds, as is demonstrated by the following equation:

$$\Delta G_{A,C}^0 - \Delta G_{A,B}^0 = S_1 T_1 = S_2 T_2 = S_3 T_3 \quad (5)$$

TABLE VII

EFFECT OF COLUMN TEMPERATURE ON *S* INDEX FOR SOME POLYCYCLIC AROMATICS WITH METHANOL-WATER AS MOBILE PHASEColumn, Finepak-SIL-C<sub>18</sub>; eluent, methanol-water (methanol from 65 to 80%, v/v). Data were recalculated from ref. 24.

Compound	Column temperature (°C)							
	70		60		50		40	
	<i>S</i>	<i>ST</i>	<i>S</i>	<i>ST</i>	<i>S</i>	<i>ST</i>	<i>S</i>	<i>ST</i>
Naphthalene	2.46	844	2.49	829	2.78	898	2.78	870
Acenaphthylene	2.70	926	2.70	899	3.00	969	3.09	967
Phenanthrene	3.26	1118	3.31	1102	3.68	1189	3.57	1117
Anthracene	3.36	1152	3.43	1142	3.81	1231	3.93	1230
Fluoranthene	3.71	1273	3.60	1199	4.03	1302	4.15	1299
Benzo[ <i>a</i> ]pyrene	4.42	1516	4.40	1465	4.90	1583	5.01	1568

where  $S_1$ ,  $S_2$  and  $S_3$  are *S* values at temperatures  $T_1$ ,  $T_2$  and  $T_3$ , respectively. Therefore, the *S* values decrease with increasing column temperature in order to keep *ST* almost constant for a particular solute, which means that there is a larger solute-water than solute-methanol free-energy change, as it can be seen in Tables VII and VIII.

Tables VII and VIII illustrate the effect of temperature on the *S* index for polycyclic aromatic hydrocarbons and some non-ionic compounds in methanol-water as mobile phase. The values of *ST* for

each compound at different temperatures are also given.

Table IX demonstrates the effect of dead time measurements on the *S* index. As can be seen, the effect of dead time measurements using methanol and sodium nitrite on the *S* index is not obvious, at least for the solutes tested in this experiment.

We conclude that the *S* index is mainly determined by the difference between solute-weak solvent and solute-strong solvent free-energy changes. *S* values are nearly constant even when column

TABLE VIII

EFFECT OF COLUMN TEMPERATURE ON *S* INDEX FOR SOME NON-IONIC COMPOUNDSColumn, C<sub>8</sub>; eluent, methanol-water (methanol from 50 to 70%, v/v). Data are calculated from refs. 28 and 29.

Compound	Column temperature (°C)							
	30		41		51		59.5	
	<i>S</i>	<i>ST</i>	<i>S</i>	<i>ST</i>	<i>S</i>	<i>ST</i>	<i>S</i>	<i>ST</i>
<i>p</i> -Nitrophenol	2.73	827	—	—	2.36	765	2.26	752
Phenol	2.57	779	2.30	722	2.23	723	2.09	695
Acetophenone	2.93	888	2.66	835	2.51	813	2.38	791
Methyl benzoate	3.28	994	3.07	964	2.85	923	2.83	941
Anisole	2.97	900	2.74	860	2.60	842	—	—
Benzene	2.88	873	2.63	826	2.55	826	2.43	808
Phenetole	3.39	1027	3.18	999	3.03	982	2.97	988
Toluene	3.35	1015	3.09	970	2.98	966	2.98	991
Ethylbenzene	3.80	873	3.59	826	3.46	826	3.30	808

corrected 7/10/35

TABLE IX  
EFFECT OF DEAD TIME MEASUREMENTS ON S INDEX

Column, Polygosil-C<sub>18</sub>; eluent, methanol-water. Dead times were measured using sodium nitrite and methanol as a non-retained compound. For experimental conditions, see text.

Compound	Non-retained compound	Methanol concentration (% v/v)			S
		90	0.90 80	0.70	
Nitrobenzene	Methanol	0.35	0.64	1.26	2.75
	Sodium nitrite	0.29	0.55	1.08	2.84
Naphthalene	Methanol	0.81	1.80	4.55	3.75
	Sodium nitrite	0.73	1.64	4.12	3.77
Toluene	Methanol	0.61	1.25	2.77	3.29
	Sodium nitrite	0.54	1.12	2.48	3.33
Acenaphthene	Methanol	1.47	3.64	10.33	4.23
	Sodium nitrite	1.36	3.37	9.47	4.21

Handwritten note: Sodium nitrite is not a retained compound. Methanol

systems with different packing materials are used. S varies with the strong solvent used, and hence it represents the solvent strength to the eluent only for a specific solute. A more detailed examination of S values as a function of molecular structure parameters will be discussed in a further paper.

REFERENCES

- 1 Cs. Horváth, W. Melander and I. Molnar, *J. Chromatogr.*, 125 (1976) 129.
- 2 A. Nahum and Cs. Horváth, *J. Chromatogr.*, 203 (1981) 53.
- 3 X. Geng and F. E. Regnier, *J. Chromatogr.*, 296 (1984) 15.
- 4 X. Geng and F. E. Regnier, *J. Chromatogr.*, 332 (1985) 147.

- 5 P. J. Schoenmakers, H. A. H. Billiet, R. Tijssen and L. de Galan, *J. Chromatogr.*, 149 (1978) 518.
- 6 P. J. Schoenmakers, H. A. H. Billiet and L. de Galan, *J. Chromatogr.*, 282 (1983) 107.
- 7 B. L. Karger, *J. Chromatogr.*, 128 (1976) 65.
- 8 L. R. Snyder, J. W. Dolan and J. R. Gant, *J. Chromatogr.*, 165 (1979) 3.
- 9 J. W. Dolan, J. R. Gant and L. R. Snyder, *J. Chromatogr.*, 165 (1979) 31.
- 10 L. R. Snyder and M. A. Quarry, *J. Liq. Chromatogr.*, 10 (1987) 1789.
- 11 L. R. Snyder, M. A. Quarry and J. L. Glajch, *Chromatographia*, 24 (1987) 33.
- 12 D. E. Martire and R. E. Boehm, *J. Phys. Chem.*, 87 (1983) 1045.
- 13 J. G. Dorsey and K. A. Dill, *Chem. Rev.*, 89 (1989) 331.
- 14 K. A. Dill, *J. Phys. Chem.*, 91 (1987) 1980.
- 15 P. Lu and X. Lu, *J. Chromatogr.*, 292 (1984) 169.
- 16 N. Tanaka, H. Goodell and B. L. Karger, *J. Chromatogr.*, 158 (1978) 233.
- 17 S. M. Petrovic and S. M. Lomic, *Chromatographia*, 27 (1989) 378.
- 18 S. M. Petrovic and S. M. Lomic, *J. Liq. Chromatogr.*, 12 (1989) 59.
- 19 R. M. Smith and C. M. Burr, *J. Chromatogr.*, 475 (1989) 75.
- 20 Th. Braumann, H. G. Genieser and D. Luumann, *Chromatographia*, 24 (1987) 777.
- 21 Th. Braumann, *J. Chromatogr.*, 373 (1986) 191.
- 22 M. Czok and H. Engelhardt, *Chromatographia*, 27 (1989) 5.
- 23 H. Engelhardt and M. Jangheim, *Chromatographia*, 29 (1990) 59.
- 24 K. Jinno and M. Kuwajima, *Chromatographia*, 22 (1986) 13.
- 25 T. L. Hafkenscheid and C. Tomlinson, *J. Chromatogr.*, 218 (1981) 409.
- 26 N. Chen, Y. Zhang and P. Lu, *Chin. J. Chromatogr.*, 6 (1988) 325.
- 27 N. El Tayar, N. van de Waterbeemd and B. Testa, *J. Chromatogr.*, 320 (1985) 293.
- 28 J. R. Gant, J. W. Dolan and L. R. Snyder, *J. Chromatogr.*, 185 (1979) 153.
- 29 J. W. Dolan, D. C. Lommen and L. R. Snyder, *J. Chromatogr.*, 535 (1990) 55.

# Dispersion in stacked-membrane chromatography

Douglas D. Frey, Robert Van de Water and Beibing Zhang

*Department of Chemical Engineering, Yale University, New Haven, CT 06520 (USA)*

(First received December 4th, 1990; revised manuscript received February 25th, 1992)

## ABSTRACT

A study was conducted of the separation efficiency of a chromatography column consisting of layers of porous polyvinyl chloride membranes incorporating submicron silica particles. It was determined that dispersion inside the membrane was the dominant band-broadening mechanism under most conditions. Experimental data are discussed and compared with previous work.

## INTRODUCTION

Conventional chromatography columns containing porous particles suffer from several deficiencies which hamper their large-scale use. Chief among these is the fact that high mass-transfer efficiencies are most readily achieved through the use of small particles, which in turn leads to high operating pressures and large capital costs. To circumvent this difficulty, a variety of novel chromatographic processes have been considered in which high efficiencies and low operating pressures are potentially achieved. Examples include aligned-fiber columns [1], columns employing bundles of hollow fibers [2,3], and columns composed of layers of flat porous membranes [4–6].

The purpose of this study was to investigate the separation efficiency of a commercial stacked-membrane chromatography column. Several previous investigations have demonstrated the usefulness of these columns for biomolecule separations. In particular, Piotrowski and Scholla [4] have shown that stacked-membrane columns incorporating submicron silica particles can attain adsorption capacities in the range required for preparative chromatography. However, previous investigations of these

columns have not included systematic measurements of column efficiency.

## EXPERIMENTAL

Fig. 1 illustrates the construction of the stacked-membrane columns used in this study. The columns were provided by Kontes Life Science Products and

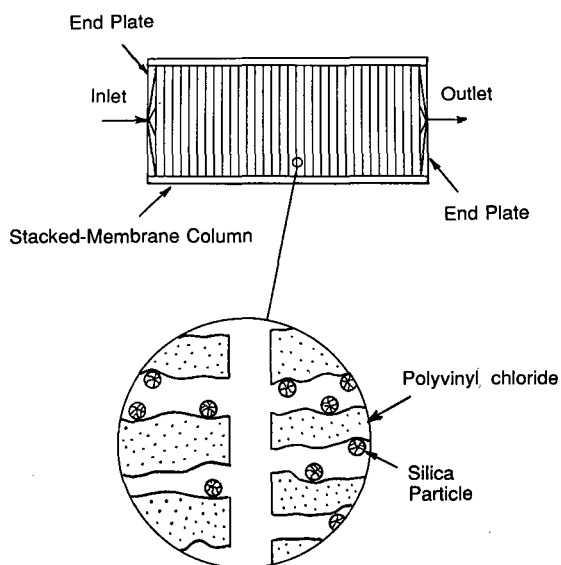


Fig. 1. Construction of a stacked-membrane chromatography column.

*Correspondence to:* Dr. D. D. Frey, Department of Chemical Engineering, Yale University, New Haven, CT 06520, USA.

consisted of layers of polyvinyl chloride membranes (MPS Microporous Sheets, FMC) having a thickness of 600  $\mu\text{m}$  and a diameter of 2.5 cm. The majority of the adsorption capacity of the column is provided by submicron silica particles embedded in the membrane. For the columns used in this study, the silica particles and polyvinyl chloride membranes were coated with polyethyleneimine such that the columns could be used for anion-exchange chromatography. Columns having lengths of 1 and 5 cm were employed. The columns were housed in a plastic cylinder and were connected to PTFE tubing using "high-resolution" end plates supplied by the column manufacturer.

Standard laboratory procedures and chromatographic equipment were used to evaluate the columns. The solvent used in all the experiments was 50 mM phosphate buffer, pH 7, which had been passed through a 0.45- $\mu\text{m}$  nylon filter. The tubing used was 1/16 in. (0.16 cm) O.D. and was composed of PTFE. A solvent pump (Model RP-SY with a Model RH1CKC pump head, Fluid Metering) and pulse dampener (Model PD-60-LF, Fluid Metering) were used to deliver the solvent to the column. Feed slugs were injected into the membrane column using a six-port sample injection valve (Model 7010, Rheodyne). The effluent from the column passed through a variable-wavelength UV detector (Model LC-85, Perkin Elmer) which was set to either 210 or 254 nm. The signal from the detector was stored and processed on an AT-class microcomputer using an IBM data acquisition and control adapter board.

The first absolute ( $\mu_1$ ) and second central ( $\mu_2$ ) moments of the effluent concentration profiles were determined by numerical integration as follows:

$$\mu_1 = \frac{\sum_{i=1}^n t_i C(t_i)}{\sum_{i=1}^n C(t_i)} \quad (1)$$

$$\mu_2 = \frac{\sum_{i=1}^n (t_i - \mu_1)^2 C(t_i)}{\sum_{i=1}^n C(t_i)} \quad (2)$$

where  $C(t_i)$  denotes the solute concentration in the effluent for data point  $i$  and  $n$  is the total number of data points.

## THEORY

For a membrane column incorporating silica particles, the second central moment of the effluent concentration profile which results from the injection of a feed slug of width  $t_{\text{feed}}$ , is given by eqn. 3 [7]:

$$\mu_{2,\text{total}} = \mu_{2,\text{dispersion}} + \mu_{2,\text{extra}} + \mu_{2,\text{fluid}} + \mu_{2,\text{particle}} + t_{\text{feed}}^2/12 \quad (3)$$

The terms  $\mu_{2,\text{dispersion}}$ ,  $\mu_{2,\text{extra}}$ ,  $\mu_{2,\text{fluid}}$ , and  $\mu_{2,\text{particle}}$  in eqn. 3 account, respectively, for band broadening from fluid velocity variations in the column, extra-column effects, mass transfer from the mobile liquid filling the membrane pores to the silica particles, and diffusion in the pores of the silica particles. Eqn. 3 ignores the kinetics for surface adsorption and axial molecular diffusion since they are both negligible compared to other mechanisms for band spreading in ion-exchange chromatography. Each term on the right side of eqn. 3 can be divided by the square of the average retention time (*i.e.*,  $\mu_1^2$ ) and multiplied by the column length to yield the corresponding plate height increment. The total plate height ( $H$ ) resulting from the broadening mechanisms inside the column is therefore given by:

$$H = H_{\text{fluid}} + H_{\text{particle}} + H_{\text{dispersion}} \quad (4)$$

If the entire adsorption capacity of the column results from adsorption in the silica particles, then the equations describing band broadening for chromatography [7] lead to the following expressions for  $H_{\text{particle}}$  and  $H_{\text{fluid}}$ :

$$H_{\text{particle}} = \frac{d_p^2 \tau (1 - \alpha) v}{30 D \epsilon \alpha} \frac{\lambda^2}{(1 + \lambda)^2} \quad (5)$$

$$H_{\text{fluid}} = \frac{2 v}{k_1 a} \frac{\lambda^2}{(1 + \lambda)^2} \quad (6)$$

where  $d_p$  is the average diameter of the silica particles,  $k_1$  is the coefficient for mass transfer between the liquid in the membrane pores and the silica particles,  $a$  is the corresponding area per unit volume, and  $\lambda$  is the ratio of the amount of adsorbate within the exterior surface of the silica particles to the amount of adsorbate in the membrane pores per unit volume of bed. The quantity  $\lambda$  is therefore given by

$$\lambda = k' \left( \frac{\alpha + \epsilon \sigma}{\alpha} \right) + \frac{\epsilon \sigma}{\alpha} \quad (7)$$

where  $\alpha$  is the volume fraction of mobile fluid in the membrane,  $\sigma$  is the volume fraction of silica particles in the column, and  $\varepsilon$  is the void fraction in the silica particles. The equilibrium parameter  $k'$  in eqn. 7 is defined as

$$k' \equiv \frac{t_R - t_0}{t_0} = K_{eq} \frac{\sigma(1 - \varepsilon)}{\alpha + \varepsilon\sigma} \quad (8)$$

where  $t_R$  is the retention time of the solute in the column,  $t_0$  is the retention time of a solute which has access to the entire pore network but which does not interact with the sorbent surface, and  $K_{eq}$  is the adsorption equilibrium constant defined as the amount of adsorbed solute per unit volume of silica divided by the solute concentration in the bulk solution at equilibrium. The retention time in the column is related to the superficial velocity ( $v_s$ ) by the relation:

$$t_R = (\alpha + \varepsilon\sigma)(1 + k')L/v_s \quad (9)$$

## RESULTS AND DISCUSSION

Scanning electron microphotographs of the membranes used in this study indicated that the membrane pores are highly tortuous and have a wide size distribution. The majority of the pores appeared to have diameters between 1.0 and 5.0  $\mu\text{m}$ . The pore size which would yield a solute velocity equal to the average solute velocity in the membrane can be determined from the membrane permeability using the Hagen–Poiseuille law as follows [8]:

$$d_{\text{pore}} = \sqrt{\frac{32BT}{\alpha}} \quad (10)$$

In eqn. 10,  $B$  is the Darcy's law permeability given by the quantity  $v_s \mu L / \Delta P$  and  $T$  is the average length of the flow path in the membrane divided by the membrane thickness. In order to use eqn. 10, an approximation for  $T$  is required. According to Dullien [9], a volume-average pore diameter for a bed of unconsolidated spheres can be estimated by equating the pore area per unit total volume for a medium containing cylindrical pores to the same ratio for a bed of spherical particles, *i.e.*,  $4\alpha/d_{\text{pore}} = 6(1 - \alpha)/d_p$  where  $d_p$  is the diameter of a spherical particle. If this relation is used to eliminate  $d_{\text{pore}}$  and introduce  $d_p$  into eqn. 10, then that equation becomes equivalent to the Karmen–Kozeny equation

[10] if  $T = 2.1$ , which will be the value for  $T$  assumed here. The Darcy's law permeability of the membrane columns was measured to be  $8.3 \cdot 10^{-10} \text{ cm}^2$ . The void fraction was measured to be 0.60 by weighing a column when it was full of buffer and weighing it again after complete drying in a desiccator. A similar value for the void fraction was obtained using eqn. 9 and measuring the retention time for urea, which is presumably unadsorbed under the conditions used. In both determinations the product  $\varepsilon\sigma$  was assumed small compared to  $\alpha$ . From these measurements it follows from eqn. 10 that  $d_{\text{pore}} = 3.0 \mu\text{m}$ .

If properties characteristic of the membranes used in this study are substituted into eqns. 4–8 (*e.g.*,  $d_{\text{pore}} = 3 \cdot 10^{-4} \text{ cm}$ ,  $\tau = 10$ ,  $d_p = 5 \cdot 10^{-4} \text{ cm}$ ,  $\alpha = 0.60$ ,  $\sigma = 0.2$ ,  $\varepsilon = 0.4$ ) and if the mass-transfer correlation of Wilson and Geankoplis [11] is employed to predict  $k_1$  [*i.e.*,  $k_1 = 0.83 D^{2/3} v^{1/3} (1 - \alpha)^{-2/3} d_{\text{pore}}^{-2/3}$  and  $a = 6 \sigma d_p^{-1}$ ], the resulting values of  $H_{\text{fluid}}$  and  $H_{\text{particle}}$  for strongly adsorbed solutes ( $k' > 1$ ) are at least two orders of magnitude smaller than the experimentally observed second central moment. For this reason, this section considers the evaluation of the term  $H_{\text{dispersion}}$  in eqn. 4, which largely determines the overall column efficiency. In order to investigate  $H_{\text{dispersion}}$  as accurately as possible, experimental conditions were chosen so that very little adsorption occurred, *i.e.*,  $k' \ll 1$ . In particular, the basic protein cytochrome *c* and the amino acid tryptophan were used together with a 50 mM phosphate buffer at pH 7. Under these conditions  $k'$  was 0.1 for the former solute and 0.2 for the latter solute while  $H_{\text{fluid}}$  and  $H_{\text{particle}}$  as determined by eqns. 4–8 were in both cases at least three orders of magnitude smaller than the experimentally observed second central moment.

Fig. 2 shows measurements of extra-column band broadening at several flow-rates. These experiments were performed by removing the column from the end plates and replacing it with a thin, solid PTFE disk with the same diameter as the column and with 24 holes drilled through it around the periphery. The response to an injection of benzoic acid was then measured and the value  $t_{\text{feed}}^2/12$  was subtracted from the result. As shown in Fig. 2,  $\mu_{2,\text{extra}}$  is a linear function of  $v_s^{-2}$  which implies that when a column is inserted between the end plates,  $H_{\text{extra}}$  will be independent of  $v_s$ .

Plate height measurements for tryptophan and

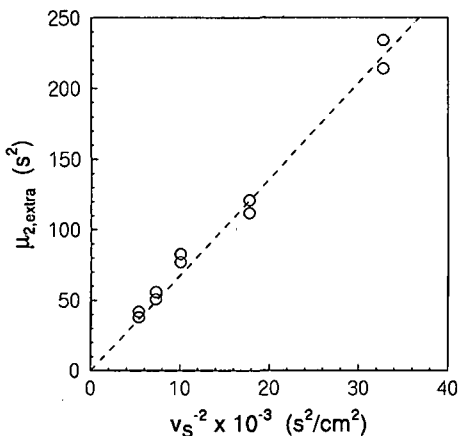


Fig. 2. Extra-column band broadening measured by replacing membrane column with thin insert.

cytochrome *c* for both 1- and 5-cm columns are shown in Fig. 3. The plate height in Fig. 3 was determined by subtracting from the experimentally measured second central moment the sum of  $t_{f,ced}^2/12$  and  $\mu_{2,extra}$  from Fig. 2, multiplying that difference by the ratio of the column length to the square of the average retention time in the column, and then non-dimensionalizing the result using the pore diameter from eqn. 10 (left vertical axis) and the membrane thickness (right vertical axis). The interstitial velocity in Fig. 3 is non-dimensionalized using the pore diameter and solute diffusivity. The major sources of experimental error in these measurements appear to be the uncertainty introduced by the signal

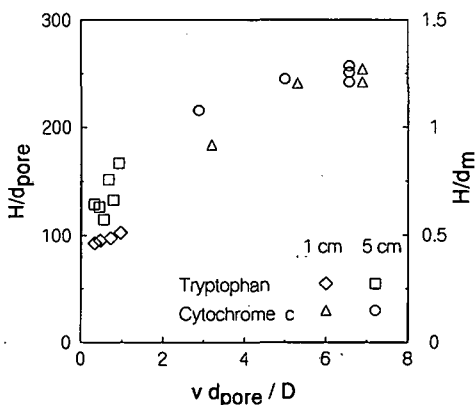


Fig. 3. Reduced plate height as a function of the reduced velocity for 1- and 5-cm columns.  $d_{pore} = 3.0 \mu\text{m}$ ,  $d_m = 600 \mu\text{m}$ .

noise when determining the baseline and the uncertainty introduced by subtracting  $\mu_{2,extra}$  as determined from Fig. 2 from the measured second moment.

The plate height measurements for the 5-cm column appear to be the more reliable of the data sets shown in Fig. 3 since  $\mu_{2,extra}$  is insignificant for a column of that length. As shown in Fig. 3, the plate height for the 5-cm column increases from a minimum of 150 pore diameters to a maximum of 240 pore diameters as the flow-rate increases. As mentioned earlier, plate heights for the membrane columns are three orders of magnitude larger than the sum of  $H_{fluid}$  and  $H_{particle}$  as predicted by eqns. 5-8. This indicates that mass transfer from the membrane pores to the silica particles does not play a significant role in these experiments. Instead, axial dispersion is the dominant band-broadening mechanism and any increase in plate height with flow-rate is likely due to the coupling which generally exists between molecular diffusion and axial dispersion [7].

The data in Fig. 3 can be compared to results for a packed bed of non-porous spheres where, depending on the method used to pack the bed, the plate height increases from a minimum at low flow-rates which is between 2 and 6 pore diameters to a maximum at high flow-rates which is between 4 and 40 pore diameters [12-14]. In accordance with the earlier discussion of the relation between  $d_{pore}$  and  $d_p$ , these results assume that the average pore size is approximately  $d_p/2$  for a bed of randomly packed spheres (*i.e.*, when  $\alpha \approx 0.35$ ). The larger values of  $H_{dispersion}/d_{pore}$  observed for membranes are apparently due to the reduced degree to which the membrane pores are interconnected as compared to the pores of a particulate bed. This permits a convective velocity bias for a particular solute molecule to persist for a much larger number of pore diameters. Nevertheless, in spite of the limited degree to which the membrane pores are apparently interconnected, individual pores contact each other often enough such that an increase in the solute diffusivity decreases the distance that a convective velocity bias is maintained for a particular solute molecule.

Fig. 3 indicates that as few as one theoretical plate is observed per membrane. This suggests that the residence time distribution for an unadsorbed solute in an individual membrane is very broad, reaches a

maximum at relatively small residence times, and approaches zero at large residence times very slowly (*i.e.*, the distribution has a significant tail at large times), since distributions having these characteristics correspond to a number of theoretical plates near unity.

Finally, Fig. 3 can be compared to results reported recently by Briefs and Kula [6]. Those workers investigated a stack of 97 nylon-based membranes having a total thickness of 1.7 cm and a Darcy's law permeability of  $3.4 \cdot 10^{-10}$  cm<sup>2</sup> which, according to eqn. 10, yields an average pore size of 1.9  $\mu$ m. Fig. 8 from Briefs and Kula [6] illustrates the response to a step change in influent concentration as compared to theoretical calculations for the case where axial dispersion is the dominant band-spreading mechanism. If the tailing shown in the figure is ignored, the figure indicates that the effective axial dispersion coefficient is between  $5 \cdot 10^{-8}$  and  $1 \cdot 10^{-7}$  m<sup>2</sup> s<sup>-1</sup> for a superficial flow-rate of 4 cm/min. Since the corresponding value of  $H_{\text{dispersion}}$  is given by the quantity  $2 D_{\text{axial}}/\nu$  (see ref. 7), this implies that  $H_{\text{dispersion}}/d_{\text{pore}}$  and  $H_{\text{dispersion}}/d_m$  as measured by Briefs and Kula [6] are between 50 and 100 and between 0.52 and 1.04, respectively, which are both comparable to the values obtained in this study.

#### SYMBOLS

$a$	area per unit volume, cm <sup>-1</sup>
$B$	Darcy's law permeability, cm <sup>2</sup>
$D$	diffusion coefficient in mobile phase, cm <sup>2</sup> s <sup>-1</sup>
$D_{\text{axial}}$	axial dispersion coefficient, cm <sup>2</sup> s <sup>-1</sup>
$d_m$	membrane thickness, cm
$d_p$	particle diameter or silica particle diameter, cm
$d_{\text{pore}}$	pore diameter, cm
$H$	height of theoretical plate, cm
$K_{\text{eq}}$	equilibrium constant
$k'$	equilibrium parameter
$k_1$	mass-transfer coefficient, cm s <sup>-1</sup>
$L$	column length, cm
$N$	number of theoretical plates
$\Delta P$	pressure drop across column, g cm <sup>-1</sup> s <sup>-2</sup>
$T$	empirical ratio between pore length and membrane thickness
$t_0$	retention time for an unadsorbed solute, s
$t_{\text{feed}}$	size of solute injection slug, s
$t_R$	retention time for a solute in the column, s

$\nu$	interstitial fluid velocity, cm s <sup>-1</sup>
$\nu_s$	superficial fluid velocity, cm s <sup>-1</sup>

#### Greek symbols

$\alpha$	volume fraction occupied by mobile fluid in membrane
$\varepsilon$	porosity of silica particles
$\lambda$	equilibrium constant defined in eqn. 7
$\mu$	viscosity, g cm <sup>-1</sup> s <sup>-1</sup>
$\mu_1$	first absolute moment, s
$\mu_2$	second central moment, s <sup>2</sup>
$\sigma$	volume fraction of silica particles
$\tau$	diffusional tortuosity

#### ACKNOWLEDGEMENTS

Financial support for this work was provided by the National Science Foundation under Grants CTS 9008746 and BCS 9014119 and by a 1988 Yale Science and Engineering Association grant. Columns used in this study were donated by Kontes Life Sciences Products. Some of the experimental work reported in this paper was performed by Mr. Minghua Lu and by Mr. Michael Raftery.

#### REFERENCES

- 1 R. Hegedus, *J. Chromatogr. Sci.*, 26 (1988) 425.
- 2 S. Brandt, R. A. Goffe, S. B. Kessler, J. L. O'Connor and S. E. Zale, *Bio/Technology*, 6 (1988) 779.
- 3 H. Ding, M.-C. Yang, D. Schisla and E. L. Cussler, *AIChE J.*, 35 (1989) 814.
- 4 J. J. Piotrowski and M. H. Scholla, *BioChromatography*, 3 (1988) 161.
- 5 *MemSep Chromatography Cartridge Technical Bulletin*, Millipore, Bedford, MA, 1991.
- 6 K.-G. Briefs and M.-R. Kula, *Chem. Eng. Sci.*, 47 (1992) 141.
- 7 J. C. Giddings, *Dynamics of Chromatography, Part 1, Principles and Theory*, Marcel Dekker, New York, 1965.
- 8 R. E. Kesting, *Synthetic Polymer Membranes*, McGraw-Hill, New York, 1971.
- 9 F. A. L. Dullien, *Porous Media Fluid Transport and Pore Structure*, Academic Press, New York, 1979.
- 10 R. B. Bird, W. E. Stewart and E. N. Lightfoot, *Transport Phenomena*, Wiley, New York, 1960.
- 11 E. J. Wilson and C. J. Geankoplis, *Ind. Eng. Chem. Fundam.*, 5 (1966) 9.
- 12 Cs. Horváth and H.-J. Lin, *J. Chromatogr.*, 126 (1976) 401.
- 13 P. Magnico and M. Martin, *J. Chromatogr.*, 517 (1991) 31.
- 14 S. F. Miller and C. J. King, *AIChE J.*, 12 (1966) 767.



CHROM. 24 079

# Reduction in large-scale adsorption chromatography unit costs by use of 30-Å Sorbsil C30 silica

I. Chappell and P. Baines

*Crosfield Chromatography, P.O. Box 26, Warrington (UK)*

P. K. Carpenter

*ICI Agrochemicals, Bracknell (UK)*

(First received November 22nd, 1991; revised manuscript received January 31st, 1992)

---

## ABSTRACT

Adsorption chromatography is being increasingly used to purify products on an industrial scale. A major cost factor is the purchase, recycling and disposal of the large volumes of solvents used in the process. Silicas of higher loading capacity are required to reduce the solvent costs and we have shown that specifically designed silicas with a pore size of 30 Å can provide the capacity increase. Although historically it has been believed that silica of pore size less than 60 Å cannot perform satisfactorily, it is shown that Sorbsil C30 gives good kinetic performance ( $h < 2$ ), and that the significantly higher surface area per unit column volume leads to much higher loading capacities. Data from small-scale breakthrough curves for laboratory- and pilot-scale elution chromatography show increases in capacity between 50 and 250% compared with conventional 60-Å silicas. Data models for large-scale operations show a significant reduction in processing costs from the use of Sorbsil C30, owing to decreased solvent consumption and a smaller sample recovery plant with the additional benefit of reduced contamination of the sample by solvent impurities.

---

## INTRODUCTION

Interest in and the use of process-scale chromatography have been growing steadily as the regulatory demands on product purity exceed the ability of conventional process purification steps to meet those demands. Although reversed-phase process chromatography has been on the increase [1], by far the largest utilization on the process scale is adsorption chromatography using silica. Over the last few years, interest has focused on the use of smaller particle silicas with an average size range of 10–20 μm [2]. These smaller particles give higher efficiency, leading to better separation of complex mixtures. For simpler mixtures, the higher efficiency can be put to good effect by increasing the solvent strength

to reduce capacity factors and save on solvent consumption.

The use of small-particle media, particularly in the 10-μm range, is not without problems as media, equipment and maintenance costs are high. Although in some instances these costs can be justified, many processes run with larger particles and cannot at this stage in their life justify the capital investment required for their change. One area which has received little attention is the improvement in the loading capacity of the media. Such improvements can benefit users of materials of all particle sizes and can be implemented at no capital cost as no modifications are required to the chromatographic plant to achieve a higher throughput. A higher surface area, provided that it is accessible to the solute, would allow a potentially higher loading capacity as deviation from the linear part of the adsorption isotherm occurs at a particular surface

---

*Correspondence to:* Dr. I. Chappell, Crosfield Chromatography, P.O. Box 26, Warrington, UK.

concentration for a given phase system. One way of achieving a higher surface area is to use a silica of small pore size as surface area tends to increase as the pore size is decreased. Historically, 60-Å, 500 m<sup>2</sup> g<sup>-1</sup> silicas have become the standard for high-capacity adsorption chromatography. The use of media of smaller pore size has been discouraged by the assertion that “micropores” cause slow diffusion kinetics and hence poor efficiency [3,4]. Although this may occur with some media, the use of a specifically designed particle with a mean size of 30 Å and a minimum of pores in the <20 Å range can give a high surface area with excellent mass transfer kinetics. This paper discusses the development, properties and application of a novel silica of high surface area and small pore size that shows significant loading advantages over conventional 60 Å silica, giving a higher throughput and substantial solvent savings.

## EXPERIMENTAL

### Materials

The materials used were obtained from the following sources: Sorbsil C30 and C60, 15–20, 20–40 and 40–60 μm, Crosfield Chromatography (Warrington, UK); Kieselgel 60, 40–60 μm (9385), E. Merck (Poole, UK); Spherisorb X and W, 10 μm, Phase Separations (Queensferry, UK); Pro 10 and Zorbax, 10 μm, DuPont (Warrington, UK); Matrex 60A, 10 μm, Amicon (Stonehouse, UK); Partisil, 10 μm, Whatman (Maidstone, UK); hexane, Rathburn (Walkerburn, UK); heptane, ethyl acetate, 2-propanol and tetrahydrofuran, Rhône Poulenc Laboratory and Products (Manchester, UK); and Agrochemical Exploratory Herbicide (Mw 400), ICI Agrochemicals (Jealott's Hill, UK).

### Equipment

The chromatographic system consisted of a Pye Unicam PU 4010 pump, Pye Unicam PU 4020 UV detector, Rheodyne Model 7125 injection valve and Hewlett-Packard HP 3393A reporting integrator.

Large-scale chromatography was carried out on a Prochrom 150 preparative liquid chromatograph with a 15 cm I.D. axially compressed column.

### Procedure

Stainless steel columns (12.5 cm × 0.46 cm I.D.

for Sorbsil C30 and 12.5 cm × 0.50 cm I.D. for Kieselgel 60) were dry packed with the 40–60-μm silica (1.32 g per column). Media of smaller particle size were slurry packed into 25 × 0.46 cm I.D. columns.

Samples of phthalate esters were prepared as either 10% (w/w) solutions in the relevant mobile phase or as neat mixtures of 50% (w/w).

Columns were purged with 2-propanol (20 column volumes) prior to purging with eluent (30 column volumes). The eluent was 2-propanol in heptane, adjusted in flow-rate to give equal linear velocities (1.8 ml min<sup>-1</sup> for Sorbsil C30, 2.2 ml min<sup>-1</sup> for Kieselgel) and in composition to give similar capacity factors for the dimethyl phthalate peak (e.g., 3% 2-propanol for C30 and 1% propanol for Si 60). Size-exclusion chromatography was carried out at 1 ml min<sup>-1</sup> with tetrahydrofuran (THF) using 0.25% w/v solutions of polystyrene standards.

The breakthrough curves of methanol in ethyl acetate were obtained by purging the columns with twelve column volumes of ethyl acetate. The column was then disconnected and the system purged with 1% methanol in ethyl acetate. The column was re-connected and purged with 1% methanol in ethyl acetate at 1 ml min<sup>-1</sup>. The retention volume to 50% breakthrough corrected for the column void volume was recorded.

The capacity factor of an experimental herbicide was measured for a range of silicas using 25% ethyl acetate in hexane. The breakthrough curves were measured for this compound on these silicas in an analogous manner to that described above.

Large-scale chromatography was carried out on a Prochrom 150 system using a 15 cm I.D. column. A 5-kg amount of 20–40-μm packing was axially compressed and eluted with hexane–ethyl acetate (75:25) at 2 l min<sup>-1</sup>. Increasing amounts of herbicide were injected and the major component (ca. 85%) was collected and assayed. The loading capacity was defined when the purity just dropped below 98%.

## RESULTS AND DISCUSSION

### Physical properties of Sorbsil C30

The standard BET-derived pore diameter plots (Fig. 1) show the narrow pore-size distribution of the Sorbsil C30 gel with a notable reduction in

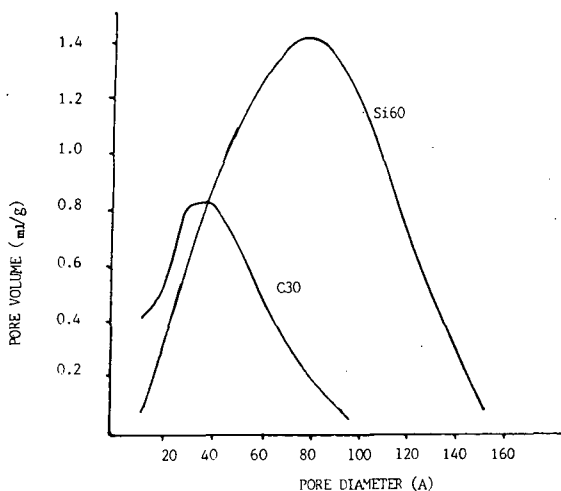


Fig. 1. Nitrogen adsorption pore volume plots for Sorbsil C30 and Merck Si 60.

pores of  $<25 \text{ \AA}$ . This lack of small pores in the 10–20  $\text{\AA}$  range contributes to excellent kinetics, as is shown by the Van Deemter plot obtained for Sorbsil C30 (15–20  $\mu\text{m}$ ). This shows (Fig. 2) an optimum

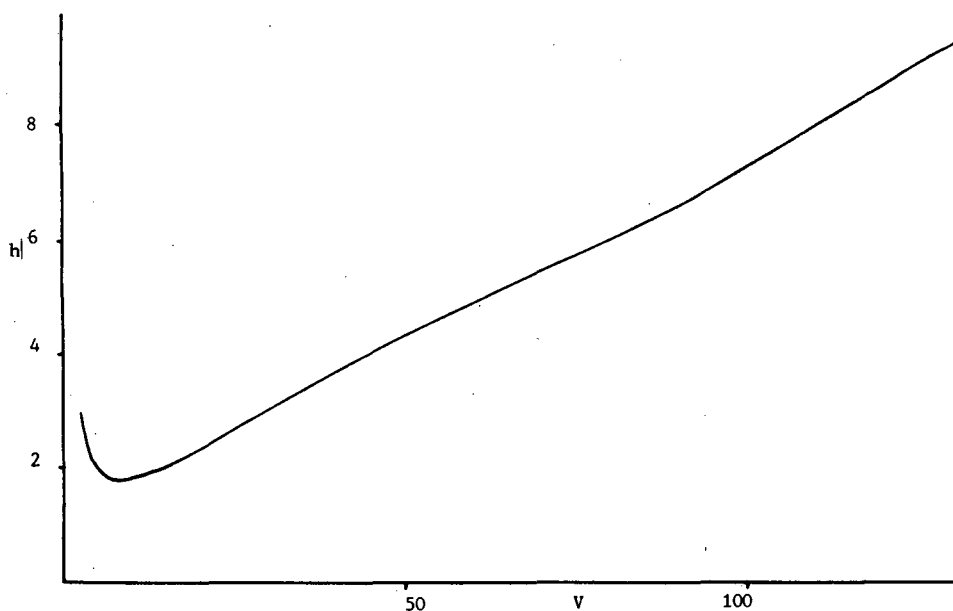


Fig. 2. Plot of reduced plate height versus reduced velocity for Sorbsil C30 (15–20  $\mu\text{m}$ ). Column, 12.5  $\times$  0.46 cm I.D.; eluent, methanol–heptane (1:99); solute, nitrobenzene.

reduced plate height of 1.7 and a low  $C$  term (0.07).

Size-exclusion curves (Fig. 3) show that both the 30- and 60- $\text{\AA}$  gels exhibit exclusion behaviour from MW 200 upwards. The curves start to show significant divergence in the MW range 700–1000 and this marks the molecular weight range where the potential loading capacity advantage of the high-surface-area 30- $\text{\AA}$  gel would be expected to diminish.

The low pore volume ( $0.6 \text{ g ml}^{-1}$ ) of Sorbsil C30 together with the optimized processing route gives a gel of very high mechanical strength. Using the equations developed by Meissner [5], the crush strength is estimated to be 28 000 p.s.i. The Sorbsil C30 gel has been re-used extensively in a Prochrom system without noticeable mechanical attrition. Sorbsil C silicas are manufactured using deionized water and show a significant improvement in impurity levels compared with technical-grade silicas (Fig. 4).

#### Overload performance

Loading capacity in adsorption chromatography is, to a first approximation, proportional to accessible surface area per unit column volume. Table I

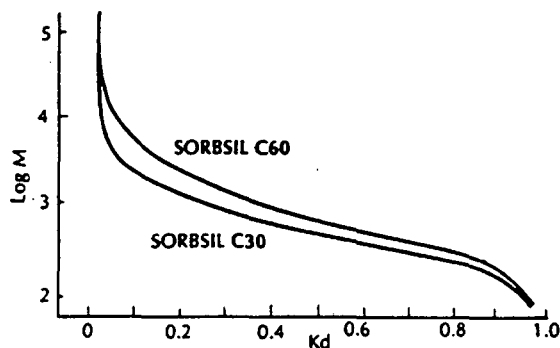


Fig. 3. Size-exclusion curves for linear polystyrene in THF on Sorbsil C30 and C60.  $K_d$  = Fraction of pore volume accessible.

gives typical values for various silicas taken from manufacturers' literature.

Breakthrough curves of 1% methanol in the ethyl acetate (Fig. 5) which give a measure of relative loading capacity gave a good correlation with relative surface areas (Table II).

The extension of this study to solutes of higher molecular weight will be reported subsequently, but initial data show that the capacity advantage of

Sorbsil C30 is maintained up to at least MW 500. The study was extended to a wider range of silica supports and the saturation capacity of an exploratory herbicide was measured by the breakthrough technique. In Fig. 6, the saturation capacity is plotted against the capacity factor of the herbicide on the same column. This gives a remarkably linear plot and indicates the usefulness of simple capacity factor measurements in predicting relative loading capacities. Further work is required to establish the generality of this result, but if confirmed it provides a means of rapid product screening for maximum loading capacity.

In order to study overload effects of the 30-Å *versus* conventional media in the elution mode, the solvent composition had to be adjusted to give similar  $k'$  values on columns of different retentivity for the most retained compound. As Sorbsil C30 is more retentive owing to the high surface area, a stronger solvent is required than for conventional 60-Å media (*e.g.*, 3% vs. 1% 2-propanol). This provides an additional benefit in large-scale use as the stronger solvent aids sample solubility, reducing the sample volume for low-solubility samples.

The loading capacity under elution conditions

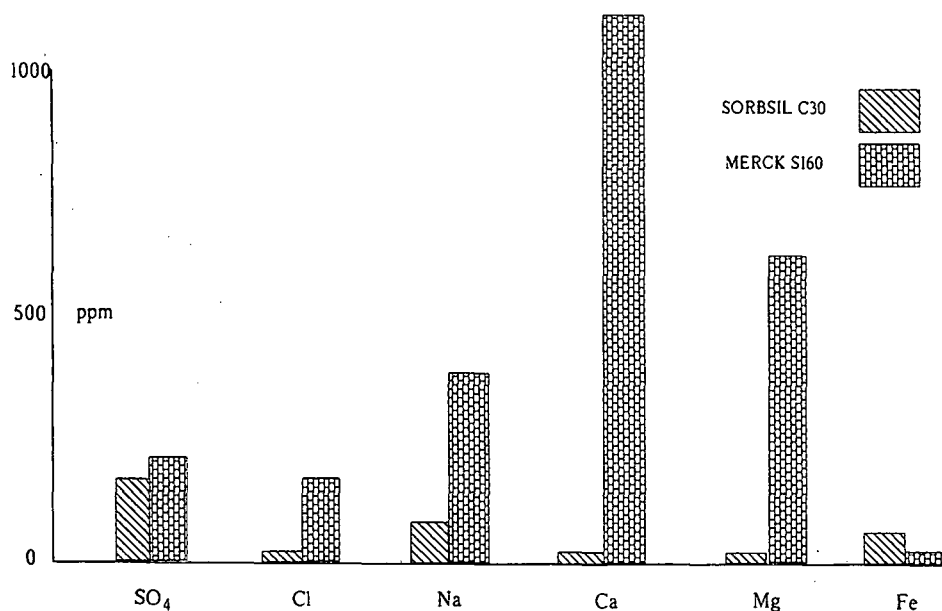


Fig. 4. Impurity profiles (ppm) for Sorbsil C30 and Merck Si 60.

TABLE I  
PROPERTIES OF DIFFERENT SILICAS

Packing	Surface area (m <sup>2</sup> g <sup>-1</sup> )	Packing density (g ml <sup>-1</sup> )	Surface area (m <sup>2</sup> ml <sup>-1</sup> )
Spherical 120 Å	220	0.62	130
Spherical 100 Å	340	0.50	170
Irregular 60 Å	500	0.55	275
Irregular 60 Å	540	0.55	297
Sorbsil C60	550	0.55	303
Sorbsil C30	700	0.63	441

was established for two solvent strengths by chromatographing a 50:50 (w/w) mixture of dibutyl and dimethyl phthalates up to 16 mg of each ester per ml of column volume (25 mg g<sup>-1</sup> of packing) (Figs. 7 and 8). Although of similar structure, the two esters show different adsorption isotherms. The butyl ester shows Langmuir-type adsorption with decreasing retention and peak tailing on overload whereas the dimethyl ester shows anti-Langmuir adsorption with increasing retention time and peak fronting. Visual inspection indicates that approximately twice the amount of ester is required to give a similar degree of peak tailing/fronting on the Sorbsil C30. Plots of retention time against mass injected (Figs. 9 and 10) show a much greater resistance to overload for the 30-Å material and similar results were obtained using the weaker solvent system. The change in capacity factor on a range of overload criteria, 10%, 25% or 50%, shows the 30-Å material to be less sensitive to overload by factors between 2 and 5.

TABLE II  
CAPACITIES AND SURFACE AREAS OF 60- AND 30-Å SILICAS

Packing	Methanol adsorbed per ml of column (mg)	Measured relative capacity	Relative surface area per ml (%)
Merck Si 60	120	91	91
Sorbsil C60	132	100	100
Sorbsil C30	197	149	146

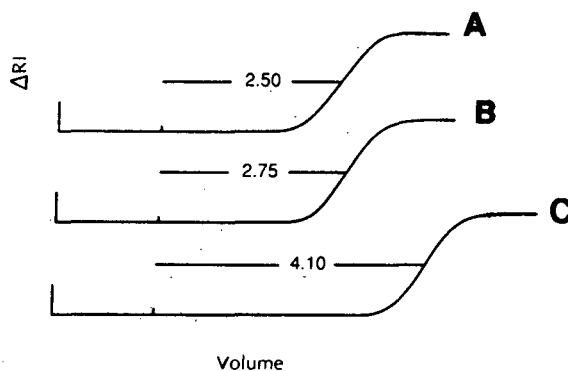


Fig. 5. Breakthrough curves on methanol–ethyl acetate (1:99) on (A) Merck Si 60, (B) Sorbsil C60 and (C) Sorbsil C30.

Most theoretical models have assumed that the critical pair(s) of compounds have similar-shaped adsorption isotherms [6–8]. However, our findings, which are by no means unique, illustrate the need to determine the isotherm shape for each application. This observation goes some way to explaining the range of increased loading capacities found in practice. These range from 0 to 300%, although the nominal increase in surface area per ml of Sorbsil C30 over Merck Si 60 is 60%. Part of this discrepancy is probably due to the difference in the shapes of the adsorption isotherms. In the phthalate ester case, the peaks move apart as they overload and the overloading of the lower capacity phase is partially compensated for by this peak shift. For the other extreme, where the first peak moves back and the second peak moves forward, resolution will be lost on the lower capacity phase at a much reduced sample loading. An understanding of this phenomenon is crucial in selecting the most appropriate phase system for a preparative separation and will be the basis for future experimentation.

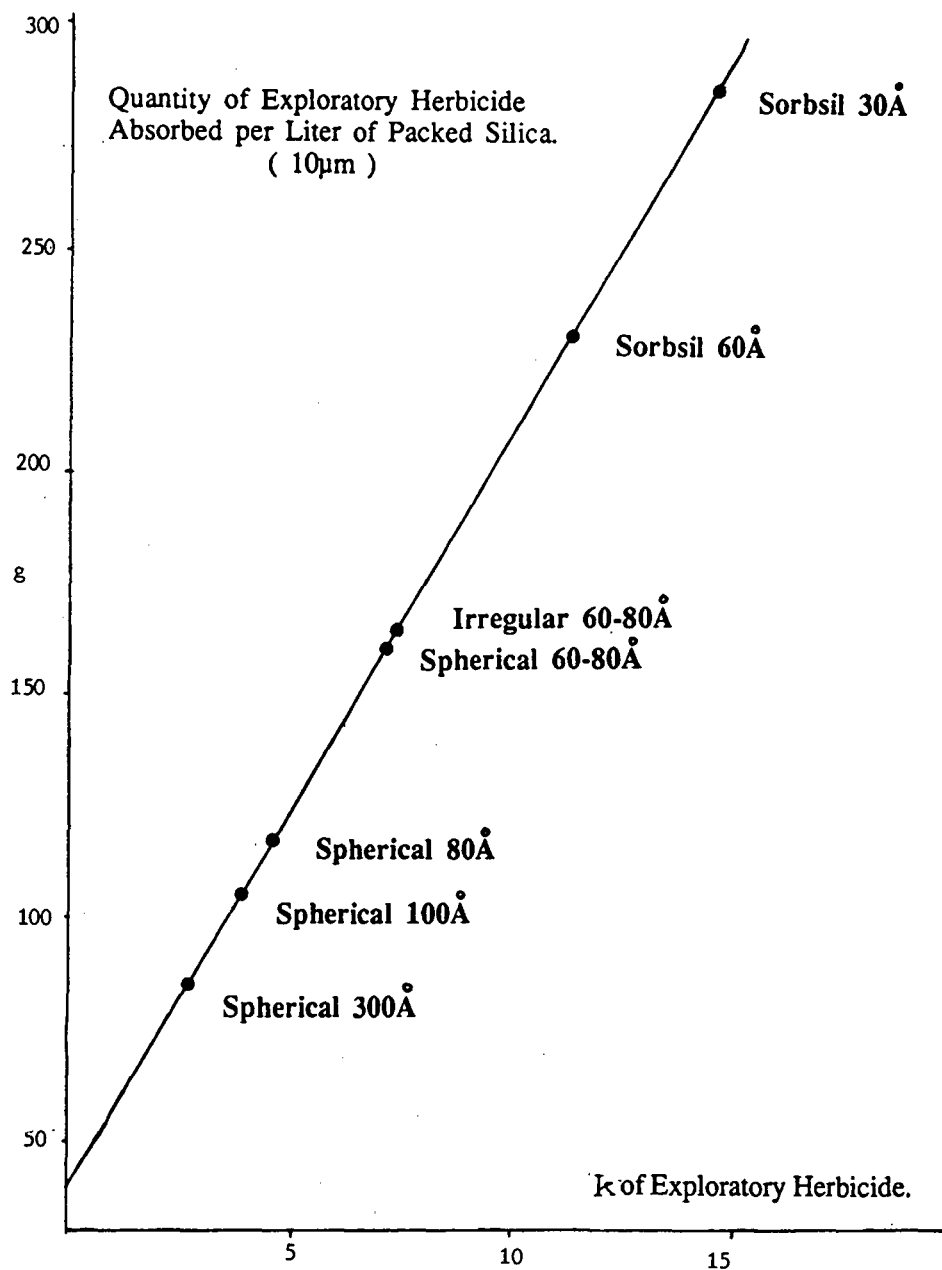


Fig. 6. Plot of amount of exploratory herbicide adsorbed per unit column volume against capacity factor of herbicide.

For a 64-mg injection, the dimethyl phthalate peak was collected and subsequently analysed by high-performance liquid chromatography. The results are given in Table III, and clearly show that

the Sorbsil C30 provides higher purity, lower solvent consumption and higher fraction concentration, all of which, as will be discussed, provide substantial cost reduction benefits in large-scale chro-

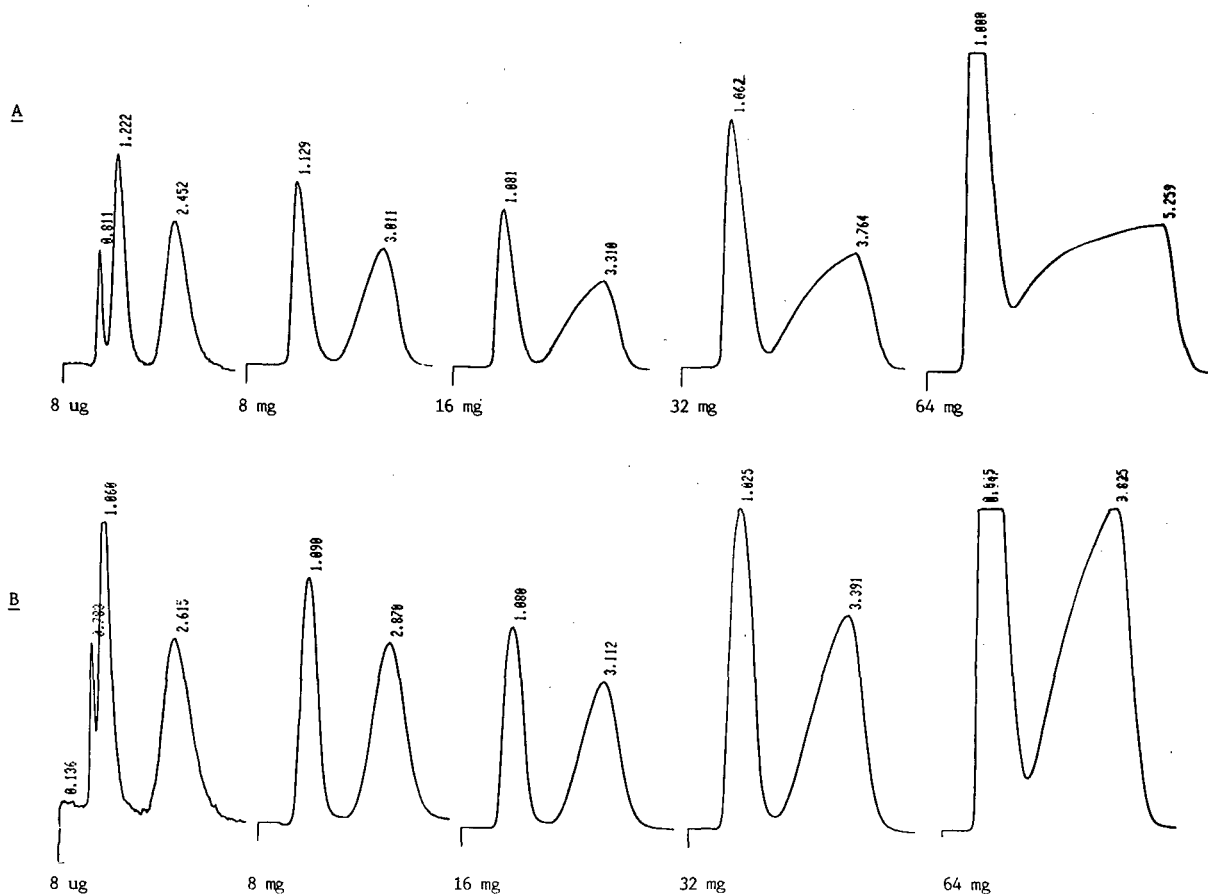


Fig. 7. Separation of 8  $\mu\text{g}$ , 8 mg, 16 mg, 32 mg and 64 mg of phthalate esters on (A) Merck Si 60 and (B) Sorbsil C30 (40–60  $\mu\text{m}$ ). Solvent: heptane–2-propanol, 1:99 for Si 60 and 3:97 for Sorbsil C30. Numbers at peaks indicate retention times in min.

matography. If a smaller mass of 32 mg were to be used on the Si 60 column, the purity would increase but the throughput would halve, the solvent consumption per unit throughput would double and the fraction volume would double.

#### Large-scale evaluation

Sorbsil C30 (20–40  $\mu\text{m}$ ) was compared with a conventional silica of high surface area (Matrex 60  $\text{\AA}$ ) in a Prochrom 150 system for the purification of an exploratory herbicide. The purity of the starting material was 85% (Fig. 11) and a minimum of 98.7% final product purity was required. The sample mass injected on to the 60- $\text{\AA}$  column was increased as the purity of the collected material was determined.

The results show that up to 200 g could be loaded on to the column before the purity fell to below 98.7% (Table IV), Figs. 12 and 13). The recovery at this load was 82%.

A similar-sized column of Sorbsil C30 (20–40  $\mu\text{m}$ ) required a slightly stronger solvent to give equivalent performance in terms of efficiency, capacity factor, selectivity and back-pressure, but allowed a sample load of 520 g and a recovery of 79%, which gave a purity of 98.8% (Figs. 14 and 15). This gives a 250% increase in product throughput with the potential for substantial cost savings.

Subsequent studies with smaller particle Sorbsil C30 15–20  $\mu\text{m}$  showed that at lower loadings, relatively high plate counts can be achieved in the Prochrom system 18 000 plates  $\text{m}^{-1}$ ,  $h = 3$ ) (Fig. 16).

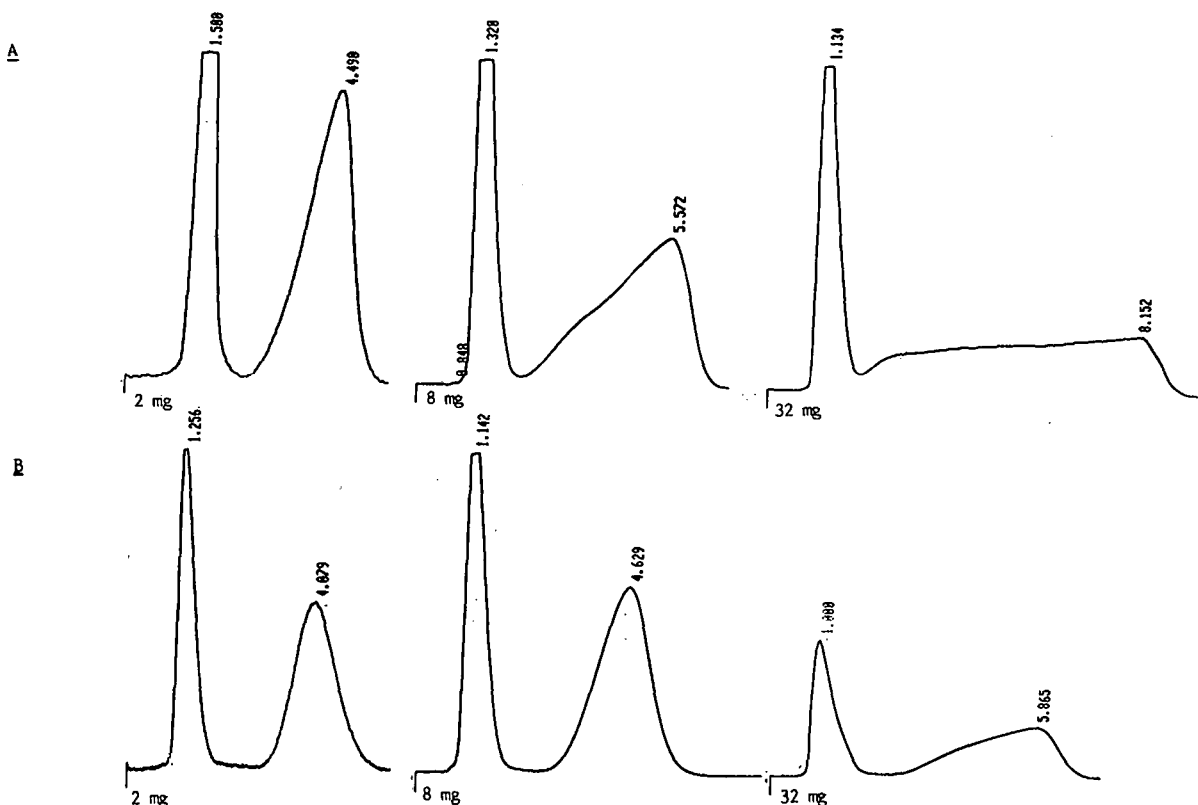


Fig. 8. Separation of 2, 8 and 32 mg of phthalate esters on (A) Merck Si 60 and (B) Sorbsil C30 (40–60  $\mu\text{m}$ ). Eluent: 2-propanol-heptane, 0.5:99.5 for Si 60 and 1:99 for Sorbsil C30. Numbers at peaks indicate retention times in min.

In some preparative systems (CEDI, 25  $\times$  10 cm I.D.) plate heights of less than 1.5 (40 000 plates  $\text{m}^{-1}$ ) have been achieved (Fig. 17) with Sorbsil C60 (15–20  $\mu\text{m}$ ).

#### Process economics of elution chromatography

Media of high loading capacity will provide cost savings from two main sources: solvents and plant.

*Solvent savings.* For a given throughput, less Sorbsil C30 will be required. The exact reduction will depend on the actual increase in capacity. This reduced volume of silica will require a similarly reduced volume of solvent for unit throughput. The solvent requirement is also reduced by the slightly lower relative column void volume of Sorbsil C30 (0.72 ml of solvent per ml of empty column) compared with 60- $\text{\AA}$  media (0.76).

Numerically, the cost saving per annum ( $S$ ) on solvents is given by the equation

$$S = a b c d [f - g / (1 + e)]$$

where  $a$  = mass of 60- $\text{\AA}$  silica used per annum;  $b$  = number of column volumes of solvent used per run;  $c$  = cost of solvent per litre (purchase, recycle, disposal);  $d$  = number of cycles before media replacement;  $e$  = fractional increase in loading capacity; and  $f$  and  $g$  = respective solvent volume in 1 g of packing. For a 60- $\text{\AA}$  packing with relative void volume 0.76 and a packing density of 0.55  $\text{g ml}^{-1}$   $f$  is 0.76/0.55 = 1.38 and for Sorbsil C30 the value of  $g$  is 0.72/0.63 = 1.14.

Three worked examples are given in the Appendix and demonstrate significant savings (45%) in

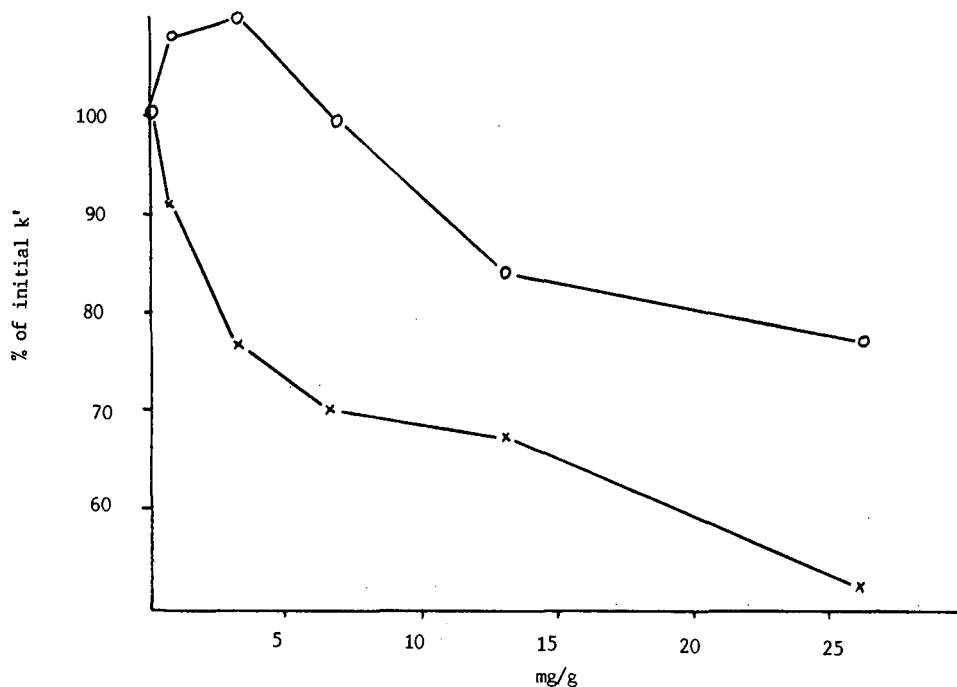


Fig. 9. Percentage change in capacity factor for dibutyl phthalate as a function of load ( $\text{mg g}^{-1}$ ) for (x) Merck Si 60 and (o) Sorbsil C30. Eluent: 2-propanol-heptane (1:99).

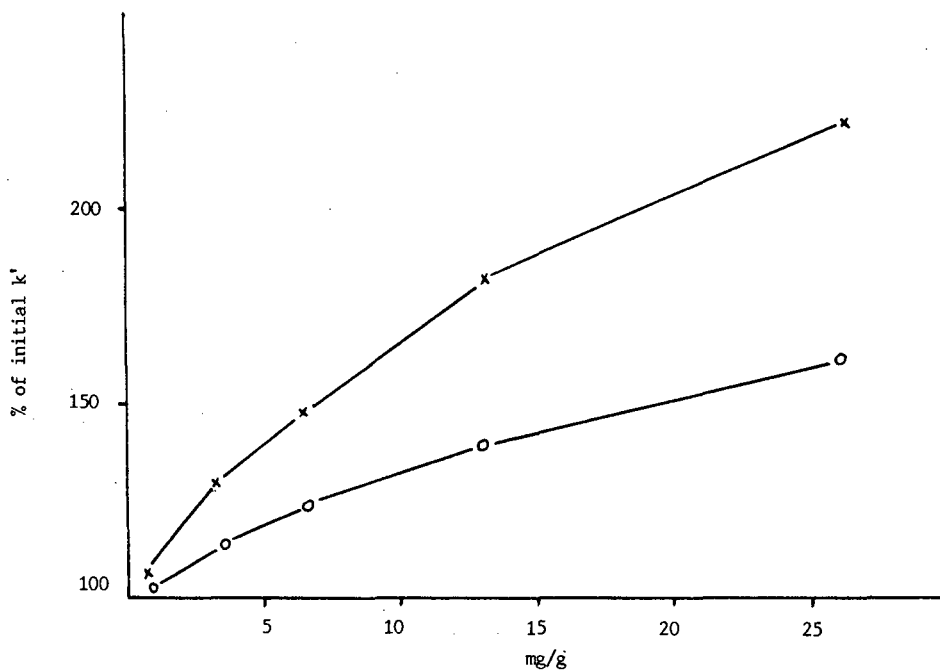


Fig. 10. Percentage change in capacity factor for dimethyl phthalate as a function of load ( $\text{mg g}^{-1}$ ) for (x) Merck Si 60 and (o) Sorbsil C30. Eluent: 2-propanol-heptane (1:99).

TABLE III  
PARAMETERS OF DIMETHYL PHTHALATE PEAKS  
FROM 64-mg INJECTION

Parameter	Si 60	Sorbsil C30
Peak volume (ml)	10.1	5.8
Mass recovered (mg)	32.8	33.8
Recovery (%)	98.5	101
Purity (%)	97.3	99.1
Concentration (mg ml <sup>-1</sup> )	3.24	5.86
Total solvent consumption per run (ml)	14.3	9.18

TABLE IV  
PURITY VS. MASS INJECTED FOR HERBICIDE ON MA-  
TREX 60 Å (20-40 µm) IN PROCHROM COLUMN

Sample load (g)	Product purity (%)
100	99.99
150	99.91
200	98.99
250	98.63

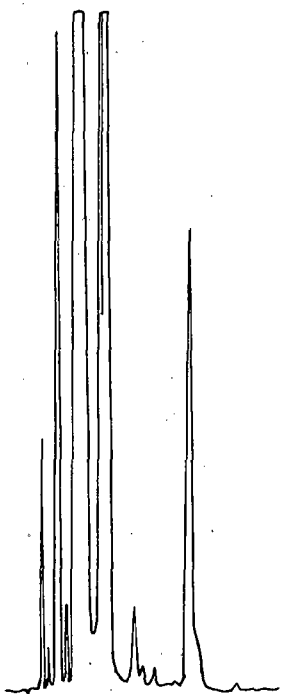


Fig. 11. Analysis of starting exploratory herbicide.

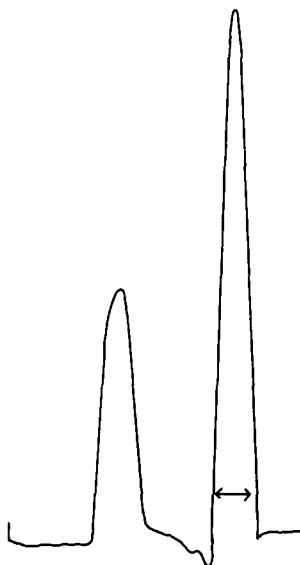


Fig. 12. Separation of 200 g of herbicide on a 68 × 15 cm I.D. column of Matrex 60 Å (20-40 µm). Eluent, ethyl acetate-hexane (20:80) at 2300 ml min<sup>-1</sup>; backpressure, 23 bar; chart speed, 300 mm h<sup>-1</sup>; injection volume, 2.5 l. Product fraction collected between arrows. Throughput 0.6 kg/h.

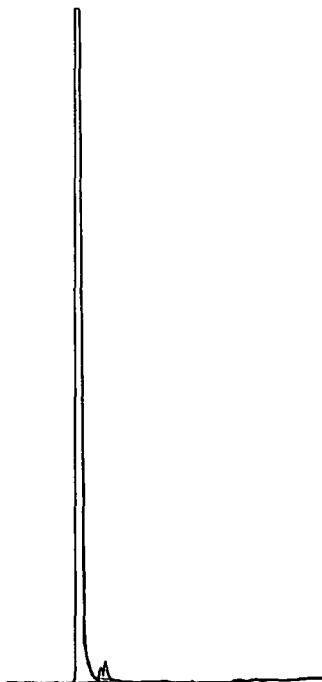


Fig. 13. Analysis of product fraction collected between arrows in Fig. 12 from application of 200-g of herbicide on a Matrex 60 Å (20-40 µm) column. Product purity 98.7%.

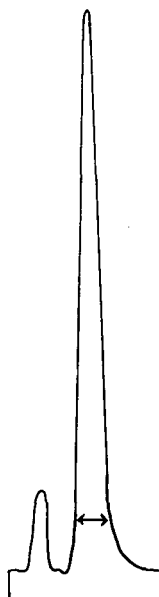


Fig. 14. Separation of 520 g of herbicide on a  $62 \times 15$  cm I.D. column of Sorbsil C30 ( $20\text{--}40 \mu\text{m}$ ). Eluent, ethyl acetate–hexane (25:75) at  $2000 \text{ ml min}^{-1}$ ; back-pressure, 20 bar; chart speed,  $180 \text{ mm h}^{-1}$ ; injection volume, 6 l. Product fraction collected between arrows. Throughput 1.5 kg/h.

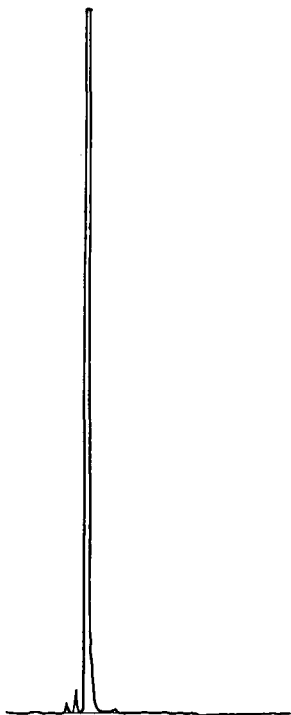


Fig. 15. Analysis of product fraction collected between arrows in Fig. 14 from application of 520 g of herbicide on a Sorbsil C30 ( $20\text{--}40 \mu\text{m}$ ) column. Product purity 98.8%.

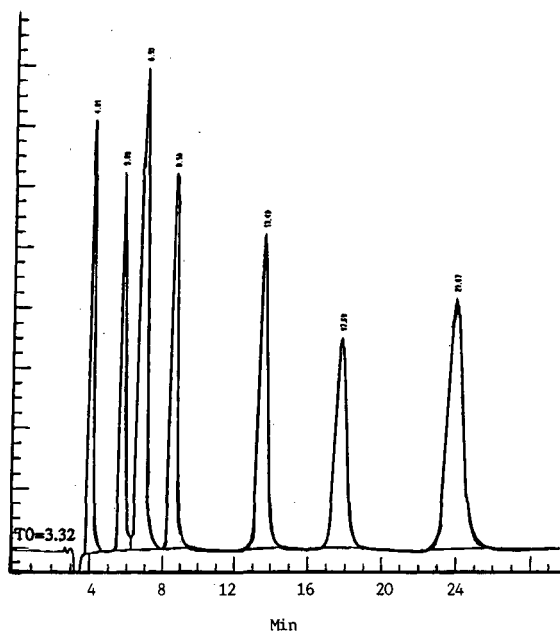


Fig. 16. Separation of test mixture on a  $21 \times 15$  cm I.D. Prochrom column packed with Sorbsil C60 ( $15\text{--}20 \mu\text{m}$ ). Eluent, ethyl acetate–hexane (10:90) at  $1000 \text{ ml/min}^{-1}$ .

variable costs. The three examples cover the following operating conditions: (1) large-particle ( $40\text{--}60 \mu\text{m}$ ), low-pressure system with the material used once and then discarded with a low solvent consumption,  $k' \approx 2$ ; (2) as (1) but with multiple use of the material and a higher solvent requirement due to column washing step between runs; and (3) small-particle ( $15\text{--}20 \mu\text{m}$ ), high-pressure system with multiple use of the material.

*Plant savings.* In a “green-field” site, considerable savings can be made owing to the reduction in the total amount of solvent which needs processing. Storage tanks, solvent pumps, chromatographic column, solvent recovery plant and sample recovery unit can all be sized smaller, leading to savings in both fixed and variable costs. At an estimated 20% reduction in plant costs resulting from a 50% increase in media loading capacity, and a plant cost of \$3 million, the capital saving would be \$600 000 with proportionate savings on depreciation and cost of capital. If buildings and facilities for solvent handling already exist, the scope for capital savings

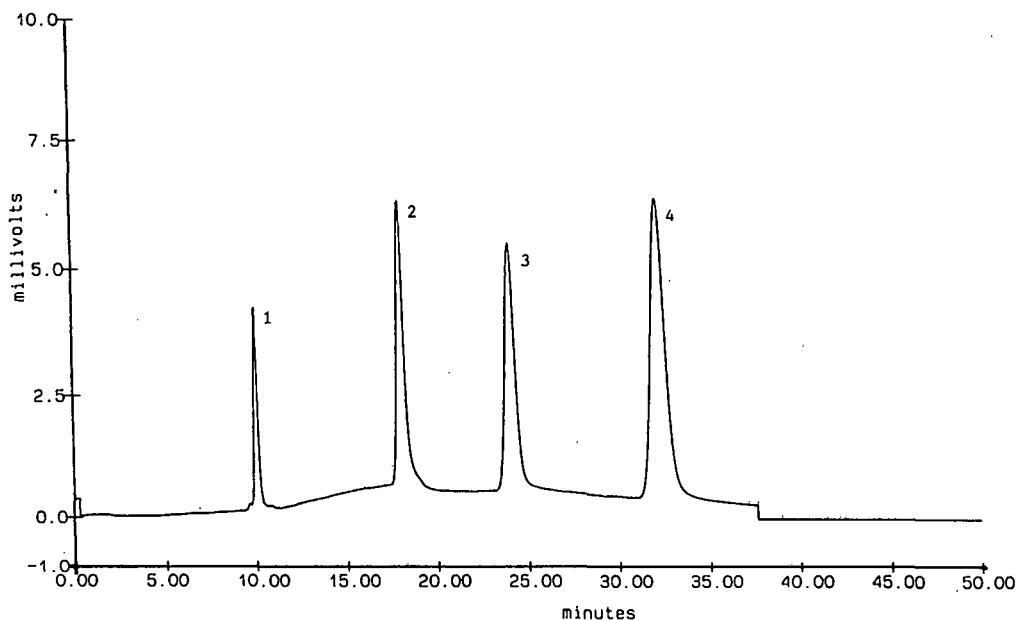


Fig. 17. Separation of toluene (1), nitrobenzene (2), phenyl acetate (3) and acetophenone (4) on a  $30 \times 10$  cm I.D. CEDI cartridge column of Sorbsil C60 (15–20  $\mu\text{m}$ ). Eluent, ethyl acetate–hexane (3:97) at  $200 \text{ ml min}^{-1}$ .

are proportionately reduced, but can still be significant.

For current processes, Sorbsil C30 offers increased throughput at no additional capital cost. Although the prime benefit is one of lower operating costs, the high capacity gives additional benefits: the concentrations of fractions are higher and lead to a reduction in the contamination of the purified material from solvent-borne impurities; and the total amount of media and solvent used will be reduced and hence the environmental impact will be minimized. This impact results from solvent and media disposal, loss of solvent to the atmosphere and the energy input into the raw materials and the separation process. Although the reduction in impact by use of a 30-Å material will not be large compared with the total environmental impact of the whole manufacturing site, significant improvements in total discharges will result from the sum of large number of smaller steps taken by individual units.

## CONCLUSIONS

This paper has demonstrated that, contrary to popular belief, silicas of small pore size can exhibit excellent mass transfer kinetics provided that the pore-size distribution does not contain a significant proportion of micropores of less than 20 Å. Sorbsil C30 has such a pore-size distribution and, owing to its high surface area and high packing density, it is capable of significantly increasing the loading capacity per unit column volume in preparative chromatography. This improved capacity can be used to increase the capacity of an existing plant or to decrease the size of plants at the design stage. Either way, processing costs are reduced primarily through the reduction in solvent consumption and reprocessing. A material of pore size 30 Å appears to be the optimum for preparative adsorption chromatography with solute molecular weights of <1000.

## ACKNOWLEDGEMENTS

We acknowledge the provision of the data on the CEDI system by Dr. N. Herbert of Jones Chromatography (Hengoed, Wales, UK).

## APPENDIX

Assume a 50% higher loading capacity for Sorbsil C30 and we require same sample throughput per annum.

A 1000-kg amount of 60-Å material occupies 1818 l of empty column ( $\rho_p = 0.55 \text{ g ml}^{-1}$ ), which at a porosity of 0.76 needs 1380 l of solvent per unit column volume.

Owing to the increased capacity of Sorbsil C30: 660 kg of Sorbsil C30 = throughput to 1000 kg of 60-Å material and

660 kg of Sorbsil C30 occupies 1047 l of column ( $\rho_p = 0.63 \text{ g ml}^{-1}$ ), which at a porosity of 0.72 needs 754 l of solvent per unit column volume.

Examples:	1	2	3
	40–60- $\mu\text{m}$ silica, solvent not recycled	40–60- $\mu\text{m}$ silica, solvent not recycled	15–20- $\mu\text{m}$ silica, solvent recycled
No. of samples before column replacement	1	150	50
No. of column volumes per run	6	15	15
Solvent cost (\$/l)	5	5	0.5
Volume of solvent (l)	8280	1 035 000	1 035 000
Sorbsil C30 (l)	4524	565 500	565 500
Solvent costs:			
60 Å	US\$ 41 250	US\$ 5 175 000	US\$ 517 500
Sorbsil C30	US\$ 22 620	US\$ 2 827 500	US\$ 282 750
Solvent savings p.a.	US\$ 18 630 = 45%	US\$ 2 347 500 = 45%	US\$ 234 750 = 45%
<i>Media costs</i>			
1000 kg of 60-Å material	US\$ 29 000	US\$ 29 000	US\$ 200 000
660 kg of Sorbsil C30	US\$ 23 000	US\$ 23 000	US\$ 200 000
Saving p.a.	US\$ 6 000	US\$ 6 000	—
Total savings p.a.	US\$ 24 000 = 34%	US\$ 2 353 000 = 45%	US\$ 234 750 = 33%

## REFERENCES

- E. P. Kroeff, R. A. Owens, E. L. Campbell, R. D. Johnson and H. I. Marks, *J. Chromatogr.*, 461 (1989) 45–61.
- M. Nyström and P. Jageland, *Ind. Chromatogr. News*, 2 (1990) 16–22.
- M. Verzele and C. Dewaele, in M. Verzele and C. Dewaele (Editors), *Preparative High Performance Liquid Chromatography*. TEC. Gent, 1986. p. 79.
- H. Engelhardt and H. Elgass, in Cs. Horváth (Editor), *High Performance Liquid Chromatography, Advances and Perspectives, Vol. 2*, Academic Press, New York, 1980, p. 67.
- P. Meissner, *Ind. Eng. Chem., Process Des. Dev.*, 3 (1964) 202.
- J. H. Knox and H. M. Pyper, *J. Chromatogr.*, 363 (1986) 1–30.
- L. R. Snyder, J. W. Dolan and G. B. Cox, *J. Chromatogr.*, 540 (1991) 21–40.
- C. A. Lucy, T.-L. Luong and S. Elchuck, *J. Chromatogr.*, 546 (1991) 27–36.



# Solvent–stationary phase interactions in normal bonded phase high-performance liquid chromatographic columns

## I. Investigation of system peaks in amino bonded phase columns

C. W. Hsu and W. T. Cooper

*Department of Chemistry, Florida State University, Tallahassee, FL 32306-3006 (USA)*

(First received November 5th, 1991; revised manuscript received February 25th, 1992)

---

### ABSTRACT

System peaks in normal bonded phase high-performance liquid chromatography (NBP-LC) have been used to characterize solvent–stationary phase interactions in an aminopropyl (amino) NBP column. Mobile phases (“solvents”) consisted of binary mixtures of hexane and a polar modifier. The term “system peak” is used to describe peaks arising from mobile phase components under isocratic conditions. These peaks can be either positive or negative, depending on the absorbance of the component relative to that of the bulk mobile phase. This study indicates that at high modifier concentrations the partition model seems to be more appropriate in describing retention in amino NBP columns than the adsorption–displacement model.

---

### INTRODUCTION

The introduction of bonded phases has significantly broadened the utility of normal-phase high-performance liquid chromatography (HPLC) because of the distinct selectivities made possible by varying both mobile phase components as well as the polar functional groups of the stationary phase [1]. However, predicting solute retention in normal bonded phase liquid chromatography (NBP-LC) has proven to be more difficult than when solid adsorbents such as silica or alumina are used. This difficulty is due in large part to the complexity of associations possible between solvent molecules and the chemically and physically heterogeneous bonded phase surface. Unfortunately, it is this very complexity which gives rise to much of the suggested

potential of NBP-LC and which must ultimately be incorporated into predictive retention models [2,3].

At this point there seems to be no generally accepted mechanism of retention in NBP-LC, unlike reversed-phase LC where solvophobic partitioning is the acknowledged starting point. A number of models of retention in NBP-LC have been proposed [5–10], but there still remain unsettled questions such as realistic modelling of adsorbent heterogeneity and the functional dependence of retention on mobile-phase composition in mixed-solvent systems. However, the most commonly accepted retention mechanism is Snyder’s adsorption–displacement model [4–6], which assumes competitive adsorption between solutes and solvent molecules in a monolayer at the surface of a homogeneous surface. As we will discuss later, polar mobile phase modifier molecules tend to accumulate on (or in) the stationary phase in concentrations far beyond a monolayer, and thus the assumption of competitive monolayer

---

*Correspondence to:* Dr. W. T. Cooper, Department of Chemistry, Florida State University, Tallahassee, FL 32306-3006, USA.

adsorption on the stationary phase is probably not suitable at high modifier concentrations (*ca.* 60%). Under these conditions, the uptake of organic modifier increases the thickness of the stationary phase, which then behaves more like an amorphous bulk fluid than a homogeneous surface. Consequently, the driving force for retention will change as solute molecules can become fully embedded within the stationary phase; that is, partitioning rather than adsorption–displacement becomes the dominant retention process.

## THEORY

System peaks [11–13] appear in liquid chromatography when the mobile phase contains more than one component. When a compound is injected into an LC system from a solution that does not precisely match the mobile phase composition, the sample that arrives at the head of the column is relatively vacant in one or both of the mobile phase components compared to the rest of the bulk mobile phase. This results in desorption of the depleted mobile phase component(s) from the stationary phase surface into the bulk, flowing mobile phase. Each of the desorbed components migrates through the column with a characteristic velocity dictated by its distribution coefficient, and they appear as peaks in the chromatogram. These peaks can be either in the negative or positive direction, relative to the detector base line, depending on the response of the particular component with regard to the bulk mobile phase. It has been shown [11,12] that system peaks are directly related to the adsorption of mobile phase components on the stationary phase surface and they can be utilized in the calculation of adsorption isotherms. Thus, by changing the modifier concentration and using one of the system peaks as a reference, it is possible to semi-quantitatively evaluate the amount of desorbed component in the vacant sample zone. This amount is related to the quantity adsorbed on the stationary phase prior to the injection, which in turn is related to the adsorption isotherm of the modifier.

In normal phase LC the hexane peak is normally used as the void volume marker. It is thus assumed that neither partitioning nor adsorption will occur for hexane molecules into (onto) the stationary phase. In order for the hexane molecules to experi-

ence partitioning, the stationary phase has to behave like an amorphous bulk fluid. However, due to the strong adsorption sites of the normal bonded phase at low modifier concentrations (<60%), the stationary phase is far from a homogeneous bulk fluid. While there is the possibility of hexane adsorption onto polar amino sites through weak dispersion forces, this should be minimal. Even if hexane is adsorbed to some extent, the resulting error in  $t_0$  (dead time) will not change the *relative* shapes and positions of the isotherms for the three solvent modifiers. Comparison of the relative behavior of the three modifiers is really the goal of this work. We therefore believe that the use of hexane as the  $t_0$  marker is suitable in this situation.

Chromatographic retention involves solute transfer from a mobile phase into or onto a stationary phase. Partitioning, adsorption, or both can be involved in the association of the solute with the stationary phase. The distinction between partitioning and adsorption is that “partitioning” implies the solute is approximately fully embedded within the stationary phase, whereas “adsorption” implies the solute is only in surface contact with the stationary phase and not fully embedded. In either case, transfer is characterized by an exchange of the environment at the surface of the solute molecule: solute is initially surrounded by neighboring mobile phase molecules and is finally surrounded, fully or partially, by neighboring molecules of the stationary phase. As proposed by Snyder and Poppe [4–6], in NBP-LC solute retention is assumed to involve a competition of solute and mobile phase molecules for a place on the stationary phase surface. In such a case the retention of a solute molecule S can be described by



where S refers to the solute, M to the solvent, m to the mobile phase and s to the stationary phase. The coefficient  $n$  is used to adjust the model for solutes and solvents of differing cross-sectional areas. From this model, the net energy of adsorption can be written as

$$\log K = E = (E_{S,s} - nE_{M,s}) + (nE_{M,m} - E_{S,m}) \quad (2)$$

(i)
(ii)

where  $K$  is the equilibrium constant of eqn. 1. Solute

retention (which is proportional to the equilibrium constant  $K$ ) is seen to be determined by partial molar solute free energies in each phase; term i corresponds to interactions in the stationary phase, and term ii groups similar interactions in the mobile phase. Thus, the compositions of each phase contribute to retention. From the thermodynamic point of view eqn. 2 does not involve any particular retention mechanism. However, it is often useful to assume that either term i or ii dominates solute retention as mobile phase composition is varied.

If term i is dominant, then eqn. 2 becomes

$$E \approx E_{S,s} - nE_{M,s} \quad (3)$$

which is Snyder's basic equation for NBP-LC. In the Snyder model, the adsorption surface is considered to be energetically homogeneous (no solute or solvent localization [4–6]) and solute-solvent interactions in the mobile phase are assumed to be cancelled by corresponding interactions in the adsorbed phase. That is, the acceptor cavity in the stationary phase is far more important than the donor cavity in the mobile phase. However, if term ii is more important then eqn. 2 becomes

$$E \approx nE_{M,m} - E_{S,m} \quad (4)$$

Eqn. 4 is in perfect agreement with the solvophobic [14–16] concept which postulates that the hydrophobic effect plays a fundamental role in reversed bonded phase liquid chromatography (RBP-LC). It also suggests that the main contribution to solute retention originates from the mobile phase ( $E_{M,m}$ ).  $E_{M,m}$  is directly related to the energy of cohesion between solvent molecules and represents the energy necessary to create a cavity in the solvent to accommodate for solute molecules.  $E_{S,m}$  is associated with the specific interaction between solute and mobile phase. Obviously, the solvophobic theory is based on the premise that the only cavity which is relevant to retention is that in the mobile phase solvent; it neglects the acceptor cavity in the stationary phase. However, as popular as it might be in RBP-LC, the solvophobic theory is not an entirely satisfactory model for chromatographic retention processes because it requires a change of cavity size in only a single phase [17] (the mobile phase). For NBP-LC under certain circumstances, not only the mobile phase but also the acceptor cavity in the stationary phase should be involved in the retention

process. In such cases, the partitioning model [17,18] will prevail, *i.e.*, the contributions from both stationary (term i) and mobile phases (term ii) are important in retention.

If the transfer process is dominated by partitioning rather than adsorption, the simplest model of retention is based on the assumption that the stationary phase is an amorphous bulk fluid and that retention resembles ordinary bulk-phase partitioning. In this case, the principal driving force for the transfer of solute is its relative chemical affinity for mobile and stationary phases; *i.e.* solute transfer involves (i) the creation of a solute-sized cavity in the stationary phase, (ii) the transfer process, and (iii) the closing of a solute-sized cavity in the mobile phase (see Fig. 1). As we will discuss later, it appears that the amino bonded exhibits dual retention characteristics: adsorption dominates at low modifier contents, with partitioning becoming important as the modifier reaches a mobile phase concentration that saturates the stationary phase.

## EXPERIMENTAL

### Equipment

All measurements were obtained with an HPLC system consisting of a IBM 9533 programmable ternary gradient liquid chromatographic system, Beckmen 506 Autosampler with 20- $\mu$ l sample loop, Gilson Model 111 UV detector (254 nm), Nelson 900 Series interface and an IBM-compatible AT computer.

### Analytical columns

The aminopropyl column (25 cm  $\times$  46 mm I.D., 5  $\mu$ m packing) was purchased from E. M. Science (Cherry Hill, NJ, USA). The column was used as received.

### Solutes and solvents

Hexane, methyl *tert.*-butyl ether (MTBE), chloroform and dichloroethane, each HPLC grade, were obtained from Fisher Scientific (Pittsburgh, PA, USA). Aromatic hydrocarbon solutes (phenanthrene, chrysene and perylene) and alkyl aryl ketone homologous series (propiophenone, butyphenone, hexanophenone, heptanophenone and octanophenone) were both obtained from Aldrich (Milwaukee, WI, USA). Phenol, nitrobenzene and aniline (re-

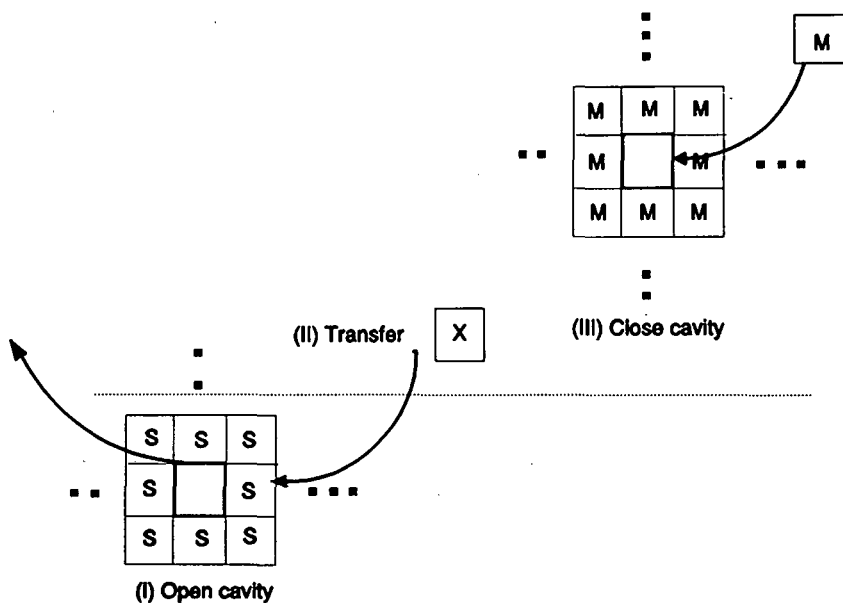


Fig. 1. Mechanics of molecule exchange in transfer processes such as partitioning or adsorption. The transfer of solute molecule X requires the opening of a cavity in stationary phase S and the closing of a cavity in mobile phase M.

agent grade) were obtained from Mallinckrodt (St. Louis, MO, USA). Aniline and nitrobenzene were purified by distillation, while phenol was used without further purification.

#### Procedures

Repeated injections of perylene and phenanthrene were used to measure the reproducibility of retention times. Reported  $t_0$  values are the result of at least three replicate injections. The flow-rate was maintained at 0.5 ml/min during the course of these studies. No less than fifteen column volumes were allowed for column equilibration upon a change of mobile phase.

In the system peaks studies, pure hexane was injected as a solute. Hexane's negative system peak was also used as the  $t_0$  marker.

## RESULTS AND DISCUSSION

#### System peaks

The deflection (positive or negative) of the system peak, as mentioned before, depends on that component's absorbance relative to the bulk mobile

phase at the detector wavelength. Fig. 2 is an illustration of the system peak in a real chromatogram, where the positive peak is due to chloroform, which absorbs significantly at 254 nm, while the negative peak is due to hexane.

Hexane is generally thought to be the least adsorbed mobile phase component available for NBP-LC. Thus, the retention volume of hexane is usually used to represent the mobile phase volume  $V_m$  (or void volume  $V_0$ ). However, the total column volume must remain constant, and any decrease of the mobile phase volume must therefore result in a corresponding increase in the volume of the stationary phase. As can be seen in Fig. 2b, the retention of hexane decreased as the modifier concentration increased from 20% to 40%. It has been suggested by Scott [19] that mobile phase can accumulate near the polar surface of the stationary phase, forming a stagnant layer. The statistical mechanical theories of retention [19-22] also predict what has been referred to as "breathing" [22]. These predictions are supported by evidence of decreasing void volumes as the modifier concentration is increased. Uptake of the polar modifier in this way could affect the driving

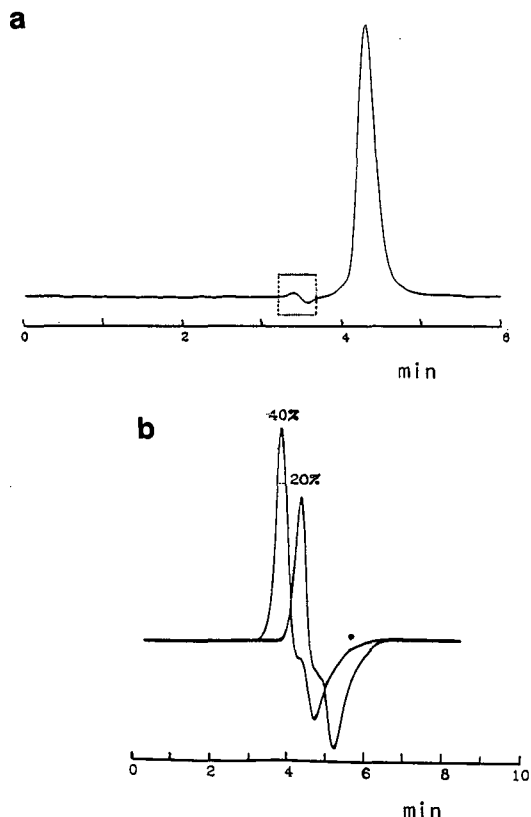


Fig. 2. (a) System peaks of a real chromatogram, with chloroform (20%, v/v) as the solvent modifier. The positive peak is due to chloroform, while the negative peak is due to hexane. (b) Enlargement of the system peak from (a). A system peak with chloroform at 40% is included for comparison. (see text for detail).

force for retention of solutes. Solutes could partition between this layer and the bulk mobile phase without directly interacting with the stationary phase.

Fig. 3 shows the trends in void volume decrease for three different modifiers. At about 60% polar modifier content, the void volume decreases reach a plateau. If the void volume at 0% modifier content is used as the reference point, the absolute value of the void volume differences can be interpreted as the degree of stationary phase accumulation under different modifier concentrations (Fig. 4). If the plateau in Fig. 4 is taken as the maximum coverage of stationary phase by modifier, then Fig. 4 can be replotted as the fractional coverage of the stationary phase (Fig. 5).

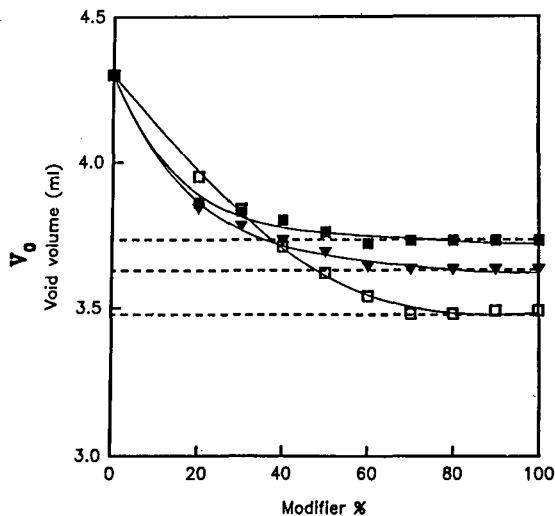


Fig. 3. Void volume changes vs. % modifier for three different solvent modifiers.  $\square$  = Chloroform;  $\blacktriangledown$  = dichloroethane;  $\blacksquare$  = methyl *tert.*-butyl ether. Amino column.

While the fractional surface coverage plots of Fig. 5 are not in actuality adsorption isotherms, they are related to isotherms. It is not our intention here to use the data of Figs. 4 and 5 for quantitative

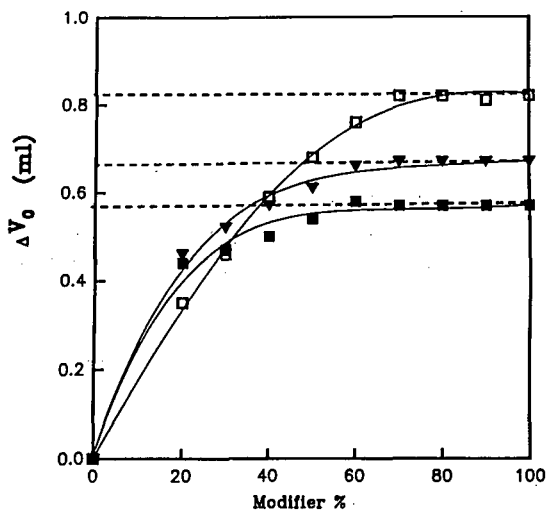


Fig. 4. If the void volume at 0% modifier content is used as the reference point, the absolute value of the void volume differences can be interpreted as the degree of modifier accumulation in the stationary phase. At about 60%, modifier ceases to accumulate in the stationary phase. Symbols as in Fig. 3. Amino column.

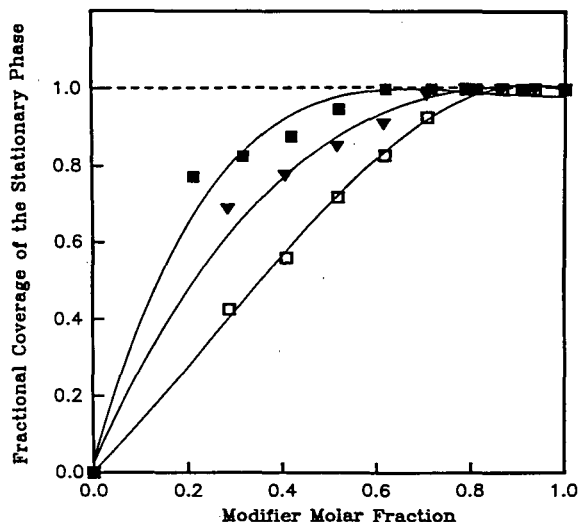


Fig. 5. Fractional coverage of the stationary phase. The plateau of Fig. 3 is taken as maximum surface coverage. Symbols as in Fig. 3.

isotherm calculations. Rather, we are interested in the *relative* affinities of the modifiers for the amino stationary phase. Clearly, chloroform shows both a higher stationary phase saturation concentration than the other two modifiers (greater  $V_0$  in Fig. 4), and more rapid approach to this saturation concentration (Fig. 5). Dichloroethane exhibits an intermediate affinity for this bonded phase, while MTBE has the lowest. Chloroform is categorized as an acidic solvent. Thus, its interaction with a basic column (amino) is expected to be the largest among these three modifiers. The observed trends for dichloroethane (dipolar solvent) and MTBE (basic solvent) are also in agreement with expectations and previous characterizations of the amino phase [23]. These data are also consistent with pure solvent strength calculations (chloroform 0.14, dichloroethane 0.12 and MTBE 0.10).

#### Partition vs. adsorption

Models of the surface structure of bonded phases help in visualizing LC retention mechanisms. For example, the surface of monomerically derivatized silica particles of the type used in this study may be pictured as a forest of organic functional groups standing on end. Thus, they are sometimes referred to as "brushes". As will be discussed, not only the

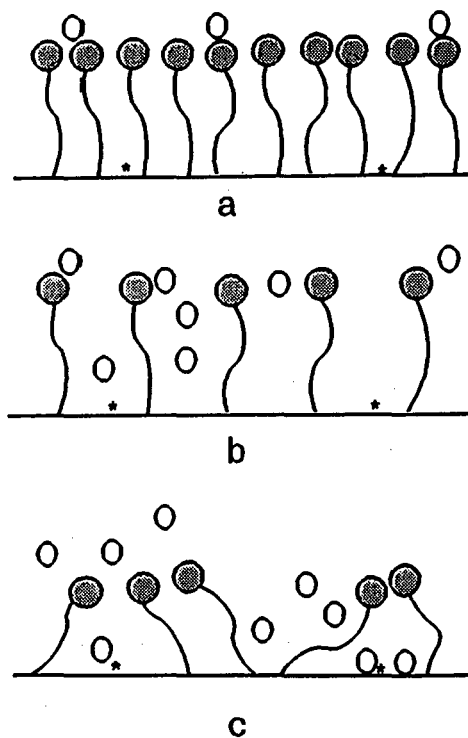


Fig. 6. Three different types of stationary phase configurations: (a) picket fence, (b) fur and (c) stack. In the "stack" structure, the grafted alkyl chains of NBP-LC stationary phases are not perpendicular to the surface, are in close contact with each other, and are less mobile than those in the "fur" configuration. Asterisks represent the strong adsorption sites (silanol groups).

character of the polar functional groups but also the mobility of the alkyl chains (alkyl "spacers") affect the retention behavior of normal bonded phases.

A number of models describing the configuration of these surface molecular brushes have been proposed [17,18,24–26]. Fig. 6 illustrates schematically three possible configurations at the silica gel surface. If a sufficiently dense stationary phase structure existed, solute molecules could not fit between the brushes and would interact only with the tip of the three-dimensional "picket fence". The nature of polar functional groups at the stationary phase surface would thus be the dominant retention factor. Obviously, the adsorption–displacement model would be applicable for such a structure, and the chromatographic effect of silanol groups at the silica surface would be negligible. However, because of steric constraints, the "fur" configuration (Fig.

6b) appears to be more realistic. This model implies that the distance between the alkyl chains is sufficiently large for certain solute molecules to bind to the chains laterally. In this configuration, both the polar functional groups and the strong adsorption sites on silica (silanol groups) can be involved in the retention process. Thus, the adsorption-displacement model needs to be modified to account for these effects [3,4,27]. In the “stack” structure, which is illustrated in Fig. 6c, the alkyl chains are not perpendicular to the surface but are in close contact with each other. In this arrangement, the alkyl chains are less mobile than those in the “fur” configuration. Instead of a distinct mobile-stationary phase boundary, the polar bonded phase and adsorbed mobile phase components are forming a “stationary phase layer”. In this fashion, an adsorbed solute molecule is not just in surface contact with the stationary phase anymore. Instead, it is more likely to partition between the three-dimensional stationary phase layer and the free-flowing, bulk mobile phase. Notice that here the alkyl chains of the bonded phase have a certain mobility, unlike the rigid rod approximation. It is the mobility of these polar functional groups which accounts for the dual behavior of this stationary phase.

Dill and Dorsey [17,18] have pointed out that in RBP-LC the “fur” models predict the grafted chains are fully exposed to the mobile-phase solvent. In light of the strength of the hydrophobic effect it should be prohibitively expensive in free energy terms for the chains to configure themselves to permit such a large degree of exposure. However, mobile phases in normal-phase LC are generally organic solutions. Thus, free energy prohibitions against “fur” and “stack” configurations do not exist in NBP-LC. In addition, strong polar interactions between active functional groups of the stationary phase and polar modifiers only enhance solvent-bonded phase mixing.

The existence of a distinct, bulk stationary phase in a fur or stack arrangement would suggest partitioning rather than adsorption would be the dominant retention process. In the bulk-phase partitioning model, retention is described as a process of transfer between bulk media of solute S from a single-component mobile phase A. However, for real chromatographic retention processes, the mobile phase is not generally a single-component

solvent; typical mobile phase solvents for the NBP-LC are mixtures of hexane with organic modifiers such as chloroform or dichloroethane. Thus, the partitioning model can be readily generalized to account for mobile phase mixtures of components A and B, with relative concentrations  $\varphi_A$  and  $\varphi_B$ , respectively, provided A and B are randomly dispersed. Thus, the partition model predicts [17,18] that there is a quadratic, not linear, relationship between  $\ln k'$  and the volume composition of the modifiers ( $\varphi$ ).

$$\ln k' = A - B\varphi + C\varphi^2 \quad (5)$$

or

$$(1/\varphi) \ln(k'/k'_0) = -B + C\varphi \quad (6)$$

where  $k'$  is the capacity factor,  $\varphi$  is modifier fraction and  $k'_0$  is the value of  $k'$  when  $\varphi = 0$ ;  $A$ ,  $B$  and  $C$  are constants.

The  $A$  constant of eqn. 5 has been replaced in eqn. 6 by the logarithm of the capacity factor of the solute in a purely hexane mobile phase. This constant cannot normally be determined directly since, without organic modifier in the mobile phase and thus no modifier adsorbed on the stationary phase, the nature of the stationary phase is considerably altered [28].

Interestingly, a similar relationship between the retention of acidic (phenol), basic (aniline), and dipolar (nitrobenzene) solutes and mobile composition has been observed for the amino column at high modifier contents (Fig. 7). The bulk phase partitioning model predicts that a plot of  $(1/\varphi) \ln(k'/k'_0)$  vs.  $\varphi$  should be linear (eqn. 6), provided the random mixing approximation [20–22] holds. However, when the modifier concentration is below ca. 10%, dispersive intermolecular interactions of the polar stationary phase result in a reduction of the effective chromatographic surface area and reduced retention behavior [29]. Once these “brush-type” phases are in contact with a mobile phase containing ca. 10% of an organic modifier, they exhibit normal retention. From the data of Fig. 6, with modifier contents between 10 and 50%, eqn. 6 does not adequately describe retention. However, as the modifier concentration increases beyond 50% the linear prediction appears valid, implying that the partition model seems to be suitable under these conditions. These retention data correlate nicely

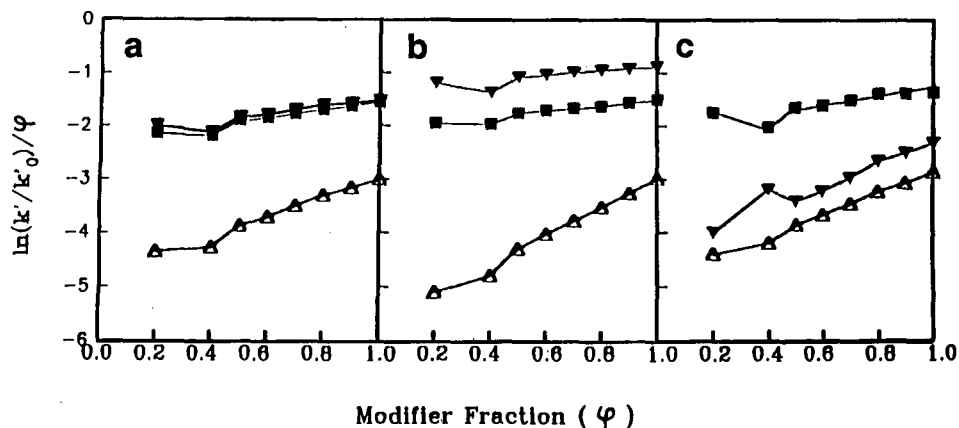


Fig. 7. Retention data for phenol ( $\Delta$ ), aniline ( $\blacktriangledown$ ) and nitrobenzene ( $\blacksquare$ ) in three different solvent modifiers plotted according to eqn. 6. Amino column. (a) Chloroform; (b) methyl *tert.*-butyl ether; (c) dichloroethane.

with the data obtained from system peaks (Figs. 3-5), where the fractional coverage of the stationary phase reached 100% at about 60% modifier concentration. At low concentrations of modifier the bonded stationary phase is not well-solvated, and alkyl chains with their polar ends are largely ordered. As modifier content in the mobile phase increases, modifier molecules begin to penetrate the bonded phase, essentially solvating it. Apparently, at *ca.* 60% modifier content, the stationary phase can now be considered a randomly mixed bulk phase, and retention is best described as partitioning rather than adsorption.

There is another retention feature that is diagnostic of bulk-phase partitioning [17,18,30-32]: the logarithm of the capacity factor depends approximately linearly on the size of the solute molecule, as does the partition coefficient, since the volume(s) of the cavity(s) created in the mobile (and possibly stationary) phase(s) to accommodate the solute molecule is (are) a significant term in the overall free energy change (eqns. 2 and 4 and Fig. 1). This dependence of retention on molecular volume in partitioning systems has been widely observed [30-32]. In order to see if such a dependence was operating here, the retention of a series of describe (propiophenone, butyrophenone, hexaphenone, heptanophenone and octanophenone) was measured with MTBE as the polar modifier (Fig. 8). Below 60% modifier concentration, the  $\log k'$  vs. the carbon number ( $n_c$ ) plots seem to be somewhat

random, although a distinct trend is observed. However, for modifier contents greater than 60%, a strong linear relationship between  $\log k'$  and  $n_c$  is obvious. We believe this data further supports the argument that at polar modifier concentrations above *ca.* 60%, partitioning rather than adsorption is the dominant retention mechanism. It should be noted that only MTBE data is shown here. The other two modifiers are too strong for retention of the alkyl aryl ketone homologues to be observed at concentrations above 60%. However, all data point to chloroform and dichloroethane behaving qualitatively exactly like MTBE.

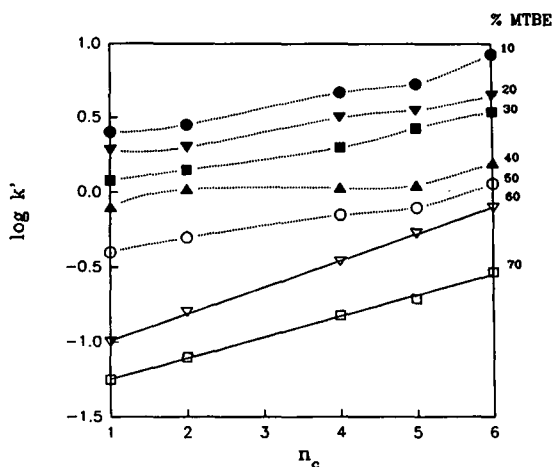


Fig. 8.  $\log k'$  vs. solute size of alkyl aryl ketone homologues. Amino column.

## CONCLUSIONS

We have concluded that two different retention mechanisms are possible in an aminopropyl NBP-LC column. At low modifier concentrations the adsorption–displacement model appears to work, provided certain modifications are included. However, when the concentration of modifier reaches 60%, a bulk partitioning process seems to result. These conclusions are based on three lines of evidence. First, hexane system peaks indicate that stationary phase volumes increase with increasing mobile phase modifier concentrations up to ca. 60%. Thus, the assumption of a monolayer of mobile phase at the surface of the stationary phase does not appear to be valid. Above 60%, however, where the volume expansion of stationary phase ceases, retention data indicate that the partition model is obeyed quite nicely. It is at this level of modifier that the stationary phase is completely solvated and the random mixing approximation holds. Finally, the retention data of the describe also suggest that the creation of the mobile phase cavity is important for modifier concentrations above 60%. It is the unique character of NBP-LC which accounts for the dual behavior of the stationary phase. For modifier concentrations < 60%, adsorption dominates. However, as modifier kept accumulates in the stationary phase, a bulk stationary phase layer forms, with partitioning becoming the dominant retention process.

## ACKNOWLEDGEMENT

The authors would like to acknowledge the support of the Environmental Protection Agency, Office of Research and Development, Grant R-814485-01-0.

## REFERENCES

- 1 S. R. Abbott, *J. Chromatogr. Sci.*, 18 (1980) 540.
- 2 R. E. Majors, *J. Chromatogr. Sci.*, 18 (1980) 488.
- 3 W. T. Cooper and P. L. Smith, *J. Chromatogr.*, 249 (1987) 410.
- 4 L. R. Snyder and H. Poppe, *J. Chromatogr.*, 184 (1980) 363.
- 5 L. R. Snyder, *Principles of Adsorption Chromatography*, Marcel Dekker, New York, 1968.
- 6 L. R. Snyder, *Anal. Chem.*, 46 (1974) 1384.
- 7 R. P. W. Scott and P. Kucera, *J. Chromatogr.*, 142 (1977) 213.
- 8 M. Jaroniec and J. A. Jaroniec, *J. Liq. Chromatogr.*, 4 (1976) 2121.
- 9 M. Jaroniec and J. Oscik, *J. High Resolut. Chromatogr. Chromatogr. Commun.*, 5 (1982) 3.
- 10 L. R. Snyder, in Cs. Horváth (Editor), *High-Performance Liquid Chromatography—Advances and Perspectives*, Vol. 3, Academic Press, New York, 1983, p. 157.
- 11 S. Levin and E. Grushka, *Anal. Chem.*, 57 (1985) 1830.
- 12 S. Levin and E. Grushka, *Anal. Chem.*, 58 (1986) 1602.
- 13 J. J. Stranahan and S. N. Deming, *Anal. Chem.*, 54 (1982) 1540.
- 14 P. Jandera, H. Colin and G. Guiochon, *Anal. Chem.*, 54 (1982) 435.
- 15 Cs. Horváth, W. Melander and I. Molnar, *J. Chromatogr.*, 129 (1976) 15.
- 16 Cs. Horváth and W. Melander, *J. Chromatogr. Sci.*, 15 (1977) 339.
- 17 K. A. Dill, *J. Phys. Chem.*, 91 (1987) 1980.
- 18 K. A. Dill and J. G. Dorsey, *J. Chem. Rev.*, 89 (1989) 337.
- 19 R. P. W. Scott, *J. Chromatogr. Sci.*, 18 (1980) 297.
- 20 D. E. Martire and R. E. Boehm, *J. Phys. Chem.*, 84 (1980) 3620.
- 21 D. E. Martire and R. E. Boehm, *J. Liq. Chromatogr.*, 3 (1980) 753.
- 22 D. E. Martire and R. E. Boehm, *J. Phys. Chem.*, 87 (1983) 1045.
- 23 W. T. Cooper and P. L. Smith, *J. Chromatogr.*, 355 (1986) 57.
- 24 W. R. Melander and Cs. Horváth, in Cs. Horváth (Editor), *High-Performance Liquid Chromatography—Advances and Perspectives*, Vol. 2, Academic Press, New York, 1980, p. 113.
- 25 L. C. Sander, J. B. Callis and L. R. Field, *Anal. Chem.*, 55 (1980) 1068.
- 26 K. K. Unger, N. Becker and P. Roumeliotis, *J. Chromatogr.*, 125 (1976) 115.
- 27 L. R. Snyder, *J. Chromatogr.*, 255 (1983) 3.
- 28 L. B. Rogers and M. E. McNally, *J. Chromatogr.*, 17 (1985) 879.
- 29 R. P. W. Scott and C. F. Simpson, *J. Chromatogr.*, 197 (1980) 11.
- 30 H. Colin, A. M. Krstulovic, M. F. Gonnord, G. Guiochon and Z. Yun, *Chromatographia*, 17 (1983) 9.
- 31 G. E. Berendsen and L. de Galan, *J. Chromatogr.*, 196 (1980) 21.
- 32 B. A. Bidlingmeyer, S. N. Deming, W. P. Price, Jr., B. Sachok and M. Petrusek, *J. Chromatogr.*, 186 (1980) 419.



# Supports for liquid–liquid partition chromatography in aqueous two-phase systems: a comparison of Superdex and LiParGel

Christer Wingren, Ulla-Britt Hansson and Kerstin Andersson

*Department of Biochemistry, Lund University, S-221 00 Lund (Sweden)*

(First received December 20th, 1991; revised manuscript received February 17th, 1992)

---

## ABSTRACT

The ability of Superdex 200, a gel filtration matrix consisting of dextran-grafted beads, to act as a support for liquid–liquid partition chromatography (LLPC) in aqueous polyethylene glycol (PEG)–dextran two-phase systems was examined. The gel adsorbed the dextran-rich bottom phase readily and retained it during elution with the PEG-rich top phase. In contrast to LiParGel 650, a matrix designed for LLPC, the entire Superdex matrix seemed to form an immobilized stationary phase. Ideal partitioning of proteins was observed only for molecules partitioning towards the stationary phase on Superdex and for those favouring the mobile phase on LiParGel. Hence, the choice of matrix depends on the separation problem at hand.

---

## INTRODUCTION

Partitioning in aqueous two-phase systems has been used for many years to separate and isolate cells, organelles and macromolecules. The method may also provide information about conformational changes occurring upon interactions between molecules [1], as the distribution of a molecule in these systems depends on its conformation and general surface properties [2–5]. By optimizing the composition of the phases, separation may be achieved in only a few steps. However, finding such optimum systems may pose difficulties and in most instances multiple extractions are required in order to obtain an adequate separation. As this procedure is tedious, various forms of automated counter-current extraction have been developed [6–8]. The time required for the analyses may be further reduced by employing column chromatography. A column

chromatographic approach would also increase the plate number and, hence, the sensitivity of the method.

An early attempt to immobilize one of the phases was made by merely soaking agarose beads in the bottom phase of the most thoroughly studied system formed by polyethylene glycol (PEG) and dextran, using the top phase as a mobile phase [9]. Since then, several materials have been studied and rejected as supports for liquid–liquid partition chromatography in aqueous two-phase systems (LLPC) [10]. In the end, hydrophilic vinyl particles grafted with polyacrylamide were found to be able to adsorb the dextran-rich bottom phase of PEG–dextran systems in amounts sufficient for partitioning [10,11]. LLPC on this matrix, LiParGel, has been shown to be a powerful tool for the qualitative structural analysis of, for instance, immunoglobulins [12].

However, as the bottom phase is adsorbed mainly as microdroplets inside the pores of the LiParGel particles [10], the volume of stationary phase available for partitioning of a protein is dependent on its

---

*Correspondence to:* Dr. Kerstin Andersson, Department of Biochemistry, Chemical Centre, Lund University, P.O. Box 124, S-221 00 Lund, Sweden.

ability to enter the pores. Hence, we were interested in finding an alternative support for LLPC in PEG–dextran two-phase systems which might be more evenly coated than LiParGel. The idea of a matrix resembling one of the phases, *i.e.*, an immobilized stationary phase, was appealing in order to avoid bleeding of the columns. Hubert *et al.* [13] have reported successful fractionations by LLPC on a matrix to which polyethylene oxide was bound covalently using a dextran-containing mobile phase. However, as was pointed out, the viscosity of dextran solutions may become a considerable drawback. This problem would be circumvented by binding the dextran to the support and eluting the columns with the PEG-rich phase, which is less cumbersome to handle.

Superdex was recently developed for size-exclusion chromatography. The matrix consists of macroporous agarose beads grafted with dextran. The mobility of these chains gives the gel the character of a dextran solution bound to the agarose support [14]. Hence Superdex particles may be expected to provide an immobilized stationary phase for LLPC in PEG–dextran systems.

In this work we compared the properties of Superdex 200 with those of LiParGel 650 with respect to their ability to adsorb the dextran-rich bottom phase of aqueous PEG–dextran two-phase systems and the influence of the supports on the elution of proteins in these LLPC columns.

## EXPERIMENTAL

### Materials

Dextran T 500 ( $M_r = 500\,000$ ) was supplied by Pharmacia LKB Biotechnology (Uppsala, Sweden). Polyethylene glycol 8000 (PEG) ( $M_r = 6000\text{--}7500$ ) was obtained from Union Carbide (New York, USA). LiParGel 650 was a gift from Merck (Darmstadt, Germany) and Superdex 200 prep grade was a gift from Pharmacia LKB Biotechnology. Horseradish peroxidase was obtained from Merck and whale skeletal muscle myoglobin from Sigma (St. Louis, MO, USA). Human albumin, rabbit aldolase, bovine catalase and bovine thyroglobulin were produced by Pharmacia LKB Biotechnology. Human transferrin was obtained from Sigma. Human immunoglobulin G (IgG) (Sandoglobulin) was obtained from Sandoz (Basel, Switzerland). Rabbit

IgG (rabbit anti-human albumin) was supplied by Dakopatts (Glostrup, Denmark).

### The two-phase system

All experiments were performed in a 4.4% (w/w) PEG 8000–6.2% (w/w) dextran T 500 two-phase system at pH 7.0. The compositions of the phases are given in Fig. 1. Two compositions of salts were used: 50 mM sodium phosphate–0.1 M NaCl–0.1 M glycine (the 0.1 M glycine system) and 10 mM sodium phosphate–0.1 M NaCl–0.2 M glycine (the 0.2 M glycine system). The concentrations of dextran in the top and bottom phases were not affected by the changes in the salt content as determined polarimetrically. Titration of the phases with 1 M HCl and/or 1 M NaOH showed that glycine was equally distributed between the phases.

### Determination of partition properties

The partition properties of the proteins were determined as their partition coefficients in batch experiments. A 4-g amount of the two-phase system described above was thoroughly mixed with 4 mg of protein and allowed to separate at 20°C overnight. The partition coefficient,  $K_{\text{batch}}$ , was defined in accordance with the notation commonly used for aqueous two-phase partitioning [2], *i.e.*,

$$K_{\text{batch}} = C_{\text{top phase}}/C_{\text{bottom phase}}$$

where  $C_{\text{top phase}}$  and  $C_{\text{bottom phase}}$  are the concentrations of the protein in the top and bottom phases, respectively, determined spectrophotometrically at 280 nm. The presence of polymers in the solvent did not affect the molar absorptivities of the proteins. It should be noted that no precipitates could be observed in the interphase after incubation overnight.

### Interactions of proteins with the matrices

A 3-mg amount of albumin or 2 mg of IgG dissolved in 0.9% NaCl were mixed with 1 ml of gel (LiParGel or Superdex) for 1 h at room temperature. The amount of protein remaining in/on the matrix was determined by measuring the concentration of the protein in the supernatant spectrophotometrically at 280 nm ( $\epsilon_{\text{IgG}} = 1.3 \text{ ml mg}^{-1} \text{ cm}^{-1}$ ,  $\epsilon_{\text{albumin}} = 0.6 \text{ ml mg}^{-1} \text{ cm}^{-1}$ ).

### Preparation of LLPC columns

The preparation of the LLPC columns is shown

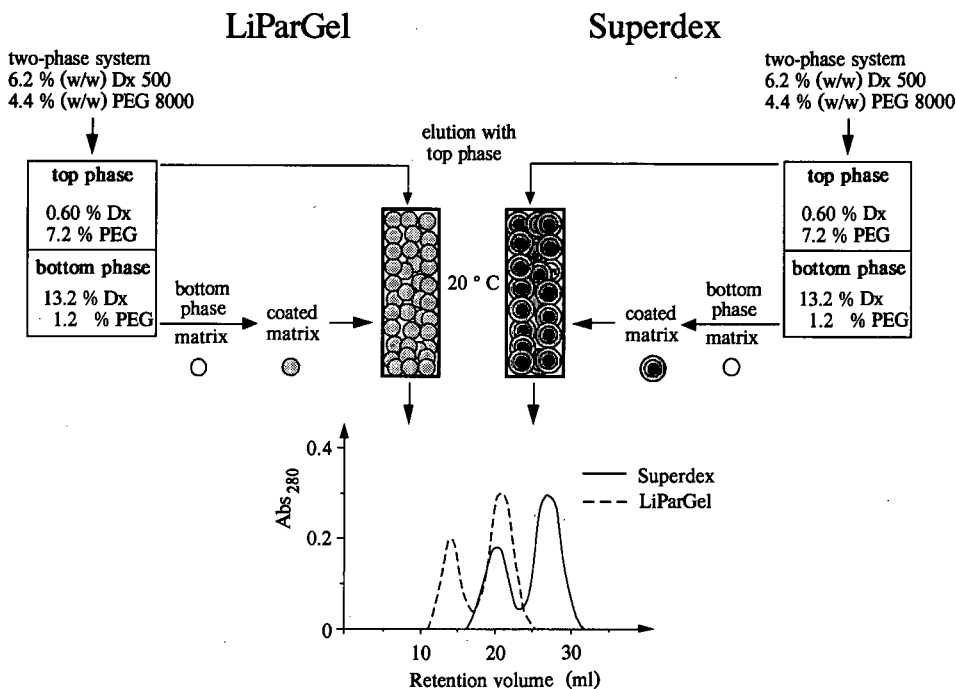


Fig. 1. Schematic diagram of the preparation of LLPC columns. The chromatograms for the references, peroxidase and myoglobin, on (solid line) Superdex and (dashed line) LiParGel, respectively, obtained in the 0.1 M glycine system are shown.

schematically in Fig. 1. The two-phase system, prepared as described previously [15], was equilibrated at 20°C for 72 h and the clear phases were separated. The matrix, LiParGel 650 or Superdex 200 prep grade, was allowed to equilibrate with the dextran-rich bottom phase (stationary phase) at room temperature. Excess of bottom phase was removed by rinsing the coated matrix with the PEG-rich top phase (mobile phase). The coated matrix was suspended in 3–4 volumes of mobile phase and poured into a thermostated (20°C) glass column (35 × 1 cm I.D.) with a filling reservoir. The columns were packed at a flow-rate of 0.2–0.6 ml min<sup>-1</sup> and equilibrated with about 3 volumes of the mobile phase at a flow-rate of 0.2 ml min<sup>-1</sup> until the eluates were almost clear. Samples were applied in 1.0 ml of mobile phase with the addition of about 5 mg of glycine. Eluates were monitored continuously at 280 nm.

In order to examine the ability of Superdex to act as a stationary phase in itself, uncoated Superdex 200 was packed in a column and equilibrated with 7.2% PEG–50 mM sodium phosphate–0.1 M

NaCl–0.1 M glycine (pH 7.0) (i.e., a solution corresponding to the top phase of the 0.1 M glycine system but without any dextran). Samples were applied to the column as described above.

#### Calculations

The parameters of the LLPC columns were determined as described earlier [10] using peroxidase and myoglobin as references. The distribution of the references between the phases in the LLPC column was assumed to be identical with their partitioning in batch, i.e., the inverted value of  $K_{\text{batch}}$  equalled  $K_C$  for the references, where  $K_C$  is the ratio of the concentration of a molecule in the stationary (dextran-rich) phase to that in the mobile (PEG-rich) phase:

$$K_C = C_{\text{stationary phase}}/C_{\text{mobile phase}}$$

The volumes of the stationary and mobile phases,  $V_S$  and  $V_M$ , were calculated from the retention volumes for the references,  $V_R$ , according to

$$V_R = V_M + K_C V_S \quad (1)$$

The standard deviation of the retention volumes for the two references was less than 5%. The volumes of stationary and mobile phases were averaged for all columns used, accounting for the number of runs on each column, with a variation less than 6% of the column volume.

The plate number,  $N$ , was calculated from the peak width at half-height ( $w_h$ ) of the myoglobin peak according to

$$N = 5.54(V_R/w_h)^2 \quad (2)$$

The resolution,  $R_s$ , of the peroxidase and myoglobin peaks was calculated as

$$R_s = (\sqrt{N/4})[k/(1+k)](\alpha - 1) \quad (3)$$

where  $k$  is the capacity factor and  $\alpha$  is the ratio of the partition coefficients of the references ( $\alpha = K_{\text{batch, peroxidase}}/K_{\text{batch, myoglobin}}$ ).

In order to facilitate the comparison of chromatograms from columns with different parameters, the retention volume of each component was expressed as  $K_C$  using eqn. 1. In cases where the protein was fractionated into more than one component by LLPC,  $K_C$  was calculated from the average retention volumes for all components.

## RESULTS

The properties of Superdex as a support for liquid–liquid partition chromatography (LLPC) was compared with those of LiParGel in a salt-containing aqueous two-phase system formed by polyethylene glycol 8000 (PEG) and dextran T 500. The two compositions of salts used are referred to as 0.1  $M$  glycine and 0.2  $M$  glycine as described under Experimental. The changes in the salt content did not affect either the volume ratio of the two-phase system or the composition of the phases, as indicated by a constant concentration of dextran. Titration of the phases showed that glycine was equally distributed. However, the distribution of the proteins tended to shift towards the dextran-rich phase in the 0.2  $M$  glycine system (Table I).

In order to examine the ability of the dextran-grafted Superdex particles to form a two-phase system with a PEG-containing mobile phase, albumin, human IgG (HIgG) and the two references, peroxidase and myoglobin, were applied one by one on a Superdex column equilibrated with a solution cor-

TABLE I

SIZE, NET CHARGE AND PARTITIONING PROPERTIES OF THE PROTEINS STUDIED, TAKEN AS THE RELATIVE MOLECULAR MASS, THE ISOELECTRIC POINT (IEP) AND THE PARTITION COEFFICIENTS DETERMINED IN BATCH EXPERIMENTS, RESPECTIVELY

Protein	$M_r$	IEP	$K_{\text{batch}}^a$	
			0.1 $M$ glycine	0.2 $M$ glycine
Thyroglobulin	670 000	4.5	0.92	0.70
Catalase	230 000	5.4	0.69	0.40
Aldolase	160 000	6.1	0.48	0.32
RIgG	160 000	5.8	1.3	1.1
HIgG	160 000	6.8	0.66	0.67
Transferrin (–Fe)	80 000	6.2	0.46	0.27
Albumin	70 000	4.9	0.32	0.21
Peroxidase	40 000	7.2	1.2	1.1
Myoglobin	17 000	7.0	0.61	0.56

$$^a K_{\text{batch}} = C_{\text{top phase}}/C_{\text{bottom phase}}$$

responding to the top phase of the 0.1  $M$  glycine system but without any dextran. Although the separation was poor, the retention volumes for the four proteins differed slightly (Fig. 2). However, the retention volumes could not be correlated either to the partition properties of the proteins or to their sizes (Table I), in spite of Superdex being a gel filtration matrix. The volume of stationary phase per unit column volume, calculated from eqn. 1, was only 0.06 ml ml<sup>-1</sup>. Using the complete top phase of the equilibrated two-phase system as a mobile phase did not improve the resolution, indicating

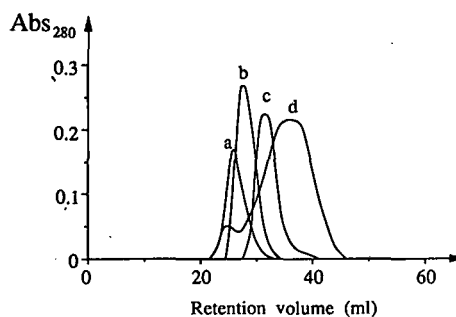


Fig. 2. Chromatogram for (a) peroxidase, (b) myoglobin, (c) albumin and (d) HIgG (0.8–1.1 mg) obtained on Superdex 200 in 7.2% PEG 8000–50 mM sodium phosphate–0.1  $M$  NaCl–0.1  $M$  glycine (pH 7.0).

TABLE II

## PARAMETERS OF THE COLUMNS USED

$V_C$  = column volume (ml);  $V_S$  = volume of the stationary phase (ml);  $V_M$  = volume of the mobile phase (ml);  $N$  = plate number per metre;  $R_s$  = resolution of peroxidase and myoglobin;  $n$  = number of runs (number of columns) for which the values are averaged.

Column	System	$V_S/V_C$ (ml ml <sup>-1</sup> )	$V_M/V_C$ (ml ml <sup>-1</sup> )	$N$ (m <sup>-1</sup> )	$R_s$	$n$
Superdex 200	0.1 M glycine	0.44 ± 0.01	0.71 ± 0.02	1700 ± 300	1.9 ± 0.2	4(2)
	0.2 M glycine	0.28 ± 0.04	0.81 ± 0.06	1800 ± 300	1.2 ± 0.2	18(7)
LiParGel 650	0.1 M glycine	0.37 ± 0.03	0.46 ± 0.03	1000 ± 200	1.5 ± 0.2	20(10)
	0.2 M glycine	0.32 ± 0.01	0.40 ± 0.01	1080 ± 150	1.7 ± 0.2	6(3)

that the amount of dextran on the Superdex particles was not large enough to form a two-phase system with the PEG-containing mobile phase. Thus, in order to obtain sufficient amounts of the two phases to allow a separation based on partitioning in this system, the Superdex particles were coated with the bottom phase of the PEG–dextran two-phase system. The preparation of LLPC column is depicted schematically in Fig. 1.

The parameters of the Superdex LLPC columns were calculated as described under Experimental and compared with those of LiParGel columns (Table II). The variation in the volumes of the stationary and mobile phases in a column, averaged for the columns used in this study, was less than 6% of the column volume for either of the matrices.

The volume of stationary phase adsorbed on the Superdex per unit column volume was smaller in the 0.2 M than in the 0.1 M glycine system. The changes were even more pronounced at slightly elevated pH (data not shown), indicating the involvement of ionic interactions in the coating of this matrix. It was also of interest that the total volume of the two phases equalled the column volume, indicating an extremely small volume of the support. In contrast to Superdex, the coating of LiParGel was only slightly affected by changes in the concentration of salts (Table II). Although the volume ratio, *i.e.*, the ratio of the stationary to the mobile phase, was constant, the total volume of the phases in the LiParGel columns was slightly smaller in the 0.2 M glycine system. This may indicate a swelling of the matrix in the presence of higher concentrations of salts.

Proteins were generally found to have a larger retention volume on the Superdex columns than on

LiParGel, which is exemplified by the chromatogram for the two references in Fig. 1. The resolution of the two reference proteins decreased with decreasing volume of stationary phase on Superdex, in spite of a constant plate number, whereas the reverse tendency was observed on LiParGel (Table II). As the flow-rate was similar in all experiments, the larger plate number in the Superdex columns indicated a larger surface area of stationary phase available for partitioning on these particles.

Fig. 3 shows the chromatogram for albumin, HlgG and rabbit IgG (RIgG) obtained by LLPC on

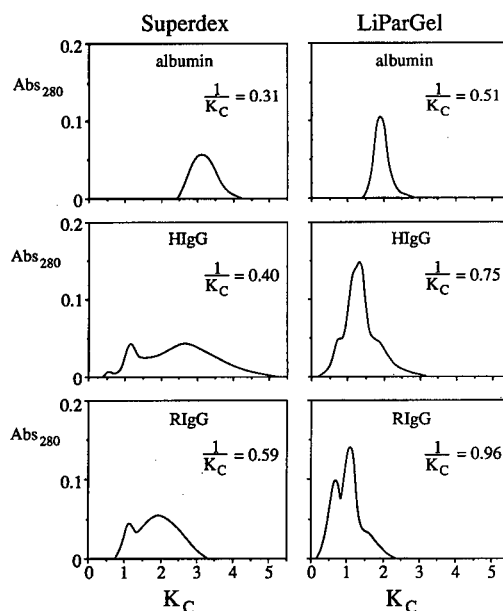


Fig. 3. Chromatograms for albumin, HlgG and RIgG (0.6–1.0 mg) obtained on Superdex and LiParGel in the 0.1 M glycine system. The average retention volume for each protein is given as an inverted value of  $K_C$ , which may be compared with  $K_{C, \text{batch}}$ .

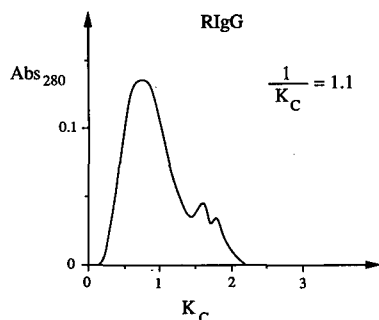


Fig. 4. Chromatogram for RIgG obtained on LiParGel in the 0.2 M glycine system. The average retention volume is expressed as  $1/K_C$ .

Superdex and LiParGel in the 0.1 M glycine system. The retention volumes were expressed as  $K_C$  (see Experimental) in order to facilitate the comparison of chromatograms obtained from columns with different parameters. Human albumin was eluted as a single peak on both matrices. IgG was fractionated into three poorly resolved components on LiParGel whereas Superdex gave a two-peak pattern, the peak with the largest retention volume being very broad. The elution profiles obtained in the 0.2 M glycine system were similar to those obtained in the 0.1 M system for all proteins except RIgG. On LiParGel, the characteristic three-peak pattern usually obtained for immunoglobulins on this matrix was shifted for RIgG into a pattern completely dominated by a peak with a small retention volume (Fig. 4). The difference between the elution patterns for IgGs on Superdex and those on LiParGel indicated a profound influence of the properties of the support on the results obtained by LLPC.

In order to evaluate the influence of the matrices on LLPC of proteins, the retention volumes were compared with those calculated from eqn. 1,  $V_{R, calc.}$ , using the inverted values of  $K_{batch}$  as  $K_C$ . A plot of the calculated retention volumes against the inverted values of  $K_{batch}$  is linear, the slope and the intercept of the line equalling the volumes of stationary and mobile phases, respectively. In Fig. 5, the calculated retention volumes for albumin, HIgG and RIgG are plotted together with those obtained experimentally, averaged for duplicate applications. It should be stressed that for IgG, and also for any protein that was fractionated into more than one component, all calculations refer to the average retention volume for the entire population.

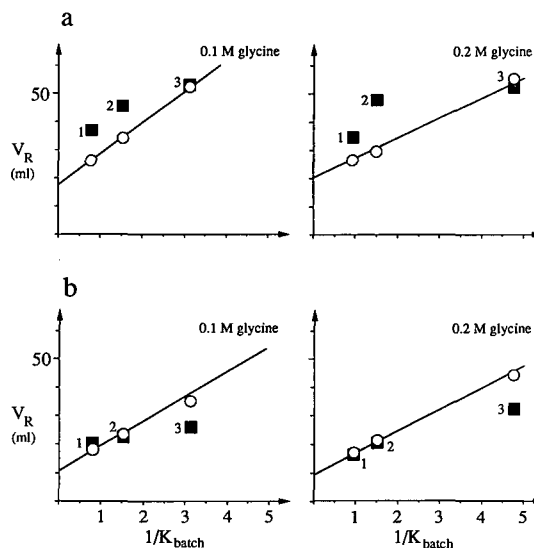


Fig. 5. Retention volumes calculated from eqn. 1 using the inverted values of  $K_{batch}$  as  $K_C$  (open symbols) as a function of the inverted values of  $K_{batch}$ , plotted together with the experimentally obtained retention volumes (closed symbols), for (a) Superdex and (b) LiParGel. The slope and the intercept of the lines equal the volumes of stationary and mobile phases, respectively, averaged for all columns used in each system referring to a column volume of 25 ml. 1 = RIgG; 2 = HIgG; 3 = albumin.

The retention volume for albumin on Superdex agreed with the calculated value whereas the IgGs were strongly retarded (Fig. 5a). In contrast, whereas the average retention volumes for IgG on LiParGel were in accordance with the theoretical values, the retention volume obtained for albumin on this matrix was considerably smaller than the calculated value (Fig. 5b). The results might be due to

TABLE III

AMOUNT OF ALBUMIN OR HUMAN IgG RETAINED IN/ON SUPERDEX 200 AND LIPARGEL 650 IN THE ABSENCE OF PHASE-FORMING POLYMERS

The proteins were added in excess to 1 ml of gel in 0.9% NaCl. The exclusion limits of the matrices are  $M_r$  600 000 and 5 000 000, respectively.

Column	Amount of protein retained (nmol ml <sup>-1</sup> gel)	
	Albumin	Human IgG
Superdex 200	8.1	11
LiParGel 650	5.1	5.9

differences in the capacity of the matrices or to an affinity of the proteins for the Superdex particles. In order to examine this point, HIgG and albumin were mixed with Superdex or LiParGel at low ionic strength (0.9% NaCl) in the absence of phase-forming polymers. Superdex was found to retain more protein than LiParGel (Table III). Furthermore, whereas LiParGel retained equimolar amounts of both proteins, the interaction of Superdex with IgG appeared to be stronger than that with albumin.

In an attempt to elucidate the properties responsible for the partitioning of proteins on the two matrices, another four proteins (aldolase, catalase, thyroglobulin, and transferrin) were applied to the columns. The salt concentrations were chosen to give the least ideal conditions in order to emphasize the deviations, *i.e.*, the 0.1 M glycine system on LiParGel and the 0.2 M system on Superdex (*cf.*, Fig. 5). The differences between the obtained retention volumes and the calculated values are shown in Fig. 6 as a function of the inverted values of  $K_{\text{batch}}$ . This difference may be considered to describe the influence of the chromatographic system on the partitioning of the molecules. The deviation from ideal elution of proteins on Superdex was not related to

either the partition properties in batch of the molecules or their isoelectric points (*cf.*, Fig. 6 and Table I). However, large proteins ( $M_r > 100\,000$ ) seemed to be retained whereas small molecules ( $M_r < 100\,000$ ) were eluted as expected. The discrepancy between the experimentally obtained retention volume and the calculated value decreased slightly for RIgG at higher concentrations of salts whereas it increased for HIgG. Hence the unexpected elution behaviour on Superdex was not related merely to the size or shape of the protein.

On LiParGel, the retention volumes agreed fairly well with the expected values although there was a tendency for early elution of molecules partitioning towards the dextran-rich phase, *e.g.*, albumin (Fig. 6). The deviation of albumin from the calculated retention volume was larger at higher concentrations of salts and even more pronounced at pH 4.5 (data not shown), which is close to the isoelectric point of the molecule. This observation would eliminate the possibility of an electrostatic repulsion of albumin from LiParGel in the LLPC columns.

## DISCUSSION

We have previously used LiParGel 650 as a support for liquid–liquid partition chromatography of immunoglobulins in aqueous PEG–dextran two-phase systems at pH 7.0 [12]. The hydrophilic vinyl particles grafted with polyacrylamide are able to retain the dextran-rich bottom phase of PEG–dextran two-phase systems during elution with the PEG-rich top phase as a mobile phase [11]. Superdex has, to our knowledge, so far been used only as a matrix for size-exclusion chromatography. The gel consists of macroporous agarose beads with an average size similar to that of the LiParGel particles (30–36  $\mu\text{m}$ ) [11,14]. The exclusion limit is reduced by binding dextran covalently to the surface of the beads and also to the walls of the pores. As these dextran chains retain a large degree of mobility, Superdex may be regarded as a solution of dextran immobilized to the agarose support [14]. Thus, resembling the bottom phase of PEG–dextran systems closely, Superdex would be expected to form a two-phase system with a PEG-containing mobile phase, *i.e.*, to constitute an immobilized stationary phase for LLPC. This expectation was supported by the fact that the elution of proteins on Superdex in a salt-

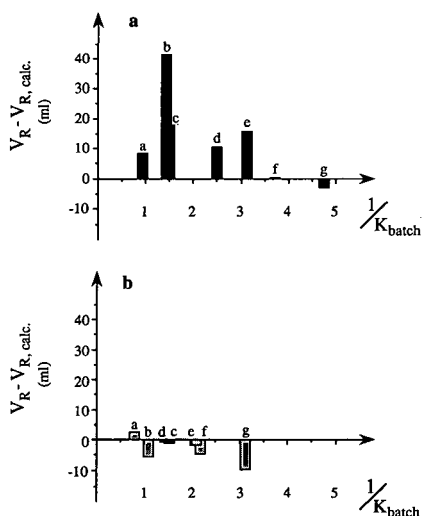


Fig. 6. Differences between the experimentally obtained retention volumes ( $V_R$ ) and those calculated as described in Fig. 5 ( $V_{R, \text{calc.}}$ ) as a function of the inverted values of  $K_{\text{batch}}$  for (a) Superdex in the 0.2 M glycine system and (b) LiParGel in the 0.1 M system. a = RIgG; b = thyroglobulin; c = HIgG; d = catalase; e = aldolase; f = transferrin; g = albumin.

containing solution of PEG was not related to their sizes (Fig. 2). However, the amount of dextran on the particles seemed to be insufficient to give an adequate resolution of proteins upon LLPC in the two-phase system used.

The coating of LiParGel is suggested to be due to the strong incompatibility of the polyacrylamide on the particles with PEG in the mobile phase rather than to an attraction of the dextran-rich phase to the matrix [10]. However, the volume of the stationary phase adsorbed on the matrix was found to be smaller at pH 4.5 than at neutral pH, indicating the involvement of electrostatic forces between the stationary phase and the LiParGel particles. This is in accordance with the observation of negative charges on LiParGel by others [16].

The stationary phase is considered to be adsorbed on LiParGel mainly as microdroplets inside the pores [10]. The exclusion limit for globular proteins on LiParGel being  $M_r$  5000 (information leaflet from Merck), all proteins used in this study should be able to penetrate the pores to gain access to the stationary phase. Nevertheless, large molecules may be partially excluded as the distribution of pore sizes of supports based on organic polymers easily ranges over one order of magnitude [15]. Considering the size of the phase-forming polymers, the accessibility of a molecule to the inside of the particles may be further reduced by the polymers in the stationary phase blocking the pores. However, the deviation from ideal elution observed on LiParGel could not be ascribed merely to exclusion phenomena (*cf.*, Fig. 6 and Table I).

Coating Superdex, we found that the matrix readily adsorbed the dextran-rich bottom phase of our two-phase system. This may seem surprising as dextran has been shown to elute well on Superdex in ordinary gel filtration buffers [14]. However, in the presence of PEG, the formation of a two-phase system would be expected as outlined above. The adsorption of the bottom phase may be due simply to mixing of dextran in the phases with that on the particles, which would give a phase system with a composition different from that of the original system. Hence the comparison of the observed elution behaviour on this matrix with that expected from the partitioning properties observed in batch experiments may be inaccurate. The chemical properties of the covalently bound dextran chains may also

differ from those of free dextran in solution owing to processing during the preparation of the matrix, implying the possibility of a three-phase system formed by immobilized dextran, free dextran and PEG, or by the core of the matrix (agarose), dextran and PEG.

As the dextran is bound both on the surface of the particles and on the walls inside the pores [14], the stationary phase would be more evenly distributed and more easily accessible on Superdex than that of LiParGel. The larger plate number for Superdex columns, in spite of similar flow-rates, also implies a larger surface of stationary phase available for partitioning. The total volume of phases in the Superdex columns was found to be equal to the column volume. This is in accordance with the extremely small relative volume of the matrix, *i.e.*, the volume of the support divided by the total volume of the support and the pores, reported [14]. Hence the entire support may be regarded as an immobilized stationary phase for LLPC.

In contrast to LiParGel, the degree of coating of Superdex was markedly reduced at higher concentrations of salts. In addition, the volume of the stationary phase was smaller at elevated pH (pH 8.2), indicating the involvement of ionizable groups with  $pK_a$  values in the range 7–8 in the adsorption of the stationary phase.

The influence of the supports on LLPC of a set of proteins was examined. For each matrix, the salt composition giving the least ideal results was chosen in an attempt to emphasize the deviations from ideal partitioning. It should be noted that the partitioning of a protein in PEG–dextran systems is related to the surface properties of the molecule, *e.g.*, its charge, size, shape and hydrophobicity [2–5, 12]. Hence the retention of a protein on an LLPC column is governed by a combination of these, and probably other still unknown, properties unless the experiment is designed to select a single parameter.

The retention volumes obtained on LiParGel were generally slightly smaller than those calculated and the deviation was more pronounced for molecules partitioning towards the bottom phase (Fig. 6). The differences between the experimentally obtained retention volume for a molecule and the calculated value may reflect a distortion of its conformation due to the repeated translocation over the interphase. It is conceivable that this effect would be

more pronounced for molecules favouring the dextran-rich stationary phase. However, as these molecules were found to elute earlier than expected, the non-linearity may rather be ascribed to non-equilibrium conditions in the columns due to difficulties in passing the interphase, *i.e.*, proteins are not allowed to partition properly between the phases.

On Superdex, all proteins except the smallest were eluted with a larger retention volume than that calculated (Fig. 6). The influence of the carboxyl groups present on Superdex on the retention of proteins may be neglected at ionic strengths higher than 0.2 M [17], which agrees with the lack of correlation between the retention of a molecule and its net charge (Fig. 6). A more plausible explanation for the retardation of large molecules emerges from the view of the phases as a network of polymers. In contrast to the situation in the LiParGel columns, this network is “immobilized” and fairly rigid in Superdex columns, restricting the free movement of large molecules. This hypothesis is supported by the extreme retention of thyroglobulin although the deviations from ideal elution could not be ascribed solely to the size of the molecules (Fig. 6). Taken together, LLPC of a molecule both on Superdex and on LiParGel is likely to reflect a combination of its surface properties, although the two matrices influence the partitioning in different ways.

The non-ideal partitioning of proteins on the two matrices might apply also to the two proteins used as references, peroxidase and myoglobin. In order to determine the parameters of a column properly, a set of standard proteins should be used, which has previously been pointed out by others [16]. Thus, the comparison of the parameters of Superdex columns with those of LiParGel columns may be deceiving. However, as the retention volume for each protein is related to those for the references run on the same column, the elution behaviour relative to the other molecules would not be affected.

Although the parameters governing the partitioning in the columns are still obscure, LLPC has turned out to be a powerful and yet simple method for acquiring qualitative information concerning the conformation of molecules and also conformational changes following interactions between mole-

cules (unpublished observations). Here, we have shown that LLPC of proteins on LiParGel agrees fairly well with the partition properties of molecules favouring the PEG-rich phase whereas ideal elution was observed on Superdex only for molecules partitioning towards the dextran-rich phase. However, the deviations from ideal behaviour are not necessarily a disadvantage but may be exploited as an additional parameter for separation. Hence the two matrices are complementary to each other and the choice depends on the separation problem at hand.

#### ACKNOWLEDGEMENT

This work was supported by grants from the Swedish National Board for Technical Development.

#### REFERENCES

- 1 L. Backman, in H. Walter, D. E. Brooks and D. Fisher (Editors), *Partitioning in Aqueous Two-Phase Systems*, Academic Press, Orlando, FL, 1985, pp. 267–314.
- 2 P.-Å. Albertsson, *Partition of Cell Particles and Macromolecules*, Wiley, New York, 3rd ed., 1986.
- 3 G. Johansson, in H. Walter, D. E. Brooks and D. Fisher (Editors), *Partitioning in Aqueous Two-Phase Systems*, Academic Press, Orlando, FL, 1985, pp. 161–226.
- 4 P.-Å. Albertsson, *J. Chromatogr.*, 159 (1978) 111.
- 5 H. Walter, G. Johansson and D. E. Brooks, *Anal. Biochem.*, 197 (1991) 1.
- 6 B. Andersson and H.-E. Åkerlund, *Biochim. Biophys. Acta*, 503 (1978) 462.
- 7 P.-Å. Albertsson, B. Andersson, C. Larsson and H.-E. Åkerlund, *Methods Biochem. Anal.*, 28 (1982) 115.
- 8 H.-E. Åkerlund, *J. Biochem. Biophys. Methods*, 9 (1984) 133.
- 9 H. S. Anker, *Biochim. Biophys. Acta*, 229 (1971) 290.
- 10 W. Müller, *Liquid-Liquid Partition Chromatography of Biopolymers*, GIT, Darmstadt, 1988.
- 11 W. Müller, *Eur. J. Biochem.*, 155 (1986) 213.
- 12 U.-B. Hansson, K. Andersson, Y. Liu and P.-Å. Albertsson, *Anal. Biochem.*, 183 (1989) 305.
- 13 P. Hubert, R. Mathis and E. Dellacherie, *J. Chromatogr.*, 539 (1991) 297.
- 14 L. Kågedal, B. Engström, H. Ellegren, A.-K. Lieber, H. Lundström, A. Sköld and M. Schenning, *J. Chromatogr.*, 537 (1991) 17.
- 15 W. Müller, *Bioseparation*, 1 (1990) 265.
- 16 A. Walsdorf and M. R. Kula, *J. Chromatogr.*, 542 (1991) 55.
- 17 I. Drevin, L. Larsson, I. Eriksson and B.-L. Johansson, *J. Chromatogr.*, 514 (1990) 137.



# Systematic study on the resolution of derivatized amino acids enantiomers on different cyclodextrin-bonded stationary phases

Sun Haing Lee<sup>☆</sup>, Alain Berthod<sup>☆☆</sup> and Daniel W. Armstrong

Department of Chemistry, University of Missouri-Rolla, Rolla, MO 65401 (USA)

(First received July 17th, 1991; revised manuscript received February 21st, 1992)

## ABSTRACT

The chiral separation of amino acids by liquid chromatography using cyclodextrin-bonded stationary phases was studied systematically. Six types of native and chemically modified  $\beta$ -cyclodextrin-bonded stationary phases have been used to separate enantiomers of some derivatized amino acids in the reversed-phase high-performance liquid chromatography mode. Chiral separations with (*R*)- and (*S*)-naphthyl-ethylcarbamate- $\beta$ -cyclodextrin (NEC- $\beta$ -CD) bonded phases were compared with similar separations with the native  $\beta$ -CD stationary phase. Racemic dansyl amino acids were separated best on  $\beta$ -CD column while 3,5-dinitro-2-pyridyl-, dansyl-, and 3,5-dinitrobenzoyl-amino acids were resolved best on the (*R*)- or (*S*)NEC- $\beta$ -CD column. The role of the mobile phase was studied. Effects of organic modifiers, ionic strength, and pH of the mobile phase on retention and enantioselectivity of the analytes were investigated on three stationary phases. The enantiomer elution order of all dansyl amino acids on native and NEC- $\beta$ -CD bonded stationary phases was L before D enantiomer, while a reverse elution order for dansyl amino acids was observed. Hence, elution order can be controlled by choosing the appropriate functional group. This provides an alternative to the current method of changing retention order by changing the stationary phase (*i.e.*, obtaining a different column). It appears that the NEC- $\beta$ -CD bonded phases are highly effective multimodal chiral stationary phases. The chiral recognition model involving inclusion complexation and  $\pi$ - $\pi$  interactions is discussed.

## INTRODUCTION

Two general approaches for the direct liquid chromatographic separation of enantiomers have been used. One involves use of chiral stationary phases (CSPs) and the other makes use of chiral mobile phase additives (CMAs). A number of new and improved CSPs and CMAs have been introduced to solve problems involving enantiomeric separations. A series of the recently developed bonded stationary phases derive from cyclodextrins (CDs), which are cyclic oligosaccharides containing

D(+)-glucopyranose units. There are three naturally occurring CDs,  $\alpha$ -cyclodextrin,  $\beta$ -cyclodextrin and  $\gamma$ -cyclodextrin commercially available. Since all of the primary and secondary hydroxyl groups of CDs are on the outside of this toroidal shaped molecule, the cavity is relatively non-polar, thus allowing CDs to form inclusion complexes with a variety of polar or non-polar molecules. It is apparent that the size and geometry of a guest molecule in relation to that of the cyclodextrin cavity is an important factor in inclusion complex formation. Inclusion complex formation is determined by the several different factors which include hydrophobic effect, hydrogen bonding, Van der Waals interactions, release of high-energy water from the CD cavity, and a change in ring strain upon complexation [1,2]. CD was attached to silica gel via a linkage chain to form an effective high-performance CSP [3–7]. The  $\beta$ -CD

Correspondence to: Dr. D.W. Armstrong, Department of Chemistry, University of Missouri-Rolla, Rolla, MO 65401, USA.

<sup>☆</sup> On leave from Kyung National University, South Korea.

<sup>☆☆</sup> On leave from Laboratoire des Sciences Analytiques, UA CNRS 435, 69622 Villeurbanne Cedex, France.

bonded phases has been the most widely used of these columns. Enantiomeric resolution of a series of amino acids, barbiturate dioxolane, phenyl acetic acid derivatives, nicotine analogues, and many other compounds were successfully obtained with  $\beta$ -CD CSPs under reversed phase conditions.

Recently, derivatized cyclodextrin bonded phases were introduced for enantiomeric high-performance liquid chromatographic (HPLC) separations in the normal-phase mode [8,9]. They were able to separate a variety of racemates with either hexane-isopropanol or mobile phases of pure alcohol or acetonitrile. These CSPs seems to resemble more closely the cellulosic stationary phases than the native cyclodextrin bonded phase. In contrast to the native  $\beta$ -CD stationary phase, the enantiomeric separation mechanism for the derivatized phases was not thought to be dependent on inclusion complexation. It was reported that derivatized CD stationary phases and native CD phases, operated in different modes, resolved different types of racemates [8–11]. The derivatized cyclodextrin bonded phases were utilized in reversed-phase separations due to their stability. It was found that completely different types of enantiomers were resolved by these columns in the reversed-phase mode [10].

Amino acids are found in all known living organisms. Proteins are made by association of twenty primary amino acids which are always L-amino acids. It may be important to be able to detect the presence of D-amino acids in biological systems [12]. The enantiomer separation of some aromatic amino acids was carried out on a  $\alpha$ -CD-CSP [11]. Racemic dansyl-amino acids (5-dimethylamino-1-naphthalene sulfonyl or Dns) and 2,4-dinitrobenzoyl (DNP)-amino acids were resolved on  $\beta$ -CD bonded CSPs [13–15].

The goal of this paper is to obtain a better knowledge of the chiral recognition mechanism of amino acids by  $\beta$ -CD bonded CSPs. The stationary phase, the mobile phase and the solute itself are all three strongly involved in the chiral recognition mechanism. In the first part of this work, the effect of the stationary phase is studied using six different  $\beta$ -CD and derivatized  $\beta$ -CD CSPs. The second part examines the effect of solute derivatization. Amino acids were derivatized with five different reagents and analyzed on the three best CSPs. The final aspect of this study deals with the mobile phase. The effects

of the organic modifier nature (methanol, acetonitrile or tetrahydrofuran) and concentration were studied. The pH and buffer concentration effects also were investigated.

## EXPERIMENTAL

### *Chemicals and methods*

Amino acids and other compounds were obtained from Sigma (St. Louis, MO, USA) or Aldrich, (Milwaukee, WI, USA). HPLC-grade methanol (MeOH), tetrahydrofuran (THF) and acetonitrile (ACN) were purchased from Fisher Scientific (St. Louis, MO, USA). Water was deionized by passing distilled water through a Barnstead water purification system. Free amino acids were dried and dabsylated according to the procedure described [16]. A 1-ml dabsyl (4-dimethylaminoazobenzene-4'-sulfonyl) chloride solution (0.65 mg/ml in ACN) was mixed with 1 ml of 0.1 M sodium carbonate solution containing excess free amino acid. The reaction mixture was shaken in water bath at 70°C for 30 min. The resulting solution was directly introduced to the injector of the liquid chromatograph. In the 3,5-dinitrobenzoyl (DNB) derivatization, approximately 2–5 mg of amino acid were dissolved in 2 ml acetone. Next, 2–3 mg of 3,5-dinitrobenzoyl chloride derivatizing agent were added. The reacting solution was heated at 60°C for 10 min under gentle stirring. The resulting solution was cooled and injected directly into the liquid chromatograph.

### *Apparatus*

A liquid chromatographic system containing a Shimadzu LC-6A chromatograph (Columbia, MD, USA) was used in this study. A variable-wavelength detector, Model SPD-6AV, was also used and interfaced with a CR601 Chromatopac data system. Dabsyl-amino acids were detected at 436 nm. All other compounds were detected at 254 nm. Rheodyne's Model 7125 sample injection valve with a 20- $\mu$ l loop was used.

The six different 25-cm columns (4.6 mm I.D., 5  $\mu$ m particle diameter) are listed in Table I. The first column was a Cyclobond I column (BC) with  $\beta$ -CD molecules chemically bonded to silica gel with a five-atom, non-nitrogen-containing spacer. The second column was a Cyclobond I Acetylated (AC)

TABLE I  
COLUMNS USED

All columns: 25 cm × 4.6 mm I.D., 5 μm particle diameter.

Designation	Bonded moiety	Number of substitutes per β-CD ring
RN	( <i>R</i> )NEC-β-CD	6.7
SN	( <i>S</i> )NEC-β-CD	3.5
HSN	( <i>S</i> )NEC-β-CD	6.6
TC	Toluoyl-β-CD	ca. 13
BC	Native β-CD	0
AC	Acetyl-β-CD	ca. 16

column which is the peracetylated form of the bond β-CD column. Both columns were obtained from Astec (Whippanny, NJ, USA). Four more 25-cm columns were packed with CSPs prepared in the laboratory. Two (*S*)-1(1-naphthyl)-ethyl carbamate [(*S*)NEC]-derivatized β-CD bonded phase columns (SN and HSN), one (*R*)-1(1-naphthyl)-ethyl carbamate (*R*)NEC-derivatized β-CD bonded phase column (RN), and one toluoyl-derivatized β-CD column (TC) were prepared according to the procedure described in previous papers [8,9].

## RESULTS AND DISCUSSION

### Resolution of racemic derivatized amino acids on five CD stationary phases

Dansyl-amino acids and 3,5-dinitro-2-pyridyl (DNPy)-amino acids (DNPy) were analyzed on the six stationary phases listed in Table I. Two mobile phases were used (A and B, Table II). Table III lists the results, retention, expressed with the capacity factor,  $k'$ , and enantioselectivity, expressed with the ratio of the  $k'$  values of the two enantiomers,  $\alpha$ .

TABLE II  
MOBILE PHASES USED

ACN = Acetonitrile; TEAA = triethylammonium acetate.

Designation	Composition (v/v)	pH
A	ACN-1% TEAA buffer (65:35)	4.5
B	ACN-1% TEAA buffer (50:50)	4.5
C	ACN-0.5% TEAA buffer (50:50)	4.1
D	ACN-0.5% TEAA buffer (21:79)	4.1

TABLE III  
CAPACITY FACTOR ( $k'$ ) AND SELECTIVITY  $\alpha$  OF SOME DERIVATIZED AMINO ACID ENANTIOMERS ON SEVERAL CHIRAL STATIONARY PHASES

Capacity factor ( $k'$ ) given for the first eluting enantiomer. PhG = Phenylglycine.

Compound	Column	$k'$	$\alpha$	Mobile phase
<i>Dansyl-amino acids</i>				
Dns-Glu	RN	4.77	1.05	B
	SN	1.94	1.05	A
	HSN	5.77	1.04	A
	TC	3.42	1.03	A
	BC	2.26	1.11	A
	AC	1.15	1.04	A
Dns-Leu	RN	5.38	1.00	B
	SN	1.66	1.00	A
	HSN	6.55	1.00	B
	TC	4.60	1.00	B
	BC	0.91	1.19	B
	AC	0.70	1.00	B
Dns-Met	RN	4.69	1.00	B
	SN	1.46	1.00	A
	HSN	6.13	1.00	B
	TC	3.98	1.00	B
	BC	0.73	1.10	B
	AC	0.61	1.00	B
Dns-Nle	RN	5.46	1.00	B
	SN	1.58	1.00	A
	HSN	3.38	1.00	A
	TC	4.87	1.00	B
	BC	0.76	1.11	A
	AC	0.66	1.00	B
Dns-Nva	RN	4.51	1.00	B
	SN	1.46	1.00	A
	HSN	6.97	1.00	B
	TC	4.07	1.00	B
	BC	0.78	1.10	B
	AC	0.66	1.00	B
Dns-Phe	RN	7.01	1.09	B
	SN	1.94	1.08	A
	HSN	4.43	1.11	A
	TC	5.65	1.05	B
	BC	0.99	1.13	B
	AC	0.76	1.00	B
Dns-Ser	RN	2.48	1.04	B
	SN	1.01	1.06	A
	HSN	1.86	1.00	A
	TC	2.03	1.00	B
	BC	0.79	1.11	A
	AC	0.44	1.00	A
Dns-Thr	RN	2.96	1.06	B
	SN	1.09	1.08	A

(Continued on p. 86)

TABLE III (continued)

Compound	Column	$k'$	$\alpha$	Mobile phase
	HSN	2.04	1.10	A
	TC	2.45	1.00	B
	BC	0.92	1.19	B
	AC	0.62	1.00	B
Dns-Trp	RN	6.71	1.05	B
	SN	1.91	1.00	A
	HSN	9.42	1.09	B
	TC	5.98	1.00	B
	BC	0.95	1.00	B
	AC	0.44	1.00	A
Dns-Val	RN	4.50	1.06	B
	SN	1.48	1.09	A
	HSN	2.93	1.05	A
	TC	2.24	1.04	A
	BC	0.66	1.18	A
	AC	0.71	1.00	B
<i>3,5-Dinitro-2-pyridyl-amino acids</i>				
DNP <sub>2</sub> -Ala	RN	3.17	1.06	B
	SN	1.26	1.00	A
	HSN	4.69	1.00	B
	TC	2.99	1.00	B
	BC	0.51	1.00	B
	AC	0.49	1.00	B
DNP <sub>2</sub> -Leu	RN	4.88	1.10	B
	SN	1.55	1.00	A
	HSN	7.31	1.00	B
	TC	4.73	1.00	B
	BC	0.62	1.13	B
	AC	0.59	1.00	B
DNP <sub>2</sub> -Met	RN	4.49	1.06	B
	SN	1.45	1.00	A
	HSN	7.22	1.08	B
	TC	4.06	1.00	B
	BC	0.63	1.00	B
	AC	0.51	1.00	B
DNP <sub>2</sub> -Nva	RN	4.30	1.09	B
	SN	1.38	1.00	A
	HSN	6.97	1.00	B
	TC	4.20	1.00	B
	BC	0.57	1.10	A
	AC	0.52	1.00	B
DNP <sub>2</sub> -Phe	RN	7.46	1.02	B
	SN	2.41	1.04	A
	HSN	4.76	1.08	A
	TC	6.39	1.02	B
	BC	0.89	1.00	B
	AC	0.69	1.00	B
DNP <sub>2</sub> -Trp	RN	6.57	1.05	B
	SN	1.93	1.00	A
	HSN	10.64	1.00	B

TABLE III (continued)

Compound	Column	$k'$	$\alpha$	Mobile phase
	TC	6.20	1.00	B
	BC	0.52	1.00	B
	AC	0.61	1.00	B
<i>Other derivatized amino acids</i>				
DNB-Leu	RN	4.08	1.06	A
	SN	1.33	1.00	A
	HSN	5.72	1.03	B
	TC	3.27	1.00	B
	BC	0.49	1.00	A
	AC	0.50	1.00	B
DNB-PhG	RN	4.73	1.17	B
	SN	1.36	1.25	A
	HSN	6.78	1.39	B
	TC	3.70	1.00	A
	BC	0.36	1.00	A
	AC	0.37	1.00	A
Benzoyl-Ala	RN	1.37	1.00	B
	SN	0.75	1.00	A
	HSN	1.50	1.00	B
	TC	1.10	1.00	B
	BC	1.04	1.00	A
	AC	0.55	1.00	A
Carbobenzoxy-Phe	RN	4.09	1.06	B
	SN	1.43	1.00	A
	HSN	2.78	1.08	A
	TC	3.19	1.00	B
	BC	0.94	1.00	B
	AC	0.60	1.00	B

*Retention.* The polarity for the six CSPs used increased from the less polar naphthylethylcarbamate derivatized  $\beta$ -CD CSPs (RN, SN and HSN), the toluoyl-derivatized  $\beta$ -CD CSP (TC), the bare  $\beta$ -CD CSP (BC), to the most polar peracetylated  $\beta$ -CD CSP (AC). The longer retention times were observed on the less polar RN, SN and HSN stationary phases. The retention differences between the SN and the HSN phases were due to the differing bonding density (Table I). The HSN CSP had a higher number of naphthylethyl units per CD ring which made it less polar than the SN CSP. Mobile phase A was richer in organic modifier than mobile phase B. The retention times obtained with A were shorter than the ones obtained with B.

*Enantioselectivity.* The most polar peracetylated  $\beta$ -CD CSP (AC) did not separate any racemic amino acids, but Dns-glutamic acid with a low 1.04

factor (Table III). The toluoyl-derivatized  $\beta$ -CD CSP (TC) was a little better and could separate three racemic amino acids out of the 20 listed in Table III. The  $\alpha$ -values were low. The NEC-derivatized  $\beta$ -CD and the original  $\beta$ -CD CSPs gave the best results with 15 and 11 amino acids-resolved, respectively. For three amino acids, Dns-Leu, Dns-Met and Dns-Nle, the underivatized  $\beta$ -CD CSP was the only one able to separate the enantiomers with selectivity higher than 1.1. Six racemates, Dns-Trp, DNP<sub>Py</sub>-Met, DNP<sub>Py</sub>-Phe, DNP<sub>Py</sub>-Trp, DNB-PhG and carbobenzoxy-Phe, were separated only by the NEC-derivatized  $\beta$ -CD CSPs. When a racemic amino acid pair was separated on both NEC-derivatized and underivatized  $\beta$ -CD CSP, the selectivity was always higher than the underivatized  $\beta$ -CD phase (Dns-Glu or DNP<sub>Py</sub>-Leu, for example, Table III). Fig. 1 shows that the 5% average gain in selectivity could produce a doubling (100% increase) in resolution of the BC chromatogram (Fig. 1A).

The RN and SN columns are both NEC-derivatized  $\beta$ -CD CSPs. The RN column was obtained from the (*R*)NEC enantiomer derivative. The SN column was obtained from the (*S*)NEC derivative (Table I). The RN and SN columns behaved different. Four racemates were separated on the *R* column and not on the *S* version (Fig. 2). All four compounds are DNP<sub>Py</sub> derivatives (DNP<sub>Py</sub>-Ala, DNP<sub>Py</sub>-Leu, DNP<sub>Py</sub>-Nva and DNP<sub>Py</sub>-Trp, Table III). Any racemate that was separated on *S* columns was

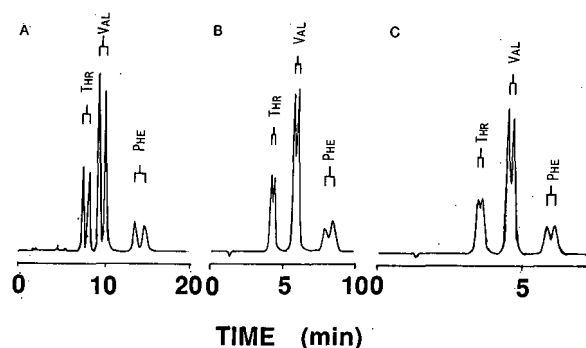


Fig. 1. Chromatograms of the separation of racemic dansyl-amino acids on three different chiral stationary phases. (A) BC column; mobile phase, ACN–0.5% TEAA buffer, pH 4.48 (25:75), 2 ml/min. (B) RN column; mobile phase, ACN–0.7% TEAA buffer, pH 4.48 (50:50), 2 ml/min. (C) SN column; mobile phase, ACN–0.7% TEAA buffer, pH 4.48 (50:50), 2 ml/min. Detection, UV at 254 nm.

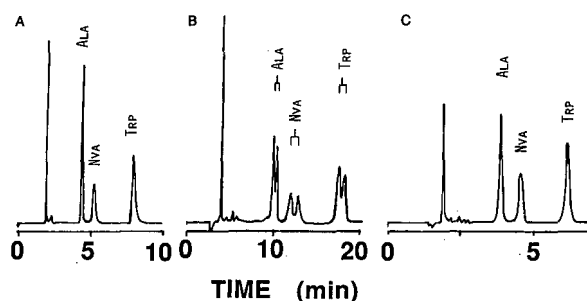


Fig. 2. Chromatograms of the separation of racemic DNP<sub>Py</sub>-amino acids on three different chiral stationary phases. All experimental conditions as in Fig. 1.

also separated on the *R* column. However, the Dns-serine racemate was separated on the SN column and not on the HSN. Conversely, Dns-Trp, DNP<sub>Py</sub>-Met, DNB-Leu and carbobenzoxy-Phe racemates were separated on the HSN column and not on the SN one.

These results show that the chiral mechanism of CDs is intricate. Inclusion complexation and chiral interaction with secondary alcohols located at the mouth of the CD cavity are parts of the mechanism. When the chiral recognition by  $\beta$ -CD disappears upon NEC derivatization (Dns-Leu, Dns-Nle and Dns-Met, Table III), a predominance of the inclusion complex formation may be suspected. Conversely, when the NEC-derivatized  $\beta$ -CD phases can separate racemates not separated by the native  $\beta$ -CD phase, a reversed-phase Pirkle-type recognition mechanism may be part of the chiral resolution process.

The peracetylated  $\beta$ -CD column (AC) and the toluoyl  $\beta$ -CD column (TC) were abandoned due to the poor enantioselectivity obtained in derivatized amino acid resolution. The highly substituted (*S*) NEC column (HSN) was also discarded due to long retention times compared to the similar SN column. Only three columns, the RN, SN and  $\beta$ -CD columns (Table I) were used to investigate solute derivatization effects (next part) and mobile phase effects (last part).

#### *Amino acid derivatization effects on chiral recognition by $\beta$ -CD columns*

*The derivatives.* The amino acids were derivatized using four different reagents: dansyl chloride (Dns) DNB, DNP<sub>Py</sub> and dabsyl chloride. All derivatiza-

TABLE IV

CAPACITY FACTOR ( $k'$ ) AND SELECTIVITY ( $\alpha$ ) OF 3,5-DINITROBENZOYL AMINO ACID ENANTIOMERS ON SOME CHIRAL STATIONARY PHASES

Np = Naphthyl; F = Fluoro; Hphe = homophenylalanine; PhG = phenylglycine.

DNB-Amino acid	Column	$k'$	$\alpha$	Mobile phase
Ala	RN	2.90	1.03	C
	SN	1.88	1.06	C
3-(1-Np)-Ala	RN	11.3	1.09	C
	SN	5.42	1.11	C
	BC	5.44	1.00	D
3-(2-Np)-Ala	RN	9.80	1.05	C
	SN	5.49	1.13	C
Asn	RN	2.26	1.03	C
	SN	1.52	1.07	C
	BC	1.22	1.00	D
Asp	RN	6.91	1.00	C
	SN	3.71	1.07	C
	BC	2.52	1.00	D
Glu	RN	6.39	1.00	C
	SN	3.18	1.09	C
	BC	2.29	1.00	D
Leu	RN	5.34	1.05	C
	SN	3.01	1.03	C
	BC	2.67	1.00	D
Met	RN	4.60	1.08	C
	SN	2.66	1.06	C
	BC	1.98	1.00	D
Nle	RN	5.30	1.09	C
	SN	2.81	1.06	C
	BC	2.61	1.00	D
Phe	RN	7.89	1.11	C
	SN	4.06	1.07	C
	BC	3.40	1.06	D
Hphe	RN	13.58	1.31	C
	SN	5.03	1.00	C
	BC	6.42	1.06	D
o-F-Phe	RN	7.00	1.07	C
	SN	3.53	1.07	C
	BC	3.28	1.06	D
PhG	RN	4.73	1.17	B
	SN	1.36	1.25	A
	BC	0.36	1.00	A
Pro	RN	2.92	1.00	C
	SN	1.84	1.00	C
	BC	2.15	1.00	D

TABLE IV (continued)

DNB-Amino acid	Column	$k'$	$\alpha$	Mobile phase
Ser	RN	2.35	1.00	C
	SN	1.65	1.08	C
	BC	1.22	1.00	D
Thr	RN	3.08	—	C
	SN	1.73	1.07	C
	BC	1.28	1.00	D
Trp	RN	7.58	1.09	C
	SN	4.08	1.12	C
	BC	3.34	1.03	D

tions make the amino acids highly UV detectable. The Dns derivatization adds a somewhat  $\pi$ -basic group on one branch of the amino acid's stereogenic center. The DNB derivatization adds a  $\pi$ -acid group to the amino group of amino acids. The DNPy group has an intermediate  $\pi$ -acidity with an electron rich ( $\pi$ -basic) pyridine ring and two electron attracting nitro groups ( $\pi$ -acid). The dabsyl derivative is rather  $\pi$ -basic, it was chosen for its long and rigid azobenzene backbone which may favor CD inclusion. Tables III and IV and V list the capacity factors and enantioselectivity factors of the four derivatized amino acids on the selected columns.

**Retention.** As a general rule, the retention order for any derivative was RN > SN > BC. It corresponds to the CSP polarity order. The underivatized  $\beta$ -CD column has the highest polarity. The retention times of the solutes were so short that it was necessary to use a water-rich polar mobile phase (solution D, 79%, v/v, water, Table II) to increase them. As far as polarity is concerned, the RN and SN columns have the same type of substituent. However, they do have differing polarities because the NEC bonding density is different (Table I). For a given amino acid, the retention times were similar for the DNB, DNPy and Dns derivatives. The dabsyl derivatives always had significantly higher retention times.

**Enantioselectivity.** The highest enantioselectivity coefficients were obtained with dabsyl derivatives. For example,  $\alpha$  values of 1.56, 1.29, 1.23 or 1.22 were obtained for dabsyl-Leu, dabsyl-Glu, dabsyl-NvA or dabsyl-Thr, respectively, on the (R)NEC or (S)NEC columns (Table V). The data of Tables

TABLE V  
CAPACITY FACTOR ( $k'$ ) AND SELECTIVITY ( $\alpha$ ) OF DABSYL-AMINO ACID ENANTIOMERS ON SOME CHIRAL STATIONARY PHASES

Dabsyl-amino acid	Column	$k'$	$\alpha$	Mobile phase
Ala	RN	4.08	1.13	A
	SN	2.27	1.04	A
	BC	2.01	1.00	A
3-(1-Np)-Ala	RN	5.65	1.11	A
	SN	2.60	1.08	A
	BC	1.29	1.07	B
3-(2-Np)-Ala	RN	7.97	1.13	A
	SN	3.16	1.00	A
	BC	1.46	1.00	B
Glu	RN	10.57	1.29	A
	SN	4.39	1.09	A
	BC	5.07	1.00	A
His	RN	1.46	1.16	A
	SN	1.01	1.15	A
	BC	1.24	1.09	B
Leu	RN	—	—	A
	SN	8.12	1.56	A
	BC	—	—	B
Nva	RN	—	—	A
	SN	2.61	1.23	A
Phe	RN	10.99	1.00	A
	SN	4.25	1.07	A
	BC	2.01	1.00	B
<i>o</i> -F-Phe	RN	6.93	1.12	A
	SN	3.19	1.04	A
	BC	1.65	1.00	A
<i>m</i> -F-Phe	RN	8.46	1.00	A
	SN	3.34	1.07	A
Pro	RN	5.10	1.10	A
	SN	2.52	1.00	A
	BC	2.93	1.00	B
Ser	RN	3.33	1.17	A
	SN	1.77	1.06	A
	BC	2.21	1.00	B
Thr	RN	4.22	1.22	A
	SN	2.19	1.07	A
	BC	2.50	1.00	B
Trp	RN	5.59	1.12	A
	SN	2.68	1.06	A
	BC	1.61	1.10	B
Tyr	SN	3.14	1.15	A
Val	RN	—	—	A
	SN	5.04	1.18	A
	BC	2.49	1.00	B

III-V lead to the following observations. The dansyl-amino acid derivatives were best separated on the underivatized  $\beta$ -CD CSP (Table III). The DNB-amino acid derivatives were best separated on the (*S*)NEC- $\beta$ -CD column (SN) (Table IV). The dabsyl and DNPy derivatives were best separated on the (*R*)NEC- $\beta$ -CD column (RN) (Tables III and V).

The dansyl derivatives, with a naphthyl group, seem to fit well in the  $\beta$ -CD cavity. It is difficult to access this cavity when bulky NEC groups are grafted on its mouth.  $\pi$ - $\pi$  interactions (Pirkle-type) and steric hindrance can be involved to explain the chiral recognition of DNB derivatives on the SN column. Most compounds also were separated, with a somewhat lower enantioselectivity, by the corresponding *R* column (RN). Circular dichroism studies showed opposite elution orders between the *D* and *L* forms of some DNB derivatives eluted on the RN and SN columns. The *D* forms eluted first on the RN column and the *L* forms on the SN column. The chiral mechanism for DNB derivatives recognition seems to be dominated by  $\pi$ - $\pi$  interaction of the Pirkle-type. Fig. 3 is an example of DNB derivative separation on the BC and RN columns. The *L* form of all dansyl derivatives eluted first on the three CSPs used. Conversely, the *D* form of all dabsyl derivatives eluted first on the three CSPs (RN, SN and BC). Inclusion complexation seems to predominate in the chiral recognition mechanism of these derivatives because there was no significant difference between the RN and SN columns. Dabsyl and DNPy derivatives have somewhat intermediate  $\pi$ -acidities. The RN column separated these analytes better than the SN column did. This shows that steric hindrance and  $\pi$ - $\pi$  interactions due to the NEC moieties cannot be neglected: the (*R*)NEC density was higher than the (*S*)NEC density (Table I). This point is illustrated by Fig. 4 which shows a dabsyl derivative separation on RN and SN columns. One exception: dabsyl-phenylalanine was better separated by the SN column. It should be noted that the observed efficiency for all dabsyl-amino acid peaks was about 50% lower than the efficiency observed for the other derivatives. The dabsyl peaks appeared broader (Figs. 3 and 4). This was due to a slow mass transfer. It is a possible sign of CD inclusion complexation. All this shows that the chiral recognition mechanism for  $\beta$ -CD-CSPs and specially for NEC-derivatized  $\beta$ -CD CSPs cannot be simply reduced to one kind of behavior, rath-

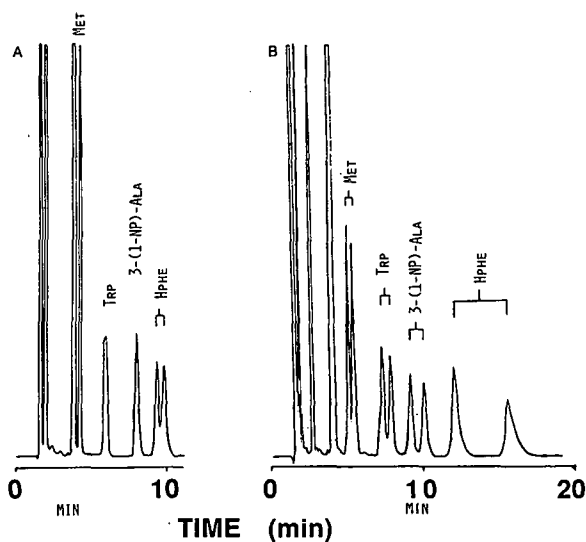


Fig. 3. Chromatograms of the separation of DNB-amino acids on the BC (A) and RN (B) chiral stationary phases. All experimental conditions as in Fig. 1.

er it involves several types. From these results, it appears that NEC- $\beta$ -CD CSP columns are particularly effective and versatile.

#### Mobile phase and enantioselectivity

The mobile phase solvates the stationary phase and the solutes. It is most often a mixture of solvents, which means that the solvation may be different when the local polarity is changing. Despite

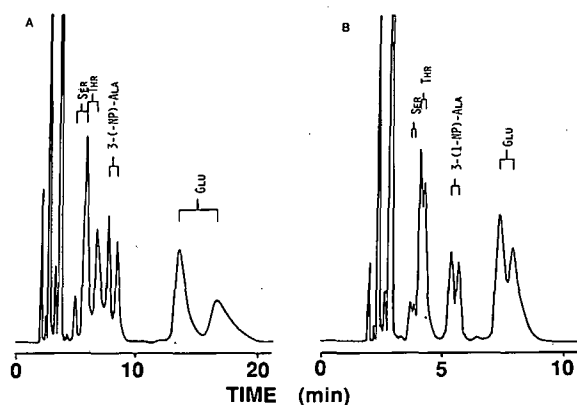


Fig. 4. Chromatograms of the separation of racemic dabsyl-amino acids on the RN and SN derivatized  $\beta$ -CD stationary phases. The mobile phase is ACN-0.7% TEAA buffer, pH 4.48 (65:35), 2 ml/min. (A) RN column. (B) SN column.

its importance, the mobile phase is probably the least known and studied parameter in chiral recognition mechanism studies. In this work, three mobile phase parameters were studied (i) the organic modifier nature, (ii) the pH effect, (iii) the ionic strength effect through buffer concentration.

*Nature of the organic modifier.* Table VI lists the

TABLE VI

ENANTIOMERIC SEPARATION DATA FOR DERIVATIZED AMINO ACIDS ON THE DIFFERENT ORGANIC MODIFIERS

Column RN and 1% TEAA buffer (pH 4.1) solutions are used.

Compound	50% ACN		50% MeOH		40% THF	
	$k'$	$\alpha$	$k'$	$\alpha$	$k'$	$\alpha$
Dns-Glu	2.42	1.03	4.84	1.00	2.41	1.00
Dns-Leu	2.73	1.00	5.25	1.00	2.75	1.00
Dns-Met	2.75	1.00	5.81	1.00	3.06	1.00
Dns-Nle	2.86	1.00	—	—	3.10	1.00
Dns-Nva	2.52	1.00	4.82	1.00	2.75	1.00
Dns-Phe	3.71	1.07	9.32	1.00	3.92	1.00
Dns-Ser	1.76	1.00	3.65	1.00	1.93	1.00
Dns-Thr	1.90	1.06	3.77	1.00	2.24	1.00
Dns-Trp	3.38	1.04	9.00	1.00	3.63	1.00
Dns-Val	2.47	1.04	4.55	1.00	2.59	1.00
DNB-PhG	3.05	1.19	8.72	1.25	5.28	1.16
Benzoyl-Ala	1.10	1.00	1.54	1.00	1.02	1.00
Carbobenzoxy-Phe	2.43	1.05	4.82	1.04	2.53	1.00
DNPpy-Ala	2.36	1.05	5.47	1.06	3.88	1.00
DNPpy-Met	3.03	1.05	8.33	1.07	5.33	1.00
DNPpy-Nva	2.81	1.08	6.68	1.09	4.87	1.00
DNPpy-Phe	4.48	1.00	13.47	1.00	6.24	1.00
DNPpy-Trp	4.03	1.04	14.36	1.07	6.34	1.00
Dabsyl-Ala	4.81	1.10	7.72 <sup>a</sup>	1.28	3.22	1.00
Dabsyl-3(1-Np)-Ala	7.65	1.08	10.84 <sup>a</sup>	1.13	5.77	1.00
Dabsyl-3(2-Np)-Ala	10.75	1.12	16.88 <sup>a</sup>	1.17	6.34	1.00
Dabsyl-Glu	7.25	1.42	16.13 <sup>a</sup>	1.00	3.69	1.00
Dabsyl-His	1.19	1.14	2.21 <sup>a</sup>	1.13	0.56	1.00
Dabsyl-Nva	7.67	1.00	8.95 <sup>a</sup>	1.00	—	—
Dabsyl-Phe	7.43	1.00	—	—	5.32	1.00
Dabsyl- <i>o</i> -F-Phe	9.41	1.10	—	—	5.10	1.00
Dabsyl- <i>m</i> -F-Phe	7.71	1.09	17.73 <sup>a</sup>	1.00	—	—
Dabsyl-Pro	6.00	1.09	11.56 <sup>a</sup>	1.07	3.19	1.00
Dabsyl-Ser	3.94	1.16	7.90 <sup>a</sup>	1.13	2.71	1.00
Dabsyl-Thr	4.70	1.18	8.87 <sup>a</sup>	1.21	2.83	1.00
Dabsyl-Trp	6.92	1.10	11.56 <sup>a</sup>	1.14	—	1.00
Dabsyl-Tyr	10.01	1.00	10.54 <sup>a</sup>	1.00	3.82	1.00

<sup>a</sup> The mobile phase of methanol-buffer (75:25) is used for all the dabsyl-amino acid separations.

retention and enantioselectivity obtained for the derivatized amino acids on the RN column. Three mobile phases were prepared with the same buffer solution (water + 1%, v/v, triethylamine (TEA) adjusted to pH 4.10 adding acetic acid) and ACN, MeOH or THF. The results are straightforward: as far as retention is concerned, THF was the strongest eluting solvent and MeOH was the weakest. However, THF should not be used because it did not give any enantioselectivity. We think the low polarity ether ring of THF may enter the  $\beta$ -CD cavity and/or associate with  $\pi$ -systems hindering both the inclusion complex formation and  $\pi$ - $\pi$  interac-

tions. Clearly, ACN gave the best enantioselectivity. It was able to resolve some Dns derivatives that were not resolved with MeOH or THF modifiers. It resolved most of the DNPy and dabsyl-amino acid derivatives, somewhat better than MeOH and with shorter retention times.

*pH effects.* It has been reported that the  $pK_a$  value of the carboxylic acid group of amino acids varies from 1.7 to 2.7 [15,17]. Substitution of the amino acid's amino group with electron acceptor moieties (Dns, DNPy, DNB or dabsyl) should increase the acid dissociation constant. All derivatized amino acids exist in the anionic form over the pH range 4.1 to 7.0. Table VII shows rapid amino acid retention decreases with pH increases. In the reversed-phase mode, such a decrease means either the solute becomes more polar or the mobile phase strength increases or the stationary phase becomes more polar. Since the solute ionization and the mobile phase becomes more polar. Since the solute ionization and the mobile phase composition are not supposed to change much, pH changes are suspected to induce stationary phase changes. The silica network underneath the  $\beta$ -CD layer is pH sensitive. Upon pH increase, residual silanols may ionize, rendering the stationary phase somewhat negatively charged. Triethylammonium ions ( $TEA^+$ ) should cancel negative charges. They may not cancel all negative charges. The good point is that, for these particular analytes, enantioselectivity is little affected by pH changes (Table VII). The chiral recognition is due to solute- $\beta$ -CD interactions that take place far enough from the silica surface. Elevated mobile phase pH values may make the chiral analysis faster. However, it should not be forgotten that silica solubilization occurs from pH 7. To extend column life, it is safer to work below pH 6.

*Buffer concentration effect.* Table VIII lists the effects of buffer concentration on retention and resolution of amino acid derivatives on the RN column. A dramatic retention decrease was observed when the TEAA concentration increased. An efficiency increase was also observed at high TEAA concentration, that is why resolution factors were listed in Table VIII instead of selectivity factors. This indicates that the solute, the mobile phase and the stationary phase were modified by TEAA. Hydrophilic  $TEAA^+$ -derivatized [amino acid] $^-$  ion pairs may be formed and eluted faster at high TEAA concen-

TABLE VII

## pH EFFECT FOR ENANTIOMERIC SEPARATION OF DERIVATIZED AMINO ACIDS

The mobile phase contains ACN-1% TEAA buffer (65:35) unless indicated otherwise; column RN.

Compound	pH 4.50		pH 6.10		pH 7.00	
	$k'$	$\alpha$	$k'$	$\alpha$	$k'$	$\alpha$
Dns-Glu	4.77 <sup>a</sup>	1.05	1.12	1.07	0.54	1.00
Dns-Phe	7.01 <sup>a</sup>	1.09	1.23	1.11	0.95	1.11
Dns-Ser	2.48 <sup>a</sup>	1.04	0.60	1.00	0.42	1.00
Dns-Thr	2.96 <sup>a</sup>	1.06	0.65	1.09	0.49	1.09
Dns-Trp	6.71 <sup>a</sup>	1.05	1.18	1.07	0.93	1.07
Dns-Val	4.50 <sup>a</sup>	1.06	0.94	1.10	0.74	1.24
DNPy-Ala	3.17 <sup>a</sup>	1.06	0.77	1.00	0.49	1.00
DNPy-Leu	4.88 <sup>a</sup>	1.10	0.99	1.10	0.66	1.12
DNPy-Met	4.49 <sup>a</sup>	1.06	0.90	1.05	0.59	1.09
DNPy-Nva	4.30 <sup>a</sup>	1.09	0.86	1.09	0.57	1.09
DNPy-Phe	7.46 <sup>a</sup>	1.02	1.40	1.00	0.93	1.00
DNPy-Trp	6.57 <sup>a</sup>	1.05	1.21	1.05	0.82	1.05
Carbobenzoxy-Phe	4.09 <sup>a</sup>	1.06	0.98	1.00	0.64	1.00
DNB-Leu	3.33	1.17	1.43	1.19	0.95	1.20
DNB-PhG	4.22 <sup>a</sup>	1.22	1.86	1.24	1.20	1.06
Dabsyl-Ala	5.10	1.10	2.25	1.10	1.47	1.09
Dabsyl-3-(1-Np)-Ala	5.65	1.11	2.36	1.14	1.57	1.11
Dabsyl-3-(2-Np)-Ala	7.97	1.13	3.47	1.14	2.21	1.13
Dabsyl-Glu	4.73 <sup>a</sup>	1.17	0.92	1.16	0.63	1.18
Dabsyl- <i>o</i> -F-Phe	6.93	1.12	3.16	1.15	2.01	1.15
Dabsyl-Pro	4.08 <sup>a</sup>	1.06	0.90	1.08	0.61	1.10
Dabsyl-Ser	10.57	1.29	3.35	1.16	1.58	1.13
Dabsyl-Thr	4.08	1.13	1.82	1.14	1.17	1.14
Dabsyl-Trp	5.59	1.12	2.60	1.13	1.69	1.13

<sup>a</sup> ACN-1% TEAA buffer (50:50), (mobile phase B in Table II).

TABLE VIII

EFFECT OF TEAA BUFFER CONCENTRATION IN THE MOBILE PHASE ON THE RETENTION AND RESOLUTION

Mobile phase: ACN-buffer, pH 4.10 (50:50); column RN.

Compound	0.2% TEAA		0.5% TEAA		1.0% TEAA	
	$k'$	$R_s$	$k'$	$R_s$	$k'$	$R_s$
Dns-Glu	16.74	0.7	5.13	0.5	2.42	0.5
Dns-Leu	10.49	0.5	4.70	0.0	2.73	0.0
Dns-Nva	9.71	0.0	4.40	0.0	2.52	0.0
Dns-Phe	15.18	1.0	6.67	0.8	3.71	0.9
Dns-Ser	6.97	0.6	3.09	0.3	1.76	0.0
Dns-Thr	7.51	0.9	3.34	0.7	1.90	0.6
Dns-Trp	13.32	0.9	5.98	0.6	3.38	0.5
Dns-Val	9.25	0.8	4.25	0.6	2.47	0.6
DNPY-Ala	9.22	1.0	4.24	0.7	2.36	0.8
DNPY-Leu	12.34	1.5	5.63	1.2	—	—
DNPY-Met	12.36	1.0	5.53	0.8	3.03	0.7
DNPY-Nva	11.44	1.5	5.16	1.1	2.81	1.0
DNPY-Phe	19.28	0.3	8.52	0.0	4.48	0.0
DNPY-Trp	17.20	1.0	5.65	1.2	4.03	0.8
DNB-Leu	9.53	0.9	4.50	0.5	2.60	0.3
DNB-PhG	12.77	3.5	5.69	3.0	3.05	3.0
Dabsyl-Ala	19.87	2.0	8.86	1.2	4.81	1.1
Dabsyl-3(1-Np)-Ala	34.10	2.0	14.86	1.5	7.65	1.0
Dabsyl-Glu	—	—	17.02	2.5	7.25	1.5
Dabsyl- <i>o</i> -F-Phe	—	—	17.41	0.5	9.41	0.4
Dabsyl-Pro	23.75	1.0	10.97	0.8	6.00	0.9
Dabsyl-Ser	16.47	4.0	7.24	2.0	3.94	1.7
Dabsyl-Thr	19.55	2.0	8.51	1.2	4.70	1.3
Dabsyl-Trp	29.66	2.0	13.06	1.0	6.92	1.0

trations. Mobile phases were prepared by putting the quoted amount (v/v) of liquid triethylamine in water and adding acetic acid to the desired pH. The 1% (v/v) TEAA water solution at pH 4.1 contained about 3% (v/v) of organic modifiers (TEA and acetic acid). Mobile phase ionic strength changed much upon TEAA concentration changes. The TEAA ion pair may enter the  $\beta$ -CD cavity thus weakening the strength of derivatized amino acid's inclusion complex. 1% (v/v) TEAA concentrations produced a decrease in enantioselectivity that was not compensated by the efficiency increase, *i.e.* the overall resolution decreased (Table VIII).

## CONCLUSIONS

The classical native  $\beta$ -CD CSP column (BC) is well-suited for dansyl-derivatized amino acid analysis. However, the NEC- $\beta$ -CD CSP columns (RN, SN and HSN), and especially the (R)NEC derivatized  $\beta$ -CD CSP column (RN) gave excellent results with  $\pi$ -acid derivatized amino acids (DNB-amino acids). The RN column was also able to resolve dansyl-amino acids and DNPY-amino acids. The linear azobenzene group of the dansyl derivative makes dansyl-amino acids easy to resolve by the RN column. ACN is better than MeOH as an organic mobile phase modifier. TEAA buffer concentrations of 0.5% (v/v) and a pH around 5 are the best mobile phase conditions to resolve racemic derivatized amino acids. Clearly the (R)NEC- $\beta$ -CD column (RN) was the most widely useful derivatized cyclodextrin based CSP. The chiral recognition mechanism of this CSP involves (i) inclusion complexation with the  $\beta$ -CD cavity, (ii)  $\pi$ - $\pi$  interaction (Pirkle type) with the naphthylethyl moiety, (iii) interactions with remaining chiral secondary alcohols at the CD-mouth and (iv) steric hindrance.

## ACKNOWLEDGEMENT

Support of this work by the Department of Energy, Office of Basic Science (DE FG02 88ER13819) and the Korean Ministry of Education is gratefully acknowledged.

## REFERENCES

- 1 D. W. Armstrong, *US Pat.*, 4 539 399 (1985).
- 2 D. W. Armstrong and W. DeMond, *J. Chromatogr. Sci.*, 22 (1984) 411.
- 3 D. W. Armstrong, W. DeMond, A. Alak, W. L. Hinze, T. E. Riehl and K. H. Bui, *Anal. Chem.*, 59 (1985) 234.
- 4 D. W. Armstrong and W. Y. Li, *Chromatography*, 2 (1987) 43.
- 5 T. Ward and D. W. Armstrong, in M. Zief and L. J. Crane (Editors), *Chromatographic Chiral Separations (Chromatographic Science Series, Vol. 40)* Marcel Dekker, New York, 1988, p. 131.
- 6 W. L. Hinze, *Sep. Purif. Methods*, 10 (1981) 159.
- 7 S. M. Han and D. W. Armstrong, in A. M. Krstulovic (Editor), *Chiral Separations by HPLC*, Wiley, New York, 1989, p. 208.
- 8 D. W. Armstrong, A. M. Stalcup, M. L. Hilton, J. D. Duncan, J. R. Faulkner and S. C. Chang, *Anal. Chem.*, 62 (1990) 1610.

- 9 A. M. Stalcup, S. C. Chang and D. W. Armstrong, *J. Chromatogr.*, 540 (1991) 113.
- 10 D. W. Armstrong, C. D. Chang and S. H. Lee, *J. Chromatogr.*, 539 (1991) 83.
- 11 D. W. Armstrong, X. Yang, S. M. Han and R. A. Menges, *Anal. Chem.*, 59 (1987) 2594.
- 12 D. W. Armstrong, J. M. Duncan and S. H. Lee, *Amino Acids*, 1 (1991) 1.
- 13 W. L. Hinze, T. E. Riehl, D. W. Armstrong, W. DeMond, A. Alak and T. J. Ward, *Anal. Chem.*, 57 (1985) 237.
- 14 K. Fujimura, S. Suzuki, K. Kayashi and S. Masuda, *Anal. Chem.*, 62 (1990) 2198.
- 15 S. Li and W. Purdy, *J. Chromatogr.*, 543 (1991) 105.
- 16 S. H. Lee, T. S. Oh and Y. C. Lee, *Bull. Korean Chem. Soc.*, 11 (1990) 411.
- 17 G. C. Barrett, in *Chemistry and Biochemistry of the Amino Acids*, Chapman & Hall, London, 1985, p. 19.



# Protein purification using combined streptavidin (or avidin)-Sepharose and thiopropyl-Sepharose affinity chromatography

Franck Desarnaud, Jacky Marie, Renée Larguier, Colette Lombard, Serge Jard and Jean-Claude Bonnafous

*Centre CNRS-INSERM de Pharmacologie-Endocrinologie, Rue de la Cardonille, 34094 Montpellier Cedex 5 (France)*

(First received October 21st, 1991; revised manuscript received February 7th, 1992)

---

## ABSTRACT

The major problem usually encountered in the application of the (strept)avidin-biotin system to the purification of proteins (or other biological molecules) lies in the difficult reversion of the interaction between immobilized (strept)avidin and the adsorbed biotinylated protein. Among the proposed solutions is the selective biotinylation of the entity to be purified by a disulphide-containing biotinylated reagent which allows its recovery from (strept)avidin gels by dithiothreitol (DTT) treatment. As emphasized by the example of angiotensin II receptor purification, achieved using this strategy, optimum reduction of this disulphide bridge may require improvement of its accessibility using denaturing agents such as sodium dodecyl sulphate or urea. However, these agents release important amounts of (strept)avidin. Two general ways of solving this problem are proposed. One solution takes advantage of the absence of cysteine in the streptavidin sequence: the protein to be purified is selectively re-adsorbed to thiopropyl-Sepharose through the thiol function generated on DTT cleavage of the biotinylated reagent. The other solution is an empirical approach to make possible the use of avidin, which possesses cysteine residues: combined avidin-Sepharose and thiopropyl-Sepharose chromatography proved efficient when carried out in the presence of urea as denaturing agent.

---

## INTRODUCTION

The so-called avidin-biotin system has been used during the last decade for the detection and purification of biomolecules. The principle consists in selective biotinylation of either the protein to be detected or purified or a ligand which interacts with this protein, followed by interaction of the biotinylated entity with derivatized or immobilized avidin or streptavidin [1–5]. Among the most striking examples are the numerous attempts to purify hormone receptors, which generally represent a small fraction of proteins and therefore require highly se-

lective procedures for their isolation. In some instances hormone biotinylation has been used as a convenient way for its controlled immobilization on avidin or streptavidin gels, thus allowing the development of classical direct affinity chromatography [6–9].

More interestingly, hormone receptors have been covalently labelled with a biotinylated hormone before adsorption to immobilized avidin [10,11]; this type of indirect affinity chromatography is required when protein solubilization is accompanied by a loss of ligand binding. This situation includes our own work on angiotensin II (AII) receptor purification [12], which will be commented upon in this paper. In these instances, the extremely high affinity of biotin for avidin raised problems for the recovery of hormone-receptor covalent complexes. Several ways of overcoming this difficulty have been pro-

---

*Correspondence to:* Dr. J.-C. Bonnafous, Centre CNRS-INSERM de Pharmacologie-Endocrinologie, Rue de la Cardonille, 34094 Montpellier Cedex 5, France.

posed: a first possibility is to use biotin derivatives which display decreased affinity for avidin (dethio-biotin) [10] or pH-sensitive affinity (iminobiotin) [13]. Another possibility is to use biotinylated ligands possessing a disulphide bridge, as exemplified by the work of Shimkus and co-workers [14–16] and Roseman *et al.* [17], who used Bio-S-S-dUTP (Bio = biotinyl) for nucleosome or transcriptionally active DNA purification.

Our work on AII receptor purification was based on the photolabelling of the receptor with biotinylated azido probes and the adsorption of solubilized probe-receptor complexes on (strept)avidin gels [12]. In this instance iminobiotin-containing probes were not suitable as they displayed too high non-specific binding to starting rat liver membranes. Successful experiments were carried out using synthetic probes containing a cleavable disulphide bridge; these probes were obtained by reaction of an azido AII derivative with the commercially available NHS-SS-Bio [14–18]. Efficient receptor recovery by dithiothreitol (DTT) required the presence of sodium dodecyl sulphate (SDS), the major effect of which was to increase the accessibility of the disulphide bridge of the probe [12]. However, SDS released avidin or streptavidin from the affinity gels, so that these proteins were in large excess over the protein to be purified. We present in this paper quantitative data demonstrating the possibility of eliminating released streptavidin through thiopropyl-Sepharose chromatography. We also envisaged the possibility of using avidin gels and to reduce released avidin in the two affinity steps through the use of various denaturing agents and detergents. The potential generalization of combined streptavidin (or avidin)-Sepharose and thiopropyl-Sepharose affinity chromatography is discussed, together with the advantages of the various experimental conditions examined.

## EXPERIMENTAL

### Materials

The probe used for AII receptor photolabelling and purification, Bio-NH(CH<sub>2</sub>)<sub>2</sub>-S-S-(CH<sub>2</sub>)<sub>2</sub>CO-[Ala<sup>1</sup>-Phe(4N<sub>3</sub>)<sup>8</sup>]AII [Bio-S-S-AII(N<sub>3</sub>)], was synthesized as described previously [19]. Solutions of the azido probes were calibrated by UV spectrophotometry ( $\epsilon_{250\text{ nm}} = 12\,500$ ). The radioiodinated

probe and unlabelled monoiodo derivative of the probe were obtained as described previously [12,20]. Probe samples of appropriate specific radioactivities were obtained by mixing labelled and unlabelled compounds.

Biotin, avidin and streptavidin were obtained from Sigma, [<sup>125</sup>I]streptavidin from Amersham, cyanogen bromide-activated Sepharose 4B and thiopropyl-Sepharose 6B from Pharmacia-LKB, YM 30 Diaflo membranes and Centricon P30 microconcentrators from Amicon, Triton X-100 (octylphenol polyethylene glycol ether) from Pierce, 3-[(3-cholamidopropyl)dimethylammonio]-1-propanesulphonate (CHAPS) from Boehringer and SDS from Bio-Rad Labs.

Electrophoresis reagents were obtained from Serva and Bio-Rad Labs. and a low-molecular-mass standard kit (14 400–97 400) from Pharmacia-LKB.

### AII receptor purification

AII receptor was purified from rat liver plasma membranes using the biotinylated photoactivatable probe as described previously [12]; when applied to lower starting receptor amounts (20–100 pmol), the two affinity steps were carried out in batchwise procedures, without significant changes in their yields. Combined (strept)avidin-Sepharose and thiopropyl-Sepharose chromatography were achieved under two types of experimental conditions: apart from previously established conditions which are based on the use of DTT in the presence of SDS [12] (see details below, conditions A), some experiments involved urea (see below, conditions B) as denaturing agent in Triton X-100 or CHAPS as detergents.

### Preparation of immobilized streptavidin or succinylavidin

The preparation of avidin-Sepharose (1 mg of protein/ml of gel) and succinylation of immobilized avidin were carried out according to Finn *et al.* [6]. The succinylation step, introduced to reduce the basic character of avidin and its resulting non-specific binding to proteins [3,6], can be omitted in the preparation of streptavidin-Sepharose (1 mg/ml of gel) [3].

[<sup>125</sup>I]Avidin was obtained using the chloramine T method: avidin (75  $\mu\text{g}$ ) in 150  $\mu\text{l}$  of 50 mM phos-

phate buffer (pH 7.4) was iodinated with 1 mCi of  $\text{Na}^{125}\text{I}$  and 40  $\mu\text{g}$  of chloramine T. Radioiodinated avidin and streptavidin were diluted with unlabelled proteins so as to obtain specific radioactivities of 4.0 and 2.9  $\mu\text{Ci}/\text{mg}$  respectively, and immobilized as indicated above.

#### *Behaviour of streptavidin and avidin released from affinity gels*

Determinations of avidin and streptavidin contaminations achieved using immobilized [ $^{125}\text{I}$ ]avidin and [ $^{125}\text{I}$ ]streptavidin.

In order to mimic conditions usually applied for AII receptor purification, 30 ml of hydroxyapatite elution buffer [0.3 M phosphate (pH 6.0), 0.5% Triton X-100, 1% SDS, 5 mM EDTA, 1 mM phenylmethylsulphonyl fluoride (PMSF) and 0.5 mM N-ethylmaleimide (NEM)] were applied to a 3-ml column of radioactive gel initially equilibrated in the same buffer without SDS. After an initial wash in the presence of 1% SDS, the column was thoroughly rinsed with several buffers containing 0.5% Triton X-100, as described previously [12]. At this stage several conditions were checked for elution from these gels and for the thiopropyl-Sepharose chromatography of the (strep)avidin eluates:

*Conditions A.* Elution was achieved by gentle agitation (15 min at room temperature) with 15 ml of 10 mM phosphate buffer (pH 8.0)–50 mM DTT, 1% SDS. The eluates were freed from most their DTT content by three successive ultrafiltration steps through YM 30 Diaflo membranes, separated by fivefold dilution with 10 mM phosphate buffer (pH 6.0) and 0.1% Triton X-100.

The samples were adsorbed, with gentle agitation for 2 h, on 250  $\mu\text{l}$  of thiopropyl-Sepharose 6B (the pH of the sample was adjusted to 7.5–7.8). The gels were then washed with 10 mM phosphate buffer (pH 8.0)–0.1% SDS; elution was achieved with the same buffer supplemented with 50 mM DTT. The thiopropyl-Sepharose eluates were submitted to ultrafiltration in Amicon Centricon P30 microconcentrators [three cycles separated by fivefold dilution with 10 mM phosphate buffer (pH 8.0)–0.1% SDS].

*Conditions B.* In experiments involving immobilized avidin the gel was presaturated with 6  $\mu\text{M}$  biotin before elution with 10 mM phosphate buffer (pH 8.0)–50 mM DTT–8 M urea in 0.1% Triton

X-100. DTT and urea removal by ultrafiltration and sample adsorption to thiopropyl-Sepharose were carried out as for conditions A. The thiopropyl-Sepharose gel was then washed with 10 mM phosphate buffer (pH 8.0) containing either 0.1% SDS or 8 M urea in 0.1% Triton X-100 or 1% CHAPS; elutions were achieved with the same buffers supplemented with 50 mM DTT. The eluates were ultrafiltered as for conditions A, except that SDS was replaced with Triton X-100 or CHAPS.

#### *SDS–polyacrylamide gel electrophoresis (PAGE)*

Purified AII receptor, avidin and streptavidin were analyzed under reducing conditions by SDS-PAGE according to the method of Laemmli [21]. Samples were treated for 1 h at 30°C in a medium containing 80 mM Tris–HCl (pH 6.8), 2% (w/v) SDS, 10% (w/v) glycerol, 0.1 M DTT and bromophenol blue. A 12.5% acrylamide running gel overlaid by a 5% acrylamide stacking gel was used (electrophoresis conditions: 14–16 h, 50 V). Gels were stained using silver or Coomassie Brilliant Blue. Dried gels were autoradiographed at  $-80^\circ\text{C}$  with Kodak XAR-5 films and intensifying screens.

## RESULTS

#### *Principle of protein purification through combined (strep)avidin-Sepharose and thiopropyl-Sepharose chromatography: the example of the angiotensin II receptor*

We recently published a detailed protocol for AII receptor purification, based on covalent labelling of the membrane receptor with a biotinylated photoactivatable hormone derivative, followed by solubilization and selective adsorption of the solubilized probe–receptor complexes on immobilized streptavidin [12]; we adopted this strategy because it appeared impossible to bind AII to the solubilized receptor so that purification through classical affinity chromatography had to be ruled out; the difficulty in reversing the streptavidin–biotin interaction led us to synthesize a probe containing a disulphide bridge between biotin and angiotensin II: Bio–NH(CH<sub>2</sub>)<sub>2</sub>–S–S–(CH<sub>2</sub>)<sub>2</sub>CO–[Ala<sup>1</sup>–Phe(4N<sub>3</sub>)<sup>8</sup>]AII. The synthesis of this probe [19] was facilitated by the commercial availability (Pierce) of the disulphide containing biotin derivative Bio–NH(CH<sub>2</sub>)<sub>2</sub>–S–S–(CH<sub>2</sub>)<sub>2</sub>COOR (R = succinimidyl) (NHS–S–

TABLE I

## BEHAVIOUR OF BIOTINYLATED AII RECEPTOR COVALENT COMPLEXES THROUGHOUT COMBINED AVIDIN OR STREPTAVIDIN-SEPHAROSE AND THIOPROPYL-SEPHAROSE CHROMATOGRAPHY

AII receptor was purified from rat liver plasma membranes using [<sup>125</sup>I]Bio-S-S-AII(N<sub>3</sub>) (initial concentration, 8 nM; specific radioactivity, 180 Ci/mmol as mentioned under Experimental. Hydroxyapatite eluates containing 0.5% Triton X-100 were adsorbed on avidin or streptavidin gels in the presence or absence of 1% SDS. Receptor adsorption to thiopropyl-Sepharose and its elution from streptavidin or avidin gels and thiopropyl-Sepharose were carried out under various conditions as described under Experimental. The values given in this table were obtained with streptavidin-Sepharose gels. Similar values were obtained with avidin-Sepharose gels.

Step	Receptor adsorption yield (%)			Receptor elution yield (%) (DTT)		
	SDS	Triton X-100	CHAPS	SDS	Urea	
					Triton X-100 <sup>a</sup>	CHAPS
Streptavidin-Sepharose	83	71	N.D. <sup>b</sup>	82	81	N.D. <sup>b</sup>
Thiopropyl-Sepharose	66	84	91	87	75	90

<sup>a</sup> The elution yield was 97% in the absence of urea.

<sup>b</sup> N.D. = Not determined.

S-Bio), a starting compound previously used for the preparation of biotinylated nucleotides [14].

Covalent complexes specifically obtained by AII receptor labelling with the radioiodinated probe were easily adsorbed on immobilized avidin or streptavidin [12]; however, receptor recovery through DTT treatment was not completely satisfactory when carried out in Triton X-100 as detergent [12]. A first possibility of solving this problem would have been to synthesize other probes displaying increased accessibility of their disulphide bridges with respect to receptor or streptavidin steric requirements. Alternatively, we choose to try to improve accessibility of this S-S bond through the use of denaturing agents. The first experiments carried out in the presence of SDS were satisfactory in terms of receptor recovery (82% yield, Table I). However, SDS treatment released avidin or streptavidin in amounts that were unsuitable for subsequent accurate electrophoretic analysis and separation. Analysis of the streptavidin peptide sequence [22] surprisingly revealed that this protein does not contain any cysteine residue. We took advantage of this to eliminate contaminating streptavidin by selectively adsorbing the receptor to thiopropyl-Sepharose through the SH function which results from DTT cleavage of the spacer arm of the probe

(see Fig. 2, Scheme 1 for illustration). The possible receptor re-adsorption through the thiol functions resulting from DTT reduction of its intramolecular disulphide bridges cannot be excluded; however, the thiol function of the cleaved probe, which occupies an "antennary" position, is probably the most accessible to the activated thiol functions of thiopropyl-Sepharose.

The 6000-fold purification allowed by this protocol was established by measurement of radioactive receptor and total protein content of the samples [12]. As a consequence of the initial covalent labelling of the binding site, it was not possible to characterize pharmacologically the purified receptor; the identity of the purified glycoprotein to the AII receptor was assessed by the following criteria: the specificity of labelling in purified samples has been demonstrated [12]; the purified receptor displayed an electrophoretic pattern [average molecular mass (*M<sub>r</sub>*) 65 000] similar to that of starting solubilized receptor; deglycosylation of non-purified and purified receptor led to the same *M<sub>r</sub>* 40 000 entity [12]. Obviously these patterns cannot result from an artifact involving contaminating streptavidin (streptavidin is not glycosylated; see also the next paragraph).

The purpose of this work was to validate this

strategy of purification (see Fig. 2 for a detailed general scheme of the procedure); pilot experiments described in the next section confirmed the prediction that thiopropyl-Sepharose chromatography is a convenient way of eliminating released streptavidin. Moreover, taking into account that streptavidin is much more expensive than avidin, an important constraint for large-scale experiments, we tried to establish conditions that would allow protein purification through combined avidin-Sepharose and thiopropyl-Sepharose chromatography with acceptable final avidin contaminations. The rational solution would have consisted in reducing avidin disulphide bridges and alkylating the resulting thiol functions, in order to suppress their ability subsequently to react with thiopropyl-Sepharose; however, it appeared impossible, consistent with the work of Green [23], who found that disulphide reduction only occurred on denatured avidin, and that alkylation prevents renaturation. In this respect, one must mention that adsorption of biotin-tagged AII receptor to monomeric avidin gels [24] was not successful. As a consequence, we used an empirical approach which consisted in limiting the release of avidin at the first affinity step and limiting its adsorption and release at the thiopropyl-Sepharose step. Based on the fact that tetrameric avidin is fairly stable in urea [25,26] or on biotin binding [27], we checked the possibility of saturating the avidin gel with biotin prior to its DTT treatment, and used urea instead of SDS as denaturing agent to improve accessibility of the disulphide bridge of the biotinylated reagent to be cleaved.

#### *Behaviour of streptavidin and avidin during (strept) avidin-Sepharose and thiopropyl-Sepharose chromatography*

Pilot experiments consisted in the use of immobilized radioiodinated avidin and streptavidin, which allowed the easy determination of the amounts of these proteins initially released from affinity gels by denaturing agents, then subsequently adsorbed to and released from the thiopropyl-Sepharose matrix.

*Streptavidin-Sepharose.* In a first series of experiments we evaluated the release of avidin and streptavidin and demonstrated subsequent elimination of streptavidin, under conditions strictly identical with those established for AII receptor purification; the results, expressed in  $\mu\text{g}$  of protein/ml of starting

gel, are given in Table II. Treatment of avidin or streptavidin gels with DTT in 1% SDS released less streptavidin (35  $\mu\text{g}$ ) than avidin (83  $\mu\text{g}$ ). To underline the importance of this contamination, it must be noted that under similar conditions, using the minimum amount of gel required for optimum receptor adsorption, the amount of eluted AII receptor was about 300 ng (a minor fraction of immobilized (strept)avidin is involved in receptor binding; for details see the next section); the intrinsic amount of released avidin or streptavidin precludes accurate electrophoretic elimination in large-scale preparations.

DTT removal by ultrafiltration through YM 30 Diaflo membranes was carried out in Triton X-100-containing buffers because this detergent unexpectedly allowed more efficient AII receptor re-adsorption to thiopropyl-Sepharose (84%) compared with SDS (66%) (Table I); this finding should not necessarily be extended to other proteins to be purified. Some streptavidin or avidin was eliminated in the first ultrafiltration cycles, probably by dialysis of monomers (which might cease when the Triton/SDS ratio reached values allowing subunit reassociation).

As expected, streptavidin was poorly and non-specifically adsorbed to thiopropyl-Sepharose (10%), while the bulk of avidin was specifically adsorbed (82%) and DTT eluted (93%) (Table II); the amount of recovered streptavidin (1.4  $\mu\text{g}$ ) can be considered as acceptable inasmuch it is exclusively found in monomeric form when treated with SDS and analysed by SDS-PAGE; Fig. 1A illustrates the absence of residual tetrameric radioiodinated streptavidin; the protein to be purified can be freed from residual contamination by electroelution, provided its molecular mass is in the suitable range (65 000 for AII receptor, see Fig. 1A).

*Avidin-Sepharose.* Biotin presaturation of the avidin-Sepharose gel and the use of urea instead of SDS as denaturing agent in the elution medium proved equally efficient in reducing the amount of released avidin (not shown), their combination being slightly more advantageous (Table II). Although most of the avidin contained in the ultrafiltered sample was adsorbed to thiopropyl-Sepharose, only 30% was eluted with DTT in the presence of SDS, and less than 10% with DTT in the presence of urea in Triton X-100; the interpretation is

TABLE II

## BEHAVIOUR OF AVIDIN OF STREPTAVIDIN THROUGHOUT COMBINED AVIDIN OR STREPTAVIDIN-SEPHAROSE AND THIOPROPYL-SEPHAROSE CHROMATOGRAPHY

3 ml of [ $^{125}$ I]avidin (4.0  $\mu$ Ci/mg of protein) and [ $^{125}$ I]streptavidin (2.9  $\mu$ Ci/mg of protein) gels were treated under various conditions designed for AII receptor purification as described in under Experimental. The amounts of recovered avidin or streptavidin were measured in the various steps involved in the purification procedure.

Step	Streptavidin ( $\mu$ g/ml of starting streptavidin-Sepharose gel)	Avidin ( $\mu$ g/ml of starting avidin-Sepharose gel)	
	Conditions for elution from streptavidin gel	Conditions for elution from avidin gel	
	DTT-SDS	DTT-SDS	Biotin presaturation + DTT-urea-Triton X-100
Elution from avidin or streptavidin gel	35	83	13.5
YM 30 ultrafiltration	17.5	72	5.9
Thiopropyl-Sepharose adsorption	1.8	59	5.3
Thiopropyl-Sepharose elution			
DTT-SDS	1.4	55	1.6
DTT-urea-Triton X-100	N.D. <sup>a</sup>	N.D. <sup>a</sup>	0.5

<sup>a</sup> N.D. = Not determined.

that the disulphide bridge joining thiopropyl-Sepharose to avidin displays different DTT accessibilities under the two conditions, and that this accessibility is systematically decreased when SDS has been omitted in the preceding step. As a final result, the residual avidin contamination was lowered to a value close to, or even lower (0.5  $\mu$ g/ml of starting gel, *i.e.*, less than 1/1000 of immobilized avidin) than that previously obtained for streptavidin (1.4  $\mu$ g/ml of starting gel). Remaining avidin was exclusively found as its monomeric form after SDS denaturation and SDS-PAGE (Fig. 1B).

#### General schemes for protein purification

That conclusions drawn from the above-described control experiments should be valid for protein purification assays can be inferred from the following evidence: only 1/1000 of immobilized avidin or streptavidin is involved in the adsorption of biotinylated AII receptor complexes, as previously established in gel saturation experiments [12]; avidin or streptavidin is stabilized upon biotin binding [27]; it was confirmed, in AII receptor purification

experiments, by the lack of receptor elution during SDS washing of the gels: not more than 1-1.5% (five experiments) of the adsorbed probe-receptor complexes were eluted on washing with four column volumes of buffer containing 1% SDS.

We have verified that initial replacement of SDS with urea in Triton X-100 did not have a significant effect either on AII receptor elution from avidin or streptavidin gels or on its readsorption or re-elution in the thiopropyl-Sepharose step, which emphasizes the validity of this new set of experimental conditions (various yields are given in Table I and electrophoretic patterns of the purified receptor are shown in Fig. 1C).

As a consequence, we can propose two general schemes (Fig. 2) for the purification of a protein which has been selectively derivatized with NHS-S-Bio or which has reacted (covalently or not covalently) with the appropriate biotinylated ligand.

Although the initial covalent labelling of the protein with the biotinylated reagent and the use of denaturing agents might not allow purified protein displaying all its native properties to be obtained.

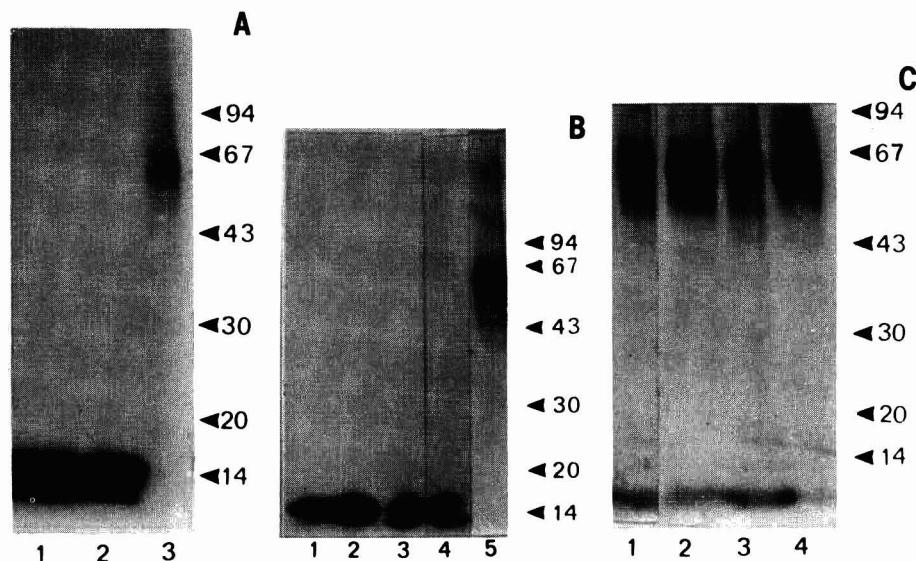


Fig. 1. Electrophoretic mobilities of purified AII receptor and streptavidin or avidin released in control experiments. A 3-ml volume of immobilized [<sup>125</sup>I]streptavidin-Sepharose (2.9  $\mu$ Ci/mg protein) or [<sup>125</sup>I]avidin (4.0  $\mu$ Ci/mg) was treated under conditions usually applied in AII receptor purification as described under Experimental. AII receptor was purified from rat liver plasma membranes using [<sup>125</sup>I]Bio-S-S-AII(N<sub>3</sub>) (initial concentration, 6–8 nM; specific radioactivity, 180–1800 Ci/mmol) as mentioned under Experimental. AII receptor, released [<sup>125</sup>I]streptavidin and [<sup>125</sup>I]avidin were analysed by SDS-PAGE (12.5% acrylamide gel) and autoradiography. (A) Released [<sup>125</sup>I]streptavidin (2.8  $\mu$ g): lane 1 = DTT elution from [<sup>125</sup>I]streptavidin-Sepharose in the presence of SDS; lane 2 = DTT elution from [<sup>125</sup>I]streptavidin-Sepharose and thiopropyl-Sepharose in the presence of SDS (see Experimental, conditions A); lane 3 = purified AII receptor (51 fmol). (B) Released [<sup>125</sup>I]avidin (1.2  $\mu$ g): lane 1 = DTT elution from [<sup>125</sup>I]avidin-Sepharose in the presence of SDS; lane 2 = DTT elution from [<sup>125</sup>I]avidin-Sepharose and thiopropyl-Sepharose in the presence of SDS (see Experimental, conditions A); lane 3 = DTT elution from biotin-presaturated [<sup>125</sup>I]avidin-Sepharose in the presence of urea in Triton X-100; lane 4 = DTT elution from biotin-presaturated [<sup>125</sup>I]avidin-Sepharose and thiopropyl-Sepharose in the presence of urea in Triton X-100 (see Experimental, conditions B); lane 5 = purified AII receptor (38 fmol). (C) Electrophoretic pattern of AII receptor purified under various elution conditions from streptavidin-Sepharose and thiopropyl-Sepharose. Purified AII receptor (1–2 fmol, 1800 Ci/mmol) was analysed by SDS-PAGE (12.5% acrylamide gel) and by autoradiography. Lane 1 = DTT elution from streptavidin-Sepharose and thiopropyl-Sepharose in the presence of SDS (see Experimental, conditions A); lanes 2–4 = DTT elution from biotin-presaturated streptavidin-Sepharose in the presence of urea, followed by DTT elution from thiopropyl-Sepharose in the presence of either SDS (lane 2), or urea in Triton X-100 (lane 3) or CHAPS (lane 4) (see Experimental, conditions B). Numbers on the right are molecular masses of protein standards ( $\times 10^{-3}$ ).

many structural applications are consistent with these constraints (antibody production, obtaining partial peptide sequences from purified intact protein or fragments for cloning or mapping studies, recognition of the protein or fragments by specific antibodies, etc).

Combinations between the two purification schemes can easily be imagined; for instance, although these modifications have not been checked for streptavidin gels, one can postulate that biotin saturation followed by the use of urea might further improve the elimination of contaminating streptavidin.

Efficient AII receptor elution from thiopropyl-

-Sepharose could be achieved in Triton X-100-containing buffers in the absence of urea (Table I). Interestingly, AII receptor could be efficiently adsorbed to thiopropyl-Sepharose in CHAPS as detergent and DTT eluted in presence of urea in CHAPS (Table I). This emphasizes the various possible conditions for obtaining purified proteins essentially freed from contaminating avidin or streptavidin, and the various media in which purified samples can be finally handled.

## DISCUSSION

Among the numerous applications of the avidin-

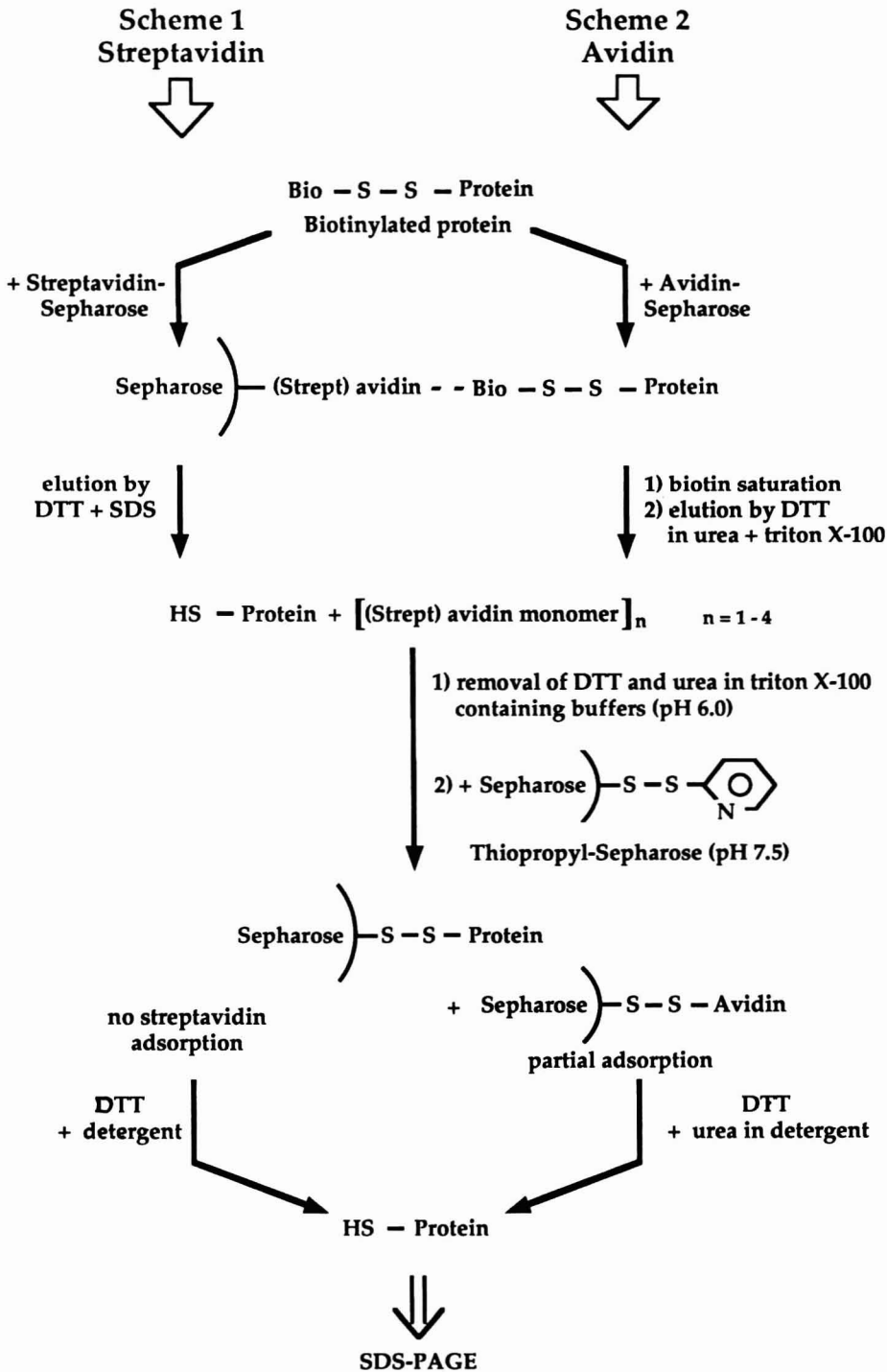


Fig. 2.

biotin system, those involving detection and quantitative evaluations of biotinylated entities using appropriate avidin derivatives have been the most straightforward [1–5]; many examples refer to the study of interactions between biomolecules. The wide use of this system essentially results from the extremely high affinity of avidin for biotin, which generally allows high residual affinity when biotin has been linked to one of the interacting partners. Conversely, purification purposes, which involve reversal of the biotin–avidin interaction, have been achieved with difficulty. Solutions to these problems based on the use of chemically modified biotin (iminobiotin [13], dethiobiotin [10]) cannot be generalized without raising new problems; for instance, our strategy for AII receptor purification [12] could not be developed with iminobiotin hormone derivatives which display prohibitive non-specific binding to membranes; the use of a dethiobiotin–ACTH derivative for receptor purification [10] did not eliminate the need for denaturing treatment in

the recovery step from affinity gels, which induced release of important amounts of avidin. Another possibility is to use biotin derivatives containing a disulphide function which can be reduced under mild conditions [14–18]. The data obtained with several Bio–S–S–dUTP derivatives emphasize that optimization of the length of the linkers joining biotin to dUTP was required to favour accessibility of the S–S bond to DTT [16].

The biotinylated photoactivatable probe that we have designed for AII receptor purification [12] was obtained by reaction of azido AII derivatives with the commercially available NHS–S–S–Bio [19]: covalent complexes between this probe and rat liver receptor could be efficiently adsorbed to (strept)avidin gels, under conditions where premature cleavage of the probe was suppressed by NEM alkylation of the thiol functions of the membrane preparations [12]; however, high recoveries of these complexes by DTT treatment required the accessibility of the probe S–S bond to SDS to be improved; this latter induced the release of unacceptable amounts of avidin or streptavidin. Instead of searching for an ideal synthetic probe possessing an accessible S–S bond, we tried to find convenient ways for avidin or streptavidin elimination. We could propose two kinds of solutions. The most rational one takes advantage of the fortuitous absence of cysteine in the streptavidin protein sequence [22]; this made possible selective re-adsorption of the protein to be purified through the thiol function generated on DTT cleavage of the spacer arm (additional re-adsorption through the other thiol functions of the protein, if any, constitutes a favourable factor); as predicted, residual streptavidin was lowered to acceptable values. The second solution is an empirical approach to make possible the use of avidin, which possesses cysteine residues [28] but is much less expensive than streptavidin; the proposed procedure involves limitation of initial avidin release by biotin saturation of avidin–Sepharose before DTT elution and the use of urea (in Triton X-100) instead of SDS to favour this elution. These initial elution conditions greatly influence the behaviour of avidin in the recovery step from thiopropyl–Sepharose gel; the use of DTT in the presence of urea leaves the bulk of adsorbed avidin unreleased, as a probable result of poor accessibility of the disulphide bridge involved, under these less denaturing conditions.

---

Fig. 2. Combined (strept)avidin–Sepharose and thiopropyl–Sepharose affinity chromatography applied to protein purification. The proposed purification schemes are applied to a protein which has previously been selectively biotinylated using the commercially available reagent NHS–S–S–Bio (or another synthetic reagent possessing a disulphide bridge). The biotinylated protein is adsorbed to streptavidin–Sepharose or avidin–Sepharose, then recovered by DTT treatment in the presence of either SDS (Scheme 1) or urea in Triton X-100 (Scheme 2); these denaturing agents favour the accessibility of the disulphide bridge of the biotinylated reagent, but at the same time release non-negligible amounts of streptavidin or avidin subunits (evaluation of the degree of subunit reassociation is beyond the scope of the paper); biotin presaturation of the gel and the use of urea greatly reduce the amount of released avidin (see text). Most of the DTT and urea are eliminated by ultrafiltration–dilution cycles carried out at pH 6.0 to avoid reoxidation of the thiol function generated on the spacer arm of the biotinylated reagent; this thiol function allows re-adsorption of the protein to an activated thiol–matrix: thiopropyl–Sepharose (after pH readjustment to 7.5). Released streptavidin, devoid of any cysteine residue, is not adsorbed (Scheme 1); although significantly adsorbed to thiopropyl–Sepharose through its thiol functions, avidin (possibly reassociated into subunits) is poorly eluted by DTT + urea, probably because of reduced accessibility of the disulphide bridge which joins it to thiopropyl–Sepharose (Scheme 2). The protein is once again efficiently recovered by DTT treatment (see the example of AII receptor commented upon in Table I), before possible analysis and further purification by SDS–PAGE. Although not having been systematically checked, combinations between these two schemes can be imagined.

The small amounts of (strept)avidin remaining after application of one of the proposed solutions can be further eliminated, if required, by SDS-PAGE.

As urea exerts little denaturing effect on avidin and streptavidin [25,26], its effect on AII receptor recovery from affinity gels results from an increase in the accessibility of the probe S–S bond through receptor denaturation; this emphasizes that avoiding denaturing agents would imply the chemical design of biotin derivatives possessing an S–S bond in the right position with respect to their receptor anchorage sites; as a consequence, generalization of the use of a given biotinylated reagent would not necessarily be possible as the steric requirements would obviously depend on the protein to be purified.

As a result of our investigations, initiated by difficulties encountered for AII receptor purification, we can propose the possible extension of the following purification scheme: selective biotinylation of the entity to be purified by a classical disulphide bridge-containing reagent, and development of combined streptavidin (or avidin)-Sepharose and thiopropyl-Sepharose chromatography. The latter step, introduced to eliminate (strept)avidin, may provide by itself additional purification; moreover, it offers the possibility of finally handling the purified entity in appropriate detergents, when required.

The reported experiments refer to conditions adapted to membrane protein purification; there is little doubt that the proposed ways of eliminating (strept)avidin might be applied to soluble proteins even when DTT recovery of the entity to be purified would not require the use of denaturing agents. In addition, leakage of ligands immobilized to cyanogen bromide-activated agarose cannot always be ignored; thiopropyl-Sepharose might constitute a convenient tool for eliminating released multimeric or monomeric streptavidin.

#### ACKNOWLEDGEMENTS

The authors thank M. Passama for preparing the figures. This work was supported by the Centre National de la Recherche Scientifique, Institut National de la Recherche Médicale and Fondation pour la Recherche Médicale.

#### REFERENCES

- 1 D. M. Boorsma, in G. R. Bullock and P. Petrusz (Editors), *Techniques in Immunocytochemistry*, Vol. 2, Academic Press, London, 1983, p. 155.
- 2 M. Wilcheck and E. A. Bayer, *Immunol. Today*, 5 (1984) 39.
- 3 E. A. Bayer and M. Wilcheck, *J. Chromatogr.*, 510 (1990) 3.
- 4 M. Wilcheck and A. B. Bayer (Editors), *Methods in Enzymology*, Vol. 184, Academic Press, San Diego, London, 1990.
- 5 M. Wilcheck and E. A. Bayer, *Trends Biol. Sci.*, 14 (1989) 408.
- 6 M. F. Finn, G. Titus, D. Horstman and K. Hofmann, *Proc. Natl. Acad. Sci. U.S.A.*, 81 (1984) 7328.
- 7 K. Hofmann, H. Titus, K. Ridge, J. A. Raffensperger and F. M. Finn, *Biochemistry*, 26 (1987) 7384.
- 8 E. Hazum, I. Schwartz, Y. Waskman and D. Keinan, *J. Biol. Chem.*, 261 (1986) 13043.
- 9 K. Wada, H. Tabuchi, R. Ohba, M. Satoh, Y. Tachiana, N. Akiyama, O. Hiraoka, A. Asakura, C. Miyamoto and Y. Furuichi, *Biochem. Biophys. Res. Commun.*, 167 (1990) 251.
- 10 K. Hofmann, C. J. Stehle and F. M. Finn, *Endocrinology*, 123 (1988) 1355.
- 11 D. P. Brennan and M. A. Levine, *J. Biol. Chem.*, 262 (1987) 14796.
- 12 J. Marie, R. Seyer, C. Lombard, F. Desarnaud, A. Aumelas, S. Jard and J. C. Bonnafous, *Biochemistry*, 29 (1990) 8943.
- 13 G. A. Orr, G. C. Heney and R. Zeheb, *Methods Enzymol.* 122 (1986) 83.
- 14 M. L. Shimkus, J. Levy and T. Herman, *Proc. Natl. Acad. Sci. U.S.A.*, 82 (1985) 2593.
- 15 M. L. Shimkus, P. Guaglianone and T. M. Herman, *DNA*, 5 (1986) 247.
- 16 T. M. Herman, E. Lefever and M. Shimkus, *Anal. Biochem.*, 156 (1986) 48.
- 17 B. Roseman, J. Lough, E. Houkom and T. Herman, *Biochem. Biophys. Res. Commun.*, 137 (1986) 474.
- 18 D. R. Gretch, M. Suter and M. F. Stinski, *Anal. Biochem.*, 163 (1987) 270.
- 19 R. Seyer and A. Aumelas, *J. Chem. Soc., Perkin Trans. 1*, (1990) 3289.
- 20 J. C. Bonnafous, M. Tence, R. Seyer, J. Marie, A. Aumelas and S. Jard, *Biochem. J.*, 251 (1988) 873.
- 21 U. K. Laemmli, *Nature (London)*, 335 (1970) 437.
- 22 C. E. Argarana, I. D. Kuntz, S. Birken, R. Axel and C. R. Cantor, *Nucleic Acids Res.*, 14 (1986) 1871.
- 23 N. M. Green, *Biochem. J.*, 89 (1963) 609.
- 24 R. A. Kohansky and M. D. Lane, *Methods Enzymol.*, 184 (1990) 194.
- 25 H. Fraenkel-Conrat, N. S. Snell and E. D. Duca, *Arch. Biochem. Biophys.*, 39 (1952) 97.
- 26 G. P. Kurzban, E. A. Bayer, M. Wilcheck and P. M. Horowitz, *J. Biol. Chem.*, 266 (1991) 14470.
- 27 N. M. Green, *Adv. Protein Chem.*, 29 (1975) 85.
- 28 R. J. De Lange and T. S. Huang, *J. Biol. Chem.*, 246 (1971) 698.

CHROM. 24 098

# Conalbumin-conjugated silica gel, a new chiral stationary phase for high-performance liquid chromatography

Nariyasu Mano and Yoshiya Oda

*Department of Physical and Analytical Chemistry, Tsukuba Research Laboratories, Eisai Co., Ltd., 5-1-3 Tokodai, Tsukuba, Ibaraki 300-26 (Japan)*

Toshinobu Miwa

*Department of Pharmaceutical Research Laboratory, Eisai Co., Ltd., 2-1 Takehaya-machi, Kawashima-cho, Hashima-gun, Gifu 483 (Japan)*

Naoki Asakawa, Yutaka Yoshida and Tadashi Sato

*Department of Physical and Analytical Chemistry, Tsukuba Research Laboratories, Eisai Co., Ltd., 5-1-3 Tokodai, Tsukuba, Ibaraki 300-26 (Japan)*

(First received January 17th, 1992; revised manuscript received February 12th, 1992)

---

## ABSTRACT

A new chiral stationary phase using conalbumin (from chicken egg white) was developed for high-performance liquid chromatography. Chiral resolution of racemic azelastine, an antiallergic drug, was achieved on a conalbumin-conjugated silica gel column. The effects of the pH, the concentration of organic solvents and salts in the mobile phase, and the temperature on the capacity factor and resolution of racemic azelastine were examined. This column shows good stability and can separate optical isomers with an aqueous mobile phase. It should be very useful in studies on pharmacokinetics and in clinical chemistry.

---

## INTRODUCTION

Chiral discrimination has been a problem in the development and use of pharmaceutical drugs, because drug enantiomers can have different pharmacokinetic properties and cause different physiological responses. For this reason, many studies on optical resolution by high-performance liquid chromatography (HPLC) have been conducted, and the direct resolution of racemic compounds has been achieved by use of chiral stationary phases. However, many of them are used under normal-phase

conditions, and laborious pretreatments are required to eliminate water in samples. At present cyclodextrin-conjugated columns [1] and protein-conjugated columns, which can be used in reversed-phase mode, are commercially available. The usefulness of protein-conjugated columns in HPLC has been demonstrated by Allenmark *et al.* [2] and Hermansson [3]. Allenmark *et al.* [2] have successfully resolved acidic compounds by using a bovine serum albumin-conjugated column, and Hermansson [3] resolved racemic amines with an  $\alpha_1$ -acid glycoprotein-conjugated column. However, these columns do not have sufficient durability. Miwa *et al.* [4] have developed a highly effective column for chiral recognition by using ovomucoid, an acid glycoprotein found in chicken egg white. An ovomucoid col-

---

*Correspondence to:* Dr. N. Mano, Department of Physical and Analytical Chemistry, Tsukuba Research Laboratories, Eisai Co., Ltd., 5-1-3 Tokodai, Tsukuba, Ibaraki 300-26, Japan.

umn can achieve the chiral resolution of acidic and basic compounds [5,6], is quite resistant to variations in pH, to heat and to organic solvents [4,7], and has been proved to have higher stability and chiral resolution than the  $\alpha_1$ -acid glycoprotein-conjugated column described by Kirkland *et al.* [8]. Oda *et al.* [9] have recently performed on-line simultaneous determination and resolution of enantiomers of verapamil and its metabolites in plasma by employing an ovomucoid column with a column-switching technique.

In this study we used azelastine (AZE), which is a phthalazinone derivative, as a model compound. AZE is an antiallergic drug with a wide spectrum of pharmacological activities. It inhibits the action of many chemical mediators such as leukotriene [10] and histamine [11]. AZE has an asymmetric carbon (Fig. 1), and Kajima *et al.* [12] have achieved the separation of enantiomeric AZE by ion-pair chromatography under normal-phase conditions. However, optical resolution of this drug has not been achieved by HPLC with an aqueous mobile phase, which would be required for studies of the pharmacokinetics of enantiomeric AZE by HPLC. In this paper, we describe a new stationary phase for chiral resolution, conalbumin-conjugated silica gel, which allows the separation of AZE enantiomers by means of reversed-phase HPLC.

## EXPERIMENTAL

### Apparatus

A Shimadzu LC-9A pump (Shimadzu, Kyoto, Japan) equipped with an SPD-6A variable-wavelength UV monitor was used. A stainless-steel col-

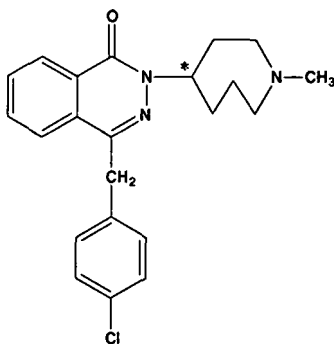


Fig. 1. Structure of *d,l*-azelastine. The chiral centre is indicated by an asterisk.

umn of 150 mm  $\times$  4.6 mm I.D. was packed with conalbumin-conjugated silica gel. The sample was injected with a Model 7125 (Rheodyne) injector. The pH was measured with a TDA HM-60S pH meter (TOA Electronics, Tokyo, Japan).

### Preparation of conalbumin column

Conalbumin-conjugated silica gel was prepared as follows: Unisil Q NH<sub>2</sub> (2 g) and N,N-dissuccinimidyl carbonate (3 g) were made to react for 6 h in acetonitrile (50 ml) at room temperature using a magnetic stirrer. The activated silica gel was washed with acetonitrile and then with the coupling buffer (50 mM potassium phosphate buffer, pH 7.5). Conalbumin (2 g) was dissolved in 50 ml of coupling buffer and then the activated silica gel was added. The mixture was stirred for 6 h at room temperature with a magnetic stirrer. After reaction, the conalbumin-conjugated silica gel was collected by filtration and washed with water and 2-propanol–water (1:2), then packed into a stainless-steel column (150 mm  $\times$  4.6 mm I.D.) by a conventional high-pressure slurry-packing procedure.

### Reagents and materials

Racemic AZE [(+)-4-(4-chlorobenzyl)-2-(hexahydro-1-methyl-1H-azepin-4-yl)-1(2H)-phthalazinone] and optically active AZE were prepared in our laboratories (Fig. 1). Conalbumin was purified from chicken egg white. N,N-Dissuccinimidyl carbonate was purchased from Wako Pure Chemical Industries (Osaka, Japan). Unisil Q NH<sub>2</sub> was purchased from Macherey-Nagel (Düren, Germany). Organic solvents and water were of HPLC grade.

### Sample

A known amount of racemic AZE was dissolved in methanol and the solution was diluted with water to a concentration of 20 ng/ $\mu$ l.

## RESULTS AND DISCUSSION

Conalbumin is an egg-white protein that is also known as ovotransferrin. This protein binds iron, copper, manganese and zinc [13–15] at pH 6 or above, and has an action that blocks the growth of bacteria. Its molecular weight is about 70 000–78 000, and its pI value is 6.1–6.6. In this study we

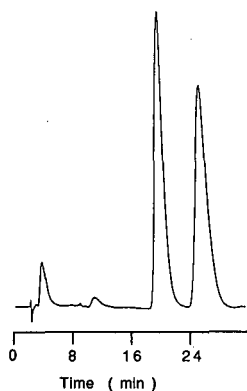


Fig. 2. Separation of *d,l*-azelastine on a conalbumin column. Chromatographic conditions: mobile phase, 50 mM potassium phosphate buffer (pH 5.0) containing 8% ethanol; detection, UV 230 nm; flow-rate, 1.0 ml/min; column temperature, room temperature; sample amount, 200 ng.

prepared conalbumin-conjugated silica gel as an HPLC stationary phase, and used the basic compound AZE as a model compound for chiral separation. The optimum conditions for chiral resolution were found to be 50 mM potassium phosphate buffer (pH 5.0) containing 8% ethanol, as shown in Fig. 2.

In this column, the pH of the mobile phase greatly affected the capacity factor ( $k'$  values) and chiral separation, as shown in Table I. The  $k'$  values of racemic AZE increased with an increase in the pH. The  $pK$  value of AZE is around 8.5, as determined by neutralization analysis, so its hydrophobicity should not change much in the pH range 4–7. As

TABLE I

EFFECT OF THE pH OF THE MOBILE PHASE ON ENANTIOSELECTIVITY FOR *d,l*-AZELASTINE ON THE CONALBUMIN COLUMN

$k'_1$  = capacity factor of *d*-azelastine;  $k'_2$  = capacity factor of *l*-azelastine;  $n$  = plate number of *d*-azelastine. Chromatographic conditions: the pH of the mobile phase was as shown in the table, and other conditions were the same as in Fig. 2.

pH	$k'_1$	$k'_2$	$\alpha$	$R_s$	$n$
3.0	0.70	0.70	1.00	0.00	908
3.5	1.41	1.64	1.17	0.98	1313
4.5	5.15	6.50	1.26	1.84	1346
5.5	10.32	13.60	1.32	1.99	1138
6.0	16.58	21.30	1.29	1.92	968
6.5	26.55	34.59	1.30	1.86	617

noted above, the  $pI$  value of conalbumin is 6.1–6.6, so the hydrophobicity of this solid phase is maximum in this pH range, and the retention of AZE is strongest at around pH 6.5 in the pH range 3.0–6.5. The reason for this seems to be related to the dissociation of the carboxylic acid moieties of amino acids and the sialic acid moieties of the glycoprotein (conalbumin). On the other hand, the separation factor ( $\alpha$ ) and resolution ( $R_s$ ) of AZE were almost constant at pH 4.5–6.5. It was very interesting that the  $\alpha$ -value and  $R_s$  value were not greatly changed in the pH range 4.5–6.5, although the retention was decreased with a decrease in pH in this range. This seems to show that the interaction between AZE and the chiral recognition site was not changed in spite of variation in the hydrophobicity of the total protein molecule. That is to say, the chiral recognition site of this column for AZE may be dissociated if it has an acidic function or not dissociated if it has a basic function, and its  $pK$  value may be around 4.5. So the enantioseparation for AZE may constant in this pH range in spite of the decrease in the retention with decreasing pH.

The performance of this column was also affected by the concentration of salts in the mobile phase (pH 5.0). As shown in Table II, the  $k'$  values of AZE increased with increasing salt concentration, though the  $\alpha$ -value was not much changed. In general, the hydrophobicity of drugs is little affected by the salt concentration of phosphate buffer in

TABLE II

EFFECT OF THE CONCENTRATION OF SALTS IN THE MOBILE PHASE ON ENANTIOSELECTIVITY FOR *d,l*-AZELASTINE ON THE CONALBUMIN COLUMN

$k'_1$  = capacity factor of *d*-azelastine;  $k'_2$  = capacity factor of *l*-azelastine;  $n$  = plate number of *d*-azelastine. Chromatographic conditions: the concentration of salts in the mobile phase was as shown in the table, and other conditions were the same as in Fig. 2.

Concentration (mM)	$k'_1$	$k'_2$	$\alpha$	$R_s$	$n$
5	2.39	2.75	1.15	0.95	823
10	3.06	3.57	1.17	0.99	852
20	4.31	5.12	1.19	1.17	802
50	6.14	7.11	1.16	1.06	921
100	7.68	8.83	1.15	1.09	1061
250	8.82	9.93	1.13	1.03	1345
500	11.45	12.76	1.12	0.82	1027

HPLC. So the increase in  $k'$  values may be related to the increase in hydrophobicity of the solid phase by the salting out of conalbumin, although the chiral recognition ability was not greatly changed.

This column was also very much affected by the concentration of organic solvents in the mobile phase; the separation mode of this column was reversed phase, as shown in Fig. 3. The hydrophobic retention of AZE on the conalbumin column was very weak compared with that on an octadecylsilane (ODS) column, and the mechanism of the retention in this column seems to involve various interactions, such as hydrophobic and ionic interactions, between conalbumin and AZE. Table III shows the effect of mobile phase modifiers on  $k'$  values and enantioselectivity. When the  $k'$  values of methanol, ethanol, 1-propanol and 1-butanol were compared, they clearly increased with decreasing hydrophobicity of the organic solvents, and this result agrees well with that in Fig. 3. In the cases of methanol and ethanol, lower hydrophobicity gave better  $R_s$  values than were obtained with 1-propanol or 1-butanol. But in the case of branched-chain

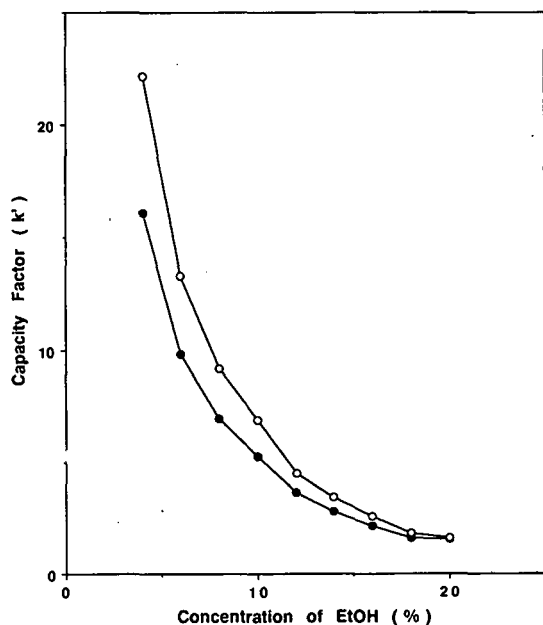


Fig. 3. Effect of concentration of ethanol (EtOH) in the mobile phase on capacity factor of *d,l*-azelastine on the conalbumin column. ● = *d*-azelastine; ○ = *l*-azelastine. Chromatographic conditions: concentration of ethanol in the mobile phase was as shown in the figure and other conditions were the same as in Fig. 2.

TABLE III

EFFECT OF THE MOBILE PHASE MODIFIERS ON ENANTIOSELECTIVITY FOR *d,l*-AZELASTINE ON THE CONALBUMIN COLUMN

$k'_1$  = capacity factor of *d*-azelastine;  $k'_2$  = capacity factor of *l*-azelastine;  $n$  = plate number of *d*-azelastine. Chromatographic conditions: the concentration of organic solvents was 8%, and other conditions were the same as in Fig. 2.

Solvents	$k'_1$	$k'_2$	$\alpha$	$R_s$	$n$
Methanol	14.21	21.17	1.49	1.61	270
Ethanol	6.92	9.17	1.33	1.78	1238
1-Propanol	3.04	3.24	1.07	0.30	342
2-Propanol	5.39	6.74	1.25	1.05	507
1-Butanol	3.01	3.01	1.00	0.00	1160
<i>tert.</i> -Butanol	6.67	8.18	1.23	2.01	1082
Acetonitrile	3.59	4.34	1.21	0.72	497

organic solvents such as 2-propanol or *tert.*-butanol, the above rule did not necessarily hold. As shown in Table III, *tert.*-butanol, which has a larger molecular weight, was more strongly retained than 2-propanol, and *tert.*-butanol likewise had a better  $R_s$  value than 2-propanol. Acetonitrile, lacking a hydroxyl group, gave poor resolution of racemic AZE, its  $\alpha$ -value, 1.21, being almost the same as that of *tert.*-butanol, 1.23. But its  $R_s$  value was only 0.72. It is clear that the resolution of the conalbumin column depends strongly on the kind of organic solvents used. Therefore we consider that organic solvents must be carefully selected whenever a pro-

TABLE IV

EFFECT OF COLUMN TEMPERATURE ON ENANTIOSELECTIVITY FOR *d,l*-AZELASTINE ON THE CONALBUMIN COLUMN

$k'_1$  = capacity factor of *d*-azelastine;  $k'_2$  = capacity factor of *l*-azelastine. Chromatographic conditions: the column temperature was given in the table, and other conditions were the same as in Fig. 2.

Temperature (°C)	$k'_1$	$k'_2$	$\alpha$	$R_s$
4	23.87	28.86	1.21	1.06
10	16.79	20.43	1.22	1.08
20	9.26	11.11	1.20	1.12
25	7.31	8.56	1.17	1.08
30	6.08	6.95	1.14	0.94
37	4.87	5.40	1.11	0.72

tein-conjugated column such as a conalbumin column is used.

In the conalbumin column, the retention of racemic AZE decreased with an increase in the column temperature (Table IV). This may reflect the partition of molecules into the mobile phase, leading to an increase in partition ratio into the aqueous phase at high temperature. However, the  $\alpha$ -value was not much changed. Considering the influence of the column temperature on the stereoselectivity and on the chromatographic efficiency, the optimum temperature was around 20°C in the analysis of AZE.

Conalbumin is labile to heat and acid, unlike chicken egg-white ovomucoid, which is relatively resistant to variation in pH, to heat and to organic solvents. However, conalbumin-conjugated silica gel was stable as a stationary phase for HPLC. Because the conalbumin-coupled silica gel column was injected with samples 400–500 times over 3 months, and although the  $R_s$  values of racemic AZE decreased from 1.7 to 1.1, the chiral recognition ability of this column was well retained. This seems to be related to the interesting property of conalbumin that it is stabilized to heat when combined with iron, copper, manganese and zinc [13–15]. That is to say, the conformation of this protein may be fixed by complexation with these metals. Thus, we considered that fixing the conformation of this protein by conjugating it to silica gel would improve its stability, and we expect that this protein can be used as a reversed phase for chiral resolution by HPLC. Even better durability may be attainable by using another method of fixation of conalbumin.

In a protein-conjugated column, the loading limit is generally much lower than that in an ODS column, because the conjugated protein only covers the external region of silica gel, and only limited regions of the protein are effective for chiral recognition. As expected, the conalbumin column showed a low loading limit. The  $R_s$  value when 200 ng were injected was about 1.1, and the  $R_s$  value when 1  $\mu$ g was injected about 0.9 (only 20% less). In addition, all retentions were almost the same. However, when 10  $\mu$ g of racemic AZE were injected, the isomers were not resolved in this column.

The chiral resolution of racemic AZE has not previously been achieved directly by using reversed-phase HPLC. The implication is that chiral resolution ability varies greatly according to the nature of the protein conjugated to silica gel. If the relation between ligand structure and drug structure can be better understood, it should be possible to prepare columns with highly efficient chiral recognition ability for specific purposes.

#### ACKNOWLEDGEMENT

We are profoundly grateful to Mr Hiroshi Inoue, Kawashima Factory, Eisai Co., Ltd., for the purification and supply of conalbumin.

#### REFERENCES

- 1 J. I. Seeman, H. V. Secor, D. W. Armstrong, K. D. Timmons and T. J. Ward, *Anal. Chem.*, 60 (1988) 2120.
- 2 S. Allenmark, B. Bomgren and H. Boren, *J. Chromatogr.*, 264 (1983) 63.
- 3 J. Hermansson, *J. Chromatogr.*, 269 (1983) 71.
- 4 T. Miwa, M. Ichikawa, M. Tsuno, T. Hattori, T. Miyakawa, M. Kayano and Y. Miyake, *Chem. Pharm. Bull.*, 35 (1987) 682.
- 5 T. Miwa, T. Miyakawa, M. Kayano and Y. Miyake, *J. Chromatogr.*, 408 (1987) 316.
- 6 T. Miwa, H. Kuroda, S. Sakashita, N. Asakawa and Y. Miyake, *J. Chromatogr.*, 511 (1990) 89.
- 7 J. Iredale, A. F. Aubry and I. Wainer, *Chromatographia*, 31 (1991) 329.
- 8 K. M. Kirkland, K. L. Neilson and D. A. McCombs, *J. Chromatogr.*, 545 (1991) 43.
- 9 Y. Oda, N. Asakawa, T. Kajima, Y. Yoshida and T. Sato, *Pharm. Res.*, 8 (1991) 997.
- 10 M. M. Little and T. B. Casale, *J. Allergy Clin. Immunol.*, 79 (1987) 204.
- 11 N. Chand, J. Pillar, W. Diamantis, J. L. Perhach and R. D. Sofia, *Eur. J. Pharmacol.*, 96 (1983) 227.
- 12 T. Kajima, N. Asakawa, T. Hattori, T. Sato and Y. Miyake, *Yakugaku Zasshi*, 109 (1989) 570.
- 13 R. C. Warner and I. Weber, *J. Am. Chem. Soc.*, 75 (1953) 5094.
- 14 J. J. Windle, A. K. Wiersema, J. R. Clark and R. E. Feeney, *Biochemistry*, 2 (1963) 1341.
- 15 A. T. Tan and R. C. Woodworth, *Biochemistry*, 8 (1969) 3711.



# High-performance affinity chromatography of oligonucleotides on nucleic acid analogue immobilized silica gel columns

Eiji Yashima, Tetsuro Shiiba, Tomohiro Sawa, Noriyuki Miyauchi and Mitsuru Akashi

*Department of Applied Chemistry and Chemical Engineering, Faculty of Engineering, Kagoshima University, 1-21-40 Korimoto, Kagoshima 890 (Japan)*

(First received November 19th, 1991; revised manuscript received February 5th, 1992)

---

## ABSTRACT

The nucleic acid analogues poly(9-vinyladenine) (PVAd), poly(9-adenylethyl methacrylate) and poly(thymylethyl methacrylate) (PTM) were chemically bonded to porous silica gel, which had been pretreated with 3-trimethoxysilylpropyl methacrylate, by free radical copolymerization to produce novel packing materials for affinity chromatographic columns. The columns separated nucleosides and nucleotide dimers on the basis of hydrophobic interaction using an aqueous buffer and complementary hydrogen bonding interaction in methanol as an eluent. The PVAd- and PTM-silica gel columns gave a nucleobase-selective separation of oligonucleotides differing in length from mixtures of oligoadenylic and oligouridylic acids. On the PVAd-silica gel column terminal phosphate isomers of oligouridylic acid up to seven mer were resolved and the elution order of the isomers was different from that on an ODS column.

---

## INTRODUCTION

During the past decade, the separation of nucleic acids has been increasingly performed by high-performance liquid chromatography (HPLC) in the fields of molecular biology and genetics [1–4], because the availability of numerous separation columns makes HPLC an attractive alternative to conventional separating techniques for nucleic acids and oligonucleotides. Polynucleotides with a wide range of chain lengths have easily been separated with high resolution using ion-exchange [5–7], reversed-phase [8–11], and mixed-mode [12–15] stationary phases, with separation based on differences in the size, charge, hydrophobicity, shape, base sequence and base composition of the nucleic acids. In ion-exchange chromatography, the elution order

of nucleic acids relies on the number of phosphodiester residues and is largely independent of sequence. Reversed-phase chromatography successfully separates oligonucleotides on the basis of hydrophobicity. Mixed-mode chromatography allows the separation of nucleic acids by size and, in part, by nucleobase sequence [15]. However, these present certain problems as it is difficult to predict the chromatographic behaviour and to control the elution order.

As polynucleotides naturally form double-stranded complexes by the specific interactions, *i.e.* complementary hydrogen bonding and stacking interactions, the development of a stationary phase in which one strand of the polynucleotide is immobilized on a support such as cellulose, agarose and silica gel allows the specific separation of the complementary strand in mixtures of polynucleotides. Chromatographic behaviour is easily predictable in HPLC using such stationary phases and the elution order of polynucleotides is simply controlled by designing an appropriate sequence of immobilized

---

*Correspondence to:* Dr. E. Yashima, Department of Applied Chemistry, Faculty of Engineering, Nagoya University, Chikusa-ku, Nagoya 464-01, Japan (present address).

polynucleotides because of the highly specific formation of duplexes between two strands of complementary polynucleotides.

Conceptually, this is affinity chromatography, which has been available for over 25 years [16–18]. Affinity chromatography is a powerful technique for the specific base recognition of polynucleotides, but its use in HPLC has developed slowly due to the low durability of packing materials for affinity chromatography. Recently, Goss *et al.* [19] prepared the octadecamer of thymidylic acid [(dT)<sub>18</sub>] covalently coupled to macroporous silica gel and separated oligoadenylic acid (A<sub>12–18</sub>) by high-performance affinity chromatography (HPAC). The high resolution of separation shows that HPAC has potentially significant advantages in the purification and separation of nucleic acids. Most packing materials for affinity chromatography and HPAC will resolve nucleic acids with high specificity, but there is a problem of the stability for the nucleic acids attached to the stationary phases. Nucleic acids are decomposed by enzyme-catalysed hydrolysis. To overcome the defect and to apply the HPAC system easily, the immobilization of nucleic acid bases [20–24] and their polymeric analogues, which are stable against chemical and enzymatic hydrolysis, to silica gel [25–27] has been performed, and nucleic acid bases, nucleosides and oligonucleotides were separated on the columns.

We have found that poly(9-vinyladenine) (PVAd)-immobilized silica gel possesses a potent ability for the nucleobase-selective separation of nucleosides and sequence isomers of oligonucleotide dimers for HPLC [28]. Moreover, an agarose-PVAd-conjugated gel showed nucleobase-selective separation of RNA and could discriminate between single- and double-stranded DNA in affinity electrophoresis [29].

In this paper, we report the immobilization of PVAd, poly(9-adenylethyl methacrylate) (PAM) and poly(thymylethyl methacrylate) (PTM) to silica gel and the separation of nucleosides, nucleotide dimers and oligoadenylic [oligo(A)] and oligouridylic [oligo(U)] acids based on complementary hydrogen bonding interactions between the stationary phases and oligonucleotides for HPAC.

## EXPERIMENTAL

### Materials

Nucleosides (A, G, C, U, dA, dG, dC, dT), nucleotide dimers [ApA; adenylyl(3'→5')adenosine, ApG, ApC, ApU, UpU], polyadenylic acid [poly(A)] and polyuridylic acid [poly(U)] were purchased from Sigma (St. Louis, MO, USA) and Yamasa Shoyu (Chiba, Japan). Nuclease S1 and micrococcal nuclease, and tris(hydroxymethyl)aminomethane (Tris) were also obtained from Sigma. Adenine and thymine were purchased from Tokyo Kasei Kogyo (Tokyo, Japan). Ethylenediaminetetraacetate (EDTA) and other chemicals were of analytical-reagent grade from Nakarai Tesque (Kyoto, Japan). Azobisisobutyronitrile and benzoyl peroxide (BPO) were recrystallized from ethanol. Triethylamine was distilled and then stored on NaOH pellets. Benzene was purified in the usual manner and distilled over sodium metal. N,N-Dimethylformamide was distilled with a small amount of dried benzene and distilled under reduced pressure and then stored over molecular sieves. HPLC-grade acetonitrile was used for HPLC.

The preparation of 9-vinyladenine was previously reported [30]. 9-Adenylethyl methacrylate and thymylethyl methacrylate were prepared according to the previously reported method [31]. IR and NMR spectra and melting points were in reasonable agreement with reported values.

### Preparation of oligo(A) and oligo(U)

Freshly autoclaved distilled water was used in all experiments. Oligo(A) was prepared by alkaline hydrolysis of poly(A) (5 mg in 2 ml of 0.15 M KOH solution) at 37°C. A portion (150 µl) of the reaction mixture was withdrawn at an appropriate time and the reaction was stopped by the addition of 3.8 µl of 6 M acetic acid; the resulting oligomer was analyzed on an ODS column [Shim-pack CLC-ODS (M), 150 × 4.6 mm I.D. or Tosoh, TSK-Gel ODS-120T, 150 × 4.6 mm I.D.] as soon as possible. It was found that the hydrolyzed oligo(A) had 2'- and 3'-terminal phosphates and the 2',3'-cyclic terminal phosphate of oligo(A) could not be detected under these conditions.

Oligo(U) with 5'-terminal phosphate was prepared by enzymatic hydrolysis of poly(U) with nuclease S1. To a solution of poly(U) (1 mg) in an

acetate buffer (0.5 ml) with 0.3 M NaCl and 3 mM ZnCl<sub>2</sub> (pH 4.5; S1 buffer) was added an aliquot (33 μl) of nuclease S1 (1 U/μl in S1 buffer) and the solution was allowed to react at 37°C for 120 min. The reaction was stopped by the addition of 0.25 ml of 0.1 M Tris-HCl buffer with 20 mM EDTA (pH 8.8).

Oligo(U) with 3'-terminal phosphate was prepared by micrococcal enzyme hydrolysis. To a solution of poly(U) (1 mg) in 0.1 M Tris buffer (0.50 ml) with 10 mM CaCl<sub>2</sub> (pH 8.8) was added an aliquot (7.5 μl) of micrococcal nuclease (1 U/μl in Tris buffer) and the solution was allowed to react at 37°C for 10 min. The reaction was stopped by the addition of 0.75 ml of 0.1 M Tris buffer with 20 mM EDTA (pH 8.8).

Alkaline hydrolyzed oligo(U) was prepared in a similar manner as oligo(A) [14,32] and the resulting oligomer was analyzed on an ODS column as soon as possible. A portion of the alkaline-hydrolyzed oligo(U) was incubated at a pH less than 2 by addi-

tion of HClO<sub>4</sub> to eliminate 2',3'-cyclic phosphates (60°C for 10 min) [8]. This sample [a mixture of 2'- and 3'-oligo(U)] and 3'-oligo(U), 5'-oligo(U) and 2'-, 3'-, and 2',3'-cyclic phosphate unimers of uridine were used as authentic samples to assign the peaks in a chromatogram of the alkaline hydrolyzed oligo(U). The terminal phosphates of the alkaline hydrolyzed oligo(U) were a mixture of 2'-, 3'- and 2',3'-cyclic phosphates. All samples were stored at -20°C until use.

#### Preparation of stationary phase

Four stationary phases with nucleic acids bases were prepared and the structures are schematically shown in Fig. 1. The preparation of adenine-immobilized silica gel (Si-A) and poly(9-vinyladenine) (PVAd)-immobilized silica gel (Si-PVAd) were previously reported [28].

PAM and PTM were chemically bonded to silica gel (Wako gel LC-10K, 100 Å pore size, 10-μm, beads) pretreated with 3-trimethoxysilylpropyl

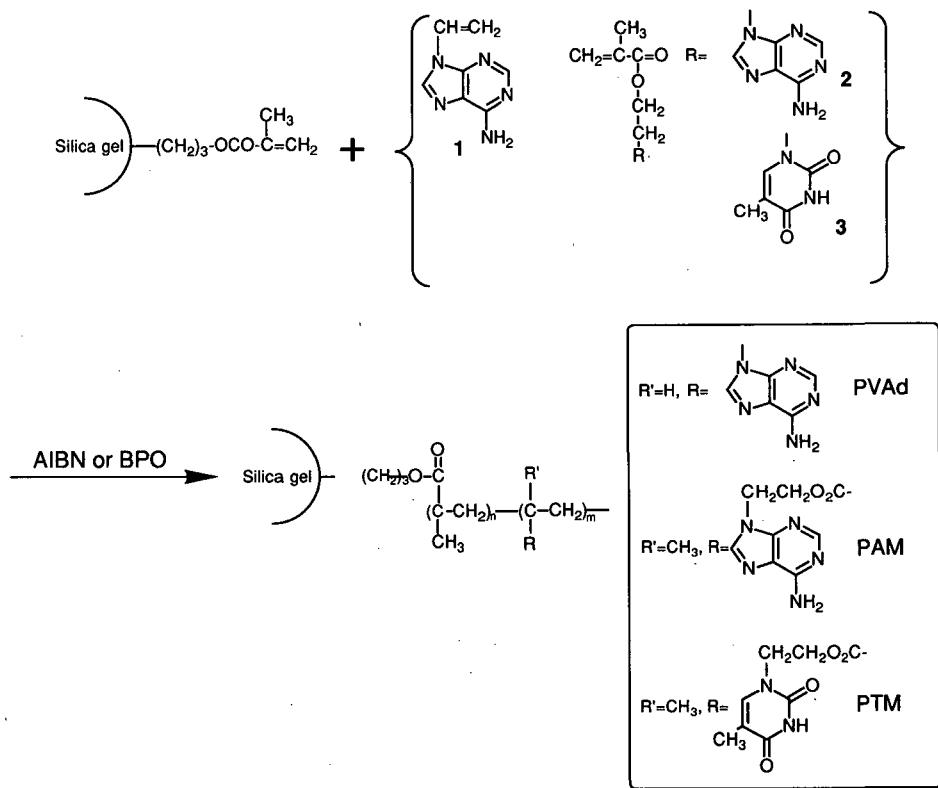


Fig. 1. Structures of the nucleic acid analogue immobilized silica gels.

methacrylate by free radical copolymerization. The typical copolymerization method is as follows: silica gel (1.5 g) was dried at 200°C for 6 h *in vacuo* and then treated with 3-trimethoxysilylpropyl methacrylate (4 ml) in toluene containing 80  $\mu$ l of triethylamine; the suspension mixture was refluxed for 4 h under nitrogen atmosphere. The silanized silica gel was filtered, washed with toluene, acetone and diethyl ether, and then dried *in vacuo*.

To a silanized silica gel (1.5 g) suspended in dioxane (25 ml) was added a solution of 9-adenylethyl methacrylate (0.75 g) in dioxane (40 ml) and azobisisobutyronitrile (0.04 g). The mixture was refluxed for 6 h under nitrogen and the resulting PAM-immobilized silica gel (Si-PAM) was filtered, washed with dioxane, dimethylsulfoxide, ethanol, diethyl ether and acetone, and then dried at 60°C for 12 h *in vacuo*. The amount of the adenyl group coupled to the silica gel was estimated on the basis of the content of the nitrogen determined by the micro-Kjeldahl method (the amounts of the adenyl group were 0.49, 0.49 and 0.47 mmol/g for Si-PAM, Si-PVAd and Si-A, respectively). PTM was immobilized to silica gel (Si-PTM) by the same method. The amount of the thymyl group coupled to silica gel was 0.62 mmol/g.

The packing materials thus obtained were packed in a stainless-steel tube (125  $\times$  4.6 mm I.D.) at 350

kg/cm<sup>2</sup> by a slurry method as reported previously [33]. The plate numbers of these columns were 2000–5000 for acetone with methanol (0.5 ml/min) as an eluent at 25°C.

#### Apparatus

Melting points were determined on a Yamato melting point apparatus Model MP-21 and not corrected. <sup>1</sup>H NMR spectra were recorded on a JEOL GSX-400 (400 MHz) instrument and tetramethylsilane (TMS) was used as the internal standard. IR spectra were measured on a Jasco A-3 infrared spectrometer.

Chromatographic analysis was performed on a Shimadzu LC-6A chromatograph equipped with a gradient controller (Shimadzu SLC-6B) and UV detector (Shimadzu SPD-6A, 260 nm) at a flow-rate of 0.5 or 1.0 ml/min and a temperature of 25 or 30°C unless stated otherwise. A Shimadzu CR-3A instrument was used as a data processor for HPLC. All gradients were performed with a binary gradient elution technique.

#### RESULTS AND DISCUSSION

##### Separation of nucleosides and nucleotide dimers

Table I shows the results of separation of various ribo- and deoxyribonucleosides on Si-A, Si-PVAd.

TABLE I  
RETENTION TIMES OF NUCLEOSIDES

Conditions: column, 125  $\times$  4.6 mm I.D.; flow-rate, 0.5 ml/min; temperature, 20°C.

Column	Eluent <sup>a</sup>	Retention time (min)							
		Ribonucleoside				Deoxyribonucleoside			
		A	G	C	U	dA	dG	dC	dT
ODS	A	6.0	4.2	3.6	3.8	6.5	4.5	3.8	5.2
	B	3.6	3.6	3.6	3.6	3.7	3.7	3.7	3.7
Si-A	C	16.9	11.5	4.7	4.6	18.8	12.5	5.2	6.7
	B	4.5	4.5	3.4	5.1	3.4	3.7	3.1	4.0
Si-PVAd	C	9.6	8.0	3.5	4.0	11.8	8.5	3.9	5.8
	B	4.0	5.6	5.6	7.3	3.2	4.1	3.8	4.1
Si-PAM	C	15.2	9.1	4.0	4.6	17.8	10.2	4.2	7.4
	B	4.4	4.5	4.2	7.7	3.7	3.9	3.4	4.7
Si-PTM	C	11.1	5.4	3.4	3.3	14.2	6.4	3.8	4.6
	B	4.0	3.3	3.3	2.9	3.9	3.2	3.1	2.8

<sup>a</sup> Eluent A, water-methanol (3:1, v/v); B, methanol; C, 1/15 M phosphate buffer (pH 7.0).

Si-PAM, Si-PTM and commercially available ODS columns. An aqueous phosphate buffer and methanol were used as an eluent. The retention times of nucleosides in an aqueous eluent revealed that purine nucleosides were retained more than pyrimidine nucleosides and deoxyribonucleosides were retarded more than the corresponding ribonucleosides ( $dA > A$ ,  $dG > G$ ,  $dT > U$  and  $dC > C$ ). These indicate that the hydrophobic base-base interaction between the stationary phases and nucleic acid bases of nucleosides plays an important part in the separation of nucleosides in an aqueous eluent, as seen in reversed-phase chromatography. On the other hand, when methanol was used as an eluent, the elution order was altered. Uridine was adsorbed most strongly on Si-A, Si-PVAd and Si-PAM, and thymidine was more retained than the other deoxyribonucleosides. In non-aqueous eluent such as methanol or chloroform, the hydrogen bonding interaction between complementary nucleic acid bases seems to be favoured rather than the hydrophobic interaction [34]. Therefore, U and T were more retained on the columns with adenylyl groups. The Si-PVAd column is superior to the Si-A column on a rapid separation of nucleosides. On the Si-PTM column, A and dA were found to have longer retention times than the other nucleosides. In this instance, both hydrophobic and complementary hydrogen bonding interactions may take part in the separation of nucleosides. We have

reported similar results previously [28], as have Nagae *et al.* [24], who prepared nucleic acid bases containing resins or silica gel and nucleoside-immobilized silica gel columns and separated nucleic acid bases and nucleosides on these columns.

There was a similar tendency in the separation of nucleotide dimers. In an aqueous eluent, five dimers were almost completely separated on all columns and purine-purine dimers such as ApA and ApG were more retained than purine-pyrimidine dimers (ApU, ApC); however, ApU and UpU dimers were adsorbed most strongly on the columns except Si-PTM when 0.5 M triethylammonium acetate (TEAA) in methanol was used as an eluent. The results of the separation of nucleotide dimers on Si-A, Si-PVAd, Si-PAM and Si-PTM using TEAA are summarized in Table II. It was evident that the retardation of ApU and UpU on the columns packed with silica gel containing adenine was due to the hydrogen bonding interaction between the adenylyl group and bases, whereas in an aqueous eluent reversed-phase mode separation proceeded. Therefore, the elution order of nucleosides and nucleotide dimers could be controlled on the nucleic acid analogue immobilized silica gel columns by an alteration of the eluents.

#### *Separation of oligo(A) and oligo(U)*

In these results, it was found that in an aqueous eluent, nucleosides and nucleotide dimers interact

TABLE II  
RETENTION TIMES OF DINUCLEOTIDES

Conditions: column, 125 × 4.6 mm I.D.; flow-rate, 1.0 ml/min; temperature, 25°C.

Column	Eluent <sup>a</sup>	Retention time (min)					
		CpA	ApC	ApG	ApU	ApA	UpU
Si-A	A	17.9	20.5	50.9	21.7	<sup>b</sup>	6.6
	B	2.8	2.7	3.1	3.4	3.3	4.0
Si-PVAd	A	2.4	2.6	4.6	3.2	4.9	2.4
	B	2.0	2.2	2.3	3.2	2.7	5.7
Si-PAM	A	4.1	4.7	10.1	6.8	12.7	2.6
	B	2.0	2.2	2.3	4.1	2.9	6.4
Si-PTM	A	2.4	3.0	4.1	2.8	5.8	1.5
	B	2.0	2.2	2.3	2.2	3.4	1.9

<sup>a</sup> Eluent A, 0.1 M TEAA in water; B, 0.5 M TEAA in methanol.

<sup>b</sup> Not detected.

with the adsorbents with nucleic acid bases not via a hydrogen bonding interaction, but via a hydrophobic interaction. However, we have already found that PVAd can form a complex with poly(U) by complementary base-pairing (hydrogen bonding) in water based on UV and imino-proton NMR spectroscopic analysis of the PVAd–poly(U) complex [35]. This may indicate that oligo(U) with a particular chain length will interact with the PVAd on silica gel by hydrogen bonding in water. The complementary base-pairing ability of nucleic acid analogues might become a powerful technique for the separation and isolation of DNA and RNA [36]. To examine such an ability, oligo(A) and oligo(U) were applied to the columns.

The retention times of oligo(A) and oligo(U) on ODS, Si–A, Si–PVAd, Si–PAM and Si–PTM columns were plotted against the degree of polymerization (DP) of the oligomers (Fig. 2). The ODS column separated oligo(A) and oligo(U) (DP = 1–10) with high resolution and the elution order depended on the chain length and hydrophobicity; oligo(A) with a particular chain length was more retained than the corresponding oligo(U). A similar tendency was observed with Si–A, although the differences in the elution times between oligo(A) and oligo(U) decreased. On the Si–PVAd column, the elution time of oligo(U) drastically increased with an increase in the DP (Fig. 2C). This strongly suggests that the oligo(U) with DP > 4–5 can interact with PVAd by complementary hydrogen bonding.

On the Si–PAM column the chromatographic behaviour of the oligomers was different from that on the Si–PVAd and was similar to that on the ODS column. Si–A and Si–PAM columns may be classified as mixed-mode columns (base-pairing and reversed-phase). In an aqueous system, only the reversed-phase mode seems to appear. The reason for the different separation properties between Si–PVAd and Si–PAM was not clear, but the structures of the polymers and the spacer effect for using PAM might influence the separation behaviour.

On the other hand, oligo(A) with DP = 3–8 was adsorbed strongly on the Si–PTM column, but the oligo(U) (DP = 1–10) was eluted within about 10 min under these conditions. The Si–PTM column seems to be the closest to an ideal base-pairing column. Both hydrogen and hydrophobic (stacking) interactions between oligo(A) and PTM must have

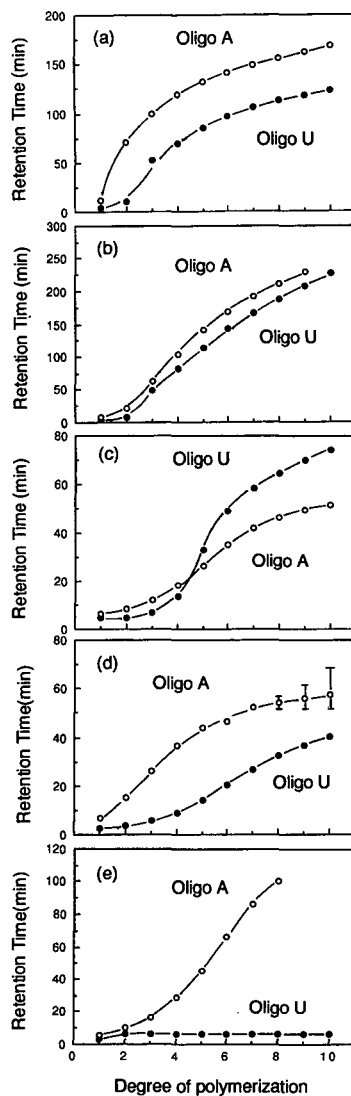


Fig. 2. Relationships between the retention times of oligo(A) and oligo(U) and the degree of polymerization of the oligonucleotides on (a) ODS, (b) Si–A, (c) Si–PVAd, (d) Si–PAM and (e) Si–PTM. The terminal phosphates of oligo(U) and oligo(A) were 3'- and a mixture of 2'- and 3'-phosphates, respectively. Column: ODS, 150 × 4.6 mm I.D.; other modified columns, 125 × 4.6 mm I.D. Eluents and gradient programme: (a) linear gradient from A [0.1 M ammonium acetate (pH 7.0) (100% at 0 min)] to 15% acetonitrile in 0.1 M ammonium acetate (100% at 270 min); (b) linear gradient from A (100% at 0 min) to B [water (100% at 270 min)]; (c) 0–15 min from 3.0 M ammonium acetate (pH 7.0) (100% 0 min) to 8% B with linear gradient, 15–120 min from 8 to 100% B with convex type gradient; (d) 0–120 min from 1.5 M ammonium acetate (pH 7.0) (100% at 0 min) to 100% B with convex type gradient; (e) 0–120 min from 1.5 M ammonium acetate (pH 7.0) (100% at 0 min) to 100% B with linear gradient. Flow-rate, 0.5 ml/min; temperature, 30°C.

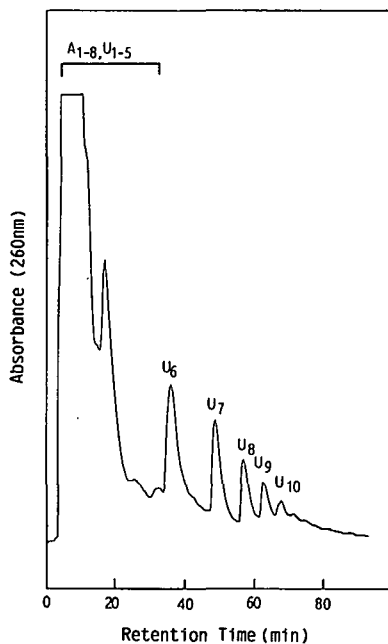


Fig. 3. Separation of mixtures of oligo(U) (DP = 1–11) and oligo(A) (DP = 1–13) on Si-PVAd column (125 × 4.6 mm I.D.). The terminal phosphates of oligo(U) and oligo(A) were 3'- and a mixture of 2'- and 3'-phosphates, respectively. Eluents and gradient programme: 0–15 min from (A) 1.5 M ammonium acetate (pH 7.0) (100% at 0 min) to (B) water (8% at 15 min) with linear gradient, 15–120 min from 8 to 100% B with convex type gradient. Flow-rate, 0.5 ml/min; temperature, 30°C.

a significant effect, as hydrophobic interaction between nucleic acid bases in an aqueous system decreases in the order purine–purine > purine–pyrimidine > pyrimidine–pyrimidine.

The chromatographic conditions described in Fig. 2 were not optimized. The optimization of the salt gradient gave a rapid and nucleobase specific HPAC. Fig. 3 shows the separation of a mixture of oligo(A) and oligo(U) on an Si-PVAd column. A mixture of oligo(A) (DP = 1–10; mixture of 2'- and 3'-terminal phosphates) and oligo(U) (DP = 1–12; 3'-terminal phosphate) was loaded and the column temperature was kept at 30°C. Most of the oligo(A) (DP = 1–8) was eluted, together with oligo(U) (DP = 1–5), within 30 min, and the remaining oligo(U) (DP > 5) was eluted slowly with high resolution. Fig. 4 shows the separation of a mixture of oligo(A) (DP = 1–15) and oligo(U) (DP = 1–10) on the Si-PTM column at 30°C using the salt gradient

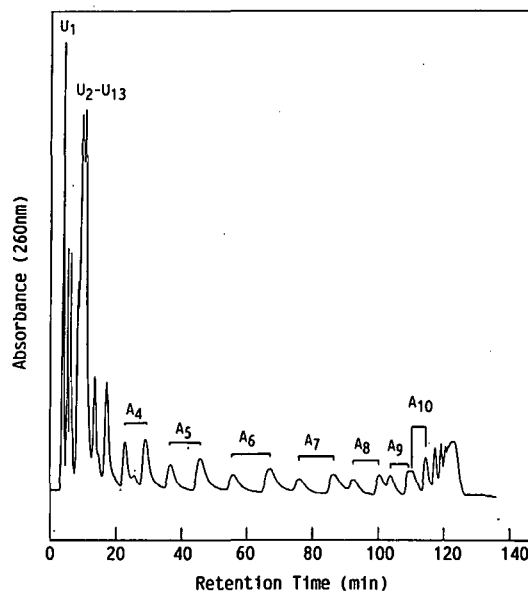


Fig. 4. Separation of mixtures of oligo(A) (DP = 1–12) and oligo(U) (DP = 1–13) on Si-PTM column (125 × 4.6 mm I.D.). The terminal phosphates of oligo(U) and oligo(A) were 3'- and a mixture of 2'- and 3'-phosphates, respectively. Eluents and gradient programme: 0–120 min from 1.5 M ammonium acetate (pH 7.0) (100% at 0 min) to 100% water with linear gradient. Flow-rate, 0.5 ml/min; temperature, 30°C.

technique. As is expected from Fig. 2e, oligo(A) with DP 4–15 was separated from the mixture of the oligonucleotides. Si-PVAd and Si-PTM can separate and isolate a desired oligomer (A or U) by the choice of the column. The [(dT)<sub>18</sub>] covalently coupled silica gel prepared by Goss *et al.* [19] will also separate oligo(A) specifically in a similar manner. The present columns seem to be superior to the nucleic acid-immobilized columns in regard to the stability against nuclease and ease of preparation. Moreover, our system should also be applicable to affinity electrophoresis and HPAC of polynucleotides, RNA and DNA. Si-PTM especially could be used to isolate m-RNA.

The Si-PAM column was not effective for the nucleobase-specific separation of oligo(U) from a mixture of oligo(A) and oligo(U). However, the Si-PAM column was found to separate oligo(U) rapidly with high resolution (Fig. 5).

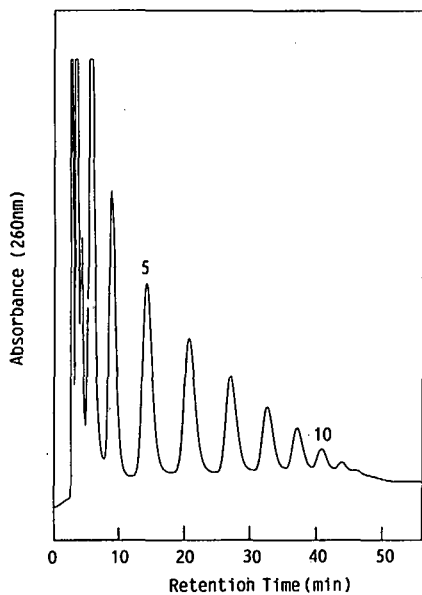


Fig. 5. Separation of 3' oligo(U) (DP = 1-13) on Si-PAM column (125 × 4.6 mm I.D.). Eluents and gradient programme: 0-120 min from 1.5 M ammonium acetate (pH 7.0) (100% at 0 min) to 100% water with convex type gradient. Flow-rate, 0.5 ml/min; temperature, 30°C.

### Separation of terminal phosphate isomers of oligo(U)

The reversed-phase ODS column separates terminal phosphate isomers of oligonucleotides in a wide range of chain lengths (at least DP = 1-7 from our experiments); however, as the oligonucleotides increase in length, the resolving power of ODS slowly decreases. Therefore, the separation of terminal phosphate isomers of oligonucleotides is difficult by ODS and ion exchange chromatography. To examine the ability of the terminal phosphate recognition on the Si-PVAd column, alkaline hydrolysed oligo(U) was loaded onto the column. Fig. 6 shows the separation of oligo(U) (DP = 1-7) prepared by alkaline hydrolysis, the terminal end of which was a mixture of 2', 3'- and 2',3'-cyclic phosphates. The peak assignment in Fig. 6 was carried out carefully using authentic samples (see under Experimental). The conditions of the alkaline hydrolysis were similar to those reported by Bischoff and McLaughlin [14] except for the concentration of KOH. Bischoff and McLaughlin stated that most of the hydrolyzed oligo(U) contained a 2',3'-cyclic phosphate and the

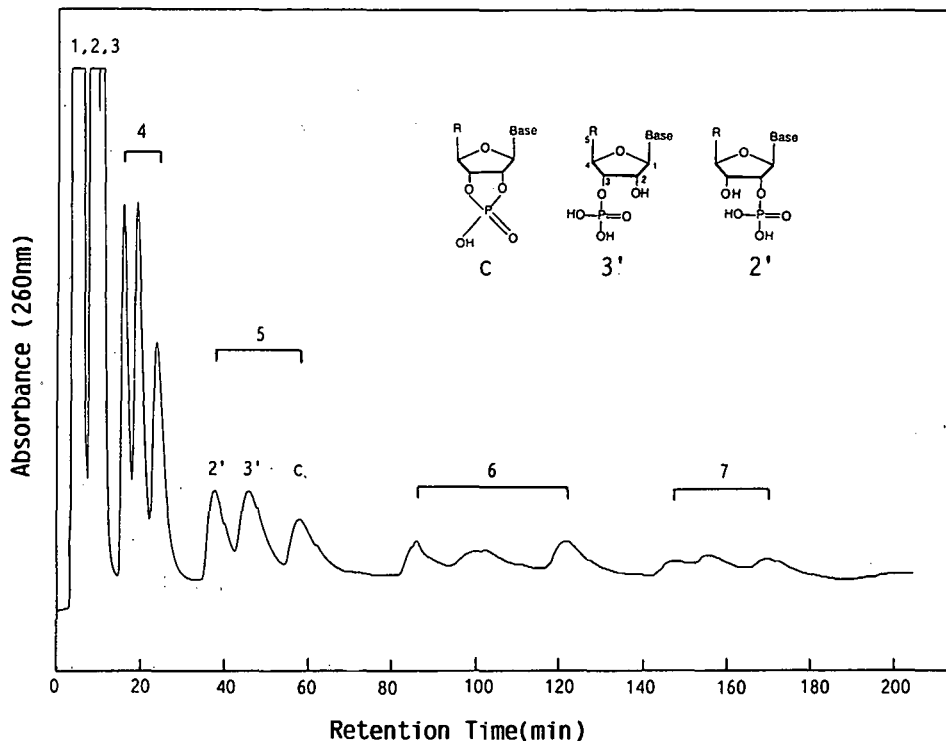


Fig. 6. Separation of terminal phosphate isomers of oligo(U) (DP = 1-7) on Si-PVAd column (125 × 4.6 mm I.D.). Eluents and gradient programme: linear gradient from 1.5 M ammonium acetate (pH 7.0) (100% at 0 min) to water (100% at 240 min). Flow-rate, 0.5 ml/min; temperature, 30°C.

amount of 2'- or 3'-terminal phosphate was roughly 5%. The ratio of the terminal phosphates of the oligo(U) in Fig. 6 varied much less with the DP and was roughly estimated to be 2'-U/3'-U/cyclicU = 1:1:1.

The terminal phosphate isomers of oligo(U) were well resolved on the Si-PVAd column and the resolution was only slightly dependent on the DP of oligo(U), although the peaks broadened as the oligonucleotides increased in length. The elution order was cyclicU > 3'-U > 2'-U. This was different from the elution order on the ODS column (2'-U > cyclic U > 3'-U).

In conclusion, nucleic acid analogues, especially polymer analogues immobilized on silica gels, are effective for the nucleobase-selective separation of nucleosides, nucleotides and oligonucleotides. The elution order of the nucleosides and nucleotide dimers can be controlled by eluents and the desired oligomers (A or U) could be separated by using Si-PVAd or Si-PTM columns. Moreover, these stationary phases have significant advantages in stability against enzyme-catalysed hydrolysis and ease of preparation compared with other nucleic acid immobilized resins and will be applicable to the separation of longer polynucleotides with nucleobase-selectivity.

#### ACKNOWLEDGEMENTS

The authors thank Professor Tshuko and Dr. Baba of Kobe Women's College of Pharmacy for useful suggestions and continuing interest and encouragement.

#### REFERENCES

- H. Schott, in A. Henschen, K.-P. Hupe, F. Lottspeich and W. Voelter (Editors), *High Performance Liquid Chromatography in Biochemistry*, VCH, Weinheim, 1985, p. 413.
- L. W. McLaughlin and R. Bischoff, *J. Chromatogr.*, 418 (1987) 51.
- R. Hecker and D. Riesner, *J. Chromatogr.*, 418 (1987) 97.
- P. R. Brown, *Anal. Chem.*, 62 (1990) 955A.
- Y. Kato, T. Kitamura, A. Mitsui, Y. Yamasaki, T. Hashimoto, T. Murotsu, S. Fukushige and K. Matsubara, *J. Chromatogr.*, 447 (1988) 212.
- Y. Kato, Y. Yamasaki, A. Onaka, T. Kitamura, T. Hashimoto, T. Murotsu, S. Fukushige and K. Matsubara, *J. Chromatogr.*, 478 (1989) 264.
- Y.-F. Maa, S.-C. Lin, Cs. Horváth, U.-C. Yang and D. M. Crothers, *J. Chromatogr.*, 508 (1990) 61.
- G. D. McFarland and P. N. Borer, *Nucleic Acid Res.*, 7 (1979) 1067.
- H. Moriyama and Y. Kato, *J. Chromatogr.*, 445 (1988) 225.
- M. Hummel, H. Herbst and H. Stein, *J. Chromatogr.*, 477 (1989) 420.
- J.-M. Egly, *J. Chromatogr.*, 215 (1981) 243.
- H. Sawai, *Nucleic Acid Res.*, 15 (1984) 105.
- R. Bischoff and L. W. McLaughlin, *J. Chromatogr.*, 270 (1983) 117.
- R. Bischoff and L. W. McLaughlin, *Anal. Biochem.*, 151 (1985) 526.
- L. W. McLaughlin, *Chem. Rev.*, 89 (1989) 309.
- W. B. Jakoby and M. Wilchek, *Methods Enzymol.*, 34 (1974).
- P.-O. Larsson, M. Glad, L. Hansson, M.-O. Mansson, S. Ohlson and K. Mosbach, *Adv. Chromatogr.*, 21 (1983) 41.
- G. Fassina and I. M. Chaiken, *Adv. Chromatogr.*, 27 (1987) 247.
- T. A. Goss, M. Bard and H. W. Jarrett, *J. Chromatogr.*, 508 (1990) 279.
- Y. Kato, T. Seita, T. Hashimoto and A. Shimizu, *J. Chromatogr.*, 134 (1977) 204.
- K. Kondo, K. Hyodo, T. Horiike and K. Takemoto, *Nucleic Acid Res. Symp. Ser.*, 10 (1981) 125.
- Y. S. Yu, K. Kondo and K. Takemoto, *Makromol. Chem.*, 186 (1985) 2311.
- M. Akashi, T. Tokiyoshi, N. Miyauchi and K. Mosbach, *Nucleic Acid Res. Symp. Ser.*, 16 (1985) 41.
- S. Nagae, T. Miyamoto, Y. Inaki and K. Takemoto, *Polym. J.*, 21 (1989) 19.
- Y. Inaki, S. Nagae, T. Miyamoto, Y. Sugiura and K. Takemoto, *Polym. Mater. Sci. Eng.*, 57 (1987) 286.
- S. Nagae, Y. Inaki and K. Takemoto, *Polym. J.*, 21 (1989) 425.
- S. Nagae, Y. Suda, Y. Inaki and K. Takemoto, *J. Polym. Sci. A: Polym. Chem.*, 27 (1989) 2593.
- M. Akashi, M. Yamaguchi, H. Miyata, M. Hayashi, E. Yashima and N. Miyauchi, *Chem. Lett.*, (1988) 1093.
- E. Yashima, N. Suehiro, M. Akashi and N. Miyauchi, *Chem. Lett.*, (1990) 1113.
- M. Akashi, H. Iwasaki, N. Miyauchi, T. Sato, J. Sunamoto and K. Takemoto, *J. Bioact. Compat. Polym.*, 4 (1989) 126.
- M. Akashi, Y. Kita and K. Takemoto, *Makromol. Chem.*, 178 (1977) 1211.
- R. Bischoff and L. W. McLaughlin, *J. Chromatogr.*, 296 (1984) 329.
- Y. Okamoto, E. Yashima, M. Ishikura and K. Hatada, *Bull. Chem. Soc. Jpn.*, 61 (1988) 255.
- K. Kyogoku, R. C. Lord and A. Rich, *J. Am. Chem. Soc.*, 89 (1967) 496.
- E. Yashima, T. Tajima, N. Miyauchi and M. Akashi, *Biopolymers*, (1992) in press.
- Y. Inaki and K. Takemoto (Editors), *Functional Monomers and Polymers*, Marcel Dekker, New York, 1987, p. 413.



# Practical approach to the miniaturization of chiral separations in liquid chromatography using packed fused-silica capillary columns

Hans Wännman, Agneta Walhagen and Per Erlandsson<sup>☆</sup>

Department of Technical Analytical Chemistry, University of Lund, P.O. Box 124, S-221 00 Lund (Sweden)

(First received November 23rd, 1991; revised manuscript received March 16th, 1992)

---

## ABSTRACT

A micro liquid chromatographic system was evaluated and the possibility of transferring some established methods of chiral separation to this system was examined. Fused-silica columns (0.32 mm I.D.) were slurry packed using an ordinary isocratic high-performance liquid chromatographic (HPLC) pump. Reversed-phase C<sub>18</sub> columns with an average reduced plate height of 3.5 could be packed reproducibly. The chiral selectors chosen were  $\beta$ -cyclodextrin, used as a mobile phase additive, bovine serum albumin adsorbed on silica and a Pirkle phase, covalently bound L-dinitrobenzoyl-phenylglycine. Enantiomeric separations gave results in good agreement with those obtained on conventional HPLC columns.

---

## INTRODUCTION

The use of liquid chromatographic (LC) columns with small inner diameters has increased in the last few years. Since the pioneering work of Scott and Kucera [1] on microbore columns and of Tsuda and Novotny [2], Ishii *et al.* [3] and Yang [4] on packed fused-silica capillary columns, a number of reports have been published describing different kinds of microcolumns in LC. For routine use, slurry-packed capillary columns, often also referred to as micro-LC columns [5], seem to attract the most interest [6-8]. The advantages and disadvantages of micro-LC have been discussed in detail by, *e.g.*, Novotny [9] and Verzele *et al.* [5].

An area where the use of micro-LC columns is of particular interest is in the separation of enantiomers. Much research has been focused on chiral separations, especially in the pharmaceutical industry, and interest is growing with the demands on documentation of drug safety. Optical isomers differ markedly in bioavailability, biological activity and metabolism [10]. A racemic mixture is therefore to be considered as a mixture of two different substances. Consequently, it is of great importance to determine the relative abundance of each isomer, possibly through stereoselective LC. Some chiral selectors in LC have been extensively studied, *e.g.*,  $\beta$ -cyclodextrin ( $\beta$ -CD) [11], bovine serum albumin (BSA) [12], triacetylcellulose [13] and the so-called Pirkle phases [14], and are also commercially available.

Although most of the work on enantiomeric separations so far has been done using conventional LC, miniaturization of the chromatographic system makes it possible to experiment with new stationary phases that are too valuable to use in larger columns, *e.g.*, monoclonal antibodies or receptor proteins.

---

Correspondence to: H. Wännman, Kabi Pharmacia Therapeutics AB, P.O. Box 941, S-251 09 Helsingborg, Sweden (present address).

<sup>☆</sup> Present address: Svensk Oljeextraktion AB, P.O. Box 3, S-374 21 Karlshamn, Sweden.

The reduced consumption of solvents also makes stereoselective additives in the mobile phase less costly. Further, the use of long fused-silica columns will make it possible, owing to increased efficiency, to separate stereoisomers with very low chromatographic separation factors ( $\alpha$ ). The aim of this study was to examine the suitability of micro-LC columns (0.32 mm I.D.) in stereoselective separations. To explore possible new chiral phases, a simple and straightforward method of packing both chiral and non-chiral columns in the laboratory is required. Three established methods for chiral separation were transferred to 0.32 mm I.D. packed fused-silica columns and the results obtained were compared with those previously reported using conventional-sized columns. The methods utilized either  $\beta$ -CD as a mobile phase additive [15], BSA as a stationary phase adsorbed on underivatized silica [16] or a commercially available Pirkle phase, covalently bound L-dinitrobenzoyl-phenylglycine [17], as chiral selectors.

## EXPERIMENTAL

### Chemicals

Terbutalin, in the (+)- and (–)-forms and the racemate, was a gift from Draco (Lund, Sweden) and ( $\pm$ )-oxazepam was a gift from Kabi-Vitrum (Stockholm, Sweden). ( $\pm$ )-Chlorthalidone, ( $\pm$ )-benzoin and BSA were purchased from Sigma (St. Louis, MO, USA). D,L- and L-tryptophan were obtained from E. Merck (Darmstadt, Germany) and D-tryptophan from United States Biochemical (Cleveland, OH, USA).  $\beta$ -Cyclodextrin was purchased from Stalex (Malmö, Sweden). ( $\pm$ )-2,2,2-Trifluoro-1-(9-anthryl)ethanol was obtained from Serva (Heidelberg, Germany), ( $\pm$ )- and (+)-propranolol from Fluka (Buchs, Switzerland) and  $\alpha$ -naphthyl isocyanate from Eastman Kodak (Rochester, NY, USA). All other chemicals used were of analytical-reagent grade and the solvents were of high-performance liquid chromatographic (HPLC) or spectrographic grade. Deionized water was obtained from a Milli-Q water purification system (Millipore, Bedford, MA, USA). Prior to use, the mobile phases were filtered through a 0.45- $\mu$ m HV filter (Millipore) and degassed by purging with helium for 30 min.

### Chromatography

A Jasco (Tokyo, Japan) Model 880-PU reciprocating pump was used for both column preparation and chromatography. The pump is capable of delivering flow-rates in the range 0.001–10 ml/min. In order to obtain low ( $< 1 \mu\text{l}/\text{min}$ ) and reproducible flow-rates under all conditions, a split-flow system was used. A three-way union connected between the pump and the injector divided the flow and the splitting ratio was adjusted by the use of a Whitey (Highland Heights, OH, USA) SS-22R2 micrometering valve. The excess flow was returned to the solvent reservoir. UV detection was performed with a Jasco 875-UV spectrophotometric detector equipped with an optional capillary cell holder. The samples were injected with a Valco (Houston, TX, USA) CI4W internal loop injector with a rotor volume of 0.06, 0.2, 0.5 or 1.0  $\mu\text{l}$ . The optimum detection wavelength for each solute was determined by recording the UV spectrum with a Shimadzu (Kyoto, Japan) UV-160 A spectrophotometer.

### Column preparation

Column blanks were prepared from fused-silica capillaries according to a previously described method [18], with minor modifications. Capillaries of 0.32 mm I.D. (Scientific Glass Engineering, Ringwood, Australia) were cut into lengths between 200 and 500 mm using a capillary cleaving tool (Supelco, Bellefonte, PA, USA). The column end frit was made from a GF/D glass-fibre filter (Whatman, Maidstone, UK) by rotating the column while pressing its end gently against the filter disc. The filter was then pushed 10 mm into the column with a short length (150 mm) of 0.10 mm I.D. connecting capillary. Finally, the capillaries were fixed with epoxy glue. In order to achieve a connection between the column and the slurry reservoir that could withstand the high packing pressures, a short length of 1/16 in. O.D. and 0.5 mm I.D. stainless-steel tubing was threaded over the column and fixed with epoxy 2 mm below the top (Fig. 1). The slurry reservoir consisted of a 20 mm  $\times$  3 mm I.D. stainless-steel column (volume *ca.* 0.14 ml) (Upchurch Scientific, Oak Harbor, WA, USA). A funnel was made out of Kel-F and inserted in the reservoir to facilitate the delivery of the slurry (Fig. 2).

Reversed-phase columns were packed using either Nucleosil 100-5 C<sub>18</sub> (5  $\mu\text{m}$ , 100 Å, 350 m<sup>2</sup>/g)

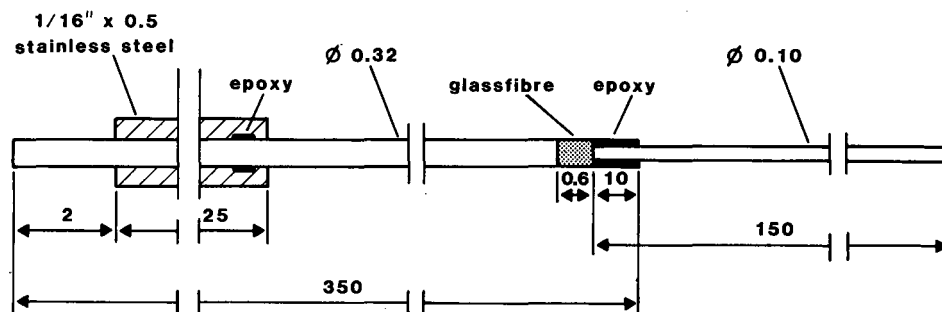


Fig. 1. Schematic diagram of the fused-silica column blank. All dimensions are in millimetres unless indicated otherwise.  $\phi$  = Diameter; " = inch.

(Macherey–Nagel, Düren, Germany), Nucleosil 120-3  $C_{18}$  ( $3 \mu\text{m}$ ,  $120 \text{ \AA}$ ,  $200 \text{ m}^2/\text{g}$ ) or Spherisorb ODS 2 ( $5 \mu\text{m}$ ,  $80 \text{ \AA}$ ,  $220 \text{ m}^2/\text{g}$ ) (Phase Separations, Norwalk, CT, USA) and columns containing underivatized silica were prepared using Nucleosil ( $5 \mu\text{m}$ ,  $300 \text{ \AA}$ ,  $120 \text{ m}^2/\text{g}$ ) (Macherey–Nagel). The Pirkle phase columns were packed with Daltosil 100 L-DNB-phenylglycine ( $4 \mu\text{m}$ ,  $90 \text{ \AA}$ ,  $300 \text{ m}^2/\text{g}$ ) (Serva). The packing material was suspended in carbon tetrachloride–2-propanol (50:50, v/v) for reversed-phase material and in chloroform–methanol (2:1, v/v) for underivatized silica and Pirkle phase material. The slurry concentration was 27% (w/w). After sonication for 2 min, the slurry was transferred to the reservoir. The pump, with aceto-

nitrile as displacing medium (methanol for underivatized silica and Pirkle phases), was started immediately with an initial pressure of zero and a flow-rate of 0.5 ml/min. Within 1 min the pressure had risen to 400 atm and the flow-rate was successively decreased to obtain a stabilized pressure of 450 atm. After 30 min, the pump was turned off and the pressure returned to zero. The column was then cut off below the steel capillary and mounted on the injector using a polyimide ferrule and liner (Valco). The reversed-phase columns were conditioned overnight with mobile phase [acetonitrile–water (80:20, v/v)] and then submitted to a column performance test. The test mixture contained toluene (0.12 mg/ml), biphenyl (0.12 mg/ml) and anthracene (0.18 mg/ml).

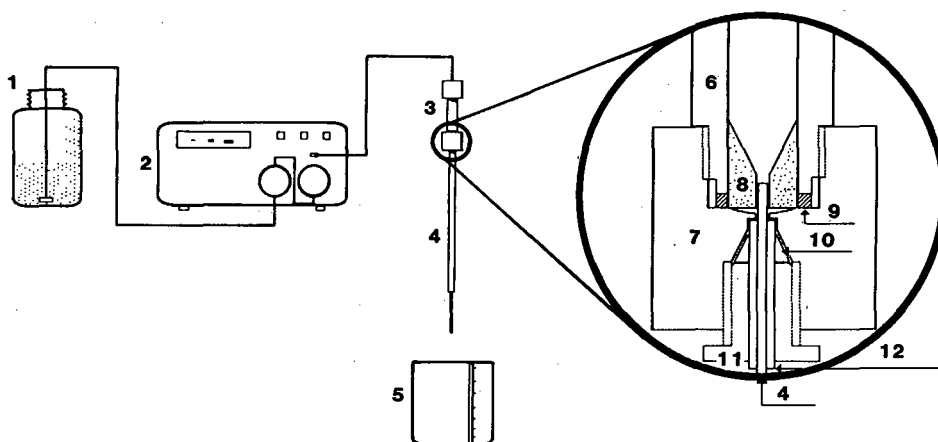


Fig. 2. Set-up for the packing of capillary columns. 1 = Solvent reservoir; 2 = pump; 3 = slurry reservoir; 4 = fused-silica column; 5 = waste; 6 = column tubing (3 mm I.D.); 7 = column end-fitting; 8 = funnel (Kel-F); 9 = seal (PEEK); 10 = ferrule (stainless steel); 11 = nut; 12 = 1/16 in. I.D. tubing (stainless steel).

ml) dissolved in acetonitrile–water (80:20, v/v). The Pirkle phase columns were conditioned with 2-propanol followed by mobile phase [*n*-hexane–2-propanol (95:5, v/v)].

#### Adsorption of BSA

Columns with underivatized silica were packed as described above. After washing with *ca.* 50 column volumes of water and equilibration with the same volume of 0.05 *M* phosphate buffer (pH 5.0), sodium nitrite was injected. The eluted peak was symmetrical and showed an efficiency of about 4000 theoretical plates/m. The immobilization of BSA by adsorption was performed as described previously [16]. A solution of 1 mg/ml BSA in 0.05 *M* phosphate buffer (pH 5.0) was pumped through the column until breakthrough of BSA was detected at 280 nm. The column was then equilibrated with BSA-free buffer until a stable UV baseline was obtained. From the point of breakthrough the amount of BSA adsorbed on the column was calculated.

#### Calculations

Experimentally, the retention time of a non-retained compound,  $t_0$ , was determined by injecting either sodium nitrite solution or water or by observing the first baseline disturbance. The plate number  $N$  was calculated according to the equation  $N = 5.54 (t_R/w_{0.5})^2$ , where  $t_R$  is the retention time and  $w_{0.5}$  is the band width at half-height. The capacity factor,  $k'$ , the plate height,  $H$ , the reduced plate height,  $h$ , and the asymmetry factor,  $A_s$ , were all calculated using standard equations [19]. The flow resistance parameter  $\phi$  was calculated as  $\phi = (\Delta p t_0 d_p^2)/(L^2 \eta)$  where  $\Delta p$  is the pressure drop,  $d_p$  is the average particle diameter,  $L$  is the column length and  $\eta$  is the dynamic viscosity of the mobile phase. The separation impedance,  $E$ , is defined as  $E = h^2 \phi$ . The total column porosity,  $\varepsilon$ , was calculated from  $\varepsilon = (4F t_0)/(\pi d_c^2 L)$ , where  $F$  is the volumetric flow-rate and  $d_c$  is the column inner diameter. The stereoselectivity,  $\alpha$ , was calculated as  $k'_2/k'_1$  and the equation  $R_s = 2(t_{R2} - t_{R1})/(w_1 + w_2)$ , where  $w$  is the band width, was used in the calculation of the resolution of wholly and partially resolved peaks [19]. This method of determining the resolution might give erroneous results with poorly resolved peaks, but with  $R_s$  exceeding unity the error is negligible.

## RESULTS AND DISCUSSION

### Instrumentation

The Jasco Model 880-PU pump is designed with a lower flow-rate limit of 1  $\mu$ l/min. However, the use of mobile phases with high concentrations of  $\beta$ -cyclodextrin led to deterioration of the plunger seals and check valves of the pump. Although this was not noticeable at high flow-rates (*e.g.*, >0.5 ml/min), it prevented a steady mobile phase delivery near the lower flow-rate limit (1  $\mu$ l/min). This problem was circumvented by the use of a split-flow system. Such a system also permits the use of pumps with a higher minimum flow-rate (*e.g.*, 0.01 ml/min). Further, a split-flow system makes it possible to deliver flow-rates well under 1  $\mu$ l/min provided that the back-pressure is sufficiently high. The use of a metering valve instead of a dummy column to set the splitting ratio makes the adjustment of the pressure (or flow-rate) easier and exchange of the mobile phase faster.

The standard 8- $\mu$ l flow cell of the detector is far too large for a micro-LC system. In order to avoid excessive band broadening, the volume of the detector cell must be well under 1  $\mu$ l. Low cell volumes can be obtained by so-called on-column detection [4,5]. This means mounting the connecting capillary directly in the light path as close as possible to the column end frit. However, after removal of the polyimide coating, the fused-silica capillary becomes very fragile and the risk of breakage is obvious. A more convenient method, although the increased dead volume gives a slightly higher band broadening contribution, is to use a separate capillary tube mounted in the detector to which the column outlet can be connected via a piece of PTFE tubing. The influence of the dead volume of this connection on the overall efficiency is shown in Table I. In all instances the direction of light is perpendicular to the solvent flow. As can be seen, the use of a wider capillary (0.32 mm I.D.) as a measuring cell reduces the efficiency and increases the peak asymmetry compared with the case where detection is made directly on the 0.10 mm I.D. connecting capillary. The limit of detection, however, is decreased fourfold. Reducing the inner diameter of the connecting capillary to 0.05 mm allows the use of a 0.20-mm flow cell without any loss of efficiency. The increased path length provides

TABLE I

## EFFECT ON COLUMN PERFORMANCE OF DIFFERENT CONNECTIONS BETWEEN THE COLUMN AND DETECTOR

Column, 440 mm × 0.32 mm I.D. packed with Nucleosil 100-5 C<sub>18</sub>; mobile phase, acetonitrile–water (80:20, v/v); sample, anthracene, 0.18 mg/ml in mobile phase; volume injected, 60 nl; detection wavelength, 215 nm; flow-rate, 2.0 μl/min.

Parameter	A	B	C
Connection:			
Length × I.D. (mm)	120 × 0.10	120 × 0.10	120 × 0.05
Volume (μl)	1.10	1.10	0.39
Cell:			
Length × I.D. <sup>a</sup> (mm)	3 × 0.10 <sup>b</sup>	3 × 0.32	3 × 0.20
Volume (μl)	0.024	0.24	0.094
<i>k'</i>	4.00	4.01	4.16
<i>N</i> (plates/m)	50 200	48 200	50 600
<i>A<sub>s</sub></i>	1.0	1.1	1.1
Limit of detection <sup>c</sup> (ppm)	6.1	1.6	2.5

<sup>a</sup> The inner diameter of the cell equals the pathlength of the light.

<sup>b</sup> Measured directly on the 0.10 mm I.D. connecting capillary.

<sup>c</sup> Limit of detection = 2/signal-to-noise ratio.

a 2.5-fold increase in detectability. Narrow connecting capillaries (<0.05 mm I.D.) can be used in lengths up to a few decimetres without any apparent reduction of the overall efficiency [20]. The geometry of the flow cell, on the other hand, has a great influence on the overall efficiency and care should be taken to avoid unswept volumes in the connection between the cell and the capillary (Fig. 3).

#### Micro-LC system

The performance characteristics of five reversed-phase columns are listed in Table II. Although the value of the reduced plate height, *h*, shows some variation and is higher than 2, which is usually considered to be the minimum value [9], it is clear that columns of reasonable efficiency can be packed without difficulty using an ordinary isocratic HPLC pump. The column resistance parameter,  $\phi$ , is at or below the lower limit of the typical range 500–1000 whereas the separation impedance [21] ranges from 4000 to 8000, mainly owing to the influence of high reduced plate heights. The value of the total porosity,  $\epsilon$ , is below the expected value of 0.8–0.9 for porous silica [6,22]. The discrepancy indicates that the nitrite ion used as a dead-time marker is in fact being partly excluded from the pores of the silica. Nevertheless the value can be used in comparisons between different columns. A typical test chromatogram

is shown in Fig. 4. Reversed-phase C<sub>18</sub> columns packed in lengths between 100 and 450 mm showed similar reduced plate heights.

Van Deemter plots, *H* vs. *u*, from three different columns and/or mobile phases are shown in Fig. 5. As can be seen, the use of low-viscosity mobile phases and small particle sizes is favourable owing to the increase in the optimum linear velocity. A high linear velocity and hence a high volumetric flow-rate

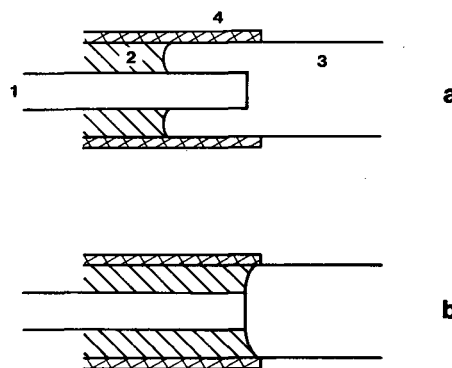


Fig. 3. Connection between connecting capillary and the flow cell in the detector. 1 = Connecting capillary; 2 = epoxy glue; 3 = flow-cell capillary; 4 = polyimide coating. The connection shown in (a) should be avoided owing to the formation of unswept volumes. The low unswept volume in (b) is obtained by withdrawing the connecting capillary through the partially hardened epoxy.

TABLE II  
COLUMN PERFORMANCE CHARACTERISTICS

Column, 0.32 mm I.D.; stationary phase, (A-C) Nucleosil 100-5 C<sub>18</sub>, (D and E) Spherisorb 5 μm C<sub>18</sub>; mobile phase, acetonitrile-water (80:20, v/v); sample, anthracene, 0.18 mg/ml in mobile phase; volume injected, 60 nl; detection wavelength, 215 nm; flow-rate, 1.5 μl/min.

Column	<i>h</i>	<i>φ</i>	<i>E</i>	<i>ε</i>
A	3.47	445	5356	0.454
B	3.32	370	4077	0.431
C	4.22	465	8283	0.510
D	3.19	532	5423	0.394
E	3.50	324	3970	0.371
Mean	3.54	427	5422	0.432
S.D.	0.40	81.6	1740	0.054
R.S.D. (%)	11.3	19.1	32.1	12.5

give shorter analysis times and less stringent demands on the lower flow-rate limit and the flow stability of the solvent-delivery system.

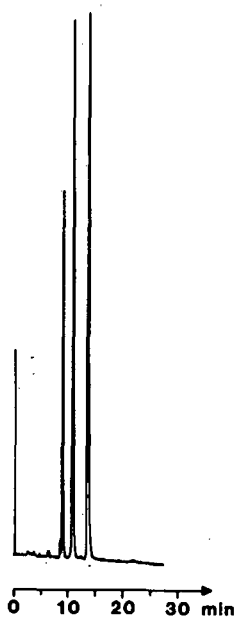


Fig. 4. Test chromatogram showing the resolution of toluene (first eluted), biphenyl and anthracene (last eluted). Column, 200 mm × 0.32 mm I.D. packed with Spherisorb 5 μm C<sub>18</sub>; mobile phase, acetonitrile-water (80:20, v/v); flow-rate, 1.8 μl/min; back-pressure, 18 kg/cm<sup>2</sup>; a.u.f.s., 0.04; volume injected, 60 nl; sample concentration, toluene 0.12, biphenyl 0.12, anthracene 0.18 mg/ml; UV detection at 215 nm. *N* (anthracene) = 13 260.

In order to reduce the extra-column band broadening due to dispersion in the injector, it is important to keep the injection volume low. If the sample is dissolved in a solvent identical with the mobile phase the column performance rapidly deteriorates with increasing injection volume (Table III). The use of larger injection volumes is possible, however, if an injection medium of lower solvent strength is used. Using this technique, up to 1 μl has been injected with only a minor reduction in the plate number. However, there is a tendency towards an increased peak asymmetry and an upward shift of the capacity factor.

Small injection volumes generally requires concentrated samples which in turn increases the risk of column overload. Table IV shows the effect on the capacity factor (*k'*), plate number (*N*) and asymmetry factor (*A<sub>s</sub>*) of increasing the sample concentration. As expected, both *k'* and *N* are affected by increased sample concentrations whereas *A<sub>s</sub>* remains almost unaffected. Plotting *N* against log (sample concentration) reveals a break point around 1 mg/ml corresponding to 5 · 10<sup>-6</sup> g solute/g packing material. In the evaluation of the microcolumns the sample concentration is generally kept five to ten times below this value.

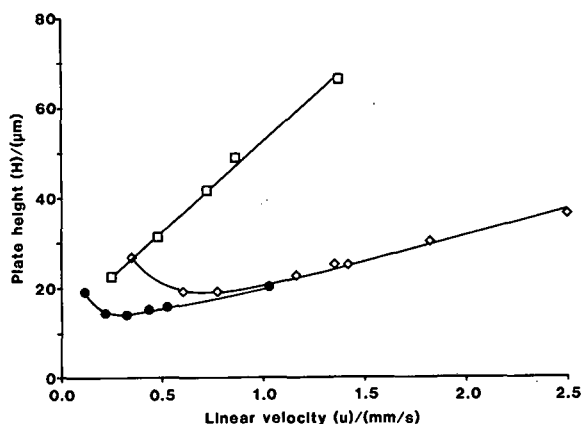


Fig. 5. Comparison between van Deemter plots from three different columns. Column, 200 mm × 0.32 mm I.D. packed with Nucleosil C<sub>18</sub>; solute, biphenyl 0.12 mg/ml in mobile phase; UV detection at 215 nm. Mobile phase and particle diameter: column I (□) = methanol-water (70:30, v/v) and 5 μm; column II (◇) = acetonitrile-water (80:20, v/v) and 5 μm; column III (●) = methanol-water (70:30, v/v) and 3 μm.

TABLE III

## EFFECT ON COLUMN PERFORMANCE OF DIFFERENT INJECTION VOLUMES AND SAMPLE SOLVENTS

Column, 255 mm × 0.32 mm I.D. packed with Nucleosil 100-5 C<sub>18</sub>; mobile phase, acetonitrile–water (80:20, v/v); sample, biphenyl in mobile phase; amount injected, 6 ng; detection wavelength, 215 nm; flow-rate, 2.0 μl/min.

Sample solvent <sup>a</sup>	60 nl			500 nl			1000 nl		
	<i>k'</i>	<i>N</i>	<i>A<sub>s</sub></i>	<i>k'</i>	<i>N</i>	<i>A<sub>s</sub></i>	<i>k'</i>	<i>N</i>	<i>A<sub>s</sub></i>
80:20	2.13	12 500	1.0	2.04	6 400	1.3	1.76	3 000	1.5
40:60	2.11	12 000	1.0	2.15	11 800	1.1	2.22	10 500	1.1
20:80	2.15	11 100	1.1	2.20	11 100	1.1	2.24	10 800	1.2

<sup>a</sup> Acetonitrile–water (v/v).

*Chiral separation*

Microcolumns are well suited for stereoselective separations with β-cyclodextrin as a chiral mobile phase additive. ODS reversed-phase columns of high efficiency can be prepared according to the above method and a low volumetric flow-rate reduces the consumption of the additive. In the separation of (±)-terbutalin with β-CD as a chiral mobile phase additive, the retention time (*t<sub>R</sub>*) and the separation factor (*α*) are dependent on the β-CD concentration (Fig. 6, Table V). The values of *α* and *R<sub>s</sub>* are in good agreement with those reported previously [15]. The separation of the enantiomers of chlorthalidone is shown in Fig. 7. The relatively

high lipophilicity of the substance results in a long retention time in spite of the high content of organic modifier.

BSA adsorbed on underivatized silica was used as a chiral stationary phase. The amount of BSA adsorbed was calculated from the breakthrough curve and found to be 1.3 mg. With about 12 mg of silica in the column, the adsorption is *ca.* 0.1 g/g, which is in good agreement with a previous report [16].

The *α* and *R<sub>s</sub>* values of the separations obtained for D,L-tryptophan, (±)-benzoin and (±)-oxazepam (Fig. 8, Table VI) are similar to those reported previously [16,23] using 1.6 and 4.6 mm I.D. stainless-steel columns. As shown in Fig. 8a, the separation of D- and L-tryptophan is highly dependent on the pH of the mobile phase. A pH of at least 7 is required to obtain reasonable selectivity. A further increase in pH leads to an even better separation. Unfortunately, the increased alkalinity also leads to breakdown of the silica and desorption of the BSA. The separation of (±)-benzoin (Fig. 8b), on the other hand, is almost independent of the pH of the mobile phase in the range 5–7 (not shown). The enantiomers of the benzodiazepine derivative oxazepam rapidly racemize in aqueous solutions [24]. This leads to coalescence, the formation of a diffuse zone between the two separated peaks containing a mixture of the enantiomers. This is particularly pronounced for separations with long retention times and results in an absence of baseline separation in spite of an apparently high resolution. Although increasing the flow-rate reduces the efficiency of the column, the resulting reduced intra-

TABLE IV

EFFECT ON CAPACITY FACTOR (*k'*), PLATE NUMBER (*N*) AND ASYMMETRY FACTOR (*A<sub>s</sub>*) OF INCREASING SAMPLE AMOUNT

Column, 260 mm × 0.32 mm I.D. packed with Nucleosil 100-5 C<sub>18</sub>; mobile phase, acetonitrile–water (80:20, v/v); detection wavelength, 215 nm; sample, biphenyl in mobile phase; injection volume, 60 nl; flow-rate, 2.0 μl/min.

Concentration (mg/ml)	Amount injected (μg)	<i>k'</i>	<i>N</i>	<i>A<sub>s</sub></i>
0.05	0.003	2.14	15 000	1.1
0.1	0.006	2.13	14 900	1.1
0.5	0.03	2.08	14 500	1.0
1.0	0.06	2.02	14 300	1.1
2.0	0.12	1.97	13 900	1.0
5.0	0.30	1.88	13 100	1.0
10	0.60	1.86	12 400	0.9

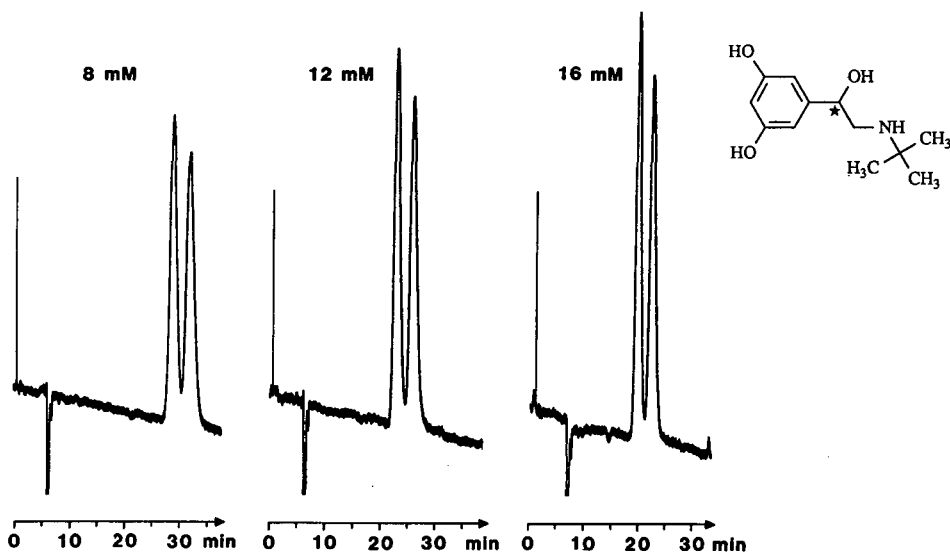


Fig. 6. Chromatograms showing the resolution of ( $\pm$ )-terbutalin with different concentrations of  $\beta$ -cyclodextrin in the mobile phase. Column, 190 mm  $\times$  0.32 mm I.D. packed with Nucleosil 100-5  $C_{18}$ ; mobile phase, 0.05 M ammonium acetate (pH 6.0) with 2% methanol as modifier; flow-rate, 1.8  $\mu$ l/min; volume injected, 60 nl of a 0.75 mM solution in water; UV detection at 215 nm.

column racemization results in a better separation (Fig. 8c).

In contrast to the previous two phases, the Pirkle phase L-DNB-phenylglycine is of the normal-phase type and runs with a hexane–isopropanol mixture as mobile phase. The Pirkle phase in question has been used in the separation of a large number of different substances such as aryl alcohols, aryl sulphoxides, bi- $\beta$ -naphthol derivatives and  $\beta$ -amino alcohols. As solutes 2,2,2-trifluoro-1-(9-anthryl)ethanol, [17] and the naphthyl isocyanate derivative of propranolol [25] were chosen (Fig. 9, Table VII). A 100 mm  $\times$  4 mm I.D. stainless-steel column was packed and used analogously to the capillary columns using the

same batch of L-DNB-phenylglycine. The separation of ( $\pm$ )-2,2,2-trifluoro-1-(9-anthryl)ethanol yielded results similar to those reported in Table VII ( $k'_1 = 1.89$ ,  $\alpha = 1.28$ ).

## CONCLUSIONS

This work has shown that 0.32 mm I.D. slurry-packed fused-silica capillary columns can be packed using an ordinary isocratic HPLC pump as a packing unit. The same pump was also used together with a UV detector equipped with an optional capillary cell holder in a chromatographic system on which the packed columns were tested. Efficient reversed-phase  $C_{18}$  columns were reproducibly packed and showed an average reduced plate height of 3.5. Enantiomeric separations on these columns with  $\beta$ -cyclodextrin as a chiral mobile phase additive gave results similar to those reported for conventional columns under the same conditions. This correlation was also found with columns using either BSA or the Pirkle phase L-DNB-phenylglycine as a chiral stationary phase. In our opinion, almost every method originally developed for use on a conventional HPLC system can be transferred with little effort to a micro-LC system such as that described here. This switch to micro-LC in routine analyses leads to

TABLE V

### CHROMATOGRAPHIC DATA FROM FIG. 6

Chiral separation of ( $\pm$ )-terbutalin with  $\beta$ -cyclodextrin ( $\beta$ -CD) as chiral mobile phase additive.

[ $\beta$ -CD] (mM)	$k'_1$ <sup>a</sup>	$k'_2$	$\alpha$	$R_s$	$N_1$
8	4.14	4.70	1.14	1.17	2300
12	3.00	3.53	1.18	1.39	2100
16	2.31	2.78	1.20	1.38	2000

<sup>a</sup> (+)-Terbutalin.

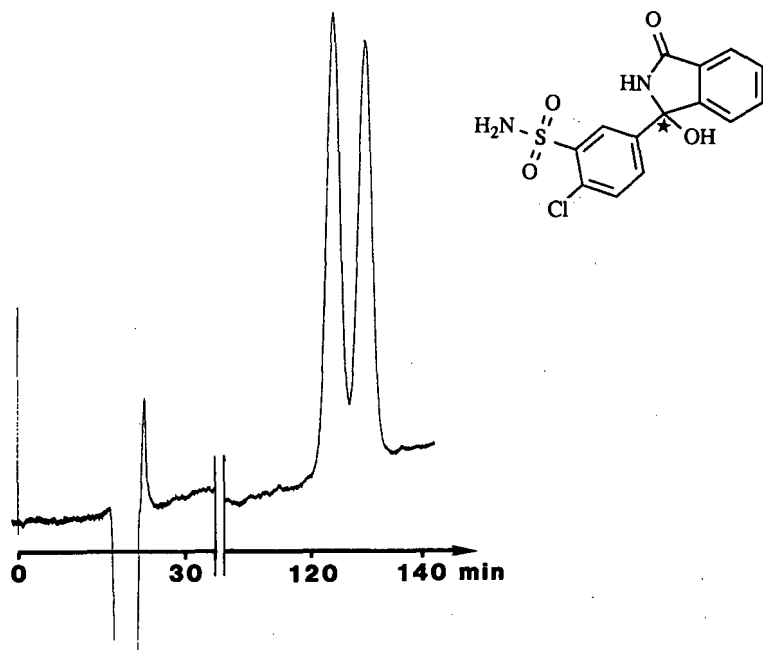


Fig. 7. Resolution of ( $\pm$ )-chlorthalidone on a 300 mm  $\times$  0.32 mm I.D. column packed with Nucleosil 100-5 C<sub>18</sub>. Mobile phase, 8.4 mM  $\beta$ -cyclodextrin in 0.05 M ammonium acetate (pH 4.7) with 20% of ethanol as modifier; flow-rate, 1.1  $\mu$ l/min; volume injected, 200 nl of a 0.01 mg/ml solution in water; UV detection at 218 nm.  $k'_1 = 6.32$ ;  $k'_2 = 6.65$ ;  $\alpha = 1.05$ ;  $R_s = 1.19$ ;  $N_1 = 13\,300$ .

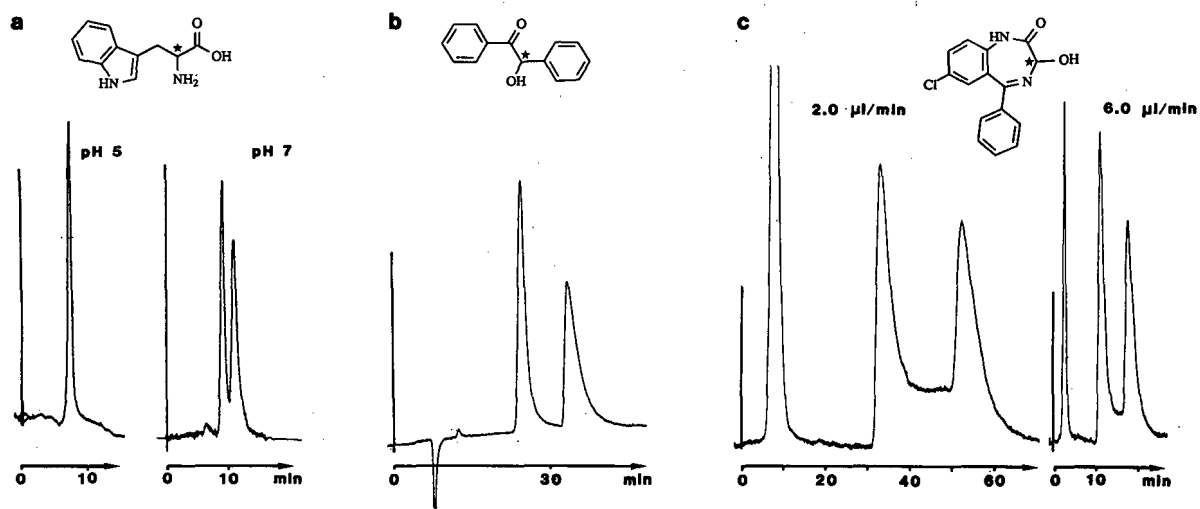


Fig. 8. Resolution of (a) D,L-tryptophan, (b) ( $\pm$ )-benzoïn and (c) ( $\pm$ )-oxazepam on a 250 mm  $\times$  0.32 mm I.D. column packed with 5- $\mu$ m BSA-silica. (a) Mobile phase, 0.05 M phosphate buffer (pH 5.0 and 7.0) with 2% of *n*-propanol as modifier; flow-rate, 2.5  $\mu$ l/min; volume injected, 200 nl of a 0.02 mg/ml solution in the mobile phase; UV detection at 279 nm. (b) Mobile phase, 0.05 M phosphate buffer (pH 5.0) with 2% of *n*-propanol as modifier; flow-rate, 2.4  $\mu$ l/min; volume injected, 200 nl of a 0.02 mg/ml solution in water-methanol (98:2, v/v); UV detection at 279 nm. (c) Mobile phase, 0.05 M phosphate buffer (pH 7.0) with 2% of *n*-propanol as modifier; flow-rate, 2.0 and 6.0  $\mu$ l/min; volume injected, 200 nl of a 0.02 mg/ml solution in water-methanol (75:25, v/v); UV detection at 249 nm.

TABLE VI  
CHROMATOGRAPHIC DATA FROM FIG. 8

Chiral separation on a BSA column.

Substance	pH	$k'_1$	$k'_2$	$\alpha$	$R_s$	$N_1$
Tryptophan	5	0.10	—	—	—	1400
	7	0.28 <sup>a</sup>	0.55	1.95	1.20	1100
Benzoin	5	2.37	3.61	1.52	2.45	1600
Oxazepam	7 <sup>b</sup>	3.40	5.84	1.72	2.6	450
	7 <sup>c</sup>	3.69	6.40	1.73	2.1	360

<sup>a</sup> D-Tryptophan.

<sup>b</sup> 2  $\mu$ l/min.

<sup>c</sup> 6  $\mu$ l/min.

a drastic reduction in the costs of solvent purchase and disposal.

It should be stressed, however, that although micro-LC generally shows a higher mass sensitivity than conventional HPLC, its concentration sensitivity is poorer owing to the small injection volumes. Quantitative analysis at low concentrations can therefore be more difficult to perform using micro-columns. Furthermore, microcolumns are usually operated at lower signal-to-noise ratios and problems with detector noise and drift are therefore more likely to occur. However, this issue is a subject for further research.

Micro-LC is likely to open up new possibilities in

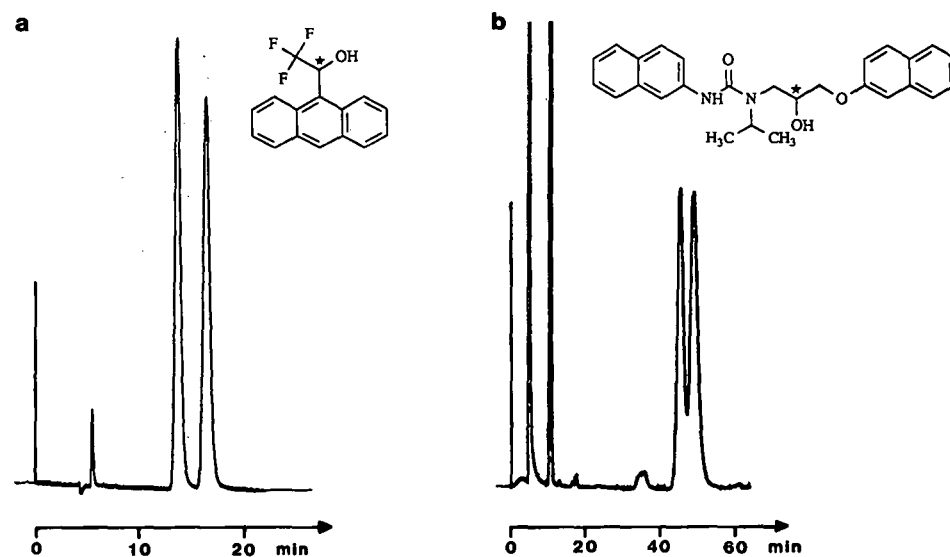


Fig. 9. Resolution of (a) ( $\pm$ )-2,2,2-trifluoro-1-(9-anthryl)ethanol and (b) ( $\pm$ )-propranolol as its naphthyl isocyanate derivative on a 260 mm  $\times$  0.32 mm I.D. column packed with 4- $\mu$ m L-DNB-phenylglycine. (a) Mobile phase, *n*-hexane–2-propanol (95:5, v/v); flow-rate, 1.9  $\mu$ l/min; volume injected, 60 nl of a 0.08 mg/ml solution in 2-propanol; UV detection at 253 nm. (b) Mobile phase, *n*-hexane–2-propanol–acetonitrile (90:10:2, v/v/v); flow-rate, 1.9  $\mu$ l/min; volume injected, 60 nl of a 2-propanol-diluted reaction mixture (less than 1.5 mM); UV detection at 214 nm.

TABLE VII  
CHROMATOGRAPHIC DATA FROM FIG. 9

Chiral separation on a Pirkle column.

Substance	Mobile phase <sup>a</sup> (v/v/v)	$k'_1$	$k'_2$	$\alpha$	$R_s$	$N_1$
Tri-F <sup>b</sup>	95:5:—	2.22	2.87	1.29	2.54	3200
Propranolol	90:10:2	12.0 <sup>c</sup>	13.3	1.11	1.12	2500

<sup>a</sup> Mobile phase: *n*-hexane–isopropanol–acetonitrile.

<sup>b</sup> 2,2,2-Trifluoro-1-(9-anthryl)ethanol.

<sup>c</sup> (+)-Propranolol.

the development of separation methods utilizing expensive or rare mobile and stationary phases such as monoclonal antibodies or receptor proteins.

#### ACKNOWLEDGEMENTS

We thank Dr. Staffan Folestad for introducing us to the preparation of packed fused-silica columns and Professor Karl-Gustav Wahlund for valuable discussions. This work was supported by grants from the Swedish Natural Science Research Council, the Crafoord Foundation and the Royal Physiographic Society of Lund.

#### REFERENCES

- 1 R. P. W. Scott and P. Kucera, *J. Chromatogr.*, 169 (1978) 51.
- 2 T. Tsuda and M. Novotny, *Anal. Chem.*, 50 (1978) 271.
- 3 D. Ishii, K. Asai, K. Hibi and T. Jonokuchi, *J. Chromatogr.*, 144 (1977) 157.
- 4 F. Yang, *J. Chromatogr.*, 236 (1982) 265.
- 5 M. Verzele, C. Dewaele and M. De Weerd, *LC·GC*, 6 (1988) 966.
- 6 J. Gluckman, A. Hirose, V. L. McGuffin and M. Novotny, *Chromatographia*, 17 (1983) 303.
- 7 C. Borra, S. M. Han and M. Novotny, *J. Chromatogr.*, 385 (1987) 75.
- 8 W. H. Wilson, H. M. McNair and K. J. Hyver, *J. Chromatogr.*, 540 (1991) 77.
- 9 M. Novotny, *Anal. Chem.*, 60 (1988) 500.
- 10 E. J. Ariens, *Eur. J. Clin. Pharmacol.*, 26 (1984) 663.
- 11 D. W. Armstrong, T. J. Ward, R. D. Armstrong and T. E. Beesley, *Science*, 232 (1986) 1132.
- 12 S. Allenmark, *J. Liq. Chromatogr.*, 9 (1986) 425.
- 13 R. Isaksson, P. Erlandsson, L. Hansson, A. Holmberg and S. Berner, *J. Chromatogr.*, 498 (1990) 257.
- 14 W. H. Pirkle and J. M. Finn, *J. Org. Chem.*, 46 (1981) 2935.
- 15 A. Walhagen and L.-E. Edholm, *Chromatographia*, 32 (1991) 215.
- 16 P. Erlandsson, L. Hansson and R. Isaksson, *J. Chromatogr.*, 370 (1986) 475.
- 17 W. H. Pirkle, D. W. House and J. M. Finn, *J. Chromatogr.*, 192 (1980) 143.
- 18 S. Einarsson, S. Folestad, B. Josefsson and S. Lagerkvist, *Anal. Chem.*, 58 (1986) 1638.
- 19 L. R. Snyder and J. J. Kirkland, *Introduction to Modern Liquid Chromatography*, Wiley, New York, 2nd ed., 1979.
- 20 H. E. Schwartz, *J. Chromatogr. Sci.*, 24 (1986) 285.
- 21 P. A. Bristow and J. H. Knox, *Chromatographia*, 10 (1977) 279.
- 22 C. A. Cramers, J. A. Rijks and C. P. M. Schutjes, *Chromatographia*, 14 (1981) 439.
- 23 P. Erlandsson and S. Nilsson, *J. Chromatogr.*, 482 (1989) 35.
- 24 Y. Aso, S. Yoshioka, T. Shibasaki and M. Uchiyama, *Chem. Pharm. Bull.*, 36 (1988) 1834.
- 25 Q. Yang, Z.-P. Sun and D.-K. Ling, *J. Chromatogr.*, 447 (1988) 208.



# Enantiomeric separation of racemic isoflavanones and related compounds on (+)-poly(triphenylmethyl methacrylate)-coated silica gel

Sándor Antus

*Research Group for Alkaloid Chemistry, Hungarian Academy of Sciences, P.O. Box 91, H-1521 Budapest (Hungary)*

Rudolf Bauer

*Institut für Pharmazeutische Biologie der Universität München, Karlstrasse 29, D-8000 Munich (Germany)*

Ágnes Gottsegen

*Research Group for Alkaloid Chemistry, Hungarian Academy of Sciences, P.O. Box 91, H-1521 Budapest (Hungary)*

Hermann Lotter, Otto Seligmann and Hildebert Wagner

*Institut für Pharmazeutische Biologie der Universität München, Karlstrasse 29, D-8000 Munich (Germany)*

(First received November 12th, 1991; revised manuscript received February 18th, 1992)

---

## ABSTRACT

(+)-Poly(triphenylmethyl methacrylate)-coated silica gel [Chiralpack OT(+)] was used for the separation of enantiomers of racemic isoflavanone, homoisoflavanone, isoflavan and 2-benzyltetralone derivatives. All the enantiomers of the above-mentioned compounds were separable. The efficiency of the separation depended on both the skeleton and substitution pattern of the racemic compounds. A relation between the number and polarity of substituents in the aromatic rings and the resolution and separation factors was observed.

---

## INTRODUCTION

Isoflavanones, being the biosynthetic precursors of pterocarpin phytoalexins, are synthesized mostly by *Leguminosae* species in response to stress-induced microbial infection [1–5]. The stereochemistry of the isoflavanones involved in pterocarpin biosynthesis has been deduced from the configuration of the pterocarpan [6–8]. Thus, in the case of

(6a*R*,11a*R*)-maackiain, the intermediate is (3*R*)-(+)-sophorol (Fig. 1).

3*R*-(+)-Sophorol [9], 3*S*-(-)-7,4'-dihydroxyisoflavanone [10], (-)-sophoraïsoflavanone A [11], (-)-isosophoranone [12] and (-)-erosenone [13] are the only isoflavanones hitherto isolated from natural sources in optically active form. That the number of optically active isoflavanones is small is probably because they are rapidly racemized by keto-enol tautomerism in the course of their isolation.

Although isoflavanones have a less rigid conformational structure than the corresponding pterocarpan, a study of their Dreiding models [14] suggested that in one of their conformers, when the

---

*Correspondence to:* Dr. S. Antus, Research Group for Alkaloid Chemistry, Hungarian Academy of Sciences, P.O. Box 91, H-1521 Budapest, Hungary.

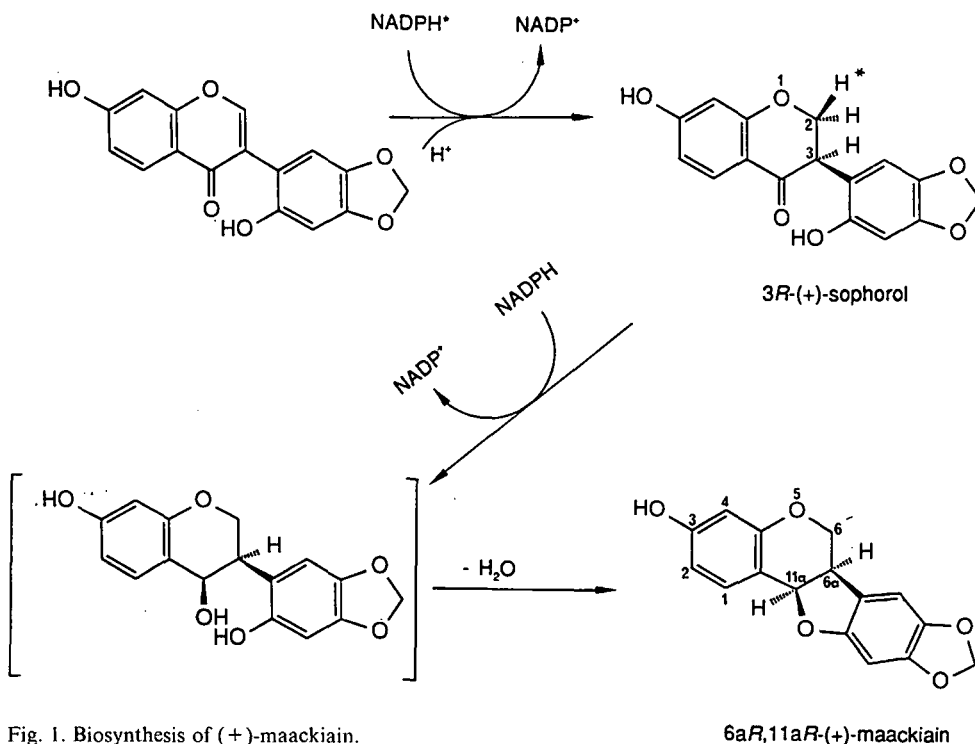


Fig. 1. Biosynthesis of (+)-maackiain.

aromatic ring at C-3 is in the *equatorial* position, the presumably dihedral angle is nearby, as it is in the homochiral pterocarpan:

Therefore, as a continuation of our work on the enantiomeric separation of pterocarpan [15], an efficient optical resolution of isoflavanones and related compounds would also be expected using (+)-poly(triphenylmethyl methacrylate) (PTrMA)-coated silica gel [Chiralpack OT(+)]. In this paper we report the enantiomeric separation of synthetic racemic isoflavanones and related compounds (Fig. 2) and the influence of their substitution patterns on the efficiency of the chromatographic resolution.

## EXPERIMENTAL

### Materials

The racemates of the isoflavanones **1**, **3–6**, **8–11** and **13** were synthesized from the appropriately substituted isoflavones by reduction with diisobutylaluminium hydride [16]. The same procedure was followed for synthesizing the homoisoflavanone **15**

and 2-(4-methoxybenzyl)indanone (**16**) from the corresponding benzylidene derivatives. The isoflavanone derivatives **2**, **7** and **12** were prepared from **5**, **9** and **13** by acidic deprotection. Preparative separation of the enantiomers **1** [**3*R*-(+)-1**, **3*S*-(-)-1**] and **14** [**3*R*-(+)-14**, **3*S*-(-)-14**] was achieved via the isoflavanone dimethylethylene thioetals (**17a** and **17b**) [17] using the method of Corey and Mitra [18].

### High-performance liquid chromatography (HPLC)

HPLC separation was carried out with a Hewlett-Packard HP 1090M liquid chromatograph with an HP 1040A photodiode-array detection system and an HP 3329A integrator. Chiralpack OT(+), 250 mm × 4.6 mm I.D. (Daicel), was used as the stationary phase. The mobile phase was methanol (HPLC grade) at a regular flow-rate of 0.5 ml/min (20°C). The injection volume was 10  $\mu$ l (*ca.* 10  $\mu$ g). The peaks of the enantiomeric separation of **1** and **14** were verified by co-chromatography of the (-) and (+)-enantiomers.

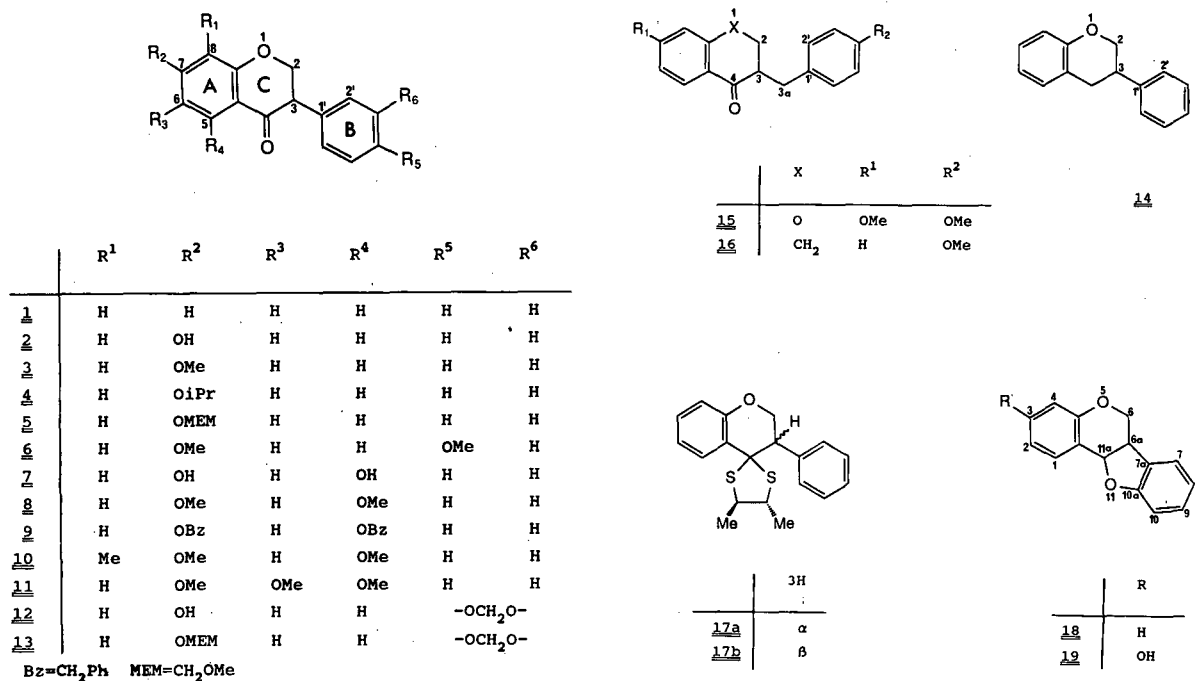


Fig. 2. Isoflavanones and related compounds studied.

## RESULTS AND DISCUSSION

Chromatographic data for the enantiomers of isoflavanones **1-13** and related compounds (**14-16**)

separated on PTrMA at room temperature using methanol as the mobile phase at 0.5 ml/min are given in Table I (formulae in Fig. 2).

To allow comparison of these data with those of

TABLE I

## CHROMATOGRAPHIC DATA FOR RACEMIC ISOFLAVANONES AND RELATED COMPOUNDS

$t_R$  = retention time (min);  $R_s$  = resolution factor =  $2 \times$  (distance between the peaks of the enantiomers/sum of band widths of two peaks);  $k'$  = capacity factor = (retained volume of enantiomer/void volume of column)/void volume of column;  $\alpha$  = separation factor =  $k'_2/k'_1$ ;  $R_s^*$ ,  $\alpha^*$  = corrected resolution and separation factors (Table II) ( $R_s^* = R_s \times 1.67$ ;  $\alpha^* = \alpha \times 1.12$ )

Compound	$t_R^1$	$k'_1$	$t_R^2$	$k'_2$	$\alpha$	$\alpha^*$	$R_s$	$R_s^*$
<b>1</b>	11.33(-)	2.37	12.29(+)	2.66	1.12	1.30	0.66	1.10
<b>2</b>	7.99	1.38	8.46	1.52	1.10	1.28	0.43	0.71
<b>3</b>	11.29	2.36	13.07	2.89	1.22	1.42	0.64	1.06
<b>4</b>	10.24	2.05	12.12	2.61	1.27	1.47	0.58	0.96
<b>5</b>	8.36	1.49	8.79	1.62	1.08	1.25	0.50	0.83
<b>6</b>	10.34	2.08	10.82	2.22	1.08	1.25	0.53	0.88
<b>7</b>	8.01	1.38	8.49	1.53	1.12	1.30	0.33	0.55
<b>8</b>	11.01	2.28	11.62	2.46	1.07	1.24	0.54	0.90
<b>9</b>	27.28	7.12	30.66	8.13	1.14	1.32	0.57	0.95
<b>10</b>	10.80	2.21	12.29	2.66	1.20	1.39	1.03	1.76
<b>11</b>	10.97	2.26	13.27	2.95	1.31	1.52	0.96	1.61
<b>12</b>	7.85	1.34	8.29	1.47	1.09	1.26	0.61	1.01
<b>13</b>	10.66	2.17	11.51	2.43	1.12	1.30	0.76	1.26
<b>14</b>	13.01(-)	2.87	15.28(+)	3.55	1.23	1.43	0.78	1.29
<b>15</b>	12.34	2.67	15.12	3.50	1.31	1.52	0.83	1.38
<b>16</b>	12.81	2.81	17.85	4.31	1.53	1.77	0.55	0.91

the pterocarpan derivatives determined by us previously [14], we checked the activity of our column by measuring the separation values ( $\alpha$ ) of the unsubstituted pterocarpan and of maackiain, to establish whether or not the separation efficiency of the column had considerably changed.

A significant decrease in the resolution factor ( $R_s$ ) was detected in both cases (Table II); this must have been the result of the decreased activity of the column (by about 40%), which was used for 150 h at room temperature. The most likely explanation for this decline is the solvolysis of PTrMA by methanol. It is also interesting to note that the decrease in the retention time ( $t_R$ ) of the more strongly retained enantiomer with 6aR,11aR absolute configuration was double (without a considerable change of its capacity factor) that of the less retained one. We therefore introduced corrected resolution and separation factors,  $R_s^*$  and  $\alpha^*$ , which were calculated using factors derived from the change in the separation efficiency of maackiain and **18** (Table I).

Since isoflavanone **1** could be just baseline resolved ( $\alpha^* = 1.30$ ), the intensity of the  $\pi$ - $\pi$  type

non-polar interaction between the aromatic parts of the substrate and the pendant trityl groups of the chiral stationary phase seemed to be remarkably smaller than in case of **18** ( $\alpha = 2.44$ ). Correlation of the configuration with the elution order revealed that the more strongly retained enantiomer [3R-(+)-**1**,  $t_R = 12.9$  min] was homochiral at C-3 with the 6aR,11aR-configured pterocarpan.

Since the chiral recognition mechanism of PTrMA is not yet understood in detail [19], it appeared to be of great interest to study the influence of the substitution pattern of a molecule on chiral recognition.

The presence of a hydroxy group at C-7 had a less significant influence (**2**,  $\alpha^* = 1.28$ ) on the chiral recognition process than in the pterocarpan series (cf. **19**,  $\alpha = 1.35$ ). The lowest enantioselectivity was observed for the 5,7-dihydroxylated isoflavanone (**7**,  $R_s^* = 0.55$ ). Reducing the polar character of the molecule by etherification of the hydroxy group(s) improved the enantiomeric separation ( $R_s^*$  values: **2** < **5** < **4** < **3**, **7** < **8** < **9** and **12** < **13**) but not as efficiently as in the case of pterocarpan. The type of protecting groups caused different retention behaviours. Replacing the hydroxy group by a methoxy, isopropoxy or methoxymethoxy group increased the retention time, which averaged up to ca. 2.7 and 3.5 min for the first- and second-eluted enantiomers, respectively. The retention times of these compounds (**3–6**, **8**, **13**) corresponded quite well to those of unsubstituted isoflavanone (**1**). In the case of **9**, a significant increase in retention time was observed for both enantiomers ( $t_R = 27.28$  and 30.66 min) as a result of the presence of benzyloxy groups at C-5 and C-7, but the separation and the resolution factor ( $\alpha^* = 1.32$ ,  $R_s^* = 0.95$ ) were similar to those found for **1** ( $\alpha^* = 1.30$ ,  $R_s^* = 1.10$ ). These data clearly indicated that  $\pi$ - $\pi$  interaction plays an important role in the separation, but this structural feature does not make any contribution to chiral recognition.

The  $\pi$ -electron density of the A- and B-rings of the isoflavanones seems to be very important for the recognition process, although a general rule cannot be derived from the results obtained so far.

The presence of a methylenedioxy group in ring B increased the enantiomeric separation ( $R_s^*$  for **2** < **12**,  $\Delta R_s^* = 0.30$ ). The same tendency with a significantly larger effect was observed in the series of

TABLE II

DETAILED CHROMATOGRAPHIC DATA FOR EXPERIMENTS REPEATED BECAUSE OF THE OBSERVED CHANGE IN COLUMN ACTIVITY

- (a) *Maackiain*  
 $t_R(-) = 8.95$  min,  $t_R(+)$  = 8.01 min;  $k'(-)$  = 2.01,  
 $k'(+) = 1.59$ ;  $\alpha = 1.26$ ;  $R_s = 1.13$
- (b) **18**  
 $t_R(-) = 18.55$  min,  $t_R(+)$  = 10.10 min;  $k'(-)$  = 5.20,  
 $k'(+) = 2.47$ ;  $\alpha = 2.10$ ;  $R_s = 2.84$

Changes in resolution values resulting from the decrease in the column activity in the case of:

- (a) *Maackiain*  
 $R_s = 2.20$  [14] - 1.13 = 1.07 (49%)  
 Correction factor for  $R_s = 2.20/1.13 = 1.94$   
 $\alpha = 1.35$  [14] - 1.26 = 0.09 (7%)  
 Correction factor for  $\alpha = 1.35/1.26 = 1.07$
- (b) **18**  
 $R_s = 4.00$  [14] - 2.84 = 1.16 (29%)  
 Correction factor for  $R_s = 4/2.84 = 1.40$   
 $R_s^* =$  corrected resolution factor  
 $= R_s \times [(1.40 + 1.94)/2] = R_s \times 1.67$   
 $\alpha = 2.44$  [14] - 2.10 = 0.34 (14%)  
 Correction factor for  $\alpha = 2.44/2.10 = 1.16$   
 $\alpha^* =$  corrected separation factor  
 $= \alpha \times [(1.15 + 1.07)/2] = \alpha \times 1.12$

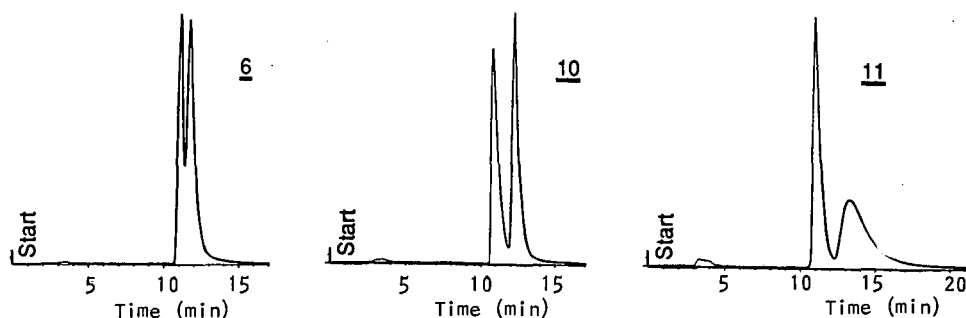


Fig. 3. Enantiomeric separation of **6**, **10** and **11** on Chiralpack OT(+) (Daicel). Mobile phase, methanol; flow-rate, 0.5 ml/min.

pterocarpan [ $R_s$  for 3-hydroxypterocarpan (**19**) < maackiain,  $\Delta R_s = 1.20$ ]. Electron-donating groups in ring A, e.g. methyl at C-8 (**10**) or methoxy at C-6 (**11**), also improved the separation ( $R_s^*$  values **6** < **11** < **10**). Moreover, the methoxy group changed the chromatographic profile strikingly, as illustrated in Fig. 3. The reason for this behaviour is still not known.

In order to obtain more information on the recognition mechanism of isoflavanones on PTrMA-coated silica gel, we also tested the resolution of some closely related compounds (**14–16**). Comparison of the separation of **1** with that of **14** ( $\alpha^* = 1.30$  and 1.43, respectively;  $R_s^* = 1.10$  and 1.29, respectively) indicated that the introduction into the isoflavanoid skeleton of a carbonyl group possessing a large dipole moment disturbed chiral recognition. It is remarkable that the polarity of the mobile phase plays an important role in the separation process. Using *n*-hexane as the mobile phase at a flow-rate of 1 ml/min, the isoflavan **14** could be just baseline resolved ( $R_s^* = 1.14$ ), and none of the examined isoflavanones were separable.

The homoisoflavanone **15** could be better resolved on PTrMA with methanol at a flow-rate of 0.5 ml/min ( $\alpha^* = 1.52$ ) than the corresponding isoflavanone **6** ( $\alpha^* = 1.25$ ) or the unsubstituted compound (**1**,  $\alpha^* = 1.30$ ). Substitution of the oxygen in ring C by  $\text{CH}_2$  (**16**) gave a similar chromatographic profile as shown for **11** in Fig. 3, but the peak shape of its better-retained enantiomer was even more asymmetric, thus reducing the resolution factor significantly ( $R_s^* = 0.91$ ).

In conclusion, PTrMA-coated silica gel is a suitable chiral stationary phase for resolving isoflavanones and homoisoflavanones. The enantioselectiv-

ity of the separation depends on different structural changes in the substituents and/or skeleton. Homoisoflavanones are better resolved than isoflavans or isoflavanones. Considerations on the chiral recognition mechanism based on computer-assisted molecular design will be published in a separate paper.

#### REFERENCES

- H. Grisebach, in J. W. Bennett and A. Ciegler (Editors), *Secondary Metabolism and Differentiation in Fungi*, Marcel Dekker, New York, 1983, pp. 377–428.
- J. C. Ingham, *Phytopathol. Z.*, 87 (1976) 353.
- P. M. Dewick, *Phytochemistry*, 16 (1977) 93.
- T. P. Denny and A. D. van Etten, *Physiol. Plant Pathol.*, 19 (1981) 419.
- V. J. Higgins, *Physiol. Plant Pathol.*, 2 (1972) 289.
- P. M. Dewick and D. Ward, *J. Chem. Soc., Chem. Commun.*, (1977) 338.
- W. Bless and W. Barz, *FEBS Lett.*, 235 (1988) 47.
- D. Schlieger, K. Tiemann and W. Barz, *Phytochemistry*, 29 (1990) 1519.
- H. Sugimoto, *Bull. Chem. Soc. Jpn.*, 39 (1966) 1544.
- M. A. Fitzgerald, P. J. M. Gunning and D. M. X. Donnelly, *J. Chem. Soc. Perkin Trans. 1*, (1976) 186.
- M. Kamatsu, I. Yokoe and Y. Shirataki, *Chem. Pharm. Bull.*, 26 (1978) 3863.
- G. Delle Monache, F. Delle Monache, G. B. Marini-Bettolo, M. M. Albuquerque, J. F. de Mello and O. G. de Lima, *Gazz. Chim. Ital.*, 107 (1977) 189.
- A. J. Kalra, M. Krishnamurti and M. Nath, *Indian J. Chem.*, 15B (1977) 1084.
- A. S. Dreiding, *Helv. Chim. Acta*, 42 (1959) 1339.
- S. Antus, R. Bauer, Á. Gottsegen and H. Wagner, *J. Chromatogr.*, 508 (1990) 212.
- S. Antus, Á. Gottsegen, M. Nógrádi, *Synthesis*, (1981) 574.
- S. Antus, E. Baitz-Gács, J. Cseri, Á. Gottsegen, O. Seligmann and H. Wagner, in preparation.
- E. J. Corey and R. B. Mitra, *J. Am. Chem. Soc.*, 84 (1962) 2938.
- A. M. Krstulovic (Editor), *Chiral Separations by HPLC*, Vol. 12, Wiley, New York, 1989, p. 316.



# Separation of oligogalacturonic acids by high-performance gel filtration chromatography on silica gel with diol radical

J. Naohara

*Environmental Resources Research Centre, Okayama University of Science, Okayama 700 (Japan)*

M. Manabe

*Faculty of Agriculture, Kagawa University, Kagawa 761-02 (Japan)*

(First received November 1st, 1991; revised manuscript received February 6th, 1992)

---

## ABSTRACT

Oligogalacturonic acids (OLGAs) ranging from two to nineteen residues in length were separated using high-performance gel filtration chromatography on a silica gel with diol radical. The optimum conditions (eluent, column temperature) for separation of OLGAs by high-performance gel filtration chromatography were investigated. The column used in this experiment allowed a high pressure of 4900 p.s.i. and a flow-rate of 2 ml/min. The stationary phase of silica gel stabilized the separation of OLGAs. The peaks of OLGAs separated using this column were assigned by comparing retention times with standards, and the molecular weights of the corresponding OLGAs were determined by fast atom bombardment mass spectrometry.

---

## INTRODUCTION

The separation of oligogalacturonic acids (OLGAs) from chemically and enzymatically degraded polygalacturonic acid is important in the structural analysis of the cell wall in plants. It is also important for studying the mechanism of action of pectin-degrading enzymes. The oligomers are recognized to be capable of regulating a number of physiological responses in plants, including the endogenous elicitation and induction of phytoalexin [1–3], an increase in the activity of phenylalanine ammonia lyase [4], the production of a proteinase inhibitor [5], lignification, and the induction of chitinase and  $\beta$ -1,3-glucanase [6]. OLGAs are involved in the fixation of extensin and lignin into the

cell wall in plants [7]. It is reported that OLGAs have antimicrobial action [8]. Therefore, it is necessary to be able to separate OLGAs rapidly and to detect OLGAs with a wide range of degree of polymerization (DP) in these investigations.

OLGAs have been analysed by thin-layer chromatography [9–11], ion-exchange chromatography [12–21], gel filtration chromatography [22,23], reversed-phase chromatography [13,17,24–26], electrophoresis [27], ultracentrifugation [27] and gas-liquid chromatography [28]. However, these analyses have the disadvantages of a long analysis time, a low distribution coefficient and poor sensitivity of longer OLGAs.

High-performance gel filtration (HPGF) chromatography is one of the best methods of analysing oligosaccharides, especially longer-DP oligomers, in a short time. HPGF chromatography has the advantage that no sample derivatization is required. In the present work, HPGF chromatography was per-

---

*Correspondence to:* Dr. J. Naohara, Environmental Resources Research Centre, Okayama University of Science, Okayama 700, Japan.

formed using a column packed with hydrophilic and porous spherical silica gel of 5  $\mu\text{m}$  particle size covered with a high degree of alcoholic OH radicals. This column allows the continuous use of high pressure and high flow-rate, and the separation of samples is stabilized as a result of the fact that silica gel is harder than polymer gels. The column can endure pressures as high as 4900 p.s.i. The pH of eluents can be between 5 and 8. The temperature of the column can range from 4 to 40°C.

The optimum conditions for the separation of OLGAs were investigated and the molecular weights of OLGAs were determined by fast atom bombardment mass spectrometry (FAB-MS).

## EXPERIMENTAL

### Materials

$\alpha$ -D-Galacturonic acid, digalacturonic acid, trigalacturonic acid, polygalacturonic acid and endo-polygalacturonase (endo-PG) (EC 3.2.1.15) were from Sigma (St. Louis, MO, USA).

### Preparation of OLGAs

A mixture of OLGAs was produced by enzyme digestion of polygalacturonic acid at 30°C for 40 min with endo-PG. The reaction mixture was heated at 100°C for 10 min to terminate the reaction. Ethyl alcohol was added to the reaction mixture at a final concentration of 65% after cooling. The resulting precipitates of OLGAs separated by centrifugation (4530 g, 20 min) were dissolved in water and lyophilized. The OLGAs were treated with 0.05 *M* sodium hydroxide at 0°C for 90 min. The de-esterified OLGAs were precipitated and separated by centrifugation (4530 g, 20 min). They were dissolved in water and lyophilized.

### HPGF chromatography

HPGF chromatography was performed on a Waters isocratic manual system (Waters, Division of Millipore, Tokyo, Japan) with a Waters R-401 refractive index (RI) detector. For the DP analysis of OLGAs, a YMC Diol 120 column (500  $\times$  8 mm I.D.) and a precolumn (30  $\times$  8 mm I.D.) (YMC, Kyoto, Japan) were used. A column oven was used to maintain the temperature at 25–50°C (Sugai U620, Sugai, Wakayama, Japan). An acetate buffer and a phosphate buffer were used in elution. Vol-

umes of 25  $\mu\text{l}$  of the liquid oligomers were injected. Chromatographic data were plotted and integrated using a Waters 714 data module.

### Measurement of the fractionation parameter

The distribution coefficient,  $K_{\text{av}}$ , was calculated from the retention time of each peak as follows:

$$K_{\text{av}} = (V_e - V_0)/(V_t - V_0)$$

where  $V_e$  is elution volume of OLGAs or standards,  $V_0$  is the void volume (verified by polygalacturonic acid) and  $V_t$  is the total bed volume.

### Preparation of authentic OLGAs

The OLGAs were separated according to the modified method of Nothnagel *et al.* [1]. High-performance ion-exchange chromatography was performed using a Waters automatic gradient system with an SF-2120 Advantec fraction collector (Advantec Toyo, Tokyo, Japan). For the separation of the oligomers QAE-Sephadex A-25 in a Waters AP-1 glass column (600  $\times$  10 mm I.D.) was used. The mixture of OLGAs (ca. 500 mg) was dissolved in 20 ml of 0.2 *M* imidazole–hydrochloric acid buffer, pH 7.0, and the solution was injected into the column. The OLGAs were eluted with a linear gradient of 0.2 *M* to 1.0 *M* imidazole–hydrochloric acid buffer, pH 7.0. The flow-rate was 2 ml/min and the volume of the collected fractions was 10 ml. The collected fractions were concentrated and desalted by a Microacilyzer S1 (Asahi Kasei, Tokyo, Japan), an automatic desalting device using AC-210-10 ion-exchange films. Each purified OLGA fraction was lyophilized.

### FAB-MS analysis

The molecular weights of fractionated and purified OLGAs were analysed by FAB-MS. The device used was a Jeol JMS-GX 303HF (Jeol, Tokyo, Japan). Xenon was used as the bombarding gas, and an atom gun was operated at 6 kV, 20 mA. Samples were dissolved in methanol–water (1–5  $\mu\text{g}/\mu\text{l}$ ) and 1  $\mu\text{l}$  of each sample solution was added to a drop of glycerol on the stainless-steel target.

## RESULTS AND DISCUSSION

### Effect of the ionic strength of the eluent

The effect of ionic strength (sodium chloride) on

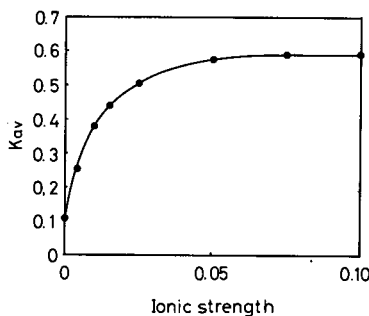


Fig. 1. Variation in the  $K_{av}$  value of galacturonic acid (amount injected: 25  $\mu$ l of a 10 mg/ml solution) with the ionic strength of eluent.

the  $K_{av}$  of galacturonic acid (10 mg/ml, 25  $\mu$ l) is shown in Fig. 1. The  $K_{av}$  of galacturonic acid increased with an increase in the ionic strength of the eluent, and the  $K_{av}$  of galacturonic acid attained an almost constant value of 0.56 when the ionic strength of the eluent was higher than 0.05. This tendency was the same as that of the effect of ionic strength on the  $K_{av}$  of galacturonic acid using the Bio-Gel P2 column [18].

The effect of the injected volume (5–100  $\mu$ l) on the retention time of galacturonic acid (10 mg/ml) was examined. When a 0.05 M sodium chloride solution was used as the eluent, the retention time of galacturonic acid lengthened a little as the volume injected increased, but the increase was negligible under the experimental conditions. The retention times were between 19.1 and 19.2 min.

*Effect of the pH of the eluent*

The effect of the pH of the acetate buffers on the retention time of the OLGAs is shown in Fig. 2. The retention times of OLGAs with different DP values increased as the pH of the acetate buffer solution was increased. The retention times of OLGAs in 0.2 M acetate buffer were longer than those in 0.05 M acetate buffer.

*Effect of the temperature of the eluent*

The effects of the column temperature on the relationship between the DP of OLGAs and  $-\log K_{av}$  are shown in Fig. 3. The relationship between the DP of OLGAs and  $-\log K_{av}$  was linear at column temperatures in the range 25–50°C. The observed DP was highest at 40–45°C. The  $-\log K_{av}$  value of

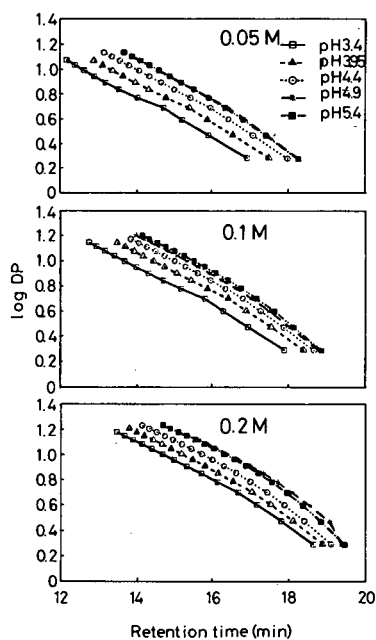


Fig. 2. Effect of pH of acetate buffers on retention time.

OLGAs with the Bio-Gel P2 column [18] increased with the increase in the column temperature. This column was stable under these temperature conditions.

*Quantification of oligogalacturonic acid*

The monomer, dimer and trimer standards (purchased from Sigma) could be quantified in the 2000- $\mu$ g region in a given sample applied to the column. When the signal-to-noise ratio was 3, the detection limits of the monomer, dimer and trimer standards were 1.0 ng. It is thought that oligomers

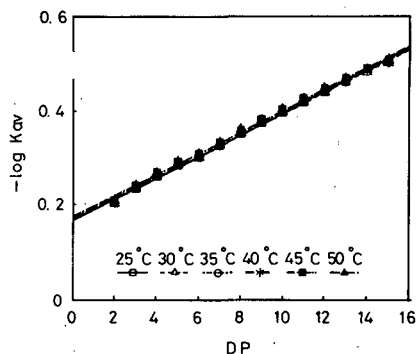


Fig. 3. Relationship between  $-\log K_{av}$  and DP.

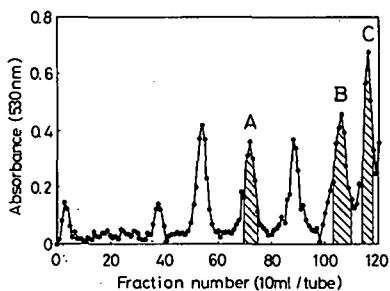


Fig. 4. HPLC of oligogalacturonic acid on QAE-Sephadex A-25.

with DP values larger than 4 may be quantified in the 2000- $\mu$ g region in a standard solution even though those oligomers are not commercially available.

This column can be used for the identification and quantification of OLGAs in the isocratic elution mode. In the reports that described the separation of

OLGAs by ion-exchange column [13,16,21] and reversed-phase columns [13,25,26], the highest DP value of the OLGAs separated in the isocratic elution mode [16] was 10. Since the pressure used for the (cation-exchange) column was limited to only 300 p.s.i. and a high flow-rate led to high back-pressures and to the loss of resolution, it seemed this method using a cation-exchange column was not practical.

The silica gel column used in this experiment allowed the use of high pressure, 4900 p.s.i., and a high flow-rate, 2-ml/min. The separation of OLGAs of DP 19 could be possible (see Fig. 6), by using porous (120 Å) spherical silica gel of 5  $\mu$ m particle size covered with a high degree of alcoholic OH radicals. This simple and rapid method by which OLGAs with DPs of 19 may be separated has not yet been reported.

#### Molecular weight of each fraction

The OLGAs in the mixture were separated by high-performance ion-exchange chromatography using a QAE-Sephadex A-25 column. Each peak fraction was pooled, desalted with the Microacilyzer S1 and lyophilized. The molecular weights of lyo-

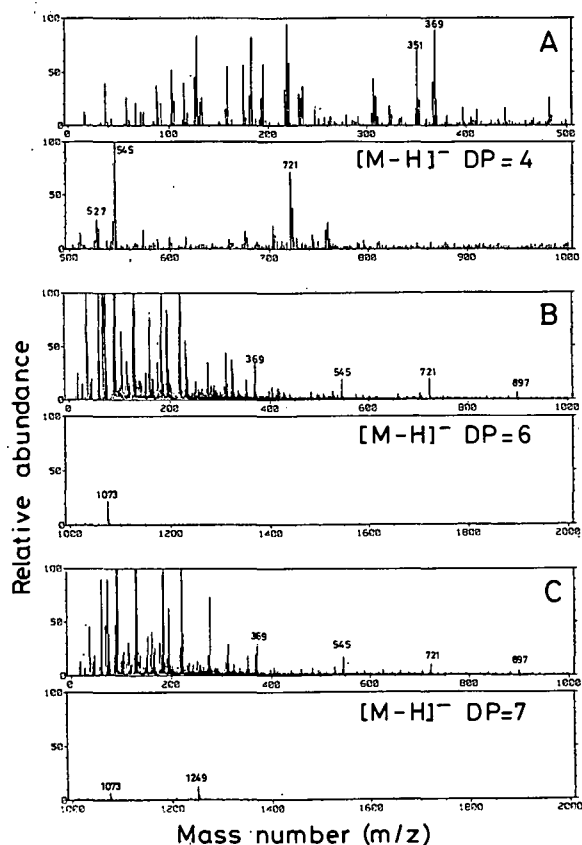


Fig. 5. FAB-MS analysis of oligogalacturonic acid.

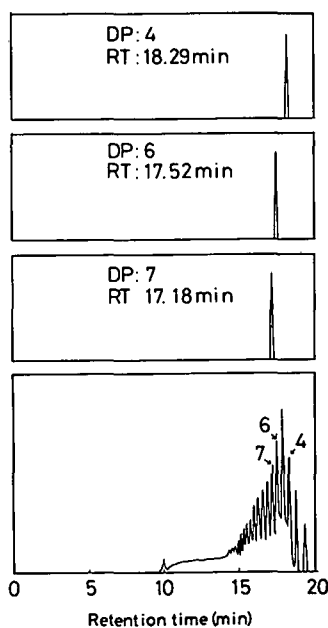


Fig. 6. High-performance gel filtration chromatographic analysis of oligogalacturonic acid. RT = Retention time.

philized OLGAs were measured by FAB-MS. The results obtained are shown in Fig. 4. These fractions gave distinct molecular ions ( $[M - H]^-$ ). Fraction A had a molecular ion at  $m/z$  721 that corresponds to a molecular weight of 722, as shown in Fig. 5A. This signal should represent a tetragalacturonic acid. Consecutive losses of galacturonosyl residues from  $[M - H]^-$  gave signals at  $m/z$  545 and 369. As shown in Fig. 5B and C, the similar spectra of the oligogalacturonic acids in fractions B and C, having molecular ions at  $m/z$  1073 and 1249, correspond to hexa- and heptagalacturonic acid, respectively. These results are in agreement with the results obtained by Komae *et al.* [19]. The retention times of tetra-, hexa- and heptagalacturonic acid analysed by the HPGF chromatography with the YMC Diol 120 column were 18.31, 17.52 and 17.19 min, respectively (Fig. 6). Some peaks could be detected when the mixture of OLGAs was analysed; the peak at a retention time of 18.29 min was possibly tetragalacturonic acid, that at 17.52 min hexagalacturonic acid and that at 17.18 min heptagalacturonic acid.

#### REFERENCES

- 1 E. A. Nothnagel, M. McNeil, P. Albersheim and A. Dell, *Plant Physiol.*, 71 (1983) 916.
- 2 D. F. Jin and C. A. West, *Plant Physiol.*, 74 (1984) 989.
- 3 K. R. Davis, A. G. Darvill, P. Albersheim and A. Dell, *Plant Physiol.*, 80 (1986) 568.
- 4 G. De Lorenzo, A. Ranucci, D. Bellincampi, G. Salvi and F. Cervone, *Plant Sci.*, 51 (1987) 147.
- 5 P. D. Bishop, G. Pearce, J. E. Bryant and C. A. Ryan, *J. Biol. Chem.*, 259 (1984) 13172.
- 6 C. A. Ryan, *Annu. Rev. Cell Biol.*, 3 (1987) 295.
- 7 B. Robertsen, *Physiol. Mol. Plant Pathol.*, 28 (1986) 137.
- 8 H. Yokotsuka, T. Matsudo, T. Kushida, N. Inamine and T. Nakashima, *Hakkou Kougaku*, 62 (1984) 1 (in Japanese).
- 9 Y. K. Liu and B. S. Luh, *J. Chromatogr.*, 151 (1978) 39.
- 10 O. Markovič and A. Slezárik, *J. Chromatogr.*, 312 (1984) 492.
- 11 L. W. Dower, P. L. Irwin and M. J. Kurantz, *Carbohydr. Res.*, 172 (1988) 292.
- 12 C. Hatanaka and J. Ozawa, *J. Agric. Chem. Soc. Japan*, 46 (1972) 417 (in Japanese).
- 13 A. G. J. Voragen, H. A. Schols, J. A. de Vries and W. Pilnik, *J. Chromatogr.*, 244 (1982) 327.
- 14 M. R. Hardy and R. R. Townsend, *Proc. Natl. Acad. Sci. U.S.A.*, 85 (1988) 3289.
- 15 A. T. Hotchkiss, K. B. Hicks, L. W. Doner and P. L. Irwin, presented at the 3rd Chemical Congress of North America, Toronto, 1989, Abstract 95.
- 16 K. B. Hicks and A. T. Hotchkiss, Jr., *J. Chromatogr.*, 411 (1988) 382.
- 17 K. B. Hicks, *Adv. Carbohydr. Chem. Biochem.*, 46 (1988) 17.
- 18 M. O. Maness and A. J. Mort, *Anal. Biochem.*, 178 (1989) 248.
- 19 K. Komae, A. Komae and A. Misaki, *Agric. Biol. Chem.*, 54 (1990) 1477.
- 20 A. T. Hotchkiss, Jr. and K. B. Hicks, *Anal. Biochem.*, 184 (1990) 200.
- 21 A. T. Hotchkiss, Jr., K. B. Hicks, L. W. Doner and P. L. Irwin, *Carbohydr. Res.*, 215 (1991) 81.
- 22 J. H. McClendon, *J. Chromatogr.*, 171 (1979) 460.
- 23 J. F. Thibault, *J. Chromatogr.*, 194 (1980) 315.
- 24 A. Heyraud and C. Rochas, *J. Liq. Chromatogr.*, 5 (1982) 403.
- 25 A. Heyraud and C. Leonard, *Carbohydr. Res.*, 215 (1991) 105.
- 26 J. F. Preston III and J. D. Rice, *Carbohydr. Res.*, 215 (1991) 137.
- 27 A. J. Barrett and D. H. Northcote, *Biochem. J.*, 94 (1965) 481.
- 28 W. R. Raymond and C. W. Nagel, *Anal. Chem.*, 41 (1969) 1700.



# Determination of hydroxylamine in aqueous solutions of pyridinium aldoximes by high-performance liquid chromatography with UV and fluorometric detection<sup>☆</sup>

W. D. Korte

*US Army Medical Research Institute of Chemical Defense (USAMRICD), Aberdeen Proving Ground, MD 21010-5425 (USA)*

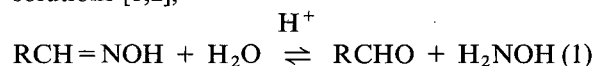
(First received February 11th, 1991; revised manuscript received March 3rd, 1992)

## ABSTRACT

A high-performance liquid chromatographic assay using UV and fluorescence detection was developed that monitored hydroxylamine as the vanillin oxime derivative while simultaneously monitoring concentrations of a complex mixture of a pyridinium aldoxime and its degradation products. The technique should be useful for measuring hydroxylamine levels in other aqueous systems.

## INTRODUCTION

During the investigation of the stability of dosage concentrations of various organic aldoximes that have potential pharmaceutical application as antidotes to organophosphorus anticholinesterase poisoning, there arose a need to monitor the concentration of hydroxylamine in the acidic aqueous solutions of degrading aldoximes. Although the equilibrium associated with the hydrolysis of aldoximes (eqn. 1) usually lies far to the left in weakly acidic solutions [1,2],



participation of the components of the equilibrium in side reactions during long term storage can lead to a significant loss of pharmacologically active al-

doxime [3–6]. For example, hydroxylamine was reported to be a reactant in the hydrolysis of the amide group during the degradation of several pyridinium aldoximes under pharmaceutical evaluation which contained both aldoxime and amide functional groups [6]. While studying these complex reactions of aldoximes, a convenient high-performance liquid chromatography (HPLC) method that allowed simultaneous determination of hydroxylamine, a pyridinium aldoxime, and the major degradation products was developed.

Numerous methods have been reported for measuring the concentration of hydroxylamine [7–12]; however, only Lombardi and Crolla [12] addressed the possibility of an HPLC assay. Although their paper primarily focused on a gas chromatographic (GC) procedure for hydroxylamine found in medicinal preparations containing hydroxamic acids, they did briefly mention that a similar method involving the pre-chromatographic formation of the 4-methoxybenzaldehyde oxime derivative of hydroxylamine had been applied to HPLC with some success.

This report will describe how the more water soluble aldehyde vanillin was used as the derivatizing agent to enhance the ultraviolet (UV) and fluores-

*Correspondence to:* Professor William D. Korte, Department of Chemistry, California State University, Chico, CA 95929, USA (present address).

<sup>☆</sup> The opinions or assertions contained herein are the private views of the author and are not to be construed as official or as reflecting the views of the Army or the Department of Defense.

cence detectability of hydroxylamine in solutions of three pyridinium aldoximes with different degradative pathways. The aldoximes selected for investigation were 2-[(hydroxyimino)methyl]-1-methylpyridinium chloride (2-PAM chloride), 1,1'-[oxybis(methylene)]bis{4-[(hydroxyimino)methyl]-pyridinium} dichloride (toxogonin), and 1-([3-(aminocarbonyl)pyridinio]methoxy)-methyl-2-[(hydroxyimino)methyl]pyridinium dichloride (**I**, HS-6). Degradation pathways for these aldoximes have been extensively studied and the concentration of hydroxylamine present under several reaction conditions determined [4,5,13,14] by modifications of the Csaky method [7] so that comparisons with the procedure described herein could be made.

## EXPERIMENTAL

### Equipment

The HPLC system included a reversed-phase 10- $\mu\text{m}$   $\mu\text{Bondapak C}_{18}$  column (30 cm  $\times$  3.9 mm I.D.), Model 6000A pump, a WISP 710B autoinjector, a Lambda-Max 481 spectrophotometer, and a Model 730 data module, all from Waters Assoc. (Milford, MA, USA). A McPherson FL-749 spectrofluorimeter (McPherson, Acton, MA, USA) equipped with a 200-W xenon–mercury lamp and a 12- $\mu\text{l}$  flow cell was used for fluorescence detection with the HPLC system. Fluorescence spectra were obtained with a Perkin-Elmer MPF-44B fluorescence spectrofluorimeter (Perkin-Elmer, Norwalk, CT, USA), and UV spectra were obtained with a Carey Model 219 spectrophotometer (Varian, Palo Alto, CA, USA).

### Materials

1-Heptanesulfonic acid, sodium salt, was purchased from Sigma (St. Louis, MO, USA), tetramethyl ammonium chloride (TMAC) from Mallinkrodt (Paris, KY, USA), and potassium dihydrogen phosphate ( $\text{KH}_2\text{PO}_4$ ), 85% phosphoric acid, sodium acetate, and vanillin were purchased from Fisher Scientific (Pittsburgh, PA, USA) and used without purification. Vanillin has UV absorption maxima [molar absorptivity ( $1 \text{ mol}^{-1} \text{ cm}^{-1}$ ) in parentheses] in ethanol at 309 nm ( $10.5 \cdot 10^3$ ), 279 nm ( $10.2 \cdot 10^3$ ) and 232 nm ( $14.4 \cdot 10^3$ ) [15]. The broad emission band was centered at 412 nm. Vanillin oxime was synthesized from vanillin and hydroxyl-

amine hydrochloride according to the procedure of Vogel [16], and recrystallized from ethanol (m.p. 121–122°C, Lit. [17] 121–122°C). UV absorption maxima in water–ethanol (5:1, v/v) were at 298 nm ( $9.6 \cdot 10^3$ ), 268 nm ( $13.8 \cdot 10^3$ ) and 213 nm ( $21.0 \cdot 10^3$ ). The broad emission band was centered at 367 nm. Hydroxylamine hydrochloride was obtained from Eastman (Rochester, NY, USA) and recrystallized from a mixture of ethanol and methanol (m.p. 151–152°C, Lit. [18] 151–152°C). 4-Cyanophenol was obtained from Aldrich (Milwaukee, WI, USA). Acetonitrile was obtained from Burdick & Jackson (Muskegon, MI, USA).

2-PAM chloride was obtained from Ayerst (New York, NY, USA) and toxogonin and **I** (HS-6) were obtained from the Walter Reed Army Institute of Research (Washington, DC, USA). HPLC analysis indicated that the three crystalline pyridinium aldoximes contained less than 1% of the starting material and were used without further purification. Outdated 2-PAM chloride autoinjectors manufactured by Survival Technology (Bethesda, MD, USA) were obtained from the Safety Officer (USAMRICD, Aberdeen Proving Ground, MD, USA).

### Derivatization procedure

Vanillin [200  $\mu\text{l}$ , 0.1 M in ethanol–water (1:1, v/v)], sodium acetate (100  $\mu\text{l}$ , 0.2 M) and the aldoxime solution to be tested (10–100  $\mu\text{l}$ ) were mixed in a 1-ml reaction vial and allowed to stand at room temperature for 30 min. At hydroxylamine concentrations greater than  $5 \cdot 10^{-5} \text{ M}$ , the reaction took less than 10 min to obtain a constant concentration of the hydroxylamine derivative, vanillin oxime. The entire contents of the vial were then transferred to a 10-, 25- or 50-ml volumetric flask, depending on the expected concentration of hydroxylamine, and diluted with water to the desired volume for HPLC analysis.

### Chromatography

Several different mobile phases were used during the study to optimize the separation of components in the mixtures of the different aldoximes and degradation products. The data in Table I were collected from separations using three different mobile phases varied only by the quantity of acetonitrile used in the solvent mixture. These mobile phases

were prepared by taking from 90 to 120 ml of acetonitrile (90 ml for I assays, 100 ml for toxogonin assays and 120 ml for 2-PAM assays), 5 ml of 0.1 M  $H_3PO_4$ , 0.2 ml of 1.0 M TMAC, 120 mg of 1-heptanesulfonic acid, sodium salt, and 70 mg of  $KH_2PO_4$  and mixing them with water to make 1 l of solution. The flow-rate was 0.5 ml/min and the chart speed on the data module set at 0.2 cm/min. The UV detector was set at 255 nm and the fluorescence detector set at 270 nm (16 nm slitwidth) for excitation and 355 nm (8 nm slitwidth) for emission. The sample size was usually 10  $\mu$ l, but it was increased to as much as 50  $\mu$ l for samples with low concentrations of hydroxylamine.

The vanillin oxime standard solutions and the vanillin reagent were prepared fresh daily. 4-Cyanophenol was a satisfactory internal standard for UV

detection with a retention time greater than that of vanillin; however, the fluorescence signal was very small at the excitation/emission wavelengths used for this study.

#### Degradation reactions

Solutions of pyridinium aldoximes (0.8 ml) at various concentrations (see Table I) were placed in one ml reaction vials and either heated in an oven at 60°C or left at room temperature for the desired period of time. The heated vials were cooled before testing. The rate of the reverse reaction, hydroxylamine with the pyridinium aldehyde (eqn. 1), has been shown to be slow at the low pH of the degradation reactions [1]; therefore, the concentration of hydroxylamine was expected to remain constant during the short cooling period.

TABLE I

HYDROXYLAMINE LEVEL IN PYRIDINIUM ALDOXIME SOLUTIONS RELATIVE TO THE INITIAL CONCENTRATION OF PYRIDINIUM OXIME<sup>a</sup> AND AS A FUNCTION OF TEMPERATURE, pH AND TIME

Oxime (concentration)	Temperature	pH	Hydroxylamine (%)				
			24 h	48 h	96 h	144 h	Other time
2-PAM (0.5 M)	60°C	1.1	2.38	2.62	2.66	2.63	2.38 <sup>b</sup>
		2.0	0.75	0.81	0.66	0.65	0.52 <sup>b</sup>
		3.1	0.15	0.13	0.15	0.17	0.05 <sup>b</sup>
	Room temperature	1.1	1.68	2.05	2.13	2.26	
		2.0	0.18	0.41	0.61	0.62	
		3.1	0.01	0.03	0.10	0.14	
2-PAM (1.8 M)	AT <sup>c</sup>	2.5					0.17 <sup>c</sup>
Toxogonin (0.25 M)	60°C	1.1	2.64	2.62	2.81	2.83	2.50 <sup>b</sup>
		1.9	0.44	0.67	0.80	0.84	
		2.9	0.08	0.11	0.19	0.17	
	Room temperature	1.1	2.55	2.46	2.44	2.56	
		1.9	0.07	0.49	0.70	0.72	
		2.9	0.01	0.08	0.15	0.17	
I (0.5 M)	60°C	1.1	0.60	1.44	1.64	1.32	
		2.7	— <sup>d</sup>	0.01	1.06	0.70	
	Room temperature	1.1	0.84	1.86	1.84	1.80	
		2.7	— <sup>d</sup>	— <sup>d</sup>	— <sup>d</sup>	0.01	

<sup>a</sup> Calculated as per cent yield of hydroxylamine from the initial concentration of pyridinium oxime: (mol hydroxylamine/mol oxime) × 100. All values are averages of two or more determinations.

<sup>b</sup> Measured after heating 2 h.

<sup>c</sup> Average value of samples from two six-year-old autoinjectors maintained at ambient temperature (AT).

<sup>d</sup> Not detectable with this assay.

## RESULTS AND DISCUSSION

This HPLC assay was designed to measure hydroxylamine in concentrations ranging from  $5 \cdot 10^{-2}$  to  $5 \cdot 10^{-5}$  M in aqueous solutions containing high concentrations of pyridinium aldoximes and their degradation products. By using an HPLC procedure instead of a GC procedure, the ionic aldoximes and both ionic and neutral decomposition products could be monitored simultaneously with the hydroxylamine.

Initial aldoxime concentrations, 0.25 M for toxogonin and 0.5 M for 2-PAM and I for the degradation reactions, were selected to reflect dosage preparations. The 1000-fold range of concentrations for hydroxylamine was expected based on previous studies concerning the degradation of pyridinium aldoximes [4,5,13,14].

*Derivatization*

Vanillin reacted readily, in less than 10 min at room temperature, with hydroxylamine in the presence of sodium acetate to form vanillin oxime over the entire expected concentration range. A large excess, at least 40-fold, of vanillin and an extended reaction time of 30 min was used to ensure reaction. Hydroxylamine was derivatized in yields between 92 and 95% when tested with either a standard solution of hydroxylamine hydrochloride or a standard solution containing hydroxylamine hydrochloride and the freshly dissolved pyridinium aldoxime. Fresh solutions of the three pyridinium aldoximes contained less than  $1 \cdot 10^{-5}$  M hydroxylamine. A yield less than 100% was expected for the derivatization reaction because a small amount of material assumed to be the *anti*-stereoisomer of vanillin oxime was also formed.

With the 30-min derivatization time, the presence of the derivatization reagents did not lead to the formation of significant quantities of base promoted pyridinium aldoxime degradation products. The chromatograms of the aging pyridinium oxime solutions were consistent with previously reported HPLC analysis at low pH (<4) [19,20]. If the derivatization reaction was extended past 1 h or subjected to heat, additional products generated from the decomposition of the pyridinium oximes at high pH (>4), particularly for the relatively base-sensitive I, were observed in the chromatogram.

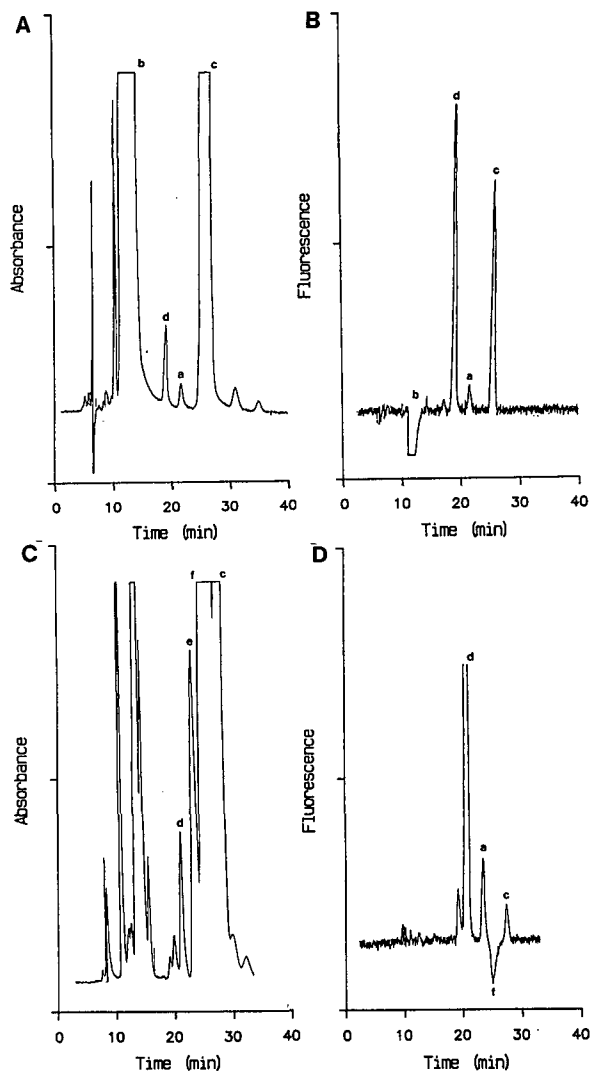


Fig. 1. (A) Chromatogram of a sample of a 2-PAM solution (pH 3.1) after 2 h at room temperature followed by derivatization with vanillin and analyzed with the UV detector (10  $\mu$ l injected), (B) the same sample as in (A) but analyzed with the fluorometric detector, (C) a sample of a solution of I (pH 2.7) after 48 h at 60°C followed by derivatization with vanillin and analyzed with the UV detector (10  $\mu$ l injected) and (D) the same sample as in (C) but analyzed with the fluorometric detector. Peaks: a = vanillin oxime; b = 2-PAM; c = vanillin; d = a by-product of vanillin presumed to be vanillin hydrate; e = a decomposition product of I; f = I. The mobile phases are described in the *Chromatography* section under Experimental.

*Chromatography*

Chromatograms A and B in Fig. 1 show the relative intensities of the components in the 0.5 M 2-

PAM (pH 3.1) solution when the concentration of hydroxylamine was near the detection limit of the assay. The vanillin oxime (peak a) represents hydroxylamine at the 0.01% level (a 1/10 000 mol ratio of hydroxylamine to 2-PAM, peak b). The large excess of vanillin (peak c), did not interfere with quantitation of vanillin oxime or 2-PAM with either UV or fluorescence detection.

Because the retention times for toxogonin and **I** were considerably greater than the retention time of 2-PAM and closer to that of vanillin oxime under many chromatographic conditions, there was a distinct advantage to using fluorescence detection for monitoring the vanillin oxime in the mixture of degrading bis(pyridinium)aldoximes, toxogonin and **I**. In Fig. 1C, the vanillin oxime signal was buried under a decomposition product of **I** (peak e), and a UV measurement was impossible even at high concentrations of vanillin oxime. With fluorescence detection, Fig. 1D, the vanillin oxime (peak a) is free from interference even when measured near the detection limit and in the presence of high concentrations of **I** (peak f).

Fluorescence detection also had the additional capability of observing fluorescent degradation products, such as the pyridones, which are formed in weakly acidic solutions of pyridinium oximes [3].

#### Quantitation

To minimize the effect of the large signal from the excess of vanillin on the vanillin oxime signal in both UV and fluorescence detection, the ratio of the two signals was optimized by the selection of detector wavelengths. The ratio of the vanillin oxime to vanillin signal was 3:1 with the UV detector set at 255 nm and the ratio was 250:1 with the fluorimetric detector set at 270 nm for excitation and 355 nm for emission. With these detector parameters, the limit of detection (a 2:1 signal-to-noise ratio) for vanillin oxime was 0.8 ng using the UV detector and 1.5 ng using the fluorimetric detector. Both detector responses were linear over the range of on-column quantities (20–2000 ng) monitored.

The precision of the assay was tested at several conditions with relative standard deviations ranging from 1 to 2% when the stable 2-PAM and toxogonin solutions at equilibrium were monitored to as high as 27% when the rapidly decomposing samples of **I** with low concentrations of hydroxylamine were

monitored. Insight into the accuracy of the method was gained by the observation that 92 to 95% of the hydroxylamine added to solutions of pyridinium aldoximes was monitored after derivatization. In addition, hydroxylamine levels measured by this HPLC method in decomposing solutions of pyridinium aldoximes, described below, were compared with hydroxylamine levels reported [5,13] using Csaky's colorimetric method for hydroxylamine [7].

#### Application: pyridinium aldoxime decompositions

Table I summarizes some selected data for the hydroxylamine level found in aged oxime samples. The data collected over a six-day period indicated that equilibrium for the hydrolysis process (eqn. 1) was attained quite slowly with 2-PAM and toxogonin, about six days at room temperature and pH 3.1, and about 4 days at room temperature and pH 2.0. Both the 0.5 M 2-PAM and 0.25 M toxogonin solutions showed similar concentrations of hydroxylamine at corresponding pH values after reaching equilibrium and the hydroxylamine levels were clearly pH dependent as expected [1,2]. At pH 1.1 and 60°C the hydroxylamine level was 2.63% for 2-PAM and 2.83% for toxogonin, at pH 2 the levels were 0.65% and 0.84% respectively, and at pH 3 the levels were 0.17% for both 2-PAM and toxogonin solutions.

The anomalous lack of pH dependence reported by Christenson [5] for a 0.28 M toxogonin solution analyzed by Csaky's method was not observed in this study. However, the hydroxylamine level (2.83%) at pH 1.1 with 0.25 M toxogonin was reasonably consistent with a value of 3.9% for a 0.28 M solution at pH 1.7 calculated from Christenson's data [5]. The hydroxylamine level of 0.17% obtained for the 2-PAM solution at pH 3 was slightly higher than a value of 0.11% calculated from Barkman's [13] data for a buffered pH 3 2-PAM methanesulfonate solution (0.6 M) stored for two years and analyzed by Csaky's method. Two six-year-old samples of buffered (pH 2.5 when opened) 1.8 M 2-PAM chloride from out-dated autoinjectors also contained 0.17% hydroxylamine and only small quantities of by-products were detected which indicated that further chemical change occurred very slowly once the hydrolysis equilibrium was attained.

A previous report of the degradation of **I** over the

pH range 0 to 3 indicated that both the degradation mechanism and hydroxylamine levels as measured by the Csaky method were similar for both toxogonin and **I** [14]. In this study, the assay of 0.5 M **I** at pH 2.7 led to unexpectedly low levels of hydroxylamine and a more complicated degradation pattern than at pH 1.1. At pH 1.1 and room temperature, **I** appeared to be relatively stable and the hydroxylamine level of 1.86% after 48 h was similar to the 2.46% level observed with toxogonin. At the higher pH (2.7) at room temperature only a trace of hydroxylamine was observed over the entire six day reaction period and a new major degradation product, the carboxylic acid derivative of **I** was identified [6]. The 60°C reaction at pH 2.7 also showed only trace quantities of hydroxylamine for the first 48 h and then an increase to 1.06% by 96 h. However, by 96 h approximately 50% of **I** had decomposed to a complex mix of by-products. The low levels of hydroxylamine in the reactions at pH 2.7 may be accounted for by the previous observations that hydroxylamine reacted with either formaldehyde formed from the cleavage of the aminal-acetal bridge which links the two pyridinium rings [4], or the amide group [6] found in **I**.

#### ACKNOWLEDGEMENTS

The author appreciates the generous support of the USAMRICD under the provisions of the Intergovernmental Personnel Act of 1970 and the cooperation and technical assistance of Dr. Ming L. Shih, Rick Smith and George Salem.

#### REFERENCES

- 1 E. G. Sander and W. P. Jencks, *J. Am. Chem. Soc.*, 90 (1968) 6154.
- 2 I. Christenson, *Acta Pharm. Suecica*, 9 (1972) 351.
- 3 D. Utley, *J. Chromatogr.*, 396 (1987) 237.
- 4 I. Christenson, *Acta Pharm. Suecica*, 5 (1968) 23.
- 5 I. Christenson, *Acta Pharm. Suecica*, 5 (1968) 249.
- 6 W. D. Korte and M. L. Shih, *Proceedings of the 1989 Medical Defense Review, Columbia, MD, August 15–17, 1989*, USAMRICD Contract Office, Aberdeen Proving Ground, MD, 1989 p. 655.
- 7 T. Z. Csaky, *Acta Chem. Scand.*, 2 (1948) 450.
- 8 T. Kalasa and W. Wardenky, *Talanta*, 21 (1974) 845.
- 9 D. J. Darke and W. E. W. Roediger, *J. Chromatogr.*, 181 (1980) 449.
- 10 M. T. von Breymann, M. A. de Angelis and L. I. Gordon, *Anal. Chem.*, 54 (1982) 1209.
- 11 P. Pietta, A. Calatroni and C. Zio, *Analyst (London)*, 107 (1982) 341.
- 12 F. Lombardi and T. Crolla, *J. Pharm. Sci.*, 77 (1988) 711.
- 13 R. Barkman, *Rev. Int. Serv. Sante Armees Terre Mer Air*, 36 (1963) 91.
- 14 I. Christenson, *Acta Pharm. Suecica*, 9 (1972) 323.
- 15 J. G. Grasselli and W. M. Ritchey (Editors), *Atlas of Spectral Data and Physical Constants for Organic Compounds*, Vol. II, CRC Press, Cleveland, OH, 2nd ed., 1975, p. 226.
- 16 A. I. Vogel, *Textbook of Practical Organic Chemistry*, Longman, New York, 4th ed., 1978, p. 1113.
- 17 A. Rappoport (Compiler), *Handbook of Tables for Organic Compound Identification*, CRC Press, Cleveland, OH, 3rd ed., 1967, p. 156.
- 18 R. C. Weast (Editor-in-Chief), *CRC Handbook of Chemistry and Physics*, CRC Press, Boca Raton, FL, 65th ed., 1984, p. B-100.
- 19 D. Utley, *J. Chromatogr.*, 265 (1983) 311.
- 20 N. D. Brown, L. Kayzah, B. P. Doctor and I. Hagedorn, *J. Chromatogr.*, 351 (1986) 599.

# Separation of benz[*f*]isoindole derivatives of amino acid and amino acid amide enantiomers on a $\beta$ -cyclodextrin-bonded phase

A. L. L. Duchateau, G. M. P. Heemels, L. W. Maesen and N. K. de Vries

DSM Research, Department FA, P.O. Box 18, 6160 MD Geleen (Netherlands)

(Received February 11th, 1992)

## ABSTRACT

A liquid chromatographic method for the determination of amino acid enantiomers and related amino acid amide enantiomers is presented. Fluorescent derivatives were formed by reaction with naphthalene-2,3-dicarboxaldehyde–cyanide reagent. The resulting benz[*f*]isoindole amino acid enantiomers and amino acid amide enantiomers were separated on a  $\beta$ -cyclodextrin-bonded phase. The separations were performed with ammonium nitrate buffer containing methanol as mobile phase. The influence of methanol, pH and buffer concentration in the mobile phase on retention, enantioselectivity and resolution were examined and are discussed. Remarkable differences in retention behaviour were found for the amino acids and amino acid amides studied on changing mobile phase parameters such as buffer concentrations and pH. With this method, the separation of an amino acid, together with the corresponding amino acid amide, into their enantiomers can be achieved in a single isocratic run. The method is suitable for monitoring the enantiomeric purity of an amino acid obtained by enantioselective hydrolysis of the corresponding acid amide using an aminopeptidase.

## INTRODUCTION

Optically pure  $\alpha$ -amino acids are important intermediates for the production of pharmaceuticals, food chemicals and agrochemicals. One of the routes to optically pure  $\alpha$ -amino acids is through organic synthesis of racemic  $\alpha$ -amino acid amides followed by an enantioselective hydrolysis using a peptidase with relaxed substrate specificity to achieve resolution on a large scale. In conjunction with this synthesis, analytical methods are required for the control of the enantiomeric purity of both  $\alpha$ -amino acids and  $\alpha$ -amino acid amides.

Several high-performance liquid chromatographic (HPLC) methods for the enantiomeric resolution of  $\alpha$ -amino acids have been described. These methods can be divided into three categories: (a) enantioseparation on chiral stationary phases (CSPs) di-

rectly or by using precolumn derivatization; (b) resolution of the enantiomers by means of a chiral mobile phase, *e.g.*, ligand-exchange methods; and (c) precolumn derivatization with a chiral reagent, followed by chromatographic analysis of the resulting diastereomers.

The aim of this work was to evaluate the potential of a  $\beta$ -cyclodextrin ( $\beta$ -CD)-bonded stationary phase for the enantioseparation of  $\alpha$ -amino acids and  $\alpha$ -amino acid amides obtained by enantioselective synthesis.

In earlier studies [1], it was shown that  $\beta$ -CD-bonded phases can form inclusion complexes with derivatized and underivatized  $\alpha$ -amino acids. However, derivatized  $\alpha$ -amino acids containing two or more aromatic rings are separated the most effectively. The enantioselectivity of the following types of  $\alpha$ -amino acid derivatives has been studied on  $\beta$ -CD phases: dansyl- $\alpha$ -amino acids [2–4],  $\alpha$ -amino acid  $\beta$ -naphthylamides [2–4],  $\alpha$ -amino acid  $\beta$ -naphthyl esters [2–4], isoindole  $\alpha$ -amino acids [5], N-(3,5-

Correspondence to: Dr. A. L. L. Duchateau, DSM Research, Department FA, P.O. Box 18, 6160 MD Geleen, Netherlands.

dinitrobenzoyl)- $\alpha$ -amino acids [6] and N-(2,4-dinitrophenyl)- $\alpha$ -amino acids [7]. Except for the N-(3,5-dinitrobenzoyl) and N-(2,4-dinitrophenyl) derivatives, all of the above-mentioned derivatives contained two rings.

The reaction of  $\alpha$ -amino acids with naphthalene-2,3-dicarboxyaldehyde (NDA) and cyanide results in the formation of N-substituted 1-cyanobenz[*f*]isoindole (CBI) derivatives [8], which can subsequently be analysed by reversed-phase chromatography.

In this paper, we report on the use of a  $\beta$ -CD phase for the enantioseparation of CBI derivatives of several  $\alpha$ -amino acids and  $\alpha$ -amino acid amides. The effects of pH, methanol and buffer concentration in the mobile phase and the structural features of the solutes on the retention, enantioselectivity and resolution were examined.

## EXPERIMENTAL

### Materials

Butyrine (But), valine (Val), norvaline (NVal), *p*-hydroxyphenylglycine (HPG), phenylglycine (PG) and phenylalanine (Phe) were obtained from Sigma (St. Louis, MO, USA). The corresponding acid amides were synthesized in our laboratory [9]. For each compound, both the racemic form and at least one optically pure enantiomer were available. Naphthalene-2,3-dicarboxyaldehyde was supplied by Polysciences (Warrington, PA, USA). Water was purified with a Milli-Q system (Millipore). HPLC-grade methanol was obtained from Merck and used as supplied. All other chemicals were of analytical-reagent grade.

### Instrumentation

HPLC was performed using a Gilson (Villiers-le-Bel, France) Model 302 pump and a Gilson Model 231-401 autosampling injector for derivatization and injection. The injection loop had a 20- $\mu$ l capacity. The  $\beta$ -cyclodextrin-bonded column (Cyclobond I, 250  $\times$  4.6 mm I.D.) was obtained from Advanced Separation Technologies (Whippany, NJ, USA). The column was thermostated at 22°C. The derivatives were monitored with a Hitachi (Tokyo, Japan) Model F-1050 fluorescence detector using an excitation wavelength of 420 nm and an emission wavelength of 520 nm.

### Mobile phases and derivatization procedure

Ammonium nitrate buffers were prepared by dissolving the required amount of ammonium nitrate in water. Mobile phases were prepared by mixing the buffer solutions with the required amount of methanol.

For derivatization, NDA reagent was prepared by dissolving 0.2 mg of NDA per ml of methanol. For the cyanide reagent, 0.2 mg of potassium cyanide was dissolved per ml of 0.4 M potassium borate buffer (pH 9.4).  $\alpha$ -Amino acids and  $\alpha$ -amino acid amides were dissolved in water. Derivatization was performed automatically with a Gilson Model 231-401 system. The reaction mixture consisted of 200  $\mu$ l of NDA reagent, 200  $\mu$ l of cyanide reagent and 20  $\mu$ l of the analyte solution. The reaction mixture was allowed to stand for at least 2 min at room temperature before an aliquot was injected into the HPLC system.

## RESULTS AND DISCUSSION

The enantioselectivity of the CBI derivatives of a series of aliphatic and aromatic  $\alpha$ -amino acids and  $\alpha$ -amino acid amides on a  $\beta$ -CD-bonded phase column was examined. In Table I, the capacity factors

TABLE I

SEPARATION DATA FOR THE ENANTIOMERS OF CBI-AMINO ACIDS AND AMINO ACID AMIDES

Chromatographic conditions: flow-rate, 0.8 ml/min; mobile phase, 0.04 M ammonium nitrate solution (pH 7.0) containing 45% (v/v) methanol. For other conditions, see Experimental.

$\alpha$ -amino acid or amide	$k'_{\alpha}$	$\alpha$	$R_s$
But	13.35	1.05	0.94
But-NH <sub>2</sub>	3.71	1.07	0.96
Val	15.76	1.05	0.85
Val-NH <sub>2</sub>	4.46	1.10	1.31
NVal	14.06	1.03	<0.50
NVal-NH <sub>2</sub>	3.88	1.04	<0.50
HPG	17.72	1.07	1.26
HPG-NH <sub>2</sub>	4.75	1.05	<0.50
PG	30.97	1.06	1.13
PG-NH <sub>2</sub>	6.02	1.04	0.54
Phe	20.03	1.09	1.59
Phe-NH <sub>2</sub>	4.73	1.09	1.18

<sup>a</sup> Capacity factor of the first-eluted enantiomer.

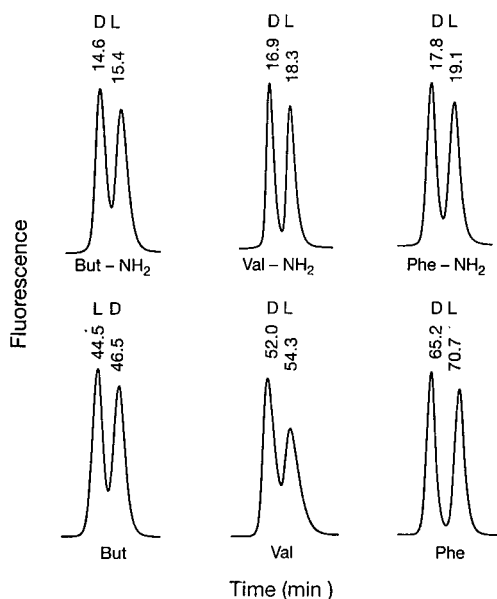


Fig. 1. Enantiomeric separation of the CBI derivatives of But, But-NH<sub>2</sub>, Val, Val-NH<sub>2</sub>, Phe and Phe-NH<sub>2</sub>. For conditions, see Table I.

( $k'$ ), selectivities ( $\alpha$ ) and resolutions ( $R_s$ ) obtained for these compounds are shown. Some typical chromatograms are shown in Fig. 1.

From Table I, it can be seen that enantioselectivity is obtained for all compounds listed. For the aliphatic  $\alpha$ -amino acid amides (But-NH<sub>2</sub>, Val-NH<sub>2</sub>, NVal-NH<sub>2</sub>), higher  $\alpha$  values are obtained compared with the corresponding  $\alpha$ -amino acids. On the other hand, the  $\alpha$  values for the aromatic  $\alpha$ -amino acid amides (HPG-NH<sub>2</sub>, PG-NH<sub>2</sub>, Phe-NH<sub>2</sub>) are lower than or equal to those of the  $\alpha$ -amino acid analogues. The elution order of the enantiomers was as follows: D before L for But-NH<sub>2</sub>, Val, Val-NH<sub>2</sub>, NVal, NVal-NH<sub>2</sub>, Phe and Phe-NH<sub>2</sub>; L before D for But, HPG, HPG-NH<sub>2</sub>, PG and PG-NH<sub>2</sub>. For all the  $\alpha$ -amino acids studied, higher  $k'$  values were obtained in comparison with the corresponding  $\alpha$ -amino acid amides.

An explanation for this phenomenon may be found in the presence of the amide functionality in the  $\alpha$ -amino acid amides and the carboxylic group present in the  $\alpha$ -amino acids. For the latter type of compounds, it may be expected that they exist in the form of anions at pH 7.0. As both the amide group and the carboxylate anion can form hydrogen

bonds with the hydroxyl groups of the CD, the higher  $k'$  values for the  $\alpha$ -amino acids may result from stronger hydrogen bonding of the carboxylate function compared with the amide function. This, however, does not result in a better enantioselectivity with regard to the  $\alpha$ -amino acid amides.

The benz[*f*]isoindole group is considered to form an inclusion complex with the CD cavity and is therefore assumed to be a major factor in determining the retention and enantioselectivity of the analytes studied. The R substituent in the side-chain of the  $\alpha$ -amino acid is also considered to play a role in the retention [10].

From Table I, it can be seen that the  $k'$  values of the CBI derivatives of the  $\alpha$ -amino acids and  $\alpha$ -amino acid amides increased, in general, with increasing hydrophobicity of the R substituent (ethyl < propyl < isopropyl < benzyl). This can be explained in terms of a decrease in mobile phase solubility of the CBI derivatives with increasing hydrophobicity of the R substituent, and hence increasing attraction to the CD stationary phase. However, the retention observed for PG and PG-NH<sub>2</sub> cannot be explained by the above-mentioned mechanism. The high  $k'$  values for PG and PG-NH<sub>2</sub> can be explained if both the benz[*f*]isoindole group and the phenyl substituent of PG or PG-NH<sub>2</sub> are considered to be included in the CD cavity. If the R group and the derivative group were both included to the same extent, no chiral recognition would occur [10]. From Table I, it can be seen that enantioselectivity is obtained for PG and PG-NH<sub>2</sub>, but less than for Phe and Phe-NH<sub>2</sub>. A partial inclusion of the phenyl substituent of PG and PG-NH<sub>2</sub> would therefore provide a reasonable explanation for the retention behaviour and enantioselectivity observed.

#### Effect of methanol

The influence of the methanol content of the mobile phase on the retention and resolution of CBI derivatives of  $\alpha$ -amino acid and  $\alpha$ -amino acid amide enantiomers has been studied. In all instances, a decrease in the capacity factor of the enantiomers was observed as the percentage of methanol increased.

In addition to the  $k'$  values, both the separation factors and resolutions also decreased. Typical plots of  $k'$  and  $R_s$  versus methanol concentration for some CBI derivatives of  $\alpha$ -amino acids and  $\alpha$ -amino acid amides are shown in Figs. 2 and 3. The effect of

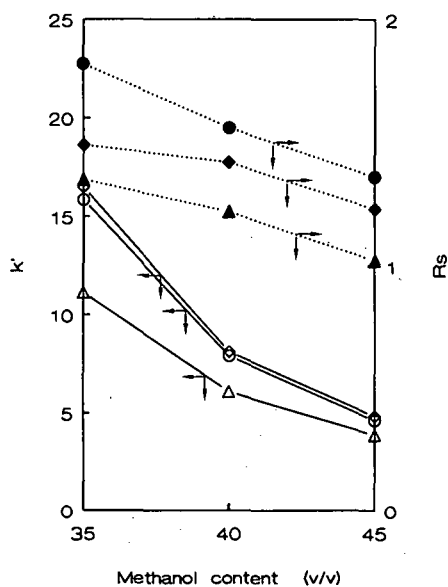


Fig. 2. Influence of methanol content in the mobile phase on the capacity factor (solid lines) and resolution (dotted lines) of the CBI derivatives of ( $\Delta$ ,  $\blacktriangle$ )But-NH<sub>2</sub>, ( $\circ$ ,  $\bullet$ )Val-NH<sub>2</sub> and ( $\diamond$ ,  $\blacklozenge$ )Phe-NH<sub>2</sub>. Mobile phase, 40 mM ammonium nitrate buffer (pH 5.4); flow-rate, 0.8 ml/min.  $k'$  is the capacity factor of the first-eluted enantiomer.

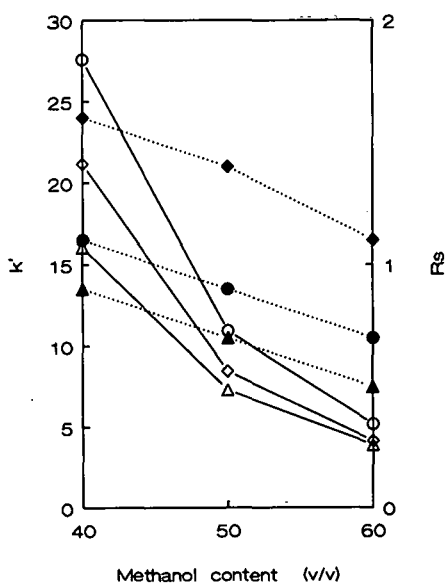


Fig. 3. Influence of methanol content in the mobile phase on the capacity factor (solid lines) and resolution (dotted lines) of the CBI derivatives of ( $\Delta$ ,  $\blacktriangle$ )Val-NH<sub>2</sub>, ( $\circ$ ,  $\bullet$ )But-NH<sub>2</sub> and ( $\diamond$ ,  $\blacklozenge$ )Phe-NH<sub>2</sub>. Mobile phase, 80 mM ammonium nitrate buffer (pH 5.3); flow-rate, 1.0 ml/min.  $k'$  is the capacity factor of the first-eluted enantiomer.

methanol content on the retention of CBI- $\alpha$ -amino acids shows the same tendencies as those observed with dansyl- $\alpha$ -amino acids [3,10] and DNP- $\alpha$ -amino acids [7]. With respect to the effect on the resolution, our data agree well with those for dansyl- $\alpha$ -amino acids [3] and DNP- $\alpha$ -amino acids [7]. However, in another study on dansyl- $\alpha$ -amino acids [10] an increase in resolution was observed when the methanol content was increased.

#### Effect of pH

The effect of pH on the retention and resolution was investigated by varying the pH of the mobile phase from 4.0 to 7.0. For the CBI derivatives of Val, But and Phe and the corresponding acid amides, the results are shown in Figs. 4 and 5. In the case of the CBI- $\alpha$ -amino acids (Fig. 5), a decreased retention with increase in pH is observed. The same observations were made for DNP- $\alpha$ -amino acids [7] and dansyl- $\alpha$ -amino acids [10].

Because of the electron-withdrawing properties of the benz[*f*]isoindole group, the  $pK_a$  values of the CBI- $\alpha$ -amino acids studied are expected to be lower

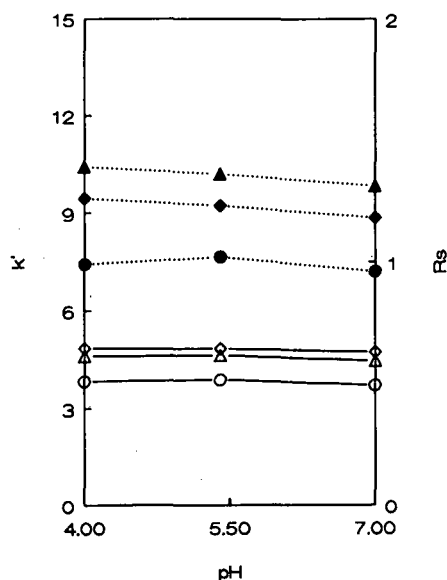


Fig. 4. Influence of pH of the mobile phase on the capacity factor (solid lines) and resolution (dotted lines) of the CBI derivatives of ( $\Delta$ ,  $\blacktriangle$ )Val-NH<sub>2</sub>, ( $\circ$ ,  $\bullet$ )But-NH<sub>2</sub> and ( $\diamond$ ,  $\blacklozenge$ )Phe-NH<sub>2</sub>. Mobile phase, 40 mM ammonium nitrate buffer containing 45% (v/v) methanol; flow-rate, 0.8 ml/min. pH measured in the aqueous part of the mobile phase.  $k'$  is the capacity factor of the first-eluted enantiomer.

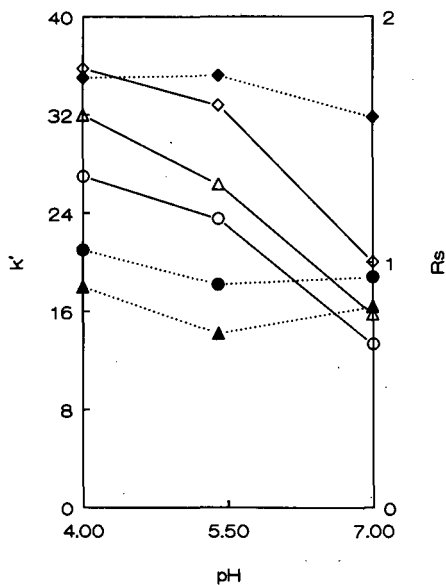


Fig. 5. Influence of pH of the mobile phase on the capacity factor (solid lines) and resolution (dotted lines) of the CBI derivatives of ( $\Delta$ ,  $\blacktriangle$ )Val, ( $\circ$ ,  $\bullet$ )But and ( $\diamond$ ,  $\blacklozenge$ )Phe. Conditions and definitions of pH and  $k'$  as in Fig. 4.

than those of the native  $\alpha$ -amino acids. Therefore, no significant change in the carboxylic acid/carboxylate anion ratio is expected in the pH range studied; the CBI- $\alpha$ -amino acids will be mainly present as anions. Hence, the binding strength of the CBI- $\alpha$ -amino acids with the CD stationary phase should not be affected by changes in pH. For DNP- $\alpha$ -amino acids, the decrease in  $k'$  has been explained by assuming competition between the DNP- $\alpha$ -amino acid anions and the  $\text{OH}^-$  ions for binding with the hydroxyl groups of the CD [7]. This mechanism may also explain the data obtained for CBI- $\alpha$ -amino acids. The increase in  $\text{OH}^-$  ions that occurs when the pH is increased will weaken the binding strength of the carboxylate anions and hence that of the CBI- $\alpha$ -amino acid solutes. Consequently, a decrease in  $k'$  with increase in pH is observed. On changing the pH, no significant change in the  $R_s$  values of the CBI- $\alpha$ -amino acids was observed.

In contrast to the CBI- $\alpha$ -amino acids, the  $k'$  values of the CBI- $\alpha$ -amino acid amides remained constant in the pH range 4.0–7.0. This may be explained by assuming that in the presence of  $\text{OH}^-$  and buffer anions, the hydrogen-bonding ability of the neutral acid amide group is too small to bind to

the hydroxyl groups of the CD. Consequently, the overall interaction of the CBI- $\alpha$ -amino acid amides with the CD cavity will not be affected by a change in pH.

#### Effect of buffer concentration

The ammonium nitrate concentration in the eluent was varied in order to study its influence on the retention and resolution of both CBI- $\alpha$ -amino acid and CBI- $\alpha$ -amino acid amides. The results for Val, But, HPG and the corresponding  $\alpha$ -amino acid amides are presented in Figs. 6 and 7. For the CBI- $\alpha$ -amino acid amides (Fig. 6), no significant changes in either the  $k'$  or the  $R_s$  values were observed with varying buffer concentration. For the CBI- $\alpha$ -amino acids, on the other hand (Fig. 7), the  $k'$  values decreased with increasing buffer concentration. With respect to the resolution, there was a slight increase for HPG, whereas a slight decrease occurred for But and Val.

As cyclodextrins have the ability to bind inorganic anions such as nitrate [11], the buffer anions may compete with the CBI- $\alpha$ -amino acid anions for

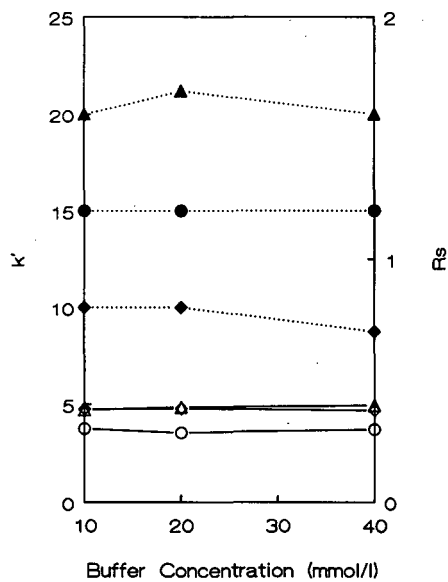


Fig. 6. Influence of buffer concentration of the mobile phase on the capacity factor (solid lines) and resolution (dotted lines) of the CBI derivatives of ( $\Delta$ ,  $\blacktriangle$ )Val- $\text{NH}_2$ , ( $\circ$ ,  $\bullet$ )But- $\text{NH}_2$  and ( $\diamond$ ,  $\blacklozenge$ )HPG- $\text{NH}_2$ . Mobile phase, ammonium nitrate buffer (pH 5.6) containing 45% (v/v) methanol; flow-rate, 1.0 ml/min.  $k'$  is the capacity factor of the first-eluted enantiomer.

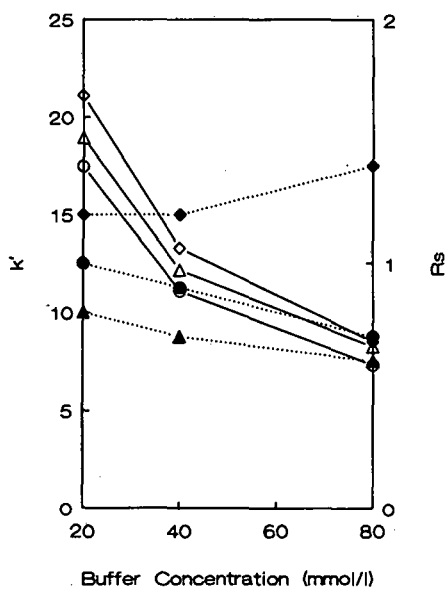


Fig. 7. Influence of buffer concentration of the mobile phase on the capacity factor (solid lines) and resolution (dotted lines) of the CBI derivatives of ( $\Delta$ ,  $\blacktriangle$ )Val, ( $\circ$ ,  $\bullet$ )But and ( $\diamond$ ,  $\blacklozenge$ )HPG. Mobile phase, ammonium nitrate buffer (pH 5.4) containing 50% (v/v) methanol; flow-rate, 1.0 ml/min.  $k'$  is the capacity factor of the first-eluted enantiomer.

binding with the hydroxyl groups of the CD. The decrease in the retention can therefore be explained by increased exclusion of the negatively charged CBI- $\alpha$ -amino acid from the CD cavity at higher ionic strength of the eluent.

For the CBI- $\alpha$ -amino acid amides it is expected that even at the lowest buffer concentration studied (10 mM), the nitrate anions will interfere with the hydrogen bonding of the neutral acid amide functionality with the hydroxyls of the CD. This situation evidently does not change at higher nitrate concentrations. Analogous to the effect of  $\text{OH}^-$ , the overall interaction of the CBI- $\alpha$ -amino acid amides with the CD cavity will therefore not be affected by variation of the buffer concentration.

## CONCLUSIONS

The results indicate that on-line derivatization of  $\alpha$ -amino acids and the corresponding  $\alpha$ -amino acid amides with NDA-cyanide reagent, followed by separation on a  $\beta$ -CD column, is a useful assay for the control of the enantiomeric purity of both  $\alpha$ -amino acids and  $\alpha$ -amino acid amides.

Among the mobile phase parameters studied, the methanol content in the mobile phase is the most effective parameter for adjusting the enantiomeric resolution of both  $\alpha$ -amino acids and  $\alpha$ -amino acid amides. By adapting the elution conditions, the method described may also be useful for the enantioseparation of other  $\alpha$ -amino acids and related  $\alpha$ -amino acid amides.

## REFERENCES

- 1 D. W. Armstrong, X. Yang, S. M. Han and R. A. Menges, *Anal. Chem.*, 59 (1987) 2594.
- 2 D. W. Armstrong, A. Alak, K. Bui, W. DeMond, T. Ward, T. E. Riehl and W. L. Hinze, *J. Includ. Phenom.*, 2 (1984) 533.
- 3 W. L. Hinze, T. E. Riehl, D. W. Armstrong, W. DeMond, A. Alak and T. Ward, *Anal. Chem.*, 57 (1985) 237.
- 4 D. W. Armstrong and W. DeMond, *J. Chromatogr. Sci.*, 22 (1984) 411.
- 5 R. Kupferschmidt and R. Schmid, presented at the 12th International Symposium on Column Liquid Chromatography, Washington, D.C., 1988.
- 6 D. W. Armstrong, Y. I. Han and S. M. Han, *Anal. Chim. Acta*, 208 (1988) 275.
- 7 S. Li and W. C. Purdy, *J. Chromatogr.*, 543 (1991) 105.
- 8 P. de Montigny, J. F. Stobaugh, R. S. Givens, R. G. Carlson, K. Srinivasachar, L. A. Sternson and T. Higuchi, *Anal. Chem.*, 59 (1987) 1096.
- 9 E. M. Meijer, W. H. J. Boesten, H. E. Schoemaker and J. A. M. van Balken, in J. Tramper, H. C. van der Plas and P. Linko (Editors), *Biocatalysis in Organic Synthesis*, Elsevier, Amsterdam, 1985, p. 135.
- 10 K. Fujimura, S. Suzuki, K. Hayashi and S. Masuda, *Anal. Chem.*, 62 (1990) 2198.
- 11 E. A. Lewis and L. D. Hansen, *J. Chem. Soc., Perkin Trans. 2*, (1973) 2081.

# High-performance liquid chromatography–thermospray mass spectrometry of gibberellins

Eugene B. Hansen, Jr., Joaquin Abian<sup>☆</sup> and Timothy A. Getek<sup>☆☆</sup>

*Department of Health and Human Services, Food and Drug Administration, National Center for Toxicological Research, Jefferson, AR 72079 (USA)*

John S. Choinski, Jr.

*Department of Biology, University of Central Arkansas, Conway, AR 72032 (USA)*

Walter A. Korfmacher<sup>☆☆☆</sup>

*Department of Health and Human Services, Food and Drug Administration, National Center for Toxicological Research, Jefferson, AR 72079 (USA)*

(Received February 7th, 1992)

---

## ABSTRACT

Seven tetracyclic monocarboxylic acid gibberellins (GA<sub>1</sub>, GA<sub>3</sub>, GA<sub>4</sub>, GA<sub>5</sub>, GA<sub>7</sub>, GA<sub>9</sub> and GA<sub>30</sub>) and the methyl ester derivatives of GA<sub>1</sub>, GA<sub>3</sub>, GA<sub>4</sub>, GA<sub>7</sub> and GA<sub>9</sub> were analyzed using combined high-performance liquid chromatography–thermospray mass spectrometry or direct injection thermospray mass spectrometry. The seven free acid GAs were resolved using a 25-min water–acetonitrile (0.1 M ammonium acetate) gradient mobile phase and a 5 μm, 150 mm × 4.6 mm, ODS column. Positive-ion thermospray mass spectra of these compounds typically showed intense [M + NH<sub>4</sub>]<sup>+</sup> ions and few, if any, fragment ions. In the negative-ion mode (filament on) the free acid GAs showed [M – H]<sup>–</sup> or [M + HCO<sub>2</sub>]<sup>–</sup> ions as the base peaks. Negative-ion spectra of the methyl ester GAs showed the [M + HCO<sub>2</sub>]<sup>–</sup> ions, however, the base peaks were [M]<sup>–</sup> or [M + HCO<sub>2</sub>H]<sup>–</sup> ions attributed to electron capture processes. Thermospray tandem mass spectra were obtained for GA<sub>1</sub>, GA<sub>3</sub> and GA<sub>30</sub> from the collisionally activated dissociation (CAD) of their [M + NH<sub>4</sub>]<sup>+</sup> ions. The CAD mass spectra show differences which allow the differentiation of the isomers GA<sub>3</sub> and GA<sub>30</sub> without the chromatographic separation. The daughter ions resulting from fragmentation processes corresponded to varying losses of CO, CO<sub>2</sub>, ammonia and water.

---

*Correspondence to:* E. B. Hansen, Jr., Department of Health and Human Services, Division of Chemistry (HFT-230), Food and Drug Administration, National Center for Toxicological Research, Jefferson, AR 72079, USA.

<sup>☆</sup> Present address: Department of Neurochemistry, Centro de Investigacion y Desarrollo, CSIC, Jordi Girona Salgado 18-26, 08034 Barcelona, Spain.

<sup>☆☆</sup> Present address: Department of Chemical Measurement and Methods, Battelle, 505 King Avenue, Columbus, OH 43201-2693, USA.

<sup>☆☆☆</sup> Present address: Department of Drug Metabolism, Schering-Plough Research, 60 Orange Street, Bloomfield, NJ 07003, USA.

## INTRODUCTION

Gibberellins (GAs) are a group of naturally occurring plant hormones responsible for a variety of biological activities, such as growth promotion, and are generally thought to be ubiquitously present in plants [1]. Numerous GAs have been analyzed, typically in low concentrations, from biological sources including spruce [2], begonia leaves [3], apricot seeds [4], peas [5], fungi [6] and soil [7]. The analysis of specific GAs in biological samples routinely involves the use of high-performance liquid chroma-

tography (HPLC), primarily as an isolation and purification step, prior to analysis by gas chromatography GC—mass spectrometry (MS). Methods for GA separations utilizing normal- and reversed-phase HPLC have been reported [8–11]. Although GC–MS is a sensitive method for the determination of GAs, the procedure requires two derivatization steps typically via methylation and silylation reactions. On-column permethylation of GAs has been reported as one alternative to the previous procedures [12]; however, the MS analysis is still of a structurally altered GA. Ideally, a method for GA analysis involving no structural alterations is preferred.

The development of combined HPLC and thermospray (TSP) MS technology has allowed new opportunities for the mass spectral analysis of compounds which cannot be analyzed by GC–MS without prior derivatization [13]. Limited data concerning the HPLC–MS analysis of GAs have been reported in the literature [14–16]. This report describes the analysis of a set of seven free acid GAs and five methyl ester GA derivatives by HPLC–TSP–MS, HPLC–TSP–MS–MS, or direct injection TSP–MS.

## EXPERIMENTAL

### Chemicals

Gibberellic acid (GA<sub>3</sub>) and the methyl esters of GA<sub>1</sub>, GA<sub>3</sub>, GA<sub>4</sub>, GA<sub>7</sub> and GA<sub>9</sub> were obtained from Sigma (St. Louis, MO, USA). The free acid gibberellins GA<sub>1</sub>, GA<sub>4</sub>, GA<sub>5</sub>, GA<sub>7</sub>, GA<sub>9</sub> and GA<sub>30</sub> were the generous gift of Dr. Noboru Murofushi, Department of Agricultural Chemistry, University of Tokyo, Tokyo, Japan. The compounds were dissolved in methanol and an aliquot diluted with 0.1 M ammonium acetate. The organic solvents used were of HPLC grade and all other chemicals were of the highest purity available. Deionized water (18 MΩ/cm) was obtained from a Milli-Q water purification system (Millipore, Bedford, MA, USA).

### High-performance liquid chromatography

Two HPLC systems were utilized during this study.

System 1 employed a 250 mm × 4.6 mm I.D., 5 μm ODS column (Beckman Instruments/Altex Scientific Operations, San Ramon, CA, USA). The

mobile phase was aqueous 0.1 M ammonium acetate–acetonitrile (85:15) maintained at a flow-rate of 1.25 ml/min by an Isco LC-5000 syringe pump (Isco, Lincoln, NE, USA). Typically, 50–100-μl volumes were injected on-column utilizing a Model 7125 injector (Rheodyne, Cotati, CA, USA).

System 2 consisted of a SP8700XR programmer and pumping system (Spectra-Physics, Santa Clara, CA, USA) and a 5 μm (150 mm × 4.6 mm I.D.) Spherisorb ODS-2 column (Phase Separations, Norwalk, CT, USA). Gradient eluents were ratios of 0.1 M ammonium acetate (adjusted to pH 4 with formic acid) and either acetonitrile or methanol as the organic modifier. The flow-rate was maintained at 1.0 ml/min and sample injections were made using a Rheodyne Model 7125 injector.

### Direct injection thermospray mass spectrometry

The liquid carrier for direct injection TSP–MS analysis was 0.1 M aqueous ammonium acetate–methanol (90:10, v/v) and was maintained at a flow-rate of 1.25 ml/min using the Isco LC-5000 syringe pump. Typically, 100-μl volumes were injected utilizing a Rheodyne Model 7125 injector.

### Thermospray mass spectrometry

A Finnigan MAT TSQ 70 triple stage quadrupole mass spectrometer equipped with a Finnigan MAT thermospray interface and source (San Jose, CA, USA) was used. The vaporizer and block temperatures were optimized to maximize the ion intensity of the  $[M + NH_4]^+$  ion. Typically, the vaporizer was adjusted to 105°C and the ion source block was set at 220°C. Negative-ion spectra were obtained using the filament-on mode. When operated in the tandem MS mode the collision gas was argon set at approximately 0.5 mTorr and the collision energy was set at 25 eV.

## RESULTS AND DISCUSSION

Combined HPLC–TSP–MS was used to analyze the seven monocarboxylic acid gibberellins (GAs) shown in Fig. 1. The chromatographic characteristics and the positive-ion TSP–MS results are shown in Table I. The retention order observed using these chromatographic systems correlates with that reported elsewhere [11] and is consistent with the chemical structures of the compounds.

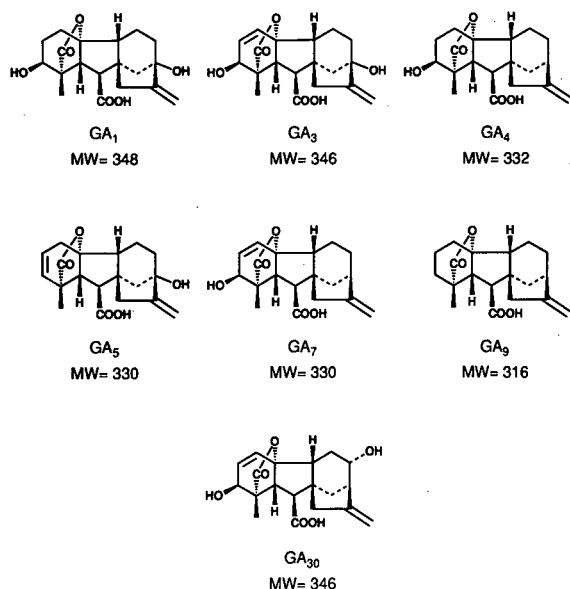


Fig. 1. Chemical structures of the gibberellins analyzed during this study. MW = Molecular weight.

Fig. 2 shows an HPLC–thermospray mass chromatogram of the seven free acid GAs analyzed. The chromatographic conditions used are given in the figure caption. The amount of each GA contained

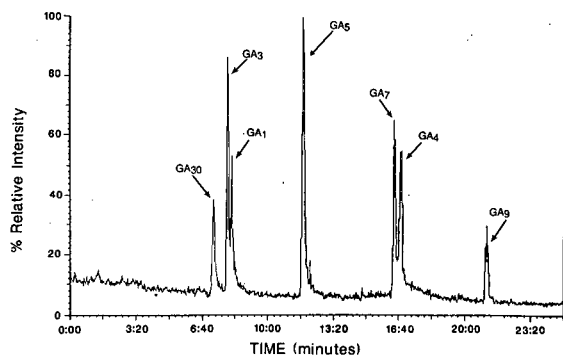


Fig. 2. Gradient HPLC–thermospray mass chromatogram of seven free acid gibberellins. HPLC system 2, mobile phase: gradient from acetonitrile–0.1 M ammonium acetate (5:95) to acetonitrile–0.1 M ammonium acetate (10:90) in 0.5 min, then to acetonitrile–0.1 M ammonium acetate (50:50) in 17 min, flow-rate: 1.0 ml/min, thermospray source: 250°C, thermospray interface temperature programming from 88°C to 85°C in 15 min. Time in min:s.

in the injection was in the range of 0.5–1.0 µg. Although gradient programming frequently results in varying thermospray conditions and probe temperature programming is needed to preserve optimal

TABLE I

SUMMARY OF THE RESULTS FROM THE HPLC–TSP–MS ANALYSIS OF GIBBERELLINS

Compound	MW	Retention time (min) <sup>a</sup>		Major ions observed	
		System 1	System 2	[M + NH <sub>4</sub> ] <sup>+</sup> (%) <sup>b</sup>	Others (%) <sup>b</sup>
GA <sub>1</sub>	348	1.3	8.2	366(100)	
GA <sub>3</sub>	346	1.3	7.9	364(100)	302(6)
GA <sub>4</sub>	332	7.0	16.8	350(100)	
GA <sub>5</sub>	330	1.8	11.8	348(100)	
GA <sub>7</sub>	330	6.3	16.4	348(100)	286(41)
GA <sub>9</sub>	316	16.0	21.1	334(100)	317(5)
GA <sub>30</sub>	346	1.3	7.2	364(100)	302(26)
GA <sub>1</sub> -methyl	362	d.i. <sup>c</sup>	d.i. <sup>c</sup>	380(100)	
GA <sub>3</sub> -methyl	360	d.i. <sup>c</sup>	d.i. <sup>c</sup>	378(100)	
GA <sub>4</sub> -methyl	346	d.i. <sup>c</sup>	d.i. <sup>c</sup>	364(100)	
GA <sub>7</sub> -methyl	344	d.i. <sup>c</sup>	d.i. <sup>c</sup>	362(100)	
GA <sub>9</sub> -methyl	330	d.i. <sup>c</sup>	d.i. <sup>c</sup>	348(100)	331(70), 299(10)

<sup>a</sup> HPLC retention times: system 1 is described in the Experimental section, system 2 is the gradient HPLC system described in the legend to Fig. 2.

<sup>b</sup> Spectral data shown were obtained using HPLC system 1. The relative intensity of the ion is listed in the parentheses after the *m/z* of the ion.

<sup>c</sup> The TSP–MS analysis was performed via direct injection of the sample.

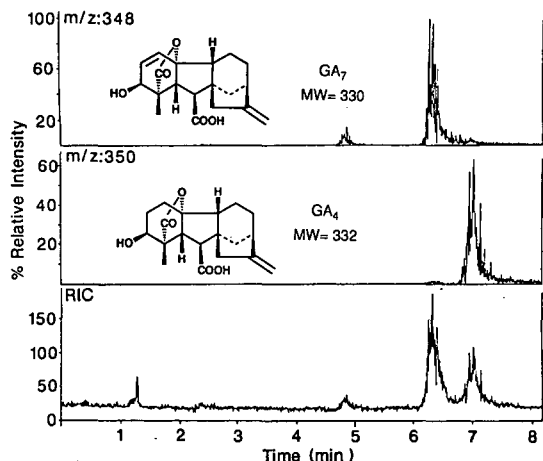


Fig. 3. Isocratic HPLC-thermospray mass chromatogram of  $GA_4$  and  $GA_7$  in admixture obtained using HPLC system 1.

response, acceptable separation of these compounds within a reasonable analysis time (22 min) required using a gradient HPLC system. Baseline separation between  $GA_4$  and  $GA_7$  was observed using HPLC system 1 (Fig. 3), however, no resolution between the more polar  $GA_3$ ,  $GA_1$  and  $GA_{30}$  was achieved (Table I).

As shown in Fig. 4 and Table I, the positive-ion thermospray mass spectra of the free acid GAs

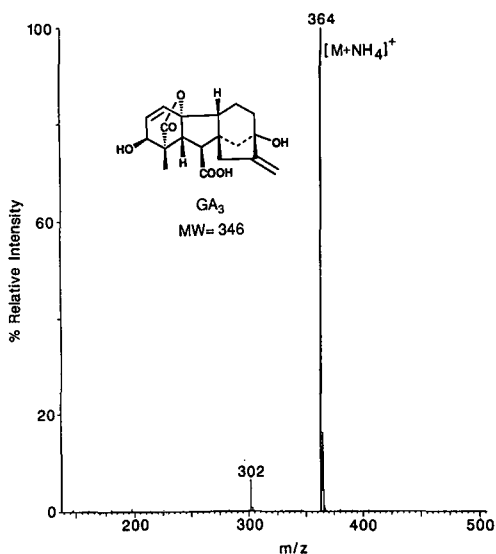


Fig. 4. HPLC-thermospray mass spectrum of  $GA_3$  obtained using HPLC system 1.

showed an intense  $[M + NH_4]^+$  ion as the base peak with few, if any, fragment ions. Although the data set is limited, two observations can be made regarding the structure of the GAs and the ions detected when the compounds were analyzed by TSP-MS. First, of the set of GAs analyzed by TSP-MS,  $GA_3$ ,  $GA_7$  and  $GA_{30}$  have a double bond across the C-3 and C-4 carbons and a hydroxyl group at the C-2 carbon (see Fig. 1). It is shown in Table I that the thermospray mass spectra for these three GAs included an  $[M + NH_4 - 62]^+$  ion in addition to the  $[M + NH_4]^+$  ion. This  $[M + NH_4 - 62]^+$  ion might be attributed to the  $[M + NH_4 - CO_2 - H_2O]^+$  ion. There appears to be a correlation between the presence of the C-3-C-4 double bond near the  $-COO-$  bridge and the removal of  $CO_2$  in combination with a loss of water resulting in a total loss of 62 daltons from the  $[M + NH_4]^+$  ion. Secondly, in Table I it is noted that  $GA_9$  is the only GA of the sample set analyzed to show an  $[M + H]^+$  ion for both the free acid and the methylated species. As seen in Fig. 1,  $GA_9$  is the only GA analyzed that does not have a double bond or a hydroxyl moiety. This suggests that even in the absence of these groups the proton affinity of  $GA_9$  is sufficient to produce an  $[M + H]^+$  ion. The abundance of the  $[M + NH_4]^+$  adducts and the absence of a  $[M + H]^+$  ion seen in the TSP-MS spectra of the GAs which have double bonds and hydroxyl groups could be explained by stabilization of the adducts with ammonia associated with the presence of the double bond and hydroxyl groups.

Fig. 5 shows the thermospray response curve obtained by injecting various amounts (0.1 to 2.0  $\mu\text{g}$ ) of  $GA_3$  and the methyl ester  $GA_3$  derivative. The thermospray response data for  $GA_3$  are shown as the peak area under the fragment ion peak seen at  $m/z$  302, the base peak at  $m/z$  364, and the combined peak areas of both. Each gave a linear thermospray response as evidenced by correlation coefficients of 0.995, 0.996 and 0.996 respectively. The linearity observed for the  $[M + NH_4]^+$  ion at  $m/z$  378 for the methyl ester of  $GA_3$  is also shown in Fig. 5. In addition to the thermospray response being more sensitive for this ion it gave the most linear response of the ions analyzed (correlation coefficient = 0.999). These data suggest that HPLC-TSP-MS could be used to detect these GAs down to levels of about 100 ng.

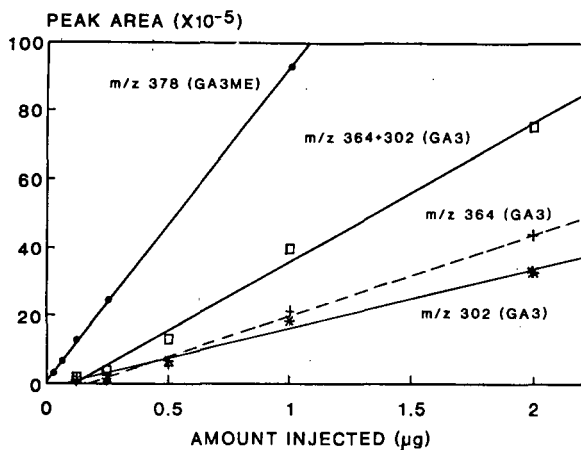


Fig. 5. Graph showing the thermospray response (peak area) vs. the amount ( $\mu\text{g}$ ) of  $\text{GA}_3$  and its methyl ester injected. HPLC system 2, mobile phase: isocratic, for  $\text{GA}_3$  acetonitrile–0.1 *M* ammonium acetate (15:85), for  $\text{GA}_3$ -methyl ester acetonitrile–0.1 *M* ammonium acetate (20:80), flow-rate 1.0 ml/min, thermospray source: 250°C, thermospray interface: 87°C for  $\text{GA}_3$ , 85°C for  $\text{GA}_3$ -methyl ester ( $\text{GA}_3\text{ME}$ ).

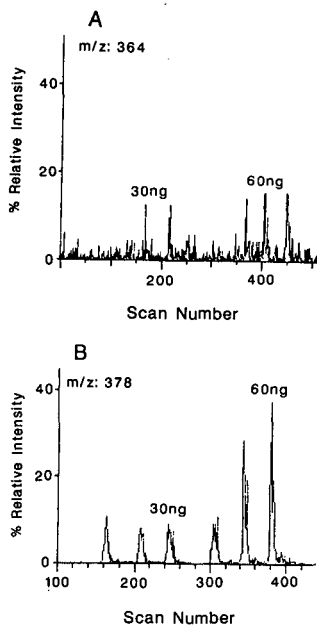


Fig. 6. Selected ion current profiles of consecutive injections of 30 ng and 60 ng each of  $\text{GA}_3$  (A) and  $\text{GA}_3$ -methyl ester (B). HPLC system 2, mobile phase: isocratic, for  $\text{GA}_3$  acetonitrile–0.1 *M* ammonium acetate (15:85), for  $\text{GA}_3$ -methyl ester acetonitrile–0.1 *M* ammonium acetate (20:80), flow-rate: 1.0 ml/min, thermospray source: 250°C, thermospray interface: 87°C for  $\text{GA}_3$ , 85°C for  $\text{GA}_3$ -methyl ester.

For comparative purposes, thermospray mass spectra of five methyl ester GA compounds were also obtained. As shown in Table I, the positive-ion thermospray mass spectra resulting from the direct injection analysis of five methyl ester GA derivatives also showed predominantly the  $[\text{M}+\text{NH}_4]^+$  ion as the base peak with few fragment ions. Fig. 6 compares consecutive injections of 30 and 60 ng  $\text{GA}_3$  (Fig. 6A) and  $\text{GA}_3$ -methyl ester (Fig. 6B) using an isocratic HPLC system. This figure clearly shows the increased sensitivity of the thermospray detector for the methyl ester  $\text{GA}_3$  derivative over that of the free acid. Detection-oriented derivatization resulting in increased thermospray response for various compounds has been reported [17–19]. Although the objective of this study was to investigate the utility of HPLC–TSP–MS to directly analyze the free acid GAs, these data suggest that the increased thermospray sensitivity gained by methylation of the free acid function may be incorporated for GA analysis in biological samples requiring higher detection sensitivity. This can be readily accomplished using diazomethane. We have previously described a simplified procedure for the preparation of diazomethane and subsequent sample derivatization [20].

Negative-ion thermospray data (filament-on mode) are presented in Table II. To our knowledge this is the first report of the negative-ion thermospray analysis of GAs. As shown in Table II, most of the free acid GAs showed the  $[\text{M}-\text{H}]^-$  or the  $[\text{M}+\text{HCO}_2]^-$  ion as the base peak or as a major peak in their negative-ion mass spectrum. The methyl ester GAs did not display an  $[\text{M}-\text{H}]^-$  ion, but showed either the  $[\text{M}]^-$  or the  $[\text{M}+\text{HCO}_2]^-$  ion as the base peak in their negative-ion thermospray mass spectra. These data demonstrate that TSP–MS in the negative-ion mode can also be used for the analysis of either free acid GAs or the methyl ester derivatives. However, positive-ion detection of these compounds was about 10 times more sensitive and did not require use of the filament-on mode.

HPLC–TSP–MS–MS spectra were obtained for the isomeric GAs  $\text{GA}_3$  and  $\text{GA}_{30}$ . As shown in Table I  $\text{GA}_1$ ,  $\text{GA}_3$  and  $\text{GA}_{30}$  co-eluted when analyzed using HPLC system 1. Figs. 7 and 8 show the collisionally activated dissociation (CAD) daughter ion mass spectra of the  $[\text{M}+\text{NH}_4]^+$  ions at  $m/z$  364 for  $\text{GA}_3$  and  $\text{GA}_{30}$ , respectively. These mass spectra

TABLE II  
NEGATIVE-ION TSP-MS SPECTRA OF GIBBERELLINS

Filament-on mode. The spectra were obtained using the following conditions: HPLC system 2, mobile phase: isocratic, for GA<sub>3</sub> acetonitrile-0.1 M ammonium acetate (15:85), for GA<sub>3</sub>-methyl ester acetonitrile-0.1 M ammonium acetate (20:80), flow-rate 1.0 ml/min, thermospray source: 250°C, thermospray interface: 87°C for GA<sub>3</sub>, 85°C for GA<sub>3</sub>-methyl ester. Me = Methyl.

[Assign] <sup>a</sup>	Relative abundance <sup>b</sup>												
	GA <sub>1</sub>	GA <sub>3</sub>	GA <sub>4</sub>	GA <sub>5</sub>	GA <sub>7</sub>	GA <sub>9</sub>	GA <sub>30</sub>	GA <sub>1</sub> Me	GA <sub>3</sub> Me	GA <sub>4</sub> Me	GA <sub>7</sub> Me	GA <sub>9</sub> Me	
M + CH <sub>3</sub> COO	11	-	4	-	2	-	-	-	5	13	-	-	
M <sub>n</sub> + HCO <sub>2</sub>	100	30	100	45	100	100	40	100	60	100	-	-	
M <sup>#</sup>	-	33	-	-	37	-	63	-	100	2	37	-	
M - H	97	44	62	100	63	95	43	-	-	-	100	-	
M + HCO <sub>2</sub> H <sup>#</sup>	-	-	-	-	28	-	-	-	42	-	25	-	
M + HCO <sub>2</sub> -44	-	38	-	-	5	-	22	-	-	-	-	-	
M + HCO <sub>2</sub> -62	-	100	-	-	6	-	100	-	-	-	-	-	
M - H - 44	-	10	-	-	-	-	16	-	-	-	-	-	
M - H - 62	-	65	-	-	-	-	54	-	-	-	-	-	

<sup>a</sup> - denotes that no signal was seen or the relative intensity of the signal was < 1%

<sup>b</sup> # denotes an ion radical probably formed by electron-capture processes.

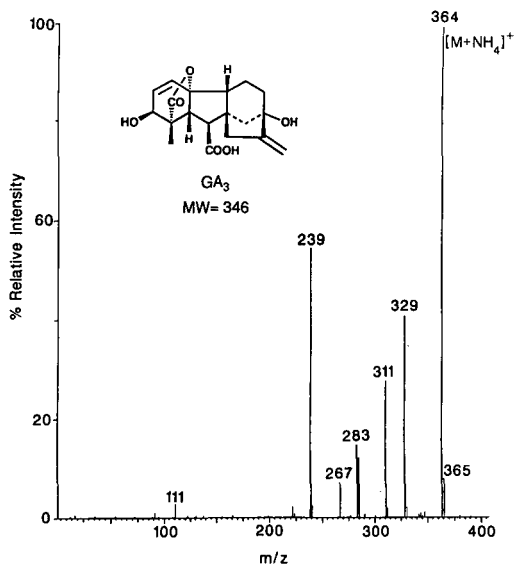


Fig. 7. Daughter ion spectrum obtained from collision activated dissociation of the  $[M + NH_4]^+$  ion at  $m/z$  364 of  $GA_3$ . HPLC system 1.

show the potential of tandem MS to differentiate these isomers without chromatographic separation. Comparison of the CAD daughter ion mass spectrum of  $GA_3$  with that of  $GA_{30}$ , shows that the

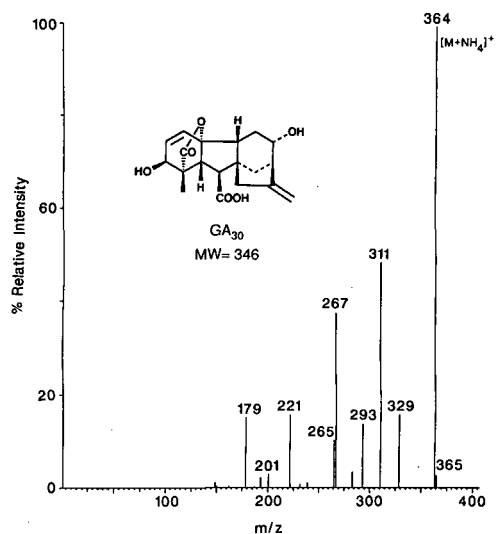


Fig. 8. Daughter ion spectrum obtained from collision activated dissociation of the  $[M + NH_4]^+$  ion at  $m/z$  364 of  $GA_{30}$ . HPLC system 1.

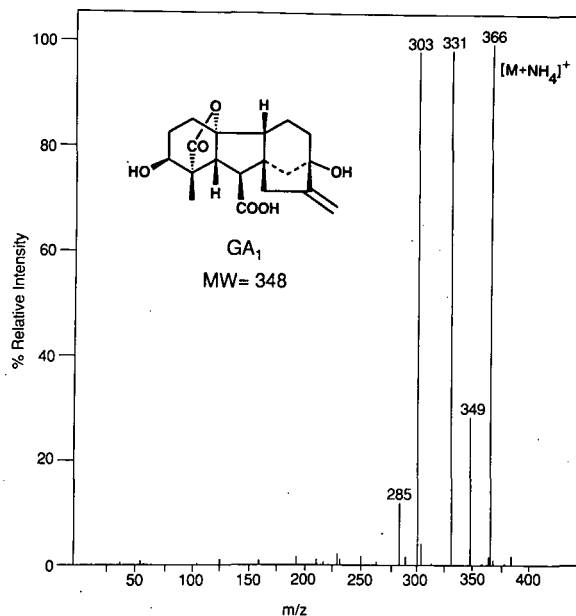


Fig. 9. Daughter ion spectrum obtained from collision activated dissociation of the  $[M + NH_4]^+$  ion at  $m/z$  366 of  $GA_1$ . HPLC system 1.

principal difference is the relative intensities of the daughter ions at  $m/z$  239,  $m/z$  265 and  $m/z$  293. In the CAD mass spectrum  $GA_3$ ,  $m/z$  239 is a prominent daughter ion, while daughter ions at  $m/z$  265 and  $m/z$  293 are not observed. In the CAD mass spectrum for  $GA_{30}$ ,  $m/z$  239 is a minor daughter ion, while daughter ions at  $m/z$  265 and  $m/z$  293 are readily observed. The differences seen in the daughter ion spectra could be explained by different fragmentation pathways involving the loss of a water molecule which is observed for  $GA_{30}$  but not for  $GA_3$ . The importance of these CAD data is that it demonstrates that TSP-MS-MS can be used to differentiate these two isomers under HPLC conditions where they co-elute and have indistinguishable thermospray mass spectra.

Because  $GA_1$  co-eluted with  $GA_3$  and  $GA_{30}$  when analysed using HPLC system 1 CAD daughter ion analysis was also performed on  $GA_1$ . Fig. 9 shows the CAD daughter ion mass spectrum of  $m/z$  366 from  $GA_1$ . This CAD daughter ion mass spectrum showed daughter ions at  $m/z$  349,  $m/z$  331,  $m/z$  303, and  $m/z$  285. These ions can be attributed to the loss of  $NH_3$ , followed by losses of  $H_2O$ , CO and

H<sub>2</sub>O. Thus both the thermospray mass spectrum and the TSP-MS-MS CAD daughter ion mass spectrum of GA<sub>1</sub> can be used to distinguish it from either GA<sub>3</sub> or GA<sub>30</sub>.

#### CONCLUSIONS

This study demonstrates TSP-MS, HPLC-TSP-MS and tandem MS to be useful for the analysis and characterization of gibberellin compounds that have one carboxylic acid group as well as their methyl ester derivatives. Elimination of the need for derivatization is one advantage of HPLC-TSP-MS over GC-MS analysis, however, the enhanced thermospray sensitivity observed with the methylated GAs suggest methylation may be advantageous for the HPLC-TSP-MS analysis of low-level GAs in biological samples. These techniques may also be applicable for the analysis of other gibberellin compounds including those containing two or more acid groups and their conjugates.

#### ACKNOWLEDGEMENTS

We thank Dr. Noboru Murofushi, Department of Agricultural Chemistry, University of Tokyo, for the samples of free acid gibberellins. We thank Dr. Jackson O. Lay Jr. (NCTR), for his helpful discussions concerning this manuscript. T.A.G. and J.A. were supported, in part, by an appointment to the ORAU Postgraduate Research Program at the National Center for Toxicological Research administered by the Oak Ridge Associated Universities through an interagency agreement between the US Department of Energy and the US Food and Drug Administration. J.S.C. was supported by the University of Central Arkansas.

#### REFERENCES

- 1 A. Crozier (Editor), *The Biochemistry and Physiology of Gibberellins*, Vols. 1 and 2, Praeger, New York, 1983.
- 2 T. Moritz, J. J. Philipson and P. C. Oden, *Physiol. Plant.*, 75 (1989) 325.
- 3 P. C. Oden and O. M. Heide, *Physiol. Plant.*, 73 (1988) 445.
- 4 R. Bottini, G. De Botini, M. Koshioka, R. P. Pharis and B. G. Coombe, *Plant Physiol.*, 78 (1985) 417.
- 5 P. J. Davis, E. Emshwiller, T. J. Gianfagna, W. M. Proevsting, N. Noma and R. P. Pharis, *Planta*, 154 (1982) 266.
- 6 J. E. N. Saucedo, J. N. Barbotin and D. Thomas, *Appl. Microbiol. Biotechnol.*, 30 (1989) 226.
- 7 S. J. Anderson and W. M. Jarrell, *Comm. Soil Sci. Plant Anal.*, 19 (1988) 617.
- 8 G. W. M. Barendse and P. H. van de Werken, *J. Chromatogr.*, 198 (1980) 449.
- 9 J. T. Lin and A. E. Stafford, *J. Chromatogr.*, 452 (1988) 519.
- 10 E. Jensen, A. Crozier and A. M. Monteiro, *J. Chromatogr.*, 367 (1986) 377.
- 11 J. T. Lin, A. E. Stafford, G. L. Steffens and N. Murofushi, *J. Chromatogr.*, 543 (1991) 471.
- 12 N. Fang and L. Rappaport, *Biomed. Environ. Mass Spectrom.*, 19 (1990) 123.
- 13 M. L. Vestal, *Methods Enzymol.*, 193 (1990) 107.
- 14 M. S. Lant, D. E. Games, S. A. Westwood and B. J. Woodhall, *Int. J. Mass Spectrom. Ion Phys.*, 46 (1983) 189.
- 15 D. E. Games, N. J. Alcock, M. S. Lant, E. D. Ramsay, R. W. Smith, S. A. Westwood and H. T. Wong, presented at the *31st Annual Conference on Mass Spectrometry and Allied Topics, Boston, MA, May 8-13, 1983*, Abstr. MOE4, pp. 117-120.
- 16 E. B. Hansen, Jr., T. A. Getek, J.S. Choinski, J. Taylor and W. A. Korfmacher, *Proceedings of the 38th ASMS Conference on Mass Spectrometry and Allied Topics, Tucson, AZ, June 3-8, 1990*, pp. 1059-1060.
- 17 R. D. Voyksner, E. D. Bush and D. Brent, *Biomed. Environ. Mass Spectrom.*, 14 (1987) 523.
- 18 J. Abian, O. Bulbena and E. Gelpi, *Biomed. Environ. Mass Spectrom.*, 16 (1988) 215.
- 19 J. Paulson and C. Lindberg, *J. Chromatogr.*, 554 (1991) 149.
- 20 L. G. Rushing, E. B. Hansen, Jr. and H. C. Thompson, Jr., *J. Chromatogr.*, 337 (1985) 37.

# High-performance liquid chromatographic investigations of stillingia oil

K. Aitzetmüller, Yaonian Xin<sup>☆</sup>, Gisela Werner and Margaretha Grönheim

Institute for Chemistry and Physics of Lipids, Federal Centre for Cereals, Potato and Lipid Research, Piusallee 76, W-4400 Münster (Germany)

(First received December 3rd, 1991; revised manuscript received February 10th, 1992)

## ABSTRACT

Stillingia oil is a Chinese raw material containing biosynthetically intriguing estolides. Oil extracted from the kernels of the seeds of *Sapium sebiferum* Roxb. was investigated using various high-performance liquid chromatographic (HPLC) techniques such as reversed-phase HPLC of the oil itself, its triacylglycerol and estolide fractions, both with refractive index and with UV detection at two different wavelengths, and using normal-phase (silica) HPLC of the tocopherols. Qualitative fingerprints and semi-quantitative results on triacylglycerols and estolides and on tocopherols are given. In the tocopherol fraction, stillingia oil contains nearly pure (92%)  $\gamma$ -tocotrienol.

## INTRODUCTION

The Chinese tallow tree *Sapium sebiferum* Roxb. is a "renewable resource" of local importance from which two totally different fats can be produced. Chinese tallow is a potential raw material for edible fats because it contains mostly symmetrical 1,3-dipalmitoyl-2-oleoylglycerol (POP)<sup>☆☆</sup> from which cocoa butter substitutes can be produced [1–4].

Stillingia oil is a liquid drying oil produced from seed kernels of the tree. In China it is used as a raw material for the local lacquer and paint industry [1,5–13]. Stillingia oil is interesting because it contains, in addition to a range of highly unsaturated

triacylglycerols (TG) [6–9] also a range of estolides (Fig. 1). Because of this remarkable feature a number of studies have been published on stillingia oil, using more conventional methods of lipid analysis [5,10–15].

Quantitative studies using HPLC with IR detection on a silica column showed that estolides amount to about 25 mol% of the oil [10]. The estolide moiety occurs exclusively in the *sn*-3-position of the glycerol [5,11].

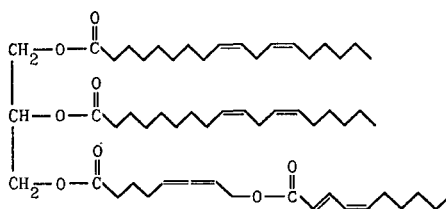


Fig. 1. A typical *Sapium sebiferum* estolide. The *sn*-3-position is esterified with the allenic  $\omega$ -hydroxy-5,6-octadienoic acid, which itself is esterified with *trans*-2,*cis*-4-decadienoic acid. Positions *sn*-1 and *sn*-2 are occupied by normal unsaturated fatty acids (O.L.Ln).

Correspondence to: K. Aitzetmüller, Institute for Chemistry and Physics of Lipids, Federal Centre for Cereals, Potato and Lipid Research, Piusallee 76, W-4400 Münster, Germany.

<sup>☆</sup> Present address: North Laodong Street 56, Xian, Shaanxi Province, China.

<sup>☆☆</sup> Fatty acids and triacylglycerols are abbreviated (as usual in high-performance liquid chromatography (HPLC) of lipids [21,22]) using S, P, O, L and Ln for stearoyl, palmitoyl, oleoyl, linoleoyl and linolenoyl residues, respectively. E stands for estolide.

## EXPERIMENTAL

Seeds of *Sapium sebiferum* were obtained from Sichuan Province, China. After removal of the seed coat fat (Chinese tallow) [1], the seeds were ground and stillingia oil (kernel oil) was extracted with hexane.

The oil as extracted was used directly for reversed-phase HPLC of the intact oil and for HPLC of the tocopherols. For further investigation, the oil was separated into two zones by preparative thin-layer chromatography (TLC) on plates of 0.5 mm thickness [20 × 20 cm, Kieselgel 60 (E. Merck, Darmstadt, Germany)] using hexane–diethyl ether (65:35, v/v). Zone I (triacylglycerols) migrated to a higher  $R_F$  value than zone II (estolides). After detection with phloxin (0.02% in ethanol), both zones were scraped off and the lipids extracted from the silica with diethyl ether.

### Gas chromatography (GC)

The GC system used was a Perkin-Elmer F 22 + AS 41 with flame ionization detection and a Silar 5 CP WCOT fused-silica (Chrompack, Middelburg, Netherlands) column (50 m × 0.22 mm I.D., film thickness 0.21 μm). The column temperature was programmed from 160 to 200°C at 1°C/min; the detector and injector temperatures were 230°C. A D-2000 chromato-integrator (Merck–Hitachi) was used.

Fatty acid methyl esters were prepared using boron trifluoride–methanol.

### Optical activity

Measurements of the specific rotation of stillingia oil, zone I and zone II were carried out in chloroform using a polarimeter (Perkin-Elmer 241 MC; chloroform blank, sodium lamp, 1.0-cm micro-cuvettes).

### Mass spectrometry

After hydrogenation (Walter F. C. Ebel 2410 Müller, hydrogen generator), zone II was investigated by mass spectrometry (Varian MAT CH 7 mass spectrometer, source temperature 250°C,  $10^{-6}$  Torr) to verify its structure.

### HPLC

HPLC was carried out using two separate re-

versed-phase (RP) systems, one with two columns and a refractive index (RI) detector, the other with only one column and a short-wavelength UV detector. HPLC of tocopherols was carried out in the usual way using a silica column with a fluorescence detector.

HPLC system 1, used for oils, triacylglycerols and estolides, with UV and RI detection, consisted of a Merck–Hitachi 655-12 pump and LC 5000 gradient controller, Superspher RP-18 end-capped column (E. Merck) (250 × 4 mm I.D., 4 μm), Rheodyne Model 7125 injection valve (20 μl) and Model 655-A-22 variable-wavelength UV monitor set at 210, 235 and 260 nm. Alternatively, an ERC-7510 RI detector was also used with HPLC system 1. The UV-transparent mobile phase used was acetonitrile–propanol–2-hexane (70:20:10, v/v/v) at 0.8 ml/min.

HPLC system 2, used for oils, triacylglycerols and estolides, with RI detection only, consisted of a Waters Model 510 pump, Rheodyne Model 7125 injector (20 μl), two Nucleosil 100 C<sub>18</sub> columns (250 mm × 4 mm I.D., 5 μm) (Knauer, Berlin, Germany) and a Knauer RI detector. The mobile phase was acetonitrile–acetone (38:62, v/v) at 0.9 ml/min.

HPLC system 3, used for tocopherols in oils with fluorescence detection, consisted of a Merck–Hitachi L-6000 pump, Rheodyne Model 7125 injection valve (20 μl), a Nucleosil 50 silica column (250 × 4 mm I.D., 5 μm) (Knauer) and a Merck–Hitachi F-1000 fluorescence detector set at 295/330 nm. The mobile phase was hexane–dioxane (95:5, v/v) at 1.0 ml/min. Dilute solutions of chinese tallow and stillingia oil were injected directly.

Peak integration was performed with a Merck–Hitachi D-2500 chromato-integrator [a drawback of such an integrator for applications of this type, however, is that they are unable to recalculate relative retention times (RRT) after one peak has been designated as having RRT = 1.000].

Palm oil, soyabean oil, linseed oil and interesterified mixtures of LnLnLn, LLL, OOO and PPP (see footnote in Introduction) and saturated TG (C<sub>30</sub>–C<sub>54</sub>) were used to identify individual peaks in TG HPLC.

## RESULTS AND DISCUSSION

Stillingia oil and tung oil are both classical Chi-

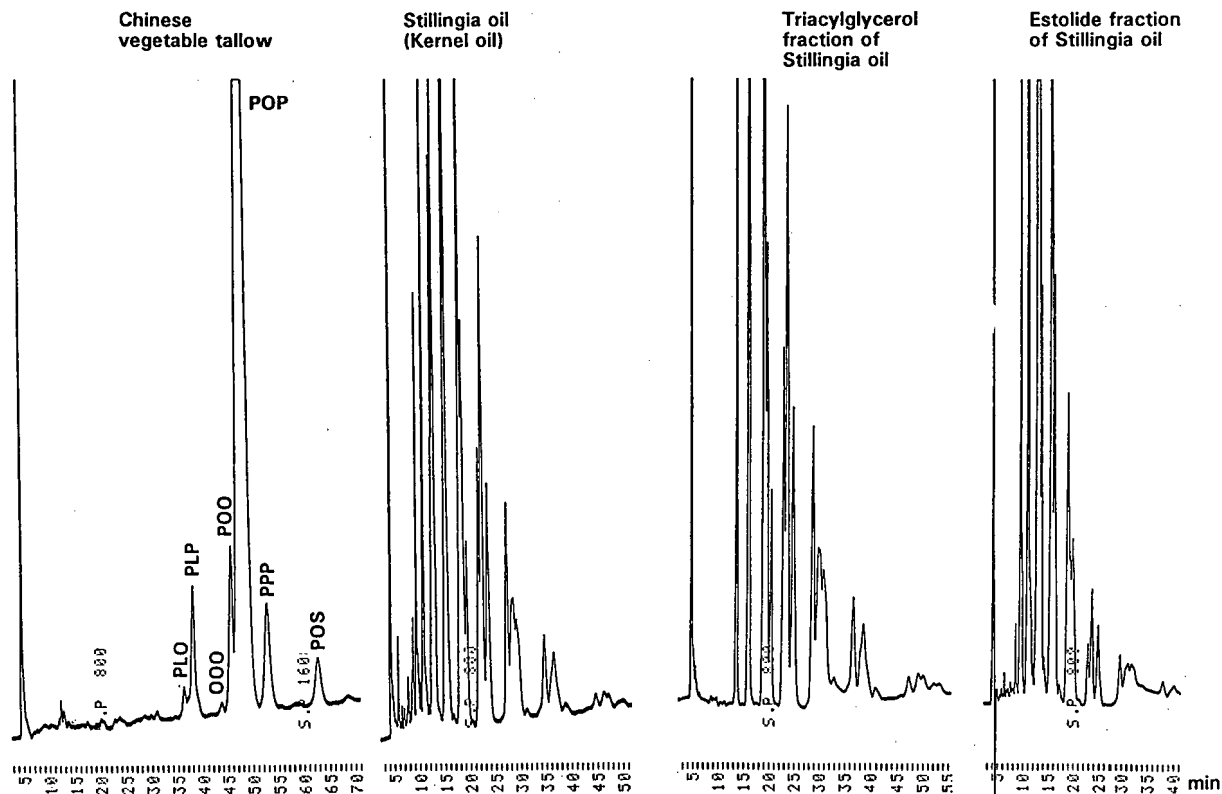


Fig. 2. RP-HPLC-RI fingerprints of Chinese tallow, stillingia oil and its triacylglycerol and estolide fractions. HPLC system 2 was used with RI detection; for HPLC conditions, see text. S, P, O, L: stearic, palmitic, oleic and linoleic acid residues, respectively.

nese drying oils. Although the content of highly unsaturated and conjugated fatty acids in tung oil is higher than in stillingia oil, the latter is the better drying oil [16]. A potential explanation for this is the presence of estolides in stillingia oil which are unstable and easily oxidized.

In conventional fingerprint RP-HPLC-RI traces of Chinese tallow, stillingia oil and its triacylglycerol and estolide fractions (Fig. 2), one notices immediately that stillingia oil and its two fractions contain much more highly unsaturated triacylglycerol and estolide molecules than Chinese tallow, which contains mostly POP.

By comparison with known oils and triacylglycerol reference mixtures, the triacylglycerol peaks in the RP-HPLC traces (UV at 210 nm and RI) were further identified as shown in Fig. 3. The identification of the estolides (--E) is tentative. Because of the

different mobile phases, the separation selectivity is slightly different (compare Fig. 3a and b).

The relative contribution of one estolide (E) moiety towards reducing retention in RP-HPLC is large, although this is caused primarily by the additional (fourth) ester group. The four double bonds are not fully available for interaction with the chromatographic system, *i.e.*, they are not contributing fully to retention time reduction in RP-HPLC, two of them because they form an allene and the other two because they are conjugated. However, exchange of an L by an E residue, as in LLE *vs.* LLL peaks, causes a dramatic decrease in retention time.

The results of the optical rotation analysis of stillingia oil (Table I) show that the optical activity is clearly caused by zone II. It has been discussed [5,11] that not the estolide in the *sn*-3-position as such but rather the allene in the C<sub>8</sub> hydroxy fatty

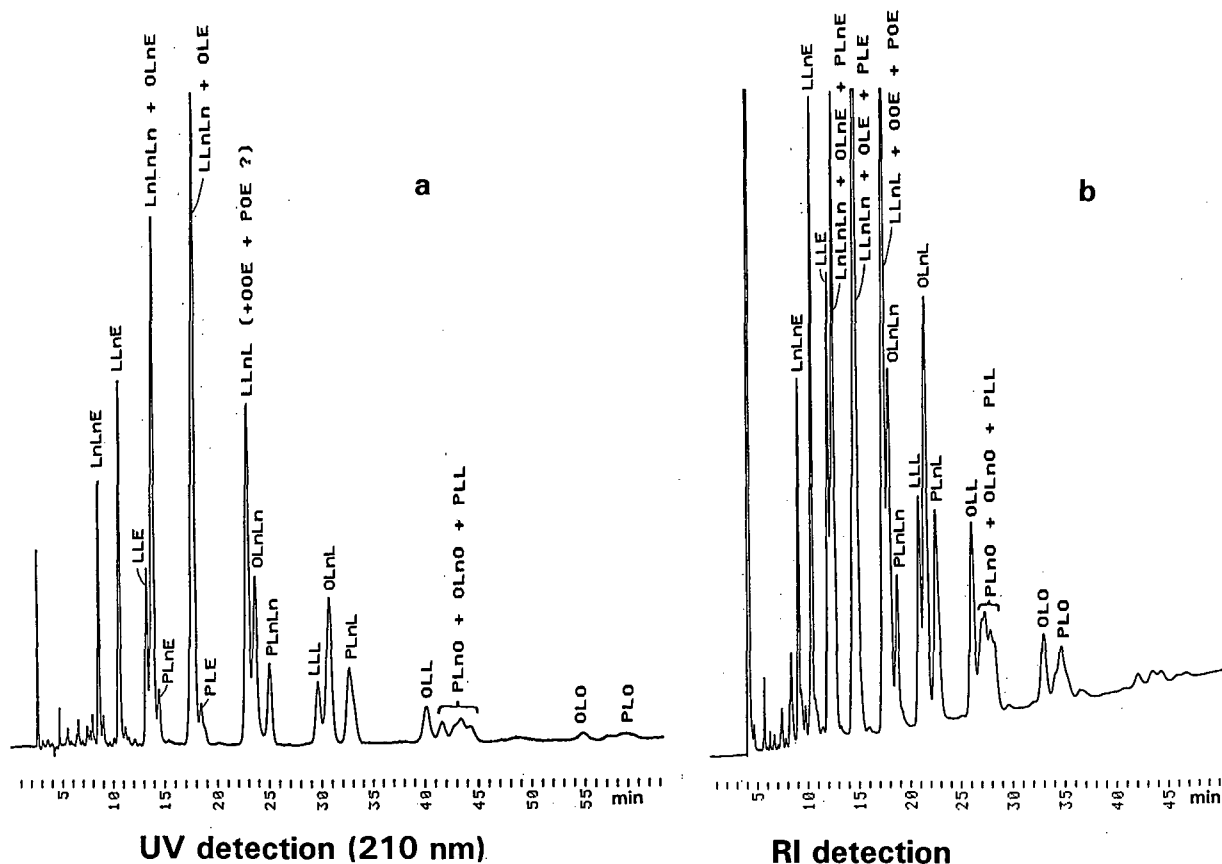


Fig. 3. RP-HPLC of intact stilingia oil: (a) with UV detection, HPLC system 1; (b) with RI detection, HPLC system 2. Triacylglycerol peaks are identified by comparison with known oils and triacylglycerol standards. Identification of estolide peaks (–E) is tentative. For HPLC conditions, see text. P, O, L, Ln: palmitic, oleic, linoleic, linolenic acid residues, respectively; E = estolide.

acid moiety of the estolides is the major cause of optical activity.

Mass spectrometry of the hydrogenated zone II showed  $M^+$  at  $m/z$  920 and fragments at  $m/z$  297, 371, 425 and 637. This result confirms the presence of estolides [5].

In the estolides, apparently the moiety consisting of 2,4-decadienoic acid and  $\omega$ -hydroxy-5,6-octadienoic acid (the allene causing the major part of the optical activity) is constant in the *sn*-3 position [5,9,11]. In RP-HPLC, the observed differences in the retention of the individual estolides are introduced by the various fatty acids (O, L, Ln) esterified at positions 1 and 2.

Fig. 4 shows GC traces of the oil and its two fractions. Table II shows the area composition

found for the fatty acids; however, no precautions were taken against losses of the  $C_8$  and  $C_{10}$  acids [11]. Compared with the results of Sprecher *et al.* [5]

TABLE I

SPECIFIC ROTATION OF STILLINGIA OIL AND ITS FRACTIONS

Component	Concentration (g per 100 ml)	Value measured	$[\alpha]_D^{20}$ (°)
Stillingia oil	1.02	–0.056	–5.49
Stillingia oil	4.98	–0.263	–5.28
Zone I	2.92	–0.011	–0.38
Zone II	1.00	–0.212	–21.20
Stillingia oil [13]			–5.01

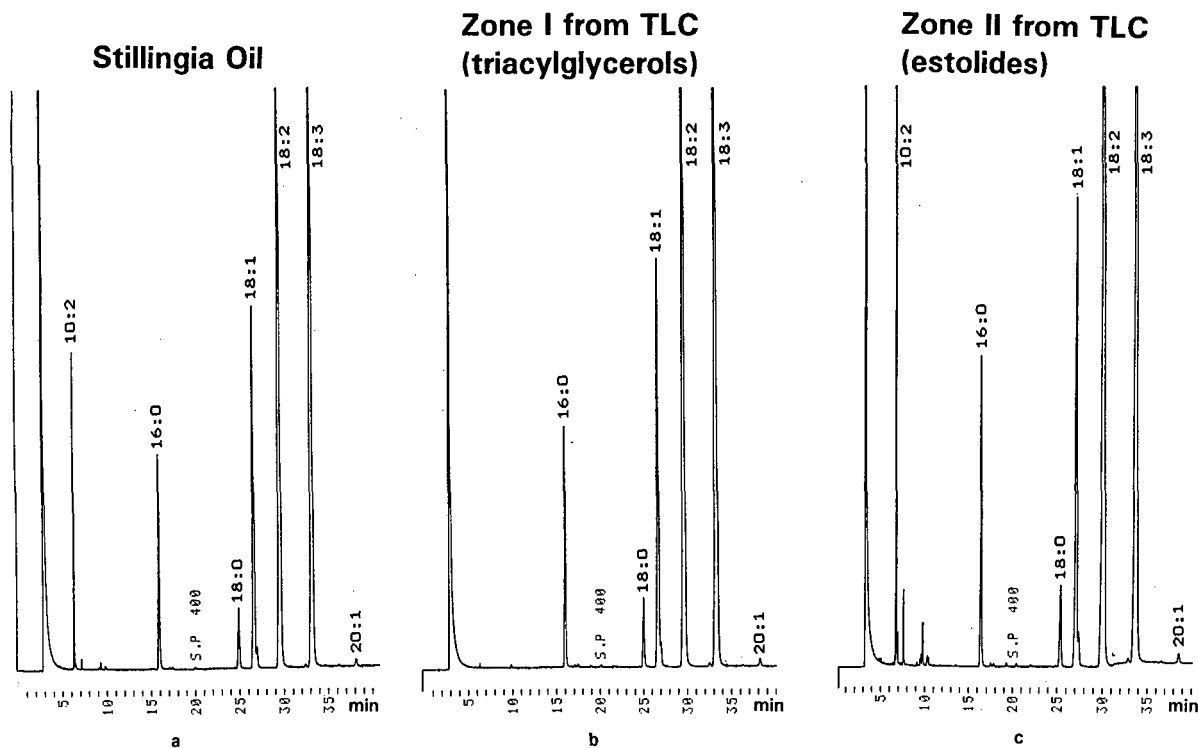


Fig. 4. GC of fatty acid methyl esters obtained from (a) stillingia oil and its (b) triacylglycerol and (c) estolide TLC-fractions. For GC conditions, see text. 16:0, 18:0, 18:1, 18:2, 18:3 and 20:1 are the usual fatty acid shorthand notations; 10:2 = 2*t*,4*c*-decadienoic acid.

and Narang and Sadgopal [8], our samples had a significantly higher linolenic acid content (38%). However, up to 50% or more linolenic acid has been found in samples from Pakistan [7] and else-

where [11]. Apart from the C<sub>8</sub> and C<sub>10</sub> acids, which have been reported to be missing in samples from India and Pakistan [7,8], the fatty acid compositions of both the TG and estolide fractions are very similar.

TABLE II

FATTY ACID COMPOSITION (AREA%) OF STILLINGIA OIL AND ITS TRIACYLGLYCEROL (ZONE I) AND ESTOLIDE (ZONE II) FRACTIONS

Sample	Fatty acids <sup>a</sup>								
	10:2	16:0	18:0	18:1 <i>n</i> -9	18:1 <i>n</i> -7	18:2 <i>n</i> -6	18:3 <i>n</i> -3	20:1 <i>n</i> -9	Unidentified <sup>b</sup>
Stillingia oil:									
Sample 1	3.3	5.9	2.3	13.8	0.8	36.1	37.3	0.3	0.2
Sample 2	2.8	5.6	2.3	13.9	0.8	35.5	38.3	0.3	0.5
Zone I (triacylglycerols)	—	6.0	2.4	14.8	0.8	35.9	39.0	0.3	0.8
Zone II (estolides <sup>a</sup> )	7.6	5.6	2.0	12.1	0.8	36.5	32.6	0.3	2.5

<sup>a</sup>  $\omega$ -Hydroxy-5,6-octadienoic acid was not determined and no special efforts were made to secure a quantitative recovery of 10:2.

<sup>b</sup> Traces of C<sub>12</sub> and C<sub>14</sub> (unsaturated) acids.

TABLE III

TENTATIVE TRIGLYCERIDE AND ESTOLIDE COMPOSITION OF *SAPIUM SEBIFERUM* FATS AND THEIR FRACTIONS

Area% (RI) from RP-HPLC with RI detection (uncorrected). *PN* = partition number, defined in the usual way [19,26] as carbon number (*CN*) minus twice the double bond number (*DB*):  $PN = CN - 2DB$ . Although *PN* is not applicable as such to the estolides (--E), with their experimentally observed equivalent partition numbers *EPN* [26] they fall within the TG *PN* ranges as indicated in the table (vertical columns).

Sample (HPLC-system/detector)	Triglycerides and estolides (--E)											
	LnLnE	LLnE	LLE	<i>PN</i> = 36			<i>PN</i> = 38			<i>PN</i> = 40 <sup>a</sup>		
				LnLnLn	OLnE	PLnE	LLnLn	OLE	PLE	LLnL	OLnLn	PLnLn
<i>Chinese tallow</i>												
Sample 1 (HPLC-2/RI)												
Sample 2 (HPLC-2/RI)												
<i>Stillingia oil</i>												
Sample 1 (HPLC-2/RI)	3.4	6.7	4.6	10.5			18.5		11.9	6.3	2.8	
Sample 2 (HPLC-2/RI)	3.0	6.9	4.6	10.3	0.2		18.0	0.1	11.5	6.6	2.7	
Sample 1 (HPLC-1/RI)	2.8	6.3	4.7	8.7	1.5		15.7	2.1	11.6	6.4	2.5	
<i>TLC zone I</i> (triglycerides)												
Plate 1 (HPLC-2/RI)	–	–	–	7.3	–	–	16.5	–	–	15.0	7.0	3.3
Plate 2 (HPLC-1/RI)	–	–	–	8.4	–	–	17.7	–	–	15.8	7.2	3.5
<i>TLC zone II</i> (estolides)												
Plate 1 (HPLC-2/RI)	8.0	17.5	14.3	–	9.7	4.3	–	13.1	6.2		<sup>f</sup>	
Plate 2 (HPLC-1/RI)	12.7	25.5	20.1	–	9.7	5.8	–	11.1	7.8		(4.4) <sup>g</sup>	
<i>TLC zone II<sup>g</sup></i> (estolides, UV)												
Plate 2 (HPLC-1/UV)	11.2	24.6	18.5	–	9.9	5.6	–	11.1	8.7		(5.5) <sup>g</sup>	

<sup>a</sup> Including OOE, POE and PPE.

<sup>b</sup> Including SLnLn, SOE and PSE.

<sup>c</sup> Including PLnO and SLnL.

<sup>d</sup> Including PLnS.

<sup>e</sup> Including PLS.

<sup>f</sup> Various smaller peaks and contaminants, possibly OOE + POE + PPE, together max. 10%, in *PN* group 40, and containing SOE + PSE, together max. 4%, in *PN* group 42.

<sup>g</sup> Using 260 nm UV. area% (uncorrected).

Table III shows the triacylglycerol and estolide compositions as found by RP-HPLC-RI for chinese tallow, stillingia oil and its two major fractions, triacylglycerols (zone I from TLC) and estolides (zone II), calculated as area% (RI detection), uncorrected. For the estolides, this is also compared with area% (UV detection at 260 nm).

In HPLC with UV detection, stillingia oil chromatograms obtained at a wavelength of 232 or 260 nm are different from those obtained at 210 nm. The unspecific absorption of C=C double bonds

and ester groups at 210 nm gives rise to chromatograms showing peaks for all the triacylglycerols and estolides present. Fig. 5 shows chromatograms at a UV detection wavelength of 210 nm for stillingia oil and its triacylglycerols (zone I) and estolides (zone II).

The same is shown in Fig. 6 for a UV detection wavelength of 260 nm. At 232 nm the conjugated diene absorption (e.g., in oxidation products, if present) would predominate. At 260 nm, extended conjugation (conjugated diene at the 2,4-position, i.e.,

<i>PN</i> = 42 <sup>b</sup>			<i>PN</i> = 44 <sup>c</sup>				<i>PN</i> = 46 <sup>d</sup>			<i>PN</i> = 48 <sup>e</sup>				<i>PN</i> = 50	
LLL	OLnL	PLnL	OLL	OLnO	PLL	PLnP	OLO	PLO	PLP	OOO	POO	POP	PPP	POS	PPS
							–	0.6	4.4	0.4	4.6	81.3	4.7	2.6	0.7
							–	0.4	3.6	0.2	5.2	83.1	4.7	2.1	
3.7	8.4	5.0	4.1	3.7	3.2	1.9	2.5	0.3	0.5	0.1					
3.5	8.5	5.1	4.1	3.6	3.2	1.8	2.5	0.3	0.4	0.4	0.4	0.3			
3.7	7.9	4.8	4.6	2.8	4.2	2.5	2.2		3.1						
5.1	11.3	6.8	5.7	5.6	4.8	1.1	2.9	3.7	0.4	0.6	1.6	1.0			
5.4	11.4	7.0	6.3	3.0	5.1	2.0	2.9	3.0							

conjugated with the carbonyl oxygen [6]) found only in the estolides containing the 2,4-decadienoic acid moiety, makes these peaks much more prominent (Fig. 6). In semi-quantitative (peak area %) calculations, it can be seen that the data for UV detection at 260 nm compare well with RI data for the estolide fraction of plate 2 (Table III). However, for truly quantitative work, individual calibration of all the peaks would be necessary.

The HPLC of tocopherols showed that chinese tallow was nearly free from tocopherols. Stillingia oil contained 700 mg/kg of total tocopherols, of which 91.8% was  $\gamma$ -tocotrienol, identified by co-

chromatography with palm oil tocotrienols (Fig. 7). Minor tocopherols also identified include  $\alpha$ -tocotrienol (1.2%),  $\beta$ -tocopherol (5.5%) and  $\delta$ -tocotrienol (0.5%).

Considerable experience has been accumulated over the years regarding experimental techniques, separation mechanisms and selectivities in the RP-HPLC of triacylglycerols using different column-solvent systems [17–25]. This work extended this to estolides, although further work is needed to draw more quantitative conclusions with regard to separation effects and retention characteristics of these and other estolides. The estolides (--E), although a



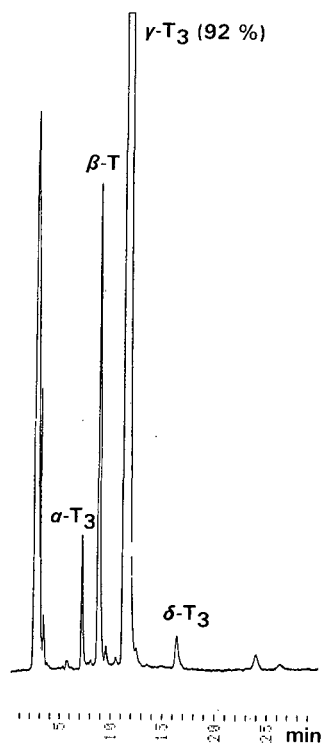


Fig. 7. HPLC of tocopherols of stillingia oil. The prominent peak (92% of total tocopherols) was tentatively identified as  $\gamma$ -tocotrienol. HPLC system 3 (silica column, fluorescence detection).  $\alpha$ -T<sub>3</sub>,  $\gamma$ -T<sub>3</sub>,  $\delta$ -T<sub>3</sub> =  $\alpha$ -,  $\gamma$ -,  $\delta$ -tocotrienols, respectively;  $\beta$ -T =  $\beta$ -tocopherol.

copherol data. Y.X. is indebted to Carl Duisberg Gesellschaft, Cologne, for financial support during his stay in Germany.

#### REFERENCES

- 1 Y. Xin and K. Aitzetmüller, *China Oils Fats (Xian)*, 1 (1991) 23.
- 2 K. Itagaki, T. Yanagihara, S. Maruzeni and N. Yasuda, *Jpn. Pat.*, 62210951 (1987); *C.A.*, 107 (1987) 235186q.
- 3 Z. Xing, *Faming Zhuanli Shenqing Gongkai Shuomingshu*, 1988; *C.A.*, 111 (1988) 152446y.
- 4 J. Wang, F. Yu, J. Li and X. Shan, *Zhiwu Xuebao*, 30 (1988) 619; *C.A.*, 111 (1988) 230926w.
- 5 H. W. Sprecher, R. Maier, M. Barber and R. T. Holman, *Biochemistry*, 4 (1965) 1856.
- 6 A. Crossley and T. P. Hilditch, *J. Chem. Soc.* (1949) 3353.
- 7 M. Y. Raie, S. Zaka, S. Iqbal, A. W. Sabir and S. A. Khan, *Fette Seifen Anstrichm.*, 85 (1983) 359.
- 8 S. A. Narang and Sadgopal, *J. Am. Oil Chem. Soc.*, 35 (1958) 68.
- 9 R. Maier and R. T. Holman, *Biochemistry*, 3 (1964) 270.
- 10 K. Payne-Wahl and R. Kleiman, *J. Am. Oil Chem. Soc.*, 60 (1983) 1011.
- 11 W. W. Christie, *Biochim. Biophys. Acta* 187 (1969) 1.
- 12 H. P. Kaufmann and B.-W. King, *Fette Seifen*, 46 (1939) 388.
- 13 P. T. Huang, R. T. Holman and W. M. Potts, *J. Am. Oil Chem. Soc.*, 26 (1949) 405.
- 14 Y. C. Chen, A. Zlatkis, B. S. Middleditch, J. Cowles and W. Scheld, *Chromatographia*, 23 (1987) 240.
- 15 W. H. Heimermann and R. T. Holman, *Phytochemistry*, 11 (1972) 799.
- 16 T. P. Hilditch, *J. Oil Colour Chem. Assoc.*, 17 (1949) 5.
- 17 A. H. El Hamdy and E. G. Perkins, *J. Am. Oil Chem. Soc.*, 58 (1981) 867.
- 18 J. P. Goiffon, C. Reminiac and D. Furon, *Rev. Fr. Corps Gras*, 28 (1981) 199.
- 19 K. Aitzetmüller, *Prog. Lipid Res.*, 21 (1982) 171.
- 20 A. Seher and H.-J. Fiebig, *Fette Seifen Anstrichm.*, 85 (1983) 333.
- 21 E. Deffense, *Rev. Fr. Corps Gras*, 31 (1975) 454.
- 22 K. Aitzetmüller, in H. Engelhardt (Editor), *Practice of High Performance Liquid Chromatography*, Springer, Berlin, 1986, pp. 287–321.
- 23 W. W. Christie, *High Performance Liquid Chromatography and Lipids*, Pergamon Press, Oxford, 1987.
- 24 K. Aitzetmüller, *Chem. Ind. (London)*, (1988) 452.
- 25 O. Podlaha and B. Töregard, *J. Chromatogr.*, 482 (1989) 215.
- 26 C. Litchfield, *Analysis of Triglycerides*, Academic Press, New York, 1972.



CHROM. 23 993

# Comparison of gas chromatographic–mass spectrometric methods for screening of chlorotriazine pesticides in soil<sup>☆</sup>

Gaël Durand

*Environmental Chemistry Department, CID-CSIC, c/Jordi Girona 18–26, 08034 Barcelona (Spain)*

Philippe Gille and Daniel Fraisse

*Service Central d'Analyse, CNRS, B.P. 22, 69290 Vernaison (France)*

Damià Barceló

*Environmental Chemistry Department, CID-CSIC, c/Jordi Girona 18–26, 08034 Barcelona (Spain)*

(First received September 18th, 1991; revised manuscript received January 3rd, 1992)

---

## ABSTRACT

The performance of a coupled technique resulting from the combination of gas chromatography with a selective mass spectrometric technique (tandem mass spectrometry) (GC–MS–MS) with collisionally activated dissociation (CAD) and multi-reaction monitoring (MRM) was compared with that of GC–low resolution MS (GC–LRMS) at a resolving power of 1000 and GC–high-resolution MS (GC–HRMS) at resolving powers of 5000 and 10 000 for the determination of atrazine, simazine, cyanazine, deethylatrazine and deisopropylatrazine in polluted soil samples. GC–MS–MS daughter ion spectra for the parent ions  $[M]^+$  and  $[M - CH_3]^+$  were generated using collisionally activated dissociation and studied. Also, by optimizing the collision energy for maximum sensitivity a method for screening chlorotriazines by MRM was developed. Analyses of soil sample extracts showed that GC–MS–MS overcomes interferences from other chlorotriazines and interfering compounds that could not be removed by GC–HRMS or GC–LRMS at resolving powers of 10 000 and 1000, respectively. The limits of detection for GC–MS–MS and GC–HRMS at a signal-to-noise ratio of 10 ranged between 1 and 24 pg, with a mean relative standard deviation of 25–30%. Soil samples known to contain chlorotriazines and their degradation products were analysed by GC–MS–MS and the results obtained were compared with those given by GC–HRMS at resolving powers of 5000 and 10 000, with quantification differences of 25–30%.

---

## INTRODUCTION

Chlorotriazines are broad-spectrum residual herbicides used widely for pre- and post-emergence weed control in corn, wheat, barley and sorghum, and also on railways and roadside verges [1]. Micro-

bial degradation and volatility are two of the main degradation processes affecting their persistence in soil [2] and yielding dealkylated metabolites which have been detected in different types of soil [3,4]. These studies on the fate of chlorotriazine pesticides in the environment have prompted the need for sensitive, specific methods for their determination.

The gas chromatographic–mass spectrometric (GC–MS) determination of chlorotriazine pesticides using a variety of ionization techniques has been approached in a number of ways. Applications reported so far include GC–MS with electron im-

---

*Correspondence to:* Dr. D. Barceló, Environmental Chemistry Department, CID-CSIC, c/Jordi Girona 18–26, 08034 Barcelona, Spain.

<sup>☆</sup> Presented at the 12th International Mass Spectrometry Conference, Amsterdam, August 26–30, 1991.

pect (EI) [3-5] and with positive- and negative-ion chemical ionization (PCI and NCI, respectively) [5,6]. Confirmation of pesticide residues is accomplished by using two or three diagnostic ions in the selected ion monitoring (SIM) mode. When higher selectivity is needed, *e.g.* to avoid false-positive identifications in environmental samples, GC-high-resolution MS (GC-HRMS) and GC-tandem MS (GS-MS-MS) are highly recommended.

Collisionally activated dissociation (CAD) MS-MS has rarely been applied to pesticide analysis. Most work reported in this respect involves the use of a triple quadrupole mass spectrometer in combination or not with GC, and with EI [7-9] or chemical ionization [10-12]. This approach has been used to confirm a variety of organic compounds [7-9] and chlorotriazine [10], organophosphorus [11,12] and carbamate [12] insecticides. In the last few years, liquid chromatography (LC)-MS-MS, also with quadrupole systems, has been applied to the determination of chlorotriazine pesticides [13,14] and organophosphorus [15] and carbamate insecticides [16], all of which testify to an increasing use of tandem MS for screening different groups of pesticides in environmental matrices. However, GC-MS-MS hybrid instruments have rarely been used in analysis for organic compounds of environmental interest [8] and only a few applications to specific compounds (*e.g.*, dioxins [17,18]) have been reported so far. By using this type of instrumentation, the high selectivity of capillary GC is enhanced as a result of the increased mass resolution of parent ions. This can be accomplished by coupling a high-resolution, double-focusing mass spectrometer in series with a quadrupole collision cell and a second quadrupole mass filter.

The lack of reports on the application of GC-MS-MS hybrid instruments to pesticide analyses prompted us to carry out a study of this nature. Thus, the aim of this work was to study the use of GC-MS-MS hybrid instruments by using CAD and different parent ions, to compare the selectivity and sensitivity of GC-MS-MS with that of GC-low-resolution MS (GC-LRMS) and GC-HRMS at resolving powers of 1000 and 10 000, respectively, and to assess the performance of different MS methods for the determination of the chlorotriazine pesticides atrazine, simazine and cyanazine and their dealkylated degradation products deethylatra-

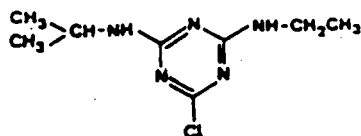
zine and deisopropylatrazine in polluted soil samples.

## EXPERIMENTAL

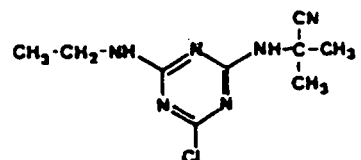
### Chemicals

The structures of the pesticides studied are given in Fig. 1. Pesticide-grade ethyl acetate, *n*-hexane, diethyl ether and dichloromethane supplied by Mallinckrodt (Paris, KY, USA) were used as solvents. Florisil (100-200 mesh) was purchased from

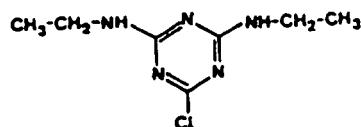
### Atrazine



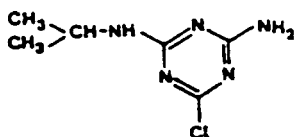
### Cyanazine



### Simazine



### Deethylatrazine



### Deisopropylatrazine

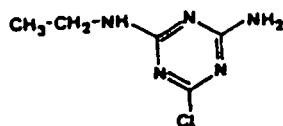


Fig. 1. Structures of the compounds.

Merck (Darmstadt, Germany). Cyanazine was supplied by Riedel-de Haën (Seelze-Hannover, Germany) and atrazine and simazine by Polyscience (Niles, IL, USA). Deethylatrazine and deisopropylatrazine were donated by Ciba-Geigy (Basle, Switzerland). Labelled atrazine (ethylamine- $d_5$ ) was purchased from Cambridge Isotope Instruments (Innerberg, Switzerland).

#### Sample preparation

Soil samples from the Ebro Delta (Tarragona, Spain) were pretreated by using a modification of a procedure commonly used at our laboratory for the residue analysis of chlorotriazine pesticides [3,5]. Thus, 10 g of soil sample were freeze-dried and sieved through a 120- $\mu$ m mesh and Soxhlet extracted with methanol for 12 h. The extracts were concentrated in a rotary evaporator to ca. 20–25 ml carefully evaporated to dryness and the residue was dissolved in 400  $\mu$ l of *n*-hexane.

Clean-up was carried out in glass columns (150 mm  $\times$  5 mm I.D.) filled with ca. 2 g of Florisil previously activated at 300°C overnight, cooled and deactivated with 2% of water. The packing material was mixed with *n*-hexane and placed on the glass column. The soil extracts in *n*-hexane (400  $\mu$ l) were placed on top of the column and eluted with diethyl ether-*n*-hexane (1:1) according to a clean-up procedure reported elsewhere [3,5]. The fractions were evaporated nearly to dryness and the residue was dissolved in 500  $\mu$ l of ethyl acetate. The volume injected into the gas chromatograph was generally 1  $\mu$ l.

#### Instrumental methods

**GC.** A Hewlett-Packard Model (Palo Alto, CA, USA) Model 5890 gas chromatograph coupled to a VG (Manchester, UK) Model 70-250-SQ mass spectrometer was used. A GC column of 15 m  $\times$  0.25 mm I.D. consisting of a fused-silica capillary coated with chemically bonded cyanopropylphenyl DB 225 (J&W Scientific, Folsom, CA, USA) with a film thickness of 0.15  $\mu$ m was used for chlorotriazines and their dealkylated metabolites. Such a column was used in previous work [5] to achieve complete separation of chlorotriazines and their degradation products. Helium was used as the carrier gas at a flow-rate of 50 cm/s. The temperature of the injector was kept at 260°C and the column temper-

ature was programmed from 70 to 220°C at 6°C/min.

**GC-LRMS and GC-HRMS.** Experiments were performed on a VG Model 70-250-SQ mass spectrometer working in the Selected Ion Recording (SIR) mode at a resolving power of 1000. HRMS experiments were performed on a VG Model 70-250-SQ mass spectrometer working in the SIR mode at resolving powers of 5000 and 10 000. The source temperature was kept at 200°C, the electron energy was 70 eV, the filament emission current was 0.2 mA and the accelerating voltage was 8 kV. The ions monitored were  $m/z$  215.0938 and 217.0908 for atrazine, 201.0781 and 203.0752 for simazine, 240.0890 and 242.0861 for cyanazine, 173.0468 and 175.0439 for deisopropylatrazine, 187.0625 and 189.0595 for deethylatrazine and 220.0938 and 222.0908 for labelled atrazine (ethylamine- $d_5$ ). Labelled atrazine, used to measure the detection sensitivity, was eluted before atrazine under the GC conditions used.

**GC-MS-MS.** A VG Model 70-250-SQ (EBqQ configuration) hybrid mass spectrometer was used for the MS-MS analyses. The monitored transitions using multi-reaction monitoring of the loss of  $CH_3^+$  from  $M^{+}$  are listed in Table I. Argon was used as the collision gas and its pressure was optimized at  $3 \cdot 10^{-6}$  mbar in the ion gauge, which resulted in a pressure of ca.  $4 \cdot 10^{-4}$  mbar in the collision cell.

TABLE I

IONS AND TRANSITIONS MONITORED IN COLLISION ENERGY EXPERIMENTS

Pesticide	$M^{+}$ ion ( $m/z$ )	Transition monitored
Deisopropylatrazine	173	$173^+ \rightarrow 158^+ + CH_3$
	175	$175^+ \rightarrow 160^+ + CH_3$
Deethylatrazine	187	$187^+ \rightarrow 172^+ + CH_3$
	189	$189^+ \rightarrow 174^+ + CH_3$
Simazine	201	$201^+ \rightarrow 186^+ + CH_3$
	203	$203^+ \rightarrow 188^+ + CH_3$
Atrazine	215	$215^+ \rightarrow 200^+ + CH_3$
	217	$217^+ \rightarrow 202^+ + CH_3$
Atrazine (ethylamine- $d_5$ )	220	$220^+ \rightarrow 205^+ + CH_3$
	222	$222^+ \rightarrow 207^+ + CH_3$
Cyanazine	240	$240^+ \rightarrow 225^+ + CH_3$
	242	$242^+ \rightarrow 227^+ + CH_3$

### Optimization of GC-MS-MS

The collision energy was optimized for each chlorotriazine studied. Argon was used as the collision gas at the pressure given above. The results obtained are shown in Fig. 2A for atrazine, simazine and cyanazine and in Fig. 2B for deethylatrazine and deisopropylatrazine. The collision energy was varied from 20 to 100 eV (Fig. 2A) and from 20 to 170 eV (Fig. 2B). The collision energy in Fig. 2B

was varied up to 170 eV, as above 80 eV the response was found to increase and give rise to a second, lower maximum between 100 and 105 eV. The optimum collision energies were found to be 50 eV for atrazine, deethylatrazine and deisopropylatrazine, 40 eV for cyanazine and 35 eV for simazine. They were optimized for each pesticide by using GC-MS-MS with MRM and monitoring of the transitions listed in Table I.

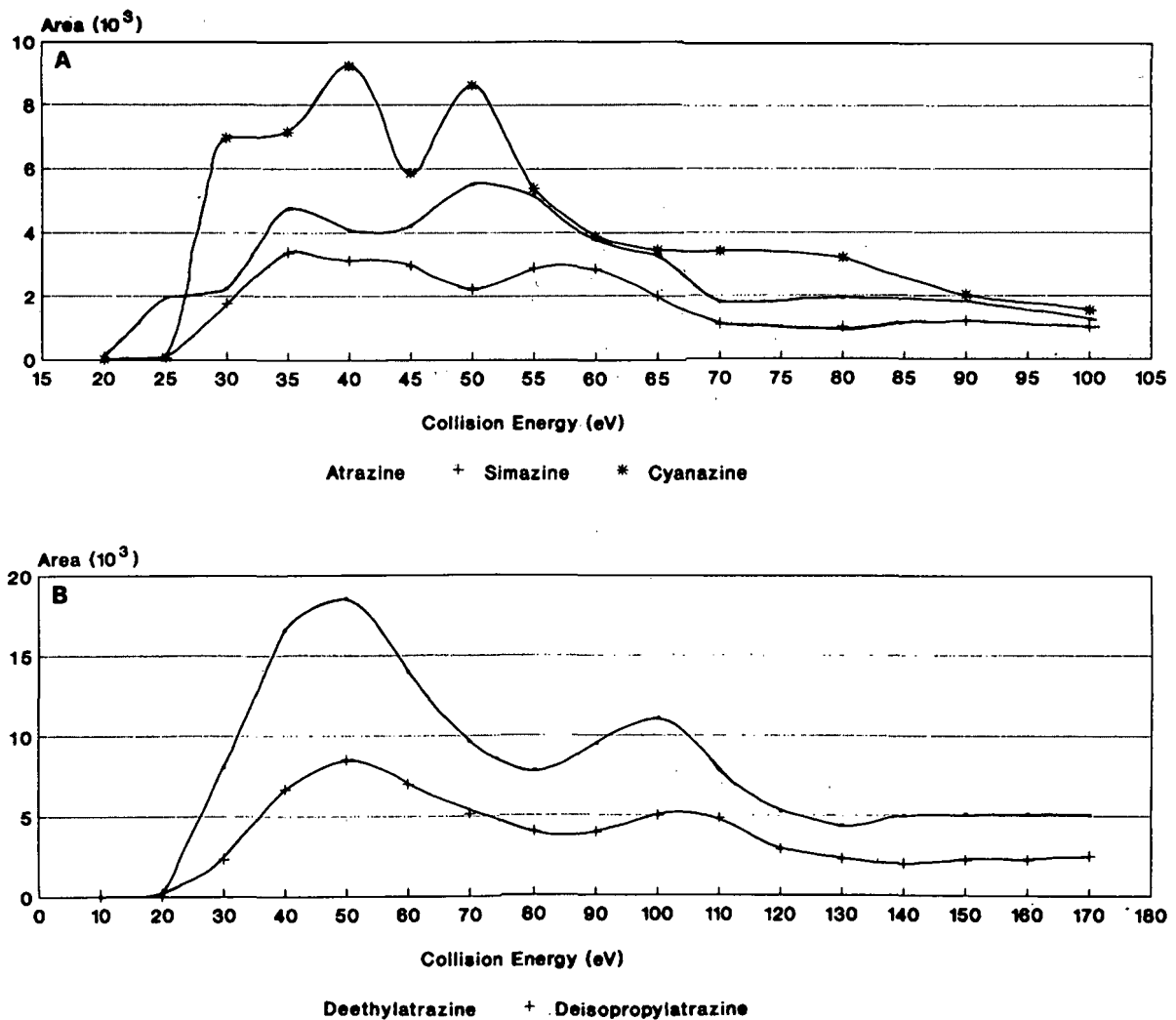


Fig. 2. Effect of the collision energy on formation of  $[M - CH_3]^+$  using GC-MS-MS with MRM for (A)  $\cdot$  = atrazine, + = simazine and \* = cyanazine and (B)  $\cdot$  = deethylatrazine and + = deisopropylatrazine.

## RESULTS AND DISCUSSION

*Tandem mass spectrometry*

Table II lists the major ions (relative abundance > 10%) in the CAD mass spectra of the chlorotriazine pesticides studied. Daughter ion spectra from the parent ion corresponding to  $[M]^{+\cdot}$  were obtained for all the compounds. Deethylatrazine, atrazine and cyanazine yielded additional daughter ions as their base peaks in their EI spectra corre-

sponded to  $[M - CH_3]^+$  ions. All the CAD spectra show characteristic ions of the structure or class of compound. It should be noted that the CAD spectra for deethylatrazine, atrazine and cyanazine for the two different parent ions,  $[M]^{+\cdot}$  and  $[M - CH_3]^+$ , are completely different.

When  $[M]^{+\cdot}$  is used as the parent ion, the daughter ion formed resembles the fragments obtained by conventional GC-MS in the EI mode [4,5,18]. Thus,  $CH_3$  loss is observed with all compounds.

TABLE II

CAD DAUGHTER IONS FROM CHLOROTRIAZINE PESTICIDES AND THEIR DEALKYLATED DEGRADATION PRODUCTS

MW	Compound	Parent ion (m/z)	Daughter ion (m/z), identification and relative abundance (%)
173	Deisopropylatrazine	173	173, $[M]^{+\cdot}$ (100) 158, $[M - CH_3]^+$ (20) 145, $[M - C_2H_4]^+$ (45) 69, $[M - NCNH - C_2H_4 - Cl]^+$ (10) 44, $[C_2H_5NH]^+$ (20)
187	Deethylatrazine	172	172, $[M - CH_3]^+$ (100) 104, $[M - HCN - C_3H_7]^+$ (20) 79, $[M - CH_3 - C_3H_6 - HCl]^+$ (10) 69, $[M - NCNH - C_3H_6 - Cl]^+$ (10)
		187	187, $[M]^{+\cdot}$ (100) 172, $[M - CH_3]^+$ (30) 145, $[M - C_3H_6]^+$ (10) 58, $[C_3H_7NH]^+$ (20)
201	Simazine	201	201, $[M]^{+\cdot}$ (100) 186, $[M - CH_3]^+$ (10) 173, $[M - C_2H_4]^+$ (70) 158, $[186 - C_2H_4]^+$ (20)
215	Atrazine	200	200, $[M - CH_3]^+$ (100) 158, $[M - C_3H_6 - CH_3]^+$ (15) 132, $[M - NCNH - C_3H_6]^+$ (45) 122, $[158 - HCl]^+$ (50) 104, $[132 - C_2H_4]^+$ (45) 96, $[132 - HCl]^+$ (20) 71, $[C_2H_5 - NH - CNH]^+$ (60)
		215	215, $[M]^{+\cdot}$ (100) 200, $[M - CH_3]^+$ (25) 173, $[M - C_3H_6]^+$ (40) 158, $[M - C_3H_6 - CH_3]^+$ (15) 58, $[C_3H_7NH]^+$ (15)
240	Cyanazine	225	225, $[M - CH_3]^+$ (100) 198, $[M - HCN - CH_3]^+$ (25) 189, $[M - HCl - CH_3]^+$ (30)
		240	240, $[M]^{+\cdot}$ (100) 225, $[M - CH_3]^+$ (50) 213, $[M - HCN]^+$ (30) 173, $[M - C(CN) - CH_3 - CH_3 + H]^+$ (15)

whereas  $C_2H_4$  loss is observed with deisopropylatrazine and simazine and  $C_3H_6$  loss with deethylatrazine and atrazine. Other fragments correspond to typical diagnostic ions with  $[C_2H_5NH]^+$  loss (e.g., deisopropylatrazine) or  $[C_3H_7NH]^+$  loss (e.g., deethylatrazine and atrazine) [4,5,19].

Other daughter ions obtained correspond to ring-opening reactions resulting in a signal at  $m/z$  132, 104 and 96 for atrazine and at  $m/z$  104 for deethylatrazine, indicating the presence of a  $C_2H_5$  group. For atrazine, this can lose a  $C_2H_4$  group to yield the fragment at  $m/z$  104. The daughter ions at  $m/z$  69 for deethylatrazine and deisopropylatrazine also correspond to the same ring-opening reactions, with an additional Cl loss for both compounds and  $C_3H_6$  and  $C_2H_5$  loss for deisopropylatrazine. The ion at  $m/z$  158 from atrazine corresponds to a loss of  $C_3H_6$  and  $CH_3$  groups, while the fragment ion at  $m/z$  71 confirms the presence of the  $C_2H_5$  group and a secondary amine structure.

The different fragmentation pattern observed for atrazine in GC-MS-MS is partly consistent with data obtained by GC-MS-MS with PCI [10], and also by other techniques such as LC-thermospray MS-MS [13] and LC-particle beam EI-MS [14]. The ions at  $m/z$  79 and 122 from deethylatrazine and atrazine, respectively, corresponding to  $CH_3$ ,  $C_3H_6$  and HCl losses, have also been observed by GC-MS with ion-trap detection [4].

The losses of  $HCN-CH_3$  and  $HCl-CH_3$  from cyanazine are consistent with results obtained by GC-EI-MS reported elsewhere [4,19]. The ion obtained at  $m/z$  173 was also observed by LC-thermospray-MS-MS [13] and corresponds to the loss of nitrile and a  $CH_3-C-CH_3$  group from cyanazine.

As triazines include a chlorine atom in their structure, the metastable transition from  $[M]^+$  to  $[M - CH_3]^+$  was monitored for each analyte by GC-MS-MS. This allowed us to use a common transition for all the chlorotriazines, which provided excellent responses and avoided the interferences between the chlorotriazines typical of other transitions (e.g.,  $[M]^+$  to  $[M^+ - C_3H_6]$  for atrazine).

### Selectivity

The selectivity of the different MS techniques studied was assessed by analysing a soil sample containing 37 ng/g of simazine and trace amounts of the other chlorotriazines. Fig. 3 shows the different

chromatograms obtained using (A) GC-LRMS, (B) GC-HRMS and (C) GC-MS-MS with MRM. The amount injected corresponds to ca. 700 pg of simazine.

As can be seen in Fig. 3A, several compounds yield the ions at  $m/z$  201.078 and 203.075, which do not allow the presence of simazine to be confirmed. Using GC-HRMS at a resolving power of 10 000 diminishes interferences from GC-HRMS traces, even though two main peaks corresponding to simazine are still obtained in the traces of the  $m/z$

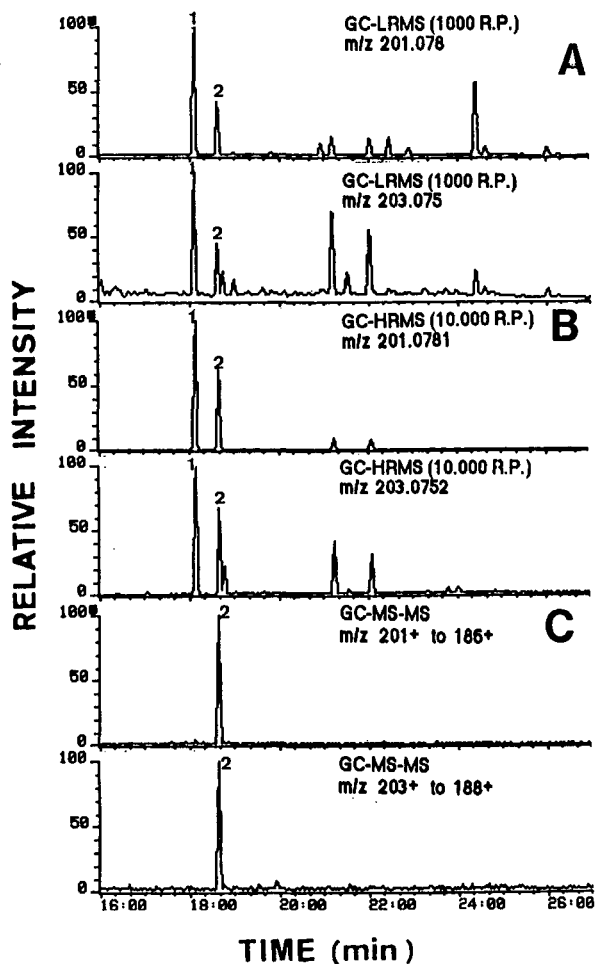


Fig. 3. Comparison of (A) GC-LRMS at a resolving power of 1000 (SIR of  $m/z$  201.078 and 203.075), (B) GC-HRMS at a resolving power of 10 000 (SIR of  $m/z$  201.0781 and 203.0752), (C) GC-MS-MS (MRM of transitions  $m/z$  201<sup>+</sup> to 186<sup>+</sup> and 203<sup>+</sup> to 188<sup>+</sup>) on a soil sample containing 270 ng/g of atrazine (peak 1) and 28 ng/g of simazine (peak 2).

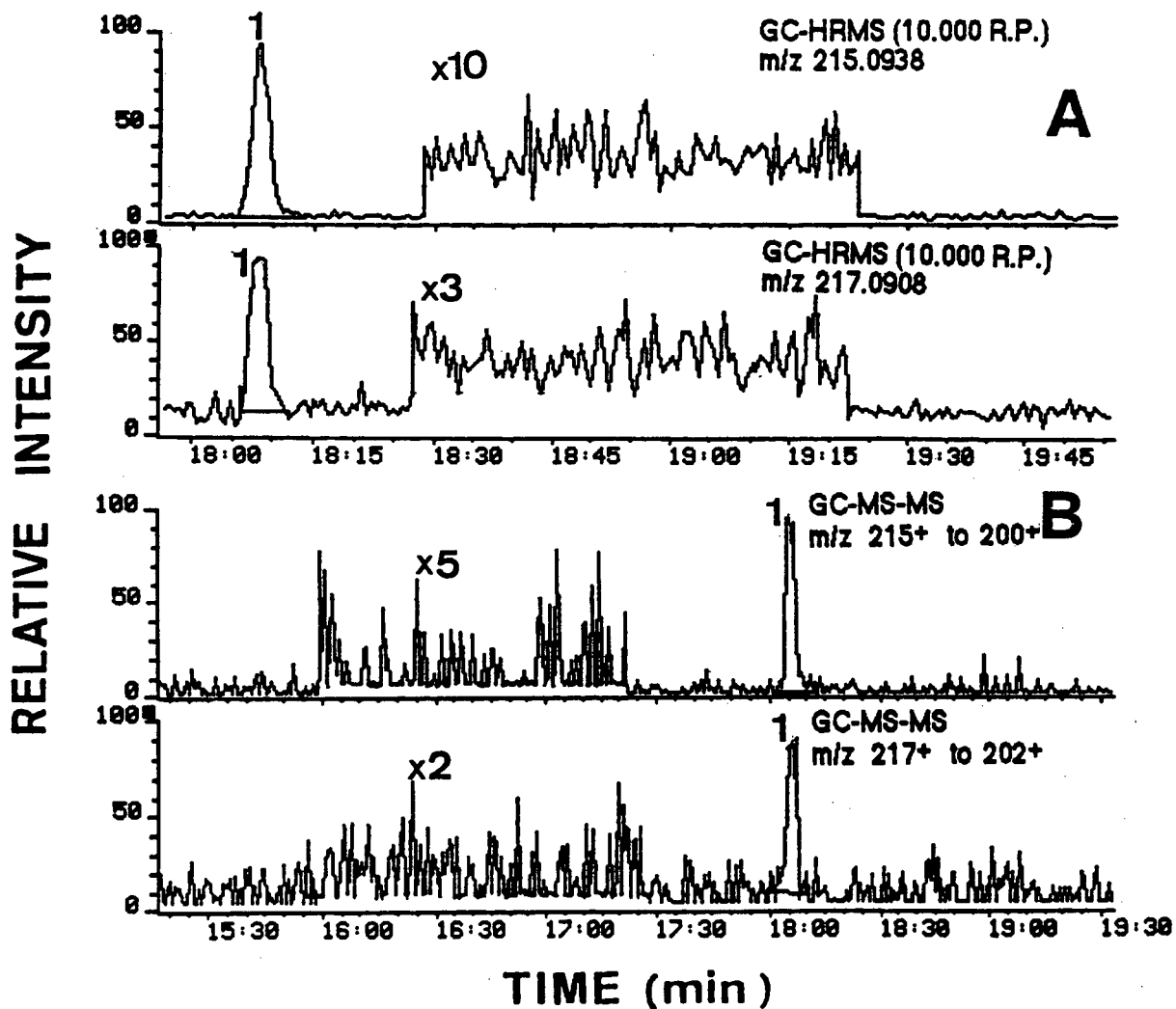


Fig. 4. Comparison of sensitivity for a 20-pg injection of atrazine using (A) GC-HRMS at a resolving power of 10 000 (SIR of  $m/z$  215.0938 and 217.0908) and (B) GC-MS-MS (MRM of transitions  $m/z$  215<sup>+</sup> to 200<sup>+</sup> and 217<sup>+</sup> to 202<sup>+</sup>). Time scale in min:s.

201.0781 and 203.0752 ions. Only GC-MS-MS provides the confirmation of simazine in soil samples with a high degree of certainty.

The problems encountered in both GC-LRMS and GC-HRMS arise from interferences from the other chlorotriazines, namely atrazine (peak 1) in the traces in Fig. 3A and B. In this example, the concentration of atrazine in the soil sample was *ca.* ten times higher than that of simazine. The appearance of the atrazine peak is to be expected when analysing for simazine residues as most formulations based on chlorotriazines contain a mixture of

the two compounds. Hence atrazine and simazine co-occur in many environmental matrices [4,5]. A second problem arises from the fact that the interference of atrazine on the simazine trace obtained by GC-HRMS at a resolving power of 10 000 is still significant. This is a result of the fragmentation of atrazine always causing  $\text{CH}_3$  loss and hence yielding traces of a compound with the same  $m/z$  as simazine, even at such a high resolving power. Therefore, GC-MS-MS is to be preferred to confirm the occurrence of different chlorotriazines in soil samples.

TABLE III

COMPARISON OF LIMITS OF DETECTION FOR THE CHLOROTRIAZINES BY GC-HRMS AND GC-MS-MS (MEAN RELATIVE STANDARD DEVIATION 25-30 %)

Pesticide	Quantitation ion ( <i>m/z</i> )	L.O.D. (pg)		
		GC-HRMS <sup>a</sup>	GC-MS-MS <sup>b</sup>	Ref. 10 <sup>c</sup>
Deisopropylatrazine	173.0468, 175.0439 173→158, 175→160	1	6	5000
Deethylatrazine	187.0625, 189.0595 187→172, 189→174	2	5	100
Simazine	201.0781, 203.0752 201→186, 203→188	4	15	100
Atrazine	215.0938, 217.0908 215→200, 217→202	4	20	100
Cyanazine	240.0890, 241.0861 240→225, 242→227	13	24	n.r. <sup>d</sup>

<sup>a</sup> Resolving power 10 000; S/N = 10.<sup>b</sup> MRM; S/N = 10.<sup>c</sup> Ref. 10: obtained with GC-MS-MS and PCI; S/N = 3.<sup>d</sup> Not reported.

### Sensitivity

Fig. 4 shows the GC-HRMS traces obtained by using the SIR of *m/z* 215.0703 and 217.0908 (Fig. 4A) and GC-MS-MS with the MRM mode of the transitions from 215 to 200 and from 217 to 202 (Fig. 4B). The amount injected corresponds to 15-20 pg of atrazine in both instances. The limits of detection (L.O.D.) at a signal-to-noise ratio (S/N)

of 10 for all the chlorotriazines are listed in Table III.

As can be seen from the chromatograms in Fig. 4, GC-HRMS and GC-MS-MS traces obtained by using <sup>37</sup>Cl are subject to higher noise levels than those obtained with <sup>35</sup>Cl because the isotope abundance of <sup>37</sup>Cl is about one third of the <sup>35</sup>Cl transition, and GC-HRMS features a slightly lower noise

TABLE IV

CONCENTRATIONS OF CHLOROTRIAZINE PESTICIDES AND THEIR DEALKYLATED DEGRADATION PRODUCTS FOUND IN SOIL SAMPLES

Pesticide	Quantitation ion ( <i>m/z</i> )	Concentration (ng/g)	
		GC-HRMS <sup>a</sup>	GC-MS-MS
Deisopropylatrazine	173.0468, 175.0439 173→158, 175→160	18	23
Deethylatrazine	187.0625, 189.0595 187→172, 189→174	109	100
Simazine	201.0781, 203.0752 201→186, 203→188	37	56
Atrazine	215.0938, 217.0908 215→200, 217→202	710	1000
Cyanazine	240.0890, 241.0861 240→225, 242→227	30	26

<sup>a</sup> Resolving power 5000 or 10 000.

level than GC–MS–MS at approximately the same response level. Hence the L.O.D. will be slightly better for GC–HRMS with SIR than for GC–MS–MS with MRM. This can be ascribed to the fact that, although MS–MS provides enhanced selectivity, as shown in Fig. 3, the chemical noise level decreases more gradually than the signal with decreasing absolute signal and noise levels, so a net reduction in S/N is observed.

GC–MS–MS is about five times less sensitive than GC–HRMS. The sensitivities are in the low picogram range (1–20 pg) S/N = 10, *i.e.*, they are better than those achieved with an L.O.D. of 100 pg at S/N = 3 using GC–MS–MS with PCI [10]. The mean relative standard deviation (R.S.D.) varied between 25 and 30%, *i.e.*, over a common range for these techniques at levels close to the L.O.D. As the two L.O.D.s were calculated at different S/N, it should be noted that the L.O.D. reported here is enhanced with respect to those obtained by GC–MS–MS with PCI by 1.5–2 orders of magnitude [10]. This increased sensitivity may be ascribed to the use of hybrid instruments rather than a triple quadrupole, the work reported in ref. 10 involved PCI with methane rather than EI and we achieved complete separation between deethylatrazine and deisopropylatrazine rather than the co-elution accomplished in ref. 10. In relation to this last point, we have reported [5] that the complete separation of atrazine, simazine and their delakylated degradation products requires a polar, short (15 m) GC column with elution profiles of increasing polarity rather than increasing molecular weight.

We analysed a soil sample by GC–HRMS at resolving powers of 5000 and 10 000 and by GC–MS–MS. The results obtained are summarized in Table IV as averages of triplicate injections, with a precision consistent to within  $\pm 10\%$ . The chlorotriazine pesticide standards yielded linear responses from 50 pg up to 10 ng. The differences in the concentrations obtained by the various techniques were between 25 and 30%, *i.e.* reasonably acceptable when compared to with determinations using coupled MS systems [15,20].

## CONCLUSIONS

GC–MS–MS with MRM and GC–HRMS at a resolving power of 10 000 are useful techniques for

the determination of chlorotriazines in polluted soil samples. GC–MS–MS has been shown to be even more selective than GC–HRMS at a resolving power of 10 000 for monitoring compounds of a given group (*e.g.*, chlorotriazines) yielding fragments of identical molecular weights. In addition, GC–MS–MS with MRM completely overcomes interferences from the polluted soil matrices containing chlorotriazines.

The L.O.D.s achieved by using either GC–HRMS with SIR or GC–MS–MS with MRM for the determination of chlorotriazines and their delakylated degradation products are a few picograms *i.e.*, 1.5–2 orders of magnitude lower than those afforded by triple quadrupole and conventional GC–MS with a single quadrupole instrument.

As all the triazines feature a common metastable transition in GC–MS–MS, namely from  $[M]^{+\bullet}$  to  $[M - CH_3]^+$ , this can be used as a common monitoring technique for screening chlorotriazines in environmental samples and provides an alternative to other GC–MS methods. In addition, unlike other MS techniques, GC–MS–MS offers two information levels for deethylatrazine, atrazine and cyanazine, which depend on the parent ion used ( $[M]^{+\bullet}$  or  $[M - CH_3]^+$ ). In each instance, completely different daughter ion spectra are obtained which can be used as complementary structural information for the identification of unknown chlorotriazine metabolites in environmental samples.

## ACKNOWLEDGEMENTS

Financial support from the BCR, Community Bureau of Reference of the Commission of The European Communities, is gratefully acknowledged. G. D. also acknowledges the award of a fellowship by the Commission of the European Communities (Contract ST2\*-0488).

## REFERENCES

- 1 A. E. Smith, D. C. G. Muir and P. Grover, in A. S. Y. Chau and B. K. Afghan (Editors), *Analysis of Pesticides in Water*, Vol. 3, CRC Press, Boca Raton, FL, 1982, Ch. 3.
- 2 H. O. Esser, G. Dupuis, E. Ebert, C. Vogel and G. J. Marco, in P. C. Kearney and D. D. Kauffman (Editors), *Herbicides, Chemistry, Degradation and Mode of Action*, Vol. 1, Marcel Dekker, New York, 1982, pp. 129–208.
- 3 G. Durand, G. R. Forteza and D. Barceló, *Chromatographia*, 28 (1989) 597.

- 4 W. E. Pereira, C. E. Rostad and T. J. Leiker, *Anal. Chim. Acta*, 228 (1990) 69.
- 5 G. Durand and D. Barceló, *Anal. Chim. Acta*, 243 (1991) 259.
- 6 L. H. Huang and M. J. I. Mattina, *Biomed. Environ. Mass Spectrom.*, 18 (1989) 828.
- 7 D. F. Hunt, J. Shabanowitz, M. Harvey and M. L. Coates, *J. Chromatogr.*, 271 (1983) 93.
- 8 K. Levsen, *Org. Mass Spectrom.*, 23 (1988) 406.
- 9 J. V. Johnson and R. A. Yost, *Anal. Chem.*, 57 (1985) 758A.
- 10 C. E. Rostad, W. E. Pereira and T. J. Leiker, *Biomed. Environ. Mass Spectrom.*, 18 (1989) 820.
- 11 J. A. Roach and L. J. Carson, *J. Assoc. Off. Anal. Chem.*, 70 (1987) 439.
- 12 S. V. Hummel and R. A. Yost, *Org. Mass Spectrom.*, 21 (1986) 785.
- 13 R. D. Voyksner, W. H. McFadden and S. A. Lammert, in J. D. Rosen (Editor), *Applications of New Mass Spectrometry Techniques in Pesticide Chemistry*, Wiley, New York, 1987, Ch. 17.
- 14 R. D. Voyksner, T. Pack, C. Smith, H. Swaisgood and D. Chen, in M. A. Brown (Editor), *Liquid Chromatography–Mass Spectrometry. Applications in Agricultural, Pharmaceutical, and Environmental Chemistry (ACS Symposium Series, Vol. 420)*, American Chemical Society, Washington, DC, 1990, Ch. 2.
- 15 L. D. Betwoski and T. L. Jones, *Environ. Sci. Technol.*, 22 (1988) 1430.
- 16 K. S. Chiu, A. Van Langenhove and C. Tanaka, *Org. Mass Spectrom.*, 18 (1989) 200.
- 17 M. J. Charles and Y. Tondeur, *Environ. Sci. Technol.*, 24 (1990) 1856.
- 18 D. Fraisse, M. F. Gonnord and M. Becchi, *Rapid Commun. Mass Spectrom.*, 3 (1989) 79.
- 19 R. Hites, *CRC Handbook of Mass Spectra of Environmental Contaminants*, CRC Press, Boca Raton, FL, 1985, pp. 1–434.
- 20 R. A. Yost, D. D. Fetterolf, J. R. Hass, D. J. Harvan, A. F. Weston, P. A. Skotnicki and N. M. Simon, *Anal. Chem.*, 56 (1984) 2223.

# Solventless determination of caffeine in beverages using solid-phase microextraction with fused-silica fibers

Steven B. Hawthorne and David J. Miller

*Energy and Environmental Research Center, University of North Dakota, Grand Forks, ND 58202 (USA)*

Janusz Pawliszyn and Catherine L. Arthur

*Department of Chemistry, University of Waterloo, Waterloo, Ontario N2L 3G1 (Canada)*

(First received December 30th, 1991; revised manuscript received February 11th, 1992)

---

## ABSTRACT

Caffeine concentrations in beverages were determined using a simple and rapid method based on microextraction of caffeine onto the surface of a fused-silica fiber. The uncoated fiber was dipped into the beverage sample for 5 min after the addition of isotopically labeled (trimethyl  $^{13}\text{C}$ )caffeine. The adsorbed caffeine was then thermally desorbed in a conventional split/splitless injection port, and the concentration of caffeine was determined using gas chromatography with mass spectrometric detection. Quantitative reproducibilities were *ca.* 5% (relative standard deviation) and the entire scheme including sample preparation and gas chromatographic analysis was completed in *ca.* 15 min per sample. The potential of the microextraction technique for the analysis of flavor and fragrance compounds in non-caffeinated beverages is also demonstrated. Since no solvents or class-fractionation steps are required, the method has good potential for automation.

---

## INTRODUCTION

Recent concerns about the use of liquid solvents for the extraction of dissolved analytes from water-based samples had led to the development of several solid-phase extraction methods in an effort to greatly reduce or eliminate the need for liquid solvents in routine laboratories [1,2]. The majority of such methods require that the sample is passed through a relatively large (several grams) sorbent packing followed by elution of the trapped analytes with a few milliliters of solvent. Present methods for the determination of caffeine in coffee, tea, and other liquids generally require pH adjustment and either liquid solvent extraction or solid-phase adsorption followed by elution of the caffeine with liquid solvents.

Analysis of the extracts is performed using gas chromatography (GC) or high-performance liquid chromatography (HPLC) [3–8]. However, methods that are solvent-free and simpler to automate for the analysis of caffeine in beverages are desirable, particularly for quality control applications and to satisfy regulatory requirements for products such as decaffeinated coffee [3,7].

A microextraction technique in which analytes are adsorbed directly onto a fused-silica fiber from water samples has recently been reported that completely eliminates the need for liquid solvents and solid-phase adsorbents [9,10]. This method utilizes a short length of fused-silica optical fiber which is mounted in a conventional GC syringe. Following exposure of the uncoated silica surface to the sample, adsorbed analytes are recovered from the fiber by thermal desorption in a conventional GC injection port. In the present study, isotopically labeled (trimethyl  $^{13}\text{C}$ ) caffeine was added as an internal

---

*Correspondence to:* Dr. S. B. Hawthorne, Energy and Environmental Research Center, University of North Dakota, Grand Forks, ND 58202, USA.

standard so that the native caffeine concentration could be directly determined without the need to obtain 100% extraction of the native caffeine onto the fiber. This approach has been developed in this study for the quantitation of caffeine in coffee, tea and carbonated beverages based on isotopic dilution analysis.

## EXPERIMENTAL

### Preparation of the fiber

The solid-phase microextraction (SPME) devices were constructed from polyimide-coated fused-silica optical fibers having outer diameters of *ca.* 170  $\mu\text{m}$  (Polymicro Technologies, Phoenix, AZ, USA) and a Hamilton series 7000 syringe. A 22-cm-long fiber was mounted in the syringe by placing a small

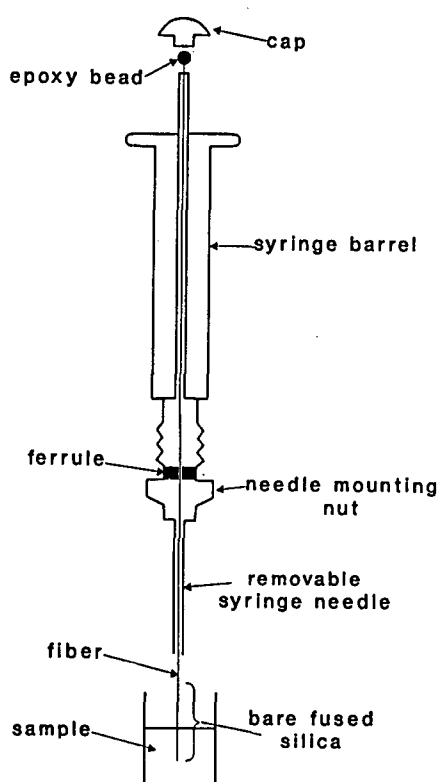


Fig. 1. Schematic of the SPME device assembled from a removable needle syringe. All components come with the syringe except for the fused-silica fiber and the epoxy bead on the end of the fiber. Construction of the device is described in the Experimental section.

drop of epoxy on one end of the fiber, allowing the epoxy to dry, and inserting the fiber through the hollow syringe plunger and the removable syringe needle. Thus, the fiber can be withdrawn into the syringe needle, or when the plunger is depressed, *ca.* 2 cm of the fiber extends out of the end of the syringe needle (Fig. 1). After the fiber was mounted in the syringe, the plunger was depressed to expose the end of the fiber, and the polyimide coating was carefully burned away from the last *ca.* 1.5 cm of the exposed end of the fiber with an oxygen-acetylene torch as shown in Fig. 1. The exposed end of the fiber was then briefly rinsed in methanol and cleaned for *ca.* 5 min by inserting into a heated (300°C) GC injection port. Mounting the fiber in the syringe in this manner provides a convenient method of protecting the uncoated portion of the fiber during storage and for inserting the fiber into the beverage samples and into the GC injection port. Construction and cleaning of a new SPME device requires *ca.* 15 min.

### Sample preparation and analysis

Regular coffee, decaffeinated coffee and tea were brewed as for normal consumption. All other beverages were used directly from the beverage container, except that they were allowed to warm to room temperature prior to analysis. No sample preparation steps were used except that, for the caffeine quantitations, 20  $\mu\text{l}$  of a methanol solution containing 150  $\mu\text{g}$  of isotopically labeled [ $^{13}\text{C}_3$ ]caffeine (trimethyl- $^{13}\text{C}_3$  purchased from Cambridge Isotope Laboratories, Woburn, MA, USA) was added to a 1-ml sample of each beverage which had been placed into a 1.5-ml autosampler vial. After brief mixing, *ca.* 1 cm of the end of the uncoated portion of the fiber was inserted into the sample to allow adsorption of the caffeine. (Mounting the syringe in a ring stand clamp prior to depressing the syringe plunger to insert the end of the fiber into the sample provides a simple way to reproducibly expose the same length of adsorbent surface for each analysis.) After the 5-min exposure period, the syringe plunger was withdrawn to pull the uncoated end of the fiber out of the sample and into the syringe needle. (Note that no water adheres to the fiber because of water's high surface tension, as described in ref. 9.) The syringe needle was then inserted into a heated (300°C) split/splitless injection

port to thermally desorb the adsorbed analytes into the GC–mass spectrometry (MS) system.

The sequential steps required to perform the method are:

(1) Pipette 1 ml of the sample beverage into a 1.5-ml autosampler vial, add the [ $^{13}\text{C}_3$ ]caffeine internal standard, and mix briefly.

(2) Depress the syringe plunger to insert *ca.* 1 cm of the uncoated end of the fused-silica fiber into the sample for 5 min (no mixing is required during the adsorption step). Then withdraw the uncoated end of the fiber out of the sample into the syringe needle.

(3) Insert the syringe needle into the GC injection port, close the split vent, and depress the syringe plunger to place the sample end of the fiber into the injection port liner.

(4) Let the adsorbed analytes thermally desorb for 1 min, withdraw the syringe plunger to pull the uncoated end of the fiber into the syringe needle, and remove the syringe from the injection port.

(5) Open the split vent, and perform a conventional GC separation.

#### GC–MS analysis conditions

All analyses were performed using a Hewlett-Packard Model 5985 GC–MS system equipped with a 25 m  $\times$  0.32 mm I.D. HP-5 column (Hewlett-Packard, 0.17  $\mu\text{m}$  film thickness) and a conventional unpacked injection port liner. No modification of the split/splitless injection port was required. During the splitless desorption step, the syringe was inserted through the injection port septum so that when the syringe plunger was depressed the sample end of the fiber was inside of the injection port liner *ca.* 1 cm above the inlet of the analytical column. (Sample desorption can also be performed in the split mode, and is preferred for samples with very high concentrations of analytes to avoid overloading the GC column stationary phase.) For the caffeine analyses, the GC column oven was maintained at 70°C during the 1 min desorption step so that the desorbed caffeine was efficiently focused at the head of the analytical column. After the desorption step was completed and the fiber was removed from the injection port, the split vent was opened, and the GC oven was heated at 30°C/min to 190°C, followed by a temperature ramp of 10°C/min to 280°C. Analyses of the non-caffeinated beverages were per-

formed in the same manner, except that the GC oven temperature was held at lower temperatures during the thermal desorption step to efficiently focus analytes that were more volatile than caffeine. All GC–MS analyses were performed using electron

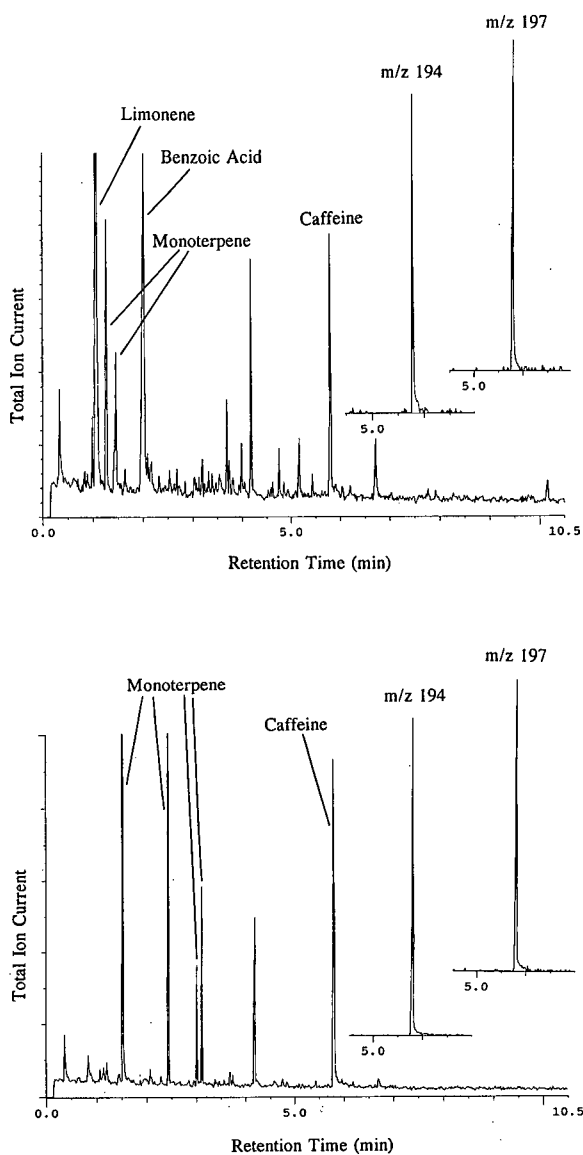


Fig. 2. GC–MS analysis of caffeine from a carbonated cola soft drink (top) and from brewed tea (bottom) using microextraction onto a fused-silica rod. The mass chromatograms for *m/z* 194 (caffeine) and *m/z* 197 ( $^{13}\text{C}_3$ ]caffeine) were generated from the reconstructed total ion current chromatograms (TIC). Microextraction and GC–MS conditions are given in the text.

impact ionization (70 eV) with a mass range of 50 to 300 a.m.u. The integrated areas from the mass chromatograms of the molecular ions (194 and 197 for caffeine and [ $^{13}\text{C}_3$ ]caffeine, respectively) were used for all quantitations.

## RESULTS AND DISCUSSION

Typical GC–MS chromatograms resulting from the SPME analysis of tea and a carbonated cola drink (Coca-Cola) are shown in Fig. 2. Both samples showed caffeine as a major peak along with several monoterpenes. The cola beverage also showed significant amounts of benzoic acid. Benzoic acid and the monoterpene, limonene, were also predominant species in many of the non-cola soft drinks tested. When the mass chromatograms were generated for the molecular ions of the native caffeine ( $m/z$  194) and the [ $^{13}\text{C}_3$ ]caffeine ( $m/z$  197), only the caffeine species showed significant chromatographic peaks for any of the caffeinated beverages tested (Fig. 2).

During the initial investigations, there was concern that adsorbed sample species, including caffeine or [ $^{13}\text{C}_3$ ]caffeine, might not be efficiently removed from the uncoated fiber during the one-minute thermal desorption step, and thus contaminate the fiber for subsequent samples. To determine whether analyte carryover could be a significant source of error, the SPME fiber was desorbed into the GC–MS a second time after the analysis of each beverage sample was completed. No carryover of analyte species could be observed in the second GC–MS analyses of any of the samples tested, demonstrating that one minute was sufficient for the thermal desorption step.

While carryover from sample to sample was not observed, two significant experimental problems were encountered during this study. First, there is a temptation for the analyst to touch the syringe needle to help guide the needle into the sample vial, or into the GC injection port. This procedure results in significant contamination, as shown by the SPME analyses of a coffee sample without touching the needle, and when the analyst guided the syringe needle into the injection port with his fingers. As shown in Fig. 3, touching the syringe needle causes significant peaks in the GC–MS chromatogram resulting from biological acids.

The second experimental problem occurs when care is not taken to protect the uncoated portion of the fused-silica fiber. Since the polyimide coating has been removed, this part of the fiber is somewhat brittle, and should be drawn into the syringe needle for physical protection unless the adsorption or desorption steps are being performed. However, with reasonable care, the fibers have good lifetimes, and all analyses in this study (> 100 microextractions) were performed with only two fibers. It is also reasonable to expect that the fiber could be deactivated from some sample matrices and, therefore, become

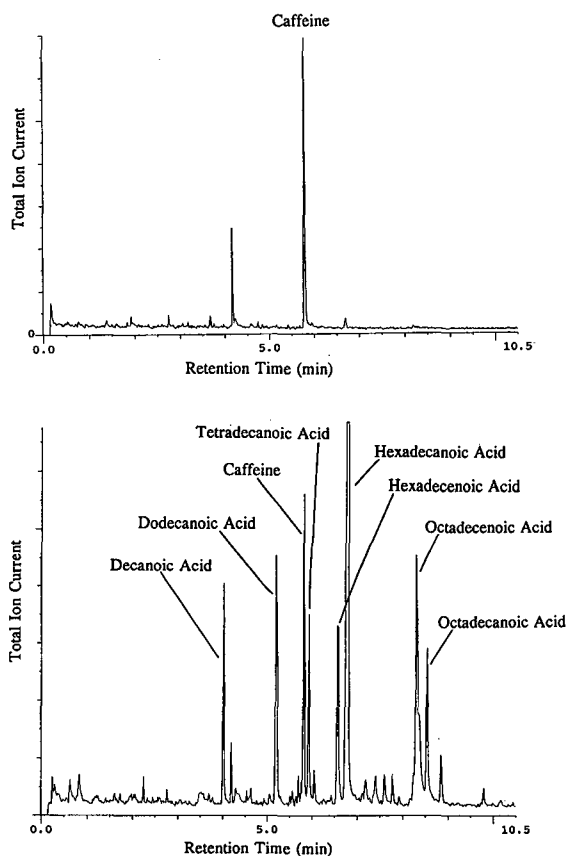


Fig. 3. Effect of touching the syringe needle on the analysis of coffee extracted using fused-silica rod microextraction followed by GC–MS. The top part of the figure shows a typical reconstructed total ion current chromatogram (TIC) of coffee. The bottom part of the figure shows the TIC chromatogram resulting from the analysis of an identical coffee sample when the analyst touched the syringe needle while inserting the needle into the GC injection port. Microextraction and GC–MS conditions are given in the text.

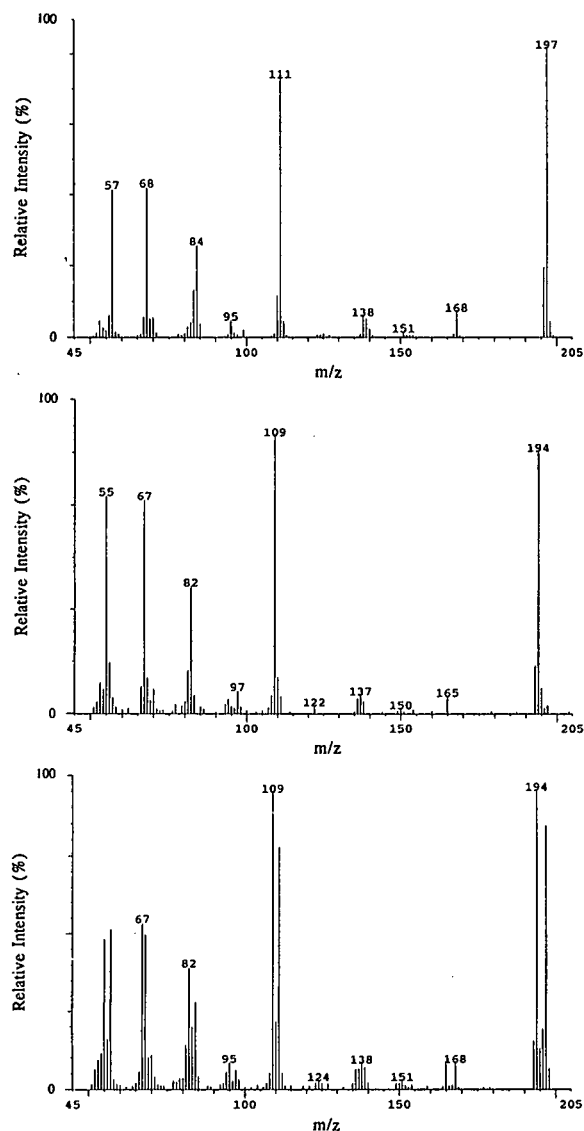


Fig. 4. Mass spectra of  $[^{13}\text{C}_3]$ caffeine (top), native caffeine from tea (middle), and the mixed caffeine- $[^{13}\text{C}_3]$ caffeine spectra from the analysis of a carbonated cola soft drink (bottom).

useless. However, no such loss of activity was observed for the samples used in this study.

Mass spectra for the native caffeine (from coffee) and the  $[^{13}\text{C}_3]$ caffeine standard are shown in Fig. 4 along with the mixed mass spectra of the caffeine chromatographic peak obtained from the analysis of the cola beverage. As shown in Fig. 4, the minimum overlap in the mass spectra occurred in the

molecular ion region. Since the molecular ions ( $m/z$  194 and 197) were also the most intense mass spectral peaks and showed no interfering chromatographic peaks in the analysis of the beverage samples, the ratio of the peak areas of  $m/z$  194 to  $m/z$  197 was used for all quantitations.

Quantitative standard curves were generated using two caffeine-free matrices, a cola drink (caffeine-free Coca-Cola), and HPLC-grade water. Standards were prepared by spiking 1-ml aliquots of the cola or water sample with 37.5, 75, 150, 375 and 750  $\mu\text{g}$  of caffeine in methanol. Each standard was then spiked with the internal standard (150  $\mu\text{g}$ ) and analyzed in a manner identical to that used for the samples. Prior to spiking with the caffeine standards, the caffeine-free cola was first analyzed using the SPME method, and no caffeine was detected.

Both the spiked caffeine-free cola and the water yielded similar standard curves, so subsequent calibration was performed using the caffeine-free cola. A typical standard curve based on the ratio of 194/197 peak areas is shown in Fig. 5, and displays acceptable linearity ( $r^2 = 0.998$ ) for quantitative calibration. It should be noted that the standard curve does not have an exact zero intercept whether the calibration matrix is pure water or caffeine-free cola. With the zero caffeine standard for both matrices, the 194/197 ratio was slightly above zero (*ca.* 0.01). This non-zero intercept was found to occur because of the presence of a small peak at  $m/z$  194 in

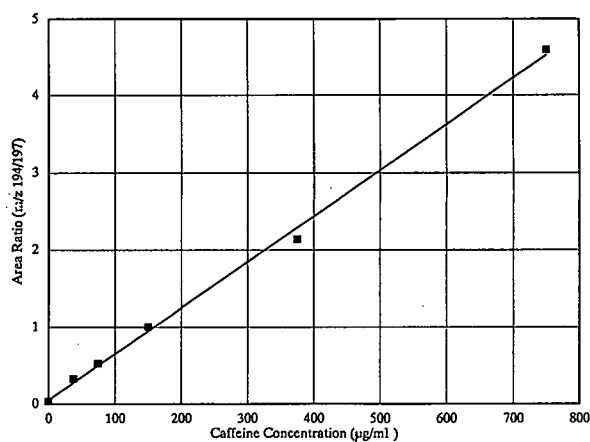


Fig. 5. Quantitative calibration curve based on the addition of caffeine to a caffeine-free cola drink containing 150  $\mu\text{g/ml}$  of  $[^{13}\text{C}_3]$ caffeine as an internal standard.

TABLE I  
QUANTITATION OF CAFFEINE IN BEVERAGES USING THE MICROEXTRACTION TECHNIQUE

Sample	Caffeine concentration ( $\mu\text{g/ml}$ )				$\bar{x} \pm \text{S.D.}^a$	Relative S.D. (%)
	Trial					
	1	2	3	4		
Coffee	295	290	291	292	$292 \pm 2$	0.7
Decaffeinated coffee	33	29	31	30	$31 \pm 1.7$	5.5
Tea	398	366	405	368	$384 \pm 20$	5.1
Diet cola	140	126	124	132	$131 \pm 7.2$	5.5

<sup>a</sup> Mean concentration  $\pm$  one standard deviation.

the mass spectra of the [ $^{13}\text{C}_3$ ]caffeine internal standard. Therefore, with the addition of 150  $\mu\text{g}$  internal standard, the practical detection limit was *ca.* 2  $\mu\text{g/ml}$  to have a 194/197 ratio twice the level of the zero calibration standard. The [ $^{13}\text{C}_3$ ]caffeine spike concentration of 150  $\mu\text{g/ml}$  was used in this study because it resulted in a concentration approximately in the range of the native caffeine in the samples studied. However, if lower detection limits are need-

ed, the sensitivity of the technique can be improved by adding less of the internal standard (and, therefore, adding less of the interfering  $m/z$  194 peak which is contributed by the [ $^{13}\text{C}_3$ ]caffeine). The analyses in this study were also performed in the full scan mode, since we were interested in identifying any species in addition to caffeine that may have been transferred to the GC by the SPME technique. However, additional sensitivity could also be

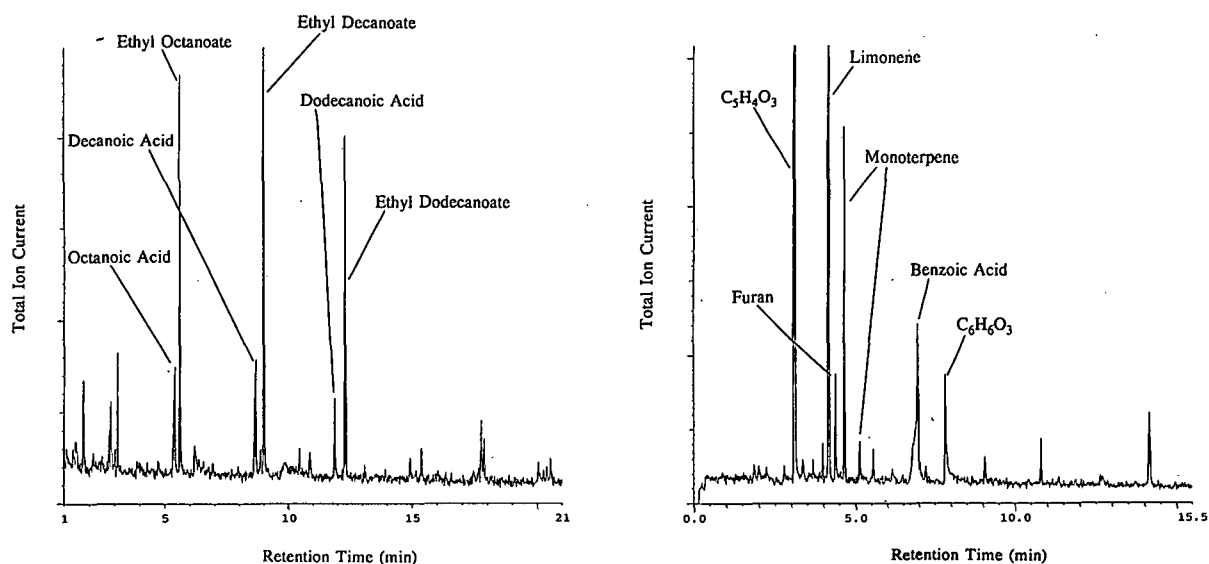


Fig. 6. SPME GC-MS analysis of flavor and fragrance compounds from lemon juice (left) and brandy (right). Both samples were extracted and analyzed as described in the Experimental section. GC oven temperature during the desorption of the fiber for lemon juice was 5°C followed by a temperature ramp of 30°C/min to 65°C, then a temperature ramp at 8°C/min. GC oven temperature during the desorption of the brandy sample was 20°C followed by a temperature ramp of 30°C/min to 80°C, then a temperature ramp at 8°C/minute. All peak identifications were based on the GC-MS analysis. The species labeled as  $\text{C}_5\text{H}_4\text{O}_3$  and  $\text{C}_6\text{H}_6\text{O}_3$  appear to be oxygenated furans.

gained by analyzing the samples using selected ion monitoring (*e.g.*, monitoring only the molecular ion of caffeine), and, with selected ion monitoring analysis, detection limits in the low ng/ml range have been achieved for caffeine in spiked water samples.

The ability of the SPME technique to yield reproducible results was investigated by performing replicate analyses of four samples including brewed coffee and decaffeinated coffee, tea, and a carbonated cola soft drink. Quadruplicate 1-ml aliquots of each sample were spiked with the internal standard and analyzed using the SPME technique. The results of these replicate analyses are shown in Table I. In general, the relative standard deviations were *ca.* 5%, which compare favorably with those reported for coffee of 2–7% using liquid solvent extraction [7] and 1–8% using solid-phase adsorption [3].

While quantitative investigations were performed only caffeine, the SPME technique may also be useful for analyzing beverages for a variety of flavor and fragrance compounds. SPME followed by GC–MS analysis of different types of samples including several carbonated soft drinks, fruit juices, and alcoholic beverages have shown acceptable chromatographic peaks for major flavor and fragrance compounds. As shown by the analysis of lemon juice and brandy in Fig. 6, SPME followed by GC analysis is a very simple and potentially useful qualitative analysis approach that requires no liquid solvents and virtually no sample preparation. However, quantitation of the individual species is not possible without the addition of an appropriate internal standard or a knowledge of the distribution

coefficient of each analyte species between the beverage sample and the fiber [9].

## CONCLUSIONS

Microextraction onto a fused-silica fiber followed by thermal desorption and capillary GC–MS isotope dilution analysis is a simple and rapid method for the quantitation of caffeine in beverages. Sample preparation consists solely of adding an internal standard, and, since all subsequent sample preparation and analysis steps are performed in a GC autosampler vial and require only the manipulation of a GC syringe, the method has good potential for automation.

## ACKNOWLEDGEMENT

The authors would like to thank the NATO Grants for International Collaboration in Research program for partial financial support.

## REFERENCES

- 1 P. R. Loconto, *LC · GC*, 9 (1991) 460.
- 2 C. Markell, D. F. Hagen and V. A. Bunnelle, *LC · GC*, 9 (1991) 332.
- 3 T. Kazi, *Colloq. Sci. Int. Cafe*, 12 (1988) 216.
- 4 S. H. Ashoor, G. J. Seperich, W. C. Monte, and J. Welty, *J. Assoc. Off. Anal. Chem.*, 66 (1983) 606.
- 5 J. L. Blauch and S. M. Tarka, *J. Food Sci.*, 48 (1983) 745.
- 6 D. S. Groisser, *Clin. Nutr.*, 31 (1978) 1727.
- 7 K. G. Sloman, *Colloq. Sci. Int. Cafe*, 9 (1980) 159.
- 8 D. W. Hill, B. T. McSharry and L. S. Trzupek, *J. Chem. Educ.*, 65 (1988) 907.
- 9 C. L. Arthur and J. Pawliszyn, *Anal. Chem.*, 62 (1990) 2145.
- 10 D. Louch, S. Motlagh and J. Pawliszyn, *Anal. Chem.*, in press.



# Characterization of a supercritical fluid chromatographic retention process with a large pressure drop by the temporal average density

Xin Zhang and Daniel E. Martire

*Department of Chemistry, Georgetown University, Washington, DC 20057 (USA).*

Richard G. Christensen

*Organic Analytical Research Division, National Institute of Standards and Technology, Gaithersburg, MD 20899 (USA)*

(First received December 31st, 1991; revised manuscript received February 27th, 1992)

---

## ABSTRACT

The characterization of supercritical fluid chromatographic retention by different forms of the average density, *viz.*, the temporal average density, the spatial average density and the arithmetic average density, is investigated in a system with appreciable pressure drop along the column. The logarithm of the capacity factor, when described in terms of the temporal average density, is independent of the pressure drop. Hence, supercritical fluid chromatographic retention processes can be characterized and represented by a hypothetical zero-pressure-drop system at a density equal to the temporal average density of the real system.

---

## INTRODUCTION

In supercritical fluid chromatography (SFC), the mobile phase is highly compressible and a pressure drop necessarily exists along the column, which usually varies from around 1 bar (1 bar =  $1 \cdot 10^5$  Pa) for a short capillary column, up to 30 bar for a conventional packed column and sometimes exceeding 150 bar for a column with small particles [1]. Therefore, there is always a density gradient along the length of an SFC column. As a solute band travels, it experiences varying conditions of mobile phase density; hence, the local retention may be significantly different at different positions along the column. At a specific column position, the local retention depends on the local density at that position. The local capacity factor,  $k'$ , which charac-

terizes solute retention in SFC, can, in general, be expressed as a function of local density,  $\rho$ , by [2]

$$\ln k' = a + b\rho + c\rho^2 \quad (1)$$

where  $a$ ,  $b$  and  $c$  are temperature-dependent quantities, independent of mobile phase density.

Eqn. 1 is a general expression for solute retention in SFC, derived from a unified theory of chromatography [2–5] and applicable to different types of SFC systems, such as those with a solid stationary phase, a fluid stationary phase or a chemically bonded stationary phase. The coefficients  $a$ ,  $b$  and  $c$  may be expressed in terms of molecular interaction parameters, which correspond to the chromatographic retention mechanism involved. Therefore, the relationship between the local retention and local density, namely, the coefficients  $a$ ,  $b$  and  $c$ , provide significant insight into the molecular interactions in the system to reveal the microscopic mechanism of retention. Unfortunately, but as is to be expected for

---

*Correspondence to:* Dr. D. E. Martire, Department of Chemistry, Georgetown University, Washington, DC 20057, USA.

an SFC system with a packed column, measurements of local retention and local density are usually not feasible. The experimentally measured or observed retention is an average of the local retention throughout the length of the column. In studying the physical chemistry of an SFC retention process using a packed column, a fundamental problem is to correlate the characteristic retention process with experimentally measured parameters.

Starting with Darcy's law, Martire [6] presented a generalized treatment of a packed column with a pressure drop and proposed three possible ways to express mobile phase average densities in an SFC column:

(1) Arithmetic average density,

$$\langle \rho \rangle_a = 0.5 (\rho_i + \rho_o) \quad (2)$$

where  $\rho_i$  and  $\rho_o$  denote the column inlet and outlet densities.

(2) Spatial average density, *i.e.*, the mobile phase density averaged over the length of the column ( $L$ ),

$$\langle \rho \rangle_x = \frac{\int_0^L \rho dx}{\int_0^L dx} = \frac{\int_{\rho_o}^{\rho_i} \rho D_x(\rho) d\rho}{\int_{\rho_o}^{\rho_i} D_x(\rho) d\rho} \quad (3)$$

where  $D_x(\rho)$  is the spatial distribution function, given by

$$D_x(\rho) = \eta^{-1} \rho \left( \frac{dP}{d\rho} \right)_T = (\eta\beta)^{-1} \quad (4)$$

where  $\eta$  is the viscosity of the mobile phase,  $P$  is the pressure,  $T$  is the temperature and  $\beta$  denotes the isothermal compressibility of the mobile phase.

(3) Temporal average density, *i.e.*, the mobile phase density averaged over the residence time ( $t_u$ ) in the column,

$$\langle \rho \rangle_t = \frac{\int_0^{t_u} \rho dt}{\int_0^{t_u} dt} = \frac{\int_{\rho_o}^{\rho_i} \rho D_t(\rho) d\rho}{\int_{\rho_o}^{\rho_i} D_t(\rho) d\rho} \quad (5)$$

where  $D_t(\rho)$  is the temporal distribution function, given by

$$D_t(\rho) = \eta^{-1} \rho^2 \left( \frac{dP}{d\rho} \right)_T = \rho(\eta\beta)^{-1} = \rho D_x(\rho) \quad (6)$$

It has also been shown [6] that the observed capacity factor is the temporal average capacity factor,

$$\langle k' \rangle_{\text{obs}} = \langle k' \rangle_t \quad (7)$$

To study the relationship between the observed retention and average density, it is reasonable to assume that the logarithm of the observed capacity factor is a quadratic function of the average mobile phase density, similar in form to the fundamental eqn. 1,

$$\ln \langle k' \rangle_{\text{obs}} = \ln \langle k' \rangle_t = a' + b' \langle \rho \rangle_y + c' \langle \rho \rangle_y^2 \quad (8)$$

where subscript  $y$  may be either  $t$  for temporal average,  $x$  for spatial average or  $a$  for arithmetic average, and  $a'$ ,  $b'$  and  $c'$  are the fitting coefficients at a given temperature, independent of mobile phase density.

There has not yet been a sound mathematical link between eqns. 1 and 8. Nevertheless, eqn. 8 can be regarded as a logical extension of eqn. 1 and as an empirical equation. In this experimental study, we demonstrate that the SFC retention process can be better characterized by the temporal average density than by either the frequently employed arithmetic average density or the spatial average density, and that the SFC retention process can be characterized and represented by a hypothetical zero-pressure-drop system at a density equal to the temporal average density of the real system.

#### EXPERIMENTAL<sup>a</sup>

The experiment was carried out on an HP 79887A SFC system (Hewlett-Packard, CA, USA). The system consisted of a variable-wavelength UV detector, a pump assembly with a refrigerated circulating bath which was maintained at  $-10$  to  $-5^\circ\text{C}$ , a back-pressure regulator which controlled the column outlet pressure, a manual injection valve and two pressure gauges for the inlet and outlet pressures of the column, respectively. The temperature control and pressure gauges of the system were carefully

<sup>a</sup> Certain commercial equipment, instruments or materials are identified in order to adequately specify the experimental procedure. This does not imply recommendation or endorsement by the National Institute of Standards and Technology.

calibrated. The temperature was controlled to within 0.2°C, and the error in the pressure readout was less than 1 bar.

The column used in this study was a silica high-performance liquid chromatography column, 25 cm × 4.6 mm I.D., 5-μm particle size. Carbon dioxide, SFC grade, was employed as the mobile phase, and benzene, methyl-, ethyl-, *n*-propyl- and *n*-butylbenzene as the probe solutes.

Since there was extra tubing between the column ends and the pressure gauges, the measured inlet and outlet pressures (the inlet and outlet pressure readouts) were different from the actual column inlet and outlet pressures. The pressure drops and the residence time of the solutes caused by this extra tubing were carefully determined through a series of calculations and by replacing the packed column by an empty column of the same diameter [7]. With these corrections, the true inlet and outlet pressures of the column, and the true solute retention times were accurately obtained.

The column void volume ( $V_0$ ) was measured by a weighing method as follows: using *n*-hexane as the solvent to fill the dry column, the void volume was calculated by dividing the difference in the column weights (in grams, obtained before and after the solvent filling), by the density of hexane (g/ml). The void volume was measured at both the beginning and the end of the experiment and the agreement between the two measurements was within 1%. The flow-rate of the mobile phase leaving the system was measured in l/min, at ambient temperature and pressure, using a wet test flow meter. This flow-rate was converted into mass flow-rate, expressed as g of carbon dioxide/min, using the equation of state of an ideal gas. The average density of carbon dioxide, in forms of the spatial, the temporal and the arithmetic averages, was calculated by a computational program, knowing the inlet and outlet pressures, and using the Benedict–Webb–Rubin (BWR) equation of state (see ref. 8). Then, the corrected solute retention volume was obtained by the following equation:

$$V_R = \frac{t_R \cdot \dot{m}}{\langle \rho \rangle_x} \quad (9)$$

where  $t_R$  is the corrected retention time (min),  $\dot{m}$  is the mass flow-rate of the mobile phase (g/min) and  $\langle \rho \rangle_x$  is the spatial average density.

Ultimately, the natural logarithm of the observed capacity factor was calculated as

$$\ln \langle k' \rangle_{\text{obs}} = \ln \left( \frac{V_R - V_0}{V_0} \right) \quad (10)$$

## RESULTS

In the experiments, the outlet pressure of the column was kept constant and the inlet pressure was varied by adjusting the flow-rate to generate the desired pressure drop. Some typical experimental results for ethylbenzene at various temperatures from 50 to 80°C are listed in Table I, corresponding to the calculated temporal, spatial, and arithmetic average density.

As seen in Fig. 1, plots of the logarithm of the observed capacity factor vs. the pressure drop give monotonically decreasing curves at constant outlet pressure. The decrease of the observed capacity factor with increasing pressure drop is due to the increase in the average density, in contrast to that observed with constant inlet density [9], where the average density decreases with increasing pressure drop.

Using the experimental data for ethylbenzene listed in Table I, plots of the logarithm of the observed capacity factor vs. the different forms of average density, as shown in Figs. 2–5, indicate that the logarithm of the observed capacity factor is better related to the temporal average density than to the other forms of average density, especially at the lower temperatures.

At the lower temperatures, as illustrated in Figs. 2 (at 50°C) and 3 (at 60°C), when characterized by the temporal average density, regardless of the outlet pressure, the observed capacity factor of ethylbenzene follows a continuous, smooth curve at a given temperature. However, if one of the other average densities is employed, each of the curves then splits up into two or three separate and incompatible curves corresponding to the different outlet pressures. The separation and incompatibility of the curves are even more pronounced when using the arithmetic average density than the spatial average density, due to the markedly non-linear distribution of the mobile phase density along the column [8]. The three forms of the average density have different dependencies on the mobile phase

TABLE I

## LOGARITHM OF THE OBSERVED CAPACITY FACTOR OF ETHYLBENZENE

$T$ (°C)	Outlet pressure (bar)	Pressure drop (bar)	Temporal average density (g/ml)	Spatial average density (g/ml)	Arithmetic average density (g/ml)	$\ln \langle k' \rangle$ ethyl- benzene
50	90	13.4	0.362	0.357	0.361	1.085
	90	18.8	0.405	0.396	0.398	0.697
	90	27.0	0.464	0.448	0.439	0.370
	90	31.2	0.493	0.475	0.457	0.178
	105	5.7	0.483	0.482	0.481	0.343
	105	11.4	0.515	0.513	0.508	0.129
	105	16.9	0.544	0.540	0.530	-0.048
	105	23.1	0.571	0.567	0.551	-0.229
	120	3.8	0.599	0.599	0.598	-0.408
	120	10.4	0.619	0.618	0.616	-0.470
	120	18.2	0.636	0.636	0.631	-0.583
	120	22.2	0.647	0.646	0.640	-0.619
	120	27.5	0.659	0.658	0.650	-0.771
	60	90	13.4	0.277	0.275	0.276
90		20.2	0.309	0.304	0.307	1.478
90		27.0	0.399	0.331	0.335	1.206
90		33.2	0.372	0.359	0.362	0.916
90		39.2	0.404	0.388	0.387	0.705
90		44.9	0.435	0.415	0.409	0.524
90		51.7	0.467	0.444	0.430	0.350
105		4.7	0.345	0.345	0.345	1.227
105		12.4	0.374	0.372	0.372	0.992
105		16.9	0.397	0.393	0.393	0.776
105		23.2	0.427	0.421	0.419	0.567
105		30.4	0.461	0.452	0.445	0.327
120		6.8	0.463	0.462	0.461	0.372
120		11.4	0.481	0.484	0.478	0.250
120		19.0	0.509	0.507	0.502	0.077
70		90	14.4	0.240	0.239	0.239
	90	23.6	0.267	0.264	0.265	1.873
	90	27.9	0.283	0.278	0.280	1.733
	90	36.1	0.312	0.303	0.306	1.481
	90	39.9	0.329	0.319	0.321	1.314
	90	49.8	0.368	0.352	0.353	1.055
	90	55.5	0.393	0.374	0.372	0.839
	105	6.7	0.288	0.287	0.287	1.568
	105	12.4	0.303	0.302	0.303	1.423
	105	17.9	0.323	0.320	0.321	1.258
	105	25.2	0.349	0.344	0.345	1.046
	105	31.4	0.372	0.365	0.365	0.877
	105	38.4	0.399	0.390	0.388	0.678
	105	43.4	0.419	0.408	0.404	0.538
	105	49.2	0.442	0.428	0.420	0.381
	120	10.4	0.379	0.378	0.378	0.916
	120	18.9	0.407	0.405	0.404	0.697
	120	25.1	0.430	0.426	0.424	0.564

TABLE I (continued)

$T$ (°C)	Outlet pressure (bar)	Pressure drop (bar)	Temporal average density (g/ml)	Spatial average density (g/ml)	Arithmetic average density (g/ml)	$\ln \langle k' \rangle$ ethyl- benzene
70	120	30.3	0.449	0.444	0.439	0.409
	120	36.6	0.470	0.463	0.456	0.270
	120	44.1	0.494	0.486	0.475	0.129
	120	53.0	0.518	0.509	0.493	-0.020
80	90	12.7	0.211	0.211	0.211	2.144
	90	18.4	0.222	0.222	0.222	2.064
	90	26.8	0.243	0.240	0.240	1.926
	90	31.1	0.255	0.251	0.251	1.779
	90	37.3	0.273	0.266	0.267	1.674
	90	43.3	0.292	0.283	0.284	1.506
	90	50.4	0.314	0.303	0.303	1.307
	90	56.2	0.334	0.320	0.319	1.114
	105	6.7	0.252	0.252	0.252	1.719
	105	13.4	0.267	0.266	0.266	1.594
	105	21.9	0.288	0.286	0.286	1.416
	105	28.2	0.306	0.302	0.302	1.277
	105	33.4	0.322	0.317	0.317	1.146
	105	40.5	0.344	0.337	0.336	0.976
	105	45.5	0.360	0.351	0.350	0.857
	105	52.2	0.383	0.371	0.368	0.681
	120	5.8	0.310	0.309	0.309	1.222
	120	10.4	0.321	0.320	0.320	1.125
	120	19.2	0.343	0.342	0.341	0.976
	120	26.3	0.364	0.361	0.360	0.809
120	29.5	0.375	0.372	0.370	0.713	
120	36.6	0.396	0.390	0.388	0.576	
120	43.6	0.417	0.410	0.405	0.431	
120	50.5	0.437	0.428	0.421	0.337	

density distribution. The temporal average density is the most sensitive to the density distribution while the arithmetic average density is totally independent of the density distribution. Therefore, when the density distribution of the mobile phase is highly non-linear, use of the arithmetic average density to characterize SFC retention will result in the largest errors.

At the higher temperatures, as illustrated in Figs. 4 (at 70°C) and 5 (at 80°C), the interesting differences in the characterization using the different forms of average density disappear, and all three forms are equally good in correlating the logarithm of the observed capacity factor of ethylbenzene. The reason is that, for a specific pressure drop, the density gradient along the column is a function of tempera-

ture, and it is smaller at high temperature (*i.e.*, when the temperature is much higher than the critical temperature) than at low temperature (*i.e.*, when the temperature is closer to the critical temperature, where the density strongly depends on the pressure). Thus, when the temperature is high, the arithmetic average density, the spatial average density and the temporal average density become nearly identical.

It has been reported that at constant mean density of the mobile phase, the observed retention is a function of the pressure drop of the system [9,10]. However, it should be noted that the reported experiment was carried out at constant arithmetic average density rather than constant temporal average density. Because the mobile phase spends relatively more time in the high density region of the

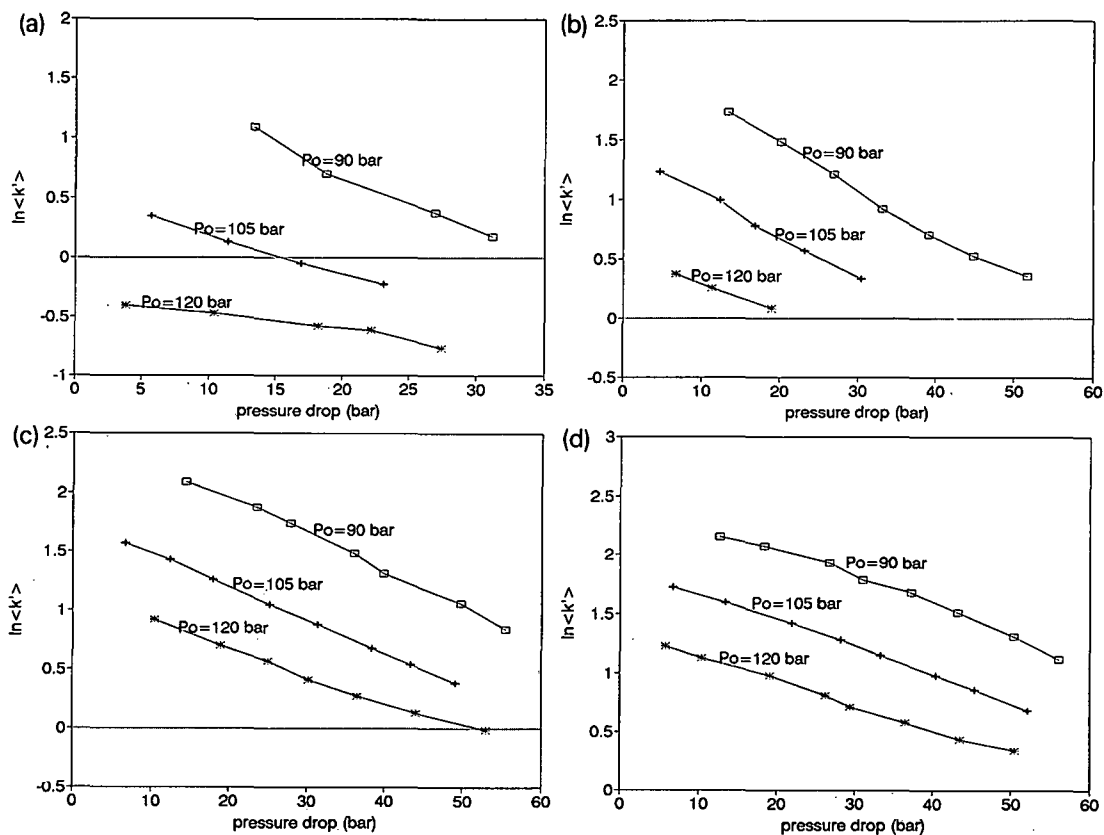


Fig. 1. Plots of the logarithm of the observed capacity factor,  $\ln \langle k' \rangle$ , vs. the pressure drop for ethylbenzene at (a) 50, (b) 60, (c) 70 and (d) 80°C, and the outlet pressure indicated.

column, the temporal average density is always higher than the arithmetic average density (see Table I), and the difference between the arithmetic average density and the temporal average density becomes more significant with a larger pressure drop [8]. At constant arithmetic average density, the temporal average density actually increases with increasing pressure drop. Therefore, at constant arithmetic average density, the observed capacity factor is expected to decrease with pressure drop due to the increase in the temporal average density.

Plots of  $\ln \langle k' \rangle_{\text{obs}}$  vs. pressure drop are illustrated in Fig. 1. Extrapolation of the plots to zero pressure drop presumably gives the  $\ln k'$  values at the set outlet density for a hypothetical column having zero pressure drop. The logarithm of the observed capacity factor can be empirically fit to a linear function of pressured drop ( $\Delta P$ ),  $\ln \langle k' \rangle_{\text{obs}} = a + b\Delta P$ , and the

intercepts are the extrapolated values of  $\ln \langle k' \rangle_{\text{obs}}$  at the outlet density. The extrapolated values of  $\ln \langle k' \rangle_{\text{obs}}$  for ethylbenzene at various outlet densities and temperatures are listed in Table II.

The extrapolated, zero-pressure-drop data approximately represent the local  $\ln k'$  values at the corresponding (outlet) densities. Incorporating the extrapolated  $\ln k'$  values into Figs. 2a–5a illustrates that the extrapolated zero-pressure-drop data fall on the curves characterized by the temporal average density. This suggests that the hypothetical curves of local  $\ln k'$  vs. local density, which are described by eqn. 1 and are supposed to pass through the extrapolated zero-pressure-drop data points, closely match the characterization curves of  $\ln \langle k' \rangle_{\text{obs}}$  vs. the temporal average density, which are expressed by eqn. 8. Accordingly, the retention process may be characterized and represented by a hypothetical

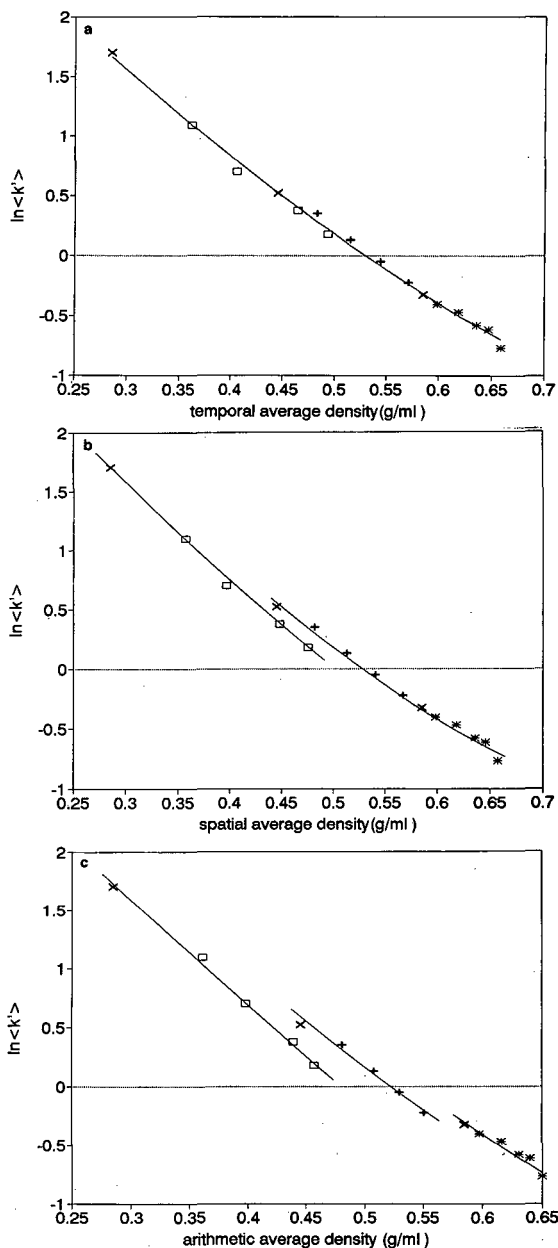


Fig. 2. Plots of the logarithm of the observed capacity factor,  $\ln \langle k' \rangle$ , vs. (a) the temporal average density, (b) the spatial average density and (c) the arithmetic average density, for ethylbenzene at 50°C;  $\times$  from extrapolation to  $\Delta P = 0$ . Symbols as in Fig. 1.

zero-pressure-drop system at a density equal to the temporal average density of the real system. Therefore, this suggests that, for a packed column SFC system, the fundamental coefficients  $a$ ,  $b$  and  $c$  in

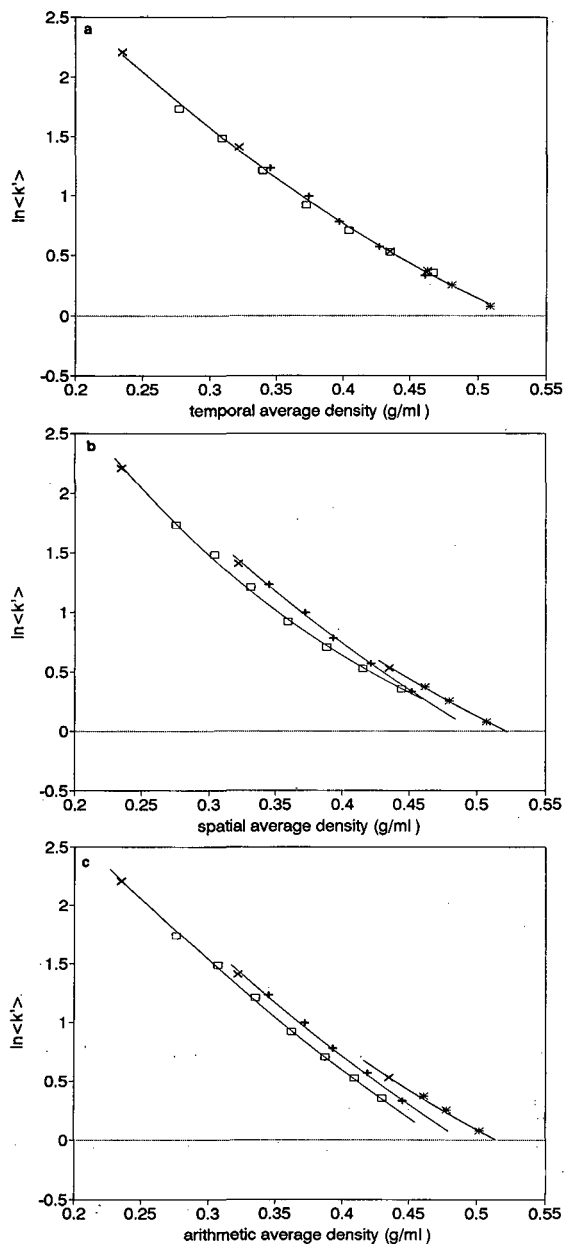


Fig. 3. Plots of the logarithm of the observed capacity factor,  $\ln \langle k' \rangle$ , vs. (a) the temporal average density, (b) the spatial average density and (c) the arithmetic average density, for ethylbenzene at 60°C;  $\times$  from extrapolation to  $\Delta P = 0$ . Symbols as in Fig. 1.

eqn. 1 should be essentially equal to the coefficients  $a'$ ,  $b'$  and  $c'$  in eqn. 8, which may be obtained from the regression of  $\ln \langle k' \rangle_{\text{obs}}$  vs.  $\langle \rho \rangle_t$  (see below).

Fig. 6 shows the behavior of homologues. The

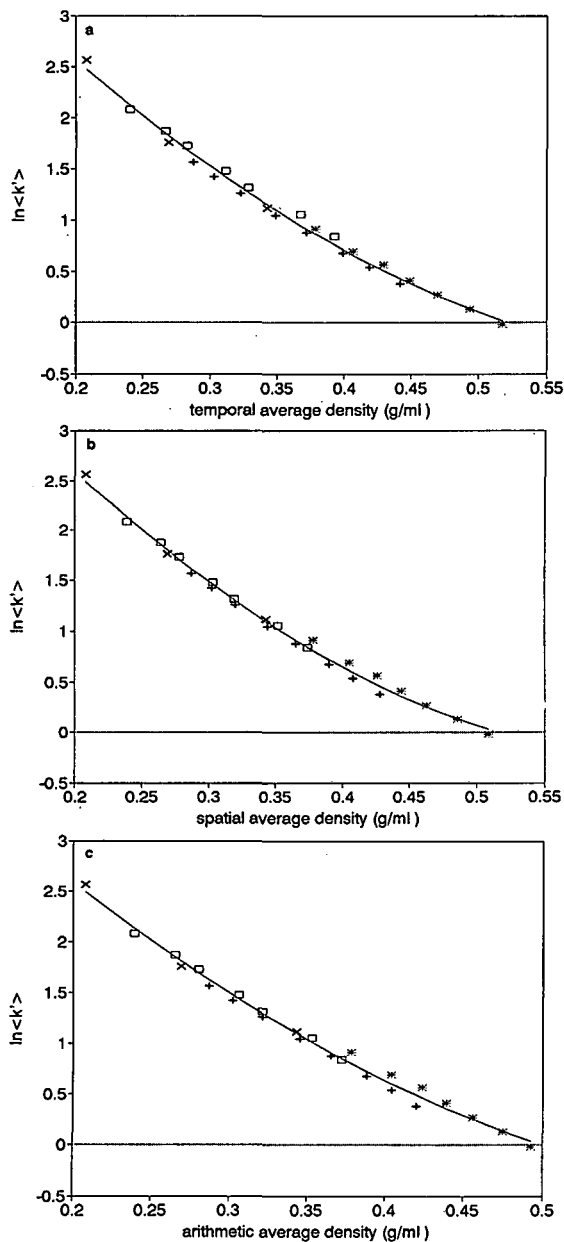


Fig. 4. Plots of the logarithm of the observed capacity factor,  $\ln \langle k' \rangle$ , vs. (a) the temporal average density, (b) the spatial average density and (c) the arithmetic average density, for ethylbenzene at 70°C;  $\times$  from extrapolation to  $\Delta P = 0$ . Symbols as in Fig. 1.

vertical distance between the curves of the solutes represents the logarithm of the selectivity factor. As long as the retention process is characterized by the temporal average density, the selectivity will be

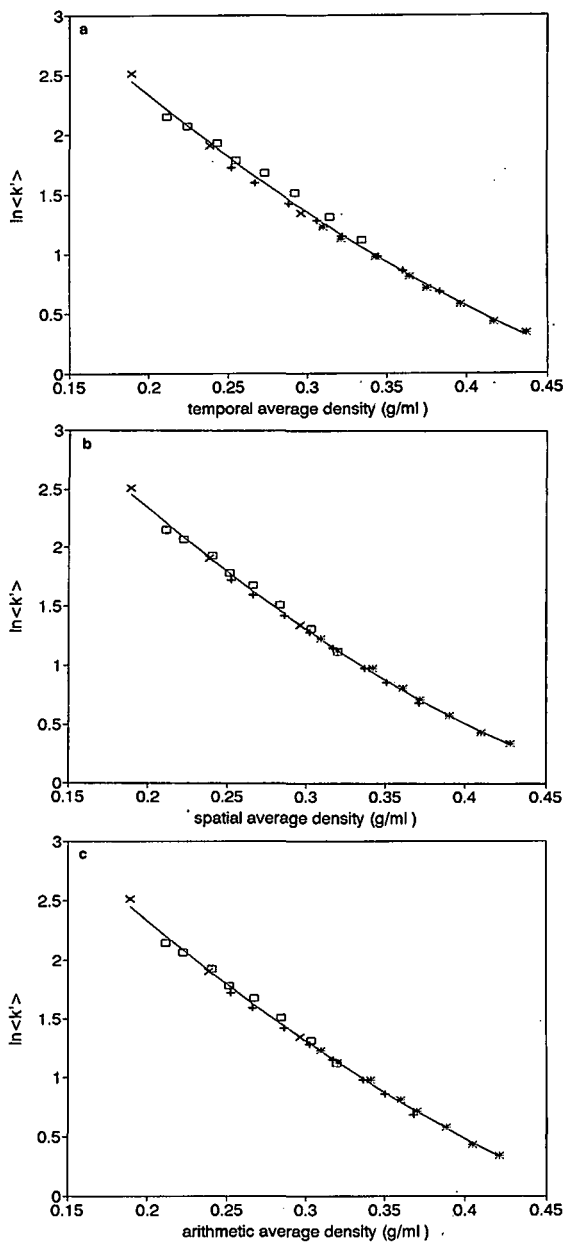


Fig. 5. Plots of the logarithm of the observed capacity factor,  $\ln \langle k' \rangle$ , vs. (a) the temporal average density, (b) the spatial average density and (c) the arithmetic average density, for ethylbenzene at 80°C;  $\times$  from extrapolation to  $\Delta P = 0$ . Symbols as in Fig. 1.

unique and exclusive at a given temperature and density, independent of the pressure drop and the outlet pressure.

TABLE II  
EXTRAPOLATED LN  $k'$  VALUES AT THE VARIOUS  
OUTLET DENSITIES AND TEMPERATURES FOR  
ETHYLBENZENE

Temperature (°C)		Outlet pressure (bar)		
		90	105	120
50	$\rho_o$ (g/ml)	0.285	0.445	0.585
	$\ln k'$	1.695	0.517	-0.331
60	$\rho_o$ (g/ml)	0.235	0.322	0.435
	$\ln k'$	2.203	1.402	0.531
70	$\rho_o$ (g/ml)	0.208	0.269	0.343
	$\ln k'$	2.568	1.762	1.117
80	$\rho_o$ (g/ml)	0.189	0.238	0.296
	$\ln k'$	2.508	1.901	1.341

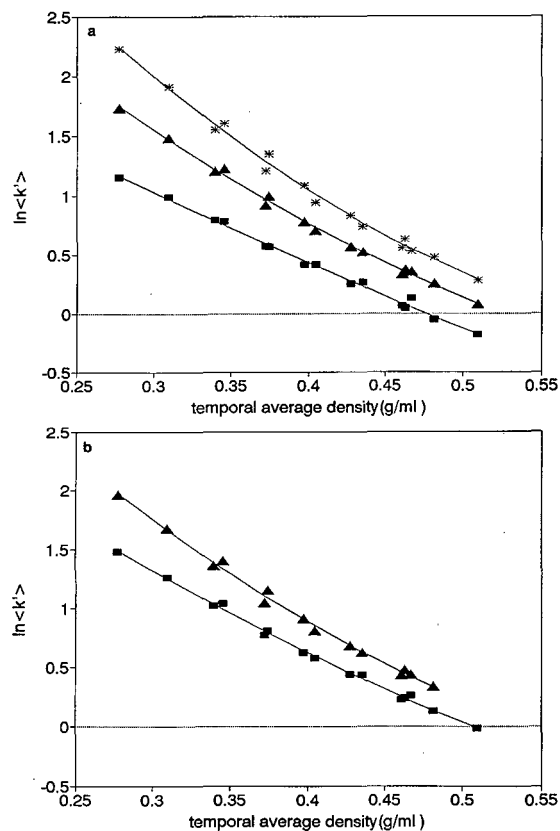


Fig. 6. The logarithm of the observed capacity factor,  $\ln \langle k' \rangle$ , characterized by the temporal average density for (a) benzene (■), ethylbenzene (▲), *n*-butylbenzene (\*), and (b) methylbenzene (■) and *n*-propylbenzene (▲), at 60°C.

## DISCUSSION

As indicated, SFC retention described in terms of the temporal average density of the mobile phase is independent of the pressure drop or the ratio of the inlet to the outlet pressure for the column. Since the plots of  $\ln \langle k' \rangle_{\text{obs}}$  vs.  $\langle \rho \rangle_t$  match the presumed plots of local  $\ln k'$  vs. local density, the true relation between  $\ln k'$  and local density (eqn. 1) may be represented by the relation between  $\ln \langle k' \rangle_{\text{obs}}$  and the temporal average density (eqn. 8). Therefore, the temporal average density is the parameter that should be chosen to characterize the retention process.

However, in practical SFC applications, *e.g.*, in SFC methods development, the arithmetic average density is often employed for simplicity. When there is a large density gradient along the column, use of the arithmetic average density to characterize SFC retention may result in large deviations leading to poor reproducibility, since at constant arithmetic average density SFC retention is also a function of the pressure drop. For example, as shown in Fig. 2, at constant temporal average density the observed capacity factor is unique, while at constant arithmetic average density the observed capacity factor can be different, depending on the pressure drop. One way to estimate potential discrepancies from the use of the arithmetic average density in correlating and representing experimental data in packed column SFC systems, instead of using the temporal average density, is to examine the relative deviation of the arithmetic average density from the temporal average density,

$$\Delta(\%) = \left( \frac{\langle \rho \rangle_t - \langle \rho \rangle_a}{\langle \rho \rangle_t} \right) \cdot 100\% \quad (11)$$

The values of the relative deviation  $\Delta(\%)$  were calculated as a function of pressure drop at various temperatures. The results are illustrated in Fig. 7, which shows that the relative deviation increases substantially with increasing pressure drop at constant temperature and a constant outlet pressure of 90 bar. For example, it approaches 10% at a practical operating condition of 40 bar in pressure drop, 90 bar in outlet pressure and 50°C. Due to the high compressibility of the supercritical fluid, the deviations become much more significant at lower temperature.

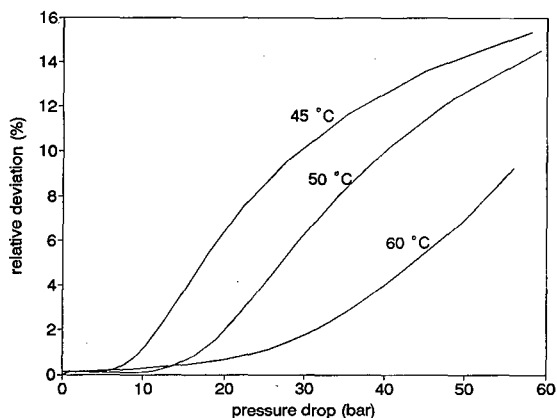


Fig. 7. The relative deviations, defined by eqn. 11, as a function of the pressure drop at an outlet pressure of 90 bar and the temperatures indicated.

The average density depends on the density gradient (density drop and density distribution) along the length of the column and the column temperature. When the density gradient is minimal and/or the density profile is relatively linear, the arithmetic average density, the spatial average density and the temporal average density are nearly identical; therefore, the three forms of density are equally valid in characterizing the observed retention, such as in the following cases,

(a) when the pressure drop along the column is small;

(b) when the temperature is substantially higher than the critical temperature [8]; and/or

(c) when the column outlet density is sufficiently greater than the critical density [8].

As mentioned in the introduction, a theoretical linkage between the expression for local retention (eqn. 1) and the expression for observed retention (eqn. 8) is lacking. It has been shown that the observed capacity factor is the temporal averaged one, as expressed by eqn. 7. According to the definition of the temporal average, the observed capacity factor ought to be expressed as

$$\langle k' \rangle_{\text{obs}} = \langle k' \rangle_t = \frac{\int_{\rho_0}^{\rho_i} k' D_t(\rho) d\rho}{\int_{\rho_0}^{\rho_i} D_t(\rho) d\rho}$$

$$\begin{aligned} &= \frac{\int_{\rho_0}^{\rho_i} [\exp(a + b\rho + c\rho^2)] D_t(\rho) d\rho}{\int_{\rho_0}^{\rho_i} D_t(\rho) d\rho} \\ &= \langle \exp(a + b\rho + c\rho^2) \rangle_t \end{aligned} \quad (12)$$

The observed capacity factors,  $\langle k \rangle_{\text{obs}}$ , were calculated according to eqn. 12, with assumed coefficients  $a$ ,  $b$  and  $c$ , and a series of given inlet and outlet densities. However, using the same set of coefficient values as  $a$ ,  $b$  and  $c$  in eqn. 12 for  $a'$ ,  $b'$  and  $c'$  in eqn. 8 (with  $\langle \rho \rangle_y = \langle \rho \rangle_t$ ), the capacity factor calculated from eqn. 12 and the capacity factor calculated from eqn. 8 become obviously different as the pressure drop substantially increases, particularly at 50 and 60°C. There are two possible explanations for this difference.

(1) The mathematical treatment leading to eqn. 12 is rigorous. Therefore, the capacity factor calculated from eqn. 12 should be the true value of the observed capacity factor for the given coefficients  $a$ ,  $b$  and  $c$ , and the given inlet and outlet densities, provided eqn. 12 can be accurately evaluated numerically. The deviation of the experimentally observed capacity factor from the characteristic value at large pressure drop might then be due to one or more of the following: (a) a thermal non-equilibrium [9] as the highly compressible mobile phase expands from the high density region near the column inlet towards the low density region near the column outlet; (b) a mass-transfer non-equilibrium [11] at large pressure drop and high flow-rate; and (c) turbulent flow in the column. (All the equations for the temporal and spatial parameters are derived based on Darcy's law which is only valid in laminar flow for apparent Reynolds number within an upper limit. The Reynolds numbers for the experiments were calculated, revealing that in some runs with very high flow-rates, thus very large pressure drops, they fell in the laminar/turbulent transition region, and therefore, turbulence might be occurring under those conditions.) If the above explanation is valid, the fitting coefficients  $a'$ ,  $b'$  and  $c'$  from eqn. 8 would not strictly represent the physicochemical parameters for an equilibrium SFC system. Instead, they would reflect the comprehensive effect of both the microscopic molecular interactions and the macroscopic flow dynamics.

(2) If the experimentally measured capacity factor is obtained under near-equilibrium conditions and it is the characteristic value of the system, then the fitting coefficients  $a'$ ,  $b'$  and  $c'$  from eqn. 8 would have physicochemical significance. The deviation of the capacity factor calculated by eqn. 12 from the experimentally measured capacity factor might then be due to error in implementing the numerical integration of eqn. 12. Involved in the integration of eqn. 12 is the core of the distribution function,  $\eta^{-1}(\partial P/\partial \rho)$ , which was evaluated using the equation of state and tabulated viscosity data, and fit to a seventh-order polynomial in reduced density at a given temperature [8]. By this method, the numerical integration of eqn. 12 becomes extremely sensitive when the inlet and outlet mobile phase densities fall in the vicinity of the minimum region in the core of the distribution function as a function of density [8], which may result in error in the observed capacity factor calculated by the numerical integration of eqn. 12.

Further investigation of these pressure-drop effects is currently underway.

#### CONCLUSIONS

This experimental study reveals that, in a packed column SFC system with a large pressure drop, (a) the chromatographic retention of solutes can be best characterized by the temporal average density of the mobile phase at a given temperature, (b) the retention processes may be represented by a hypothetical zero-pressure-drop system at a density equal to the temporal average density of the real system, and (c) when using the temporal average density to characterize the observed retention, physicochemically meaningful parameters  $a$ ,  $b$  and  $c$  in the local

retention–local density relations (eqn. 1) may be obtainable from the coefficients  $a$ ,  $b$  and  $c$ , by fitting the observed retention as a function of the temporal average density (eqn. 8, with  $y = t$ ).

#### ACKNOWLEDGEMENTS

This material is based upon work supported at Georgetown University by the National Science Foundation under Grant No. CHE-8902735. The authors are also grateful to R. L. Riester for providing an average density computation package, and to the National Institute of Standards and Technology for granting guest-researcher privileges to X.Z.

#### REFERENCES

- 1 D. R. Gere, R. Board and D. McManigill, *Anal. Chem.*, 55 (1983) 1370.
- 2 D. E. Martire, R. L. Riester and X. Zhang, in F. Bondi and G. Guiochon (Editors), *Theoretical Advancement in Chromatography and Related Separation Techniques*, Kluwer, Dordrecht, in press.
- 3 D. E. Martire and R. E. Boehm, *J. Phys. Chem.*, 91 (1987) 2433.
- 4 D. E. Martire, *J. Chromatogr.*, 452 (1988) 17.
- 5 D. E. Martire and R. E. Boehm, *J. Phys. Chem.*, 87 (1983) 1045.
- 6 D. E. Martire, *J. Chromatogr.*, 461 (1989) 165.
- 7 X. Zhang, *Doctoral Dissertation*, Georgetown University, Washington, DC, 1991.
- 8 D. E. Martire, R. L. Riester, T. J. Bruno, A. Hussam and D. P. Poe, *J. Chromatogr.*, 545 (1991) 135.
- 9 P. J. Schoenmakers and F. C. C. J. G. Verhoeven, *J. Chromatogr.*, 352 (1986) 315.
- 10 P. J. Schoenmakers and L. G. M. Uunk, *Chromatographia*, 24 (1987) 51.
- 11 J. C. Giddings, *Unified Separation Science*, Wiley, New York, 1991.



# Retention characteristics of high-molecular-weight compounds in capillary supercritical fluid chromatography

Luther D. Giddings, Susan V. Olesik and Lars A. Pekay

*Department of Chemistry, Ohio State University, Columbus, OH 43210 (USA)*

Edward Marti

*Research and Information Services, Ashland Chemical Inc., 5200 Blazer Parkway, Dublin, OH 43017 (USA)*

(First received August 27th, 1991; revised manuscript received March 3rd, 1992)

---

## ABSTRACT

The separation of oligomers of two different polymers using capillary supercritical fluid chromatography was studied. Pressure programming was used to achieve optimum separation of the oligomers. From a comparison of the separation of these oligomers with different length columns it was demonstrated that oligomer solubility was primarily controlling the separation. Accordingly, changing the stationary phase, shortening the column or not even using a stationary phase had minimal effect on the separation of the oligomers.

---

## INTRODUCTION

Supercritical fluid chromatography (SFC) provides a powerful technique for the separation of oligomers in polymer samples. A wide variety of natural and synthetic polymers have been separated. Many combinations of mobile phase, stationary phase, and operating conditions are available for use. Such diversity may make it possible to separate polymers that are presently problematic when using other techniques.

Interactions between the mobile phase and the oligomers are of primary importance to polymer separations in SFC. While the stationary phase affects retention, the mechanism by which it contributes is unclear [1]. For packed SFC columns the postulated separation process involves continuous reprecipitation and redissolution of the oligomers as they move down the column [2]. As a result of the

pressure drop across the column and the existence of threshold pressures or threshold densities for each oligomer [3], the higher-molecular-weight oligomers follow the smaller ones down the column. The validity of this retention mechanism has been substantiated by experimental results showing that the nature of the stationary phase has little impact on the selectivity of the oligomer separation [4]. Due to the nature of the retention mechanism in packed-column SFC of oligomers, gradient programming is required to achieve optimum separation of the oligomers [5]. Pressure programming and the resultant density programming were the first gradient methods used to separate polymers [3] and remains the most common gradient methods used for oligomer separations.

Capillary columns of the dimensions used in this study have negligible pressure drop across the column. The retention mechanism based on precipitation–redissolution as a function of pressure drop is therefore not applicable to capillary columns. This paper illustrates the relative importance of oligomer solubility and oligomer–stationary phase interac-

---

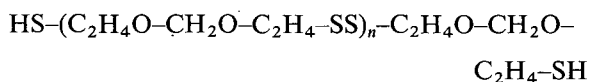
*Correspondence to:* Dr. S. V. Olesik, Department of Chemistry, Ohio State University, Columbus, OH 43210, USA.

tions for two very different polymer systems: a polydisulfide and a methylmethacrylate(MMA)-*n*-butylacrylate (BA) copolymer.

## EXPERIMENTAL

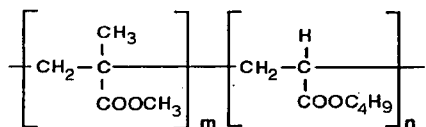
### Polymers and samples

Thiokol LP-3 is a polydisulfide elastomer that is produced by Morton Thiokol. It is used as a sealant and as an additive for high molecular weight polymer synthesis. The polydisulfides are good sealants because they exhibit high resistance to organic solvent, *i.e.* the solubility of these elastomers in organic solvents is minimal. However, we have recently demonstrated that the LP-3 polymer is soluble in supercritical CO<sub>2</sub> [6]. The approximate molecular structure of the polydisulfide repeating unit is as follows (this structure does not include any subunits due to cross-linking reactions):



Thiokol LP-3 was obtained from Polysciences (Warrington, PA, USA) and was used without further purification.

The repeating unit of the MMA-BA copolymer has the following molecular structure:



where *m* usually ranges from 10 to 18 and *n* values vary between 0 and 7, with *n* = 2 being the most common [7]. Oligomers ranging in molecular weight from 600 to 3500 have been identified using mass spectroscopy [7]. There are at least 72 oligomers theoretically possible in the molecular weight range from 1000 to 2700. These copolymers are used for the manufacture of many types of plastics. The specific MMA-BA copolymer studied was made by combining 80% (w/w) MMA and 20% (w/w) BA of the monomers. The polymer was obtained from the Marshall Laboratories of E.I. du Pont de Nemours & Co.

Table I shows other properties of the two oligomer systems used in this study. The analyzed

samples were made by diluting bulk polymer to 10% (w/w) with reagent-grade carbon disulfide (J. T. Baker). This concentration, although high, was necessary because many of the oligomers in the samples were not detectable at lower bulk sample concentrations.

### Instrumentation: MMA-BA studies

The chromatograph in the MMA-BA studies consisted of a Varian 3700 gas chromatographic oven and a Varian flame ionization detector. A 20 m × 100 μm I.D. DB-17 (polyphenylmethylsiloxane) open tubular column with a film thickness of 0.2 μm was used as purchased (J&W Scientific). A 20 m × 100 μm I.D. DB-225 (polycyanopropylphenylmethylsiloxane) open tubular column with a film thickness of 0.1 μm was also used as purchased (J&W Scientific). The mobile phase consisted of SFC-grade carbon dioxide (Matheson) modified with 0.5–1.3% (v/v) of 95–97% formic acid (Aldrich). An ISCO 260D syringe pump was used to deliver the mobile phase. Sample introduction was accomplished with a Valco CI4W injector with a 60-nl sample loop. Upon injection the sample loop was left in line with the column for the duration of the run. This is to prevent discrimination against high-molecular-weight analytes. Cycling of the valve introduces a pressure drop in the injection loop, and the concomitant density reduction may render the mobile phase solvent strength inadequate for solvation of heavier components in a sample.

### Instrumentation: polydisulfide studies

The chromatographic system and operating conditions used have been described in detail elsewhere [6]. A Hewlett-Packard 5890A gas chromatograph and a Hewlett-Packard Model 19256A flame pho-

TABLE I  
PHYSICAL PROPERTIES OF POLYMERS STUDIED

*M<sub>n</sub>* = Number-average molecular weight; *M<sub>w</sub>* = weight-average molecular weight; *D* (polydispersity) = *M<sub>w</sub>*/*M<sub>n</sub>*.

	<i>M<sub>n</sub></i>	<i>M<sub>w</sub></i>	<i>D</i>
Thiokol LP-3	540	1500	2.8
MMA-BA	750	1300	1.70

tometric detector served as the system oven and detector. A 12.2 m  $\times$  220  $\mu$ m I.D. BP-10 (polyphenylmethylsiloxane) open tubular column with a film thickness of 0.25  $\mu$ m was used (Scientific Glass Engineering, Austin, TX, USA). The stationary phase was cross-linked with azo-*tert*-butane before exposure to a supercritical fluid mobile phase. A 12.2 m  $\times$  250  $\mu$ m I.D. fused-silica capillary (Polymicro Technologies, Phoenix, AZ, USA) was also employed as a column. The fused-silica tubing was rinsed with methylene chloride and then flushed with dry nitrogen before use. The mobile phase used in the polydisulfide studies consisted of supercritical-grade carbon dioxide (Scott Specialty Gases). An ISCO  $\mu$ LC500 syringe pump delivered the mobile phase. Sample introduction was accomplished with a Valco CI4W injector with a 200-nl sample loop. As in the MMA–BA studies, upon injection the sample loop was left in line with the column for the duration of the analysis.

In all studies, integral restrictors constructed from 50  $\mu$ m I.D. fused-silica tubing (Polymicro Technologies) were used to regulate pressure and to control flow. The orifice diameter of the restricting capillary was approximately 5  $\mu$ m.

## RESULTS AND DISCUSSION

### *Polydisulfide studies*

The chromatographic separation of Thiokol LP-3 on the BP-10 column is shown in Fig. 1. Fig. 2 shows separation of the Thiokol LP-3 when the column is replaced with a fused-silica open tube with the same internal diameter and length as the column. Identical chromatographic conditions were used in the separation of LP-3 with the column and the fused-silica tube. These conditions included using carbon dioxide as the mobile phase, an oven temperature of 100°C, and an initial pressure of 102 atm for 15 min, followed by a pressure ramp of 3.4 atm/min to a final pressure of 306 atm. The polydisulfide was crudely separated in the fused-silica open tube, without the benefit of interaction with a stationary phase. The resulting chromatogram mimicked the results obtained when the BP-10 column was used under the same experimental conditions. The BP-10 column separation produced three sets of peaks, each peak being composed of one or more oligomers. The fused-silica tube separation lacked the resolution of

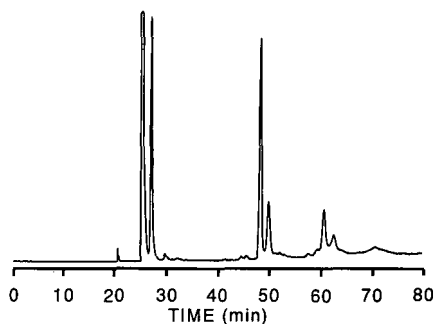


Fig. 1. Separation of Thiokol LP-3 on the 12.2-m BP-10 column. Oven temperature: 100°C. Mobile phase: carbon dioxide. Initial pressure: 102 atm for 15 min. Pressure ramp: 3.4 atm/min. Final pressure: 306 atm. Detector gas flows: 240 ml/min hydrogen, 45 ml/min oxygen. From ref. 7.

the column chromatogram, but reproduced the three principle peak clusters.

These results give insight into the retention mechanism of polymers in capillary SFC. The separations observed in the fused-silica tube can be attributed to the selective solvation of oligomers as the mobile phase density was ramped. Isobaric conditions did not permit a satisfactory separation to occur. If the initial pressure was too low, there was no sample elution. If the initial pressure was too high, the oligomers coeluted. With isobaric runs at an intermediate pressure, fewer peaks were observed. We attribute the separation achieved without stationary phase in the fused-silica tube to the selective solvation of the oligomers by the supercritical fluid. The polydisulfide must initially precipitate out onto the

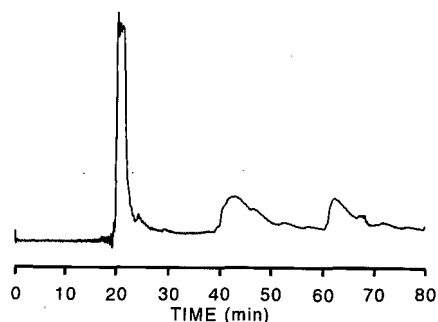


Fig. 2. Separation of Thiokol LP-3 on the 12.2-m fused-silica tube. Oven temperature: 100°C. Mobile phase: carbon dioxide. Initial pressure: 102 atm for 15 min. Pressure ramp: 3.4 atm/min. Final pressure: 306 atm. Detector gas flows: 240 ml/min hydrogen, 45 ml/min oxygen.

head of the column, due to the low solubility of the oligomer in supercritical carbon dioxide under the initial low-pressure conditions. By scanning through the threshold densities of the oligomers with a pressure or density program, selective solvation occurs. There are active sites found on fused-silica surfaces which can interact with and slow the migration of oligomers, but the number of sites is too small to be wholly responsible for the observed separations.

#### MMA–BA studies: DB-17 column

Fig. 3 shows the chromatogram resulting from the separation of the MMA–BA (80:20, w/w) copolymer on the 20-m DB-17 column. After completing initial studies on this 20-m column, the first meter was detached and used in further experiments. This was done to see if the efficiency and the resolution of the separations changed when a shorter column with a lesser amount of active stationary phase surface was used. Fig. 4 shows the separation of the MMA–BA copolymer on the 1-m column. When using either of the DB-17 columns a typical chromatogram contained from 30 to 40 peaks. The fifteen most prominent peaks on the chromatograms of both the 20-m and the 1-m columns were selected, and the chromatographic selectivities relative to one another were calculated to ensure that the same peaks were being compared between chromatograms.

The height equivalent to a theoretical plate (HETP) was calculated for each of the peaks using triangulation and is shown in Table II. In general,

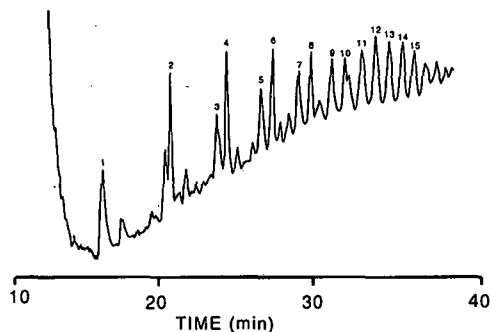


Fig. 3. Separation of MMA–BA on the 20-m DB-17 column. Oven temperature: 140°C. Mobile phase: carbon dioxide with 0.8% (v/v) formic acid. Initial pressure: 88 atm. Pressure ramp: 6.8 atm/min. Final pressure: 374 atm. Detector gas flows: 455 ml/min air, 45 ml/min hydrogen.

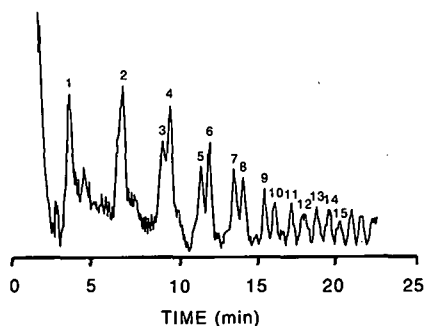


Fig. 4. Separation of MMA–BA on the 1-m DB-17 column. Oven temperature: 140°C. Mobile phase: carbon dioxide with 0.8% (v/v) formic acid. Initial pressure: 88 atm. Pressure ramp: 6.8 atm/min. Final pressure: 374 atm. Detector gas flows: 455 ml/min air, 45 ml/min hydrogen.

the 1-m column was as efficient or more efficient than the 20-m column. The same restrictor was used for the 1-m column and the 20-m column. Therefore since all other chromatographic conditions remained the same for the two separations, the linear velocity at a given pressure was also the same in each column. Minimal variation in plate height would therefore be expected with change in column length. The difference in measured plate heights for the two columns was also greatest for the compounds that

TABLE II  
HETP ( $\mu\text{m}$ ) PER PEAK

Peak No.	HETP	
	20-m column	1-m column
1	2000	1400
2	550	920
3	420	680
4	100	250
5	530	180
6	320	110
7	290	130
8	70	120
9	250	60
10	530	70
11	500	60
12	210	80
13	200	70
14	190	50
15	180	40

TABLE III  
CAPACITY FACTORS ( $k'$ ) AND SELECTIVITIES ( $\alpha$ ) FOR 20-m DB-17, 20-m DB-225 AND 1-m DB-17 COLUMNS

Peak	$k'$			$\alpha$		
	DB-17 (20 m)	DB-225 (20 m)	DB-17 (1 m)	DB-17 (20 m)	DB-225 (20 m)	DB-17 (1 m)
1	0.50	3.30	6.00	—	—	—
2	0.80	8.90	11.10	1.6	2.7	1.9
3	1.10	13.00	15.80	1.4	1.5	1.3
4	1.20	13.70	15.50	1.1	1.1	1.1
5	1.40	16.70	18.40	1.2	1.2	1.2
6	1.45	17.70	19.30	1.0	1.1	1.0
7	1.50	19.90	21.50	1.0	1.1	1.1
8	1.60	20.90	22.30	1.1	1.1	1.0
9	1.80	22.60	24.50	1.1	1.1	1.1
10	1.85	23.90	25.40	1.0	1.1	1.0
11	1.95	25.10	27.10	1.1	1.1	1.1
12	2.00	26.30	28.30	1.0	1.1	1.1
13	2.10	27.40	29.60	1.1	1.0	1.1
14	2.15	28.60	30.70	1.0	1.0	1.0
15	2.20	29.40	31.90	1.0	1.0	1.0

eluted latest. For these oligomers the plate height was significantly lower on the 1-m column than on the 20-m column.

Table III shows the capacity factors and selectivities for the 15 most prominent peaks in the chromatogram for both the 20- and 1-m columns. Since the two columns were identical in every way except in length, the capacity factor for a given oligomer should not change between the two columns. However, the measured capacity factor of a given oligomer was much larger for the longer column. This is a logical result if selective solvation significantly controls the separation of the oligomers. The dead time,  $t_0$ , of the 1-m column is 1/20 that of the longer column, while the dissolution time of an oligomer at a given pressure should be the same in each column.

The resolution for the two columns was also determined. Fig. 5 shows a comparison of these values. The long column, the less efficient of the two columns, provided superior resolution for oligomers 1-9. In typical chromatographic separations resolution is related to the square root of the total number of plates generated by a column. Although it was less efficient, the longer column still generated a far greater total number of theoretical plates. In Table IV the efficiency and the resolution of the two

columns are compared. If the experimental efficiency of each chromatographic peak on the 20-m column is divided by 20 and substituted into the resolution equation below

$$R_s = \left( \frac{\sqrt{N}}{4} \right) \left( \frac{\alpha - 1}{\alpha} \right) \left( \frac{k'}{k' - 1} \right)$$

along with the experimental selectivity and capacity factor value for the 1-m column, then the expected resolution on the 1-m column can be calculated. This is shown in Table IV. These data show that the experimental resolution obtained on the 1-m column is always higher than that expected for the larger oligomers found for peak 8 and later. We believe the major cause of this enhanced resolution to be that the separation of the higher molecular weight oligomers is predominately determined by their selective solvation in the supercritical fluid at well defined densities; this is the same mechanism as was described for the polydisulfide polymer. Interactions between the lower-molecular-weight oligomers and the stationary phase had a greater impact on their resolution. This further illustrates the relationship between the stationary phase and differential solvation in polymer separations. As seen in

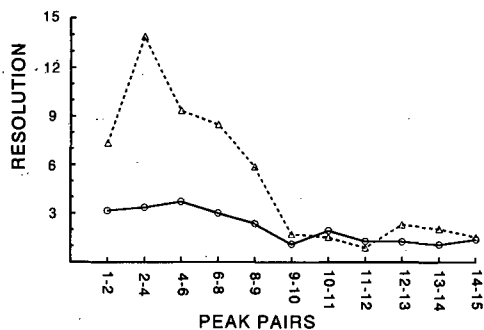


Fig. 5. Chromatographic resolution of the (○) 1-m DB-17 column and on the (△) 20-m DB-17 column.

the polydisulfide studies, stationary phase must be present to achieve anything better than a crude separation of oligomers. The interactions between the stationary phase and oligomers serve to enhance the separation that is initiated by their differential solvation in the mobile phase. At the same time, a column that is needlessly long may increase the measured plate height of the separation (as shown in Table II) because selective solvation of the oligomers is controlling the separation, especially for the higher molecular weight compounds.

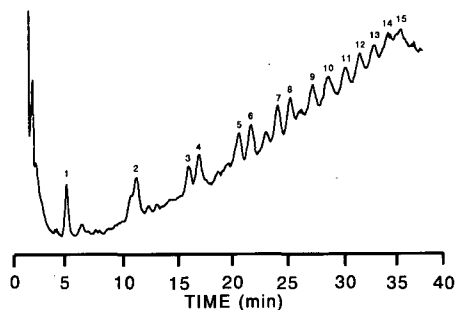


Fig. 6. Separation of MMA-BA on the 20-m DB-225 column. Oven temperature: 130°C. Mobile phase: carbon dioxide with 0.9% (v/v) formic acid. Initial pressure: 88 atm. Pressure ramp: 10.2 atm/min. Final pressure: 272 atm. Detector gas flows; 455 ml/min air, 45 ml/min hydrogen.

#### MMA-BA studies: DB-225 column

MMA-BA separations were obtained on a DB-225 column. Fig. 6 shows a chromatogram resulting from the separation. It resembles those obtained on the 20-m DB-17 column. The fifteen most prominent peaks on the DB-225 chromatogram were measured and found to have the same relative selectivity,  $\alpha$ , as the fifteen most prominent peaks observed on the 20-m DB-17 column. In Table III a comparison of the capacity factors ( $k'$ ) and the selectivities ( $\alpha$ ) for the 20-m DB-225 and the 20-m

TABLE IV

A COMPARISON OF THE NUMBER OF THEORETICAL PLATES ( $N$ ), AND RESOLUTION ( $R_s$ ) OBSERVED FOR THE 20-m DB-17 AND 1-m DB-17 COLUMNS

Peak pair	$N$		$R_s$		
	DB-17 (20 m)	DB-17 (1 m)	DB-17 (20 m)	DB-17 (1 m)	DB-17 <sup>a</sup> (20 m)
1-2	36 000	1 100	9.2	3.2	4.5
2-4	199 000	4 000	18.0	3.4	6.6
4-6	62 000	8 800	6.4	3.7	2.6
7-8	296 000	8 100	10.9	3.0	4.0
8-9	81 000	17 100	3.9	2.4	1.3
9-10	38 000	14 800	1.4	1.1	0.4
10-11	40 000	16 900	1.5	1.9	0.7
11-12	95 000	12 700	1.0	1.3	0.7
12-13	101 000	13 900	2.3	1.2	0.8
13-14	106 000	21 400	2.	1.1	0.6
14-15	109 000	23 100	1.5	1.4	0.7

<sup>a</sup> Calculated values.

DB-17 columns is shown. The elution order of the oligomers was the same regardless of the stationary phase used. These results corroborate the premise that the selectivity is controlled by selective solvation of the oligomers. Oligomer–stationary phase interactions are of lesser importance in determining retention order.

#### ACKNOWLEDGEMENTS

Financial support of this work by Ashland Chemical is gratefully acknowledged. We thank Dr. William Simonsick for providing the MMA–BA samples.

#### REFERENCES

- 1 C. R. Yonker and R. D. Smith, *J. Chromatogr.*, 459 (1988) 183.
- 2 E. Klesper and W. Hartmann, *J. Polym. Sci. Polym. Lett. Ed.*, 15 (1977) 707.
- 3 L. McLaren, M. N. Meyers and J. C. Giddings, *Science (Washington, D.C.)*, 159 (1968) 197.
- 4 J. E. Conaway, J. A. Graham and L. B. Rogers, *J. Chromatogr. Sci.*, 16 (1978) 102.
- 5 F. P. Schmitz and E. Klesper, *J. Supercrit. Fluids*, 3 (1990) 29.
- 6 L. A. Pekay and S. V. Olesik, *Anal. Chem.*, 61 (1989) 2616.
- 7 L. M. Nuwaysir, C. L. Wilkens and W. J. Simonsick, *J. Am. Soc. Mass. Spectrom.*, 1 (1990) 66.



# Reversed-phase thin-layer chromatography of diacylglycerols in the presence of silver ions

V. P. Pchelkin and A. G. Vereshchagin

Laboratory of Lipid Metabolism, Institute of Plant Physiology, Academy of Sciences, Botanicheskaya 35, Moscow 127276 (Russia)

(First received July 1st, 1991; revised manuscript received December 19th, 1991)

## ABSTRACT

Each of the SS, SL and SLe groups of 1,2-*rac*-diacylglycerols (DAGs) in which S is a residue of stearic (St) or palmitic (P) acid and L and Le are residues of linoleic and linolenic acid, respectively, were separated into individual species using reversed-phase thin-layer chromatography in the presence of silver ions ( $\text{Ag}^+$ -RP-TLC). This technique, combined with adsorption  $\text{Ag}^+$ -TLC ( $\text{Ag}^+$ -TLC +  $\text{Ag}^+$ -RP-TLC, in the form of two-dimensional TLC), afforded the complete separation of all the components of the DAG model mixture obtained by glycerolysis of St, P, L, Le and oleic acid (O) esters. All fifteen individual DAG species were identified: StSt-, StP-, StO-, PP-, PO-, OO-, StL-, PL-, OL-, LL-, StLe-, PLe-, OLe-, LLe- and LeLe-glycerols. Their  $\text{Ag}^+$ -RP-TLC mobilities relative to that of *rac*-1,2-LeLe ( $R_{1,2-\text{LeLe}}$ ) were inversely proportional to the equivalent lipophilicity of their  $\text{Ag}^+$  complexes  $L_3$  ( $R_{1,2-\text{LeLe}} = 1.47 - 0.04 L_3$ ). In terms of separation selectivity of the DAG model mixture, the  $\text{Ag}^+$ -TLC +  $\text{Ag}^+$ -RP-TLC technique exceeds reversed-phase high-performance liquid chromatography and is roughly equal to gas chromatography.

## INTRODUCTION

In previous studies on the molecular species composition of the diacylglycerol (DAG) model mixture using adsorption thin-layer chromatography of their coordination complexes with silver ions ( $\text{Ag}^+$ -TLC), we identified eight out of the fifteen theoretically possible DAG species [1,2]. At the same time, in addition to these eight individual species, we discovered three DAG groups of mixed molecular species composition, *viz.*, SLe-, SL- and SS-glycerols, where S are residues of stearic (St) or palmitic (P) acid and Le and L are linolenate and linoleate, respectively [3]. The separation of each of these groups into individual species by  $\text{Ag}^+$ -TLC has not been achieved. Therefore, we attempted to attain the same goal by using another mode of TLC, *viz.*, reversed-phase TLC in the presence of silver ions ( $\text{Ag}^+$ -RP-TLC), which has previously been report-

ed to exceed the  $\text{Ag}^+$ -TLC in terms of separation selectivity of individual DAG species [2]. Several DAG samples of a relatively simple molecular species composition (see below) served as standards to identify individual DAG species in the model mixture [3].

## EXPERIMENTAL

### *Preparation and fractionation of rac-1,2-DAGs*

The model mixture [1] and the standards [3] of DAGs were obtained as described previously [3]. All DAG preparations were separated into their positional isomers and subsequently only *rac*-1,2-DAGs were used [3]. For one-dimensional  $\text{Ag}^+$ -RP-TLC fractionation of the latter [2], the entire surface of a Silufol plate (15 × 15 cm) (Kavalier, Sklářny, Czechoslovakia) was sprayed with a 1% (w/v) methanolic solution of silver nitrate [3] and then impregnated with a 10% (v/v) benzene solution of *n*-tetradecane [1]. From 20 to 50  $\mu\text{g}$  of *rac*-1,2-DAGs were applied at the starting line of this plate. They were separated into individual spe-

Correspondence to: Dr. V. P. Pchelkin, Laboratory of Lipid Metabolism, Institute of Plant Physiology, Academy of Sciences, Botanicheskaya 35, Moscow 127276, Russia.

cies and groups of DAGs in a completely vapour-saturated chamber for continuous-flow TLC (see Fig. 1 in ref. 4) using a 5% (w/v) boric acid solution in methanol saturated with silver nitrate and *n*-tetradecane [2] as the mobile phase.

Prior to two-dimensional TLC, the entire plate was sprayed with the silver nitrate solution (see above), and 50  $\mu\text{g}$  of *rac*-1,2-DAG mixture were applied at point A (Fig. 1). DAGs were separated by continuous-flow  $\text{Ag}^+$ -TLC in direction 1 on region I of the plate for 6 h using a silver nitrate-saturated mixture of chloroform and isopropanol (99:1, v/v) as the mobile phase [3]. The plate was kept in a hood for 0.5 h, region II was impregnated with *n*-tetradecane and then SL and SLe zones formed by  $\text{Ag}^+$ -TLC were further separated as above in direction 2 by continuous-flow RP-TLC.

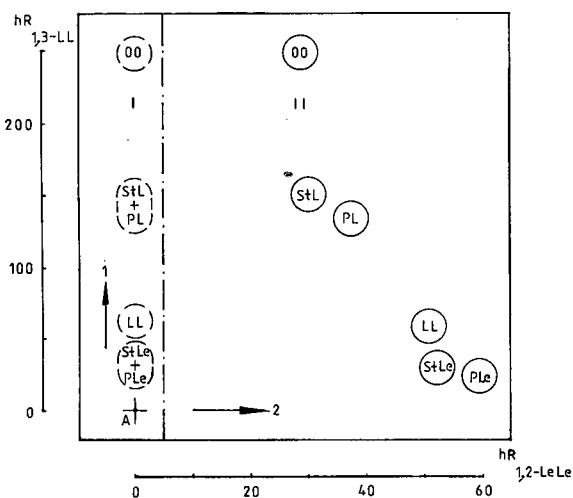


Fig. 1. Two-dimensional thin-layer chromatogram of a mixture of six *rac*-1,2-diacylglycerol species. A = starting point; I and II = regions of the plate non-impregnated and impregnated with *n*-tetradecane, respectively; 1 = direction of mobile phase [silver nitrate-saturated chloroform–isopropanol (99:1, v/v)] migration during  $\text{Ag}^+$ -TLC; 2 = direction of mobile phase [5% (w/v) boric acid solution in methanol, saturated with silver nitrate and *n*-tetradecane] migration during  $\text{Ag}^+$ -RP-TLC. Zone limits  $\text{Ag}^+$ -TLC of DAGs in region I and after  $\text{Ag}^+$ -RP-TLC in region II are indicated by broken and solid lines, respectively.  $hR_{1,3-LL} = 100R_{1,3-LL}$  = mobility of DAG zones in relation to that of *rac*-1,3-dilinoleoylglycerol [3]. For other abbreviations, see Experimental and Table III.

### Detection and identification of individual DAG species

Soluble silver salts [3] and *n*-tetradecane [1] were removed from the plate and individual TLC zones of UU- and SS-DAGs, where U is Le, L or oleate (O), were revealed with phosphomolybdic acid (PMA). SS-DAGs which did not react with PMA were revealed with a 10% copper sulphate solution in an 8% solution of phosphoric acid (CS-PA) [2]. Treatment with CS-PA also revealed SU- and UU-DAGs. The mobility of different DAG zones was expressed as  $x \pm s$ , where  $x = 100R_{1,2-LeLe} = hR_{1,2-LeLe}$  is the arithmetic mean of individual measurements of the mobility of a given zone in relation to that of the *rac*-1,2-LeLe zone ( $R_{1,2-LeLe}$ ) multiplied by 100 ( $h$ ) and  $s$  is the absolute standard deviation of these measurements; *rac*-1,2-LeLe was selected as a mobility standard because it exceeded other molecular species of the model mixture in its  $\text{Ag}^+$ -RP-TLC mobility. Other methods were the same as those used previously [1–3].

## RESULTS AND DISCUSSION

### DAG standards

Previously, we have fractionated the DAG model mixture by one-dimensional  $\text{Ag}^+$ -RP-TLC directly, without its preliminary separation into non-symmetrical and symmetrical *rac*-1,2- and *rac*-1,3-positional isomers, as the mobilities of both during reversed-phase chromatography were shown to be very similar [2]. However, the present study revealed (see below) that complete separation of the mixture could be achieved only by combining  $\text{Ag}^+$ -RP-TLC with adsorption  $\text{Ag}^+$ -TLC, *i.e.*, by two-dimensional TLC (see Experimental). In addition,  $\text{Ag}^+$ -TLC mobilities of various positional isomers within each species present in the initial model mixture were shown to be different [3]. It is clear that direct two-dimensional TLC of this mixture would result in a very complicated separation pattern which would be useless for the identification of individual DAG species, and therefore nothing but isomerically pure components of the model mixture and DAG standards (see Experimental) could be employed for both  $\text{Ag}^+$ -TLC and  $\text{Ag}^+$ -RP-TLC in the present study [1–3]. Only non-symmetrical *rac*-1,2-DAG isomers were used in the experiments described below because, on the one hand, the ultimate goal of

TABLE I  
FATTY ACID COMPOSITION OF DAG STANDARDS

Standard No.	Fatty acid composition (mol%) <sup>a</sup>				
	St	P	O	L	Le
1	3.1	67.0	29.9	–	–
2	69.3	3.2	25.3	2.2	–
3	49.6	27.8	2.1	20.5	–
4	44.0	30.1	1.2	2.2	22.5

<sup>a</sup> Data from ref. 3. For abbreviated designations of fatty acid species, see text.

our studies is the chromatographic determination of the molecular species composition of non-symmetrical *sn*-1,2-DAGs obtained from native polar glycerolipids [1] and, on the other, on liquid chromatography of DAGs of the same composition on achiral stationary phases *rac*-1,2-DAGs always coincide with *sn*-1,2-DAGs in their mobility [5].

The data on fatty acid composition in Table I demonstrate that standards 1 and 2 include large amounts of P and St, respectively, and standards 3 and 4 contain, in addition to S acid, mostly L and Le, respectively. From these data, a possible species composition of DAG standards 1–4 was calculated as shown in Table II [1–3]. From Table II it can be

TABLE II  
CHARACTERISTICS OF MOBILITY AND LIPOPHILICITY OF INDIVIDUAL DAG SPECIES ON Ag<sup>+</sup>-RP TLC AND THEIR IDENTIFICATION IN STANDARDS 1–4

Mobility of DAG zones ( $x \pm s$ ) <sup>a</sup>	DAG species content in standards 1–4: calculated (mol%) <sup>b</sup> and evaluated visually <sup>c</sup>				Staining behaviour with		Ag <sup>+</sup> -TLC data [3] <sup>d</sup>	DAG identification	$L_3$ values of DAGs <sup>e</sup>
	1	2	3	4	PMA	CS-PA			
4 ± 1		49 +++	26 +++	20 +++	–	+	A	StSt	36
10 ± 2	4 ++	5 ++	29 +++	28 +++	–	+	A	StP	34
15 ± 1	2 +	35 +++	2 +		+	+	+	StO	33
19 ± 1	45 +++		8 ++	9 ++	–	+	A	PP	32
23 ± 1	40 +++	2 +			+	+	+	PO	31
30 ± 2	9 ++	9 ++	20 +++	3 +	+	+	B	OO+ StL	30
38 ± 3			11 ++		+	+	B	PL	28
51 ± 2			4 ++	20 +++	+	+	C	LL+ StLe	24
60 ± 2				15 +++	+	+	C	PLe	22

<sup>a</sup> Arithmetic means of individual measurements of  $hR_{1,2-L_eLe}$  and absolute standard deviations are shown (see Experimental).

<sup>b</sup> Calculated from the DAG fatty acid composition data in Table I according to the theory of random distribution of fatty acid residues between DAG molecules [1]. Standard 4 also contained the LeLe zone (5 mol%).

<sup>c</sup> Results of visual evaluation of the relative intensity of DAG zone staining are designated by –, +, ++, +++ (in ascending order).

<sup>d</sup> Unambiguously proved the presence of a given DAG species (+), SS-DAGs (A), SL-DAGs (B) or SLe-DAGs (C) in the model mixture [3].

<sup>e</sup> Equivalent lipophilicity  $L_3 = m - 2p - u$ , where  $m$  and  $p$  are total number of carbon atoms and relative polarity of DAG aliphatic chains, respectively, and  $u$  is the number of unsaturated fatty acid residues in the DAG molecule [1–3]. See text for other abbreviations.

seen that these standards include mainly SS and SU species in addition to a small amount of UU species. Hence it can be suggested that these standards would be suitable for the identification of respective DAG species in SS, SL and SLe groups of the DAG model mixture. Table II shows also that the separation of each of the standards 1–4 by Ag<sup>+</sup>-RP-TLC yields 5–7 zones. Up to ten separate DAG zones were obtained.

#### Identification of individual DAG species in standards 1–4

The identification was based on the data in Table II which include both the parameters of Ag<sup>+</sup>-RP-TLC mobility of DAGs and the results of their detection (see columns 6–8) and of the identification of different DAG species and DAG groups by Ag<sup>+</sup>-TLC [3]. Below, when examining the properties of each TLC zone, these results are assumed to be known and, therefore, no detailed discussion of them is given.

Table II demonstrates that zones with  $x = 60$  and 51 (referred to below as zones 60 and 51) display the highest TLC mobility (except the  $x = 100$  zone corresponding to *rac*-1,2-LeLe). These zones occur almost exclusively in standard 4. From their staining behaviour, they belong to unsaturated DAGs, and from the comparative colour intensities of different zones of this standard they can be PLe and StLe, respectively. One must also take into account that PLe and StLe predominate among the SU-DAGs in the calculated standard 4 composition. Moreover, because the reversed-phase mobility of DAGs is known to be inversely proportional to their lipophilicity [1,2], PLe which is less lipophilic must exceed StLe in its mobility. Therefore, one must conclude that zone 60 represents an individual PLe species whereas in the standard 4 zone 51 contains StLe. At the same time, zone 51 occurs also in standard 3 as its most mobile component. This standard does not contain Le and includes only traces of O, but is rich in L (see Table I). Hence, in standard 3 zone 51 does not contain StLe, and includes only LL species. Therefore, the latter cannot be separated from StLe by Ag<sup>+</sup>-RP-TLC.

The next in rank of mobility is zone 38, which was found only in standard 3. From the fatty acid composition of the latter (Table I) and the data on DAG species content and staining characteristics

(Table II), it can be suggested that this zone belongs to the SL group and can represent only one of the two alternative molecular species of this group (PL or StL), *i.e.*, PL because it is the least lipophilic and most mobile of the SL species.

As regards zone 30, it occurs as a major component only in standard 3, in which L predominates among unsaturated fatty acids (see above). Therefore, in this instance zone 30 contains only the diacid StL species. At the same time, this zone is present in an appreciable amount in standard 1, which, apart from S, contains only O. In this standard, zone 30 is most mobile and, therefore, must contain the least lipophilic of all DAG species possible for this case. Because DAGs of this zone do not represent SS-DAGs (see columns 6 and 7), they can contain only OO- and/or PO-glycerols. If one takes into account that the calculated contents of these species in standard 1 are 40 and 9%, respectively, and that zone 3 is considerably inferior to the adjoining zones 23 and 19 in its colour intensity, one can conclude that in the case of standard 1 zone 30 includes only the one (monoacid) OO species [3]; hence, on Ag<sup>+</sup>-RP-TLC OO has the same  $x$  as StL.

The next zone, 23, be found only in standards 1 and 2 and, from the data in columns 6 and 7 (Table II), does not represent SS DAGs. Of the two major DAG zones of standard 1 which in its fatty acids contains 67% P and 30% O, this zone is the most mobile, *i.e.*, the least lipophilic. It can be concluded that this zone represents one of the two possible SO species, namely PO.

Zone 19 (of the SS type) is the major component of standard 1 in which P predominates (see above). It can also be found in standards 3 and 4 where P makes up 28 and 30% of the total fatty acids, respectively. At the same time, zone 19 is absent in standard 2 where the P content does not exceed 3.2%. Therefore, zone 19 is composed of the disaturated PP species.

Zone 15 does not belong to the SS type (see columns 6 and 7) and is present almost exclusively in standard 2. Here O appears to be the only major unsaturated fatty acid, and among S fatty acids St predominated (Table I). Because PO and OO were identified previously in zones 23 and 30, respectively, it can be concluded that zone 15 is composed of only one individual SU species, *i.e.*, StO [3].

The last but one zone, 10 (of the SS type), may

represent either StP or StSt. However, this zone was found to be intensely colored only in the standards rich in both St and P, *i.e.*, in standards 3 and 4. Therefore, this zone can consist of nothing but StP.

Finally, zone 4, which also belongs to the SS type, is present only in the standards (2–4) containing St as the major component and is absent from standard 1 where the St content does not exceed 3.1% (see Tables I and II). It is therefore evident that zone 4 is composed of the monoacid StSt species.

*Identification of StL and StLe in the DAG model mixture by Ag<sup>+</sup>-TLC followed by Ag<sup>+</sup>-RP-TLC.*

As shown in the previous section, in the course of analysis of the standards of a simple species composition, the SS group of DAGs was separated into individual StSt, StP and PP molecular species, the SL group into StL and PL and the SLe group into StLe and PLe. At the same time, these data show that during Ag<sup>+</sup>-RP-TLC StL and StLe do not differ in their mobility from OO and LL, respectively. Previously it has been shown that StL, StLe, OO and LL could be completely separated from each other by adsorption Ag<sup>+</sup>-TLC. However, the latter technique does not separate StL and StLe from PL and PLe, respectively [3]. Hence the six molecular species, *i.e.*, StL, StLe, PL, PLe, OO and LL, are close to each other in their TLC mobility and therefore the methods for their complete TLC separation must be considered in more detail.

Several variants of the qualitative composition of these DAGs in synthetic and natural mixtures are shown in Table III. It is seen that in order to deal with different variants, one must adopt different strategies. Thus, if the absence of OO and/or LL in a given DAG mixture (variants 3 and 7) has been established by Ag<sup>+</sup>-TLC, StL and/or StLe can be identified in it by the occurrence of zones 30 and/or 51, respectively, on Ag<sup>+</sup>-RP-TLC. Similarly, if PL and/or PLe were not found in a mixture by Ag<sup>+</sup>-RP-TLC (variants 1 and 5; 2 and 6), then the presence of StL and/or StLe will be unambiguously proved by Ag<sup>+</sup>-RP-TLC.

Finally, the most complicated variants which are also present in our model mixture (variants 4 and 8) include all six DAG molecular species listed above. In these instances the identification of StL and StLe species can be achieved only by two-dimensional chromatography of the mixture on the same plate

TABLE III

IDENTIFICATION OF StL AND StLe INDIVIDUAL SPECIES IN DAG MIXTURES OF DIFFERENT MOLECULAR SPECIES COMPOSITION USING THE SEPARATION OF THESE MIXTURES BY Ag<sup>+</sup>-TLC FOLLOWED BY Ag<sup>+</sup>-RP-TLC

DAG species <sup>a</sup>		Variants of DAG mixture species composition <sup>b</sup>			
A	B	1	2	3	4
StL	PL	–	–	+	+
	OO	–	+	–	+
StLe	PLe	5	6	7	8
	LL	–	–	+	+
		–	+	–	+

<sup>a</sup> A, StU species to be identified; B, DAG species accompanying StL and StLe in the model mixture and identified by Ag<sup>+</sup>-TLC (OO, LL) and Ag<sup>+</sup>-RP-TLC (PL, PLe).

<sup>b</sup> 1–8 are variant numbers; + and – indicate the presence and absence, respectively, of a given DAG species (column B) in a mixture.

(Ag<sup>+</sup>-TLC + Ag<sup>+</sup>-RP-TLC, see Fig. 1), *viz.*, by using Ag<sup>+</sup>-TLC in the first direction and Ag<sup>+</sup>-RP-TLC in the second. After separating DAGs by Ag<sup>+</sup>-TLC, OO and LL zones in addition to SL and SLe groups will be formed. In the second stage of two-dimensional TLC these groups are separated into StL, PL, StLe and PLe individual species as a result of their Ag<sup>+</sup>-RP-TLC.

Earlier, by Ag<sup>+</sup>-TLC we identified in the DAG model mixture LeLe, LLe, OLe, LL, OL, OO, PO and StO species [3], and now, by means of Ag<sup>+</sup>-TLC + Ag<sup>+</sup>-RP-TLC, PLe, StLe, PL, StL, PP, StP and StSt were also shown to be present, in addition to the species mentioned above. Hence our model mixture contains fifteen individual DAG species: LeLe, LLe, OLe, PLe, StLe, LL, OL, PL, StL, OO, PO, PP, StO, StP and StSt, *i.e.*, noting but the species which are formed as a result of the random distribution of the five fatty acid residues between molecules of glycerol [1].

It is evident that the Ag<sup>+</sup>-TLC + Ag<sup>+</sup>-RP-TLC technique which ensures complete separation of the mixture of fifteen DAG species, *i.e.*, a mixture of a very complex molecular species composition will be all the more suitable for the analysis of individual *sn*-1,2-DAGs obtained from plant polar glycerol-

lipids because in the latter instance the number of species formed is usually lower than in our mixture. For example, the identification of StL and StLe will be required only rarely because the level of St in membrane lipids does not usually exceed 4%, and therefore StL and StLe are usually present there in only trace amounts, if at all.

*Relationship between the Ag<sup>+</sup>-RP-TLC mobility of individual DAG species and the equivalent lipophilicity of their coordination complexes*

Having at our disposal the results of DAG identification and the  $x$  values<sup>a</sup> of different TLC zones (Table II), we attempted to determine the relationship between the mobility of individual DAGs on Ag<sup>+</sup>-RP-TLC and characteristics of their molecules. One of the most important is known to be lipophilicity [6]. Previously this characteristic has been shown to vary under different TLC conditions. For example, during RP-TLC of free DAGs in a methanol-trimethyl borate-*n*-tetradecane system, *i.e.*, in the absence of silver ions, lipophilicity has been defined by us as

$$L_1 = m - 2e \quad (1)$$

Where  $m$  and  $e$  are the total numbers of carbon atoms and olefinic bonds in the fatty acid chains, respectively [1]. Later, in preliminary experiments on the separation of a mixture of DAG positional isomers by Ag<sup>+</sup>-RP-TLC, the lipophilicity of DAG coordination complexes was expressed as

$$L_2 = m - 2e - u \quad (2)$$

where  $u$  is the number of unsaturated fatty acid residues in the DAG molecule [2]. However, further studies have demonstrated that the Ag<sup>+</sup>-TLC mobility of these complexes was mainly determined by their polarity,  $p$ . Like  $e$ , polarity is inversely proportional to the equivalent lipophilicity of Ag<sup>+</sup>-DAG complexes. At the same time, polarity reflects their properties more accurately than the number of olefinic bonds,  $e$  [3]. Therefore, to calculate the lipo-

philicity parameter of *rac*-1,2-DAGs on Ag<sup>+</sup>-RP-TLC,  $e$  values in eqn.2 were substituted by  $p$  values taken from Table II in ref. 3. Calculated parameters

$$L_3 = m - 2p - u \quad (3)$$

approximated to the nearest whole number are shown in Table II.

To establish which of the three lipophilicity parameters,  $L_1$  [1],  $L_2$  [2] or  $L_3$  (Table II), is the most satisfactory characteristic of DAG properties on Ag<sup>+</sup>-RP-TLC, we calculated correlation coefficients,  $r$ , between each of these parameters and  $x$  values of the respective DAG species (Table III). The values were  $-0.976$ ,  $-0.972$  and  $-0.999$ , respectively, and confirm, first of all, the above conclusion that the mobility of individual DAGs on RP fractionation is always inversely proportional to their lipophilicity. Moreover, these results show that during Ag<sup>+</sup>-RP-TLC the selectivity of DAG separation is dependent mostly on the  $L_3$  parameter. This relationship is linear ( $x = 147 - 4 L_3$ ,  $r = +0.999$ ), the number of DAG chromatographic zones is equal to the total number of different  $L_3$  values and separation between individual DAG species takes place only when their  $L_3$  values differ by  $\geq 1$ , *i.e.*, at  $\Delta L_3 \geq 1$ .

It should be emphasized that on RP-TLC of DAGs in the absence of silver ions there was also a linear relationship between their  $hR_F$  and  $L_1$  values:  $hR_F = 164 - 4 L_1$  [2]. However, under these conditions, the DAG model mixture was separated only into seven zones with  $\Delta L_1 \geq 2$ , whereas the presence of silver ions resulted in the formation of twelve zones, indicating a significant increase in the selectivity of DAG separation in the RP system [2].

*Comparison of Ag<sup>+</sup>-TLC + Ag<sup>+</sup>-RP-TLC with other chromatographic techniques in the selectivity of DAG separation*

Above it was stated that the proposed technique ensured the complete separation of a mixture containing fifteen individual DAG species and embraces a wide range of their lipophilicity. Nevertheless, for the definitive evaluation of the practical significance of this technique, it was necessary to compare it with other modern procedures for DAG fractionation [7] in the separation selectivity of natural DAGs and their derivatives. As a criterion of

<sup>a</sup> These values for pure *rac*-1,2-DAGs presented in Table II were not always equal to the respective mobility characteristics obtained earlier by the same method when using a mixture of DAG positional isomers [2].

selectivity we applied the relative retention of two neighbouring peaks or chromatographic zones as suggested by Schoenmakers [8]:

$$\alpha_{j,i} = t_{R,j}/t_{R,i} \quad (4)$$

where  $t_{R,i}$  and  $t_{R,j}$  are retention times of the first ( $i$ ) and next ( $j$ ) eluting peaks. Peaks  $i$  and  $j$  were considered to be separated only at  $\alpha_{j,i} > 1.1$ . The values of

$hR_{1,3-LL}$  [3] and  $hR_{1,2-LLeLe}$  (Table II) show that the relative retention of one or another DAG species during separation, if any, by  $Ag^+$ -TLC and  $Ag^+$ -TLC +  $Ag^+$ -RP-TLC was much in excess of  $\alpha_{j,i} = 1.1$ . Therefore, when comparing the two TLC techniques with other fractionation procedures it was assumed that the former allowed the separation of eight and the latter of fifteen DAG species (Table IV).

TABLE IV  
ESTIMATE OF SEPARATION SELECTIVITY OF INDIVIDUAL DAGs AND THEIR DERIVATIVES BY RP-HPLC

sn-3-O-Derivatives	Number of DAG species		Non-separable DAG species (fractions) <sup>a</sup>	Estimate of separation selectivity	Ref.
	Total	Separated			
Free DAGs	15	8	StSt + StP + PP, StL + PL, StLe + PLe	0.53	3 <sup>b</sup>
	15	15	–	1	This work <sup>c</sup>
	5	5	–	1	9
Acetates	7	3	II	0.43	10
	12	8	II	0.67	11
	8	6	III	0.75	12
	7	3	II, III	0.43	13
tert.-Butyldimethylsilyl ethers	9	3	II, III	0.33	14
Benzoates	7	5	II	0.71	15
	3	3	–	1	16
	8	2	II, III	0.25	17
	10	4	I–III	0.40	18
	7	4	II	0.58	19
	7	5	II	0.71	20
Methoxybenzoates	5	5	–	1	21
	12	6	I, III, LL + Ole	0.50	22
Nitrobenzoates	4	4	–	1	23
	8	3	II, III	0.38	24
	8	3	II, III	0.38	25
	8	2	I–III	0.25	26
	8	4	II, III	0.50	27
	8	2	I–III	0.25	28
	9	3	I–III	0.33	29
	3	3	–	1	30
	7	5	III	0.71	31
Naphthylurethanes	7	3	II, III	0.43	32
	9	3	I–III	0.33	33
	7	5	LL + PLe	0.71	34
Anthroates	4	4	–	1	35
	7	3	StSt + StP, II	0.43	36

<sup>a</sup> Non-separable species: I = StP + StO; II = PP + PO + OO + StL; III = PL + OL.

<sup>b</sup>  $Ag^+$ -TLC.

<sup>c</sup>  $Ag^+$ -TLC +  $Ag^+$ -RP-TLC.

The value of the “estimate of separation selectivity” (*ESS*) was expressed as the ratio between the total number of DAG species being analysed and the number of species which were separated from each other. Of course, when considering all individual DAG species referred to by other workers we took into account only those species which happened also to be present in our model mixture [1]. It is evident that a maximally accessible value of *ESS* (the case of complete separation of all the components of a DAG mixture) is 1. The shortcoming of calculating *ESS* in the way devised here is caused by the fact that analyses of DAG mixtures performed by various workers include different total numbers of individual species. Therefore, the estimates obtained by this method should be considered as preliminary values.

Let us first consider reversed-phase high-performance liquid chromatography (RP-HPLC), which is now widely used for DAG species analysis. *ESS* values of *sn*-3-O-derivatives of DAGs calculat-

ed by us using the mobility data obtained by this technique are presented in Table IV. It can be seen that in most studies *ESS* was significantly lower than 1 because many DAG species were not separated by RP-HPCL. Identical mobilities of these species were obtained because they did not differ from each other in their  $L_1$  values (see above). Previously, the same relationship was observed when separating a DAG model mixture by RP-TLC [1]. Most frequently there was no separation between the components of fractions I, II and III with  $L_1 = 34, 32$  and  $30$ , respectively (their molecular species composition is shown in Table IV). Moreover, the LL+OLe and LL+PLe pairs with the same  $L_1 = 28$  and StSt+StP also failed to be separated in some instances. Values of *ESS* = 1 were observed by only a few workers and, moreover, the number of individual DAG species which are taken into account in the present study and were included in their analyses did not exceed five (see above), *i.e.*, it was much less than in our model mixture. Hence  $Ag^+$ -TLC +

TABLE V

## ESTIMATE OF SEPARATION SELECTIVITY OF INDIVIDUAL DAG DERIVATIVES BY GC

<i>sn</i> -3-O-Derivatives	Number of DAG species		Non-separable DAG species (fractions) <sup>a</sup>	Estimate of separation selectivity	Ref.
	Total	Separated			
Acetate	3	3	—	1	37
	7	5	VI	0.71	38
	14	10	VII, LLe + LeLe	0.71	39
	3	3	—	1	40
	10	4	IV–VI	0.40	41
Trimethylsilyl ethers	4	4	—	1	42
	6	2	V, OO + LL	0.33	43
	7	3	VI, PL + OL	0.43	44
	7	5	VI	0.71	38
	3	3	—	1	45
	15	13	VII	0.87	39
	7	7	—	1	46
	6	2	VI	0.33	47
	13	9	V, OL + StLe	0.69	48
	9	6	VI	0.67	49
	14	14	—	1	50
	8	8	—	1	51
10	10	—	1	52	
<i>Tert.</i> -Butyldimethylsilyl ethers	15	13	VII	0.87	39
	6	6	—	1	53
	5	3	VI	0.60	54
	10	4	IV–VI	0.40	55

<sup>a</sup> Non-separable species: IV = StP+PO; V = PLe + StSt + StO; VI = StO + OO + StL + OL; VII = LL + OLe.

Ag<sup>+</sup>-RP-TLC significantly exceeds RP-HPLC in the selectivity of separation.

There are also a large number of studies in which DAG mixtures of different types of derivatives were simultaneously fractionated, quantified and identified by gas chromatography (GC). ESS values of *sn*-3-O-acetates and silyl ethers of DAGs separated by this method are presented in Table V. These results indicate that in general the separation selectivity achieved by GC was significantly higher than that in RP-HPLC experiments. In many instances it was close to the selectivity of separation achieved by Ag<sup>+</sup>-TLC + Ag<sup>+</sup>-RP-TLC [39,48,50,52]. At the same time, the number of DAG species separated from each other never reached fifteen because no workers succeeded in separating LL from OLE (fraction VII in Table V). In addition, the components of fractions IV–VI in Table V frequently did not differ from each other in their mobilities. Finally, it must be stressed that the selectivity of GC fractionation usually slightly decreased with increasing DAG unsaturation, whereas the reverse was true when separation was carried out using Ag<sup>+</sup>-TLC + Ag<sup>+</sup>-RP-TLC.

Hence, in the selectivity of separation of our DAG mixture, the technique of Ag<sup>+</sup>-TLC + Ag<sup>+</sup>-RP-TLC is at least equal to GC and even exceeds it in certain respects. Both methods are also about equal as regards the amount of laboratory work and manipulations required. At the same time, the advantage of Ag<sup>+</sup>-TLC + Ag<sup>+</sup>-RP-TLC as compared with HPLC and GC is that its application does not require elaborate equipment. In addition, when using Ag<sup>+</sup>-TLC and Ag<sup>+</sup>-RP-TLC there is no dependence on the synthesis of various DAG derivatives. This is essential for performing DAG separations by RP-HPLC and GC, although it is frequently accompanied by the migration of acyl residues, *i.e.*, a breakdown of the native structure of DAGs [7].

In conclusion, the possibility of simultaneous DAG determination is usually regarded as an advantage of GC as compared with planar chromatography. However, inspection of a considerable body of the results of such experiments shows that they lack sufficient accuracy [7]. Thus, the recovery of trimethylsilyl ethers of DAGs after GC is far below 100% [56]. This seems to be caused by the high-temperature oxidation of polyunsaturated DAG

molecular species and partial retention of DAG samples in the GC column [56]. Therefore, it could be assumed that it is more advisable to carry out the quantitative determination of lipids by liquid chromatography.

## REFERENCES

- 1 V. P. Pchelkin and A. G. Vereshchagin, *J. Chromatogr.*, 209 (1981) 49.
- 2 V. P. Pchelkin and A. G. Vereshchagin, *Appl. Biochem. Microbiol. USSR*, 24 (1989) 667.
- 3 V. P. Pchelkin and A. G. Vereshchagin, *J. Chromatogr.*, 538 (1991) 373.
- 4 D. H. van den Eijden, *Anal. Biochem.*, 57 (1974) 321.
- 5 P. Michelsen, E. Aronsson, G. Odham and B. Åkesson, *J. Chromatogr.*, 350 (1985) 417.
- 6 A. G. Vereshchagin, *Izv. Akad. Nauk SSSR, Ser. Biol.*, No. 1 (1981) 54.
- 7 V. P. Pchelkin and A. G. Vereshchagin, *Adv. Chromatogr.*, 32 (1991) 87.
- 8 P. J. Schoenmakers, *Optimization of Chromatographic Selectivity — a Guide to Method Development*, Elsevier, Amsterdam, 1986, p. 5.
- 9 Y. Kondoh and S. Takano, *J. Chromatogr.*, 393 (1987) 427.
- 10 Y. Nakagawa and L. A. Horrocks, *J. Lipid Res.*, 204 (1983) 1268.
- 11 Y. Nakagawa, T. Sugiura and K. Waku, *Biochim. Biophys. Acta*, 833 (1985) 323.
- 12 K. Itoh, A. Suzuki, Y. Kuroki and T. Akino, *Lipids*, 20 (1985) 611.
- 13 Y. Nakagawa, K. Waku, A. Hirose, Y. Kawashima and H. Kozuka, *Lipids*, 21 (1986) 634.
- 14 S. Pind, A. Kuskis, J. J. Myher and L. Marai, *Can. J. Biochem. Cell Biol.*, 62 (1984) 301.
- 15 M. L. Blank, M. Robinson, V. Fitzgerald and F. Snyder, *J. Chromatogr.*, 298 (1984) 473.
- 16 S. J. Robins and G. M. Patton, *J. Lipid Res.*, 27 (1986) 131.
- 17 P. V. Subbaiah and H. Monshizadegan, *Biochim. Biophys. Acta*, 963 (1988) 445.
- 18 M. Careaga-Houck and H. Sprecher, *J. Lipid Res.*, 30 (1989) 77.
- 19 B. Banerji, P. V. Subbaiah, R. E. Cregg and J. D. Bagdade, *J. Lipid Res.*, 30 (1989) 1907.
- 20 A. P. Simoes, G. N. Moll, B. Beaumelle, H. J. Vial, B. Roelofsen and J. A. F. Op den Kamp, *Biochim. Biophys. Acta*, 1002 (1990) 135.
- 21 M. Batley, N. H. Packer and J. W. Redmond, *Biochim. Biophys. Acta*, 710 (1982) 400.
- 22 D. G. Bishop, *J. Liq. Chromatogr.*, 10 (1987) 1497.
- 23 M. Batley, N. H. Packer and J. W. Redmond, *J. Chromatogr.*, 198 (1980) 520.
- 24 M. Kito, H. Takamura, H. Narita and R. Urade, *J. Biochem.*, 98 (1985) 327.
- 25 H. Takamura, H. Narita, R. Urade and M. Kito, *Lipids*, 21 (1986) 356.
- 26 M. Ishinaga and K. K. Carroll, *Biochem. Cell Biol.*, 66 (1988) 1163.

- 27 M. V. Bell, *Lipids*, 24 (1989) 585.
- 28 H. Takamura, K. Tanaka, T. Matsuura and M. Kito, *J. Biochem.*, 105 (1989) 168.
- 29 H. Takamura, H. Kasai, H. Arita and M. Kito, *J. Lipid Res.*, 31 (1990) 709.
- 30 M. Schlame, I. Horvath, Z. Forok, L. I. Horvath and L. Vigh, *Biochim. Biophys. Acta*, 1045 (1990) 1.
- 31 M. Schlame, L. I. Horvath and L. Vigh, *Biochem. J.*, 265 (1990) 79.
- 32 J. Kruger, H. Rabe, G. Reichmann and B. Rustow, *J. Chromatogr.*, 307 (1984) 387.
- 33 B. Rustow, D. Kunze, H. Rabe and G. Reichmann, *Biochim. Biophys. Acta*, 835 (1985) 465.
- 34 A. M. Justin, C. Demandre, A. Tremolieres and P. Mazliak, *Biochim. Biophys. Acta*, 836 (1985) 1.
- 35 P. Laakso and W. W. Christie, *Lipids*, 25 (1990) 349.
- 36 C. S. Ramesha, W. C. Pickett and D. V. K. Murthy, *J. Chromatogr.*, 491 (1989) 37.
- 37 Y. Ohno, I. Yano and M. Masue, *FEBS Lett.*, 50 (1975) 50.
- 38 J. Itabashi and T. Takagi, *Lipids*, 15 (1980) 205.
- 39 A. Kuksis, in H. Mangold (Editor), *CRC Handbook of Chromatography: Lipids*, CRC Press, Boca Raton, FL, 1984, p. 381.
- 40 D. A. Brengartner, *Anal. Chim. Acta*, 173 (1985) 177.
- 41 J. J. Myher, A. Kuksis, L. Marai and P. Sandra, *J. Chromatogr.*, 452 (1988) 93.
- 42 G. Casparrini, M. G. Horning and E. C. Horning, *Anal. Lett.*, 1 (1968) 481.
- 43 G. Casparrini, E. C. Horning and M. G. Horning, *Ann. Inst. Super Sanita*, 6 (1970) 189.
- 44 M. G. Horning, S. Murakami and E. C. Horning. *Am. J. Clin. Nutr.*, 24 (1971) 1086.
- 45 A. Kuksis, L. Marai and J. J. Myher, *J. Chromatogr.*, 273 (1983) 43.
- 46 A. Kuksis, J. J. Myher and L. Marai, *J. Am. Oil Chem. Soc.*, 62 (1985) 762.
- 47 M. S. Pessin and D. M. Raben, *J. Biol. Chem.*, 264 (1989) 29.
- 48 J. J. Myher and A. Kuksis, *J. Chromatogr.*, 471 (1989) 187.
- 49 J. J. Myher, A. Kuksis and S. Pind, *Lipids*, 24 (1989) 396.
- 50 T. Rezanaka and M. Podojil, *J. Chromatogr.*, 463 (1989) 397.
- 51 L.-Y. Yang, A. Kuksis and J. J. Myher, *Biochem. Cell Biol.*, 68 (1990) 480.
- 52 J. J. Myher, A. Kuksis and L.-Y. Yang, *Biochem. Cell Biol.*, 68 (1990) 336.
- 53 P. Child, J. J. Myher, F. A. Knypers, J. A. F. Op den Kamp, A. Kuksis and L. L. M. van Deenen, *Biochim. Biophys. Acta*, 812 (1985) 321.
- 54 A. Kuksis, J. J. Myher and L. Marai, *J. Am. Oil Chem. Soc.*, 62 (1985) 767.
- 55 A. Kuksis, J. J. Myher and P. Sandra, *J. Chromatogr.*, 500 (1990) 427.
- 56 A. Dyer and E. Klopfenstein, *Lipids*, 12 (1977) 889.

# Fluorescence reactions of inorganic cations heated on a porous glass sheet for thin-layer chromatography

Masanori Yoshioka and Hiroko Araki

*Faculty of Pharmaceutical Sciences, Setsunan University, 45-1, Nagaotoge-cho, Hirakata, Osaka 573-01 (Japan)*

Madoka Seki and Tadashi Miyazaki

*Japan Spectroscopic Co. Ltd. (JASCO), 2967-5, Ishikawa-cho, Hachioji, Tokyo 192 (Japan)*

Takeshi Utsuki, Takao Yaginuma and Masaaki Nakano

*Ise Chemical Industries Co., Ltd., 2-7-12, Yaesu, Chuo-ku, Tokyo 104 (Japan)*

(First received December 17th, 1991; revised manuscript received February 21st, 1992)

---

## ABSTRACT

A porous glass sheet was used as a stationary phase for the thin-layer chromatography (TLC) of inorganic cations. Some cations gave rise to fluorescent compounds when spots on the sheet were heated for detection. The fluorescent cations were screened from commercially available reagents by heating at various temperatures from 100 to 700°C for 15 min. The fluorescent cations found were Mg, Al, Ca, V, Cu, Zn, Ge, Y, Zr, Mo, Ag, Cd, In, La, Ce, Eu, Tb, Tl, Pb and Bi. Detection limits of lead, vanadium and tin were 300 pmol and that of copper was 3 pmol. Their fluorescence spectra were measured *in situ* on the sheet and showed hitherto unknown fluorescent reactions. After the separation, the fluorescent spots were overlapped with the triplicate spots detected with 8-hydroxyquinoline or dithizone, which meant that the fluorescent compounds were not due to impurities.

---

## INTRODUCTION

Thin-layer chromatographic (TLC) plates consist of inorganic or organic powders coated on supporting matrices. The inorganic powders are popularly made of silica gel or alumina. Porous glass powders have also been applied to make thin layers, giving good separations, but the separation power is no higher and the preparation of the glass layer is no more convenient than those for silica gel and alumina described by MacDonell and Williams [1] and Kramer *et al.* [2]. Papers made of glass-fibre impregnated with silica or salts were used in TLC by

Swartwout and Gross [3] and Alberti and Grassini [4]. The separations with such papers were not good enough for practical analyses.

Since the above earlier work, the technology of glass has advanced so that porous glass sheets can be made without the supporting matrices. In a previous study [5], we made a 5 cm × 5 cm × 0.5 mm square sheet of porous glass of pore diameter 700 nm. The sheet acts as both the separation layer and the supporting matrix. The surface of the sheet is mechanically and chemically stable. Further, the sheet is so rigid that it is easy to handle. Using this sheet, we obtained good separation and detection conditions for various organic and inorganic compounds. The sheet was found to be very useful even for conventional TLC. In addition, various advanced detection methods could be directly con-

---

*Correspondence to:* Dr. M. Yoshioka, Faculty of Pharmaceutical Sciences, Setsunan University, 45-1, Nagaotoge-cho, Hirakata, Osaka 573-01, Japan.

nected with these TLC sheets. It was possible to measure a Fourier transform IR spectrum and a fluorescence spectrum of a spot on the sheet, because the surface was very smooth compared with those of silica gel and alumina. Because of the large surface of the porous glass, numerous novel dry chemistry reactions were found [5].

Some metal ions became fluorescent after heating without the need for any fluorescent spray reagent. These fluorescent compounds seem to be different from hitherto known fluorescent metal ions. There are well known fluorescent organic metal ion complexes, reviewed by Udenfriend [6], crystalline fluorescent mixtures of inorganic compounds for fluorescent lamps, described by Nakamura and Tamura [7], and atomic fluorescence of metals at extremely high temperature, described by Browner [8].

In this work, we examined these novel fluorescent reactions by using many metal ions and determined the optimum heating temperature for each ion, their fluorescent spectra and their TLC characteristics.

## EXPERIMENTAL

### Materials

According to our previous method [5], we prepared a porous glass sheet of pore diameter 700 nm. The mean pore volume and specific surface area were 0.46 cm<sup>3</sup>/g and 6.6 m<sup>2</sup>/g, respectively, measured by a mercury intrusion method with a mercury penetration porosimeter. The glass consisted of 45–70% SiO<sub>2</sub>, 8–30% B<sub>2</sub>O<sub>3</sub>, 8–25% CaO, 5–15% Al<sub>2</sub>O<sub>3</sub>, 3–8% Na<sub>2</sub>O, 1–5% K<sub>2</sub>O and 0–8% MgO. The mixture was heated at 600–800°C for 20 h to effect a phase separation. The glass block was cut into a square sheet of 5 cm × 5 cm × 0.5 mm. The sheet was leached with 1 M HCl at 80–90°C for 4–10 h to etch the B<sub>2</sub>O<sub>3</sub> phase to make it porous, washed with water and dried.

The salts of the metal ions used were obtained commercially and dissolved in water, 0.1 M HCl (\*), 0.1 M HCl containing ethanol (\*\*), or 0.35% hydrogen peroxide (\*\*\*) to make 0.1 M solutions, which were further diluted with 0.1 M HCl. The following salts were obtained from Wako (Osaka, Japan) and dissolved in one of the above media: LiCl, NaCl, MgCl<sub>2</sub> · 6H<sub>2</sub>O (\*), AlCl<sub>3</sub> · 6H<sub>2</sub>O, KCl, CaCl<sub>2</sub> · 2H<sub>2</sub>O (\*), VCl<sub>3</sub>, CrCl<sub>3</sub> · 6H<sub>2</sub>O, MnCl<sub>2</sub> ·

4H<sub>2</sub>O, FeCl<sub>2</sub> · nH<sub>2</sub>O, FeCl<sub>3</sub> · 6H<sub>2</sub>O, CoCl<sub>2</sub> · 6H<sub>2</sub>O, NiCl<sub>2</sub> · 6H<sub>2</sub>O, CuCl<sub>2</sub> · 2H<sub>2</sub>O, ZnSO<sub>4</sub>, GeCl<sub>4</sub>, SeCl<sub>4</sub>, RbCl, SrCl<sub>2</sub> · 6H<sub>2</sub>O, YCl<sub>3</sub> · 6H<sub>2</sub>O, ZrOCl<sub>2</sub> · 8H<sub>2</sub>O, MoCl<sub>5</sub>, RuCl<sub>3</sub>, PdCl<sub>2</sub>, AgNO<sub>3</sub>, CdCl<sub>2</sub> · 2½H<sub>2</sub>O, InCl<sub>3</sub> · 4H<sub>2</sub>O, SnCl<sub>2</sub> · 2H<sub>2</sub>O, SbCl<sub>3</sub>, TeCl<sub>4</sub> (\*\*), CsCl, BaCl<sub>2</sub>, La<sub>2</sub>O<sub>3</sub> (\*\*\*), CeCl<sub>3</sub> · 7H<sub>2</sub>O, CeO<sub>2</sub> (\*\*\*), Pr<sub>6</sub>O<sub>11</sub> (\*\*\*), Nd<sub>2</sub>O<sub>3</sub> (\*\*\*), Sm<sub>2</sub>O<sub>3</sub> (\*\*\*), Eu<sub>2</sub>O<sub>3</sub> (\*\*\*), Gd<sub>2</sub>O<sub>3</sub> (\*\*\*), TbCl<sub>3</sub> · xH<sub>2</sub>O, YbCl<sub>3</sub> · 6H<sub>2</sub>O, WCl<sub>6</sub>, IrCl<sub>4</sub>, H<sub>2</sub>PtCl<sub>6</sub> · 6H<sub>2</sub>O, H<sub>2</sub>UO<sub>4</sub> · 4H<sub>2</sub>O, HgCl<sub>2</sub> (\*), TiCl<sub>4</sub>, Pb(NO<sub>3</sub>)<sub>2</sub> and BiCl<sub>3</sub> (\*\*).

### Fluorescent reaction by heating

A 3-μl volume of each solution was spotted on the sheet and dried. The sheet was heated in an electric muffle furnace (Advantec OPM-16S, Toyoseisakusho, Tokyo, Japan) at various temperatures from 100 to 700°C for 15 min. The spot of Sn on heating was not fluorescent, but became fluorescent by flaming the sheet in the oxidizing flame of a gas burner for 30 s. In the dark, the sheet was irradiated with an ultraviolet lamp at 254 or 366 nm to reveal the fluorescence of the spots. The fluorescence spectrum of the spots were measured with an FP-770 spectrofluorimeter (JASCO, Tokyo, Japan).

### TLC of cations

The cations showing fluorescence on heating were analysed by TLC according to our previous method [5]. For spotting the sample solutions, a 1-μl glass capillary (32 mm × 0.1 mm I.D.) (Microcaps) was cut to one tenth of the original length, *i.e.*, 3.2 mm long. The small tip of the capillary was connected with a silicon tube of 0.5 mm I.D. The tip was dipped into the sample solution and 0.1 μl was sucked into it. The tip was applied to the sheet by pushing the silicon tube, dried and developed with *n*-butanol–benzene–1 M HNO<sub>3</sub>–1 M HCl (75:69:4:2, v/v) or of acetone–3 M HCl (99:1, v/v). The triplicate spots were detected by the above heating, by spraying a solution of 0.05% dithizone in chloroform or a solution of 1% 8-hydroxyquinoline in methanol, following by exposure to ammonia gas from 28% ammonia solution.

## RESULTS

As shown in Table I, fluorescent cations were

TABLE I

## COLOURS OF FLUORESCENCES AND UV ABSORBANCES OF METAL IONS HEATED ON THE SHEETS AT VARIOUS TEMPERATURES

The plate was irradiated by a UV lamp at 254 or 366 nm. Colours are abbreviated as follows: B = blue or blueish; D = dark; G = green; L = light; O = orange; P = pink or pinkish; V = violet; W = white; Y = yellow or yellowish. Intensities of the UV absorptions were decided by eye in the increasing order  $\pm$ , + and 2+. Asterisks indicate the contour of the spot.

Ion	Irradiation (nm)	Temperature ( $^{\circ}$ C)							
		20	100	200	300	400	500	600	700
Mg <sup>2+</sup>	254					LW	W		
	366		$\pm$	$\pm$	$\pm$	LB	LB	LO	
Al <sup>3+</sup>	254						LW		
	366		$\pm$	$\pm$	$\pm$	LB	LW	$\pm$	
Ca <sup>2+</sup>	254			$\pm$	$\pm$		W*	W*	
	366		$\pm$	+	+	+	W*	WO*	LW*
V <sup>3+</sup>	254	+	2+	+	+	+	+	LY	LY
	366	+	2+	+	+	+	+	O	O
Cu <sup>2+</sup>	254	+	+	+	B	B	B	B	BG
	366	+	+	+	+	+	+	$\pm$	
Zn <sup>2+</sup>	254			LW			W*	B*	
	366			LW	LW	$\pm$	W*	LW*	LW*
Ge <sup>4+</sup>	254				$\pm$	$\pm$			
	366		+	$\pm$	LB*	LB	+	$\pm$	
Y <sup>3+</sup>	254					BW			
	366		+	$\pm$		BW	+		
Zr <sup>4+</sup>	254			LW	LW	BW	W		
	366			LW	W	BW	W		
Mo <sup>5+</sup>	254	2+	2+	2+	2+	2+	+	$\pm$	Y
	366	2+	2+	2+	2+	2+	+	+	LO
Ag <sup>+</sup>	254	+	2+	2+	+	2+	B	B	B
	366	+	2+	+	+	2+	2+	LO	LO
Cd <sup>2+</sup>	254					LOW			
	366		$\pm$	+	+	OW*	+		
In <sup>3+</sup>	254			BG	LW	BW*	LW*	LW*	LY
	366		$\pm$	LWV	W	W	LO	+	LO
La <sup>3+</sup>	254			LW	LW	LW*	LB*		
	366			LY	LW	W	+	+	+
Ce <sup>3+</sup>	254	V	V	V	+	+	+	+	+
	366		V	B	+	+	+	+	
Ce <sup>4+</sup>	254	+	LV	+	+	+	+	+	+
	366	+	$\pm$	+	+	2+	2+	$\pm$	
Eu <sup>3+</sup>	254	LP	LP	DP	P	P	P	P	P
	366	LP	DP	+	+	DP	DP	LP	LDP
Tb <sup>3+</sup>	254	YG	LYG	LYG	LY	YG	YG	YG	YG
	366	LW	$\pm$	LG	+	+	+	+	+
Tl <sup>+</sup>	254	$\pm$		LB	LB	LB	LB		
	366	LW	$\pm$	BW	LB	LB	LB	LB	
Pb <sup>2+</sup>	254	+	+	+	+	$\pm$	B	B	B
	366		$\pm$	$\pm$	$\pm$	O*	$\pm$		
Bi <sup>3+</sup>	254	+	2+	2+	+	2+	2+	2+	O2+
	366	+	2+	2+	2+	2+	+	$\pm$	$\pm$

screened from the reagents described under *Materials*. The fluorescent colours were dependent on the heating temperature and the wavelength of excitation. Some cations showed fluorescence only at high temperatures, but UV absorption at low temperatures. Vanadium showed strong UV absorption at 100°C, changing to light absorption at 200–500°C and yellow fluorescence at 600°C. Copper(II) showed UV absorption at 100–200°C, changing to blue fluorescence at 300–600°C and green fluorescence at higher temperatures. Germanium showed blue fluorescence at 300–400°C, but not at higher temperatures. Indium showed blueish-green fluorescence at 200–600°C, changing to blue fluorescence at 700°C, but no fluorescence above 700°C. Tin was not fluorescent after heating in the furnace, but gave rise to a pink fluorescence after being heated in the flame of the gas burner. The other fluorescent cations also gave rise to the same fluorescence in the flame as in the furnace. The reproducibilities of the fluorescences in the furnace were better than those in the flame. Cerium(III) showed blueish fluorescence at 100–200°C, but only absorption at the higher temperatures. Terbium was al-

ways fluorescent at any temperature. Thallium showed light blue fluorescence at 200–500°C, but no fluorescence at other temperatures. However, it showed stronger fluorescence in the flame than the furnace. Lead showed absorption at low temperatures, changing to blue fluorescence. Molybdenum showed yellow fluorescence at 700°C. Hence all these cations had characteristic temperatures for their fluorescences.

Limits of detection of these fluorescent reactions are summarized in Table II. Dilute solutions were spotted on the sheet and heated at each optimum temperature in the above manner. The detection limit of germanium was 0.3  $\mu\text{mol}$ , those of vanadium(III), tin and lead were 300 pmol and that of copper(II) was 3 pmol. This high sensitivity is comparable to that of atomic spectrometric techniques.

These fluorescent reactions were applied to detection for TLC. The metal ions shown in Fig. 1 were well separated. The  $R_F$  values of the ions are summarized in Table III. The spots detected by heating overlapped the triplicate spots detected by spraying with 8-hydroxyquinoline or dithizone solution. Hence the fluorescent compounds were not due to impurities in the metal reagents.

TABLE II  
DETECTION LIMITS PER SPOT OF CATIONS

For conditions and abbreviations, see Table I.

Cation	Heating temperature for 15 min (°C)	Amount ( $\mu\text{mol}$ )	Colour	Excitation (nm)
V <sup>3+</sup>	700	$3 \cdot 10^{-4}$	LO	254
Cu <sup>2+</sup>	400	$3 \cdot 10^{-6}$	B	254
Ag <sup>+</sup>	700	$3 \cdot 10^{-1}$	B	254
In <sup>3+</sup>	400	$3 \cdot 10^{-2}$	BG	254
Sn <sup>2+</sup>	Flame	$3 \cdot 10^{-4}$	P	254
Ce <sup>3+</sup>	100	$3 \cdot 10^{-2}$	B	254
Tb <sup>3+</sup>	700	$3 \cdot 10^{-2}$	YG	254
Tl <sup>+</sup>	Flame	$3 \cdot 10^{-2}$	LB	254
Mo <sup>5+</sup>	700	$3 \cdot 10^{-2}$	Y*	254
Mg <sup>2+</sup>	400	$3 \cdot 10^{-1}$	LB*	366
Zn <sup>2+</sup>	700	3	LO	254 or 366
Al <sup>3+</sup>	400	$3 \cdot 10^{-2}$	W	254 or 366
Zr <sup>4+</sup>	400	$3 \cdot 10^{-1}$	LB*	366
Bi <sup>3+</sup>	700	$3 \cdot 10^{-2}$	LO	254
Y <sup>3+</sup>	400	$3 \cdot 10^{-2}$	W	254 or 366
Cd <sup>2+</sup>	400	$3 \cdot 10^{-1}$	LO	366
La <sup>3+</sup>	300	3	LB	254 or 366
Pb <sup>2+</sup>	700	$3 \cdot 10^{-4}$	B	254
Ge <sup>4+</sup>	Flame	$3 \cdot 10^{-1}$	LB	254

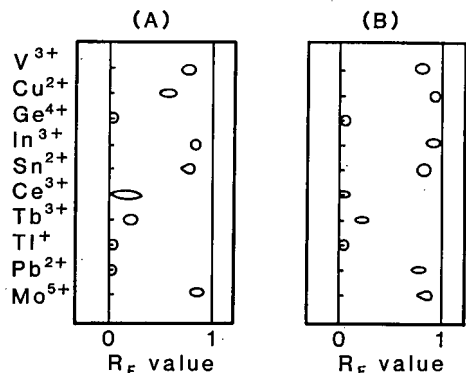


Fig. 1. Chromatograms of metal ions developed with (A) *n*-butanol-benzene-1 M HNO<sub>3</sub>-1 M HCl and (B) acetone-3 M HCl. The developed sheet was cut in the development direction into small pieces for each ion, and each piece was heated at the particular optimum temperature described in Table I.

TABLE III

*R<sub>f</sub>* VALUES OF FLUORESCENT CATIONS AS SHOWN IN FIG. 1

Cation	<i>R<sub>f</sub></i> value	
	Fig. 1A	Fig. 1B
V <sup>3+</sup>	0.78	0.81
Cu <sup>2+</sup>	0.56	0.93
Ge <sup>4+</sup>	0.04	0.06
In <sup>3+</sup>	0.81	0.93
Sn <sup>2+</sup>	0.78	0.85
Ce <sup>3+</sup>	0.15	0.04
Tb <sup>3+</sup>	0.22	0.22
Tl <sup>+</sup>	0.04	0.04
Pb <sup>2+</sup>	0.04	0.81
Mo <sup>5+</sup>	0.85	0.89

It was possible to measure fluorescence spectra *in situ* on the sheet. As shown in Fig. 2a, copper showed an excitation maximum at 254 nm and an

emission maximum at 450 nm. Lead showed an excitation maximum at 254 nm and an emission maximum at 400 nm (Fig. 2b). However, the quantum

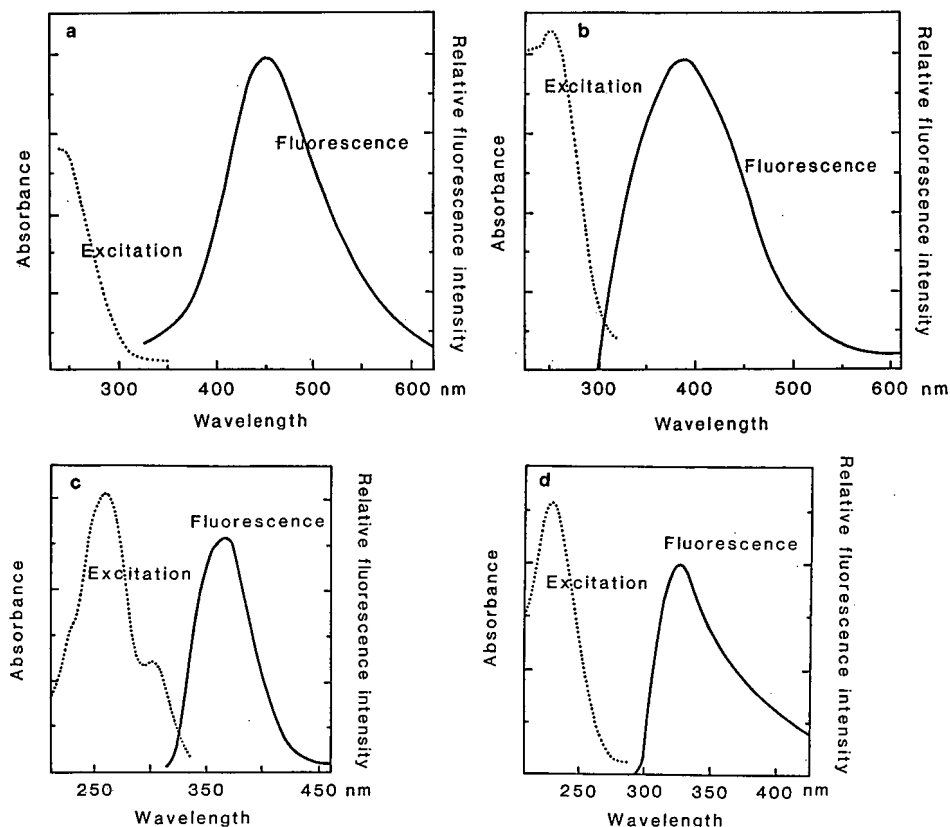


Fig. 2. Fluorescence spectra of metal ions heated on the sheet. a = Copper; b = lead; c = cerium; d = thallium.

yields of the products from both metals were only a few percent. Cerium(III) showed an excitation maximum at 260 nm and an emission maximum at 375 nm for blue fluorescence (Fig. 2c). Thallium showed an excitation maximum at 230 nm and an emission maximum at 325 nm for light blue fluorescence (Fig. 2d).

## DISCUSSION

We have found new phenomena in the fluorescence reactions of some metal ions on the new glass sheet. The fluorescent compounds produced on the sheet are stable at room temperature more than 1 month. These fluorescence reactions are not observed on thin layers of silica gel or in a test-tube heated at the temperatures used. Hence specific reactions occur on the porous glass surface. When the spot is heated, the fluorescent compounds are fused in the glass phase. In the fusion, the starting forms of the cations are essential factors for the fluorescence reactions, because endogeneous cations such as Ca, Mg and Al do not show a fluorescent background.

From the broad spectra as shown in Fig. 2, the fluorescences are different from the atomic fluorescences reviewed by Browner [8]. Many kinds of fluorescent compounds have been found. Inorganic chelating agents can be used to prepare fluorescent chelates for inorganic analyses, *e.g.*, 8-hydroxyquinoline, morin [6]. The systematic analysis of inorganic cations has been investigated by TLC using silica gel plates. The detection was based on conventional chromogenic reagents as described by Seiler and Rothweiler [9] and Ajmal *et al.* [10]. Inorganic crystalline fluorescent mixtures have been impregnated in the silica gel layer to detect some metal ions [7]. The present fluorescent reactions are simpler for TLC detection, although they are limited to the particular cations reported here. Some cations, such as copper, lead, vanadium and tin, are very sensitive with results comparable to atomic spectrometry.

Inorganic crystals of mixtures of several atoms are strongly fluorescent with almost 100% quantum yields. These crystals, such as the blueish white (Zn, Cd)S–Cu, Al + ZnS–Ag, the red phosphor  $Y_2O_3$ –S–Eu and the green phosphor  $Zn_2SiO_4$ –Mn, In, have been used for making fluorescent lamps [7]. These materials are different from the present fluorescent

products in their compositions and amorphous states. If the quantum yield in the glass can be increased, it will provide a new method to prepare fluorescent lamps.

Other photoluminescences are found in high-temperature superconductors, such as are ErBaCuO, NdBaCuO and GdBaCuO. Their photoluminescences excited by an argon ion laser are observed at 77 K and are influenced by the environmental crystalline conditions. The present fluorescent products are also different from the superconductors in principle as reported by Fujiwara and Kobayashi [11]. The new glass sheet may provide a simple way to make new materials in which the solutions of metal ions are easily combined and heated at high temperature.

It is very difficult to identify these new fluorescent compounds, because the chemical yields are not high and they are included in the glass. The glass matrix seems to stabilize the fluorescent compounds at room temperature, as seen in thermally activated delayed fluorescence of organic fluorescent substances in solid supports such as sodium acrylate polymer and filter-paper as described by Onoue *et al.* [12]. Time-resolved fluorescence spectroscopy has been applied to study the fluorescent characteristics of immobilized pyrene on an alkylated silica surface, as described by Wong *et al.* [13]. This kind of study is one of the ways to characterize fluorescent compounds. However, it is worth investigating these novel phenomena further in order to open up a new field of dry chemistry and also a new detection method for TLC.

## ACKNOWLEDGEMENTS

We express our gratitude to Mr. T. Nishimura and Mr. T. Takahara of the Electron Tube and Device Division, Horikawacho Works, Toshiba (Kawasaki, Japan) for their advice on the inorganic fluorescent compounds and the measurement of quantum yields of the fluorescence on the sheet.

## REFERENCES

- 1 H. L. MacDonell and J. P. Williams, *Anal. Chem.*, 33 (1961) 1552.
- 2 J. K. G. Kramer, E. O. Sciller and A. D. Robinson, *Anal. Chem.*, 36 (1964) 2379.
- 3 J. R. Swartwout and R. J. Gross, *J. Am. Oil Chem. Soc.*, 41 (1964) 378.

- 4 G. Alberti and G. Grassini, *J. Chromatogr.*, 4 (1960) 425.
- 5 M. Yoshioka, H. Araki, M. Kobayashi, T. Utsuki, T. Yaginuma and M. Nakano, *J. Chromatogr.*, 525 (1990) 205.
- 6 S. Udenfriend, *Fluorescence Assay in Biology and Medicine*, Vol. I, Academic Press, New York, 1962, Ch. 12.
- 7 H. Nakamura and Z. Tamura, *Bunseki Kagaku*, 22 (1973) 1356.
- 8 R. F. Browner, *Analyst (London)*, 99 (1974) 617.
- 9 H. Seiler and W. Rothweiler, *Helv. Chim. Acta*, 44 (1961) 941.
- 10 M. Ajmal, A. Mohammad and N. Fatima, *J. Liq. Chromatogr.*, 9 (1986) 1877.
- 11 Y. Fujiwara and T. Kobayashi, *Appl. Phys.*, 58 (1989) 52.
- 12 Y. Onoue, K. Hiraki, and Y. Nishikawa, *Anal. Sci.*, 3 (1987) 509.
- 13 A. L. Wong, M. L. Hunnicutt and J. M. Harris, *Anal. Chem.*, 63 (1991) 1076.



# Formation of zinc complexes during chromatography of porphyrins on fluorescent thin-layer plates

Koichi Saitoh, Chikara Kiyohara and Nobuo Suzuki

Department of Chemistry, Faculty of Science, Tohoku University, Sendai, Miyagi 980 (Japan)

(First received August 6th, 1991; revised manuscript received March 5th, 1992)

## ABSTRACT

An undesirable chemical change of a porphyrin to its zinc complex occurred on a particular silica gel thin-layer chromatographic (TLC) coating that contained a fluorescent indicator. This effect was observed for different porphyrins, such as *meso*-tetraphenylporphine, *meso*-tetrakis(*p*-tolyl)porphine, octamethylporphyrin, etioporphyrin and octaethylporphyrin in development with *m*-xylene. The zinc complex formation was attributable to the reaction of porphyrin with the zinc compound contained as a fluorescent indicator in the TLC coating.

## INTRODUCTION

Thin-layer chromatography (TLC) [1,2] and also high-performance TLC (HPTLC) [3–5] are powerful techniques for the separation and identification of porphyrins and metalloporphyrins and also common organic compounds. A TLC plate coated with an adsorbent containing a fluorescent indicator is usually particularly convenient for the detection of colourless organic compounds in chromatograms. Such fluorescent TLC coatings are applicable, of course, to the separation of coloured compounds. It is required in any event that the fluorescent indicators do not affect the chemical stability of the compounds to be chromatographed.

This work was undertaken to examine whether the fluorescent indicator contained in the TLC coating would influence the TLC behaviour of porphyrins. Six synthetic porphyrins were tested on three commercial silica gel TLC plates precoated with or without fluorescent indicator.

Correspondence to: Dr. K. Saitoh, Department of Chemistry, Faculty of Science, Tohoku University, Sendai, Miyagi 980, Japan.

## EXPERIMENTAL

### *Porphyrins and their metal complexes*

Fig. 1(a) and (b) show the general formulae of porphyrins ( $H_2P$ ) and their metal complexes  $[M(P)]$ , respectively.

Porphine ( $H_2Por$ ) ( $R_1 = R_2 = R_3 = H$  in Fig. 1) [6], *meso*-tetraphenylporphine ( $H_2 tpp$ ) ( $R_1 = \text{phenyl}$ ;  $R_2 = R_3 = H$ ) [3], *meso*-tetrakis(*p*-tolyl)porphine ( $H_2 ttp$ ) ( $R_1 = 4\text{-methylphenyl}$ ;  $R_2 = R_3 = H$ ) [4] and etioporphyrin I ( $H_2 etio$ ) ( $R_1 = H$ ;  $R_2 = \text{methyl}$ ;  $R_3 = \text{ethyl}$ ) [5] were prepared previously. Octamethylporphyrin ( $H_2 omp$ ) ( $R_1 = H$ ;  $R_2 = R_3 = \text{methyl}$ ) was synthesized from 3,4-dimethylpyrrole and formaldehyde [7]. Octaethylporphyrin ( $H_2 oep$ ) ( $R_1 = H$ ;  $R_2 = R_3 = \text{ethyl}$ ) was obtained from Strem Chemicals (Newburyport, MA, USA).

The complexes of each porphyrin with Zn(II)  $[Zn(P)]$  and Cu(II)  $[Cu(P)]$  were prepared by reaction of  $H_2P$  (1 mM) with zinc acetate (30 mM) and copper acetylacetonate (10 mM), respectively, while refluxing in chloroform.  $Zn(P)$  was purified by recrystallization from chloroform–methanol and  $Cu(P)$  by alumina column chromatography. The complexes, such as Ni(P) and Pd(P) ( $P = tpp$  [3],  $ttp$  [4],  $etio$  [5]), were synthesized previously.

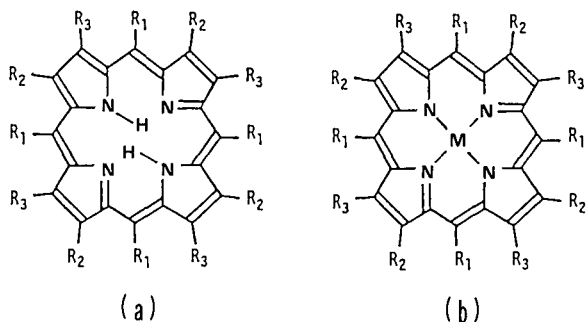


Fig. 1. General structural formulae of (a) porphyrin ( $H_2P$ ) and (b) its metal complex [(MP)].

### HPTLC

HPTLC plates (10 cm × 10 cm) were obtained from Merck (Darmstadt, Germany), including silica gel 60 (plate I), silica gel 60 F<sub>254</sub> (plate II) and silica gel 60 F<sub>254S</sub> (plate III). The first plate was free from the fluorescent indicator and the other two were of the fluorescent indicator-added type. Each HPTLC plate, after having been developed with methanol for cleaning, was activated by heating at 110°C for 30 min and then cooled in a silica gel desiccator for 2 h.

A 0.5- $\mu$ l aliquot of a chloroform solution of a porphyrin (at 0.1 mM or lower concentration) was placed on the TLC plate used. The chromatogram was developed 45 mm from the sample origin with *m*-xylene in the so-called solvent vapour saturation mode or the non-saturation mode in a horizontal sandwich chamber (Model 28510, Camag, Muttenz, Switzerland). In the former mode, a TLC plate coated with cellulose, which had been wetted with *m*-xylene, was used as a counter plate in the chamber. The temperature was 25°C. Each porphyrin was detected spectrophotometrically at about 400 nm with a Shimadzu (Kyoto, Japan) Model CS-920 densitometer.

### HPLC

A Shimadzu Model LC-6A HPLC system including an SPD-M6A photodiode-array spectrophotometric detector was used with an Inertsil ODS-2 (5  $\mu$ m) column (150 mm × 4.6 mm I.D.) (GL Sciences, Tokyo, Japan).

## RESULTS AND DISCUSSION

### HPTLC of porphyrins

*m*-Xylene was a convenient solvent for comparing the TLC behaviours of different porphyrins. Every porphyrin gave single spots with almost identical mobilities on plates I and III. On plate II, however, two poorly resolved spots appeared for each porphyrin whether it was developed in the solvent vapour saturation mode or the non-saturation mode (Fig. 2). One of the spots appeared with a migration comparable to those of the same porphyrin on plates I and III, and the other spot appeared with a larger migration. This spot was assigned to an unknown compound. When exposed to UV radiation of wavelength 365 nm, both spots found on plate II fluoresced with intense reddish colours.

A comparative study of the TLC behaviour was carried out for several examples of metalloporphyrins [M(P)], such as the Ni, Cu, Pd and Zn complexes of tpp, ttp and etio, on plate II. All the M(P)s of the first three metals moved near to the solvent front, which meant larger mobilities than the unknown compounds found with corresponding porphyrins ( $H_2P$ s) on plate II. In addition, the M(P)s of these three metals did not fluoresce under 365-nm UV radiation. However, each Zn(P) showed almost the same extent of migration as the unknown compound observed with the corresponding  $H_2P$ . Fig. 2 shows the comparative chromatograms of six  $H_2P$ s and corresponding Zn(P)s on plates I and II. In addition, it was confirmed that every Zn(P) fluoresced with a reddish colour under UV radiation.

It was considered at this stage that the unknown spot found in the chromatogram of an  $H_2P$  on plate II could be assigned to Zn(P) that was formed presumably from  $H_2P$  on the TLC coating of plate II.

### Effect of fluorescent indicator

In order to verify the hypothesis that an  $H_2P$  could be converted into its Zn complex on a particular TLC coating, the reactivities of  $H_2$ etio, which was taken as an example of  $H_2P$ , with the TLC coatings of plate I and II were compared.

About 250-mg portions of the TLC coatings (I and II) were scraped from plates I and II. Each portion of the coating, after having been activated by heating at 110°C for 30 min, was wetted with toluene and then packed in a short glass column tube of 4

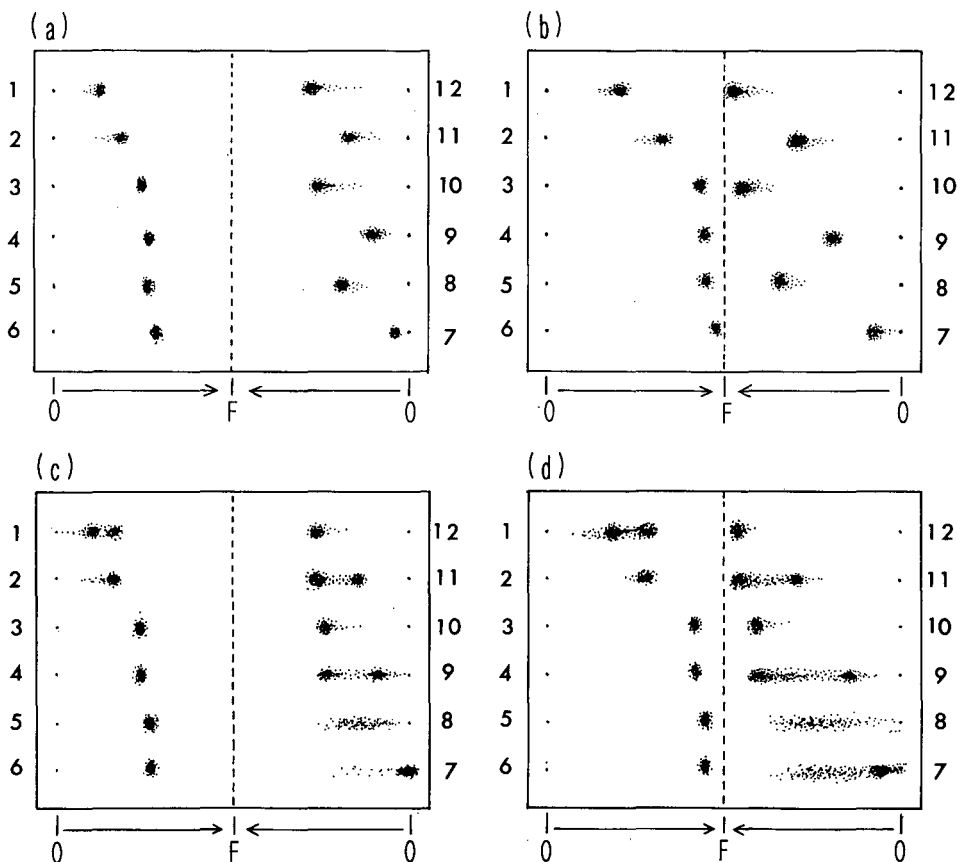


Fig. 2. HPTLC of porphyrins and their zinc(II) complexes on (a,b) plate I and (c,d) plate II. Development: 45 mm with *m*-xylene, (a,c) in the solvent vapour saturation mode with a 30-min preliminary exposure to the vapour and (b,d) the non-saturation mode. O, sample origin; F, solvent front. Compounds: 1 = H<sub>2</sub>Por; 2 = Zn(por); 3 = H<sub>2</sub>tpp; 4 = Zn(tpp); 5 = H<sub>2</sub>ttp; 6 = Zn(ttp); 7 = H<sub>2</sub>omp; 8 = Zn(omp); 9 = H<sub>2</sub>etio; 10 = Zn(etio); 11 = H<sub>2</sub>oep; 12 = Zn(oep).

mm I.D. A 50- $\mu$ l aliquot of a toluene solution of H<sub>2</sub>etio (0.1 mM) was placed on the column, which was then allowed to stand for 1 h at room temperature. Some coloured substance was eluted from the column with 0.8 ml of toluene, and the eluate was analysed by reversed-phase high-performance liquid chromatography (HPLC). The same procedures were also applied to the experiment using the TLC coating of plate II which was washed with 0.1 M hydrochloric acid in preference to the activation (hereafter denoted TLC coating II-aw).

The HPLC traces recorded for the eluate from the columns packed with different TLC coatings are compared with reference chromatograms of H<sub>2</sub>etio and Zn(etio) in Fig. 3. The eluates from coatings I and II-aw gave peaks at the same retention time as

H<sub>2</sub>etio, and that from coating II gave a peak at the retention time corresponding to Zn(etio). The visible absorption spectra recorded with the photodiode-array detector for the peaks in chromatograms (a) [and also (c)] and (b) matched perfectly those of H<sub>2</sub>etio and Zn(etio), respectively. It was reasonable to conclude that no chemical change had occurred for H<sub>2</sub>etio on TLC coating I, whereas a conversion from H<sub>2</sub>etio to Zn(etio) occurred on TLC coating II. Such an undesirable chemical change did not occur on TLC coating II-aw.

According to the manufacturer's literature (Merck), the coating on plate II contains zinc silicate as the fluorescent indicator and that on plate III some acid-resistant fluorescent indicator (more detailed information about this indicator is not

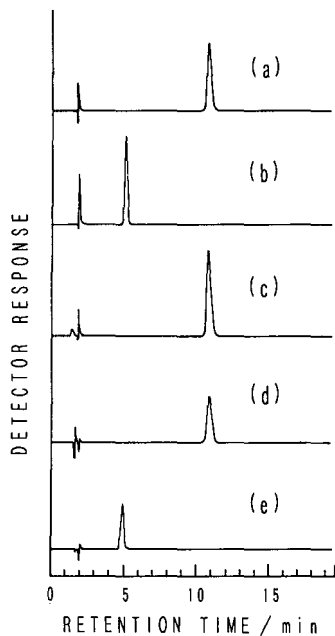


Fig. 3 HPLC of the eluate from  $H_2$ etio-charged small columns packed with adsorbents (a) I, (b) II and (c) II-aw and references chromatograms of (d)  $H_2$ etio and (e) Zn(etio). Mobile phase: methanol at 1 ml/min. Detection at 400 nm.

available). It is noted that TLC coating II, after having been washed with the acid, became non-fluorescent even on exposure to UV radiation, and the zinc washed from the coating was determined to be about 1% dry weight of the coating by atomic absorption spectrometry at 213.8 nm (Model 180-80 spectrometer, Hitachi, Tokyo, Japan).

It is considered that the foregoing peculiar HPTLC behaviour observed for porphyrins on plate II is attributable to the reactions of the porphyrins with the zinc compound (presumably zinc silicate) contained as the fluorescent indicator. Accordingly, plate II is not recommended for use in HPTLC separations of porphyrins. It should be noted that no metal complex formation was observed on plate III even though its coating contains a fluorescent indicator. HPTLC plates coated with both the non-fluorescent and the  $F_{254}S$  type of silica gel 60 (plates I and III, respectively) are recommended for the chromatography of porphyrins.

When copper complexes [Cu(P)] were tested in place of  $H_2P$ , no transmetallation from Cu(P) to Zn(P) occurred on plate II. This was attributable to the higher stability of Cu(P) than Zn(P) {the stability classes of Cu(P) and Zn(P) are II and III, respectively [8,9]}.

In conclusion, a preliminary check is required for the effect of the fluorescent indicator contained in the thin layer of adsorbent on the chemical stability of porphyrins in preference to application of the HPTLC plate to the separation of porphyrins. The formation of metal porphyrin complexes usually does not occur easily. Heating of a solution containing a high concentration of porphyrin and metal salt is applied many instances [10,11]. The formation of zinc-porphyrin complexes on an HPTLC plate is undesirable with respect to chromatography, whereas it is presumably useful for the preparation of the complex under such mild conditions in a solvent of low polarity at room temperature.

#### ACKNOWLEDGEMENT

This work was supported by Grants-in-Aid for Scientific Research from the Ministry of Education, Science and Culture.

#### REFERENCES

- 1 J.-H. Fuhrhop and K. M. Smith, in K. M. Smith (Editor), *Porphyrins and Metalloporphyrins*, Elsevier, Amsterdam, 1975, pp. 858-859.
- 2 W. I. White, R. C. Bachmann and B. F. Burnham, in D. Dolphin (Editor), *The Porphyrins*, Vol. I, Academic Press, New York, 1978, pp. 553-576.
- 3 K. Saitoh, M. Kobayashi and N. Suzuki, *Anal. Chem.*, 53 (1981) 2309.
- 4 M. Kobayashi, K. Saitoh and N. Suzuki, *Chromatographia*, 20 (1985) 417.
- 5 S. Miyake, K. Saitoh and N. Suzuki, *Chromatographia*, 22 (1986) 160.
- 6 Y. Wakui, K. Saitoh and N. Suzuki, *Chromatographia*, 22 (1986) 160.
- 7 D. O. Cheng and E. L. Gott, *Tetrahedron Lett.*, 17 (1976) 1157.
- 8 J. N. Phillips, *Rev. Pure Appl. Chem.*, 10 (1960) 35.
- 9 J. W. Buchler, in K. M. Smith (Editor), *Porphyrins and Metalloporphyrins*, Elsevier, Amsterdam, 1975, p. 197.
- 10 A. D. Adler, F. R. Longi, F. Kampas and J. J. Kim., *J. Inorg. Nucl. Chem.*, 32 (1976) 2443.
- 11 J. W. Buchler, in K. M. Smith (Editor), *Porphyrins and Metalloporphyrins*, Elsevier, Amsterdam, 1975, pp. 177-187.

# Theoretical aspects of chiral separation in capillary electrophoresis

## I. Initial evaluation of a model

Stephen A. C. Wren and Raymond C. Rowe

Pharmaceutical Department, ICI Pharmaceuticals, Macclesfield SK10 2NA (UK)

(First received December 11th, 1991; revised manuscript received February 12th, 1992)

### ABSTRACT

A simple model for the separation of pairs of enantiomeric molecules in capillary electrophoresis is presented. The model shows that the degree of separation depends on the concentration of chiral selector, and that there is an optimum concentration. The size of the optimum concentration depends inversely on the affinity of the enantiomers for the chiral selector. The model is supported by experimental results using propranolol and  $\beta$ -cyclodextrins.

### INTRODUCTION

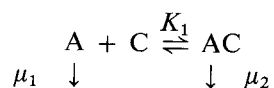
The analysis of the different enantiomeric forms of chiral molecules is an area of increasing importance in separation science. In the more conventional chromatographic procedures such as high-performance liquid chromatography, gas chromatography and thin-layer chromatography, chiral separation is brought about by the use of chiral additives in the mobile phase or the use of a chiral stationary phase.

In the newer field of capillary electrophoresis (CE), chiral separations are being undertaken by the use of chiral additives in the running buffer. A range of additives have been employed, some of which have already been successfully used in the conventional chromatographic procedures mentioned above. Examples are bile acids [1,2], chiral surfactants [3], cyclodextrins as buffer additives [4–6], cyclodextrins incorporated into a gel matrix [7] and

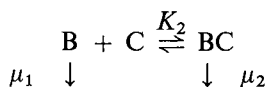
cyclodextrins mixed with other chiral selectors [8]. In several of these studies it was found that the degree of resolution obtained varied with the concentration of chiral selector [5,6,8] or the concentration of organic solvent in the buffer. As the chiral selector or organic solvent concentration was increased, the resolution could either increase, decrease or increase to a maximum before decreasing. In earlier work in this laboratory it was found that there was an optimum concentration of cyclodextrin for a particular chiral separation. It was therefore decided to investigate the underlying mechanism.

### MODEL

The following simple model is proposed and used as a working hypothesis. It is intended to cover simple situations where a freely soluble analyte interacts with a single chiral selector:



Correspondence to: Dr. S. A. C. Wren, Pharmaceutical Department, ICI Pharmaceuticals, Macclesfield SK10 2NA, UK.



where  $\mu_1$  is the electrophoretic mobility of the analyte in free solution,  $\mu_2$  is the electrophoretic mobility of the analyte-chiral selector complex and  $K_1$  and  $K_2$  are equilibrium constants. A and B are a pair of enantiomers which have the same electrophoretic mobility in free solution. They interact with a chiral selector C dissolved in the buffer to form the inclusion complexes AC and BC, which are assumed to have the same electrophoretic mobility. If the two enantiomers have different affinities for the chiral selector, *i.e.*,  $K_1$  and  $K_2$  are different, and the electrophoretic mobilities of the free and complexed enantiomers are different, then chiral resolution is possible. If the exchange of A between the free and bound forms is very rapid, then the apparent electrophoretic mobility of A will be a function of the proportion of the time when A is free and the proportion when it is complexed, *i.e.*,

$$\bar{\mu}_a = \left( \frac{[\text{A}]}{[\text{A}] + [\text{AC}]} \right) \mu_1 + \left( \frac{[\text{AC}]}{[\text{A}] + [\text{AC}]} \right) \mu_2 \quad (1)$$

$$[\text{AC}] = K_1[\text{A}][\text{C}] \quad (2)$$

and therefore

$$\bar{\mu}_a = \frac{\mu_1 + \mu_2 K_1 [\text{C}]}{1 + K_1 [\text{C}]} \quad (3)$$

The difference in the apparent electrophoretic mobility of A and B is

$$\Delta\mu = \frac{\mu_1 + \mu_2 K_1 [\text{C}]}{1 + K_1 [\text{C}]} - \frac{\mu_1 + \mu_2 K_2 [\text{C}]}{1 + K_2 [\text{C}]} \quad (4)$$

This rearranges to

$$\Delta\mu = \frac{[\text{C}](\mu_1 - \mu_2)(K_2 - K_1)}{1 + [\text{C}](K_1 + K_2) + K_1 K_2 [\text{C}]^2} \quad (5)$$

From eqn. 5, it is clear that the apparent mobility difference will be zero if  $K_1 = K_2$  or  $\mu_1 = \mu_2$ . In addition, the apparent mobility difference will be zero if  $[\text{C}] = 0$  or  $[\text{C}]$  is very large. This implies that in between these two extremes some value of  $[\text{C}]$  will give a maximum apparent mobility difference and hence a maximum separation of the two enantiomers.

This approach considers mobility difference rather

than resolution. This is because resolution is more complex mathematically as it must also consider electroosmotic mobility, band broadening due to diffusion and other factors such as injector and detector length [9]. Apart from diffusion, however, these factors will generally be independent of the chiral selector concentration and the optimum resolution would be expected to occur at a value of  $[\text{C}]$  similar to that which gives optimum separation.

This model was investigated by substituting into eqn. 5 some possible parameter values. Fig. 1 was generated with  $\mu_1 = 2$  and  $\mu_2 = 1$  using equilibrium constants of  $K_1 = 100$  and  $K_2 = 105$  and  $K_1 = 100$  and  $K_2 = 110$ . The graph shows that the apparent mobility difference reaches a maximum value as the chiral selector concentration is increased, before decreasing at higher chiral selector concentrations. The size of the difference in the apparent electrophoretic mobilities is greater the larger the difference in the equilibrium constants.

Fig. 2 shows the graphs generated by using  $\mu_1 = 2$  and  $\mu_2 = 1$  with three sets of equilibrium constants. The pairs in the sets differ by the same percentage value but have different absolute values. In each instance the resultant maximum apparent mobility difference is the same but the chiral selector concentration required to produce it is different. The greater the affinity of the enantiomers for the selector (the greater the equilibrium constants), the lower is the optimum selector concentration. This result is important as it indicates that the optimum concentration of chiral selector will be compound

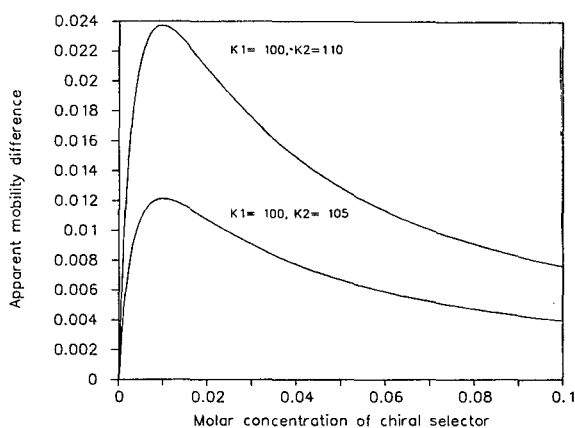


Fig. 1. Theoretical curves generated from eqn. 5 using  $\mu_1 = 2$  and  $\mu_2 = 1$  with the equilibrium constants  $K_1 = 105$  and  $K_2 = 105$  and  $K_1 = 100$  and  $K_2 = 110$ .

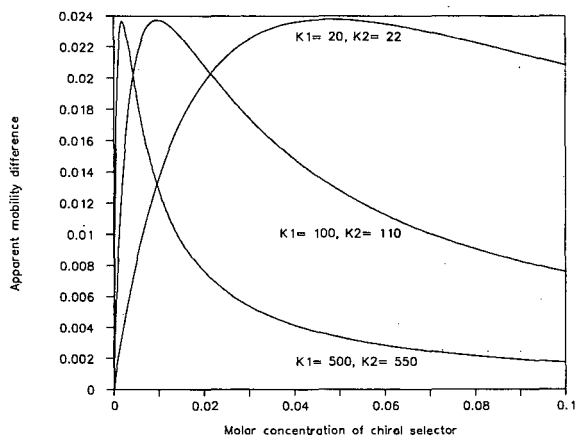


Fig. 2. Theoretical curves generated from eqn. 5 using  $\mu_1 = 2$  and  $\mu_2 = 1$  with three sets of equilibrium constants as shown.

dependent. For compounds that have a very high affinity for the chiral selector, the optimum concentration of chiral selector may well be much lower than the values of tens of millimoles typically mentioned in the previous references.

Fig. 3 shows the effect of keeping the analyte mobility constant and varying the apparent mobility of the analyte-chiral selector complex. It indicates that the apparent mobility difference between the two enantiomers will be greatest when the mobility of the analyte-chiral selector complex is in the opposite direction to that of the analyte itself. This

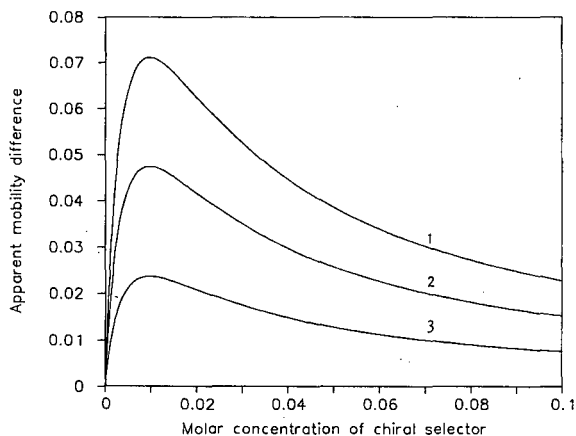


Fig. 3. Theoretical curves generated from eqn. 5 using three sets of mobility values with the equilibrium constants  $K_1 = 100$  and  $K_2 = 110$ . Curves: (1)  $\mu_1 = 2, \mu_2 = -1$ ; (2)  $\mu_1 = 2, \mu_2 = 0$ ; (3)  $\mu_1 = 2, \mu_2 = 1$ .

suggests that chiral selectors which carry a charge opposite to that on the analyte will be useful.

The optimum concentration of chiral selector can be found from eqn. 5 by the use of differential calculus. It occurs when  $d\Delta\mu/d[C] = 0$ , and this condition exists when  $(K_2 - K_1)(\mu_1 - \mu_2)(1 - K_1K_2[C]^2) = 0$ , i.e., apart from the trivial solutions when

$$[C] = \frac{1}{\sqrt{K_1K_2}} \quad (6)$$

A knowledge of the size or likely size of the equilibrium constants will therefore be of great use in selecting the correct concentration of the chiral selector. The equilibrium constant  $K_2$  will be some ratio of  $K_1$ , i.e.,  $K_2 = nK_1$ . Combining eqns. 5 and 6 will give the value of the apparent mobility difference at the optimum concentration of chiral selector:

$$\Delta\mu = \frac{(n-1)(\mu_1 - \mu_2)}{(\sqrt{n} + 1)^2} \quad (7)$$

This equation confirms the visual inferences from Figs. 1-3: the maximum apparent mobility difference between the two enantiomers will be large if the percentage difference between  $K_1$  and  $K_2$  is large and the mobility difference between the analyte and analyte-chiral selector complex is large.

## BACKGROUND

To check the model, it was decided to examine the separation of the enantiomers of propranolol (1-[(1-methylethyl)amino]-3-(1-naphthalenyloxy)-2-propanol) by the use of  $\beta$ -cyclodextrin (BCD) and "methyl"- $\beta$ -cyclodextrin (see Experimental) (MeBCD). These systems were chosen because of the good solubility of the components in water-urea or water and the results of previous work. Nuclear magnetic resonance data [10] had also shown that propranolol is included in the hydrophobic cavity of BCD and that the exchange of propranolol between the bulk solution and the cavity was rapid. Previous CE work [5,6] had shown that the resolution of the enantiomers was dependent on the concentration of BCD used and the concentration of methanol in the buffer. The work was carried out at a low pH in order to reduce the electroosmotic mobility.

## EXPERIMENTAL

Experiments were carried out on PACE 2100 and PACE 2000 systems (Beckman Instruments, High Wycombe, UK). The separation capillary was fused silica with an I.D. of 75  $\mu\text{m}$ , a total length of 57 cm and a length of 50 cm from the inlet to the detector. The samples were loaded by a 2-s pressure injection and separated at 25°C using a voltage of 20 kV. The data were recorded at 200 nm using a 2-Hz collection rate. Viscosity was measured using a Bohlin (Huntingdon, UK) VOR rheometer.

BCD and (*R*)-(+)-propranolol were obtained from Sigma (Poole, UK), lithium hydroxide from FSA Laboratory Supplies (Loughborough, UK), orthophosphoric acid from BDH (Poole, UK) and urea from Aldrich (Gillingham, UK). Racemic propranolol was made at ICI Pharmaceuticals (Macclesfield, UK) and MeBCD was a gift from Wacker Chemicals (Halifax, UK). The latter material had the 2-, 3- and 6-hydroxy groups partially substituted with methoxy groups, the average degree of substitution being 1.8. Lithium phosphate solution was prepared by adjusting the pH of a 50 mM solution of lithium hydroxide to 3.0 with orthophosphoric acid, followed by helium degassing.

The MeBCD buffers were all 40 mM in lithium phosphate (in order to reduce the current and hence power) and were prepared by mixing lithium phosphate, 370 mM MeBCD and water in the appropriate proportions to give ten buffers ranging from 0 to 74 mM in MeBCD. The BCD buffers were also 40 mM and were prepared from 50 mM lithium phosphate in 4 M urea, 80 mM BCD in 4 M urea and 4 M urea. The two most concentrated solutions were prepared directly from BCD and the other components. The buffers were measured at pH 3.12, degassed in an ultrasonic bath for 15 min, and filtered through a 0.2- $\mu\text{m}$  Anotop filter (Anotec Separations, Banbury, UK). For the MeBCD work propranolol was dissolved in water at 0.05 mg ml<sup>-1</sup>. The electroosmotic mobility was measured using a dilute propanone solution and was found to be very low, <0.04 · 10<sup>-4</sup> cm<sup>2</sup> V<sup>-1</sup> s<sup>-1</sup>; it was therefore ignored in the calculations. For BCD propranolol was dissolved at 0.01 mg ml<sup>-1</sup> in water.

Electrophoretic mobility was determined using the equation

$$\mu_{\text{ep}} + \mu_{\text{eo}} = \frac{IL}{Vt} \quad (8)$$

where  $\mu_{\text{ep}}$  and  $\mu_{\text{eo}}$  are the electrophoretic and electroosmotic mobilities, respectively,  $l$  is the capillary length to the detector and  $L$  is the total length,  $V$  is the operating voltage and  $t$  is the migration time. Duplicate propranolol injections were made at each buffer concentration and the average mobility value was used. The difference between the values from the two duplicates was typically 3%.

## RESULTS AND DISCUSSION

*Methyl- $\beta$ -cyclodextrin*

The separations of racemic propranolol achieved at six of the ten MeBCD concentrations are shown in Fig. 4. Clearly the degree of separation is dependent on the concentration and passes through a maximum value, as expected from the theory. By spiking a solution of (*R*)-(+)-propranolol into the original racemate, the (*R*)-(+)-enantiomer is shown to have the longer migration time and hence the greater affinity for MeBCD. The peaks tail due to overloading [11] but the efficiencies are still high with 115 000 theoretical plates being a typical value. There is no decrease in efficiency on adding MeBCD to the buffer. This supports the view that the exchange of propranolol between free solution and MeBCD complexation is rapid.

There is a significant difference in the heights of the peaks due to the two enantiomers. When peak areas are considered, however, the amounts become much closer to 50:50, and when the areas are divided by migration times, even closer. The migration times increase with MeBCD concentration. This has two causes: propranolol spends more time as the slowly moving propranolol–MeBCD complex and the buffer viscosity increases with increasing cyclodextrin concentration.

The buffer viscosity will affect the mobility of all the ionic species and hence the resultant current. The adjusted electrophoretic mobility of propranolol may therefore be determined by multiplying the experimentally determined value by the ratio of the current at zero MeBCD concentration by that at the concentration of interest.

The relative viscosity values determined from measuring the current agree well with those determined by direct measurement. For the buffers without MeBCD and with 75 mM MeBCD the current values are 55.5 and 42  $\mu\text{A}$ , giving a ratio of 1.32.

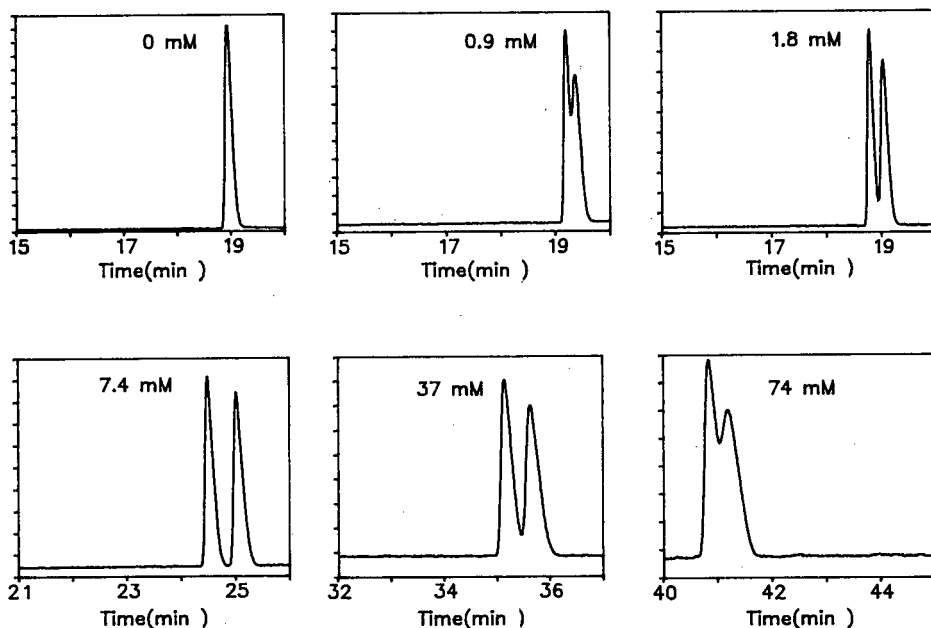


Fig. 4. Change in separation of propranolol enantiomers as the concentration of MeBCD is varied.

By direct measurement at 25°C the viscosities are 0.965 and 1.300 pascal seconds, giving a ratio of 1.35. At 35°C the relative viscosity by direct measurement is 1.34. The adjustment mentioned above was used to determine the apparent electrophoretic mobility of the (*S*)-(-)-enantiomer and the results are shown in Fig. 5. Initially the mobility decreases quickly before tending towards a limiting value at high MeBCD concentration. This reflects the fact that the propranolol spends an increasing amount of time complexed to MeBCD rather than in free solution.

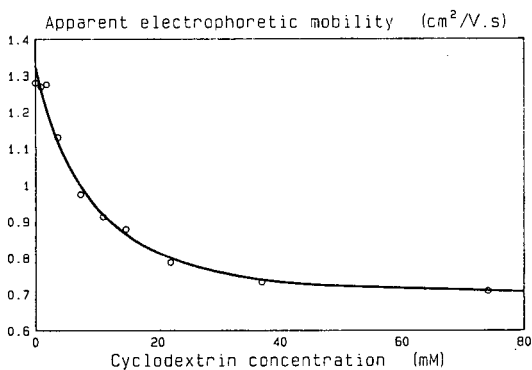


Fig. 5. Apparent electrophoretic mobility of (*S*)-(-)-propranolol as a function of MeBCD concentration.

In Fig. 6 the apparent mobility difference between the two enantiomers is plotted as a function of MeBCD concentration. The graph is very similar to the theoretical plots in Figs. 1-3, which lends strong support to the model proposed in eqn. 5. The optimum MeBCD concentration is *ca.* 5.5 mM, which implies an average value of the two equilibri-

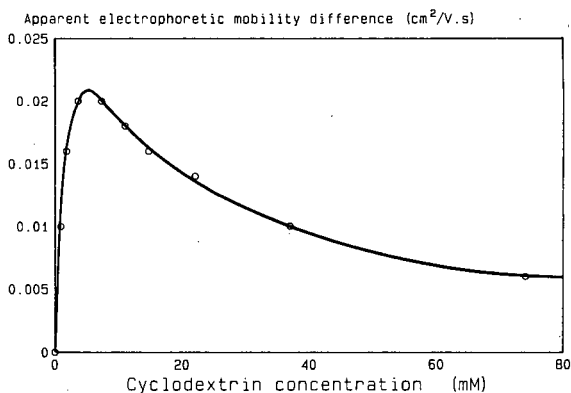


Fig. 6. Apparent electrophoretic mobility difference between the propranolol enantiomers as a function of MeBCD concentration. The apparent mobility difference was obtained via the times for the individual enantiomers after adjustment. The *R* form was identified by spiking (*R*)-(+)-propranolol into the original racemate.

um constants  $K_1$  and  $K_2$  of *ca.*  $180 \text{ mmol}^{-1}$ . The maximum mobility difference between the two enantiomers is *ca.*  $0.02 \text{ cm}^2 \text{ V}^{-1} \text{ s}^{-1}$ ; the use of this value and values of  $\mu_1$  and  $\mu_2$  of 1.3 and 0.7 (from Fig. 5) implies that the two equilibrium constants differ by about 12%.

The resolution between the enantiomers is measured by the use of the equation

$$R_s = \frac{2.354 (t_2 - t_1)}{(W_a^{\frac{1}{2}} + W_b^{\frac{1}{2}})} \quad (9)$$

where  $t_1$  = migration time of enantiomer 1 and  $W_a^{\frac{1}{2}}$  = peak width at half-height of enantiomer 1. The resultant graph is shown in Fig. 7.

As expected from Fig. 6, showing change in separation, the resolution is strongly dependent on MeBCD concentration. The optimum resolution occurs at *ca.* 4 mM, slightly lower than the concentration for optimum separation. The maximum value resolution is *ca.* 1.8. This was achieved in spite of overloading and compares favourably with the value of 1.4 from the use of two 25-cm  $\beta$ -cyclodextrin-bonded columns in series [12].

#### $\beta$ -Cyclodextrin

The variation in the apparent electrophoretic mobility difference between the two enantiomers as the BCD concentration is varied is shown in Fig. 8. The shape of the curve is again that expected on theoretical grounds. The maximum separation

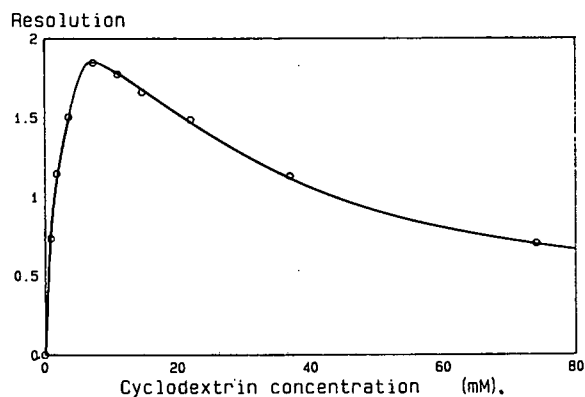


Fig. 7. Resolution between the propranolol enantiomers as a function of MeBCD concentration.

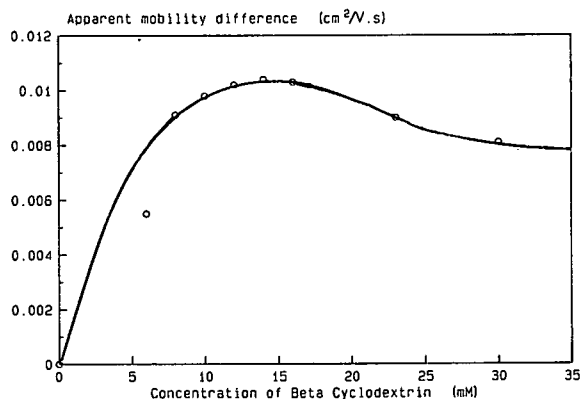


Fig. 8. Apparent electrophoretic mobility difference between the propranolol enantiomers as a function of BCD concentration.

achieved is shown in Fig. 9. A comparison with the work with MeBCD shows the optimum cyclodextrin concentration to be significantly higher and the maximum apparent mobility difference to be significantly lower. This indicates that propranolol has a lower affinity for BCD than MeBCD and that the difference between the stabilities of the two cyclodextrin-enantiomer complexes is lower. The reason for this is uncertain but it mirrors the results of Fanali's work with terbutaline [5].

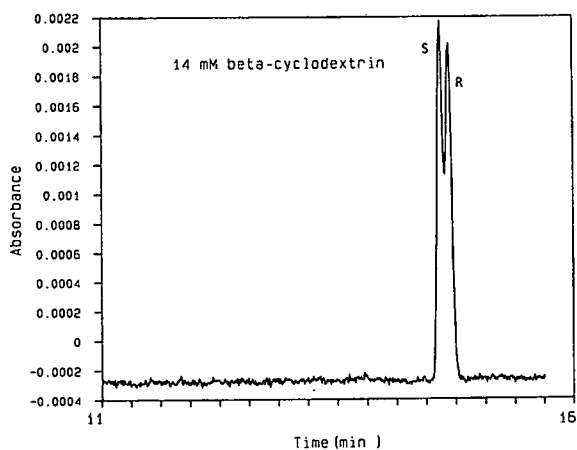


Fig. 9. Separation between propranolol enantiomers at the optimum BCD concentration.

## CONCLUSIONS

A simple model for the separation of enantiomers in CE is presented. The model is of use in the choice of chiral selector concentration and is strongly supported by work on propranolol using  $\beta$ -cyclodextrin. Further work is in progress to investigate the role of the organic solvent in the buffer and to check the applicability to other chiral molecules.

## REFERENCES

- 1 H. Nishi, T. Fukuyama, M. Matsuo and S. Terabe, *J. Microcol. Sep.*, 1 (1989) 234.
- 2 R. O. Cole, M. Sepaniak and W. L. Hinze *J. High Resolut. Chromatogr.*, 13 (1990) 579.
- 3 K. Otsuka and S. Terabe, *J. Chromatogr.*, 515 (1990) 221.
- 4 S. Fanali, *J. Chromatogr.*, 474 (1989) 441.
- 5 S. Fanali, *J. Chromatogr.*, 545 (1991) 437.
- 6 G. Persson, S. Palmarsdottir, A. Walhagen and L. E. Edholm, presented at the *15th International Symposium on Column Liquid Chromatography, Basle*, June 3-7, 1991.
- 7 A. Guttman, A. Paulus, A. S. Cohen, N. Grinberg and B. L. Karger, *J. Chromatogr.*, 448 (1988) 41.
- 8 H. Nishi, T. Fukuyama and S. Terabe, *J. Chromatogr.*, 553 (1991) 503.
- 9 X. Huang, W. F. Coleman and R. N. Zare, *J. Chromatogr.*, 480 (1989) 95.
- 10 D. Greatbanks and R. Pickford, *Magn. Reson. Chem.*, 25 (1987) 208.
- 11 F. E. P. Mikkers, F. M. Everaerts and Th. P. E. M. Verheggen, *J. Chromatogr.*, 169 (1979) 1.
- 12 D. W. Armstrong, T. J. Ward, R. D. Armstrong and T. E. Beesley, *Science (Washington, D.C.)*, 232 (1986) 1132.



# Chromogenic substrate for *endo*-polygalacturonase detection in gels

Oskar Markovič, Danica Mislovičová, Peter Biely and Kvetoslava Heinrichová

Institute of Chemistry, Slovak Academy of Sciences, Dúbravská cesta 9, 842 38 Bratislava (Czechoslovakia)

(First received February 13th, 1991; revised manuscript received February 26th, 1992)

---

## ABSTRACT

A simple, sensitive zymogram technique for the detection of *endo*-polygalacturonase (EC 3.2.1.15) in gel slabs after electrophoresis or isoelectrofocusing was developed. This technique employs a new chromogenic substrate prepared by coupling D-galacturonan DP 10 with Ostazin Brilliant Red S-5B dye. The detection of multiple forms of *endo*-polygalacturonase is based on the selective removal of depolymerized dyed substrate from the agar replicas by a solvent system that does not solubilize non-degraded dyed D-galacturonan DP 10 present in agar gel replicas.

---

## INTRODUCTION

Several methods have been described for resolving and detecting pectic enzymes and their multiple forms in electrophoretic gels; of special interest here is the detection of *endo*-polygalacturonase (EC 3.2.1.15).

The first group of these methods uses the incorporation of the substrate (pectic acid or pectin) directly into the separation gel. Following electrophoresis, the gels are incubated in a buffer to allow enzymic digestion of substrate and then stained with ruthenium red, toluidine blue or methylene blue [1–3]. This procedure is not suitable for isoelectric focusing. However, this limitation can be removed by methods using contact of the enzyme with substrate after electrophoretic separation, *e.g.*, by dipping the electrophoretic gel in substrate solution and revealing the enzymes with ruthenium red staining [4]. Even more sensitive and reproducible are methods employing the “zymogram technique”. The substrate gel is brought into close contact with

the gel in which the pectic enzymes were separated by isoelectrofocusing or sodium dodecyl sulphate electrophoresis. After detachment, the substrate gels are stained with ruthenium red or toluidine blue [5,6]. Pectic enzyme activity can also be revealed by using cetyltrimethylammonium bromide to precipitate the unhydrolysed pectin or pectic acid [7].

This paper describes the preparation of a new soluble chromogenic substrate prepared by coupling the dye Ostazin Brilliant Red S-5B with D-galacturonan and its use for the detection of *endo*-polygalacturonase in electrophoretic gels by the gel-replica technique.

## EXPERIMENTAL

### Enzyme assays

The *endo*- and *exo*-polygalacturonase activity was determined by measuring the increase in reducing groups [8] with sodium pectate ( $M_r \approx 27\,000$ ), D-galacturonan with a degree of polymerization (DP) of 10 and di-D-galactosiduronate as substrates, using D-galactopyranuronic acid as calibration standard. Activity is expressed in  $\mu$ moles of reducing groups per minute (1 U).

---

Correspondence to: Dr. O. Markovič, Institute of Chemistry, Slovak Academy of Sciences, Dúbravská cesta 9, 842 38 Bratislava, Czechoslovakia.

### Enzymes used

Commercial preparations of pectic enzymes in powder form were used: three samples of pectinase (*Aspergillus niger*) with polygalacturonase activity of 0.7–1.1 U/mg, two samples of pectofetidin (*Aspergillus foetidus*) with polygalacturonase activity of 0.8–1.3 U/mg (both preparations from the Factory of Microbiological Preparations, Botevgrad, Bulgaria; the samples used differed in date of preparation). One sample of leozyme (*Aspergillus niger* R3) with polygalacturonase activity 1.3 U/mg was the product of Slovak Canning Factory and Distilleries (Leopoldov, Czechoslovakia) and one sample of rohament P (*Aspergillus* sp.) with polygalacturonase activity 3.2 U/mg from Roehm (Darmstadt, Germany).

After dissolution in water and centrifugation, all enzyme preparations were tested with sodium pectate as substrate, reflecting both *endo*- and *exo*-polygalacturonase activities.

*exo*-Polygalacturonase (EC 3.2.1.67) isolated from carrots [9] as a freeze-dried product had specific activities of 0.52 U/mg with sodium pectate, 0.61 U/mg with D-galacturonan DP 10 and 0.13 U/mg with di-D-galactosiduronate as substrates. A fungal *exo*-polygalacturonase preferring oligomeric substrates was prepared from leozyme (*Aspergillus niger* R3) by chromatography on Sephadex G-75 and ion-exchange chromatography on DEAE-Sephadex A-50. This procedure allowed the separation of the less acidic *exo*-polygalacturonase ( $pI = 4.8$ ) from the more acidic *endo*-polygalacturonase ( $pI = 3.0$ ) [10]. This *exo*-polygalacturonase exhibited activities of 1.7 U/mg with sodium pectate, 2.3 U/mg with D-galacturonan DP 10 and 4.4 U/mg with di-D-galactosiduronate as substrates.

### Preparation of dyed substrate

D-Galacturonan (DP 10  $\pm$  2), prepared according to McCready and Seegmiller [11], was dissolved in water and mixed with an equal amount by weight of Ostazin Brilliant Red S-5B (SODB, Pardubice, Czechoslovakia). To the homogeneous solution, sodium acetate was added to a final concentration of 1% (w/v). The mixture was then made alkaline to pH 11 with sodium carbonate [1.25% (w/v) final

concentration], incubated for 2 h at 30°C and neutralized with acetic acid, and the dyed conjugate (OBR–galacturonan DP 10) was then precipitated by adding two volumes of ethanol and two volumes of acetone. The precipitated material was washed on a filter with ethanol–acetone–0.05 M acetate buffer, pH 5.0 (2:2:1), then with 96% ethanol and acetone and dried in air [12]. The products obtained contained on average 5% (w/w) of the dye (determined spectrophotometrically in aqueous solution at 540 nm by using Ostazin Brilliant Red S-5B as the calibration standard).

### Isoelectrofocusing

Isoelectrofocusing was done on ultra-thin layers of polyacrylamide gel (5% T, 3% C)<sup>a</sup> according to Radola [13], using Servalyte 3–10 (Serva, Heidelberg, Germany) as the carrier ampholyte.

### Detection of *endo*-polygalacturonase activity

OBR–galacturonan DP 10 (300 mg) was dissolved in 10 ml of distilled water by stirring and heating to 70°C. The dissolved substrate was mixed with 20 ml of hot 3% (w/v) agar solution in 0.2 M acetate buffer (pH 4.5) and poured between two polyester sheets mounted on glass plates, separated by plastic spacer bars (0.8 mm). After electrophoresis, the polyacrylamide gel was laid on the dyed substrate gel for 5–15 min at room temperature and then the substrate–agar replica was dipped in the solvent ethanol–acetone–0.1 M acetate buffer, pH 4.5 (2:1:1). It was possible to detect fungal polygalacturonase multiple forms with isoelectric points below 6 without previous preincubation of electrophoretic gels in an appropriate buffer. The zones of *endo*-polygalacturonase-degraded dyed substrate were continuously destained as a result of solubilization of dyed substrate fragments. The rate of the destaining depended on the degree of substrate digestion.

## RESULTS AND DISCUSSION

The detection of multiple forms of *endo*-polygalacturonase after electrophoresis or isoelectrofocusing in polyacrylamide gels was based on the selective removal of depolymerized dyed substrate from the substrate–agar replicas by a solvent which fixed the non-degraded dyed substrate in the gel. The principle of this method is identical with those

<sup>a</sup> C = g N,N'-methylenebisacrylamide (Bis)/%T; T = g acrylamide + g Bis per 100 ml of solution.

described for detection of *endo*-1,4- $\beta$ -glucanases, *endo*-1,4- $\beta$ -xylanases and  $\alpha$ -amylases [14,15].

The coupling of the dye Ostazin Brilliant Red S-5B with pectic acid ( $M_r \approx 27\,000$ ) and with citrus pectin ( $M_r \approx 60\,000$ ) produced a material containing only 4.5% (w/w) of the dye. This is in contrast to 15–20% of dye which can be attached to neutral polysaccharides such as hydroxyethylcellulose and partially hydrolysed starch [14,15]. Dyed pectic acid, containing *ca.* 2 mol of dye per mole of pectic acid (composed of *ca.* 150 saccharide units), and dyed citrus pectin (containing *ca.* 4 mol of dye per *ca.* 340 saccharide units), were found to be unsuitable for the detection of *endo*-polygalacturonase by the dyed substrate–agar gel overlay technique. OBR–galacturonan DP 10 containing 5.0% of the dye (*i.e.*, on average only each seventh molecule is dye bound) was suitable for the enzyme detection without previous separation of dyed and undyed D-galacturonan DP 10 molecules. An interesting feature of this short polygalacturonase substrate is that the first attack of an *endo*-acting enzyme may liberate fragments soluble in the presence of organic solvents, which would not be the case with dyed pectic acid, which required extensive digestion and overloading of the gel with polygalacturonase to generate short dyed fragments soluble in organic solvents.

Fig. 1 presents the results of isoelectric focusing and subsequent detection of *endo*-polygalacturonase in four commercial pectic enzyme preparations. The sensitivity of the method is in the range  $10^{-2}$ – $10^{-3}$  U of endopolygalacturonase. The gel replicas can be preserved by fixing on a chromatographic paper or by drying under vacuum.

OBR–galacturonan DP 10 was not a substrate for *exo*-polygalacturonases. Neither carrot nor *Aspergillus niger* *exo*-polygalacturonases produced a positive response even after incubation for 10 h of the separation gels with OBR–galacturonan DP 10–agar replicas (in a wet chamber). With high-molecular-mass substrates, *exo*-acting glycanases, for obvious reasons, do not liberate short dyed fragments from the corresponding dyed polysaccharides. For instance, amyloglucosidase does not attack Cibacron Blue–amylose [16] and Cibacron Blue–pachyman does not serve as a substrate for *exo*-1,3- $\beta$ -glucanase [17]. The pectin covalently dyed with N-(1-{4[(3,6-disulpho-1-naphthyl)azo]naphthyl})ethylenediamine is considered to be a sub-

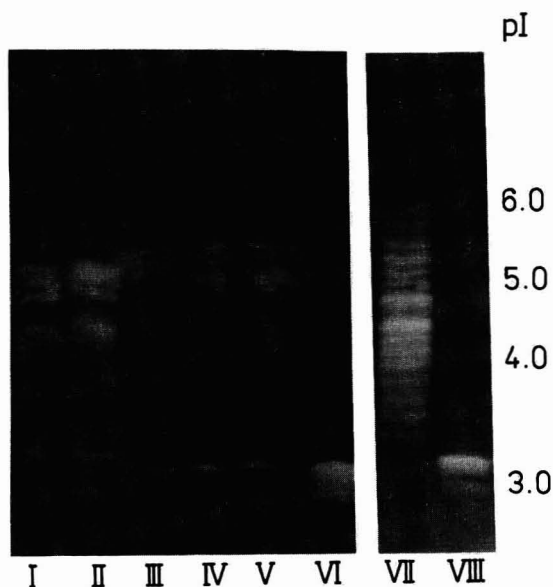


Fig. 1. Isoelectric focusing of commercial samples of pectic enzymes in ultra-thin layers of polyacrylamide gel with a pH 3–10 gradient. A 1- $\mu$ l volume of enzyme solution was applied. *endo*-Polygalacturonase was detected with OBR–galacturonan DP 10–agar detection gel kept in contact with the separation gel for 10 min. Lanes: I = pectofoetidin, sample 1 (10  $\mu$ g); II = pectofoetidin, sample 2 (10  $\mu$ g); III = pectinase, sample 1 (8  $\mu$ g); IV = pectinase, sample 2 (10  $\mu$ g); V = pectinase, sample 3 (10  $\mu$ g); VI = leozyme (12  $\mu$ g); VII = rohament (4  $\mu$ g); VIII = leozyme (7  $\mu$ g).

strate for endopeptinase only [18].

However, OBR–galacturonan DP 10 could theoretically serve also as a substrate for *exo*-polygalacturonase, as two or three subsequent cleavages from the non-reducing terminal could produce dyed fragments soluble in the presence of organic solvents, as fragments formed by the action of *endo*-polygalacturonase. Why this does not occur remains unclear, but the following possibilities are suggested: the dye is attached exclusively to D-galacturonic acid units present on the non-reducing terminus of the D-galacturonate DP 10, thus preventing the action of exopolygalacturonase; and/or the bulky dye ( $M_r = 615$ ) present on a relatively short substrate prevents the formation of the enzyme–substrate productive complex. The latter alternative finds some support in our previous observations that *exo*-polygalacturonase did not interact with partially acetylated D-galacturonic acid units in the pectic acid molecule [19].

OBR–galacturonan DP 10 was successfully used to follow the separation and purification of *Aspergillus endo-* and *exo-*polygalacturonases having different *pI* values; parallel detection of both *exo-* and *endo-*polygalacturonases was performed by using non-dyed D–galacturonan DP 10–agar gel overlay technique with subsequent ruthenium red staining [5].

OBR–galacturonan DP 10 could theoretically serve also as a substrate for *endo-*pectate lyase detection, but during these experiments a specific *endo-*pectate lyase was not available.

#### ACKNOWLEDGEMENTS

The authors are grateful to Dr. Karol Tihlárík for participation in the early attempts to prepare covalently dyed pectin and pectic acid and Mr. Tibor Lipka for excellent technical assistance.

#### REFERENCES

- 1 H. Stegemann, *Hoppe-Seyler's Z. Physiol. Chem.*, 348 (1967) 951–952.
- 2 R. H. Cruickshank and G. C. Wade, *Anal. Biochem.*, 107 (1980) 177–181.
- 3 T. A. McKeon, *J. Chromatogr.*, 455 (1988) 376–381.
- 4 N. Lisker and N. Retig, *J. Chromatogr.*, 96 (1974) 245–249.
- 5 M. D. Frey and B. J. Radola, in B. J. Radola (Editor), *Electrophoresis Forum '83, München*, Institut für Lebensmitteltechnologie und Analytische Chemie, Technische Universität München, Freising-Weihenstephan, 1983, pp. 252–257.
- 6 J. L. Ried and A. Collmer, *Appl. Environ. Microbiol.*, 50 (1985) 615–622.
- 7 Y. Bertheau, E. Madgidi-Hervan, A. Kotoujansky, C. Nguyen-The, T. Andro and A. Coleno, *Anal. Biochem.*, 139 (1984) 383–389.
- 8 M. Somogyi, *J. Biol. Chem.*, 195 (1952) 19–23.
- 9 K. Heinrichová, *Collect. Czech. Chem. Commun.*, 42 (1977) 3214–3221.
- 10 K. Heinrichová and O. Markovič, unpublished results.
- 11 R. M. McCready and C. G. Seegmiller, *Arch. Biochem. Biophys.*, 50 (1954) 440–450.
- 12 D. Mislovičová, O. Markovič and P. Biely, *Czech. Pat.*, 274 026 (1988).
- 13 B. J. Radola, *Electrophoresis*, 1 (1980) 43–56.
- 14 P. Biely, O. Markovič and D. Mislovičová, *Anal. Biochem.*, 144 (1985) 147–151.
- 15 P. Biely, D. Mislovičová, O. Markovič and V. Kaláč, *Anal. Biochem.*, 172 (1988) 176–179.
- 16 U. J. Marshall, *Anal. Biochem.*, 37 (1970) 466–470.
- 17 W. A. Philpott and J. M. Chapman, *Anal. Biochem.*, 79 (1977) 257–262.
- 18 D. R. Friend and G. W. Chang, *J. Agric. Food Chem.*, 30 (1982) 982–985.
- 19 K. Heinrichová and R. Kohn, *Collect. Czech. Chem. Commun.*, 45 (1980) 427–434.

# High-performance capillary electrophoretic analysis of chloramphenicol acetyl transferase activity

James P. Landers, Mark D. Schuchard, Malayannan Subramaniam, Tamara P. Sismelich and Thomas C. Spelsberg

*Department of Biochemistry and Molecular Biology, Mayo Clinic and Mayo Foundation, Rochester, MN 55905 (USA)*

(First received November 14th, 1991; revised manuscript received February 12th, 1992)

---

## ABSTRACT

This study highlights the potential utility of high-performance capillary electrophoresis (HPCE) for monitoring enzyme activity. Free-zone capillary electrophoresis is used to rapidly and reproducibly analyze the activity of the bacterial enzyme chloramphenicol acetyl transferase (CAT) which converts the substrates acetyl coenzyme A (CoA) and chloramphenicol to acetyl chloramphenicol and CoA. The results of this study indicate that HPCE may be an excellent tool for studying enzyme activities since it has several advantages over standard single parameters assays, most notably, the ability to monitor both loss of substrate and appearance of products simultaneously. Conditions have been identified for optimal separation of the substrate (chloramphenicol) from the products (acetylated derivatives). This presents a unique potential of HPCE for the analysis of enzymatic reactions that may be applied to areas of analytical research presently utilizing enzymatic reactions. One such analytical method is the CAT assay used for analysis of gene promoter activity. In this study, HPCE is shown to yield similar quantitative results with nonradiolabelled substrate in a fraction of the time. HPCE has several advantages over standard techniques including speed of analysis, no need for radiolabelled substrate, small sample volumes, high sensitivity/resolution and excellent quantitative capabilities.

---

## INTRODUCTION

High-performance capillary electrophoresis (HPCE) is a versatile, relatively new analytical technique that has combined the quantitative precision and instrumental control of high-performance liquid chromatography (HPLC) with the resolving power of electrophoresis. HPCE differs from other analytical separation techniques, such as HPLC, in that it is capable of unprecedented separation efficiency, *i.e.* has the potential for generating several hundred thousand theoretical plates [1]. HPCE is also capable of automated microscale electrophoretic separation of a number of samples in a reproducible manner within a relatively short period of time. Although there are some limitations with the

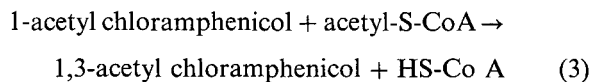
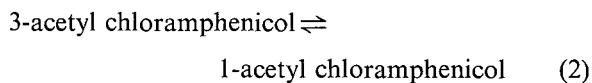
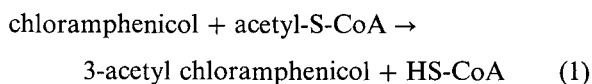
present technology, the resolving power, speed, quantitative ability, reproducibility and sensitivity at the femtomole level has made HPCE a valuable technique in the biomedical sciences (reviewed in refs. 2–4). HPCE has advanced tremendously since its conception almost a decade ago. Much of the early efforts were focussed on defining conditions for the separation of smaller molecules; a few of which include anticancer drugs [5], organic compounds [6,7] and metal ions [8]. More recent research efforts have applied the resolving power and sensitivity of HPCE to the analysis of macromolecular components of the cell such as peptides [9,10] (for review see ref. 4), proteins [2] and oligonucleotides [11–15] (for review see ref. 3).

There has been little in the literature regarding the use of HPCE for monitoring enzymatic reactions of either clinical or basic science interest. In this study we use, as a model system, the bacterial enzyme chloramphenicol acetyl transferase (CAT) to dem-

---

*Correspondence to:* Dr. J. P. Landers, Department of Biochemistry and Molecular Biology, Mayo Clinic and Mayo Foundation, Rochester, MN 55905, USA.

onstrate the utility of HPCE for monitoring enzyme activity. CAT is an enzyme synthesized in several strains of chloramphenicol-resistant bacteria [16]. The properties of the enzyme vary according to the bacterial strain from which it is purified and no CAT is representative of all the enzymes. Typically, the native enzymes have a molecular mass of 80 000, a quaternary structure of four identical subunits of 20 000 and isoelectric points ranging from 4.0–5.4 [17]. As indicated by its name, CAT catalyzes the conversion of the substrates chloramphenicol and acetyl coenzyme A (acetyl-S-CoA), to the products 3-acetyl-chloramphenicol and coenzyme A (HS-CoA) as described by eqn. 1. The acetyl group of the 3-acetylchloramphenicol congener can apparently undergo a non-enzymatic, pH-dependent migration to form the 1-acetylchloramphenicol product (eqn. 2) which then can be further acetylated enzymatically (eqn. 3).



One of the classic extensions of this particular enzyme activity is its use in the molecular biology technique that specifically exploits the enzyme-catalyzed acetylation of chloramphenicol. The CAT assay is used to characterize the transcriptional activity of a eukaryotic promoter and of regulatory sequences in the 5' flanking domains [17] found upstream of actively transcribed genes [18]. Ideally, promoter activity is measured by the amount of gene product produced in response to a regulator of the specific promoter. However, not all gene products are convenient to assay. Therefore, to circumvent this problem, the coding sequence of the bacterial CAT gene is connected to a promoter and/or 5' flanking domain in question. Cells are transfected with an expression vector containing the CAT gene downstream of the specific promoter sequence to be evaluated and the cells are treated with an activator. If the sequence has promoter activity, transcription of the CAT gene ensues and, in the presence of the

cellular translational machinery, the mRNA is translated to yield an active CAT enzyme. Because there is not a eukaryotic counterpart of the CAT gene, the enzyme activity can be directly and quantitatively measured in the extract of the cell. The level of CAT enzyme activity corresponds to the amount of CAT synthesized, which in turn reveals the level of activity of the promoter.

In this study, we show that enzyme-dependent loss of reactants and formation of products can be monitored accurately and reproducibly with HPCE. The use of borate as a buffer is necessary for this separation since its apparent complexation with chloramphenicol results in the separation of this substrate from the acetylated products. The ability to monitor CAT activity with HPCE is not only of interest from an enzymological perspective, but is discussed in terms of the potential extrapolation of these findings to improve upon a present day molecular biological technique, the CAT assay.

## EXPERIMENTAL

### *Chemicals and reagents*

Chloramphenicol was obtained from Boehringer Mannheim, the acetyl coenzyme A from Pharmacia, the diacetyl chloramphenicol, CAT (isolated from *E. coli*), coenzyme A, sodium tetraborate, dithiothreitol (DTT), glycerol and boric acid from Sigma and the Tris-Cl from ICN Chemicals. All solutions were made with Milli-Q purified distilled water. [<sup>14</sup>C]Chloramphenicol was purchased from New England Nuclear (NEN).

### *Incubation conditions for CAT activity*

CAT was stored as a stock solution in 50% glycerol, 10 mM Tris-HCl, 0.5 mM DTT, pH 7.5 at a stock concentration of 1 Unit/μl. Acetyl coenzyme A and chloramphenicol were maintained at stock concentrations of 4 mM (in water) and 11 mM (in 95% ethanol) respectively. All components were stored at –20°C, and kept on ice until added to the incubation mixture. For CAT activity, the appropriate amount of enzyme was added to Tris buffer (20 mM Tris-HCl pH 7.5) containing acetyl CoA and chloramphenicol, and incubated in a water bath equilibrated at either 27, 37, 44 or 55°C for varied times. The reaction was terminated by boiling the sample for 2 min. For stability studies at 27°C, the

sample was simply allowed to stand in a Beckman minivial within a capped 4-ml sample tube in the P/ACE 2050 unit.

#### CAT enzymatic assay

**[<sup>14</sup>C]Chloramphenicol thin-layer chromatographic (TLC) analysis.** The CAT assays using TLC were performed following the procedure of Gorman *et al.* [17] with slight modifications. The 150- $\mu$ l reaction mixture contained 20 mM Tris-Cl, pH 7.5, 0.513 mM [<sup>14</sup>C]chloramphenicol (NEN 1.3 mCi/mmol, 0.1  $\mu$ Ci), 0.533 mM acetyl coenzyme A (Pharmacia, Sweden) and 1 U CAT enzyme. The enzymatic reaction was performed at 27°C for different time periods at which point the reactions were stopped by boiling the sample. The [<sup>14</sup>C]chloramphenicol and its acetylated derivatives were extracted with 500  $\mu$ l of ethyl acetate. The organic phase was removed and dried down on a speed vac. The residue was dissolved in 30  $\mu$ l of ethyl acetate and spotted on a silica gel TLC plate. The TLC plate was placed in a tank containing chloroform–methanol (90:10) for ascending chromatography. Following the chromatography the TLC plate was autoradiographed.

**HPCE analysis.** The CAT assay mixtures were prepared for HPCE by filtration through a 0.22- $\mu$ m syringe filter. The fused-silica capillary (47 or 57 cm  $\times$  50  $\mu$ m I.D.; uncoated; 7 cm from the detector to the outlet) was equilibrated with the running buffer consisting of 100 mM borate/tetraborate buffer at pH of 8.3 (a minimum 15-min rinse or preferably overnight equilibration). Each method

involved a 1-min rinse with running buffer, injection of sample, separation, 1-min rinse with 0.1 M NaOH and finally, a 2-min rinse with running buffer. Unless otherwise noted, the sample was pressure injected for 1–5 s (*ca.* 1.3 nl/s) into the capillary and separation carried out on a Beckman P/ACE Model 2050 at 25 kV, 32  $\mu$ A, 25°C. Unless otherwise noted, detection was at wavelength  $\lambda = 200$  nm. Data were collected and peak migration time and area were analyzed using Beckman System Gold Version 6.0 software.

#### Effect of DTT on coenzyme stability

Coenzyme A (0.5 mg/ml in 100 mM borate buffer, pH 8.3) was incubated with or without 20 mM DTT at 27°C. The samples were kept at 4°C until incubation at 27°C and analysis initiated by HPCE at time 0 and 7 h.

## RESULTS

Fig. 1 shows the chemical structures of the substrates chloramphenicol and acetyl coenzyme A in their fully protonated form. Fig. 2 shows an electropherogram of standard acetyl coenzyme A, chloramphenicol, diacetyl chloramphenicol and coenzyme A. A net negative charge on coenzyme A at a pH of 8.3 accounts for the clear separation from chloramphenicol which is uncharged. Separation of the acetylated chloramphenicol from the chloramphenicol is interesting since both are neutrally charged under these conditions. Acetylated chlor-

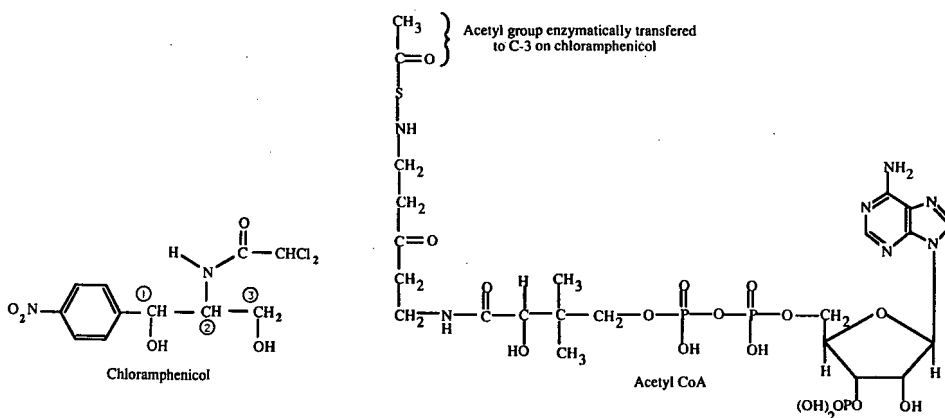


Fig. 1. Chemical structures of chloramphenicol and acetyl coenzyme A.

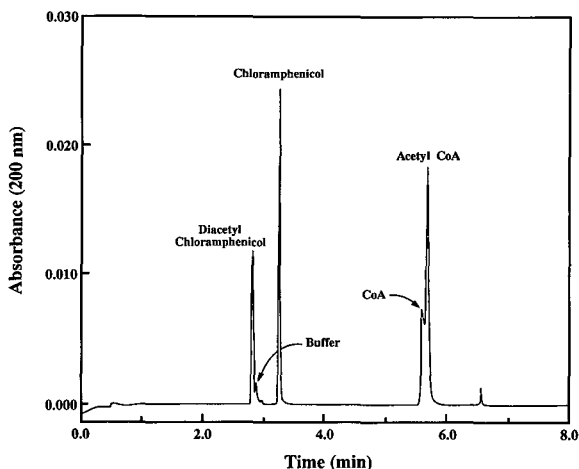


Fig. 2. HPCE separation of CAT enzyme substrates and products. Purified acetyl coenzyme A, coenzyme A, chloramphenicol and diacetylated chloramphenicol (all at a concentration of *ca.* 500 mg/ml in 20 mM Tris buffer pH 7.5) were injected by pressure for 1 s (equivalent to 1.3 nl or 650 pg) into a 57 cm  $\times$  50  $\mu$ m capillary and separated at 25 kV.

amphenicol migrates, as expected, with endosmotic flow (EOF; the bulk flow of buffer towards the cathode; neutral molecules migrate with this) but surprisingly, chloramphenicol elutes later than EOF, indicating that other variables are playing a role in the separation. Borate appears to be a variable since separation in phosphate buffer at the same pH did not lead to the resolution of chloramphenicol and the acetylated derivatives which both comigrated with EOF (data not shown). Acetyl coenzyme A and coenzyme A were found to be barely separable under these experimental conditions (coenzyme A, 5.7 min; acetyl coenzyme A, 5.8 min in the 57-cm capillary) probably as result of the thiol group of CoA not being ionized at this pH. Purified monoacetyl chloramphenicol was not commercially available as a pure standard and therefore the identity of the acetylated chloramphenicol peak was determined by a process of elimination. Using purified standards, the minimum detectable on-column mass of both the diacetylated and unacetylated forms of chloramphenicol was *ca.* 1 pg and optimal at  $\lambda = 200$  nm. Detection sensitivity for these types of compounds at  $\lambda = 200$  nm was approximately 2–3 times greater than at  $\lambda = 214$  nm (data not shown). Addition of CAT to 25 mM

Tris–Cl buffer, pH 7.5 containing a 500  $\mu$ M concentration of both chloramphenicol and acetyl coenzyme A led to a measurable loss of substrate and appearance of products. Fig. 3 illustrates the enzyme-dependent (1 Unit) loss of chloramphenicol and acetyl coenzyme A and the corresponding appearance of peaks which represent acetylated forms of chloramphenicol and coenzyme A as described by the equations in the Introduction. While a minor amount of diacetyl chloramphenicol may be produced (typically <1%), there was no indication that it was separable under these conditions from the major product, 3-acetyl-chloramphenicol. When an enzymatic reaction mix is spiked with diacetylchloramphenicol, the acetylated chloramphenicol peak is increased with no other observable peaks (data not shown). Determination of the peak area was made for calculation of the percent conversion of chloramphenicol to acetylated chloramphenicol as a function of time at this temperature and is shown in Fig. 4A. A linear rate of formation of product occurs within 30 min and thus represents the useful reaction time for kinetic studies. Conversion was complete at 2 h at 27°C even though approximately 15% of the substrate was still available. The leveling off may have been due either to the temperature-dependent inactivation of CAT or to a product feedback inhibition. The quantitative results obtained with HPCE are similar to those obtained by the more laborious TLC method using  $^{14}$ C-labelled substrate (Fig. 4A and B). The data shown in Fig. 4A were obtained by linear scanning of the autoradiogram obtained from TLC (Fig. 4B). The slight difference in the saturation level with the two assay methods may be due to inaccuracy of linear densitometry scanning of the autoradiogram. The temperature-dependency of the CAT activity is illustrated in Fig. 5. As expected, higher temperatures resulted in higher enzyme activity with optimal production of monoacetyl chloramphenicol in 1 h occurring at 44°C. A temperature of 55°C appears to be less productive, perhaps due to a more rapid inactivation of the enzyme. As expected, the CAT-catalyzed conversion was found to be dependent upon the concentration of both the reactants and the enzyme with maximal production of acetylated chloramphenicol and coenzyme A occurring at a 500  $\mu$ M concentration of both reactants with 1 Unit of CAT (data not shown). Increasing the substrate

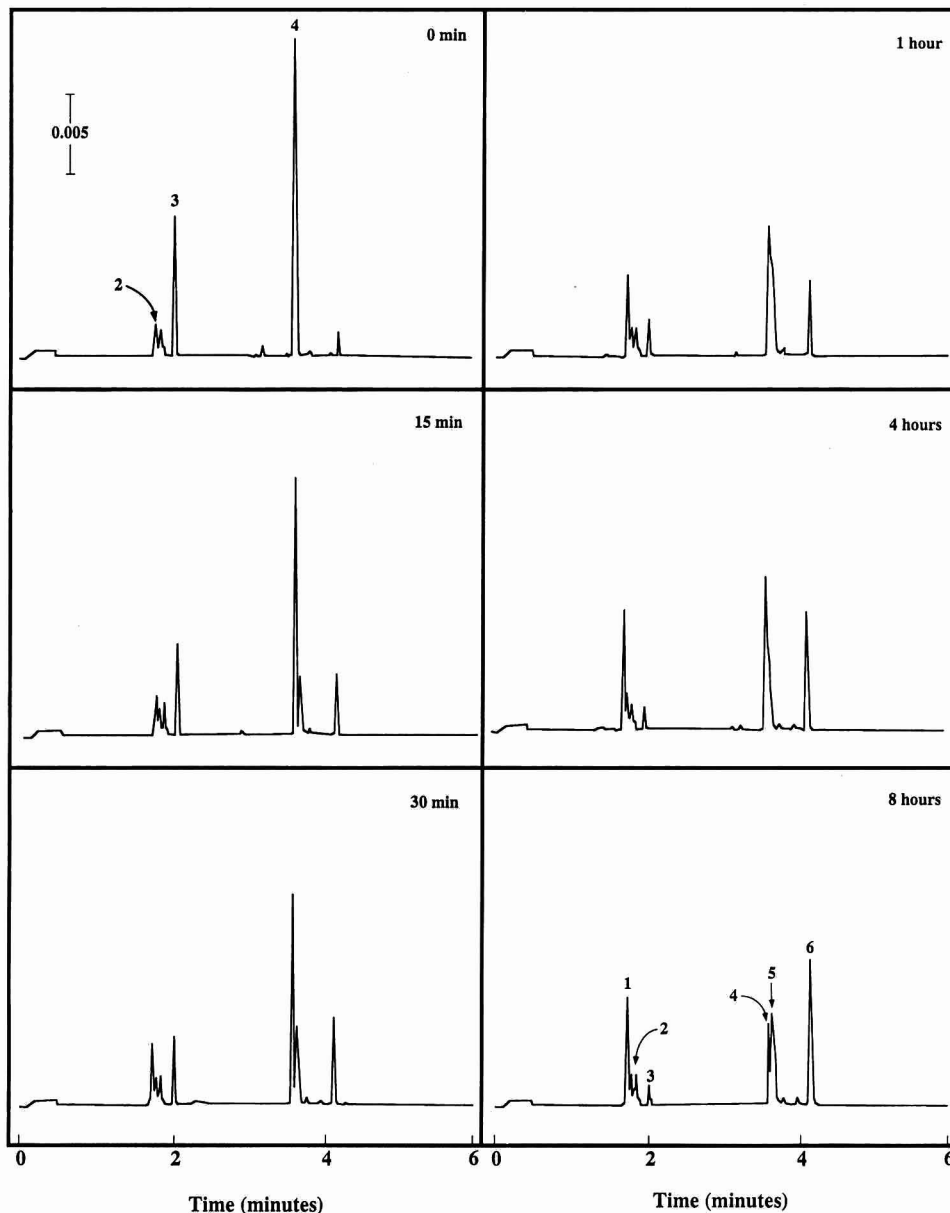


Fig. 3. HPCE analysis of the CAT-catalyzed acetylation of chloramphenicol. Chloramphenicol ( $500 \mu\text{M}$ ), acetyl coenzyme A ( $500 \mu\text{M}$ ) incubated in  $20 \text{ mM}$  Tris-Cl at  $27^\circ\text{C}$  for 0, 15, 30, 60, 240 and 480 min in the presence of 1 Unit of CAT. The reaction volume for each sample was  $150 \mu\text{l}$ . The resultant mixtures were diluted 1:1 with tetraborate buffer pH 8.3 and pressure injected for 5 s into a  $47 \text{ cm} \times 50 \mu\text{m}$  capillary and separated at 25 kV. Identified peaks: 1 = acetylated chloramphenicol; 2 = Tris-HCl; 3 = chloramphenicol; 4 = acetyl CoA; 5 = CoA; 6 = product of CoA.

beyond this concentration did not enhance production of the acetylated chloramphenicol.

Loss of substrate (chloramphenicol and acetyl coenzyme A) was due solely to the activity of the

enzyme and not to a non-enzymatic degradation since exposure to  $23^\circ\text{C}$  for 36 h or  $100^\circ\text{C}$  for 2 min had a negligible effect on the amount of each of the substrates or the shape of the peaks (data not

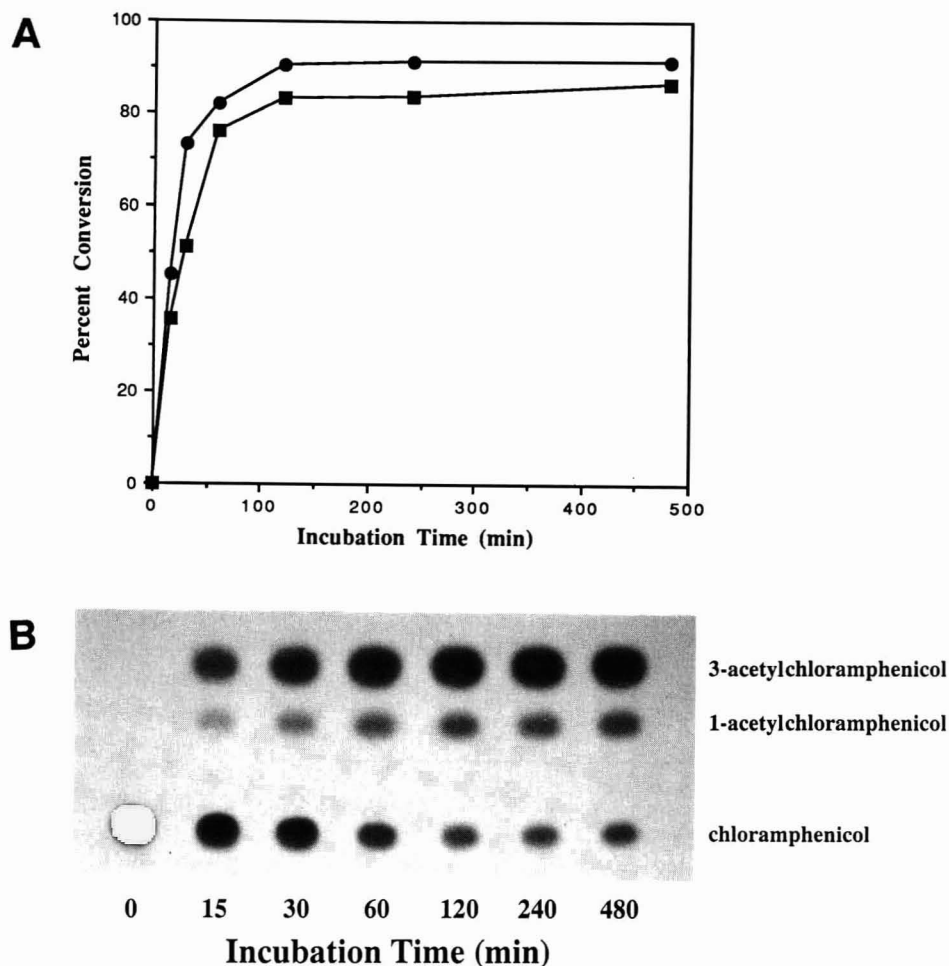


Fig. 4. CAT-catalyzed production of acetylated chloramphenicol. (A) A comparison of the percent conversion of chloramphenicol to acetyl chloramphenicol by 1 Unit of CAT at 27°C using HPLC analysis (■) and the standard TLC method (●). Percent conversion was determined by the peak area for the HPLC analysis and linear scanning densitometry of the autoradiogram for the TLC method. (B) Autoradiograph of TLC separation of the [<sup>14</sup>C]acetylchloramphenicol from the [<sup>14</sup>C]chloramphenicol substrate.

shown). This was not the case for the reaction product coenzyme A which eluted as a relatively broad peak and appeared to undergo a temperature-dependent, non-enzymatic degradation at temperatures greater than 4°C. At 27°C, the time-dependent increase in magnitude of the peak at ca. 6.0 min clearly results from the loss of coenzyme A (Fig. 6). The identity of this peak has not been determined unequivocally, but the possibility that it represents ADP, pantothenic acid or  $\beta$ -mercaptoethylamine (subcomponents of coenzyme A) has been eliminated since these standards did not co-migrate with this peak (data not shown). Interestingly, the pres-

ence of DTT appeared to prevent the loss of coenzyme A. Analysis of the samples at time 0 and 7 h of incubation at 27°C showed that the presence of DTT prevented the formation of the peak previously observed, indicating that this is most likely an oxidized form of coenzyme A (Fig. 7A). The absence of DTT led to the total conversion of coenzyme A to the oxidized product over the course of 7 h (Fig. 7B). The remarkably unstable nature of coenzyme A under these experimental conditions is highlighted in graphic form in Fig. 8 which shows the non-enzymatic loss at 27°C in comparison with the other CAT reaction components. In contrast to coenzyme

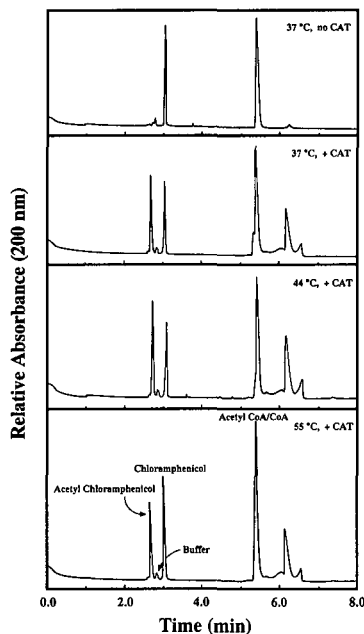


Fig. 5. Temperature-dependence of the CAT-catalyzed conversion of substrate to product. Chloramphenicol ( $500 \mu\text{M}$ ), acetyl coenzyme A ( $500 \mu\text{M}$ ) incubated in  $20 \text{ mM}$  Tris-Cl at 37, 44 and  $55^\circ\text{C}$  for 1 h. One unit of CAT was added to the indicated reactions in a total volume of  $150 \mu\text{l}$ . Samples were pressure injected (3 s) into a  $57 \text{ cm} \times 50 \mu\text{m}$  capillary and separated at 25 kV.

A, chloramphenicol, acetyl chloramphenicol and acetyl coenzyme A were very stable under similar conditions since no loss of these components was observed over the course of 8 h. The slight increase in their concentration over the course of the experiment is most likely due to a concentrating effect result from evaporation of solvent at  $27^\circ\text{C}$ . Despite the use of rubber caps on the sample vials, a loss of approximately 5% of sample volume per hour has been routinely observed (data not shown). This is a significant loss with microvials the capacity of which is approximately  $25 \mu\text{l}$ .

## DISCUSSION

In this study, we have demonstrated that both the substrates and products of the CAT enzymatic reaction can be separated rapidly by HPCE with a borate buffer system at pH 8.3. Loss of substrates (acetyl coenzyme A and chloramphenicol) and the

formation of products (acetylated chloramphenicol and coenzyme A) could be clearly observed in a manner dependent upon time and temperature, as well as reactant and enzyme concentration. The observed separation of chloramphenicol from its acetylated derivative is curious in light of the fact that they both are neutrally charged under these experimental conditions and hence would be expected to migrate with EOF. The fact that chloramphenicol elutes later than the EOF leads to two possible hypotheses. The first is based on the potential for chloramphenicol to interact with the capillary wall. It seems unlikely, based on the structure of chloramphenicol, that this molecule would be ionized at a pH of 8.3. Thus, it is possible that the presence of intact hydroxyl groups make chloramphenicol amenable to interaction (polar) with the capillary wall ( $\text{SiO}_3$ ) which would ultimately retard its migration. In contrast, acetylated chloramphenicol is less polar (especially the diacetylated derivative which has both hydroxyl groups masked), interacting with the wall to a substantially lesser degree and would thus migrate with EOF. The second hypothesis exploits the potential of chloramphenicol to interact with borate. Since borate is known to complex with vicinal hydroxyls, it is possible that it forms a complex with the two free hydroxyl groups of chloramphenicol, imparting a net negative charge to the molecule at pH 8.3. This complexation is not possible with either the mono- or diacetylated chloramphenicol and hence, this molecule comigrates with the endosmotic flow. This latter possibility appears to be the case. Separation of identical samples in phosphate and borate buffer at the same pH showed that chloramphenicol and the acetylated derivatives were not resolved in phosphate buffer but instead, comigrate with EOF (data not shown). These results suggest that, as shown by Lui *et al.* [19] with sugars, borate may be forming specific complexes with chloramphenicol but not acetylated chloramphenicol.

With respect to the monitoring of enzyme activity, HPCE has advantages over standard colorimetric or radiometric analysis which monitor changes in a single parameter. This includes not only the time required for analysis of a single sample, but also the fact that conditions can be found in which all components (substrates and products) can be monitored simultaneously. For the case of CAT, activity

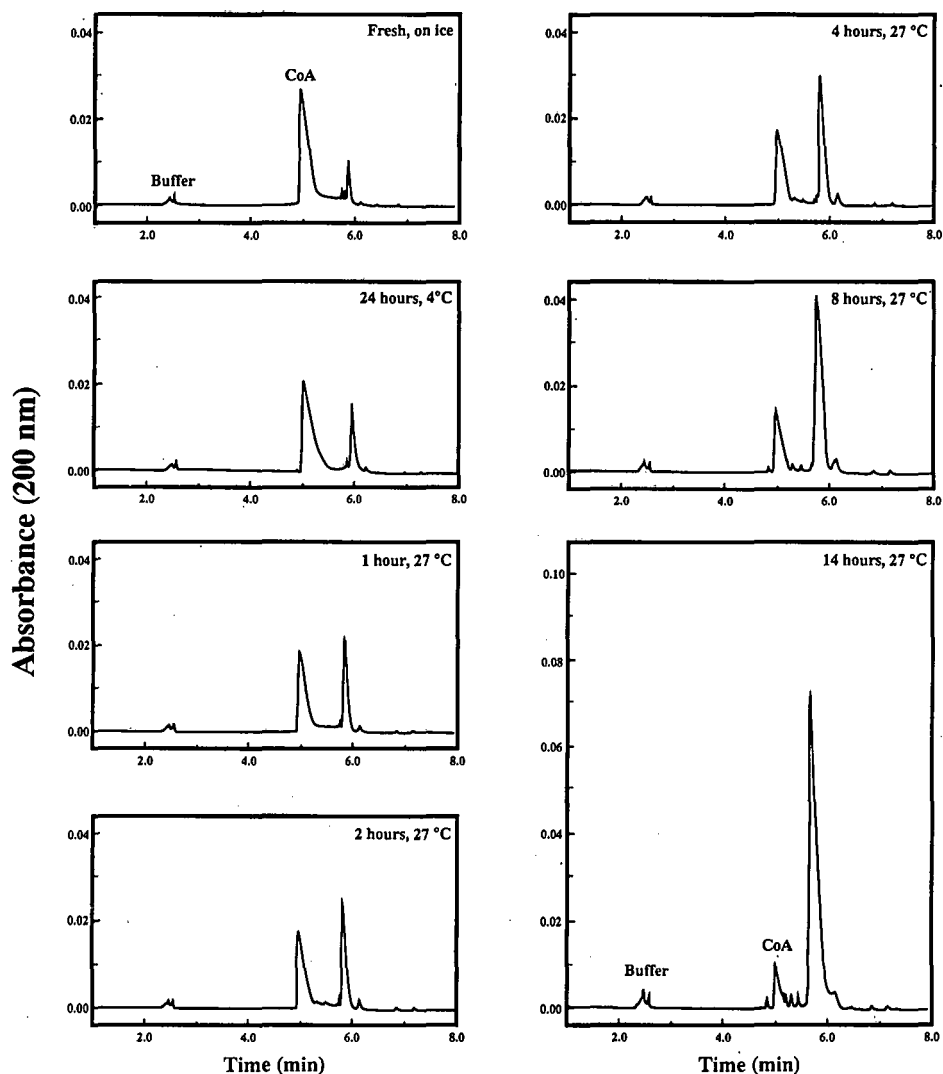


Fig. 6. HPCE monitoring of the non-enzymatic loss of coenzyme A. Coenzyme A ( $500 \mu\text{g/ml}$ ) was incubated on ice or at  $27^\circ\text{C}$  in  $20 \text{ mM}$  Tris-Cl and sampled at specific intervals. Sample injection was by pressure for 1 s into a  $57 \text{ cm} \times 50 \mu\text{m}$  capillary and separation at  $25 \text{ kV}$ .

can be followed as a function of both chloramphenicol loss and/or acetylchloramphenicol formation. Additionally, the speed of HPCE analysis allows for protocol modification to be tested rapidly. For example, a 10-min analysis determined that incubation in boiling water (*i.e.* boiling) had little or no effect on substrate stability and could thus serve to terminate enzyme activity. HPCE analysis also demonstrated that, in contrast to reports on the

stability of acetyl coenzyme A in cell extracts [20], this component was apparently very stable under our experimental conditions while the product coenzyme A was found to be very unstable. The identity of the peak resulting from prolonged exposure of coenzyme A to  $27^\circ\text{C}$  was not any of the obvious possibilities such as subcomponents of coenzyme A. Through the use of the reducing agent DTT, it became apparent that coenzyme A was

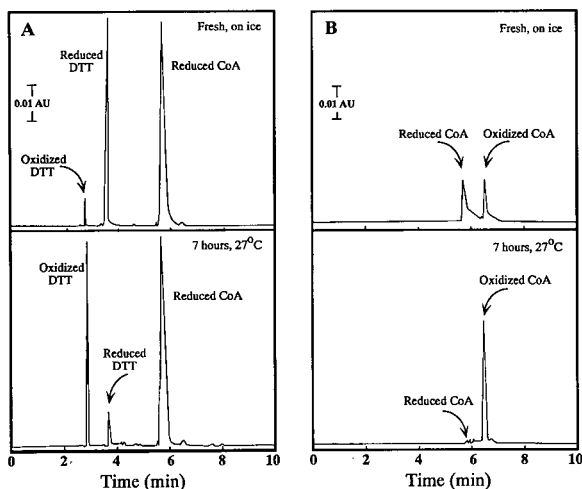


Fig. 7. Dithiothreitol stabilization of coenzyme A. Coenzyme A (0.5 mg/ml in borate buffer, pH 8.3) in the presence (A) and absence (B) of 20 mM DTT at 27°C at time 0 and 7 h. The reaction volume for each sample was 50  $\mu$ l. An aliquot was sampled by pressure injection for 3 s into a 57 cm  $\times$  50  $\mu$ m capillary and separated at 25 kV.

undergoing oxidation, possibly forming a dimer through a disulphide bond. The ability to detect the rapid loss of any reaction component is relevant to the development of an assay for enzyme activity. In the case of CAT, the estimation of enzyme activity, as measured by the appearance of coenzyme A, would be largely underestimated as a result of rapid oxidation of this molecule in a temperature-dependent, non-enzymatic manner.

Perhaps one of the more obvious extensions of the results of this study is the potential extrapolation to the molecular biology technique that has exploited the enzyme-catalyzed acetylation of chloramphenicol. With the standard CAT assay the aim is to measure the amount of enzyme (and hence the activity of the promoter) by the addition of [ $^{14}$ C]chloramphenicol and acetyl coenzyme A to an extract of the cells containing (or lacking) the enzyme. Active enzyme catalyzes the acetylation of  $^{14}$ C-labelled chloramphenicol using acetyl coenzyme A as the acetyl group donor. Labelled products (both mono- and diacetylated chloramphenicol) are separated from the substrate by TLC and results are qualitatively assessed by autoradiography. Quantitative assessment of product formation is determined by liquid scintillation counting after spots have been

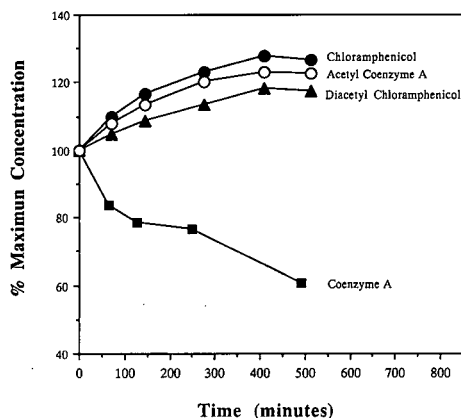


Fig. 8. HPLC analysis of the stability of CAT substrates and products in the absence of enzyme. Acetyl coenzyme A (1 mg/ml), coenzyme A (500  $\mu$ g/ml), diacetyl chloramphenicol (500  $\mu$ g/ml) and chloramphenicol (500  $\mu$ g/ml) were incubated individually at 27°C in 20 mM Tris-HCl and sampled at specific intervals (1-s injection; 57 cm  $\times$  50  $\mu$ m capillary; 25 kV). Percent maximum concentration was obtained through peak areas and plotted vs. the incubation time.

scraped from the thin-layer plate or by scanning densitometry of the autoradiogram. Another method involves a two-phase extraction of the  $^{14}$ C-labelled product into liquid scintillation cocktail using [ $^{14}$ C]acetyl coenzyme A and unlabelled chloramphenicol [21].

In the study described here, concentrations of unlabelled chloramphenicol and acetyl coenzyme A similar to those used in a standard CAT assay were used. The use of a Tris buffer concentration (20 mM) lower than that typically used in a standard CAT assay (167–570 mM; cf. refs. 20 and 22) reduced the size of the buffer peak which migrates close to acetyl chloramphenicol without affecting enzymatic activity. Parallel experiments using  $^{14}$ C-labelled chloramphenicol as substrate, followed by analysis with the standard TLC method and HPLC analysis, show that similar quantitative data are obtained. This clearly indicates that CAT-induced acetylation of chloramphenicol can be rapidly monitored with HPLC and may be a useful tool for the evaluation of the transcriptional promoting activity of specific sequences of DNA. This approach presents several potential advantages over the TLC method presently used (Table I). First, HPLC significantly decreases the amount of time needed to obtain qualita-

TABLE I  
COMPARISON OF HPCE AND TLC ANALYSIS OF CAT ENZYME ACTIVITY

	HPCE	TLC
Speed for analysis of single sample	6 min	Up to 24 h
Radioactivity required	No	Yes
Sample size ( $\mu$ l)	10	150
Quantitation: number of steps	1	3
method	Peak area analysis	Scintillation counting
Cost considerations	—	$^{14}$ C-Substrate purchase
	—	Radioactivity disposal
Automation	Yes	No
Simultaneous analysis of multiple samples	No	Yes

tive and quantitative data. Typical times for obtaining quantitative data with the TLC method may be as long as 24 h when including ethylacetate extraction, chromatography, autoradiography and scintillation counting. The data presented here indicate that, with HPCE, the equivalent quantitative data may be obtained in less than 10 min per sample. Moreover, CAT activity by any assay is measured by the presence of both the mono- and diacetylated forms of chloramphenicol. HPCE separation under the conditions described in this study results in the apparent comigration of all acetylated forms and, hence, peak area is a true quantitative representation of activity. In addition to eliminating the biohazard of working with radioactivity, all of the advantages of using a non-isotopic assay follow. The cost of the assay is dramatically reduced by eliminating the cost of purchasing [ $^{14}$ C]chloramphenicol or [ $^{14}$ C]acetyl coenzyme A and disposing of the radioactive products. Finally, a single HPCE analysis uses a smaller reaction mixture volume (as little as 10  $\mu$ l) to make nanoliter volume injections. This is substantially less than the 150  $\mu$ l typically required for TLC or liquid scintillation cocktail extraction and, hence, reduces the amount of precious cell extract needed.

#### CONCLUSIONS

These data highlight new potential uses for HPCE. First, the possibility that the rapid, reproducible nature of HPCE analysis for the evaluation of enzyme activities is identified with the particular

advantage that both loss of substrate as well as the increase in product(s) can be monitored. Finally, the potential exists for HPCE to circumvent the tedious methodology presently used to characterize the transcriptional activity of eukaryotic promoters using the CAT assay.

#### ACKNOWLEDGEMENTS

The authors would like to thank Mr. Ken Peters for graphic assistance and Ms. Colleen Allen for typing the manuscript.

J.P.L. is the recipient of a Medical Research Council (Canada) post-doctoral fellowship. M.D.S. was supported by an NIH training grant HD 07108. T.C.S. is George Eisenberg Professor of Biochemistry and Molecular Biology.

#### REFERENCES

- 1 J. W. Jorgenson and K. D. Lukacs, *Anal. Chem.*, 53 (1981) 1298-1302.
- 2 M. J. Gordon, X. Huang, S. L. Pentoney, Jr. and R. N. Zare, *Science (Washington, D.C.)*, 242 (1988) 224-228.
- 3 B. L. Karger, A. S. Cohen and A. Guttman, *J. Chromatogr.*, 492 (1989) 585-614.
- 4 P. D. Grossman, J. C. Colburn, H. H. Lauer, R. G. Nielsen, R. M. Riggin, G. S. Sittampalam, E. C. Rickard, *Anal. Chem.*, 61 (1989) 1186-1194.
- 5 M. C. Roach, P. Gozel and R. N. Zare, *J. Chromatogr.*, 426 (1988) 129-140.
- 6 T. Tsuda, K. Nomura and G. Nakagawa, *J. Chromatogr.*, 264 (1983) 385-392.
- 7 X. H. Huang, J. A. Luckey, M. J. Gordon and R. N. Zare, *Anal. Chem.*, 61 (1989) 766-770.
- 8 W. R. Jones, P. Jandik and R. Pfeifer, *Am. Lab.*, May (1991) 40-48.

- 9 P. D. Grossman, J. C. Colburn and H. H. Lauer, *Anal. Biochem.*, 179 (1989) 28–33.
- 10 J. P. Landers, *Bioessays*, 13 (1991) 253–258.
- 11 A. S. Cohen, D. Najarian, J. A. Smith and B. L. Karger, *J. Chromatogr.*, 458 (1988) 323–333.
- 12 H. Swerdlow and R. Gesteland, *Nucleic Acids Res.*, 18 (1990) 1415–1419.
- 13 A. Paulus, E. Gassmann and M. J. Field, *Electrophoresis*, 11 (1990) 702–708.
- 14 H. Drossman, J. A. Luckey, A. J. Kostichka, J. D’Cunha and L. M. Smith, *Anal. Chem.*, 62 (1990) 900–903.
- 15 J. A. Luckey, H. Drossman, A. J. Kostichka, D. A. Mead, J. D’Cunha, T. B. Norris and L. M. Smith, *Nucleic Acids Res.*, 18 (1990) 4417–4421.
- 16 W. V. Shaw, *Methods Enzymol.*, 43 (1975) 737–755.
- 17 C. M. Gorman, L. F. Moffat and B. H. Howard, *Mol. Cell. Biol.*, 2 (1982) 1044–1051.
- 18 J. P. Landers and T. C. Spelsberg, *Ann. N.Y. Acad. Sci.*, 637 (1991) 26–55.
- 19 J. Lui, O. Shirota and M. Novotny, *Anal. Chem.*, 63 (1991) 413–417.
- 20 F. M. Ausubel, R. Brent, R. E. Kingston, D. D. Moore, J. G. Seidman, J. A. Smith and K. Struhl (Editors), *Current Protocols in Molecular Biology*, Wiley, New York, 1989, p. 9.6.4.
- 21 M. J. Sleight, *Anal. Biochem.*, 156 (1986) 251–256.
- 22 M. A. Lopata, D. W. Cleveland and B. Sollner-Webb, *Nucleic Acid Res.*, 12 (1984) 5707–5717.



# Separation of sulphonamides and determination of the active ingredients in tablets by micellar electrokinetic capillary chromatography

Quan-xun Dang

*Shaanxi Institute for Drug Control, Zhu-que Street, Xian 710061 (China)*

Zeng-pei Sun and Da-kui Ling

*National Institute for the Control of Pharmaceutical and Biological Products, Temple of Heaven, Beijing 100050 (China)*

(First received July 23rd, 1991; revised manuscript received February 6th, 1992)

---

## ABSTRACT

The separation and determination of seven sulphonamides and trimethoprim by micellar electrokinetic capillary chromatography were successfully achieved, employing sodium dodecyl sulphate (SDS) as a micellar phase and tetrabutylammonium bromide as additive. The effects of surfactant and modifier concentrations, pH and applied voltage on the retention behaviour of the solutes and the column efficiency were studied. The migration time of sulphonamides increase with increasing SDS concentration and decreasing the applied voltage, but varies only slightly with pH. There is an optimum applied voltage at which a higher theoretical plate number is achieved, in contrast to the sulphonamides, the retention behaviour of trimethoprim gave a more obvious response to changes in the experimental conditions. The determination of three active ingredients in tablets was performed using sulphathiazole as an internal standard with good results. The theoretical plate number ranged between  $2.0 \cdot 10^5$  and  $2.8 \cdot 10^5$  with a 50-cm capillary.

---

## INTRODUCTION

Micellar electrokinetic capillary chromatography (MECC) was first reported by Terabe *et al.* in 1984 [1]. Several reports and reviews of the theory and application of MECC have been published [2–4]. Chiral separations of some amino acid derivatives [5] and drugs [6] have also been performed by MECC with a micelle of sodium dodecyl sulphate (SDS) and a chiral additive or with chiral cholate micelles. The determination of drugs in pharmaceutical preparations by application of MECC has been achieved by using an internal standard method [7,8]. Purity testing of diltiazem has also been reported [9].

In this paper, the separation and determination of seven sulphonamides and trimethoprim in pharmaceutical preparations by MECC with SDS is reported. The effects of pH, concentrations of surfactant and modifier and applied voltage are discussed. The application of this technique to the quantitative analysis of commercial tablets using an internal standard method is also described.

## EXPERIMENTAL

### *Apparatus*

Experiments were performed with a Bio-Rad Labs. (Richmond, CA, USA) HPE 100 apparatus equipped with a UV detector adjusted to 240 nm and a power supply able to deliver up to 12 kV D.C. Electrokinetic sampling was used to introduce samples into the capillary. A Bio-Rad Labs. 148-3014

---

*Correspondence to:* Dr. Q.-x. Dang, Shaanxi Institute for Drug Control, Zhu-Que Street, Xian 710061, China.

HPE capillary cartridge (50 cm × 50 μm I.D., uncoated) was employed and a Chromatopac C-R3A (Shimadzu, Kyoto, Japan) was used for data processing.

#### Drugs and reagents

The bulk drugs analysed are listed in Table I.

SD–SMZ–TMP tablets (nominally containing 200 mg of SD, 200 mg of SMZ and 80 mg of TMP per tablet) and SMZ–TMP tablets (nominally containing 400 mg of SMZ and 80 mg of TMP per tablet) were purchased from Beijing Pharmaceutical Factory (Beijing, China) and Xian Pharmaceutical Factory (Xian, Shaanxi, China), respectively. SDS was obtained from Nacalai Tesque (Kyoto, Japan). Tetrabutylammonium bromide (TAB) of analytical-reagent grade was a product of Beijing Chemical Factory (Beijing, China).

The buffer solutions were prepared by mixing 0.01 M sodium tetraborate solution with appropriate volume of 0.5 M sodium dihydrogenphosphate solution to give pH 9, 8, and 7, or with dilute hydrochloric acid to give pH 6 and 5. The appropriate amount of SDS was dissolved in the buffer solutions to obtain carrier solutions. The solutions were filtered through a 0.45-μm membrane filter and degassed by ultrasonication prior to their use.

#### Test solutions and procedure

Owing to the low solubility of TMP in water, all test solutions were prepared by shaking the solutes, after shaking them with an appropriate amount of methanol first, with a mixture of two volumes of

methanol and eight volumes of pH 8.5 buffer solution that was added later. A resolution test mixture was prepared by dissolving the solutes to obtain a solution containing 100 μg/ml each of SPZ, SDM, SD, SMZ, ST and TMP and 50 μg/ml each of SN and SG. For the determination of the linear range and response factor, five solutions were prepared to give a series of concentrations ranging from 45 to 225 μg/ml of SD and SMZ and from 12 to 60 μg/ml of TMP. After preparation as above, the concentrations of the solutions for the recovery tests were 36 μg/ml of SD and SMZ and 14 μg/ml of TMP and other two concentrations levels equivalent to 80% and 120% of these concentrations. The powder of SD–SMZ–TMP tablets or SMZ–TMP tablets was dissolved at a concentration of 14 μg/ml of TMP. All the solutions contained 90 μg/ml of ST as internal standard.

Sample solution was loaded by the electrokinetic method at the positive end of the capillary using a 10-kV constant voltage and a 10-s loading time. It is useful to rinse the internal wall of the capillary between individual injections. This was effected by injecting a flow of the carrier solution used into the capillary with a 100-μl syringe (Hamilton, Reno, NV, USA) at the negative end. All experiments were performed at ambient temperature.

#### RESULTS AND DISCUSSION

A typical electropherogram of the eight ingredients separated is shown in Fig. 1; each compound is completely resolved.

TABLE I  
TEST SAMPLE

Peak No.	Compound	Abbreviation	Origin
1	Sulphanilamide	SN	British Pharmacopoeia, authentic specimen
2	Sulphaguanidine	SG	
3	Sulphaphenazole	SPZ	
4	Sulphadimethoxine	SDM	
7	Sulphathiazole	ST	
5	Sulphadiazine	SD	Bulk drugs, Chinese Pharmacopoeia grade
6	Sulphamethoxazole	SMZ	
8	Trimethoprim	TMP	

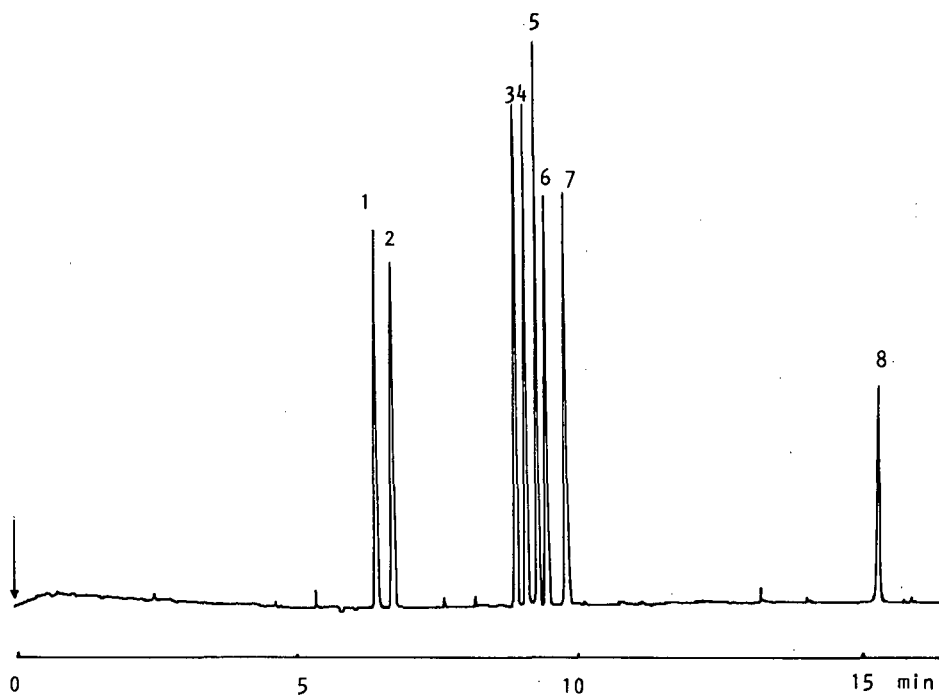


Fig. 1. Typical separation in MECC. For peak identifications, see Table I. Carrier, 0.025 *M* phosphate–borate solution (pH 8.5) containing 0.1 *M* SDS; applied voltage, 12 kV.

### Quantitative analysis

The solutions for the determination of the linear range and relative responsive factor were chromatographed using 0.025 *M* phosphate–borate buffer solution (pH 8.5) containing 0.1 *M* SDS and 0.01 *M* TAB; a 12-kV voltage was applied in the constant-voltage mode. The results were calculated by the peak-area ratio method, and the calibration plots of  $A_i/A_s$  vs.  $W_i/W_s$ , where  $A_s$  and  $A_i$  are peak areas and

$W_s$  and  $W_i$  are weights of the sample(s) and internal standard (i), showed excellent linearity in the ranges 30–150  $\mu\text{g}/\text{ml}$  for SD and SMZ and 12–60  $\mu\text{g}/\text{ml}$  for TMP. Response factors relative to ST were calculated by a conventional method (Table II).

Recoveries were examined under the experimental conditions described above. The results and their relative standard deviations are given in Table III.

The average recovery for each ingredient, with three levels and five repeated injections per level, was close to the stated composition value, and the relative standard deviation (R.S.D.), especially for SD and SMZ, was small, demonstrating that this method is sufficiently accurate and reproducible.

Determinations of each ingredient in SD–SMZ–TMP tablets and in SMZ–TMP tablets were performed according to the procedure described above. Typical chromatograms are shown in Fig. 2.

The assay results are summarized in Table IV. The results suggest that micellar electrokinetic capillary chromatography may be a useful technique in pharmaceutical analysis.

TABLE II  
RESULTS OF THE DETERMINATION OF LINEAR RANGE AND RESPONSE FACTORS ( $n = 5$ )

Parameter	SD	SMZ	TMP
Correlation coefficient ( $r$ )	0.9999	0.9995	0.9958
Intersection at area ratio axis	0.0764	0.0206	-0.3720
Slope	2.174	1.144	3.555
Response factor	0.4288	0.8353	0.5645
Relative standard deviation (R.S.D.)	2.77%	2.62%	5.88%

TABLE III  
RESULTS OF THE DETERMINATION OF RECOVERIES

Ingredient	Amount added ( $\mu\text{g/ml}$ )	Amount found ( $\mu\text{g/ml}$ )	Recovery (%)	Average (%)	R.S.D. (%)
SD	28.5	28.5	100.0	100.3	1.27
	36.1	35.8	99.2		
	41.8	42.5	101.7		
SMZ	28.8	29.3	101.7	101.6	0.50
	35.3	35.7	101.1		
	42.3	43.2	102.1		
TMP	11.5	11.1	96.5	98.6	4.26
	14.2	13.6	95.8		
	17.7	18.3	103.4		

#### Retention behaviour

The retention behaviour of solutes depends on several properties, including hydrophobicity and degree of dissociation in the solution. The depend-

ence of the migration times of seven sulphonamides and TMP on pH was examined with 0.1 M SDS solutions in the pH range 5–9 and the results are shown in Fig. 3. The migration times of all the sul-

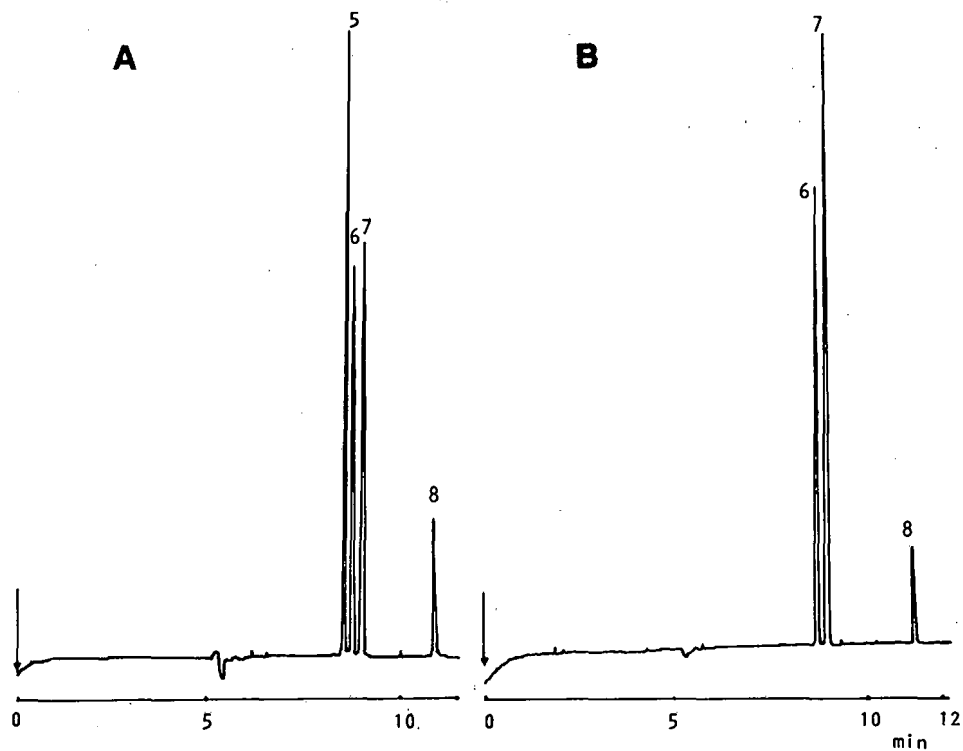


Fig. 2. Chromatogram obtained in the assay of (A) SD-SMZ-TMP tablets and (B) SMZ-TMP tablets. Conditions as in Fig. 1, with addition of 0.01 M TAB to the micellar solution. For peak identifications, see Table I.

TABLE IV

ASSAY RESULTS FOR THE PREPARATIONS OF SULPHONAMIDES ( $n=8$ )

Sample	Batch No.	Ingredient	Amount found (mg)	Label claim (mg)	Percentage of label claim	R.S.D. (%)
SD-SMZ-TMP tablets	900676	SD	202.5	200	101.3	0.31
		SMZ	205.2	200	102.6	0.99
		TMP	77.2	80	96.5	4.34
	900877	SD	196.6	200	98.3	0.72
		SMZ	201.2	200	100.6	0.82
		TMP	74.2	80	92.7	3.46
SMZ-TMP tablets	900853	SMZ	395.5	400	98.9	1.28
		TMP	79.3	80	99.1	4.91
	900811	SMZ	392.9	400	98.2	1.27
		TMP	79.6	80	99.5	3.93

phonamides except sulphathiazole increased only slightly with increasing pH, but that of trimethoprim changed dramatically. At lower solution pH, it may be possible that the sulphonamides are undissociated, and most of them are distributed in the micellar phase. At higher pH, although they are dissociated, having a negative charge owing to their acidic properties, they migrate slowly toward the cathode with an opposite electrophoretic migration giving a net migration time that is little influenced by pH. Trimethoprim can be dissolved not only in

acidic media [10] but also in basic media [11]; therefore, when the carrier solution pH changed from acidic (pH 5) to basic (pH 9), trimethoprim underwent a variation from cationic to neutral to anionic. Accordingly, the retention of trimethoprim varied from rapid (in low-pH medium) to slow (in neutral medium) and again to rapid (in high-pH medium).

In MECC, solutes partition between the aqueous and micellar phases in order of increasing hydrophobicity. The effect of SDS concentration on the retention time is shown in Fig. 4.

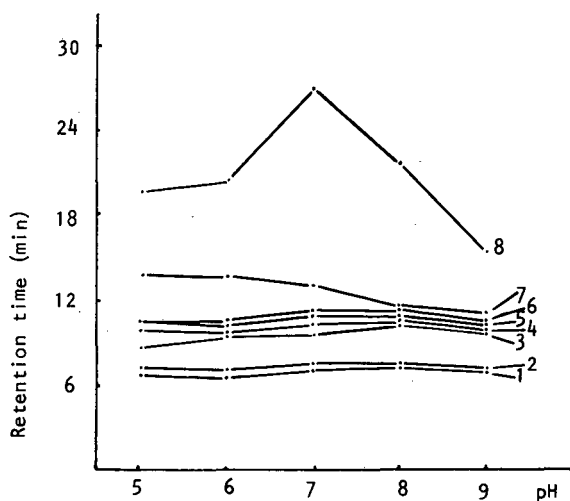


Fig. 3. Effect of pH on retention time. Other conditions as in Fig. 1. For compound identifications, see Table I.

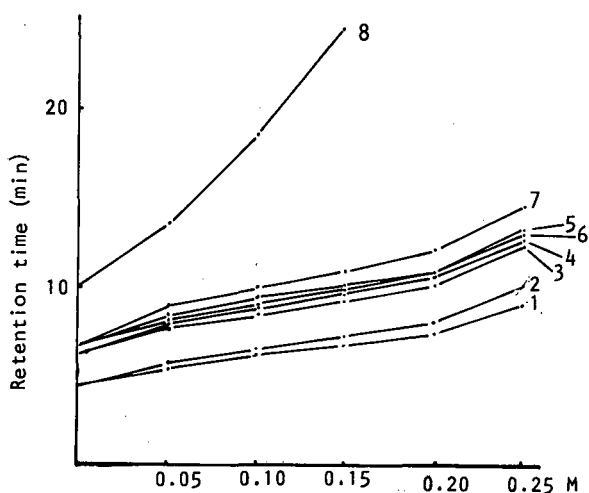


Fig. 4. Effect of SDS concentration on the retention time of ingredients. Other conditions as in Fig. 1. For compound identifications, see Table I.

The retention times of all the sulphonamides and trimethoprim increased gradually with increasing SDS concentration. SN and SG, SPZ and SDM, and SD, SMZ and ST were not resolved by electrophoresis without SDS. When the SDS concentration was above 0.05 M (above the critical micelle concentration), then they were readily separated from each other. TMP gave a longer retention time which increased faster than those of the sulphonamides (see Fig. 1), presumably owing to its higher hydrophobicity.

The dependence of the migration velocities of the solutes on the electrical field strength was examined under various applied voltages. The plots of retention time vs. applied voltage indicated, as expected, that the migration velocity of each solute increased with increasing applied voltage, but the relative retention time of each solute did not alter and did not influence the resolution of the solutes.

The addition of tetrabutylammonium salts to the SDS solution can improve the resolution of some compounds [12]. In order to optimize the separation of SD, SMZ and TMP for quantitative analysis, TAB was added to the SDS solution (pH 8.5) and the results are shown in Fig. 5. The migration times of SD, SMZ and ST gradually increased and the resolution between SD and SMZ was improved. This indicates that the addition of TAB enhances the interaction between the anionic solute and the micelle. The anionic solute and TAB tend to form

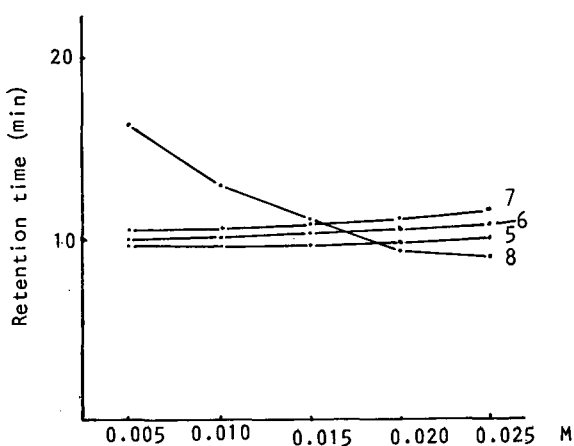


Fig. 5. Effect of TAB concentration on the retention times of (5) SD, (6) SMZ, (7) ST and (8) TMP. Other conditions as in Fig. 1.

ion pairs, which may be solubilized more easily by the anionic micelle than the free anionic solutes.

The addition of TAB to the micellar solution caused a considerable decrease in the migration time of TMP from that observed in the SDS solution alone. Cationic TAB added to the SDS solution probably combines with the anionic SDS micelle. Consequently, the addition of TAB to SDS solution could possibly prevent TMP from combining with the micelle.

#### Column efficiency

The theoretical plate number for the chromatographic peak of each ingredient that was obtained at different micellar concentrations and different applied voltages was calculated by the equation  $N = 2\pi(t_R h/A)^2$ , where  $t_R$ ,  $h$  and  $A$  are retention time, peak height and peak area, respectively [13]. The calculated results indicated that both the surfactant concentration and applied voltage influenced the column efficiency in MECC. The effect of the surfactant concentration on the theoretical plate number is illustrated in Fig. 6.

The theoretical plate number, except for SMZ and ST, increased with increasing surfactant concentration. However, it decreased with increasing micellar concentration after solute-specific levels

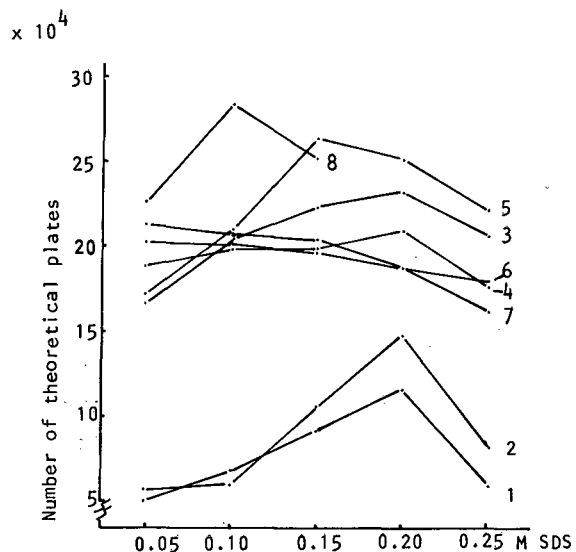


Fig. 6. Effect of SDS concentration on column efficiency. Other conditions as in Fig. 4. For compound identifications, see Table I.

TABLE V  
VARIANCE ANALYSIS FOR THE TWO CONSTANT MODES

Solute	Variance of peak area ratios in constant-voltage mode ( $n=6$ )	Variance of peak area ratios in constant-current mode ( $n=6$ )	Ratio
SD	0.000437	0.00381	8.72
SMZ	0.000225	0.00127	5.64
TMP	0.000501	0.00271	5.41

had been reached. The results indicate that for the separation efficiency of each ingredient there is always an optimum surfactant concentration.

The applied voltage also influences the efficiency of separation. The results of a study of the effect of applied voltage on efficiency for the MECC system are shown in Fig. 7.

In this work, the efficiency for most solutes increased with increasing applied voltage. Sepaniak and Cole [3] reported that there was a Van Deemter-like relationship between plate height and applied voltage, and an optimum applied voltage exists for the highest separation efficiency. In this

work, it may be that an optimum voltage for the highest theoretical plate number was not attained because the maximum voltage of the apparatus is 12 kV.

#### *Reproducibility of quantitative analysis*

HPE-100 has two operational modes, constant voltage or constant current. The reproducibility of peak-area ratios (sample to internal standard) obtained in the constant-voltage mode for six replicates, was compared with that in the constant-current mode under identical experimental conditions. The results are given in Table V.

The reproducibility of peak-area ratios obtained in the constant-voltage mode is better than those obtained in the constant-current mode.

In this experiment, the reproducibility obtained was similar to that expected from a comparable high-performance liquid chromatographic method, especially for SD and SMZ. The reproducibility of the analytical results for TMP was slightly inferior. This may be due to adverse effects of the MECC technique itself, such as variation of peak area with migration time and adsorption of the sample on the internal wall of the capillary. It may also be due to the location of the TMP peak on the chromatogram. The TMP peak is far from the internal standard peak, and the difference in peak-area value between TMP and the internal standard was also large. In future work, it may therefore be advisable to employ another internal standard located near the TMP peak to improve the reproducibility with TMP.

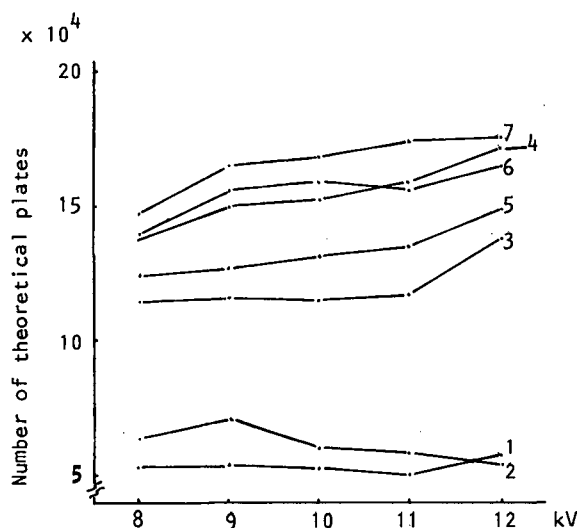


Fig. 7. Effect of applied voltage on column efficiency. Other conditions as in Fig. 1. Each point is the mean of six determinations; the R.S.D.s are between 3.6% and 5.7%. For compound identifications, see Table I.

## REFERENCES

- 1 S. Terabe, K. Otsuka, K. Ichikawa, A. Tsuchiya and T. Ando, *Anal. Chem.*, 56 (1984) 111.
- 2 S. Terabe, K. Otsuka and T. Ando, *Anal. Chem.*, 57 (1985) 834.
- 3 M. J. Sepaniak and R. O. Cole, *Anal. Chem.*, 59 (1987) 472.
- 4 G. Werner, *Anal. Chem.*, 62 (1990) 403R.
- 5 S. Terabe, M. Shibata and Y. Miyashita, *J. Chromatogr.*, 480 (1989) 403.
- 6 H. Nishi, T. Fukuyawa, M. Matsuo and S. Terabe, *J. Chromatogr.*, 515 (1990) 233.
- 7 S. Fujiwara, S. Iwase and S. Honda, *J. Chromatogr.*, 447 (1988) 133.
- 8 H. Nishi, T. Fukuyawa, and M. Matsuo, *J. Chromatogr.*, 515 (1990) 245.
- 9 H. Nishi, T. Fukuyawa, M. Matsuo and S. Terabe, *J. Chromatogr.*, 513 (1990) 279.
- 10 G. J. Manius, in K. Florey (Editor), *Analytical Profiles of Drug Substances*, Vol. 7, Academic Press, New York, 1978, p. 445.
- 11 *British Pharmacopoeia 1988*, Vol. 1, H. M. Stationery Office, London, 1988, p. 586.
- 12 H. Nishi, N. Tsumagari and S. Terabe, *Anal. Chem.*, 61 (1989) 2434.
- 13 L. R. Snyder and J. J. Kirkland, *Introduction to Modern Liquid Chromatography*, Wiley, New York, 2nd ed., 1979, p. 222–223.

# Qualitative analysis of environmental samples for aromatic sulfonic acids by high-performance capillary electrophoresis

William C. Brumley

*US Environmental Protection Agency, Environmental Monitoring Systems Laboratory, P.O. Box 93478, Las Vegas, NV 89193-3478 (USA)*

(First received January 13th, 1992; revised manuscript received March 12th, 1992)

---

## ABSTRACT

High-performance capillary electrophoresis (HPCE) is investigated as a qualitative tool in the analysis of environmental samples for aromatic sulfonic acids and related compounds. Using standard borate buffer solutions, characteristic migration times define windows wherein certain compound types will be found. Eight aromatic sulfonic acids are separated as an example of the power of the technique. A leachate from a hazardous waste site is also subjected to HPCE. Qualitative identification may be approached by use of migration times and ancillary techniques such as continuous-flow fast atom bombardment mass spectrometry.

---

## INTRODUCTION

Analytical interest in high-performance capillary electrophoresis (HPCE) has increased rapidly in the last few years [1–4], in part because it is a technique of high efficiency capable of generating theoretical plates above  $1 \cdot 10^6$  [5]. Applications of CE to the determination of organic ions have centered largely in the biological and pharmaceutical areas [6]. Thus, peptides, proteins, and DNA fragments have been separated using CE [7–9]. In pharmaceutical applications of HPCE, issues such as purity and optical isomerism have been addressed [10–12]. Within this context, HPCE as a complementary tool to high-performance liquid chromatography has been emphasized [13].

In contrast, applications of HPCE to environmental analysis have been limited. Gaitonde and Pathak [14] used micellar electrokinetic CE to deter-

mine chlorophenols in wastewater. Separations of phenols and other compounds of environmental interest were reported [15–18]. Direct determination of small organic ions in the context of inorganic anion analysis was discussed [1]. This latter paper illustrated that an important role exists for CE in inorganic analysis, and one could extend the applicability to environmental problems.

On-column detection in HPCE is most often done by UV absorption in either the direct or indirect mode. Fluorescent detection is also widely used, and reports of electrochemical and other approaches have been reviewed [6]. Detection as a result of coupling CE to mass spectrometry (MS) has been the subject of several papers. Among the techniques employed include electrospray ionization and continuous-flow fast atom bombardment (CF-FAB) MS using either a coaxial or a liquid junction interface [19–22]. These techniques may be compared to approaches using ion chromatography. Ion chromatography in conjunction with particle-beam liquid chromatography–MS was used to identify 4-chlorobenzenesulfonic acid as a major com-

---

*Correspondence to:* Dr. W. C. Brumley, US Environmental Protection Agency, Environmental Monitoring Systems Laboratory, P.O. Box 93478, Las Vegas, NV 89193-3478, USA.

ponent in the leachate from the Stringfellow Superfund site [23].

The extension of HPCE to the determination of non-volatile organics and water-soluble compounds of environmental interest seems obvious. The efficiency of HPCE in terms of the number of theoretical plates suggests a technique comparable to capillary gas chromatography. The great variety of chemistries to apply in HPCE enhances the prospect of sufficient selectivity for separations involving complex samples.

In this initial work, focus is placed on qualitative identification with the separation of eight aromatic sulfonic acids using a boric acid–borate buffer. This class of compounds presents a simple, common organic functional group that occurs in a variety of compounds. Azo dyes and anionic surfactants are two such classes of compounds that are of environmental interest. Additional results for selected azo dyes, aromatic carboxylic acids, and similar compounds defines functionally diverse moieties likely to be found in the migration window of interest. An electropherogram of the Stringfellow leachate is also presented. Finally, the qualitative identifications are supported by results from CF-FAB-MS used with direct CE interfacing and with flow-injection in an off-line mode.

## EXPERIMENTAL

### Chemicals

Compounds were used as received. Solutions of individual standards were made up at concentrations of approximately 0.5 mg/ml. Sodium dodecylbenzenesulfonate, sodium cumenesulfonate, sodium xylenesulfonate, and sodium toluenesulfonate were obtained from Chem Service (West Chester, PA, USA). Potassium phthalimide, sodium benzoate, sodium diphenylamine-4-sulfonate, orange II, boric acid, sodium tetraborate decahydrate, sodium salicylate, 4-chlorobenzenesulfonic acid, sodium 2-naphthalenesulfonate and sodium 3-nitrobenzenesulfonate were obtained from Aldrich (Milwaukee, WI, USA).

### HPCE

A Beckman Model 2050 P/ACE system was used for all CE experiments; the instrument was controlled using the Windows-based operating system,

version 2.0. A 57-cm (50 cm to the detector)  $\times$  0.050 mm capillary was used with UV detection at 214 nm. The buffer system was boric acid–borate at 50 mM (pH8.3). Generally, 5-s pressure injections were made followed by CE at 30.0 kV at a current of approximately 33  $\mu$ A with temperature maintained at 25°C. Solutions were filtered through a 0.2- $\mu$ m pore size nylon filter. Separations were carried out using a method that consisted of a 2.0-min rinse of buffer, 5.0-s pressure injection, separation, 2.0-min rinse of 0.1 M NaOH and 2.0-min rinse of deionized water.

To assess daily performance and reproducibility before running samples, a start-up sequence was established that began with 5.0-min rinses of 0.1 M NaOH followed by deionized water followed by buffer. Thereafter, a series of five runs of standards was made: two runs of Beckman's Test Mix A (benzoic acid, 4-hydroxybenzoic acid and 2-phenylacetic acid), two runs of toluenesulfonic acid and one run of pyridine. These runs provided information on separation, migration times, and electroosmotic flow.

### CF-FAB-MS and CE-MS

A VG/Fisons 7070 EQ mass spectrometer with 11-250 (11/24 based, software B22) data system was used with a standard VG CF FAB probe. Flow injection analysis used a 0.25 mm I.D. fused-silica capillary (Polymicro Technologies, Phoenix, AZ, USA) with a flow of about 1  $\mu$ l/min of FAB matrix consisting of 25% glycerol in water. Injections were made with a Valco valve (Model CI4W, Houston, TX, USA), and the flow was established with an Isco syringe pump (Model SFC-500, Lincoln, NE, USA).

Magnetic scans of 1 s/decade at an accelerating voltage of  $-6$  kV were calibrated by using negative ions from the matrix or negative ions from polyethylene glycol. The FAB gun was operated at 8 kV, 1 mA. Accurate mass measurements were performed at a resolution of 3000 scanning at 3 s/decade.

CE-MS was performed using the coaxial arrangement [21]. A 0.020 mm I.D.  $\times$  0.144 mm O.D. capillary was used for CE and was about 110 cm long. The outer capillary (0.150 mm I.D.  $\times$  0.350 mm O.D.) carried the FAB matrix at a flow-rate of about 1  $\mu$ l/min doped with ammonium acetate–triethylenetetramine (pH 9) to maintain electrical

continuity. A Glassman (Model PS/MJ30P, Whitehouse, NJ, USA) power supply was operated at 30kV (total voltage drop 36 kV) with currents generally below 15 $\mu$ A for 10 mM buffer of boric acid-borate or ammonium acetate (pH 8.3 using NH<sub>3</sub>-water). Injections were electroosmotic at 30kV for 5-15 s. During injection, the CF-FAB probe was removed from the instrument to eliminate introduction of vacuum-induced air bubbles.

#### Leachate

A concentrated methanolic solution of leachate from the Stringfellow Superfund site was obtained from M. A. Brown (California Department of Health Services). Sample work-up was briefly as follows [23]. Aqueous samples (500-2000 ml) of leachate were concentrated by freeze-drying (24-72 h). The residue was redissolved in methanol (50-200

ml) and inorganic salts precipitated by adding an equal volume of acetone. After evaporation, the filtered residue was redissolved in methanol (1-20 ml).

#### RESULTS AND DISCUSSION

An electropherogram of eight aromatic sulfonic acids shows the power of the technique (Fig. 1). The inset in Fig. 1 illustrates the improved resolution of the last three sulfonic acids as a result of decreasing the injection time from 4.8 s to 1.2 s. The immediate application of HPCE to characterization of samples for aromatic sulfonic acids is obvious. A migration time window is defined from dodecylbenzenesulfonic acid to 4-chlorobenzenesulfonic acid of about 3.2-4.8 min under these conditions.

A migration time window in CE, like a retention

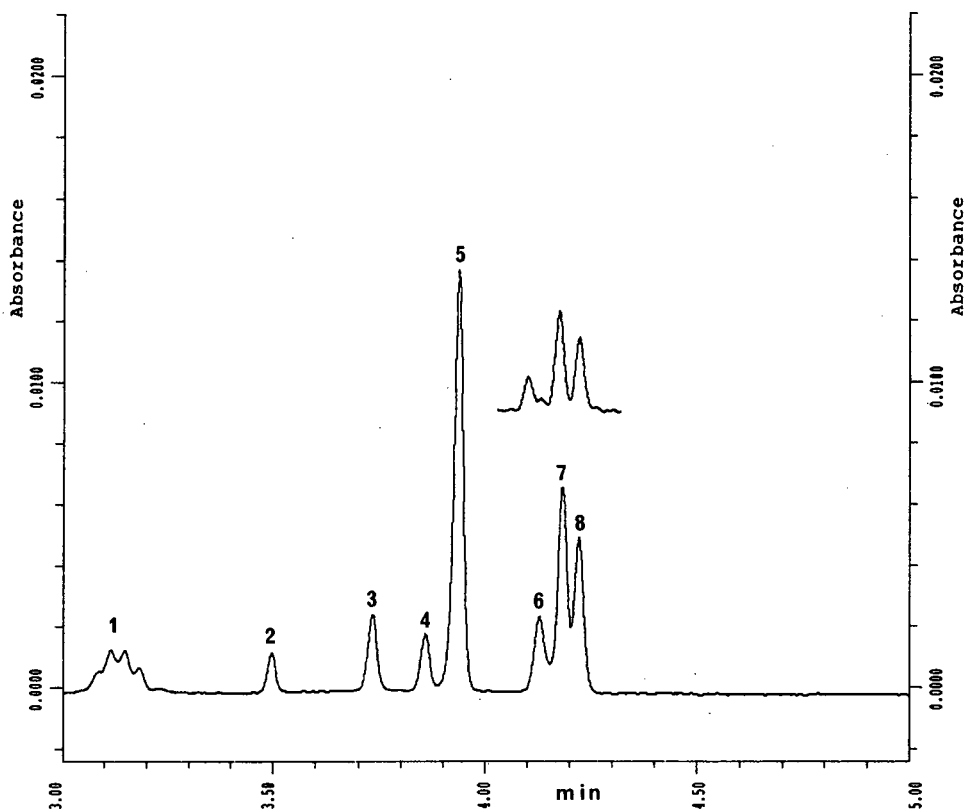


Fig. 1. Electropherogram of eight aromatic sulfonic acids using sodium borate-boric acid at pH 8.3, 57 cm (50 cm to detector)  $\times$  0.050 mm I.D. capillary, UV detection at 214 nm. Peaks: 1 = dodecylbenzenesulfonate; 2 = diphenylamine-4-sulfonate; 3 = cumenesulfonate; 4 = xylenesulfonate; 5 = 2-naphthalenesulfonate; 6 = toluenesulfonate; 7 = 4-nitrobenzenesulfonate; 8 = 4-chlorobenzenesulfonate. For inset, see text.

TABLE I  
MIGRATION TIMES OF SELECTED ANIONS USING SODIUM BORATE-BORIC ACID BUFFER AT pH 8.3

Anion	Migration time (min)
Pyridine <sup>a</sup>	2.30
Orange II	3.42
Phthalimide	3.74
Benzoate	4.19
Salicylate	4.06
2-(4-Hydroxyphenyl)acetate	3.74
4-Hydroxybenzoate	4.03
Dodecylbenzenesulfonate (center)	3.13
Diphenylamine-4-sulfonate	3.50
Cumenesulfonate	3.73
Xylenesulfonate	3.86
2-Naphthalenesulfonate	3.94
Toluenesulfonate	4.12
4-Nitrobenzenesulfonate	4.18
4-Chlorobenzenesulfonate	4.22

<sup>a</sup> Neutral marker of electroosmotic flow.

time window in gas chromatography, can be used as a qualitative tool for the identification of compound types as well as specific isomers. The multiplet labeled as dodecylbenzenesulfonate indicates the many isomers present in the standard of this compound and the ability of HPCE to resolve them.

Anions with other organic functionalities undoubtedly will be found in this migration time window. For example, Table I gives migration times for the aromatic sulfonic acids and several aromatic carboxylic acids and related compounds that elute in this window under these experimental conditions. An azo dye is also included, and it produces a strongly fronting peak which may be indicative of mismatching mobilities with the buffer counter ions [1].

Within the class of sulfonic acids, it appears that large organic constituents result in a smaller electrophoretic mobility (*i.e.*, for anions moving in opposite direction to electroosmotic flow) and a shorter migration time. Conversely, electron-withdrawing substituents such as Cl and NO<sub>2</sub> and small organic substituents such as methyl result in longer migration times of the compounds illustrated. The azo dyes, with a large organic moiety, have some of the shortest migration times of the compounds studied. It therefore remains as an objective to develop CE

conditions that are selective and appropriate for the high-efficiency separation of anions of very low mobility.

From an environmental perspective, the toxicity and other health effects associated with aromatic sulfonic acids and aromatic carboxylic acids may not be of primary concern. Nevertheless, the ability to characterize leachates or other matrices for these and similar compounds not readily amenable to gas chromatography-MS is of interest [23]. Such data help to account for total organic carbon and halogen in such matrices. An example of the potential of HPCE in this regard is the electropherogram of a leachate from Stringfellow Superfund site (Fig. 2). A large number of peaks are revealed under these buffer conditions. The simplicity and efficiency of HPCE compared with ion chromatography [23] are evident. Within the migration time window for sulfonic acids is one large peak and several lesser peaks that could indicate aromatic sulfonic or carboxylic acids of the type studied. The large peak corresponds to 4-chlorobenzenesulfonic acid [23], and this has been independently confirmed in this work by migration times of standards by HPCE, flow injection analysis using CF-FAB-MS, and by CE-MS as illustrated in Fig. 3. Differences in migration time between CE-MS and HPCE are a result of differences in column length, buffer concentrations and voltage.

The coaxial interface as presently implemented is difficult to use in practice, and further work is needed to put this approach on an equal footing with HPCE as usually carried out with commercial instruments. Comparisons of efficiencies indicate that standards and the leachate exhibit about 79 000 and 164 000 theoretical plates, respectively, for representative peaks. The CE-MS efficiency was never above 50 000 plates and ranged from 20 000 to 50 000 plates.

Medium resolution mass measurements have confirmed the elemental composition C<sub>6</sub>H<sub>4</sub>SO<sub>3</sub>Cl for the (M - H)<sup>-</sup> ion at *m/z* 191. The smaller peaks appear to be below the detection limit of the CE-MS techniques tried herein to date. Alternative approaches include automated peak collection with multiple runs followed by flow injection analysis using CF-FAB-MS.

Also evident in Fig. 2 are peaks eluting later than the aromatic sulfonic acids. These peaks likely con-

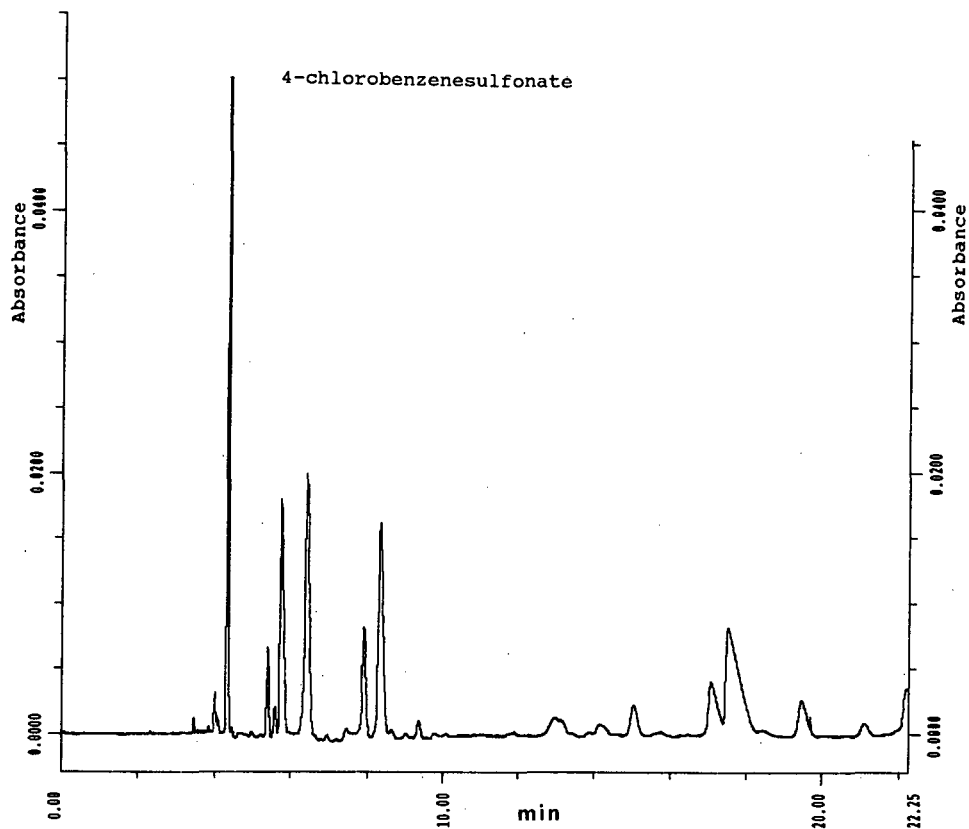


Fig. 2. Electropherogram of Stringfellow leachate using sodium borate-boric acid at pH 8.3.

sist of smaller organic anions of high mobility. The tailing evident in their peak shape again suggests an improper match with the mobility of the buffer counter ions [1]. The ability to identify these unknown ions remains an area of research.

Several issues involving analysis of environmental samples by HPCE need further investigation. Among these is the long-term reproducibility and

comparability of migration times. Another issue concerns the long-term stability of calibration curves with appropriate corrections for on-column detection in quantitative analysis by CE. Essential quality assurance/quality control tools for assessing performance in the context of these issues will need to be developed.

The extension of HPCE to other pH conditions,

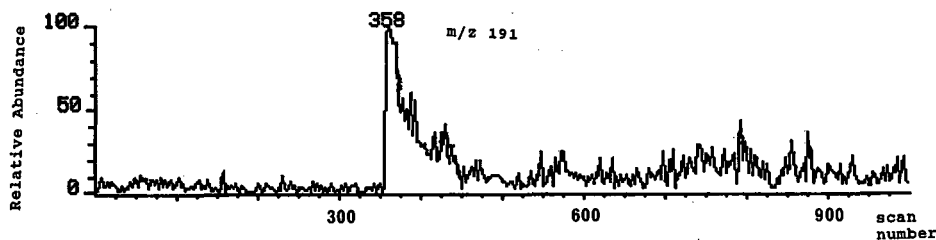


Fig. 3. Negative ion electropherogram of  $m/z$  191 from the Stringfellow leachate using sodium borate-boric acid at pH 8.3.

buffers, and analytes within the context of environmental analysis remains an active pursuit. Whether as a stand-alone technique or as a complementary tool together with high-performance liquid chromatography and thin-layer chromatography, HPCE exhibits great potential for the separation and determination of non-volatile analytes and in characterizing environmental samples for such analytes.

#### ACKNOWLEDGEMENT

The author thanks M.A. Brown (California Department of Health Services, Berkeley, CA, USA) for generously supplying the concentrated String-fellow leachate.

#### NOTICE

Although the research described in this report has been funded by the US Environmental Protection Agency, it has not been subjected to Agency review and, therefore, does not necessarily reflect the views of the Agency and no official endorsement should be inferred. Mention of trade names or commercial products does not constitute endorsement or recommendation for use.

#### REFERENCES

- 1 P. Jandik, W. R. Jones, A. Weston and P. R. Brown, *LC GC*, 9 (1991) 634-645.
- 2 D. E. Burton, M. J. Sepaniak and M. P. Maskarinec, *J. Chromatogr. Sci.*, 25 (1987) 514-518.
- 3 X. Huang, J. A. Lackey, M. J. Gordon and R. N. Zare, *Anal. Chem.*, 61 (1989) 766-770.
- 4 M. Aguilar, X. Huang and R. N. Zare, *J. Chromatogr.*, 480 (1989) 427-431.
- 5 A. G. Ewing, R. A. Wallingford and T. M. Olefirowicz, *Anal. Chem.*, 61 (1989) 212A-229A.
- 6 W. G. Kuhr, *Anal. Chem.*, 62 (1990) 403R-414R.
- 7 K. A. Cobb and M. Novotny, *Anal. Chem.*, 61 (1989) 2226-2231.
- 8 E. S. Yeung and W. G. Kuhn, *Anal. Chem.*, 63 (1991) 275A-282A.
- 9 H.-F. Yin, J. A. Lux and G. Schomburg, *J. High Resolut. Chromatogr.*, 13 (1990) 624-627.
- 10 S. Fujiwara and S. Holda, *Anal. Chem.*, 59 (1987) 2773-2776.
- 11 H. Nishi, T. Fukuyama, M. Matsuo and S. Terabe, *J. Microcolumn Sep.*, 1 (1989) 234-241.
- 12 H. Nishi, T. Fukuyama, M. Matsuo and S. Terabe, *J. Chromatogr.*, 498 (1990) 313-323.
- 13 P. D. Grossman, J. C. Colburn, H. H. Lauer, R. G. Nielson, R. M. Riggan, G. S. Sittampalam and E. C. Rickard, *Anal. Chem.*, 61 (1989) 1186-1194.
- 14 C. D. Gaitonde and P. V. Pathak, *J. Chromatogr.*, 514 (1990) 389-393.
- 15 F. Foret, V. Sustacek and P. Bocek, *Electrophoresis*, 11 (1990) 85-97.
- 16 S. Terabe, K. Otsuka, K. Ichikawa and A. Tsuchiya, *Anal. Chem.*, 56 (1984) 111-113.
- 17 S. Terabe, K. Otsuka and T. Ando, *Anal. Chem.*, 57 (1989) 834-841.
- 18 S. Terabe, Y. Miyashita, O. Shibata, E. R. Barnhart, L. R. Alexander, D. G. Patterson, B. L. Karger, K. Hosoya and N. Tanaka, *J. Chromatogr.*, 516 (1990) 23-31.
- 19 E. D. Lee, W. Mück, J. D. Henion and T. R. Corey, *Biomed. Environ. Mass Spectrom.*, 18 (1989) 253-257.
- 20 R. M. Caprioli, W. T. Moore, M. Martin, B. B. DaGue, K. Wilson and S. Moring, *J. Chromatogr.*, 480 (1989) 247-257.
- 21 M. A. Mosely, L. J. Deterding, K. B. Tomer and J. W. Jorgenson, *Anal. Chem.*, 63 (1991) 109-114.
- 22 R. D. Smith, J. A. Olivares, N. T. Nguyen and R. H. Udseth, *Anal. Chem.*, 60 (1988) 436-441.
- 23 M. A. Brown, I. S. Kim, R. Roehl, F. I. Sasinos and R. D. Stephens, *Chemosphere*, 19 (1989) 1921-1927.

## Short Communication

---

# Multiple ligand applications in high-performance immunoaffinity chromatography

Jeffrey B. Wheatley

*Rainin Instrument Company, 1780 Fourth Street, Berkeley, CA 94710 (USA)*

(First received August 19th, 1991; revised manuscript received April 3rd, 1992)

---

### ABSTRACT

A mixture of antibodies specific for albumin and transferrin, immobilized onto a single support, was used for the simultaneous extraction of albumin and transferrin from immunoglobulin G by high-performance immunoaffinity chromatography. The affinity column was coupled to a strong cation exchanger in order to monitor the success of the extraction and to demonstrate the compatibility of the two chromatographic modes. Coupling of non-affinity chromatography with multiple ligand affinity chromatography is discussed as an alternative to positive affinity chromatography for protein purification.

---

### INTRODUCTION

The chromatographic purification of a protein from a complex sample matrix often poses a difficult challenge. The bulk of the extraneous components in a mixture can usually be removed using non-affinity chromatographic modes such as ion-exchange, hydrophobic interaction and size-exclusion chromatography [1,2]. However, complex mixtures frequently contain components whose chromatographic behavior closely resembles that of the protein of interest. When this is the case purification through non-affinity methods alone is very difficult, and an affinity step is often included in the procedure. Immunoaffinity chromatography is recognized as a powerful tool in protein purification [1,3,4]. It is characterized by extremely specific se-

lectivity and is particularly valuable for separations involving components of such similar physical characteristics as to preclude resolution through other chromatographic modes. Good examples of such problematic separations include the resolution of the immunoglobulin fraction of serum according to class, or the purification of an antigen-specific antibody from the immunoglobulin fraction.

Immunoaffinity chromatography is usually associated with "positive" affinity methods in which the specificity of the immobilized affinity ligand is directed toward the compound of interest. When the sample is applied to an affinity column using this approach, the compound of interest is extracted through complexation with the affinity ligand and the other components in the sample pass through, unretained. The product is released from the affinity ligand by eluting in low-pH buffer or high concentrations of chaotropic salt solutions. An alternative to the positive displacement approach relies on the direct removal of contaminants from the compound

---

*Correspondence to:* J. B. Wheatley, Terrapin Technologies, 165 Eighth Street, Suite 306, San Francisco, CA 94103, USA (present address).

of interest by using immobilized affinity ligands specific for the contaminants instead of the product. This technique, which can be called negative affinity chromatography, is often used as a clean-up step in the final stages of a purification [5,6]. The contaminant, using this approach, is retained on the column and the product is collected in the unretained fraction.

Negative affinity chromatography can be used to extract multiple contaminants in a single step. By mixing the required antibody populations, each bearing a specificity for one of the contaminants, and immobilizing the mixture as a whole, a multiple ligand affinity column is prepared possessing a multiple specificity for the antigens against which the individual antibodies were raised. In this study multiple ligand high performance affinity chromatography is demonstrated for the single step removal of two proteins, human albumin and transferrin, from a third protein, human immunoglobulin G (IgG). This was achieved by passing a mixture of the three proteins through an affinity column containing purified anti-albumin and anti-transferrin antibodies immobilized onto the surface of a silica-based affinity support. In order to monitor the success of the purification, the affinity column was positioned as a pre-column immediately preceding and coupled to a high-performance cation-exchange column for which a method had been developed for the separation of the three proteins. The compatibility of the conditions for the affinity and cation-exchange modes suggests the possibility of single-step performance of negative-affinity and cation-exchange chromatography. Furthermore, the concept can be extended to include affinity chromatography coupled to anion-exchange, size-exclusion and hydrophobic interaction chromatographic modes. The purification of the antibodies used in the study by positive affinity methods is also described.

## EXPERIMENTAL

### *Materials*

Proteins and antisera were obtained from Sigma (St. Louis, MO, USA). Human transferrin (Sigma T 3400) was stated by the manufacturer to be 98% pure and human albumin (Sigma A 8763) was stated to be globulin free and to have been purified

from 96–99% albumin. Human IgG (Sigma I 4506) was described as at least 95% pure. Antisera to transferrin (Sigma T 6225) and albumin (Sigma A 1151) consisted of the  $\gamma$ -globulin fraction of whole goat antiserum and were tested by the manufacturer for antigen specificity. Other chemicals, all reagent grade, were from Baker.

### *Apparatus*

Chromatography and affinity purifications were performed using Rainin (Woburn, MA, USA) (Model HPX) HPLC pumps and Knauer Model 71 and Model 87 UV detectors from Rainin. Control of pumps, HPLC methods, data acquisition and treatment were accomplished with the Macintosh-based Dynamax HPLC Method Manager from Rainin. Spectrophotometric measurements were made on a Hitachi (San Jose, CA, USA) Model U-200 scanning spectrophotometer.

Hydropore-EP and Hydropore-5-SCX were obtained from Rainin. Hydropore-EP served as the affinity support in this study and is based on spherical silica (12  $\mu\text{m}$ , 300  $\text{\AA}$ ), the surface of which is chemically modified and possesses an epoxide functional group which reacts with proteins resulting in their covalent immobilization onto the support surface. Hydropore-5-SCX, based on spherical silica (5  $\mu\text{m}$ , 300  $\text{\AA}$ ), is a strong cation exchanger possessing a sulfopropyl functional group. Hydropore-EP and Hydropore-5-SCX were packed into 15 mm  $\times$  4.6 mm I.D. and 100 mm  $\times$  4.6 mm I.D. stainless-steel column modules, respectively. The column modules were coupled using Dynamax end fittings and analytical guard column hardware from Rainin.

### *Purification of anti-albumin and anti-transferrin antibodies from goat antiserum*

Antibodies specific for human albumin and transferrin were isolated from the  $\gamma$ -globulin fraction of goat antiserum according to procedures similar to those described in [7]. This was accomplished by passing the antiserum through a 100  $\times$  4.6 mm I.D. column possessing the appropriate immobilized antigen, either albumin or transferrin. After washing the column in 20 mM potassium phosphate containing 150 mM sodium chloride at a pH of 6.9 (PBS loading buffer) to remove unretained and weakly associated components, the retained,

antigen-specific antibodies were eluted from the column by switching the mobile phase to the elution buffer, 50 mM PBS, pH 2.5. The retained fraction was collected, quickly neutralized with 5% sodium hydroxide, and the absorbance was measured at 280 nm. The amount of protein was estimated by using a 0.1% extinction coefficient of 1.3. The antigen columns had been previously prepared by recirculating a solution of albumin or transferrin dissolved in 1.0 M potassium phosphate, pH 7.0, through a column packed with Hydropore-EP for about 18 h.

Fig. 1 shows a chromatogram obtained from an injection of the  $\gamma$ -globulin fraction of goat anti-human transferrin onto the transferrin column. The first peak corresponds to unretained protein while the second peak represents the retained fraction corresponding to anti-transferrin antibodies. The chromatogram from an injection of anti-albumin antiserum onto the albumin column was very similar to the one shown in Fig. 1. Injections of the purified transferrin and albumin antibody preparations onto their respective antigen columns, using the chromatographic conditions described in Fig. 1,

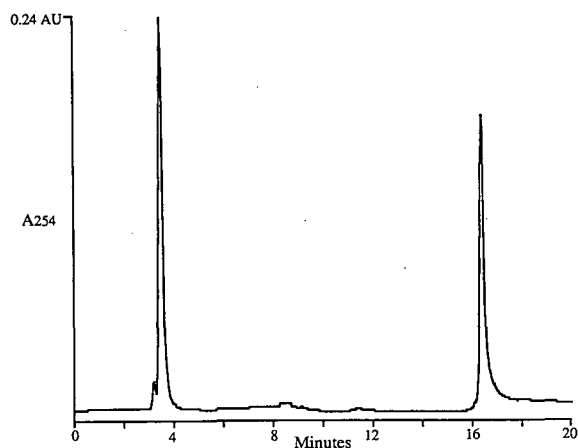


Fig. 1. Goat anti-human transferrin ( $\gamma$ -globulin fraction) injected onto the transferrin antigen column. Transferrin antibodies are found in the retained band. Sample: goat anti-human transferrin antiserum, 24.5  $\mu$ g in 20  $\mu$ l of load buffer; column: human transferrin immobilized on Hydropore-EP 100  $\times$  4.6 mm I.D.; load buffer: 150 mM sodium chloride in 20 mM potassium phosphate, pH 6.9; elution buffer: 150 mM sodium chloride in 50 mM potassium phosphate, pH 2.5; flow-rate: load and elute at 0.5 ml/min, wash at 3.0 ml/min; detection at 254 nm, 0.24 AUFS; method: step gradient from loading to elution buffer.

showed a retained band and almost no unretained protein, indicating highly pure and specific antibody populations.

#### *Preparation of the multiple ligand affinity column: immobilization of anti-transferrin and anti-albumin antibodies*

To combined solutions of purified antibodies containing equal amounts of anti-transferrin and anti-albumin antibodies was added an equal volume of saturated ammonium sulfate solution resulting in the precipitation of the antibodies. The precipitated protein was then isolated by centrifugation and reconstituted in a minimal volume of water. The anti(albumin,transferrin) affinity column was produced by introducing this solution, containing about 2.7 mg of protein, into a short cartridge packed with Hydropore-EP. The dimensions of the bed were 15 mm  $\times$  4.6 mm I.D. After 18 h at room temperature the affinity cartridge was washed several times with PBS, alternating between pH 6.9 and 2.5, after which the cartridge was ready to use. The capacity of the affinity cartridge was measured and found to be 330  $\mu$ g and 375  $\mu$ g, respectively, for transferrin and albumin when each was loaded separately. Previous studies indicate that the maximum albumin binding capacity for a cartridge of this size, at high densities of immobilized antibodies, would be 2.5–3 mg.

#### *Chromatography*

A method was developed for the separation of transferrin, albumin and IgG on the SCX stationary phase, and peaks for the individual components in the mixture were assigned by injection of the individual species. Mixtures of either (1) albumin and transferrin or (2) albumin, transferrin and IgG were injected onto either the SCX column alone or onto the SCX column coupled to the anti-(albumin, transferrin) affinity cartridge with the affinity cartridge positioned in the manner of a guard column. The chromatographic conditions, including protein concentrations, were identical for all injections and are described in Fig. 2. The proteins were eluted using a linear salt gradient formed from two pumps and a high pressure mixer; the volume of the mixer was 1.4 ml.

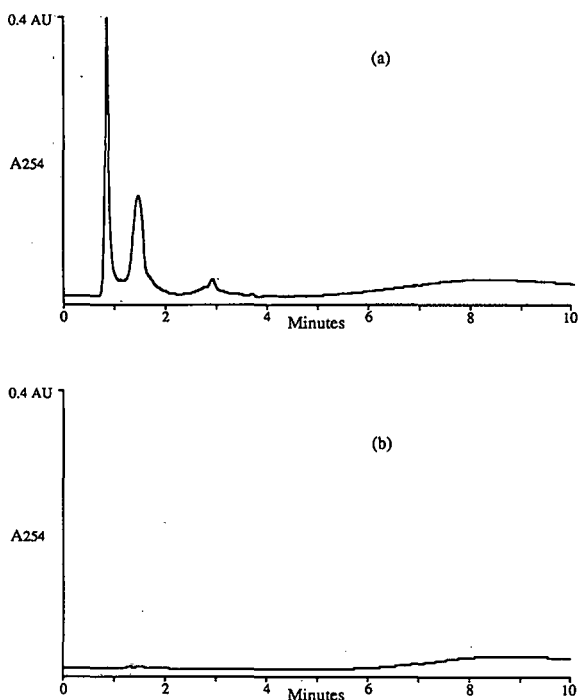


Fig. 2. (a) Mixture of albumin and transferrin injected onto the SCX column. Sample: human albumin (13.3  $\mu\text{g}$ ) and human transferrin (13.3  $\mu\text{g}$ ) in 20  $\mu\text{l}$  buffer A; column: Hydropore-5-SCX, 100  $\times$  4.6 mm I.D.; buffer A: 20 mM sodium acetate, pH 5.8; buffer B: 1.0 M sodium chloride in A; flow-rate: 1.0 ml/min; detection at 254 nm, 0.4 AUFS; method: 0-5 min, 0-70% B; 5-10 min, 70% B. (b) Same sample as in (a) injected on an anti-(albumin,transferrin) affinity column (15  $\times$  4.6 mm I.D.) coupled to and preceding the SCX column. The conditions were identical to (a).

## RESULTS AND DISCUSSION

The chromatogram shown in Fig. 2a is from the injection of a mixture of albumin and transferrin onto the SCX column. Albumin is represented by the peak appearing at 0.8 min and transferrin appears as a major peak at 1.5 min and also as a minor peak at about 2.9 min. In Fig. 2b a chromatogram is shown from the injection of the same mixture onto the anti-(albumin,transferrin) affinity cartridge coupled to and immediately preceding the SCX column. A comparison of the two chromatograms indicates the absence of albumin and transferrin in the chromatogram obtained from the coupled system as a result of their capture by the affinity pre-column. The chromatogram in Fig. 3a was

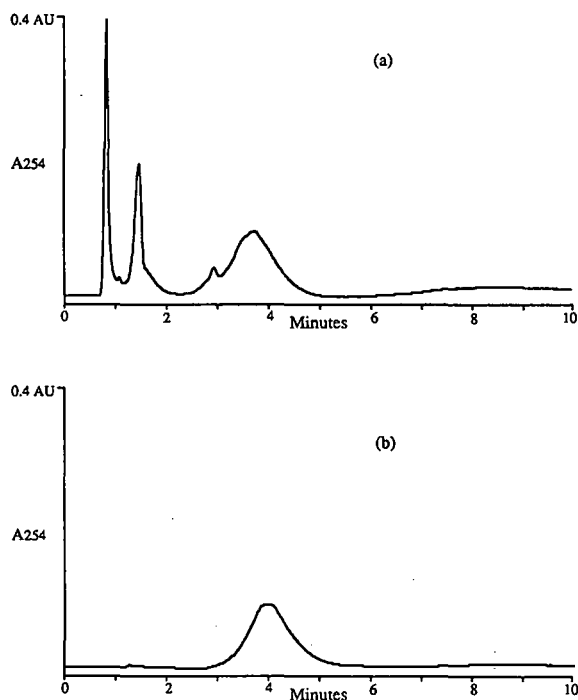


Fig. 3. (a) Mixture of albumin, transferrin and IgG injected onto the SCX column. Sample: human albumin (13.3  $\mu\text{g}$ ), human transferrin (13.3  $\mu\text{g}$ ) and human IgG (20.0  $\mu\text{g}$ ) in 20  $\mu\text{l}$  buffer A; column: Hydropore-5-SCX, 100  $\times$  4.6 mm I.D. The conditions were identical to those described in Fig. 2. (b) Same sample as in (a) injected onto the anti-(albumin,transferrin) affinity column (15  $\times$  4.6 mm I.D.) coupled to and preceding the SCX column. The conditions were identical to (a).

obtained from the injection of a mixture of albumin, transferrin and IgG onto the SCX column. Albumin and transferrin appear as in Fig. 2a and IgG appears as a broad band at about 3.7 min. Fig. 3b shows a chromatogram for the injection of the same mixture onto the coupled affinity-SCX columns, obtained under the same conditions. Conspicuously absent in the second chromatogram are the peaks corresponding to albumin and transferrin which were extracted from the mixture by the affinity pre-column. The retention of IgG in the second chromatogram, seen as a broad band at 4.0 min, was delayed by about 0.3 min relative to that seen in Fig. 3a as a result of the additional dead volume contributed by the affinity pre-column. The areas of the two IgG peaks in Fig. 3a and b are nearly the

same indicating that very little, if any, IgG was lost in its passage over the anti-(albumin,transferrin) affinity column.

The integrity of the antigen–antibody complexes formed between albumin, transferrin and their antibodies in the affinity pre-column was apparently unperturbed by application of the salt gradient, as indicated by the absence of these proteins in the chromatograms shown in Figs. 2b and 3b. The stability of the complexes under these conditions allows the extraction of components from a mixture through the affinity mode while at the same time applying the conditions required for achieving separations in either a cation-exchange or anion-exchange mode. The compatibility of these conditions thus permits the two modes to be directly coupled thereby combining their respective selectivities in a manner analogous to that which has been described for other multi-dimensional chromatographic systems [8–11]. In addition to ion-exchange chromatography, these conditions would also be compatible with size exclusion chromatography and, in some cases, hydrophobic interaction chromatography.

For a mixture of IgG, albumin and transferrin, the application of both affinity and SCX modes is unnecessary for purifying IgG from the other two components. In this mixture only two impurities are present which can be easily removed with the multiple ligand affinity cartridge alone. Even without the affinity mode, major resolution of the three components was achieved in the SCX mode, as seen in Fig. 3. In this study the non-affinity (SCX) mode was coupled to the affinity cartridge solely for the purpose of illustrating the compatibility of the two modes and for monitoring the success of the affinity extraction. A coupled system, analogous to that described in this study, would be most useful for more complex sample mixtures for which either separation mode alone would be insufficient for purification of the product. For such a hypothetical sample mixture most of the extraneous components could be separated from the compound of interest through a non-affinity mode, yielding a product in a predominantly pure state but containing a limited number of minor, but difficult to remove, contaminants. To this mode would be coupled a multiple ligand affinity column possessing immobilized antibodies with specificities corresponding to the conta-

minants co-eluting with the product in the non-affinity mode. The affinity column would thus extract the components from the mixture which, in the non-affinity mode, could not be separated from the product. For a purification scheme consisting of several non-affinity steps the affinity column would be coupled to the last mode in the sequence. The affinity cartridge in this study possessed specificities for only two proteins, but the principle can be readily extended for multi-component extraction, according to the number of contaminants present.

In this study a very short affinity pre-column (1.5 cm) was coupled directly to the SCX column, and the IgG peak eluting from the coupled column arrangement showed only slight broadening in comparison to the peak obtained from injection of the sample on the SCX column alone (Fig. 3b and a, respectively). However, for some processes direct coupling of the affinity column could result in significant losses of resolution in the non-affinity mode thereby introducing unnecessary contaminants overlapping with the product band. Undesirable interference from the coupled affinity column would arise from contributions of the affinity column to band broadening and from tailing due to weak associations between sample components and the affinity stationary phase. This would be particularly true for longer affinity columns and for complex, concentrated samples.

While the coupling arrangement used in this study might suffice for many applications, the problems described above could be avoided by the installation of one or more multiple port switching valves to control the path of the sample and mobile phase. In such an arrangement the sample would initially pass through the non-affinity column with the valves positioned such that the effluent containing any early eluting bands would by-pass the affinity column. Immediately before elution of the band containing the product, the valve configuration would be switched to re-direct the effluent from the first column through the affinity column. The product and any co-eluting impurities would then pass from the first column directly onto the affinity column which would be designed to extract the impurities co-eluting with the product. If the separation of the mixture on the first column subsequent to product elution were also of interest (for example, if it were desirable to collect more than one product

from the separation) the valve(s) could be returned to the initial configuration, once again by-passing the affinity column and preventing its interference in the final stages of the separation. Several authors have recently published papers describing system configurations designed to coordinate processes involving coupled columns [9,10,12] which could be adapted for the purposes described here.

Immunoaffinity chromatography continues to be an expensive process, and is even more so for applications in which the necessary antibodies are unavailable and must be custom produced. Purification of a product by immunoaffinity extraction of the contaminants requires antibodies specific for the contaminants. In many cases the identity of the contaminants may be either unknown or, if known, their antibodies may be unavailable. As the number of impurities increases this problem is compounded. Thus, for many processes the multiple ligand-negative affinity approach would prove impractical, and a positive affinity approach would be indicated.

For some processes, however, the amount of antibody required for the positive affinity approach could exceed by many times that needed for the removal of a few percent impurity. In these cases the reduction in antibody requirements achieved through the negative affinity approach could justify the effort to isolate the impurities and produce their purified antibodies. Whether this would be worthwhile would depend on the scale of the process, the difficulty in isolating the impurities, and on the level of in-laboratory expertise.

Another consideration which can make the positive affinity approach less attractive are factors that are associated with positive affinity chromatography but are less important in the negative affinity approach. These include the use of denaturing eluents and the non-immunospecific binding of unwanted sample components to the affinity phase along with the product [13–15]. As pointed out in ref. 14, non-specific binding of contaminants, in particular, is a common problem in positive affinity chromatography. This results in the elution of the non-specifically bound contaminants along with the product, and may necessitate additional chromatographic steps in order to reach the desired level of product purity. In negative affinity chromatogra-

phy, since the product appears in the unretained fraction this is less of a problem.

In conclusion, the compatibility of the conditions used in negative affinity chromatography with other separation modes suggests that this technique could be readily coupled with other kinds of stationary phases. In addition antibody populations of multiple specificity can be immobilized onto a single support thereby permitting single step removal of multiple impurities. Many non-affinity modes are themselves compatible and amenable to on-line coupling, as reviewed by Majors [11], so that in some cases an affinity column could be incorporated into a pre-existing coupling scheme. Currently available automation enables precise coordination of system devices and events within a coupled system through method programming, thereby providing the potential for reducing the number of steps in a complex purification scheme.

#### REFERENCES

- 1 M. T. W. Hearn, *J. Chromatogr.*, 418 (1987) 3.
- 2 W. S. Hancock (Editor), *High Performance Liquid Chromatography in Biotechnology*, Wiley, New York, 1990.
- 3 P. Mohr and K. Pommerening, *Affinity Chromatography: Practical and Theoretical Aspects*, Marcel Dekker, New York, 1985.
- 4 D. J. Winzor and J. DeJersey, *J. Chromatogr.*, 492 (1989) 377.
- 5 D. Low, in W. S. Hancock (Editor), *High Performance Liquid Chromatography in Biotechnology*, Wiley, New York, 1990, pp. 501–502.
- 6 H. A. Chase, *J. Biotechnol.*, 1 (1984) 67.
- 7 J. B. Wheatley, *J. Chromatogr.*, 548 (1991) 243.
- 8 J. C. Giddings, *Anal. Chem.*, 56 (1984) 1258A.
- 9 M. M. Bushey and J. W. Jorgenson, *Anal. Chem.*, 62 (1990) 161.
- 10 M. M. Bushey and J. W. Jorgenson, *Anal. Chem.*, 62 (1990) 978.
- 11 R. E. Majors, *J. Chromatogr. Sci.*, 18 (1980) 571.
- 12 G. Thévenon-Emeric and F. E. Regnier, *Anal. Chem.*, 63 (1991) 114.
- 13 P. O'Carra, S. Barry and T. Griffin, *FEBS Lett.*, 43 (1974) 169.
- 14 D. R. Nau, in W. S. Hancock (Editor), *High Performance Liquid Chromatography in Biotechnology*, Wiley, New York, 1990, p. 501.
- 15 W. G. Palmer, *Biochim. Biophys. Acta*, 278 (1972) 299.

## Short Communication

# Novel polymeric reagent for synthesizing 9-fluorenylmethoxycarbonyl L-prolinyl derivatives for chiral high-performance liquid chromatography of amino acids

Z. Zhang, G. Malikin and S. Lam

*Albert Einstein College of Medicine, 1300 Morris Park Avenue, Bronx, NY 10461 (USA)*

(First received November 26th, 1991; revised manuscript received March 30th, 1992)

### ABSTRACT

The synthesis of a novel polymer-supported 9-fluorenylmethoxycarbonyl-L-proline reagent for derivatizing nucleophiles is described. The new polymer, containing a 1-hydroxybenzotriazole activated ester, is highly reactive. Significant improvement in the ease of use and the rate of reaction with strong and weak nucleophiles is achieved. In this study, the utility of the solid-phase reagent for derivatizing amino acids for chiral high-performance liquid chromatography is described. Derivatization is accomplished simply by mixing a sample of the amino acid in acetonitrile with the polymer at room temperature for 10 min. Racemization of amino acids under the mild reaction conditions is not observed. Despite 9-fluorenylmethoxycarbonyl-L-prolinyl-D,L-amino acids are diastereoisomeric, the isomers are not separated by simple reversed-phase chromatography. Since these derivatives possess the necessary functional groups for metal chelation, mobile phases containing chiral Cu(II) complexes were used to resolve the optical isomers. Excellent resolution of all the D and L enantiomers of natural amino acids was achieved by using Cu(II)-L-histidine methyl ester and Cu(II)-L-proline eluents on reversed phases columns with various concentrations of acetonitrile. The separated derivatives were detected in the low-nanogram range by fluorescence at 315 nm with excitation at 275 nm.

### INTRODUCTION

Chromatographic resolution of enantiomers is generally accomplished by transforming an enantiomer pair to a diastereomer pair. In the direct resolution mode, diastereomeric transformation takes place when the enantiomers form association complexes with a chiral system ligand immobilized on the stationary phase or added to the mobile phase. The chiral ligand can be a micro-molecule or a macro-molecule like protein. The forces of association, depending on the chromatographic system,

may include  $\pi$ - $\pi$  interaction, hydrogen bonding, dipole stacking, mixed ligand metal complexation, inclusion complex formation, ion pair complexation or a combination of several of these forces as in protein binding sites. In the indirect resolution mode, optical isomers are resolved by chemical derivatization with a chiral reagent to form covalently bonded diastereomers. The differences in internal energy of the diastereomers favor the partition of one isomer over the other in the chromatographic system, and as a result, chiral separation.

As the natural L-amino acids are distinct from the D-isomers with different biological implications, there is a great deal of emphases in resolving these optical isomers and identifying their stereo-config-

*Correspondence to:* Dr. S. Lam, Albert Einstein College of Medicine, 1303 Morris Park Avenue, Bronx, NY 10461, USA.

uration. Amino acids, with a few exceptions, are known to possess poor absorption characteristics and electrochemical properties for high-performance liquid chromatography (HPLC) detection. Chemical derivatization by pre-column or post-column techniques is a standard approach for enhancing the sensitivity of detection. Recently, chemical derivatization is also recognized as an approach for enhancing both direct and indirect chiral resolution. In the indirect resolution mode, however, the derivative must introduce an additional optical center to give a diastereomer.

Among the chiral derivatization reagent for amino acids are  $N^2$ -(5-fluoro-2,4-dinitrophenyl)-L-alanine amide and modifications substituting alanine with different amino acid [1], *o*-phthalaldehyde with various chiral thiols [2,3], and a collection of other chiral reagent [4]. Recently, Patchornik and co-workers introduced polymeric active esters such as polymeric 1-hydroxybenzotriazole (HOBT) [5], polymeric 4-hydroxy-3-nitrobenzophenone (P-BP) [6], and polymeric 4-(dimethylamino)pyridine (P-DMAP) [7] as acylating reagents in peptide synthesis. Following the similar idea, Krull and co-workers synthesized several of these polymeric reagents containing 9-fluorenylmethoxycarbonyl (FMOC), FMOC-L-phenylalanine, FMOC-L-proline and 3,5-dinitrophenyl (DNB) moieties for derivatization of various nucleophiles in HPLC. They used polymeric reagents P-HOBT-FMOC [8,9], P-BP-FMOC [10], P-HOBT-DNB and P-BP-DNB [11] for labelling amines and polyamines, and P-DMAP-FMOC [12], P-BP-DNB [13] and P-HOBT-DNB [13] for labelling alcohols. Polymeric reagents containing chiral labels such as P-BP-FMOC-L-proline and P-BP-FMOC-L-phenylalanine were also used for transforming enantiomeric amines to diastereomeric amines for detection and chiral separation [14,15]. No work on labelling free amino acids with chiral polymeric reagent has been reported.

In this work, we report the synthesis of a new polymeric reagent containing HOBT ester of FMOC-L-proline for derivatization and resolution of optical isomers of amino acids by HPLC.

## EXPERIMENTAL

### Chemical and reagents

Polystyrene [styrene divinylbenzene (96:4), 200–

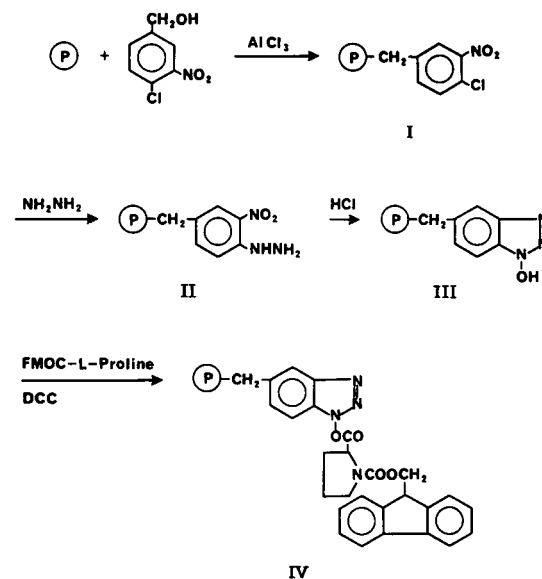
400 mesh) was purchased from Fluka (Buchs, Switzerland) and FMOC-L-proline from Chemical Dynamics (South Plainfield, NJ, USA). The amino acids were obtained from Sigma (St. Louis, MO, USA). Dicyclohexylcarbodiimide (DCC) was bought from Aldrich (Milwaukee, WI, USA) and acetonitrile, distilled in glass, from Burdick & Jackson Labs. (Muskegon, MI, USA).

### Instrumentation

The HPLC system consisted of two Altex (Berkeley, CA, USA) 110A pumps, an Altex 420 gradient microprocessor and a Rheodyne (Cotati, CA, USA) 7105 injection valve. The analytical column 15 × 0.42 cm I.D., was packed with Nucleosil-5 C<sub>18</sub> (Macherey–Nagel, Düren, Germany) by the downward slurry technique. A FMOC-L-prolinyl derivatives were monitored with a Hitachi fluorescence detector, Model F-1050 (Danbury, CT, USA) at 315 nm with excitation at 275 nm. The detector signals were output to the Model 4416 data system (Nelson Analytical, Cupertino, CA, USA). Elemental microanalyses were performed by Schwarzkoff Microanalytical Laboratory (New York, NY, USA).

### Synthesis of polymeric reagent

(3-Nitro-4-chloro)benzylated polystyrene I. To



Ⓟ : Polystyrene

10 g of dried polystyrene copolymer [styrene–divinylbenzene (96:4), 10 g] were added 50 ml of nitrobenzene, 10 g (53.3 mmol) of 3-nitro-4-chlorobenzyl alcohol and 10 g (75 mmol) of anhydrous aluminum chloride. After stirring at 65–75°C for three days, the reaction was stopped by allowing the mixture to cool to room temperature. The polymer was filtered and washed with 1 M HCl in dioxane (3 × 50 ml), N,N-dimethylformamide (DMF) (3 × 50 ml), methanol (3 × 50 ml) and methylene chloride (3 × 50 ml), and finally dried under vacuum at 80°C. The dried polymer weighed 13.8 g. Elemental analyses of the polymer found 1.76 mmol chlorine and 1.9 mmol nitrogen per gram of dry solid, indicating that about 26% of the aromatic rings of the polymer were substituted.

**1-Hydroxybenzotriazole-bound polystyrene III.** To 7 g of polystyrene I were added 24 ml of hydrazine hydrate–ethylene glycol monoethyl ether 4:6, v/v). The mixture was refluxed for 20 h. After cooling to room temperature, the polymer was filtered, washed thoroughly with water, and dried. The polymer, 3-nitro-4-hydrazine-benzylated polystyrene II, was then suspended in 36 ml of concentrated HCl–dioxane (1:1, v/v) and refluxed for 20 h. The polymer was filtered, washed with water (5 × 35 ml), methanol (3 × 35 ml) and diethyl ether (3 × 18 ml), and dried in vacuum at 80°C. The light brown polystyrene III weighed 6.34 g. Elemental analysis found 4.93% nitrogen, corresponding to 1.17 mmol 1-hydroxybenzotriazole functional group/g of dry solid.

**Polymeric Fmoc-L-proline reagent IV.** To 6 g (6.2 mmol hydroxy functional group) of polystyrene III was added a solution of 4.86 g (14.4 mmol) of Fmoc-L-proline in 45 ml methylene chloride. After equilibration to 0°C, the mixture was stirred for an additional 5 min before 2.97 g (14.4 mmol) of DCC in 15 ml of methylene chloride was added. The mixture was stirred at 0°C for 20 min. The polymer was filtered, washed with methylene chloride (4 × 100 ml) and dry diethyl ether (2 × 50 ml), and dried in vacuum at room temperature. The yield was 6.7 g polystyrene IV, containing 0.25 mmol Fmoc-L-proline per gram of dry solid.

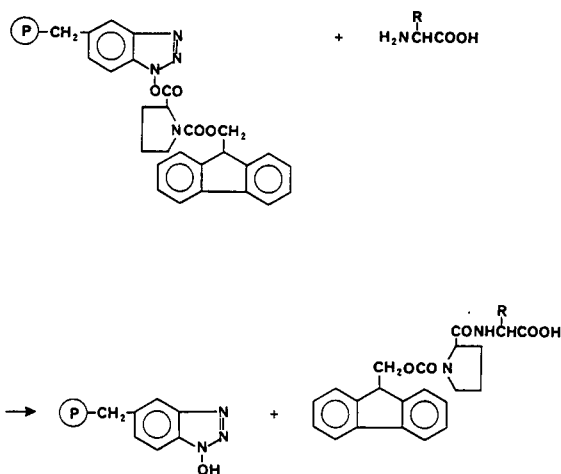
#### Derivatization of amino acid with Fmoc-L-prolinyl polystyrene

Amino acids (4 μl of a 1000-ppm solution in ace-

tonitrile were derivatized by addition to a suspension of Fmoc-L-prolinyl polystyrene (20 mg) in 200 μl of acetonitrile. The reaction was allowed to proceed for 10 min at room temperature. After centrifugation, 20 μl of the upper solution were injected into the HPLC system.

#### RESULTS AND DISCUSSION

The representative derivatization reaction of Fmoc-L-prolinyl polystyrene with a nucleophile is shown below:



The acyl carbon in this polymer is highly reactive, due to the great electron-withdrawing inductive effect of the benzotriazole ring, that it is susceptible to attack by nucleophiles. The derivative can be used for conventional sensitivity enhancement by UV or fluorescence detection, or for chromatographic enhancement by forming diastereomers for chiral separation.

#### Reaction conditions

Since the benzotriazole Fmoc-L-prolinyl polystyrene is highly reactive, the choice of appropriate solvent for supporting the derivatization reaction is critical. When methanol was used as the solvent for amines, rapid transesterification of methanol was observed as evident of the large methanol peak together with the amine peak. Methanol therefore was not an appropriate solvent for the derivatization reaction. DMF was a useful solvent for solubilizing certain amino acids, but was found to con-

tain too many impurities for a clean derivatization reaction. Acetonitrile due to its good swelling property and solvability, as reported by Gao *et al.* [10], was the best derivatization solvent, giving the highest yield with the smallest FMOC-L-proline reagent peak resulting from hydrolysis of the polymer. FMOC-L-proline peak was also observed when water, which also acts as a nucleophile in this case, is present in the sample or the solvent.

In chiral derivatization, racemization of one isomer to another under drastic reaction conditions is a major concern. Since the reaction conditions were mild and HOBT ester suppressed racemization, D-isomer was not detected when L-lysine was allowed to react with the polymeric reagent for up to 30 h (Fig. 1).

#### Chromatography of amino acids

By attaching a FMOC-L-proline group to free D,L-amino acids, diastereomeric acids are obtained. The diastereomeric pair in theory is chromatographically separable because of differences in chemical properties. When chromatographed under reversed-phase conditions using acetonitrile and water, enantiomeric resolution was not achieved. In the study of enantiomeric amines and amino alco-

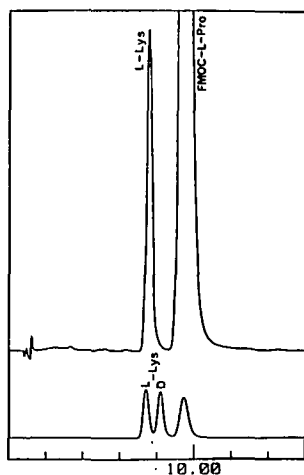


Fig. 1. Chromatogram of L-lysine after a 30-h reaction with FMOC-L-prolinyl polystyrene showing no D-isomer from racemization (upper tracing); D,L-lysine standards (lower tracing). Column: Nucleosil 5 C<sub>18</sub>, 15 × 0.42 cm I.D. Mobile phase: 2.5 mM Cu(II)-L-histidine methyl ester complex and 2 g/l ammonium acetate in acetonitrile-water (25:75). pH 7.0. Flow-rate: 2.0 ml/min. Time in min.

ols, chiral separation was achieved only when organic mobile phases were used [15]. Apparently, these derivatives with multiple keto and amino groups are much better candidates for hydrogen-bonding interaction in normal-phase separation than reversed-phase partition chromatography.

In our previous study, ligand-exchange chromatography has proven to be a most effective approach for resolving amino acid isomers. We therefore attempted the separation of FMOC-L-prolinyl amino acids using mobile phases that contained chiral copper complexes. We used L-histidine methyl ester copper complexes, since it gave both excellent

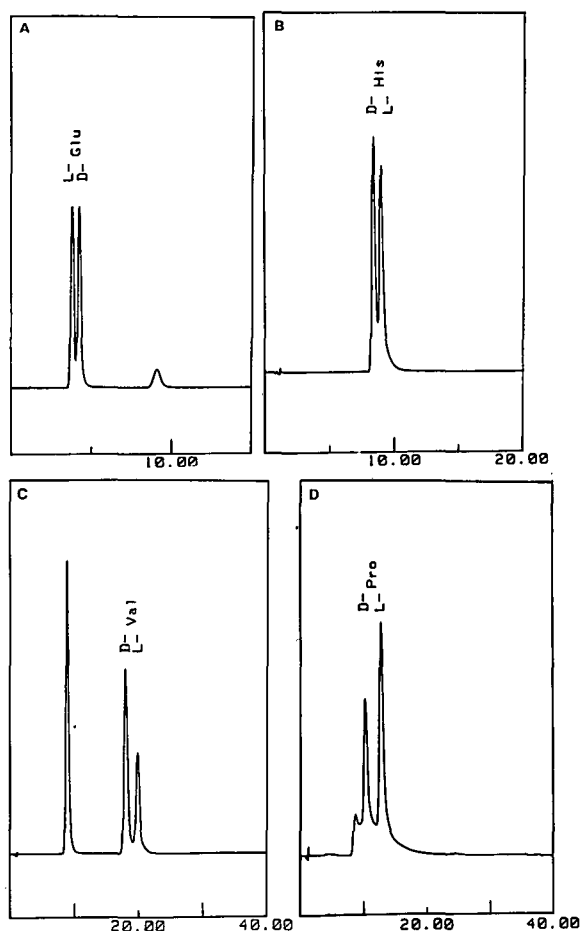


Fig. 2. Representation chromatogram of FMOC-L-prolinyl amino acids with different substituents. (A) Glutamic acid; (B) histidine; (C) valine; (D) proline. The peak at 9.5 min is FMOC-L-proline, the derivatizing agent. Conditions as in Fig. 1.

chiral and achiral selectivity in the separation of dansyl amino acids [2].

A mobile phase containing 2.5 mM Cu(II)-L-histidine methyl ester complex in acetonitrile–water (25:75) was used to effect the separation of FMOC-L-prolinyl amino acids (Fig. 2). As shown in Table I, all the amino acids are resolved into their enantiomeric pairs. FMOC-L-Prolinyl amino acids were similarly separated when 2.5 mM Cu(II)-L-proline was used. However, the capacity ratios were smaller than those observed in the histidine methyl ester system, reflecting the retention of a less hydrophobic mixed complex as a result of the contribution of a less hydrophobic system ligand (Table II). In agreement with the work on dansyl-amino acids, the higher the carbon content of the amino acids, the bulkier the alkyl substituent on the  $\alpha$ -carbon, the longer the retention.

The stereoselectivity is dependent on the immediate micro-environment, affected by the substituent

on the  $\alpha$ -amino acids. Amino acids with a basic or acidic side-chain capable of participation in metal complexation showed reversed selectivity as the amino acids with aliphatic substituents. These observations suggest that the amino acids form glycine-like coordination with the system ligand, and the prolinyl substitution may contribute axial coordination in the mixed metal complex.

Proline, unlike the other amino acids, is an imino acid. The FMOC-L-prolinyl-proline does not possess a dissociable amine proton. Like dansyl-proline, it is not expected to form a glycine-like mixed complex with copper and give chiral separation. Instead proline is resolved with an exceptional large  $\alpha$  value. The carbonyl group on the peptide linkages contributed by the FMOC-L-prolinyl moiety must be an important participant in metal coordination. The mechanism of metal complexation of the FMOC-L-prolinyl-amino acid is under investigation.

TABLE I

CAPACITY RATIO  $k'$  AND SELECTIVITY ( $\alpha = k'_D/k'_L$ ) OF FMOC-PROLINYL AMINO ACIDS

Mobile phase: 2.5 mM Cu(II)-L-histidine methyl ester complex and 2 g/l ammonium acetate in acetonitrile–water. The acetonitrile concentration is indicated. pH 7.0. Flow-rate 2.0 ml/min.

Amino acid	25% acetonitrile			30% acetonitrile		
	$k'_D$	$k'_L$	$\alpha$	$k'_D$	$k'_L$	$\alpha$
Glu	3.40	2.94	0.86	1.06	0.93	0.87
Asp	4.34	4.24	0.98	1.33	1.33	1.00
Asn	6.81	6.53	0.96	2.20	2.11	0.96
Ser	7.40	8.08	1.09	2.63	2.87	1.09
Lys	7.46	6.66	0.89	2.44	2.22	0.91
Ala	7.87	8.81	1.12	2.93	3.26	1.11
Arg	8.24	7.51	0.91	2.62	2.47	0.94
Thr	9.10	9.57	1.05	3.27	3.38	1.03
Pro	9.53	12.08	1.27	2.38	2.38	1.00
His	9.75	11.09	1.14	3.56	4.05	1.14
Tyr	16.25	16.64	1.02	4.96	4.96	1.00
Val	17.64	19.55	1.11	5.74	6.27	1.09
Nval	18.22	20.56	1.13	5.98	6.65	1.11
Met	19.45	21.48	1.10	6.52	7.11	1.09
Ileu	28.45	30.81	1.08	9.93	10.73	1.08
Leu	33.58	37.34	1.11	9.84	10.91	1.11
Nleu	34.72	38.75	1.12	9.81	10.86	1.11
Phe	54.15	60.34	1.11	14.90	15.93	1.07
Trp	58.66	64.77	1.10	15.20	16.36	1.08

TABLE II

CAPACITY RATIO  $k'$  AND SELECTIVITY ( $\alpha = k'_D/k'_L$ ) OF FMOC-PROLINYL AMINO ACIDS

Mobile phase: 2.5 mM Cu(II)-L-proline complex and 5 g/l ammonium acetate in acetonitrile-water. The acetonitrile concentration is indicated. pH 7.0. Flow-rate 2.0 ml/min.

Amino acid	25% acetonitrile			30% acetonitrile		
	$k'_D$	$k'_L$	$\alpha$	$k'_D$	$k'_L$	$\alpha$
Glu	2.89	2.46	0.85	0.88	0.77	0.88
Asp	2.97	2.82	0.95	0.87	0.87	1.00
Asn	6.60	6.40	0.90	2.03	2.03	1.00
Pro	6.68	9.98	1.49	2.09	2.59	1.24
Lys	6.97	6.14	0.88	2.14	1.95	0.91
Arg	7.92	7.18	0.90	2.32	2.32	1.00
Ser	8.20	8.20	1.00	2.47	2.47	1.00
Ala	8.87	10.04	1.13	3.22	3.22	1.00
His	9.05	9.81	1.08	2.99	2.99	1.00
Thr	9.84	10.33	1.05	3.04	3.04	1.00
Tyr	15.87	16.30	1.03	4.54	4.54	1.00
Val	17.53	19.84	1.13	5.23	5.82	1.11
Nval	18.63	21.25	1.14	5.40	6.08	1.13
Met	20.20	22.42	1.11	5.86	6.43	1.10
Ileu	27.60	30.37	1.10	7.65	8.34	1.09
Leu	31.57	35.15	1.11	8.33	9.27	1.11
Nleu	32.15	36.13	1.12	8.54	9.54	1.12
Phe	54.66	60.20	1.10	13.48	14.35	1.06
Trp	57.95	64.80	1.12	13.68	14.87	1.09

## REFERENCES

- H. Brückner and C. Keller-Hoehl, *Chromatographia*, 30 (1990) 621–629.
- S. Lam, *J. Chromatogr.*, 355 (1986) 157–164.
- H. Brückner, R. Wittner and H. Godel, in G. Lubec and G. A. Rosenthal (Editors), *Amino Acids: Chemistry, Biology and Medicine*, ESCOM, Leiden, Netherlands, 1990, pp. 143–151.
- M. Ahnoff and S. Einarsson, in W. J. Lough (Editor), *Chiral Liquid Chromatography*, Blackie, New York, 1989, p. 39.
- R. Kalir, A. Warshawsky, M. Fridkin and A. Patchornik, *Eur. J. Biochem.*, 59 (1975) 55–61.
- B. J. Cohen, H. Karoly-Hafeli and A. Patchornik, *J. Org. Chem.*, 49 (1984) 922–924.
- Y. Shai, K. A. Jacobson and A. Patchornik, *J. Am. Chem. Soc.*, 107 (1985) 4249–4252.
- C.-X. Gao, T.-Y. Chou, S. T. Colgan, I. S. Krull, C. Dorschel and B. Bidlingmeyer, *J. Chromatogr. Sci.*, 26 (1988) 449–457.
- T.-Y. Chou, C.-X. Gao, S. T. Colgan, I. S. Krull, C. Dorschel and B. Bidlingmeyer, *J. Chromatogr.*, 454 (1988) 169–183.
- C.-X. Gao, T.-Y. Chou and I. S. Krull, *Anal. Chem.*, 61 (1989) 1538–1548.
- A. J. Bourque and I. S. Krull, *J. Chromatogr.*, 537 (1991) 123–152.
- C.-X. Gao and I. S. Krull, *J. Chromatogr.*, 515 (1990) 337–356.
- A. J. Bourque and I. S. Krull, *J. Chromatogr. Sci.*, 29 (1991) 489–495.
- C.-X. Gao and I. S. Krull, *J. Pharm. Biomed. Anal.*, 7 (1989) 1183–1189.
- T.-Y. Chou, C.-X. Gao, N. Grinberg and I. S. Krull, *Anal. Chem.*, 61 (1989) 1548–1558.

## Short Communication

---

# Automated liquid chromatographic determination of ochratoxin A in cereals and animal products using immunoaffinity column clean-up

Matthew Sharman, Susan MacDonald and John Gilbert

Ministry of Agriculture, Fisheries and Food, Food Science Laboratory, Colney Lane, Norwich NR 4 7UQ (UK)

(First received February 7th, 1992; revised manuscript received April 3rd, 1992)

---

### ABSTRACT

The analysis of the fungal mycotoxin ochratoxin A in cereals and animal products is described using an immunoaffinity column clean-up and high-performance liquid chromatographic determination. The clean-up can be carried out manually or using a commercially available automated sample preparation system. The method has been applied to cereals such as wheat, rye and barley, unprocessed breakfast cereals and animal products such as pigs' kidneys and blood sausages. Recoveries ranged from 70–80% for spiked samples (10 µg/kg) and the method had a relative standard deviation of 1.3% ( $n=8$ ) for the analysis of a wheat sample naturally contaminated at 13.7 µg/kg ochratoxin A and relative standard deviation of 3.0% ( $n=8$ ) for a pig kidney sample spiked at 10 µg/kg ochratoxin A. The immunoaffinity approach was significantly faster than methods employing conventional chromatographic clean-up, and extracts were free of co-extractives giving a limit of detection of 0.2 µg/kg.

---

### INTRODUCTION

Ochratoxin A is a mycotoxin produced by *Aspergillus ochraceus* as well as by other fungi notably *Penicillium veridicatum*. The toxin has been found to occur in foods of plant origin, and through transfer from animal feeds can occur as a contaminant in edible animal tissues. Despite extensive data already in the literature concerning the occurrence of ochratoxin A there still exists a need for routine monitoring both to assess human exposure, and to test for compliance with regulations in countries such as Denmark [1]. Numerous methods have been

published for the analysis of ochratoxin A using conventional column clean-up with high-performance liquid chromatographic (HPLC) end-determination [2] or using immunological methods such as enzyme-linked immunosorbent assay (ELISA) [3,4]. Many of these methods although individually effective do have the disadvantage of being only applicable to a limited number of matrices.

There is some advantage for laboratories that have large numbers of samples to analyse for a range of different mycotoxins to standardise procedures and thereby rationalise available instrumentation. For the analysis of aflatoxins in foods and animal feeds we have recently reported [5] a fully automated sample preparation and HPLC analysis procedure based on immunoaffinity column clean-up. An identical approach can be adopted for the

---

Correspondence to: Dr. J. Gilbert, Ministry of Agriculture, Fisheries and Food, Food Science Laboratory, Colney Lane, Norwich NR4 7UQ, UK.

determination of ochratoxin A, offering the same advantages of automation, application to a range of differing matrices and allowing utilisation of the same equipment as for the aflatoxins.

Immunoaffinity columns comprise an anti-mycotoxin antibody bound to a gel material contained in a small plastic cartridge. Crude extract is forced through the column and the specific mycotoxin is left bound to the recognition site of the immunoglobulin. Extraneous material can be washed off the column with water and the mycotoxin in question can be recovered in purified form by liberating the bound analyte from the antibody with an elution solvent such as methanol or acetonitrile. Immunoaffinity columns are commercially available and have been routinely employed for determining aflatoxins B<sub>1</sub>, B<sub>2</sub>, G<sub>1</sub> and G<sub>2</sub> in nuts, nut products and dried fruit [6–8], as well as for determining aflatoxin M<sub>1</sub> in milk [9] and cheese [10]. These columns have the advantages of speed and simplicity compared to conventional clean-up and of high specificity thereby producing extracts free of interferences, although they have yet to be established by collaborative trial as satisfying requirements of official methods.

The simplicity of analysis using immunoaffinity columns makes this approach particularly amenable to automation, which in turn overcomes problems that are sometimes reported as being associated with sample loading onto the column such as poor recovery due to erratic flowrate through the columns. We previously described [5] a modification to the design of the plastic immunoaffinity cartridges to fit the rack of a commercially available automated sample preparation system (ASPEC). Changes to the software of the system which were made for aflatoxin analysis and which permitted conditioning, loading, washing and eluting operations were sufficiently flexible to allow the system to be readily extended for use for ochratoxin A analysis. The system described in this paper as previously for automated aflatoxin analysis, has been fully integrated with the HPLC determination, utilising fluorescence detection to determine ochratoxin A.

## EXPERIMENTAL

### Materials

Immunoaffinity columns (Easi-extract) for ochratoxin A were supplied by Biocode (York, UK). The manufacturer's data for the recovery from the columns was >85% when 100 ng of ochratoxin A were applied in a suitably diluted methanol extract, and a total capacity of greater than 2.7 µg of ochratoxin A when applied in phosphate-buffered saline (PBS).

Acetonitrile, methanol and chloroform were purchased from Rathburn (Walkerburn, UK). All water was deionised and distilled. Ochratoxin A was purchased from Sigma (Poole, UK) and buffer salts from BDH (Poole, UK). PBS was prepared from potassium chloride (0.2 g), potassium dihydrogenphosphate (0.2 g), anhydrous disodium hydrogenphosphate (1.16 g) and sodium chloride (8.0 g) added to distilled water (900 ml). After dissolution the pH was adjusted to 7.4 (with 0.1 M HCl or 0.1 M NaOH as appropriate) and the solution made to 1 l.

### Sample preparation

*Cereal samples.* The sample (10.0 g) was weighed into a 100-ml tall form beaker and 40 ml of PBS-methanol (50:50) were added. The mixture was homogenised at high speed for 3–5 min with an Ultra Turrax homogeniser fitted with an 18N shaft to produce a slurry. The sample was filtered through Whatman 113V filter paper and an aliquot of the supernatant (15 ml) was diluted with PBS (35 ml) prior to affinity column clean-up.

*Animal products.* For pigs' kidneys the sample (10.0 g) was weighed into a 250-ml beaker, chloroform (100 ml) and 85% phosphoric acid (0.6 g) were added and the sample was homogenised as above. For black pudding (blood sausage) the sample (10.0 g) was similarly extracted but with the addition of water (15 ml). The kidney sample was filtered through a Whatman 113V filter paper, whilst the black pudding sample was centrifuged at 4500 g (4°C) for 10 min followed by filtration through a Whatman 113V filter paper into a separating funnel. In both cases the chloroform solution (50 ml) was partitioned with 1 M sodium hydrogencarbonate (100 ml), and an aliquot of the aqueous phase (45 ml) was diluted with water (15 ml), taking 50 ml

of the resultant solution for affinity column clean-up.

**Manual immunoaffinity column clean-up.** The immunoaffinity column was conditioned with PBS (20 ml) followed by the sample extract (50 ml) pushing both through the column at a steady flow of approximately 5 ml/min. The column was washed with distilled water (10 ml), then air dried by pumping air from a disposable syringe. The ochratoxin A was eluted from the column with 2.0 ml of methanol over 2 min, collecting in a 4-ml amber vial. The sample was subsequently diluted with water (2 ml) and thoroughly mixed prior to HPLC analysis.

**Automatic clean-up and chromatography.** The automated HPLC system (from Anachem, Luton, UK) consisted of a Gilson 307 isocratic pump, a Gilson ASPEC (an automatic solid-phase extraction system fitted with a Rheodyne 7010 injector and a Gilson 401 dilutor), and a Perkin-Elmer LC240 fluorescence detector (Beaconsfield, UK). The detector, the Gilson pump and the ASPEC were linked via a Gilson 506B system interface module to an IBM Model 30 personal computer. The use of Gilson 712 HPLC software allowed both collection of data and the control of the interfaced equipment.

The sequence of operations for the automated clean-up of samples using the ASPEC were as follows:

- (a) Affinity column conditioned with PBS (20 ml) at 3.0 ml/min.
- (b) Column loaded with sample extract (50 ml) at 3.0 ml/min.
- (c) Column washed with water (10 ml) at 6 ml/min.
- (d) Column dried with air (2 ml).
- (e) Column eluted with methanol (0.5 ml) at 0.36 ml/min.
- (f) Waiting period of 1 min.
- (g) Column eluted with methanol (1.5 ml) at 0.36 ml/min.
- (h) Remaining solvent recovered from column with air (3 ml).
- (i) Total methanol eluate mixed by bubbling air (3 ml).
- (j) Eluate (1.0 ml) transferred to a vial (2.0 ml).
- (k) The remaining aliquot (1 ml) of methanol eluate diluted with 2% (v/v) acetic acid (2 ml) followed by further air mixing (3 ml).

- (l) Automated injection (400  $\mu$ l) of the diluted eluate onto HPLC by partial loop fill.

#### *High-performance liquid chromatography*

A Spherisorb ODS2 analytical column (5  $\mu$ m particle size, 250  $\times$  4.6 mm I.D.) was employed (held at 35°C) and this was protected by an inline filter (A315, Upchurch) fitted with a 2- $\mu$ m frit (A101, Upchurch) and a C<sub>18</sub> guard column (C752, Upchurch). The mobile phase of acetonitrile–water–acetic acid (99:99:2) was pumped at 1.0 ml/min. Detection was using a Perkin-Elmer LC240 fluorescence detector operated at an excitation wavelength of 333 nm and an emission wavelength of 477 nm.

#### RESULTS AND DISCUSSION

Although a single analytical procedure is desirable that can be used for both cereals and animal products, the simplified procedure that worked well for cereals using PBS–methanol extraction and then direct application of the extract onto the affinity column, gave low recoveries (*ca.* 50%) for animal products and problems with co-extractives. To increase recoveries for animal products it was necessary to use an acidified chloroform extraction solvent. To maintain solvent compatibility with the antibody and to remove some co-extractives an additional back-extraction step was needed prior to loading the extract onto the affinity column. The affinity column clean-up (manual or automated) and HPLC analysis was thereafter identical for cereal or animal product samples.

For the automated clean-up procedure the two-stage elution (stages e–g) increased the recovery of ochratoxin A from the immunoaffinity columns as the initial application of methanol permeated the gel, breaking the antibody–antigen binding, prior to final elution with the larger volume of methanol. Stage h purged all the remaining methanol from the column maintaining a quantitative recovery. Immunoaffinity columns were only used once before disposal although at least in theory multiple-use should be possible. Stage j in the sequence of operations for the ASPEC was introduced for two purposes. Firstly it minimised the amount of 2% acetic acid required in stage k and secondly it provided a spare portion of sample that could be kept as a reference to be analysed on a different instrument or at

a later date. This is of particular importance if a confirmation step such as the formation of the methyl ester is required. To avoid sample concentration by evaporation prior to HPLC, which can be time consuming and result in loss of analyte, the methanol eluate from the affinity column was diluted so that the aqueous composition of the solvent was approximately 20% greater than that of the HPLC mobile phase. This allowed a relatively large volume (400  $\mu$ l) to be injected onto the HPLC without loss of column performance.

For the fluorescence detection of ochratoxin A the emission wavelength was optimised by obtaining a spectrum of a solution in HPLC mobile phase. At an excitation wavelength of 333 nm the maximum was found to be at 477 nm, which gave a 25-fold increase in sensitivity compared with a wavelength of 420 nm which has been frequently employed in other published methods.

Performance data for the use of affinity columns were obtained using the automated system. For a wheat sample that had been shown to contain <0.2  $\mu$ g/kg ochratoxin A, spiked at 10  $\mu$ g/kg the recovery averaged 74% ( $n = 8$ ) with a relative standard deviation (R.S.D.) of 3.5%. As ochratoxin A in PBS gave a quantitative recovery from the affinity column it can only be assumed that recovery losses are occurring from the matrix possibly due to binding effects. For samples of pigs' kidney and of blood sausages again found to contain <0.2  $\mu$ g/kg ochratoxin A in both, spiked at 10  $\mu$ g/kg, the recoveries averaged 79% ( $n = 8$ ) and 74% ( $n = 8$ ) with R.S.D. of 3.0 and 6.0%, respectively. A naturally contaminated sample of pigs' kidney and blood sausages was not available but for a naturally con-

taminated sample of wheat containing 13.7  $\mu$ g/kg ochratoxin A a R.S.D. of 1.3% was obtained on repeated analysis ( $n = 8$ ). Ochratoxin A certified reference materials are not as yet available so it was not possible to demonstrate the accuracy of the method on naturally contaminated samples. The limit of detection of the method was found to be 0.2  $\mu$ g/kg for both cereal and animal products, which was comparable to most other published methods and sufficiently low for the needs of food surveillance.

The major advantage of use of immunoaffinity column clean-up for mycotoxin analysis is the ability to apply essentially the same procedure to differing matrices, to achieve high recoveries and to produce chromatograms essentially free of interferences. Typical chromatograms are shown in Fig. 1 for cereals and for pigs kidneys illustrating the high specificity of the clean-up and thus the ability to achieve low limits of detection. Animal products such as pigs' kidney and black pudding can frequently be difficult matrices to analyse by conventional methods because of co-extractives which are essentially removed with the affinity column procedure. To date in surveillance work several hundred retail samples of wheat, barley, maize, bran products, wholemeal breakfast cereals, pigs' kidneys and black pudding have been analysed using the immunoaffinity method without experiencing any matrix problems or interferences. The reliability of the automated system has been demonstrated and significant time-savings have been achieved compared with manual approaches.

The full flexibility of the automated ASPEC system can be utilised to allow for concurrent analysis

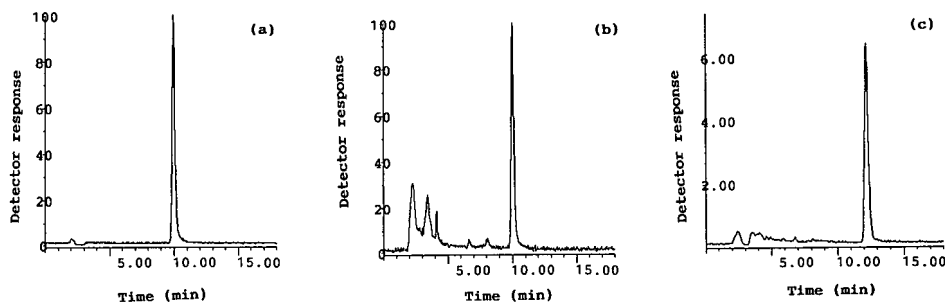


Fig. 1. HPLC chromatograms illustrating the analysis of ochratoxin A. Peaks for ochratoxin A normalised to full scale deflection in each chromatogram. (a) Standard equivalent to 20  $\mu$ g/kg; (b) naturally contaminated wheat sample containing 13.7  $\mu$ g/kg; (c) pigs' kidney spiked with 10  $\mu$ g/kg ochratoxin A.

of samples for either aflatoxins or ochratoxin A. This has been achieved by modification of the system to incorporate column switching between an ODS2 column for ochratoxin analysis and an ODS1 column (with post-column derivatization) for aflatoxin analysis. By the use of the appropriate affinity columns and application of the differing sample extraction procedures the ASPEC can be utilised to carry out both mycotoxin analyses in an unattended mode of operation. For the future it is anticipated that automated multi-mycotoxin analyses will be possible as the range of affinity columns is extended further and through the development of multi-analyte columns using mixed antibodies.

#### ACKNOWLEDGEMENTS

The authors gratefully acknowledge the assistance of P. Arnold (Biocode Ltd.) for the provision of ochratoxin A affinity columns and M. Lindsay (Anachem Ltd.) for modification of the software for the ASPEC system.

#### REFERENCES

- 1 H. P. van Egmond, in M. Castegnaro, R. Plestina, G. Dirheimer, I. N. Chernozemsky and H. Bartsch (Editors), *Mycotoxins, Endemic Nephropathy and Urinary Tract Tumors*, International Agency for Research on Cancer (IARC), Lyon, pp. 57-70.
- 2 World Health Organisation, *Environmental Health Criteria 105: Selected Mycotoxins: Ochratoxins, Trichothecenes, Ergot*, WHO, Geneva, 1990, pp. 30-32.
- 3 S. C. Lee and F. S. Chu, *J. Assoc. Off. Anal. Chem.*, 67 (1984) 45.
- 4 M. R. A. Morgan, R. McNerney and H. W.-S. Chan, *J. Assoc. Off. Anal. Chem.*, 66 (1983) 1481.
- 5 M. Sharman and J. Gilbert, *J. Chromatogr.*, 543 (1991) 220.
- 6 A. L. Patey, M. Sharman and J. Gilbert, *Food Add. Contam.*, 7 (1990) 515.
- 7 M. Sharman, A. L. Patey, D. A. Bloomfield and J. Gilbert, *Food Add. Contam.*, 8 (1991) 299.
- 8 A. A. G. Candlish, C. A. Haynes and W. H. Stimson, *Int. J. Food Sci. Technol.*, 23 (1988) 479.
- 9 D. N. Mortimer, J. Gilbert and M. J. Shephard, *J. Chromatogr.*, 407 (1987) 393.
- 10 M. Sharman, A. L. Patey and J. Gilbert, *J. Chromatogr.*, 474 (1989) 457.

## Short Communication

# Automation of a clean-up procedure for determination of trichothecenes in cereals using a charcoal–alumina column

W. Langseth and P.-E. Clasen

Department of Pharmacology and Toxicology, National Veterinary Institute/Norwegian College of Veterinary Medicine, P.O. Box 8146 Dep., N-0033 Oslo 1 (Norway)

(First received November 15th, 1991; revised manuscript received February 24th, 1992)

### ABSTRACT

Automation of the clean-up procedure for trichothecenes on a charcoal–alumina column is described. Standard high-performance liquid chromatographic equipment was used for the clean-up step. An acetonitrile–water (84 + 16, v/v) extract of the sample was cleaned up on a column packed with charcoal–alumina–Celite, which was washed with acetonitrile between each sample. The eluates were collected directly in reaction vials and evaporated to dryness. The residual water was removed azeotropically with benzene. The sample was derivatized with 1-(trimethylsilyl)imidazole and analysed by capillary gas chromatography with electron-capture detection.

### INTRODUCTION

Mycotoxins, being secondary metabolites of fungi, have caused many well-documented cases of toxicosis following consumption of fungus-contaminated cereals [1–4]. Probably the trichothecenes are the most important group produced by the genus *Fusarium*. According to studies in many countries, deoxynivalenol is the toxin that most often occurs, but other trichothecenes have also frequently been reported [1–5]. An analytical method capable of screening large numbers of samples is of great importance when cereals and feed products are to be controlled and when factors that affect the growth

of *Fusarium spp.* and toxin formation are to be established.

Thin-layer (TLC) [6,7], high-performance liquid (HPLC) [8–10] and supercritical fluid chromatography (SFC) [11] have been used for the determination of trichothecenes, but gas chromatography (GC) with electron-capture (EC) or mass spectrometric (MS) detection are probably the methods that are most commonly used [12–14].

Several clean-up procedures have been published. Most of them include a liquid–liquid extraction step and purification of the extract on a Florisil or silica gel column and different evaporation steps [15–18]. These procedures are time consuming and difficult to automate. Romer *et al.* [19] presented a clean-up method using a charcoal–alumina column. The method was later modified [7–8] and the columns can today be purchased from Romers Labs. [20]. The column can be used for most of the group A and B trichothecenes. The sample is extracted with

Correspondence to: Dr. W. Langseth, Department of Pharmacology and Toxicology, National Veterinary Institute/Norwegian College of Veterinary Medicine, P.O. Box 8146 Dep., N-0033 Oslo 1, Norway.

acetonitrile–water, the extract is transferred directly to a charcoal–alumina column, and the trichothecenes are eluted with the same solvent mixture. The column has to be connected to a vacuum system to obtain sufficient flow through the column. The first vacuum systems described were for only one column [7,8,20], but subsequently manifolds for the simultaneous connection of up to six columns have been used in many laboratories. The large elution volumes, however, restrict the number of columns that can be connected to the manifold.

The aim of this work was to automate the clean-up procedure of trichothecenes using the charcoal–alumina column so that large series of samples can be run simultaneously.

## EXPERIMENTAL

### *Reagents and apparatus*

Trichothecene standard solution was obtained from Romers Labs. and contained 100 µg/ml each of deoxynivalenol (DON), fusarenon-X (F-X), niv-alenol (NIV), neosolaniol, diacetoxyscirpenol (DAS), T-2 and HT-2 in acetonitrile. 3-Acetyl-DON was purchased from Sigma. A stock solution which contained 2 µg/ml of each compound in acetonitrile was prepared.

1-(Trimethylsilyl)imidazole (TMSI) (Fluka) was used as a derivatization agent. Acetonitrile was of HPLC grade and hexane was of Distol grade, both obtained from Fisons.

The samples were extracted with a universal flask shaking machine from Edmund Bühler, Type SM 2.5.

The equipment used for the clean-up procedure consisted of a Perkin-Elmer Series 10 pump, one of the pumps on a Perkin-Elmer Series 2 delivery system and a Perkin-Elmer ISS-101 autoinjector equipped with a 2-ml preparative loop. A Rheodyne six-port valve (Model 7000) and a Gilson fraction collector (Model 203) were controlled by an Omega-2 (Perkin-Elmer) data system via a time relay. The clean-up column was a Chromguard cartridge (50 mm × 3 mm I.D.) with a snap-open–snap-shut holder (Chrompack). The cartridge was packed with Darco G-60 activated carbon, 100–325 mesh (Aldrich), neutral aluminium oxide 90 active, 0.063–0.200 mm (Merck), and Celite, reagent grade (Supelco), in the proportions 2.33:1.67:1 (w/w/w).

GC analysis was performed on a Varian Model 3400 gas chromatograph equipped with a <sup>63</sup>Ni electron-capture detector, a splitless injector and a Model 8100 autosampler.

All chromatograms were recorded on a Varian Star data system. The capillary GC fused-silica column was 30 m × 0.32 mm I.D., coated with 0.25-µm SPB-1. The carrier gas was helium at 9 p.s.i., and the make-up gas was nitrogen. The temperatures of the injector and detector were 280 and 300°C, respectively. The oven temperature was 60°C for 2 min, then increased to 210°C at 30°C/min, to 225°C at 1°C/min and to 250°C at 20°C/min, the final temperature being maintained for 20 min.

### *Procedure*

A 25-g amount of the ground sample was extracted for 1 h with 125 ml of acetonitrile–water (84:16, v/v). Some of the extract was filtered through a folded filter-paper and 0.5 ml of the extract was injected into an HPLC system, shown in Fig. 1. The trichothecenes were eluted for 5 min with acetonitrile–water (84:16, v/v) before the column was washed for 5 min with acetonitrile. The column was then conditioned for about 2 min with acetonitrile–water before a new sample was injected. The flow-rate of both pumps was 1.0 ml/min. The eluates were collected directly in 5-ml reaction vials, which were subsequently placed in a heating module (60°C), and the eluates were evaporated to dryness under a stream of nitrogen. A 1-ml volume of benzene was added to each vial and mixed on a Whirlimixer for 30 s, and thereafter the mixture was again evaporated to dryness. The vials were sealed with screw-caps until room temperature was obtained. The residue was dissolved in 100 µl of TMSI. The vials were sealed and mixed on a Whirlimixer before being heated at 80°C for 30 min for derivatization. A 500-µl volume of hexane was added and mixed on a Whirlimixer. The hexane phase was extracted with 1 ml of water, which was discarded, and then dried with sodium sulphate. A 0.5-µl volume of the extract was injected into the GC system.

## RESULTS AND DISCUSSION

Romer [20] found that 50 ml of elution solvent, in addition to 5–10 ml of the sample extract, was required to obtain optimum recovery of the seven

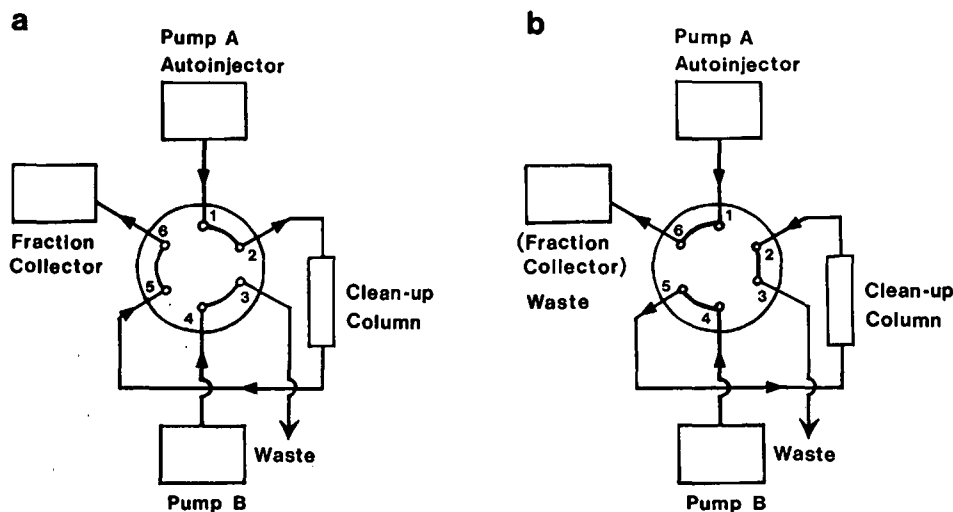


Fig. 1. Flow diagram of the Rheodyne six-port valve. (a) Direction of flow during collection of the eluent; (b) direction of flow during washing of the column.

most commonly analysed trichothecenes with a  $21 \times 19$  mm I.D. charcoal-alumina column, while 22.5 ml were used in our laboratory with a  $40 \times 0.9$  mm I.D. column. In both instances the eluent had to be evaporated to dryness in a rotary evaporator. This operation is very time consuming, as only one flask can be run at the same time. Loss of sample may also occur in connection with evaporation, because trichothecenes are easily adsorbed on the glass walls [15].

The total elution volume can be reduced to about 10 ml by using the same cartridges as commonly used for 1-ml solid-phase extraction columns ( $5 \times 0.55$  mm I.D.). By using HPLC clean-up columns, such as the Chromguard cartridge, the elution volume can be reduced to 5 ml or less, which is the volume of the reaction vials normally used for derivatization. No extra evaporation step or quantitative transfer of extract from one vial to another is then needed.

Reducing the column diameter results in a lower capacity of the column. The detection limit of trichothecenes measured by GC is, however, mostly limited by other impurities in the extract injected. Therefore, although only 0.5 ml of sample extract was injected in this procedure, which corresponds to 0.1 g of the sample, a detection limit of about 20

$\mu\text{g}/\text{kg}$  was obtained, which is satisfactory for most purposes.

Replacement of the vacuum manifold with an HPLC pump or similar equipment renders automation of the procedure possible. A more uniform flow through the column is also ensured. The pressure above the column was between 100 and 150 psi with a flow-rate of 1 ml/min. Standard HPLC equipment was used in this work for the clean-up step, except that the normal injector loop was replaced with a larger preparative loop. The fraction collector was also slightly modified so that all steps could be controlled by the data system via a time relay. Special holes for the reaction vials were also made in the rack.

The clean-up column cartridge was dry-packed with carbon, alumina and Celite, which were mixed well in the correct proportions before use. The trichothecenes were eluted with acetonitrile–water (84 + 16, v/v). By washing with acetonitrile between each injection, one cartridge could be used for about ten samples before it had to be repacked. Some of the contaminants remained on the column and restricted the lifetime of the cartridge. By using a cartridge column with a snap-open–snap-shut holder, a new cartridge can be inserted within 1 min. Much time is saved by reducing the time-consuming job of packing columns.

Nitrogen was used for evaporation to prevent decomposition. It is important that no water remains in the vials to ensure complete derivatization. Omission of the addition of benzene sometimes caused poor recoveries, even when the residue appeared dry, probably because water was occluded in the residue. Benzene forms an azeotrope with water, and thereby ensures the removal of most of the water. The vials were sealed during cooling to avoid adsorption of water. Addition of as much as 100  $\mu$ l of TMSI was necessary to ensure complete derivatization. The charcoal–alumina column does not remove many of the more polar contaminants. The washing of the hexane phase at the end of the procedure does, however, ensure the removal of many of these components [21].

At least two recovery tests were carried out for the group B trichothecenes for each set of samples analysed. An 80- or 160-ng amount of each of the trichothecenes was added to an 1-ml aliquot of sample extract. The same clean-up and GC method was used for these extracts as for the others. The recovery for 50 spiked samples was 94% ( $\sigma_{n-1} = 11$ ) for DON, F-X and NIV and 81% ( $\sigma_{n-1} = 20$ ) for 3-acetyl-DON. About 500 samples have been analysed by the method described.

## CONCLUSIONS

An automated clean-up procedure capable of screening a large number of samples for trichothecenes has been developed. A two- to threefold increase in the number of samples analysed was observed in our laboratory when the traditional clean-up method with 9 mm I.D. columns and vacuum manifold was replaced with the proposed method.

## REFERENCES

- 1 Y. Ueno, *Trichothecenes—Chemical, Biological and Toxicological Aspects (Developments in Food Science, Vol. 4)*, Elsevier, Amsterdam 1983.
- 2 A. Z. Joffe, *Fusarium Species, Their Biology and Toxicology*, Wiley, New York, 1986.
- 3 J. Chelkowski, *Fusarium, Mycotoxins, Taxonomy and Pathogenicity (Topics in Secondary Metabolites, Vol. 2)*, Elsevier, Amsterdam, 1989.
- 4 H. Kurata and Y. Ueno, *Toxigenic Fungi—Their Toxins and Health Hazard*, Elsevier, Amsterdam, 1984.
- 5 L. Sundheim, S. Nagayama, O. Kawamura, T. Tanaka, G. Brodal and Y. Ueno, *Norw. J. Agric. Sci.*, 2 (1988) 49.
- 6 H. Kamimura, M. Nishijima, K. Yasuda, K. Saito, A. Ibe, T. Nagayama, A. Ushiyama and Y. Naoi, *J. Assoc. Off. Anal. Chem.*, 64 (1981) 1067.
- 7 M. W. Trucksess, S. Nesheim and R. M. Eppley, *J. Assoc. Off. Anal. Chem.*, 67 (1984) 40.
- 8 H. L. Chang, J. W. DeVries, P. A. Larson and H. H. Patel, *J. Assoc. Off. Anal. Chem.*, 67 (1984) 52.
- 9 V. L. Sylvia, T. D. Phillips, B. A. Clement, J. L. Green, L. F. Kubena and N. D. Heidelbaugh, *J. Chromatogr.*, 362 (1986) 79.
- 10 R. D. Voyksner, W. M. Hagler and S. P. Swanson, *J. Chromatogr.*, 394 (1987) 183.
- 11 R. D. Smith, H.R. Udseth and B. W. Wright, *J. Chromatogr. Sci.*, 23 (1985) 192.
- 12 P. M. Scott, P. Y. Lau and S. R. Kanhere, *J. Assoc. Off. Anal. Chem.*, 64 (1981) 1364.
- 13 C. E. Kientz and A. Verweij, *J. Chromatogr.*, 355 (1986) 229.
- 14 R. J. Cole, *Modern Methods in the Analysis and Structural Elucidation of Mycotoxins*, Academic Press, New York, 1986.
- 15 T. Tanaka and Y. Ueno, *International IUPAC Symposium on Mycotoxins and Phycotoxins, Tokyo, Japan, 16–19th August 1988*, Elsevier, Amsterdam, 1989, p. 51.
- 16 T. Tanaka, A. Hasegawa, Y. Matsuki, K. Ishii and Y. Ueno, *Food Addit. Contam.*, 2 (1985) 125.
- 17 E. Lindfors, National Veterinary Institute, Finland, personal communication.
- 18 P. M. Scott, S. R. Kanhere and E. J. Tarter, *J. Assoc. Off. Anal. Chem.*, 69 (1986) 889.
- 19 T. R. Romer, D. E. Greaves and G. E. Gibson, paper presented at the AOAC 6th Annual Spring Workshop, May 12–14, 1981, Ottawa, Ontario, Canada.
- 20 T. R. Romer, *J. Assoc. Off. Anal. Chem.*, 69 (1986) 699.
- 21 A. F. Rizzo, L. Saari and E. Lindfors, *J. Chromatogr.*, 368 (1986) 381.

## Short Communication

---

# Gas chromatographic–mass spectrometric detection of trace amounts of organic compounds in the intravenous solution Infusio Darrowi

Jan Lesko and Tibor Jakubik

Laboratory for Mass Spectrometry, Faculty of Chemical Technology, Slovak Technical University, Radlinskeho 9, 812 37 Bratislava (Czechoslovakia)

Anna Michalkova

State Institute for Drugs Control, Kvetna 11, 825 08 Bratislava (Czechoslovakia)

(First received November 4th, 1991; revised manuscript received March 3rd, 1992)

---

### ABSTRACT

A gas chromatographic–mass spectrometric procedure was employed to confirm the presence of trace amounts of organic compounds in the intravenous solution Infusio Darrowi. Organic contaminants in the solution analysed were concentrated by microextraction with *n*-pentane. The main compounds detected were 2,6-di-*tert.*-butyl-4-methylphenol, 2,6-di-*tert.*-butyl-4-ethylphenol, 2,6-di-*tert.*-butyl-4-methoxyphenol, benzothiazole, isomeric C<sub>9</sub> alkyl phenols and di(*n*-butyl) phthalate. These impurities were leached from rubber stoppers during their sterilization into the intravenous solution at levels ranging *ca.* from  $5 \cdot 10^{-6}$  to  $5 \cdot 10^{-8}$  g/l.

---

### INTRODUCTION

Plastics are widely used in the manufacture of drugs packaging and medical devices. The most common plasticizers are phthalate esters, which may migrate from plastic devices and containers into contacting media. The leachability of plasticizers [particularly of di-(2-ethylhexyl) phthalate] from plastic devices into blood, blood products, haemo-

dialysis fluids and intravenous solutions has been extensively studied, using gas chromatography, gas chromatography–mass spectrometry (GC–MS) [1–10] and high-performance liquid chromatography [11].

The objective of this study was to examine the sources of contamination of the intravenous solution Infusio Darrowi, which had been prepared under standard conditions in a laboratory. The impurities in this intravenous solution and in the chemicals used for its preparation were determined by GC–MS analyses of the particular *n*-pentane extracts.

---

Correspondence to: Dr. J. Lesko, Laboratory for Mass Spectrometry, Faculty of Chemical Technology, Slovak Technical University, Radlinskeho 9, 812 37 Bratislava, Czechoslovakia.

## EXPERIMENTAL

*Chemicals*

The following chemicals were used: *n*-pentane of spectroscopic grade (Merck, Darmstadt, Germany), 1-chlorooctane (Aldrich-Chemie, Steinheim, Germany), sodium chloride and potassium chloride of the quality complying with the requirements of the present Czechoslovak Pharmacopoeia (Lachema, Brno, Czechoslovakia) and 1 *M* sodium lactate injection (Biotika, Slovenska Lupca, Czechoslovakia).

The final product Infusio Darrowi (sodium chloride 4.00 g, potassium chloride 2.67 g, 1 *M* sodium lactate injection 53.00 ml, redistilled water to 1000.00 ml), was prepared in the Microbiological Department of the District Laboratory for Drugs Control of Western Slovakia (Bratislava, Czechoslovakia) in accordance with the requirements of the Czechoslovak Pharmacopoeia.

*Extraction procedure*

In this study, experience with microextraction [12–15] for the concentration of trace impurities was used. Organic contaminants in the samples were concentrated by a single-stage microextraction with *n*-pentane [12]. The sodium lactate injection and Infusio Darrowi prior to and after autoclaving (121°C for 20 min) were extracted directly. Sodium chloride and potassium chloride were extracted from their solutions in redistilled water (20 g/l). The solutions were cooled to 5°C prior to the extraction, the internal standard 1-chlorooctane ( $10^{-5}$  g/l) was added and the solutions were extracted with *n*-pentane (0.5 ml/l). An aliquot of the extract was used directly for GC–MS analysis.

*GC–MS conditions*

GC–MS measurements were made with a Kratos Analytical (Manchester, UK) MS 25 RFA mass spectrometer equipped with a Carlo Erba (Milan, Italy) Model 5160 gas chromatograph. A Chrom-pack (Middelburg, Netherland) fused-silica capillary GC column (25 m × 0.32 mm I.D.) with a CP-Sil 5 CB coating (0.12 μm) was used. Helium was used as the carrier gas. The injector temperature was 250°C. The GC oven temperature was programmed as follows: 1 min at 40°C, increased at 4°C/min to 100°C, then at 10°C/min to 240°C. For

MS, electron impact ionization was used, the source temperature was 200°C, the electron energy was 70 eV and the scan speed was 0.6 s per decade.

## RESULTS AND DISCUSSION

GC separations of organic impurities in Infusio Darrowi prior to and after sterilization are shown in Fig. 1a and b, respectively. Organic compounds were identified according to their mass spectra by a library search. A comparison of Fig. 1a and b reveals that some of these compounds were detected only in the sterilized solution or that their concentration was increased on sterilization.

As the intravenous solutions are sterilized in glass bottles, the only possible source of contamination with leached organic compounds during the sterilization procedure is the black rubber stoppers. Derivatives of di-*tert*-butylphenols are known to be used as antioxidants and phthalate esters as plasticizers in the chemical industry. The source of benzothiazole (Fig. 2a) is probably 2-mercaptobenzothiazole, widely applied as a rubber accelerator. We did not succeed in identifying the compound with scan number 830 (Fig. 1b, mass spectrum in Fig. 2b). The commercially available sodium lactate injection used contained the same organic contaminants as the final Infusio Darrowi, but their levels were lower.

The main organic impurities in the potassium chloride samples, detected later also in the final intravenous solution, were C<sub>9</sub>-alkylphenols. Their content varied from batch to batch and obviously depended on the packaging material and the storage of the product (in some batches phenol and cresol were also found).

The amount of organic contaminants in the sodium chloride samples was negligible. Except for di(*n*-butyl) phthalate, no other impurities were detected. Traces of di(*n*-butyl)phthalate were the only contamination found in the extractant *n*-pentane and the redistilled water, used for the preparation of all the solutions analysed.

The semi-quantitative determination of levels of organic impurities was based on calculations using the ratio of the peak areas of these compounds to that of the internal standard. The concentrations of organic contaminants in the final intravenous solution determined this way ranged from  $5 \cdot 10^{-6}$  to  $5 \cdot 10^{-8}$  g/l.

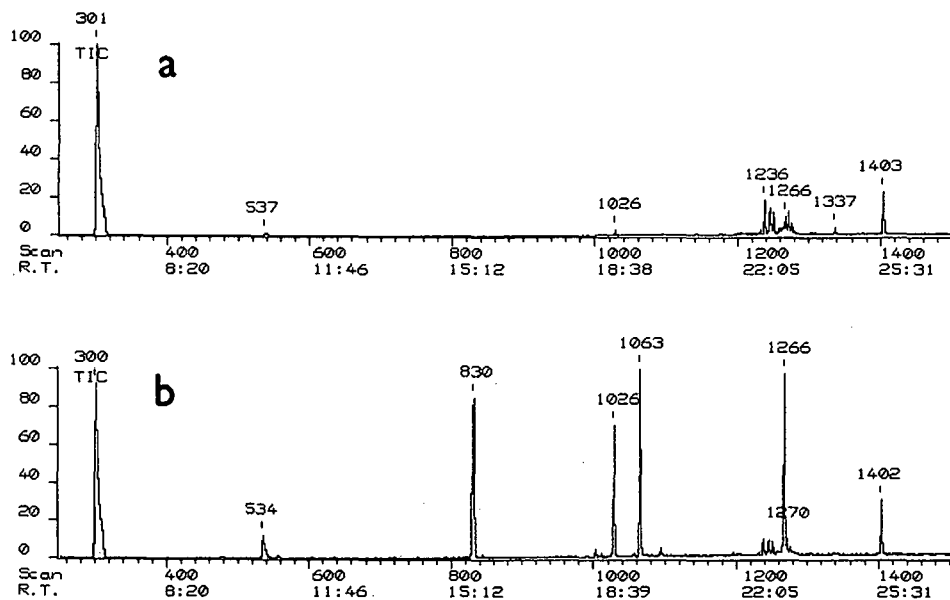


Fig. 1. Chromatogram of the *n*-pentane extract of the intravenous solution Infusio Darrowi (a) prior to and (b) after sterilization. Scan numbers: (a) 301 = 1-chlorooctane (internal standard), 537 = benzothiazole, 1026 = 2,6-di-*tert*-butyl-4-methoxyphenol, 1236–1259 = isomeric C<sub>9</sub>-alkylphenols, 1403 = di(*n*-butyl) phthalate; (b) 300 = 1-chlorooctane (internal standard), 534 = benzothiazole, 830 = unidentified, 1026 = 2,6-di-*tert*-butyl-4-methoxyphenol, 1063 = 2,6-di-*tert*-butyl-4-methylphenol, 1237–1244 = isomeric C<sub>9</sub>-alkylphenols, 1266 = 2,6-di-*tert*-butyl-4-ethylphenol, 1402 = di(*n*-butyl) phthalate. R.T. = Retention time in min:s.

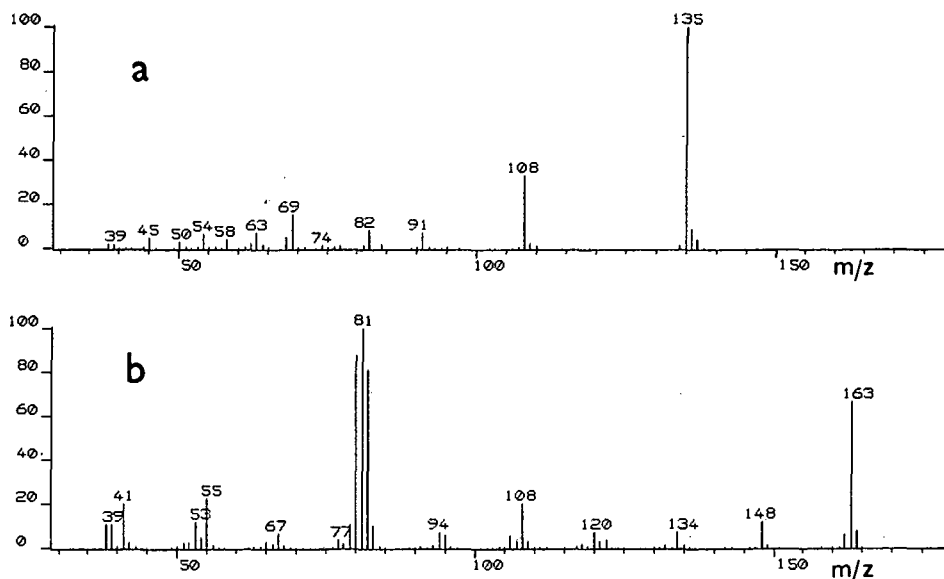


Fig. 2. Electron impact mass spectra obtained by GC–MS analysis of a Infusio Darrowi sample after sterilization. (a) Scan 534, benzothiazole; (b) scan 830, unidentified compound.

## CONCLUSIONS

A simple and rapid method was developed for the preconcentration and identification of organic contaminants in the intravenous solution Infusio Darrowi and in chemicals used for its preparation. The microextraction and consecutive GC–MS analysis can be employed as a sensitive and reliable control method for the detection of trace amounts of organic impurities. Rubber stoppers proved to be the main source of contamination with organic compounds leached into intravenous solutions during their sterilization.

## REFERENCES

- 1 L. S. Hillman, S. L. Goodwin and W. R. Sherman, *J. Med.*, 292 (1975) 381.
- 2 N. P. H. Ching, G. N. Jham, Ch. Subbarayan, D. V. Bowen, A. L. C. Smit, Jr., C. E. Grossi, R. G. Hicks, F. H. Field and T. F. Nealon, Jr., *J. Chromatogr.*, 222 (1981) 171.
- 3 A. Arbin, S. Jacobsson, K. Hänninen, A. Hagman and J. Östelius, *Int. J. Pharm.*, 28 (1986) 211.
- 4 K. Ono, R. Tatsukawa and T. Wakimoto, *J. Am. Med. Assoc.*, 234 (1975) 948.
- 5 P. O. Sjöberg, U. G. Bodesson, E. G. Sedin and J. P. Gustafsson, *Transfusion*, 25 (1985) 424.
- 6 T. P. Gibson, W. A. Briggs and B. J. Boone, *J. Lab. Clin. Med.*, (1976) 519.
- 7 L. M. Lewis, T. W. Flechtner, J. Kerkay, K. H. Pearson and S. Nakamoto, *Clin. Chem.*, 24 (1978) 741.
- 8 L. Nässberger, A. Arbin and J. Östelius, *Nephron*, 45 (1987) 286.
- 9 B. Kakac, M. Sarsunova, Z. Perina, A. Michalkova, J. Hrivnak and H. Berankova, *Pharmazie*, 44 (1989) 31.
- 10 A. Arbin and J. Östelius, *J. Chromatogr.*, 193 (1980) 405.
- 11 R. S. Labow and M. Tocchi, *J. Toxicol. Environ. Health*, 19 (1986) 591.
- 12 J. Hrivnak, *Anal. Chem.*, 57 (1985) 2159.
- 13 D. A. J. Murray, *J. Chromatogr.*, 177 (1979) 135.
- 14 D. A. J. Murray and L. W. Lockhart, *J. Chromatogr.*, 212 (1981) 305.
- 15 J. Ilavsky, Thesis, Slovak Technical University, Bratislava, 1989.

## Short Communication

# Quantitation of *l*-epinephrine and determination of the *d*-/*l*-epinephrine enantiomer ratio in a pharmaceutical formulation by capillary electrophoresis

Teresa E. Peterson and David Trowbridge

Alcon Laboratories, Inc., 6201 South Freeway, Fort Worth, TX 76134-2099 (USA)

(First received January 17th, 1992; revised manuscript received April 1st, 1992)

### ABSTRACT

A procedure for the quantitation of *l*-epinephrine and the determination of the *d*-/*l*-epinephrine ratio in a pharmaceutical formulation containing *l*-epinephrine is described. The optical isomers of epinephrine were resolved by capillary electrophoresis with a buffer containing heptakis-(2,6-di-*o*-methyl)- $\beta$ -cyclodextrin. Quantitation was achieved with the use of an internal standard, *l*-pseudoephedrine. Results with and without internal standard correction illustrate the improved reproducibility possible with an internal standard.

### INTRODUCTION

There are very few reports in the literature which show that capillary electrophoresis can be used for quantitation in a formulated product [1–3]. This report describes the quantitation of *l*-epinephrine and the determination of the *d*-/*l*-epinephrine ratio in a pharmaceutical formulation. This formulation contains *l*-epinephrine and is a sterile ophthalmic solution for the control of simple glaucoma. An analytical method which can distinguish between *d*- and *l*-epinephrine is necessary to insure that minimal racemization occurs over time. Although there are a number of high-performance liquid chromatography procedures in the literature which can distinguish between both isomers of epinephrine, they

can involve a time-consuming derivatization step [4–6].

Cyclodextrins have been used in capillary isotachophoresis to resolve ephedrine alkaloid enantiomers [7]. Recently, Fanali [8] reported the optical isomer resolution of epinephrine and related compounds by capillary electrophoresis with a 10 mM Tris-H<sub>3</sub>PO<sub>4</sub>/18 mM heptakis-(2,6-di-*o*-methyl)- $\beta$ -cyclodextrin (Me- $\beta$ -CD) pH 2.4 buffer. These separations were performed with a coated capillary. In the procedure described here an uncoated fused-silica capillary was used to perform the separation and an internal standard was added to correct for the imprecise injection system of this instrument.

### EXPERIMENTAL

#### Chemicals

Orthophosphoric acid, hydrochloric acid and sodium hydroxide were obtained from J.T. Baker

Correspondence to: Dr. Teresa E. Peterson, R1-18, Alcon Laboratories, Inc., 6201 South Freeway, Fort Worth, TX, 76134-2099, USA.

(Phillipsburg, NJ, USA). Tris(hydroxymethyl)amino methane (Tris), *d*-/*l*-epinephrine, *l*-epinephrine, *l*-pseudoephedrine and Me- $\beta$ -CD were obtained from Sigma (St. Louis, MO, USA).

#### Apparatus

The experiments were performed with a Dionex CES system (Sunnyvale, CA, USA) equipped with a UV detector set at 206 nm (0.1 a.u.f.s.). Separations were performed in an unmodified fused-silica capillary (50 cm  $\times$  0.075 mm I.D., 45 cm to detector) Polymicro Technologies, Phoenix, AZ, USA). Samples were gravity injected for 10 s at 50 mm. The injection end was the anode (+). The applied voltage was 15 kV and the observed current was 30–40  $\mu$ A. Separations were achieved with a 10 mM Tris/18 mM Me- $\beta$ -CD buffer adjusted to pH 2.4 with concentrated H<sub>3</sub>PO<sub>4</sub>. Electropherograms were recorded with a Spectra-Physics Chrom-Jet integrator (San Jose, CA, USA).

#### Procedure

At the beginning of each day, and whenever the buffer solution was changed, the capillary was pressure rinsed two times for 180 s with 0.1 M H<sub>3</sub>PO<sub>4</sub> and two times with 0.5 M NaOH. Then the entire system (capillary, source and destination vials) was rinsed four times with purified water and five times with the buffer solution. These rinse cycles were performed automatically by the instrument. Once this procedure was complete, it was only necessary to rinse the entire system with buffer one time after each injection.

#### Solutions

All solutions were diluted to volume with 0.01 M HCl to prevent epinephrine from oxidizing. Standards were stable for up to one week. The *l*-epinephrine standard solutions contained 25 ppm *l*-epinephrine and 100 ppm *l*-pseudoephedrine as the internal standard. Standard curve solutions contained approximately 12.5, 25 and 37.5 ppm *l*-epinephrine with 100 ppm *l*-pseudoephedrine added as the internal standard. The vehicle standard solutions were prepared from a vehicle solution containing everything in the formulation except *l*-epinephrine. The vehicle standard solutions contained 0.0025% *l*-epinephrine, boric acid, ascorbic acid, acetylcysteine, 0.00005% benzalkonium chloride

and sodium carbonate (monohydrate) to adjust pH.

A *d*-epinephrine standard curve at 2, 5, 8 and 10% of the *l*-epinephrine assay concentration was prepared in duplicate by spiking an *l*-epinephrine standard with a *d*-/*l*-epinephrine standard. The solution had to be prepared this way because there was no *d*-epinephrine standard available. The *l*-epinephrine standard used to prepare this curve was contaminated with about 2% (area%) *d*-epinephrine so 2% was the lowest point on the curve.

The formulations containing *l*-epinephrine were prepared so that they contained 100 ppm *l*-pseudoephedrine and 25 ppm, *l*-epinephrine after dilution with 0.01 M HCl.

#### Calculations

The percentage of *l*-epinephrine in the sample solutions can be calculated by

$$l\text{-epinephrine (\%)} = 100 [(A_f/A_p)/(A_s/A_p)]C_s/C_f$$

where  $A_f$ ,  $A_s$  and  $A_p$  are the peak areas for *l*-epinephrine in the formulation, *l*-epinephrine in the standard and *l*-pseudoephedrine, respectively.  $C_s$  and  $C_f$  are the concentrations of *l*-epinephrine in the standard and formulation solutions, respectively.

The ratio percentage of *d*-epinephrine in the pharmaceutical formulation can be calculated by

$$d\text{-epinephrine (\%)} = \frac{0.945 A_d}{0.945 A_d + A_l} \cdot 100$$

where  $A_d$  and  $A_l$  are the peak areas for *d*- and *l*-epinephrine, respectively, and 0.945 is the peak area ratio (area% *l*/area% *d*) for a racemic mixture of *d*- and *l*-epinephrine. Fanali and Boček [1] showed that a correction factor must be introduced into the equation used to calculate the percentage *d*-epinephrine because the UV absorbance coefficients of *d*- and *l*-epinephrine may not be the same when cyclodextrin is present. The presence of cyclodextrin may shift the absorbance spectra of the complexes.

#### RESULTS AND DISCUSSION

Fig. 1 shows the electropherogram of a *d*-/*l*-epinephrine standard and a formulation solution containing the internal standard *l*-pseudoephedrine. The elution order of *d*- and *l*-epinephrine in Fig. 1 agrees with Fig. 2 of Fanali's paper [8].

This method was found to be reproducible and precise. Ten separate preparations of standard were prepared on two days. The standard solutions gave relative standard deviations (R.S.D.) of 1.4 and 1.8% with internal standard correction and 3.0 and 3.4% without internal standard correction. Ten separate preparations of vehicle standard gave a mean recovery of 99% with an R.S.D. of 2.6% with

internal standard correction and 101% with an R.S.D. of 6.7% without internal standard correction.

To show that the *l*-epinephrine response is linear in this concentration range, two standard curves and two vehicle standard curves ranging from 12.5 to 37.5 ppm *l*-epinephrine were prepared in duplicate. The results with and without internal standard correction are illustrated in Table I. The two standard and vehicle standard curves for *l*-epinephrine were linear and passed near the origin. The curves had better R.S.D. values with internal standard correction than without. The R.S.D. values ranged from 0.9 to 2.5% with internal standard correction and 1.8 to 8.1% without internal standard correction. The recovery of *l*-epinephrine from vehicle standard solutions, with internal standard correction, was 99 and 101% with R.S.D. values of 1.2 and 2.0%, respectively. Without internal standard correction, the recovery was 86 and 97% with R.S.D. values of 7.9 and 2.2%, respectively.

A *d*-epinephrine standard curve was prepared at 2, 5, 8 and 10% of the *l*-epinephrine assay concen-

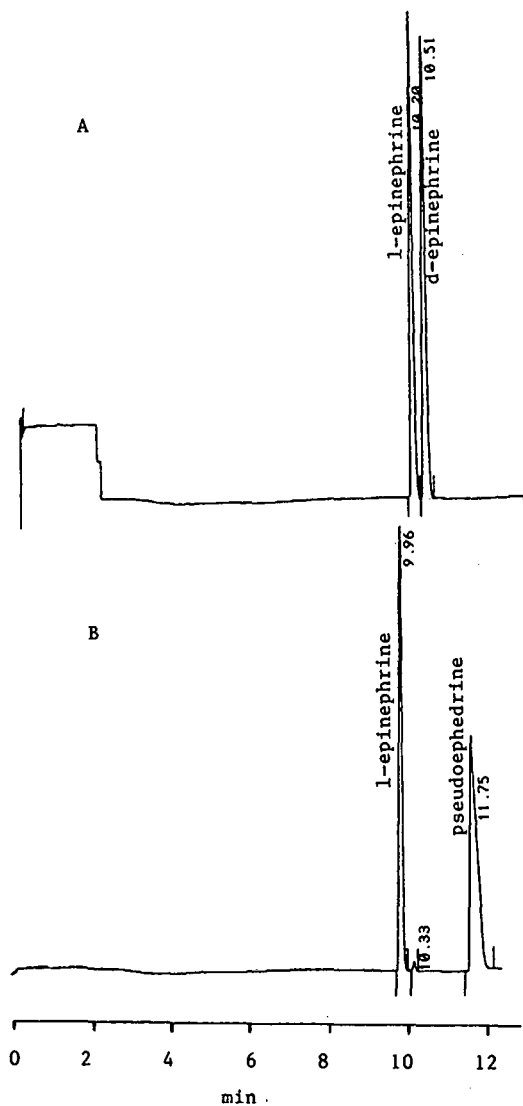


Fig. 1. Electropherograms of (A) 50 ppm *d*-/*l*-epinephrine standard and (B) pharmaceutical formulation diluted to 25 ppm *l*-epinephrine with pseudoephedrine added as an internal standard. See Table I for conditions.

TABLE I

LEAST SQUARES REGRESSION ANALYSIS FOR PLOTS OF RELATIVE PEAK AREA VS. CONCENTRATION FOR *l*-EPINEPHRINE

Conditions: buffer, 10 mM Tris-H<sub>3</sub>PO<sub>4</sub>/18 mM Me-β-CD pH 2.4; fused-silica capillary 50 cm × 0.075 mm (45 cm to detector); injection (at anode) by gravity 50 mm for 10 s; applied voltage, 15 kV; detection wavelength, 206 nm (0.1 a.u.f.s.).

<i>l</i> -Epinephrine	With internal standard		Without internal standard	
	1	2	1	2
Standard curve				
Correlation coefficient	0.9998	0.9998	0.9988	0.9985
R.S.D. (%)	2.5	0.9	2.7	2.7
Intercept (%) <sup>a</sup>	3.0	1.2	0.2	4.5
Vehicle standard curve				
Correlation coefficient	0.9988	0.9985	0.9474	0.9972
R.S.D. (%)	1.3	1.9	8.1	1.8
Intercept (%) <sup>a</sup>	0.2	4.5	9.4	2.2
Recovery (%), (R.S.D., %)	99,(1.2)	101,(2.0)	86,(7.9)	97,(2.2)

<sup>a</sup> The intercept calculation is based on the response of a 25 ppm *l*-epinephrine standard.

TABLE II

ANALYSIS OF THE PERCENTAGE OF *l*-EPINEPHRINE AND RATIO PERCENTAGE *d*-EPINEPHRINE IN A PHARMACEUTICAL FORMULATION

Conditions as in Table I. The specification for the percentage of *l*-epinephrine in this formulation is 90–115%. The formulation expires after 12 months.

Lot	Age of sample (months)	<i>n</i> <sup>a</sup>	<i>l</i> -epinephrine (%)		Ratio percentage <i>d</i> -Epinephrine
			Mean value	R.S.D. (%)	
A	5	3	110	1.4	1.4, 1.2, 1.4
B	10	3	102	1.1	1.3, 1.4, 1.4
C	29 <sup>b</sup>	3	84	2.5	2.3, 2.2, 2.2

<sup>a</sup> Number of replicate analyses.

<sup>b</sup> This sample past expiration of 12 months.

tration to show that small amounts of *d*-epinephrine could be determined in the presence of 25 ppm *l*-epinephrine and that the *d*-epinephrine response is linear in this region. The curve passed through the origin and had a correlation coefficient of 0.9998 with an R.S.D. of 1.3% after internal standard correction. Without internal standard correction the correlation coefficient was 0.9992 with an R.S.D. of 3.3%.

In all cases, internal standard correction improved the reproducibility of the method. The imprecise injection system of most commercial instruments warrants the use of an internal standard for quantitation. This method was used to assay three samples from three lots of the pharmaceutical formulation containing *l*-epinephrine. The results in Table II illustrate the reproducibility of the method. Lot C, which is 29 months old and 17 months past the expiration date, still shows very little *d*-epinephrine (2.3% or less) indicating very little racemization occurred in this formulation.

## ACKNOWLEDGEMENTS

We thank Dr. Karen B. Sentell at the University of Vermont for her many helpful comments on this manuscript. We also thank Alcon for providing us the time and facilities to complete this work.

## REFERENCES

- 1 S. Fanali and P. Boček, *Electrophoresis*, 11 (1990) 757–760.
- 2 H. Nishi, T. Fukuyama, M. Matsuo and S. Terabe, *J. Pharm. Sci.*, 79 (1990) 519–523.
- 3 P. Grossman, J. Colburn, H. Lauer, R. Nielson, R. Riggan, G. Sittampalam and E. Rickard, *Anal. Chem.*, 61 (1989) 1186–1194.
- 4 R. Kirchhoefer, G. Sullivan and J. Allgire, *J. Assoc. Off. Anal. Chem.*, 68 (1985) 163–165.
- 5 N. Nimura, Y. Kasahara and T. Kinoshita, *J. Chromatogr.*, 213 (1981) 327–330.
- 6 J. Allgire, E. Juenge, C. Damo, G. Sullivan and R. Kirchhoefer, *J. Chromatogr.*, 325 (1985) 249–254.
- 7 J. Snopek, I. Jelinek and E. Smolková-Keulemansová, *J. Chromatogr.*, 438 (1988) 211–218.
- 8 S. Fanali, *J. Chromatogr.*, 474 (1989) 441–446.

## Author Index

- Abian, J., see Hansen, Jr., E. B. 603(1992)157
- Aitzetmüller, K., Xin, Y., Werner, G. and Grönheim, M.  
High-performance liquid chromatographic investigations  
of stillingia oil 603(1992)165
- Akashi, M., see Yashima, E. 603(1992)111
- Andersson, K., see Wingren, C. 603(1992)73
- Antus, S., Bauer, R., Gottsegen, Á., Lotter, H., Seligmann, O.  
and Wagner, H.  
Enantiomeric separation of racemic isoflavanones and  
related compounds on (+)-poly(triphenylmethyl  
methacrylate)-coated silica gel 603(1992)133
- Araki, H., see Yoshioka, M. 603(1992)223
- Armstrong, D. W., see Lee, S. H. 603(1992)83
- Arthur, C. L., see Hawthorne, S. B. 603(1992)185
- Asakawa, N., see Mano, N. 603(1992)105
- Baines, P., see Chappell, I. 603(1992)49
- Barceló, D., see Durand, G. 603(1992)175
- Bauer, R., see Antus, S. 603(1992)133
- Berthod, A., see Lee, S. H. 603(1992)83
- Biely, P., see Markovič, O. 603(1992)243
- Bonnafofus, J.-C., see Desarnaud, F. 603(1992)95
- Brumley, W. C.  
Qualitative analysis of environmental samples for  
aromatic sulfonic acids by high-performance capillary  
electrophoresis 603(1992)267
- Carpenter, P. K., see Chappell, I. 603(1992)49
- Chappell, I., Baines, P. and Carpenter, P. K.  
Reduction in large-scale adsorption chromatography unit  
costs by use of 30-Å Sorbsil C30 silica 603(1992)49
- Chen, N., Zhang, Y. and Lu, P.  
The *S* index in the retention equation in reversed-phase  
high-performance liquid chromatography 603(1992)35
- Choinski, Jr., J. S., see Hansen, Jr., E. B. 603(1992)157
- Christensen, R. G., see Zhang, X. 603(1992)193
- Clasen, P.-E., see Langseth, W. 603(1992)290
- Cooper, W. T., see Hsu, C. W. 603(1992)63
- Dang, Q.-x., Sun, Z.-p. and Ling, D.-k.  
Separation of sulphonamides and determination of the  
active ingredients in tablets by micellar electrokinetic  
capillary chromatography 603(1992)259
- Desarnaud, F., Marie, J., Larguier, R., Lombard, C., Jard, S.  
and Bonnafofus, J.-C.  
Protein purification using combined streptavidin (or  
avidin)-Sepharose and thiopropyl-Sepharose affinity  
chromatography 603(1992)95
- De Vries, N. K., see Duchateau, A. L. L. 603(1992)151
- Do, D. D., see Nguyen, T. S. 603(1992)27
- Duchateau, A. L. L., Heemels, G. M. P., Maesen, L. W. and  
De Vries, N. K.  
Separation of benz[*f*]isoindole derivatives of amino acid  
and amino acid amide enantiomers on a  $\beta$ -cyclodextrin-  
bonded phase 603(1992)151
- Durand, G., Gille, P., Fraisse, D. and Barceló, D.  
Comparison of gas chromatographic-mass spectrometric  
methods for screening of chlorotriazine pesticides in soil  
603(1992)175
- Erlandsson, P., see Wännman, H. 603(1992)121
- Fraisse, D., see Durand, G. 603(1992)175
- Frey, D. D., Van de Water, R. and Zhang, B.  
Dispersion in stacked-membrane chromatography  
603(1992)43
- Getek, T. A., see Hansen, Jr., E. B. 603(1992)157
- Giddings, L. D., Olesik, S. V., Pekay, L. A. and Marti, E.  
Retention characteristics of high-molecular-weight  
compounds in capillary supercritical fluid  
chromatography 603(1992)205
- Gilbert, J., see Sharman, M. 603(1992)285
- Gille, P., see Durand, G. 603(1992)175
- Golshan-Shirazi, S. and Guiochon, G.  
Comparison of the various kinetic models of non-linear  
chromatography 603(1992)1
- Gottsegen, Á., see Antus, S. 603(1992)133
- Grönheim, M., see Aitzetmüller, K. 603(1992)165
- Guiochon, G., see Golshan-Shirazi, S. 603(1992)1
- Guiochon, G., see Ma, Z. 603(1992)13
- Hansen, Jr., E. B., Abian, J., Getek, T. A., Choinski, Jr., J. S.  
and Korfmacher, W. A.  
High-performance liquid chromatography-thermospray  
mass spectrometry of gibberellins 603(1992)157
- Hansson, U.-B., see Wingren, C. 603(1992)73
- Hawthorne, S. B., Miller, D. J., Pawliszyn, J. and Arthur, C.  
L.  
Solventless determination of caffeine in beverages using  
solid-phase microextraction with fused-silica fibers  
603(1992)185
- Heemels, G. M. P., see Duchateau, A. L. L. 603(1992)151
- Heinrichová, K., see Markovič, O. 603(1992)243
- Hsu, C. W. and Cooper, W. T.  
Solvent-stationary phase interactions in normal bonded  
phase high-performance liquid chromatographic columns.  
I. Investigation of system peaks in amino bonded phase  
columns 603(1992)63
- Hu, S.-G., see Nguyen, T. S. 603(1992)27
- Jakubik, T., see Lesko, J. 603(1992)294
- Jard, S., see Desarnaud, F. 603(1992)95
- Kiyohara, C., see Saitoh, K. 603(1992)231
- Korfmacher, W. A., see Hansen, Jr., E. B. 603(1992)157
- Korte, W. D.  
Determination of hydroxylamine in aqueous solutions of  
pyridinium aldoximes by high-performance liquid  
chromatography with UV and fluorometric detection  
603(1992)145
- Lam, S., see Zhang, Z. 603(1992)279
- Landers, J. P., Schuchard, M. D., Subramaniam, M.,  
Sismelich, T. P. and Spelsberg, T. C.  
High-performance capillary electrophoretic analysis of  
chloramphenicol acetyl transferase activity 603(1992)247
- Langseth, W. and Clasen, P.-E.  
Automation of a clean-up procedure for determination of  
trichothecenes in cereals using a charcoal-alumina  
column 603(1992)290

- Larguier, R., see Desarnaud, F. 603(1992)95
- Lee, S. H., Berthod, A. and Armstrong, D. W.  
Systematic study on the resolution of derivatized amino acids enantiomers on different cyclodextrin-bonded stationary phases 603(1992)83
- Lesko, J., Jakubik, T. and Michalkova, A.  
Gas chromatographic-mass spectrometric detection of trace amounts of organic compounds in the intravenous solution Infusio Darrowi 603(1992)294
- Ling, D.-k., see Dang, Q.-x. 603(1992)259
- Lombard, C., see Desarnaud, F. 603(1992)95
- Lotter, H., see Antus, S. 603(1992)133
- Lu, P., see Chen, N. 603(1992)35
- Ma, Z. and Guiochon, G.  
Comparison between the hodograph transform method and frontal chromatography for the measurement of binary competitive adsorption isotherms 603(1992)13
- MacDonald, S., see Sharman, M. 603(1992)285
- Maesen, L. W., see Duchateau, A. L. L. 603(1992)151
- Malikin, G., see Zhang, Z. 603(1992)279
- Manabe, M., see Naohara, J. 603(1992)139
- Mano, N., Oda, Y., Miwa, T., Asakawa, N., Yoshida, Y. and Sato, T.  
Conalbumin-conjugated silica gel, a new chiral stationary phase for high-performance liquid chromatography 603(1992)105
- Marie, J., see Desarnaud, F. 603(1992)95
- Markovič, O., Mislovičová, D., Biely, P. and Heinrichová, K.  
Chromogenic substrate for *endo*-polygalacturonase detection in gels 603(1992)243
- Marti, E., see Giddings, L. D. 603(1992)205
- Martire, D. E., see Zhang, X. 603(1992)193
- Michalkova, A., see Lesko, J. 603(1992)294
- Miller, D. J., see Hawthorne, S. B. 603(1992)185
- Mislovičová, D., see Markovič, O. 603(1992)243
- Miwa, T., see Mano, N. 603(1992)105
- Miyauchi, N., see Yashima, E. 603(1992)111
- Miyazaki, T., see Yoshioka, M. 603(1992)223
- Nakano, M., see Yoshioka, M. 603(1992)223
- Naohara, J. and Manabe, M.  
Separation of oligogalacturonic acids by high-performance gel filtration chromatography on silica gel with diol radical 603(1992)139
- Nguyen, T. S., Hu, S.-G. and Do, D. D.  
Batch dynamic adsorption of dipeptides onto reversed-phase silica gel 603(1992)27
- Oda, Y., see Mano, N. 603(1992)105
- Olesik, S. V., see Giddings, L. D. 603(1992)205
- Pawliszyn, J., see Hawthorne, S. B. 603(1992)185
- Pchelkin, V. P. and Vereshchagin, A. G.  
Reversed-phase thin-layer chromatography of diacylglycerols in the presence of silver ions 603(1992)213
- Pekay, L. A., see Giddings, L. D. 603(1992)205
- Peterson, T. E. and Trowbridge, D.  
Quantitation of *l*-epinephrine and determination of the *d*-/*l*-epinephrine enantiomer ratio in a pharmaceutical formulation by capillary electrophoresis 603(1992)298
- Rowe, R. C., see Wren, S. A. C. 603(1992)235
- Saitoh, K., Kiyohara, C. and Suzuki, N.  
Formation of zinc complexes during chromatography of porphyrins on fluorescent thin-layer plates 603(1992)231
- Sato, T., see Mano, N. 603(1992)105
- Sawa, T., see Yashima, E. 603(1992)111
- Schuchard, M. D., see Landers, J. P. 603(1992)247
- Seki, M., see Yoshioka, M. 603(1992)223
- Seligmann, O., see Antus, S. 603(1992)133
- Sharman, M., MacDonald, S. and Gilbert, J.  
Automated liquid chromatographic determination of ochratoxin A in cereals and animal products using immunoaffinity column clean-up 603(1992)285
- Shiiba, T., see Yashima, E. 603(1992)111
- Sismelich, T. P., see Landers, J. P. 603(1992)247
- Spelsberg, T. C., see Landers, J. P. 603(1992)247
- Subramaniam, M., see Landers, J. P. 603(1992)247
- Sun, Z.-p., see Dang, Q.-x. 603(1992)259
- Suzuki, N., see Saitoh, K. 603(1992)231
- Trowbridge, D., see Peterson, T. E. 603(1992)298
- Utsuki, T., see Yoshioka, M. 603(1992)223
- Van de Water, R., see Frey, D. D. 603(1992)43
- Vereshchagin, A. G., see Pchelkin, V. P. 603(1992)213
- Wagner, H., see Antus, S. 603(1992)133
- Walhagen, A., see Wännman, H. 603(1992)121
- Wännman, H., Walhagen, A. and Erlandsson, P.  
Practical approach to the miniaturization of chiral separations in liquid chromatography using packed fused-silica capillary columns 603(1992)121
- Werner, G., see Aitzetmüller, K. 603(1992)165
- Wheatley, J. B.  
Multiple ligand applications in high-performance immunoaffinity chromatography 603(1992)273
- Wingren, C., Hansson, U.-B. and Andersson, K.  
Supports for liquid-liquid partition chromatography in aqueous two-phase systems: a comparison of Superdex and LiParGel 603(1992)73
- Wren, S. A. C. and Rowe, R. C.  
Theoretical aspects of chiral separation in capillary electrophoresis. I. Initial evaluation of a model 603(1992)235
- Xin, Y., see Aitzetmüller, K. 603(1992)165
- Yaginuma, T., see Yoshioka, M. 603(1992)223
- Yashima, E., Shiiba, T., Sawa, T., Miyauchi, N. and Akashi, M.  
High-performance affinity chromatography of oligonucleotides on nucleic acid analogue immobilized silica gel columns 603(1992)111
- Yoshida, Y., see Mano, N. 603(1992)105
- Yoshioka, M., Araki, H., Seki, M., Miyazaki, T., Utsuki, T., Yaginuma, T. and Nakano, M.  
Fluorescence reactions of inorganic cations heated on a porous glass sheet for thin-layer chromatography 603(1992)223
- Zhang, B., see Frey, D. D. 603(1992)43

Zhang, X., Martire, D. E. and Christensen, R. G.  
Characterization of a supercritical fluid chromatographic  
retention process with a large pressure drop by the  
temporal average density 603(1992)193  
Zhang, Y., see Chen, N. 603(1992)35

Zhang, Z., Malikin, G. and Lam, S.  
Novel polymeric reagent for synthesizing 9-  
fluorenylmethoxycarbonyl L-prolinyl derivatives for chiral  
high-performance liquid chromatography of amino acids  
603(1992)279

## Errata

---

*J. Chromatogr.*, 597 (1992) 37–56

Page 52, third line: “[4,86]” should read “[84,86]”.

*J. Chromatogr.*, 597 (1992) 93–100

Page 97, sixth and fifth line from bottom should read: “That these agreements are probably irrelevant can be shown with the tripeptide Trp-Trp-Trp (Table IV).”

# Journal of Chromatography

## NEWS SECTION

### ANNOUNCEMENTS

2nd INTERNATIONAL SYMPOSIUM ON CAPILLARY ELECTROPHORESIS, YORK, UK, AUGUST 26-28, 1992

The scientific programme will consist of invited plenary lectures, contributed lectures and posters. This symposium will be of interest to scientists working in the field of CE, and those with a background in chromatography and/or electrophoresis who wish to find out more about the "state-of-the-art" in this related technique.

All are invited to submit an abstract describing original research in the area of CE. Papers presented at the conference will be published in a special symposium volume of the *Journal of Chromatography*.

The symposium will be preceded by a three-day short course in CE, August 23-26, 1992.

The cost for the meeting and accommodations will be £185 for Chromatographic Society and British Electrophoresis Society members, and £225 for non-members. The reduced fee for students is £160. A limited number of student bursaries may be offered for students providing a poster or oral contribution.

For further information contact: Dr. Terry Threlfall, Symposium Manager, Department of Chemistry, University of York, Heslington, York YO1 5DD, UK. Tel.: (+44-904) 432-576 or 432-511; Fax: (+44-904) 432-516.

1992 EUROPEAN WORKSHOP IN CHEMOMETRICS, OXFORD, UK, SEPTEMBER 20-25, 1992

This workshop commences with an optional one and a half day long course covering basic topics of pattern recognition, experimental design and univariate signal processing. The three and a half day workshop, beginning September 22 will feature structured sessions including lectures, group discussions, hands-on software, software demonstrations and videos. Delegates can participate in either the full programme of the course plus the workshop or opt for the workshop element only. In addition there will be a special case study session to which all participants can contribute: selected case studies will be sent to those requesting them as documented ASCII files, in advance of the workshop. The organizers would need to hear from those who wish to participate by July 25.

*Workshop topics* covered, in parallel sessions, will include:

- Multivariate data analysis: exploratory data analysis (e.g. PCA), factor analysis, applications;
- Decision making: decision making, cost-benefit analysis, risk analysis;
- Pattern recognition: canonical variates and linear discriminant analysis, cluster analysis, K-nearest neighbour analysis, linear learning machine, SIMCA and related approaches to soft modelling;
- Multivariate data display: principal components

analysis, correspondence analysis, biplots, spectral mapping;

- Fuzzy methods: fuzzy sets and related applications;
- Calibration: univariate calibration, ordinary least squares, principal components regression, partial least squares;
- Factor analysis: factor rotations, evolutionary factor analysis, target transform factor analysis, ITTFA, HELP, applications to HPLC and IR;
- Maximum entropy and Bayesian analysis: entropy in spectroscopy, MEM algorithm, Bayesian fundamentals;
- Advances in experimental design: MANOVA, leverage, visualising confidence bands;
- Expert systems: expert systems, neural networks;
- Multivariate image analysis: multiway calibration, image analysis.

Course topics, run as a single session, will include:

- Pattern recognition and multivariate analysis: principal components analysis, factor analysis, classification problems;
- Experimental design: factorial designs, partial factorials, simplex, response surfaces;
- Univariate signal processing: Fourier transform, time series, deconvolution, derivatives.

Software packages such as UNSCRAMBLER, SPECTRAMAP, SIRIUS, FUZZY C VARIATES, SPECTRACALC, SPIDA, FUZZY TOOLS and Xi3 will be available for hands-on use. Demonstrations of various other packages such as S+ and PARVUS will also be organized.

Fees for the workshop range from £750 to £880 depending on which parts of the workshop will be attended.

For further details contact: Mrs. S. Bladon, School of Chemistry, University of Bristol, Cantock's Close, Bristol BS8 1TS, UK. Tel.: (+44-272) 303-698; Fax: (+44-272) 251-295.

5th INTERNATIONAL SYMPOSIUM ON HIGH PERFORMANCE CAPILLARY ELECTROPHORESIS, ORLANDO, FL, USA, JANUARY 25-28, 1993

The meeting will include invited and contributed lectures, posters, and a three-day exhibition of com-

mercial HPCE systems and components. Lecture and poster topics will include:

- Zone electrophoresis
- Isoelectric focusing
- Micellar separations
- CE/Mass Spectrometry
- Control of electroosmosis
- Gel columns
- Isotachopheresis
- Detector design
- Chiral separations
- Column Coatings
- Analytical and micropreparative applications:
  - Pharmaceuticals, peptides, proteins, carbohydrates, oligonucleotides, sub-cellular structures and whole cells, speciation and detection of inorganics.

All are invited to submit an abstract. Deadline for submission is September 1, 1992. Papers presented at the symposium will be reviewed for publications in a special volume of the *Journal of Chromatography*. Complete manuscripts will be due at the time of the symposium.

For further information contact: Shirley E. Schlessinger, Symposium Manager, HPCE '93, Suite 1015, 400 E. Randolph Drive, Chicago, IL 60601, USA. Tel.: (+1-312) 527-2011.

PITTCON '93, 44th PITTSBURGH CONFERENCE AND EXPOSITION ON ANALYTICAL CHEMISTRY AND APPLIED SPECTROSCOPY, ATLANTA, GA, USA, MARCH 8-12, 1993

This five-day symposium promises to feature new technological developments and applications in analytical chemistry, spectroscopy and related sciences. Special sessions, invited symposia, contributed papers and short courses will be presented. In addition, an exposition of modern laboratory instrumentation, equipment, supplies and services will be available.

All are invited to submit a contributed paper for consideration as an oral presentation or as a poster. Papers are requested in the following categories:

**Methodology:** atomic spectroscopy, chemometrics, computers, electrochemistry, gas chromatography, liquid chromatography, magnetic resonance, mass spectroscopy, sample handling/automation, scanning probe microscopy, separation sciences, supercritical fluid separations, thermal analysis, UV/VIS absorbance/luminescence, and, vibrational spectroscopy;

**Application:** basic chemical research, bioanalytical, clinical/toxicology, environmental, food, forensic, fuels and energy, industrial hygiene, instrumental development/improvement, material characterization, and, process chemistry.

Original, unpublished papers may be contributed in all areas of analytical chemistry, spectroscopy and related scientific areas. One copy of a 250-word abstract must be submitted for review. All abstracts will be carefully evaluated. The abstract should clearly state: the objective of the work, the research plan, equipment and procedures used, sufficient experimental evidence to indicate success of the research plan, and results and/or conclusions. Abstracts must include sufficient content and organization for adequate evaluation by the Conference Program Committee. The deadline for initial abstracts is August 5, 1992.

The conference will also feature several technical sessions in which awards will be presented to distinguished scientists. Some of the awards planned are:

- Pittsburgh Spectroscopy Award;
- Maurice F. Hasler Award;
- Charles N. Reilley Award,
- Dal Nogare Award;
- Bomem-Michelson Award;
- Pittsburgh Analytical Chemistry Award;
- Keene P. Dimick Award;
- James L. Waters Symposium; and,
- The Williams-Wright Industrial Spectroscopist Award.

For further information contact: Mrs. Alma Johnson, Program Secretary, Pittsburgh Conference, 300 Penn Center Boulevard, Suite 332, Pittsburgh, PA 15235-5503, USA. Tel.: (+1-412) 825-3220.

#### 4th INTERNATIONAL SYMPOSIUM ON PHARMACEUTICAL AND BIOMEDICAL ANALYSIS, BALTIMORE, MD, USA, APRIL, 1993

All those involved in the analysis of drugs, related materials and endogenous compounds, in all areas of the pharmaceutical and biomedical sciences are cordially invited to attend this symposium series.

There will be a complete exhibition of analytical equipment, materials and facilities, allowing delegates to observe recent developments at first hand.

The scientific sessions will be preceded on Sunday morning and afternoon by a series of workshops on a number of topical themes.

The scientific program will feature invited keynote speakers, submitted lectures, posters, and poster discussion sessions. Topics for presentation will include the following:

- Advances in separation techniques – LC, CE, SFC, GC
- Analysis of bulk drug substances and formulations
- Analysis of enantiomers
- Analytical biotechnology
- Analytical considerations in preformulation and drug delivery studies
- Applications of monoclonal antibodies
- Assay validation
- Automated methods of analysis
- Bioanalysis in clinical and preclinical drug development
- Derivatization Techniques
- Drugs of abuse and sports medicine
- Electrochemical methods
- Pharmaceutical quality control
- Receptor, enzyme, immuno- and bio-assays
- Sample preparation
- Spectroscopy and spectroscopic methods – NMR, MS, CD, FT-IR, UV-VIS, CL, FL
- Therapeutic drug monitoring, clinical and forensic toxicology

For further information contact: Shirley Schlessinger, Symposium Manager, Suite 1015, 400 E. Randolph Drive, Chicago, IL 60601, USA. Tel.: (+1-312) 527-2011.

**INTERNATIONAL SYMPOSIUM ON ANALYSIS OF PEPTIDES, STOCKHOLM, SWEDEN, MAY 24-26, 1993**

The aim of the symposium is to provide state-of-the-art of the different analytical techniques useful in peptide research, as well as to highlight necessary new research directions to meet the requirements from future research and development activities on peptide drugs and endogenous peptides.

The symposium will include sessions on: separation techniques, purity and structure, immunological techniques, spectroscopic techniques, and analysis in biological material; along with discussion sessions in analytical challenges in biotechnology and strategies for the analysis of peptides in biological material.

Poster abstracts may be submitted up to March 8, 1993. Information as to whether a poster has been accepted or not will be given before April 5, 1993.

The official language of the symposium will be English.

For further information contact: Swedish Academy of Pharmaceutical Sciences, Symposium on "Analysis of Peptides", P.O. Box 1136, S-111 81 Stockholm, Sweden. Tel.: (+46-8) 245-085; Fax: (+46-8) 205-511.

**PREP '93, 10th INTERNATIONAL SYMPOSIUM ON PREPARATIVE CHROMATOGRAPHY, ARLINGTON, VA, USA, JUNE 14-16, 1993**

The three-day program of this symposium will include invited and contributed lectures, poster presentations, an exhibit of software and technical literature, and discussion sessions. All are invited to submit an abstract for consideration for inclusion in the program describing original research in areas of preparative chromatography such as:

- Theory of non-linear chromatography, overloaded elution and displacement chromatography
- Kinetics of mass transfer at high concentrations
- Stationary phases
- Applications to drugs and specialty chemicals

- Applications to recombinant and natural proteins, to peptides, other biopolymers, chiral separations, etc.
- Optimization of experimental conditions
- Economics of preparative chromatography
- Instrumentation

The deadline for submission of Abstracts is December 1, 1992. Abstracts received after December 1, 1992 will be considered for poster presentation, but will not be included in the preliminary program.

For further information contact: Washington Chromatography Discussion Group, c/o Barr Enterprises, P.O. Box 279, Walkersville, MD 21793, USA. Tel.: (+1-301) 898-3772; Fax: (+1-301) 898-5596.

**9th DANUBE SYMPOSIUM ON CHROMATOGRAPHY, BUDAPEST, HUNGARY, AUGUST 23-27, 1993**

The scientific program will cover all fundamental aspects, instrumentation, new developments and applications of the various chromatographic techniques, *i.e.* column liquid chromatography, supercritical fluid chromatography, gas chromatography, planar chromatography, hyphenated methods, and related techniques such as field flow fractionation, capillary electrophoresis and other electro-driven separation techniques.

Invited plenary and keynote lectures will be given by internationally recognized scientists. The majority of the contributed papers will be presented as posters, a limited number as oral communication. In addition, poster discussion sessions will be organized.

An exhibition of chromatographic instruments, columns, accessories, chemicals and chromatographic literature is planned in connection with the symposium.

All registered participants will receive a copy of the book of abstracts. The deadline for submission of abstracts is February 28, 1993. Submitted papers will be considered for publication in a special issue of the *Journal of Chromatography*.

The deadline for registration is June 30, 1993. The symposium language will be English.

For further information contact: Symposium Secretariat, Professor László Szepesy, Department of Chemical Technology, Technical University of Budapest, Budafoki út 8., H-1521 Budapest, Hungary. Tel.: (+ 36-1) 186-9000; Fax: (+ 36-1) 181-2755; Telex: 225931 muegy h.

12th INTERNATIONAL SYMPOSIUM ON BIOMEDICAL APPLICATIONS OF CHROMATOGRAPHY AND ELECTROPHORESIS AND 2nd INTERNATIONAL SYMPOSIUM ON THE APPLICATIONS OF HPLC IN ENZYME CHEMISTRY, VERONA, ITALY, SEPTEMBER 7-10, 1993

The program for this three-day symposium will consist of plenary lectures, oral presentations and posters. The focus will be on the following five areas:

- New methodological achievements in HPLC and CE applied to the biosciences

- HPLC and CE analysis of drugs and other toxic substances in biological media
- HPLC and CE in enzyme analysis
- HPLC and CE in immunochemistry and DNA analysis
- Use of bioreactors in HPLC and CE

The Symposium language will be English.

Submitted Abstracts should be sent to the Symposium Secretariat no later than May 15, 1993.

The papers presented at this symposium will be published in a special issue of the *Journal of Chromatography, Biomedical Applications*.

Since progress in analytical techniques is closely linked to developments in instrumentation, a technical exhibition by international suppliers is planned close to the lecture halls.

Deadline for advance registration is May 15, 1993.

For further information contact: Dr. Franco Tagliaro, Istituto di Medicina Legale, Università di Verona, Policlinico, I-37134 Verona, Italy. Tel.: (+ 39-45) 807-4618/807-4246; Fax: (+ 39-45) 505-259.

Announcements are included free of charge. Information on planned events should be sent well in advance (6 months) to: *Journal of Chromatography*, News Section, P.O. Box 330, 1000 AH Amsterdam, Netherlands, or by Fax: (+ 31 20) 5862304.

## CALENDAR OF FORTHCOMING EVENTS

### ■ June 22–24, 1992

**Research Triangle Park, NC, USA**

Annual Meeting of the Electrophoresis Society

Contact: Mrs. Janet Cunningham, Seminar Manager, Barr Enterprises, P.O. Box 279, Walkersville, MD 21793, USA. Tel.: (+1-301) 898-3772; Fax: (+1-301) 898-5596.

### July 8–10, 1992

**Amsterdam, Netherlands**

Amsterdam Summercourse on Capillary Electrophoresis

Contact: Dr. W.Th. Kok or Dr. J.C. Kraak, Laboratory for Analytical Chemistry, University of Amsterdam, Nieuwe Achtergracht 166, 1018 WV Amsterdam, Netherlands. Tel.: (+31-20) 525-6539/46/15; Fax: (+31-20) 525-5698.

### July 14–17, 1992

**Montreal, Canada**

CAC-92, 5th International Conference on Chemometrics in Analytical Chemistry

Contact: Int. Conf. on Chemometrics in Analytical Chemistry, c/o Department of Chemistry, Clarkson University, Potsdam, NY 13699-5810, USA. Tel: (+1-315) 268-3861 (Dr. Hopke); (+1-315) 268-2394 (Dr. Lavine); Fax: (+1-315) 268-6670.

### July 27–31, 1992

**New Hampton, NH, USA**

42nd Annual Gordon Research Conference on Statistics in Chemistry and Chemical Engineering

Contact: Dr. A.M. Cruickshank, Gordon Research Center, University of Rhode Island, Kingston, RI 02881, USA. Tel.: (+1-401) 783-4011; E-Mail: bcp101@uriacc.bitnet.

### ■ Aug. 18–20, 1992

**Washington, DC, USA**

Symposium on Greenhouse Gas Emissions and Mitigation Research

Contact: Sue Philpott, Acurex Environmental, P.O. Box 13109, Research Triangle Park, NC 27709, USA. Tel.: (+1-919) 544-4535; Fax: (+1-919) 544-5690.

### Aug. 23–26, 1992

**York, UK**

Capillary Electrophoresis Training Course

Contact: Dr. Terry Threlfall, Industrial Liaison Executive, Department of Chemistry, University of York, Heslington, York YO1 5DD, UK. Tel.: (+44-904) 432576/432511; Fax: (+44-904) 432516

### Aug. 24–27, 1992

**Jena, Germany**

COMPANA '92, 5th Conference on Computer Applications in Analytical Chemistry

Contact: COMPANA '92, Friedrich Schiller University Jena, Institute of Inorganic and Analytical Chemistry, Steiger 3, Haus 3, O-6900 Jena, Germany. Tel.: (+37-82) 25467 or (+37-82) 25029.

### Aug. 26–28, 1992

**York, UK**

International Symposium on Capillary Electrophoresis

Contact: Dr. Terry Threlfall, Industrial Liaison Executive, Department of Chemistry, University of York, Heslington, York YO1 5DD, UK. Tel.: (+44-904) 432576/432511; Fax: (+44-904) 432516.

### ■ Aug. 30–Sept. 3, 1992

**Cincinnati, OH, USA**

106th Annual International Meeting and Exposition of the AOAC

Contact: Margaret Ridgell, AOAC, 2200 Wilson Blvd., Suite 400, Arlington, VA 22201-3301, USA. Tel.: (+1-703) 522-3032; Fax: (+1-703) 522-5468.

### Aug. 31–Sept. 3, 1992

**Cincinnati, OH, USA**

106th Annual International Meeting and Exposition of the AOAC

Contact: Margaret Ridgell, AOAC, 2200 Wilson Boulevard, Suite 400, Arlington, VA 22201-3301, USA. Tel.: (703) 522-3032; Fax: (703) 522-5468.

### September 4–6, 1992

**Tallin, Estonia**

Chromatography and Ecology

Contact: Elle Roosaluuste, Department of Botany and Ecology, Lai 40, Tartu, Estonia. Tel.: (+7-1434) 35151; Fax: (+7-1434) 33472; E-Mail: KALEVI@ZBI.TARTU.EW.SU.

### Sept. 13–18, 1992

**Aix-en-Provence, France**

19th International Symposium on Chromatography

Contact: G.A.M.S., 88 Boulevard Malesherbes, 75008 Paris, France. Tel.: (1) 45639304; Fax: (1) 49530434

**Sept. 20–25, 1992**

**Philadelphia, PA, USA**

19th Annual Meeting of the Federation of Analytical Chemistry and Spectroscopy Societies

Contact: FACSS, P.O. Box 278, Manhattan, KS 66502, USA. Tel.: (+1-301) 846-4797.

■ **Sept. 20–25, 1992**

**Oxford, UK**

1992 European Workshop in Chemometrics

Contact: Mrs. S. Bladon, School of Chemistry, University of Bristol, Cantock's Close, Bristol BS8 1TS, UK. Tel.: (+44-272) 303-698; Fax: (+44-272) 251-295.

**Sept. 21–23, 1992**

**Noordwijkerhout, Netherlands**  
**Anabiotec '92**

Contact: ANABIOTECH '92, p/a CAOS, WG Plein 475, 1054 SH Amsterdam, Netherlands. Tel.: (+31-20) 616-5151; Fax: (+31-20) 689-0981.

**Sept. 21–24, 1992**

**Linz, Austria**

International Ion Chromatography Symposium

Contact: Century International, P.O. Box 493, Medfield, MA 02052, USA. Tel.: (+1-508) 359-8777; Fax: (+1-508) 359-8778.

**Oct. 3–4, 1992**

**Salt Lake City, UT, USA**

**FFF Workshop V**

Contact: Julie Westwood, FFF Research Center, Department of

Chemistry, University of Utah, Salt Lake City, UT 84112, USA. Tel.: (+1-801) 581-5419; Fax: (+1-801) 581-4353.

**Oct. 5–7, 1992**

**Park City, UT, USA**

3rd International Symposium on Field-Flow Fractionation (FFF)

Contact: Julie Westwood, FFF Research Center, Department of Chemistry, University of Utah, Salt Lake City, UT 84112, USA. Tel.: (+1-801) 581-5419; Fax: (+1-801) 581-4353.

**Oct. 5–8, 1992**

**Tübingen, Germany**

3rd International Symposium on Chiral Discrimination

Contact: Gesellschaft Deutscher Chemiker, Abteilung Tagungen, P.O. Box 90 04 40, D-6000 Frankfurt 90, Germany. Fax: (+49-69) 791-7475

**Oct. 6–9, 1992**

**Rome, Italy**

ITP '92, 8th International Symposium on Capillary Electrophoresis and Isotachopheresis

Contact: Dr. Salvatore Fanali, Istituto di Cromatografia del C.N.R., P.O. Box 10, 00016 Monterotondo Scalo (Rome), Italy. Tel: (+39-6) 9005328/9005836; Fax: (+39-6) 9005849; Telex: 624809 CNR ML 1.

**Oct. 19–20, 1992**

**Strasbourg, France**

1st European Symposium on FPLC of Biomolecules

Contact: Symposium Secretariat, B.O. Conference Service, P.O. Box 100 78, S-750 10 Uppsala, Sweden. Tel. and Fax: (+46-18) 30-4074.

**Oct. 20–21, 1992**

**Frederick, MD, USA**

3rd Annual Frederick Conference on Capillary Electrophoresis

Contact: Margaret L. Fanning, Conference Coordinator, PRI, NCI-FCRDC, P.O. Box B, Frederick, MD 21702-1201, USA. Tel.: (+1-301) 846-1089; Fax: (+1-301) 846-5866.

■ **Oct. 26–28, 1992**

**Munich, Germany**

Electrophoresis Forum '92

Contact: Professor B.J. Radola, Technical University Munich, W-8050 Freising-Weiherstephan, Germany. Tel.: (+49-8161) 713287; Fax: (+49-8161) 12962.

**Nov. 4–6, 1992**

**Montreux, Switzerland**

9th Montreux Symposium on Liquid Chromatography–Mass Spectrometry (LC–MS, SFC–MS, CZE–MS, MS–MS)

Contact: Marianne Frei, IAEAC Secretariat, P.O. Box 46, CH-4123 Allschwil, Switzerland. Tel.: (+41-61) 632789; Fax: (+41-61) 4820805.

■ **Nov. 11, 1992**

**Loughborough, UK**

European Radiochemistry

Contact: Dr. P. Warwick, Department of Chemistry, University of Technology, Loughborough, Leicestershire LE11 3TU, UK. Tel.: (+44-509) 263-171; Fax: (+44-509) 233-163.

**Nov. 29–Dec. 2, 1992**

**Sydney, Australia**

12th International Symposium on HPLC of Proteins, Peptides and Polynucleotides

Contact: 12 ISPPP Secretariat, GPO Box 128, Sydney NSW 2001, Australia. Tel.: (+61-2) 262-2277; Fax: (+61-2) 262-2323.

**Dec. 14–16, 1992**

**Budapest, Hungary**

Budapest Chromatography Conference

Contact: Organizing Bureau, Agnes v. Rubányi, Intercongress, Dózsa György u. 84/a, H-1068 Budapest, Hungary. Tel.: (+36-1) 122-2203; Fax: (+36-1) 142-4118; Telex: 223955 ici pv.

■ **Jan. 25–28, 1993**

**Orlando, FL, USA**

5th International Symposium on High Performance Capillary Electrophoresis

Contact: Shirley E. Schlessinger, Symposium Manager, HPCE '93, Suite 1015, 400 E. Randolph Drive, Chicago, IL 60601, USA. Tel.: (+1-312) 527-2011.

■ **March 8–12, 1993**

**Atlanta, GA, USA**

PITTCON '93, 44th Pittsburgh Conference and Exposition on Analytical Chemistry and Applied Spectroscopy

Contact: Mrs. Alma Johnson, Program Secretary, Pittsburgh Conference, 300 Penn Center Blvd., Suite 332, Pittsburgh, PA 15235-5503, USA. Tel.: (+1-412) 825-3220.

■ **April, 1993**

**Baltimore, MD, USA**

4th International Symposium on Pharmaceutical and Biomedical Analysis

Contact: Shirley Schlessinger, Symposium Manager, Suite 1015, 400 E. Randolph Drive, Chicago, IL 60601, USA. Tel.: (+1-312) 527-2011.

**April 4–7, 1993**

**Wrexham, UK**

Ion-Ex '93

Contact: Ion-Ex '93, Conference Secretariat, Faculty of Science, The North East Wales Institute, Connah's Quay, Deeside, Clwyd, CH5 4BR, UK. Tel.: (+44-244) 831-531 ext. 245 or 276; Fax: (+44-244) 814-305.

**May 9–14, 1993**

**Hamburg, Germany**

17th International Symposium on Column Liquid Chromatography

Contact: Gesellschaft Deutscher Chemiker, Abteilung Tagungen, P.O. Box 900440, Varrentrappstrasse 40-42, W-6000 Frankfurt am Main 90, Germany. Tel.: (+49-69) 7917-360; Fax: (+49-69) 7917-475.

■ **May 24–26, 1993**

**Stockholm, Sweden**

International Symposium on Analysis of Peptides

Contact: Swedish Academy of Pharmaceutical Sciences, Symposium on "Analysis of Peptides", P.O. Box 1136, S-111 81 Stockholm, Sweden. Tel.: (+46-8) 245-085; Fax: (+46-8) 205-511.

■ **May 25–27, 1993**

**Ghent, Belgium**

5th International Symposium on

Quantitative Luminescence Spectrometry in Biomedical Sciences

Contact: Dr. Willy R.G. Baeyens, Symposium Chairman, University of Ghent, Pharmaceutical Institute, Harelbekestraat 72, B-9000 Ghent, Belgium. Tel.: (+32-91) 218-951, ext. 246; Fax: (+32-91) 217-902.

■ **June 14–16, 1993**

**Arlington, VA, USA**

Prep '93, 10th International Symposium on Preparative Chromatography

Contact: Washington Chromatography Discussion Group, c/o Barr Enterprises, P.O. Box 279, Walkersville, MD 21793, USA. Tel.: (+1-301) 898-3772; Fax: (+1-301) 898-5596.

■ **July 26–29, 1993**

**Washington, DC, USA**

107th Annual International Meeting and Exposition of the AOAC

Contact: Margaret Ridgell, AOAC, 2200 Wilson Blvd., Suite 400, Arlington, VA 22201-3301, USA. Tel.: (+1-703) 522-3032; Fax: (+1-703) 522-5468.

■ **Aug. 23–27, 1993**

**Budapest, Hungary**

9th Danube Symposium on Chromatography

Contact: Symposium Secretariat, Professor László Szepesy, Department of Chemical Technology, Technical University of Budapest, Budafoki út 8., H-1521 Budapest, Hungary. Tel.: (+36-1) 186-9000; Fax: (+36-1) 181-2755; Telex: 225931 muegy h.

**Sept. 5–11, 1993**

**Edinburgh, UK**

**EUROANALYSIS VIII**, 8th European Conference on Analytical Chemistry

Contact: Miss P.E. Hutchinson, Analytical Division, The Royal Society of Chemistry, Burlington House, Piccadilly, London W1V 0BN, UK. Tel.: (071) 4378656; Fax: (071) 734-1227; Telex: 268001.

■ **Sept. 7–10, 1993**

**Verona, Italy**

12th International Symposium on Biomedical Applications of Chromatography and Electrophoresis and 2nd International

Symposium on the Applications of HPLC in Enzyme Chemistry

Contact: Dr. Franco Tagliaro, Istituto di Medicina Legale, Università di Verona, Policlinico, I-37134 Verona, Italy. Tel.: (+39-45) 807-4618/807-4246; Fax: (+39-45) 505-259.

**Sept. 8–10, 1993**

**Prague, Czechoslovakia**

4th Workshop on Chemistry and Fate of Modern Pesticides and Related Pollutants

Contact (for Eastern European countries): Dra. J. Hajslova, Department of Food Chemistry and Analysis, Institute of Chemical Technology, Suchbátarova 5,

166 28 Prague 6-Dejvice, Czechoslovakia. Fax: (+42-2) 311-4769. For all other countries, contact: IAEAC, M. Frei-Häusler, P.O. Box 46, CH-4123 Allschwil 2, Switzerland. Fax: (+41-61) 482-0805.

**June 20–24, 1994**

**Bournemouth, UK**

20th International Symposium on Chromatography

Contact: Executive Secretary, The Chromatographic Society, Nottingham Polytechnic, Burton Street, Nottingham, NG1 4BU, UK. Tel.: (0602) 500596; Fax: (0602) 500614.

---

■ Indicates new or amended entry.



# Laboratory information **new!** management

An International Journal

Section of Chemometrics and Intelligent Laboratory Systems

Editor:

**R.D. McDowall**, Beckenham, Kent, UK

Editor for North America:

**R.R. Mahaffey**, Eastman Chemicals  
Division, Kingsport, TN, USA

The journal covers all aspects of information management in a laboratory environment, such as information technology, storage, processing and flow of data. The following topics are covered:

- \* **Laboratory Information Management Systems (LIMS)**
- \* **Means of integrating and merging laboratory information**
- \* **Networks**
- \* **Regulatory Aspects**
- \* **Electronic Laboratory Notebooks**
- \* **Human aspects of laboratory automation**

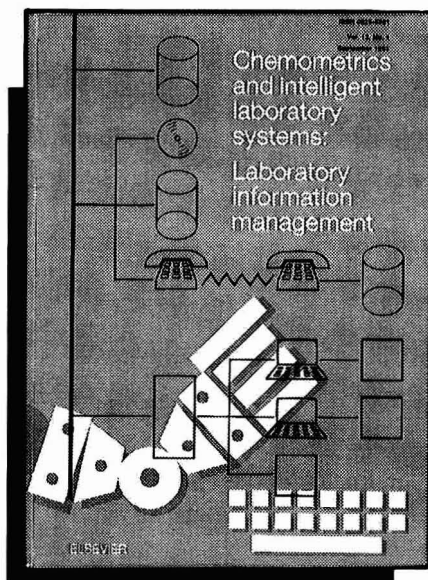
Subscription Information:

1992: Vol. 17 (3 issues)

Dfl. 406.00 / US\$ 201.00

(including postage)

ISSN 0925-5281



***A Free Sample Copy is Available on Request***

Elsevier Science Publishers  
P.O. Box 330  
1000 AH Amsterdam  
The Netherlands  
Tel: (31-20) 5862 873  
Fax: (31-20) 5862 845



in the USA and Canada  
P.O. Box 882  
Madison Square Station  
New York, NY 10159, USA  
Tel: (212) 633 3750  
Fax: (212) 633 3764

**ELSEVIER SCIENCE PUBLISHERS**

---

---

# New Developments in Ion Exchange

Materials, Fundamentals and Applications

Proceedings of the International Conference on Ion Exchange,  
ICIE '91, Tokyo, Japan, October 2-4, 1991

edited by **M. Abe**, Tokyo Institute of Technology, Tokyo, Japan,  
**T. Kataoka**, University of Osaka Prefecture, Osaka, Japan and  
**T. Suzuki**, Yamanashi University, Yamanashi, Japan

This volume contains the papers presented at the International Conference on Ion Exchange (ICIE '91). Included are reviews and original papers reflecting recent progress in new branches of science and technology based on novel ion-exchange materials and ion-exchange theory.

Topics covered include:  
Fundamentals (Ion exchange theory and process), Synthesis of New Materials, Chromatography (Ion and liquid chromatography, and associated techniques), Water Purification, Environmental, Membranes, Hydrometallurgy, Separation Science and Technology (Food, pharmaceutical, biological and others).

**Contents:**  
**Fundamentals.**  
(21 papers).

**Synthesis of New Materials.**  
(24 papers).

**Chromatography.**  
(8 papers).

**Water Purification.**  
(7 papers).

**Environmental.**  
(12 papers).

**Membranes.**  
(14 papers).

**Hydrometallurgy.**  
(8 papers).

**Separation Science and  
Technology.**  
(14 papers).

**1991 xlii + 636 pages**  
**Price: US \$ 218.00 / Dfl. 425.00**  
**ISBN 0-444-98688-X**

*Co-edition with and distributed in  
Japan by Kodansha Scientific Ltd.*



**Elsevier Science Publishers**

P.O. Box 211, 1000 AE Amsterdam, The Netherlands  
P.O. Box 882, Madison Square Station, New York, NY 10159, USA

## PUBLICATION SCHEDULE FOR 1992

*Journal of Chromatography and Journal of Chromatography, Biomedical Applications*

MONTH	O 1991-F 1992	M	A	M	J	J	
Journal of Chromatography	Vols. 585-593	594/1 + 2 595/1 + 2	596/1 596/2 597/1 + 2	598/1 598/2 599/1 + 2 600/1 600/2	602/1 + 2 603/1 + 2 604/1	604/2 605/1 605/2 606/1	The publication schedule for further issues will be published later.
Cumulative Indexes, Vols. 551-600							
Bibliography Section		610/1			610/2		
Biomedical Applications	Vols. 573 and 574	575/1 575/2	576/1	576/2 577/1	577/2	578/1 578/2	

\* Cumulative Indexes will be Vol. 601, to appear early 1993.

### INFORMATION FOR AUTHORS

(Detailed *Instructions to Authors* were published in Vol. 558, pp. 469-472. A free reprint can be obtained by application to the publisher, Elsevier Science Publishers B.V., P.O. Box 330, 1000 AH Amsterdam, The Netherlands.)

**Types of Contributions.** The following types of papers are published in the *Journal of Chromatography* and the section on *Biomedical Applications*: Regular research papers (Full-length papers), Review articles and Short Communications. Short Communications are usually descriptions of short investigations, or they can report minor technical improvements of previously published procedures; they reflect the same quality of research as Full-length papers, but should preferably not exceed five printed pages. For Review articles, see inside front cover under Submission of Papers.

**Submission.** Every paper must be accompanied by a letter from the senior author, stating that he/she is submitting the paper for publication in the *Journal of Chromatography*.

**Manuscripts.** Manuscripts should be typed in double spacing on consecutively numbered pages of uniform size. The manuscript should be preceded by a sheet of manuscript paper carrying the title of the paper and the name and full postal address of the person to whom the proofs are to be sent. As a rule, papers should be divided into sections, headed by a caption (*e.g.*, Abstract, Introduction, Experimental, Results, Discussion, etc.). All illustrations, photographs, tables, etc., should be on separate sheets.

**Introduction.** Every paper must have a concise introduction mentioning what has been done before on the topic described, and stating clearly what is new in the paper now submitted.

**Abstract.** All articles should have an abstract of 50-100 words which clearly and briefly indicates what is new, different and significant.

**Illustrations.** The figures should be submitted in a form suitable for reproduction, drawn in Indian ink on drawing or tracing paper. Each illustration should have a legend, all the legends being typed (with double spacing) together on a separate sheet. If structures are given in the text, the original drawings should be supplied. Coloured illustrations are reproduced at the author's expense, the cost being determined by the number of pages and by the number of colours needed. The written permission of the author and publisher must be obtained for the use of any figure already published. Its source must be indicated in the legend.

**References.** References should be numbered in the order in which they are cited in the text, and listed in numerical sequence on a separate sheet at the end of the article. Please check a recent issue for the layout of the reference list. Abbreviations for the titles of journals should follow the system used by *Chemical Abstracts*. Articles not yet published should be given as "in press" (journal should be specified), "submitted for publication" (journal should be specified), "in preparation" or "personal communication".

**Dispatch.** Before sending the manuscript to the Editor please check that the envelope contains four copies of the paper complete with references, legends and figures. One of the sets of figures must be the originals suitable for direct reproduction. Please also ensure that permission to publish has been obtained from your institute.

**Proofs.** One set of proofs will be sent to the author to be carefully checked for printer's errors. Corrections must be restricted to instances in which the proof is at variance with the manuscript. "Extra corrections" will be inserted at the author's expense.

**Reprints.** Fifty reprints of Full-length papers and Short Communications will be supplied free of charge. Additional reprints can be ordered by the authors. An order form containing price quotations will be sent to the authors together with the proofs of their article.

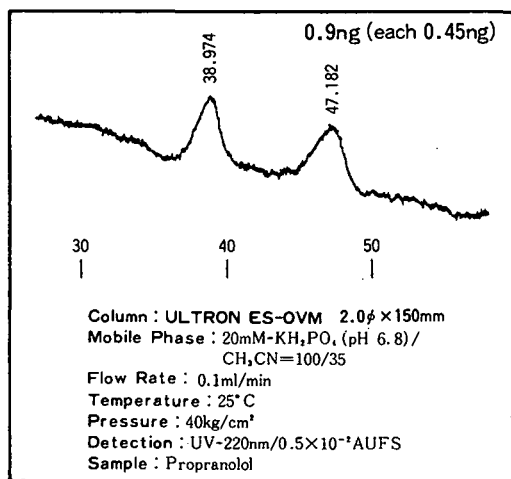
**Advertisements.** The Editors of the journal accept no responsibility for the contents of the advertisements. Advertisement rates are available on request. Advertising orders and enquiries can be sent to the Advertising Manager, Elsevier Science Publishers B.V., Advertising Department, P.O. Box 211, 1000 AE Amsterdam, Netherlands; courier shipments to: Van de Sande Bakhuizenstraat 4, 1061 AG Amsterdam, Netherlands; Tel. (+31-20) 515 3220/515 3222, Telefax (+31-20) 6833 041, Telex 16479 els vi nl. UK: T. G. Scott & Son Ltd., Tim Blake, Portland House, 21 Narborough Road, Cosby, Leics. LE9 5TA, UK; Tel. (+44-533) 753 333, Telefax (+44-533) 750 522. USA and Canada: Weston Media Associates, Daniel S. Lipner, P.O. Box 1110, Greens Farms, CT 06436-1110, USA; Tel. (+1-203) 261 2500, Telefax (+1-203) 261 0101.

# The most useful chiral separation column, ULTRON ES-OVM, for enantiomeric drugs.

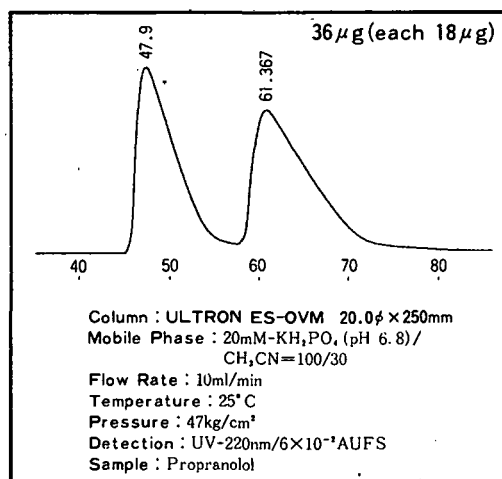
Substance	Rs	Substance	Rs	Substance	Rs
Acetylpheneturide	2.74	Disopyramid	2.04	Nisoldipine	2.36
Alimemazine	6.06	Eperisone	1.15	Nitrendipine	1.80
Alprenolol	1.09 <sup>1)</sup>	Ethiazide	1.42	Oxazepan	2.65 <sup>2)</sup>
Arotinolol	1.95	Fenoprofen	0.80	Oxprenolol	1.38
Bay K 8644	5.92	Flurbiprofen	1.27	Pindolol	2.04
Benproperine	3.27	Glutethimide	1.36	2-Phenylpropionic acid	0.80
Benzoin	8.41	Glycopyrronium	1.73	Pranoprofen	0.63
Biperiden	3.17	Hexobarbital	1.70	Prenylamine	0.86
Bunitrolol	3.08	Homochlorcyclizine	3.04	Profenamine	3.31
Bupivacaine	1.26	Hydroxyzine	2.15	Promethazine	1.42
Chlormezanone	6.48	Ibuprofen	1.72	Propranolol	1.24
Chlorphenesin	2.23	Ketoprofen	1.37	Terfenadine	2.22
Chlorpheniramine	2.36	Lorazepam	2.55 <sup>2)</sup>	Thioridazine	0.72
Chlorprenaline	2.34	Meclizine	3.71	Tolperisone	1.50
Cloperastin	2.85	Mepenzolate	1.40	Trihexyphenidyl	5.16
Dimethindene	4.33	Mephobarbital	1.70	Trimipramine	3.69
1,2-Diphenylethylamine	1.74	Methylphenidate	1.13 <sup>1)</sup>	Verapamil	1.49

NOTE: 4.6×150mm column at room temp. except<sup>1)</sup> 6.0×150mm at room temp. and<sup>2)</sup> 6.0×150mm at 10°C

From trace analysis for metabolites:



to preparative scale



## SHINWA CHEMICAL INDUSTRIES, LTD

50 Kagekatsu-cho, Fushimi-ku, Kyoto 612, JAPAN

Phone: 80-75-621-2360 Fax: 80-75-602-2660

Please contact in United States of America and Europe to:

Rockland Technologies, Inc. 538 First State Boulevard, Newport, DE 19804, U.S.A.

Phone: 302-633-5880, Fax: 302-633-5893

This product is licenced by Eisai Co., Ltd.